Experimental Condensed Matter Physics Principal Investigators' Meeting–2019

September 16–18, 2019

Marriott Washingtonian, Gaithersburg, MD

Co-chairs: Jan Musfeldt (Tennessee), Dave Hsieh (Caltech)

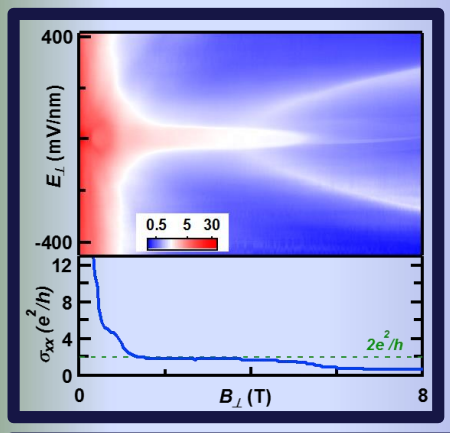

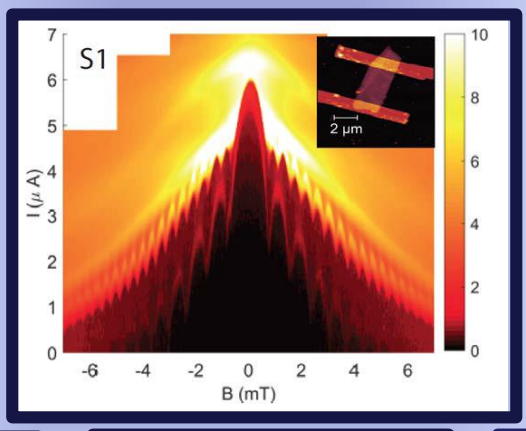

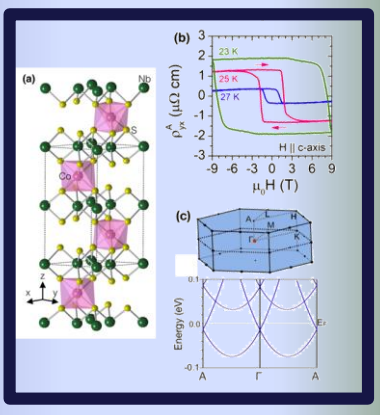

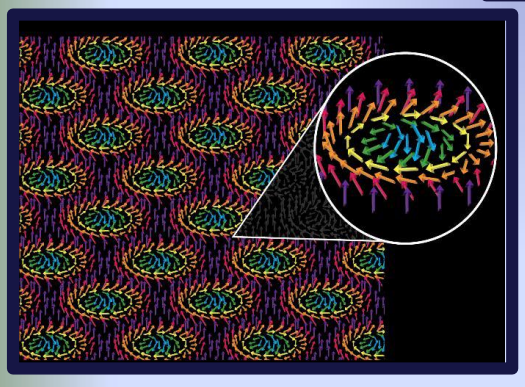

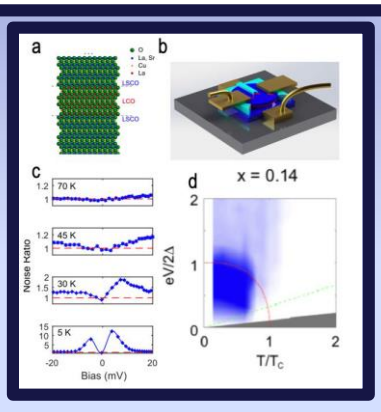

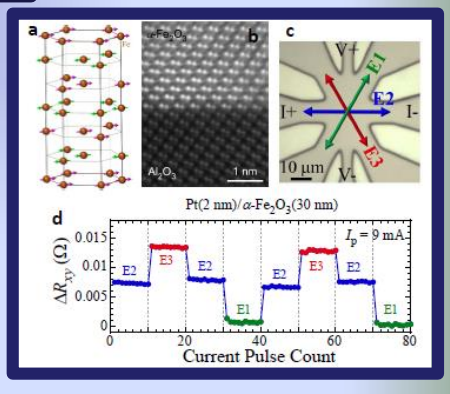

U.S. DEPARTMENT OF ENERGY | Office of Science

Office of Basic Energy Sciences
Materials Sciences and Engineering Division

On the Cover

1	2	3
4	5	6

Figures are from selected highlight slides submitted to the ECMP PI Meeting.

1. Quantum Parity Hall in Trilayer Graphene. Jeanie Lau, PI. Ohio State University.
2. Edge Supercurrent in Weyl Superconductor. Phuan Ong, PI. Princeton University.
3. Topological Hall Effect in a Magnetic Layered Dichalcogenide. John Mitchell, lead PI. Argonne National Laboratory.
4. Liberating Magnetic Vortices from the Crystal Lattice. John DiTusa, PI. Louisiana State University.
5. Pairing in the Pseudogap Regime Revealed by Shot Noise. Doug Natelson, PI. Rice University.
6. Electrical Switching of Antiferromagnetic Néel Order. Fengyuan Yang, PI. Ohio State University.

This document was produced under contract number DE-SC0014664 between the U.S. Department of Energy and Oak Ridge Associated Universities.

The research grants and contracts described in this document are supported by the U.S. DOE Office of Science, Office of Basic Energy Sciences, Materials Sciences and Engineering Division.

Foreword

This book contains abstracts for presentations made at the 2019 Experimental Condensed Matter Physics (ECMP) Principal Investigators' Meeting sponsored by the Materials Sciences and Engineering Division of the US Department of Energy, Office of Basic Energy Sciences (DOE-BES). The meeting convenes scientists supported within ECMP by the DOE-BES to present the most exciting, new research accomplishments and proposed future research directions in their BES supported projects. The meeting also affords PIs in the program an opportunity to see the full range of research currently being supported. We hope the meeting fostered a collegial environment to (1) stimulate the discussion of new ideas and (2) provide unique opportunities to develop or strengthen collaborations among PIs. In addition, the meeting provides valuable feedback to DOE-BES in its assessment of the state of the program and in identifying future programmatic directions. The meeting was attended by approximately 100 ECMP-supported scientists.

The Experimental Condensed Matter Physics program supports research that will advance our fundamental understanding of the relationships between intrinsic electronic structure and properties of complex materials. Research supported by the program focuses on systems whose behavior derives from strong electron correlation, competing or coherent quantum interactions, topology, and effects of interfaces, defects, spin-orbit coupling, and reduced dimensionality. Scientific themes include charge, spin, and orbit degrees of freedom that result in phenomena such as superconductivity, magnetism, and topological protection, and the interactions of these in bulk and reduced-dimensional systems. The program supports synthesis and characterization of new material systems required to explore the central scientific themes. This includes development of experimental techniques that enable such research. Growth areas include new and emergent quantum phenomena in topological materials, low-dimensional materials including proximity effects, and materials with targeted functionality (e.g., quantum information science and neuromorphic computing).

The meeting was organized into six oral and four poster sessions covering the range of activities supported by the program. This structure represents a change from the past, featuring fewer oral and more poster sessions, with the intent to provide enhanced PI interaction. Co-chairs for the meeting were Jan Musfeldt (Tennessee) and Dave Hsieh (Caltech). To these two I express my sincere appreciation for their invaluable help in organizing the meeting. A panel discussion entitled "*Research at World-Class BES Facilities*" was featured at the meeting. The meeting co-chairs and I thank the panelists for their investment in time and for their willingness to share their experiences and knowledge with the ECMP community. We also want to gratefully acknowledge the excellent support provided by Ms. Linda Severs of the Oak Ridge Institute for Science and Education and by Ms. Teresa Crockett of BES, for their efforts in organizing the meeting.

Dr. Michael (Mick) Pechan
Program Manager, Condensed Matter and Materials Physics
Division of Materials Sciences and Engineering
Basic Energy Sciences

Table of Contents

Session 3

Session 4

Poster Sessions

Poster Abstracts

Experimental Condensed Matter Physics
Principal Investigators' Meeting Agenda

Monday, September 16, 2019

7:30–8:15am	***Breakfast***
8:15–8:40am	*BES – Welcome* **Mick Pechan**, Department of Energy
Oral Session 1	Chair: **Amir Yacoby**, Harvard University
8:40–8:55 am	**Jie Shan**, Cornell University *Planar Systems for Quantum Information*
8:55–9:10 am	**Feng Wang**, Lawrence Berkeley National Laboratory *Van der Waals Heterostructures, Novel Materials and Emerging Phenomena*
9:10–9:25 am	**Leonid Butov**, University of California – San Diego *Cold Exciton Gases in Semiconductor Heterostructures*
9:25–9:40 am	**Dmitri Basov,** Columbia University *Electronic and Photonic Phenomena in Graphene-Based Heterostructures*
9:40–9:55 am	**Min Ouyang**, University of Maryland *Understanding a Few Spin-Based Fundamental Interactions in Colloidal Organic-Inorganic Hybrid Perovskite Nanostructures by Ultrafast Optical Spectroscopy*
9:55–10:05 am	**Posters Intro**
10:05–10:35 am	***Break***
10:35–12:25 pm	**Poster Session 1**
12:25–1:45 pm	***Lunch*** **Linda Horton**, Department of Energy *DMSE Overview*
Oral Session 2	Chair: **Ray Ashoori**, Massachusetts Institute of Technology
1:45–2:00 pm	**Mansour Shayegan**, Princeton University *Magneto-transport in GaAs Two-Dimensional Hole Systems*
2:00–2:15 pm	**Philip Kim**, Harvard University *Correlated Quasiparticles in Graphene*
2:15–2:30 pm	**Jeanie Lau**, Ohio State University *Symmetry Breaking in Two-Dimensional Flat-band Systems for Spin, Charge and Cooper Pair Transport*

2:30–2:45 pm	**Cory Dean**, Columbia University *Quantum Transport in 2D Semiconductors*
2:45–3:00 pm	**Gabor Csathy**, Purdue University *Exotic Quasiparticles in the Fractional Quantum Hall Regime*
3:00–3:10 pm	**Posters Intro**
3:10–3:40 pm	*****Break*****
3:40–5:10 pm	**Poster Session 2**
5:10–6:30 pm	**Panel**, *Research at World-Class BES Facilities* Co-chairs: **Jan Musfeldt**, Tennessee and **Dave Hsieh**, Caltech Panelists: **Valentina Bisogni**, BNL **Neil Harrison**, LANL **Saw Hla**, Ohio University/ANL **Rob McQueeney**, Ames Lab **Matteo Mitrano**, Illinois, Urbana-Champaign
6:30–7:30 pm	***** Dinner*****
7:30–9:00 pm	**Informal Discussion. Posters from Sessions 1 and 2 available.**

Tuesday, September 17, 2019

7:30–8:30 am	*****Breakfast*****
Oral Session 3	Chair: **George Hadjipanayis**, University of Delaware
8:30–8:45 am	**John DiTusa**, Louisiana State University *LaCNS: Building Neutron Scattering Infrastructure in Louisiana for Advanced Materials*
8:45–9:00 am	**Mingzhong Wu**, Colorado State University *Room-Temperature Topological Insulator α-Sn Thin Films—From Fundamental Physics to Applications*
9:00–9:15 am	**Pablo Jarillo-Hererro**, Massachusetts Institute of Technology *Interplay of Magnetism and Superconductivity in van der Waals Heterostructures*
9:15–9:30 am	**Fengyuan Yang**, Ohio State University *Spin Dynamics and Magnonic Spin Transport in Antiferromagnetic Heterostructures at High Frequencies up to 360 GHZ*
9:30–9:45 am	**Dan Ralph**, Cornell University *Effects of Lateral Broken Crystal Symmetries on Spin-Orbit Torques and Magnetic Anisotropy*
9:45–10:00 am	**Ho Nyung Lee**, Oak Ridge National Laboratory *Interfaces in Epitaxial Complex Oxides*

10:00–10:10 am	**Posters Intro**
10:10–10:40 am	*****Break*****
10:40–12:30 pm	**Poster Session 3**
12:30–1:30 pm	*****Lunch*****
Oral Session 4	Chair: **Joe Orenstein**, Lawrence Berkeley National Laboratory
1:30–1:45 pm	**Phuan Ong**, Princeton University *Experiments on Nonsymmorphic Topological and Weyl Semimetals*
1:45–2:00 pm	**Filip Ronning**, Los Alamos National Laboratory *Quantum Fluctuations in Narrow Band Systems*
2:00–2:15 pm	**Gleb Finkelstein**, Duke University *Symmetries, Interactions and Correlation Effects in Carbon Nanostructures*
2:15–2:30 pm	**Johnpierre Paglione**, University of Maryland *Topological Superconductivity in Strong Spin-Orbit Materials*
2:30–2:45 pm	**Ben Hunt**, Carnegie Mellon University *Proximity Effects and Topological Spin Currents in van der Waals Heterostructures*
2:45–3:00 pm	**Moses Chan**, Penn State University *Exploring Quantized Axion Electrodynamics in Magnetic Topological Insulator Multilayer Heterostructures*
3:00–3:10 pm	**Posters Intro**
3:10–3:40 pm	*****Break*****
3:40–5:30 pm	**Poster Session 4**
5:30–6:30 pm	**Paul Canfield**, Ames Laboratory Plenary: *New Materials Physics*
6:30–7:30 pm	***** Dinner*****
7:30–9:00 pm	**Informal Discussion. Posters from Sessions 3 and 4 available.**

Wednesday, September 18, 2019

7:30–8:30am	*****Breakfast*****
Oral Session 5	Chair: **John Xiao**, University of Delaware
8:30–8:45 am	**Valentina Bisogni**, Brookhaven National Laboratory *Revealing Collective Spin Dynamics under Device-Operating Conditions to Enhance Tomorrow's Electronics*

8:45–9:00 am	**Xiaoshan Xu**, University of Nebraska *Nonvolatile Active Control of Spin Transport using Interfaces with Molecular Ferroelectrics*
9:00–9:15 am	**Peter Schiffer**, Yale University *Exotic Frustration-Induced Phenomena in Artificial Spin Ice*
9:15–9:30 am	**Harold Hwang**, SLAC *Atomic Engineering Oxide Heterostructures: Materials by Design*
9:30–9:45 am	**Ivan Schuller**, University of California – San Diego *Nanostructured Materials: From Superlattices to Quantum Dots*
9:45–10:15 am	*****Break*****
Oral Session 6	Chair: **Ian Fisher**, SLAC
10:15–10:30 am	**Tony Valla**, Brookhaven National Laboratory *Electron Spectroscopy*
10:30–10:45 am	**Yuji Furukawa**, Ames Laboratory *Complex States, Emergent Phenomena, and Superconductivity in Intermetallic and Metal-Like Compounds*
10:45–11:00 am	**Doug Natelson**, Rice University *Nanostructure Studies of Correlated Quantum Materials*
11:00–11:15 am	**Claudia Ojeda-Aristazabal**, California State University – Long Beach *Experimental Study of Novel Relativistic Mott Insulators in the Two-Dimensional Limit*
11:15–11:30 am	**Jun Kono,** Rice University *Spectroscopy of Degenerate One-Dimensional Electrons in Carbon Nanotubes*
11:30–11:45 am	*BES – Concluding Remarks* **Mick Pechan**, Department of Energy
11:45 am	**Meeting Adjourns**

Session 1

Planar Systems for Quantum Information

PI: Jie Shan (Cornell University)
Co-PIs: Cory R. Dean (Columbia University)
James Hone (Columbia University)
Allan H. MacDonald (University of Texas at Austin)
Kin Fai Mak (Cornell University)
Tony F. Heinz (SLAC National Accelerator Laboratory/Stanford University)

Program Scope

The scope of this program is to investigate two-dimensional (2D) systems, such as the valley pseudospin degree of freedom in transition metal dichacogenides (TMDs), as a candidate for the construction of quantum bits. In particular, we will develop approaches including stimulated Raman adiabatic passage and dynamic exchange magnetic field for full control of valley pseudospin. We will seek to determine the factors controlling decoherence and develop approaches for enhancing coherence times using approaches including spin-forbidden excitons, valley polarized carriers, and arrays of localized excitons and carriers.

Recent Progress

Bose-Einstein condensate has been achieved for atoms cooled to temperatures close to absolute zero. With much smaller mass, excitons have been predicted to condense at significantly higher temperatures[1-3]. TMD semiconductors with large exciton binding energy (~ 0.5 eV) and flexibility in forming van der Waals (vdW) heterostructures provide an exciting platform for exploring high-temperature exciton condensation and condensate-based applications such as weak links in Josephson junctions to enhance coherence time for quantum computing[4].

We studied interlayer excitons in $MoSe_2/WSe_2$ double layers. The device (Fig. a) consists of two angle-aligned TMD monolayer crystals separated by a two- to three-layer hexagonal boron nitride (hBN) tunnel barrier. The barrier suppresses interlayer electron-hole recombination to achieve high exciton density while maintaining strong binding. The double layer is gated on both sides with symmetric gates that are made of few-layer graphene gate electrodes and 20-30 nm h-BN gate dielectrics. By applying equal voltages to the two gates and a bias voltage to the WSe2 layer, one can tune the carrier density in each TMD layer independently. Interlayer excitons up to 10^{12} cm^{-2} have been created electrostatically (Fig. b). The interlayer tunneling current depends only on exciton density, indicative of correlated electron-hole pair tunneling. Strong electroluminescence arises when a hole tunnels from WSe_2 to recombine with an electron in $MoSe_2$. We observed a critical threshold dependence of the EL intensity on exciton density, accompanied by a super-Poissonian photon statistics near threshold, and a large EL enhancement peaked narrowly at equal electron-hole densities (Fig. c). The phenomenon persists above 100 K,

which is consistent with the predicted critical condensation temperature. This study provides compelling evidence for interlayer exciton condensation in 2D atomic double layers.

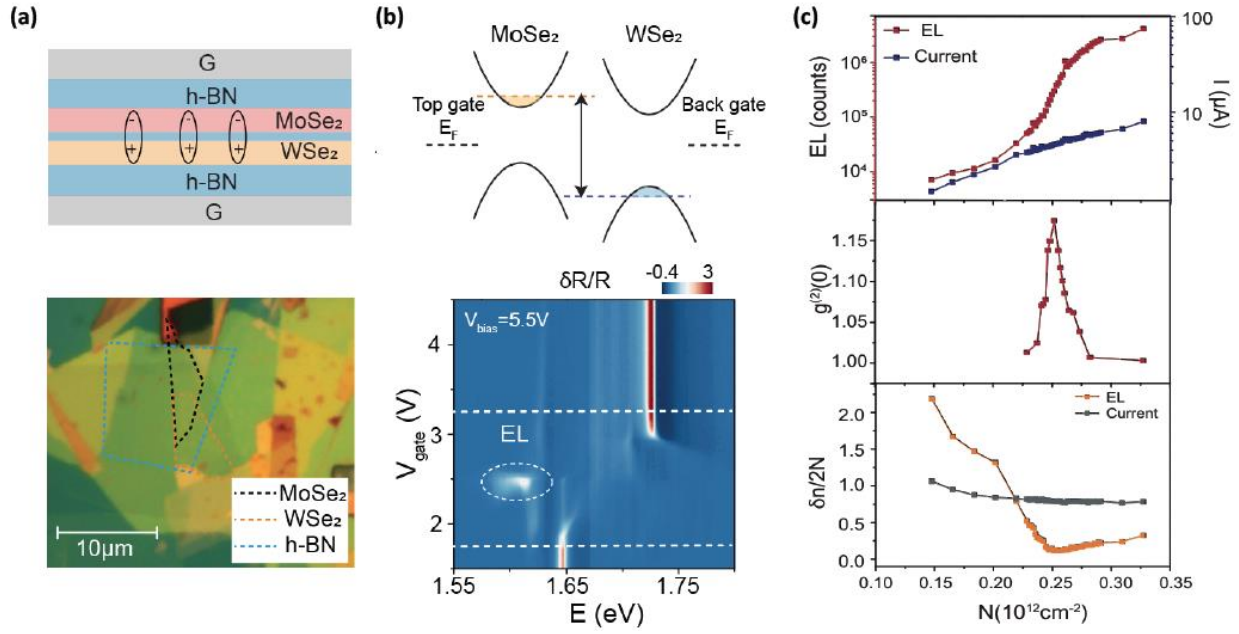

Figure on interlayer exciton condensation. (**a**) Schematics (top) and optical micrograph (bottom) of a $MoSe_2/WSe_2$ double layer with an hBN barrier and symmetric top and bottom gates made of hBN and graphite (G). Interlayer excitons (electrons in $MoSe_2$ and holes in WSe_2) are created by electrical biasing and gating. (**b**) Contour plot of the reflection contrast spectrum as a function of photon energy E and gate voltage V_{gate} (identical on both gates) under 5.5 V bias voltage. A gap is opened for the $MoSe_2$ and WSe_2 neutral exciton resonances (between the white dashed lines). It is consistent with the band alignment (upper panel). The bias voltage splits the $MoSe_2$ and WSe_2 electrochemical potentials (orange and blue dashed lines). The circled bright spot in the lower panel is electroluminescence (EL) from the tunnel junction. (**c**) Exciton density dependence of the integrated electroluminescence intensity and tunneling current (top), the electroluminescence intensity correlation at zero delay (middle), and the width of the electroluminescence and tunneling as a function of density imbalance (bottom).

Future Plans

We will continue the lines of on-going work. They include the development of high-quality bulk crystals of TMDs and vdW heterostructures of these materials, the study of the valley properties of charged excitons (trions) and dark excitons (spin-forbidden excitons) in monolayer TMDs, and interlayer excitons to seek approaches for enhancing valley coherence times. In addition, we will explore the TMD moiré systems and investigate the effect of strong interactions on the valley properties of the system. This is inspired by the progress in twisted bilayer graphene system including the recently discovered valley magnetism. The experimentalists and the theorists of this program will interact regularly with the aim to understand the strong correlation states in TMD moiré systems.

References

1. Xie, M. & MacDonald, A. H. Electrical reservoirs for bilayer excitons. *Phys. Rev. Lett.* **121**, 067702 (2018).
2. Fogler, M. M., Butov, L. V. & Novoselov, K. S. High-temperature superfluidity with indirect excitons in van der Waals heterostructures. *Nat. Commun.* **5**, 4555 (2014).
3. Wu, F.-C., Xue, F. & MacDonald, A. H. Theory of two-dimensional spatially indirect equilibrium exciton condensates. *Phys. Rev. B* **92**, 165121 (2015).
4. Peotta, S., Gibertini, M., Dolcini, F., Taddei, F., Polini, M., Ioffe, L. B., Fazio, R. & MacDonald, A. H. Josephson current in a four-terminal superconductor/exciton condensate/superconductor system. *Phys. Rev. B* **84**, 184528 (2011).

Publications

1. Tang Y., Mak K. F. & Shan, J. Long valley lifetime of dark excitons in single-layer WSe_2. *Nat. Commun.* **10**, 4047 (2019). https://doi.org/10.1038/s41467-019-12129-1.
2. Wang, Z., Rhodes, D. A., Watanabe, K., Taniguchi, T., Hone, J. C., Shan, J., & Mak, K. F. Evidence of high-temperature exciton condensation in 2D atomic double layers, *Nature* (2019) In press.

Van der Waals Heterostructures: Novel Materials and Emerging Phenomena

Feng Wang, Michael Crommie, Steven G. Louie, Zi Q. Qiu, Mike Zaletel, Alex Zettl

Materials Science Division, LBNL

Program Scope

This program aims to exploit extraordinary new scientific opportunities enabled by designing van der Waals (vdW) heterostructures that allow creation of novel functional materials with unprecedented flexibility and control. We will explore a variety of quantum phenomena in these systems, ranging from 2D magnetism and spin liquids to moiré physics and exciton Bose-Einstein condensates in van der Waals heterostructures. The proposed objectives will be achieved by an integrated team effort combining materials development, advanced experimental characterization, and state-of-the-art theoretical calculations.

Recent Progress: Moiré excitons in WS2/WSe2 heterostructures

Moiré superlattices in van der Waals heterostructures provide a powerful tool to engineer the properties of two-dimensional materials. The periodic variation of the interactions between the atomically thin layers can dramatically change the band structure of the system. For example, correlated insulating states and superconductivity have been reported in graphene-based superlattice systems[1,2,3]. In principle, the moiré superlattice can also significantly change the behavior of excitons in semiconducting vdW heterostructures.

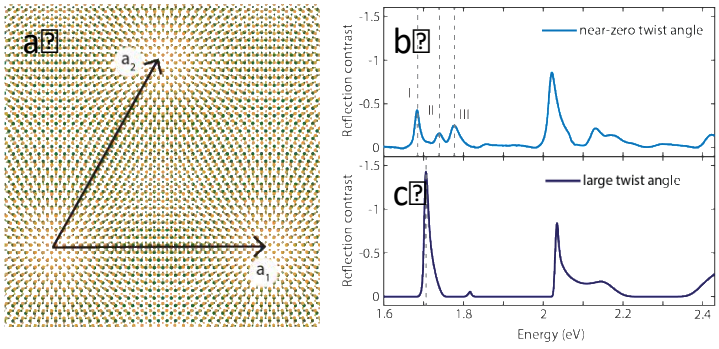

Fig. 1. (a) Schematic of the WSe_2/WS_2 moiré superlattice. (b) Optical reflection spectrum of the WSe_2/WS_2 moiré superlattice reveals three distinct moiré exciton peaks between 1.6 to 1.8 eV. (c) Only one exciton peak exists in the spectrum of large-twist-angle TMD heterostructures.

In a collaboration led by Wang and Zettl, we observed for the first time moiré superlattice exciton states in nearly aligned WSe2/WS2 heterostructures (Fig. 1)[4]. We first determined the crystallographic orientation of WSe2 and WS2 monolayers using second harmonic generation, and fabricated near-zero twist angle WSe2/WS2 heterostructures by aligning the crystallographic orientations of the two layers. The moiré superlattices of such aligned WSe2/WS2 heterostructures were directly visualized through high resolution transmission electron microscopy (TEM) imaging. Optical reflection spectroscopy revealed that multiple optical absorption peaks emerge around the original WSe2 A exciton resonance due to the moiré exciton states. These moiré exciton peaks

exhibit gate dependences that are distinctly different from that of the A exciton in WSe2 monolayers and in large-twist-angle WSe2/WS2 heterostructures. The observed phenomena can be described by a theoretical model where the periodic moiré potential is much stronger than the exciton kinetic energy and creates multiple flat exciton minibands. The moiré exciton bands provide an attractive platform to explore and control novel excited states of matter, such as topological excitons and a correlated exciton Hubbard model in TMDs.

Future Plans

We propose to further explore novel exciton states enabled by 2D Moiré superlattices in TMD heterostructures.

Our observation of intra-layer moiré excitons in WS2/WSe2 heterostructures revealed a surprisingly large effective potential generated by the moiré superlattice. However, there is still a lack of fundamental understanding of both the atomic configuration and the electronic/exciton bandstructure of the moiré superlattice. Wang, Zettl, Crommie, Louie, and Zaletel will combine advanced device fabrication, optical spectroscopy, STM, TEM, and model Hamiltonian calculations to systematically investigate novel exciton states emerging in TMD heterostructure moiré superlattices.

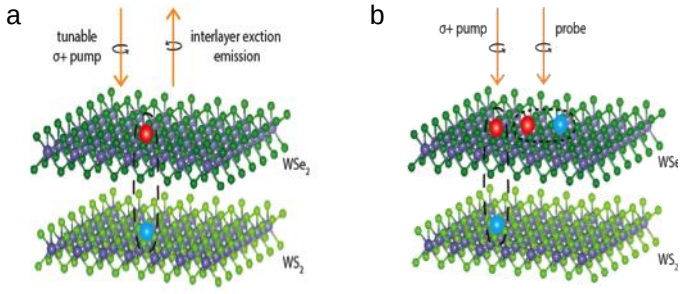

Fig. 2. (a) Photoluminescence excitation spectroscopy and (b) Interlayer exciton pump-intralayer exciton probe spectroscopy provides background free measurements of interlayer moiré

Wang and Zettl will fabricate high quality moiré heterostructures composed of different TMD layers (such as MoSe2/WSe2, WS2/WSe2, MoTe2/WSe2, etc.) using the mechanical exfoliation and stacking method. We will identify the crystallographic orientations of individual layers using second harmonic generation spectroscopy, and align the layers to control the twist angle and therefore the moiré lattice constant. Zettl and Crommie will image the local moiré superlattice structure with atomic resolution using high-resolution TEM and STM imaging, respectively. Such structural characterization will reveal the atomic reconstruction and corrugation induced by the layer-layer interactions in the moiré superlattices. Crommie will also examine the local electronic bandstructure change induced by the moiré superlattice with STS spectroscopy. Wang will employ advanced laser spectroscopy to probe both intra-layer and inter-layer moiré exciton transitions in the same devices. Recently, Wang developed a background free absorption spectroscopy based on photoluminescence excitation spectroscopy and resonant pump-probe spectroscopy (Fig. 2), which enabled a direct observation of multiple interlayer moiré exciton states and unambiguous demonstration of an emerging site-dependent moiré quasi-angular momentum. We will systematically study the dependence of intra-layer and inter-layer

moiré excitons on the TMD layer materials, twist angles, and electrostatic gating, and correlate the excited state responses to the atomic structure and electronic bands of the moiré superlattice. These experimental studies will be compared to both the ab initio theory (Louie) and model Hamiltonian calculations (Zaletel) to gain a fundamental and comprehensive understanding of the moiré exciton transitions in TMD heterostructure superlattices.

References

1. Cao, Y.; Fatemi, V.; Demir, A.; Fang, S.; Tomarken, S. L.; Luo, J. Y.; Sanchez-Yamagishi, J. D.; Watanabe, K.; Taniguchi, T.; Kaxiras, E.; Ashoori, R. C.; Jarillo-Herrero, P. Correlated insulator behaviour at half-filling in magic-angle graphene superlattices. Nature 556, 80 (2018)

2. Cao, Y.; Fatemi, V.; Fang, S.; Watanabe, K.; Taniguchi, T.; Kaxiras, E.; Jarillo-Herrero, P. Unconventional superconductivity in magic-angle graphene superlattices. Nature 556, 43 (2018)

3. G. Chen*, A.L. Sharpe*, P. Gallagher, I.T. Rosen, E.J. Fox, L. Jiang, B. Lyu, H. Li, K. Watanabe, T. Taniguchi, Z. Shi, D. Goldhaber-Gordon, Y. Zhang, F. Wang, "Signatures of Gate-Tunable Superconductivity in Trilayer Graphene/Boron Nitride Moiré Superlattice", Nature, 572, 215 (2019)

4. Jin, C., Regan, E. C., Yan, A., Utama, M. I. B., Wang, D., Qin, Y., Yang, S., Zheng, Z., Watanabe, K., Taniguchi, T., Tongay, S., Zettl, A., Wang, F. "Observation of Moiré Excitons in WSe2/WS2 Heterostructure Superlattices," Nature 567, 76–80 (2019).

Publications

1. C. Jin, J. Kim, M. I. B. Utama, E. C. Regan, H. Kleemann, H. Cai, Y. Shen, M. J. Shinner, A. Sengupta, K. Watanabe, T. Taniguchi, S. Tongay, A. Zettl, F. Wang. "Imaging of pure spin-valley diffusion current in WS2 -WSe2 heterostructures," Science 896, 893–896 (2018).

2. C. K. Yong, J.Horng, Y. Shen, H. Cai, A. Wang, C. S. Yang, C. K. Lin, S. Zhao, K. Watanabe, T. Taniguchi, S. Tongay, F. Wang. "Biexcitonic optical Stark effects in monolayer molybdenum diselenide," Nature Physics, https://doi.org/10.1038/s41567-018-0216-7 (2018).

3. H. Zhu, J. Yi, M.-Y. Li, J. Xiao, L. Zhang, C.-W. Yang, R. A. Kaindl, L.-J. Li, Y. Wang & X. Zhang. "Observation of chiral phonons," Science, 359, 579 (2018).

4. M. M. Ugeda, A. Pulkin, S. Tang, H. Ryu, Q. Wu, Y. Zhang, D. Wong, Z. Pedramrazi, A. Martín-Recio, Y. Chen, F. Wang, Z.-X. Shen, S.-K. Mo, O. V. Yazyev, and M. F. Crommie. "Observation of Topologically Protected States at Crystalline Phase Boundaries in Single-layer WSe2," Nature Communications, 9, 3401 (2018).

5. Jin, C., Regan, E. C., Yan, A., Utama, M. I. B., Wang, D., Qin, Y., Yang, S., Zheng, Z., Watanabe, K., Taniguchi, T., Tongay, S., Zettl, A., Wang, F. "Observation of Moiré Excitons in WSe2/WS2 Heterostructure Superlattices," Nature 567, 76–80 (2019).

6. T. Cao, M. Wu, and S. G. Louie. "Unifying Optical Selection Rules for Excitons in Two Dimensions: Band Topology and Winding Numbers," Phys. Rev. Lett. 120, 087402 (2018).

7. Q. Li, M. Yang, C. Gong, R. V. Chopdekar, A. T. N'Diaye, J. Turner, G. Chen, A. Scholl, P. Shafer, E. Arenholz, A. K. Schmid, S. Wang, Kai Liu, N. Gao, A. S. Admasu, S.-W. Cheong, C. Hwang, J. Li, F. Wang, X. Zhang, and Z. Q. Qiu. "Patterning-induced ferromagnetism of Fe3GeTe2 van der Waals materials beyond room temperature," Nano Letters, published online. DOI: 10.1021/acs.nanolett.8b02806

8. Y. Wang, J. Xiao, H. Zhu, Y. Li, Y. Alsaid, K. Y. Fong, Y. Zhou, S. Wang, W. Shi, Y. Wang, A. Zettl, E. J. Reed & X. Zhang. "Structural phase transition in monolayer MoTe2 driven by electrostatic doping," Nature, 550, 487, (2017).

9. H. Ryu, Y. Chen, H. Kim, H.-Z. Tsai, S. Tang, J. Jiang, F. Liou, S. Kahn, C. Jia, A. A Omrani, J.-H. Shim, Z. Hussain, Z.-X. Shen, K. Kim, B. I. Min, C. Hwang, M. F. Crommie, S.-K. Mo. "Persistent Charge-Density-Wave Order in Single-Layer TaSe2," Nano Letters 18, 689 (2018).

10. Z. Li, T. Cao, and S. G. Louie. "Two-dimensional ferromagnetism in few-layer van der Waals crystals: Renormalized spin-wave theory and calculations," J. of Mag. and Mag. Mat. 463, 28-35 (2018).

11. Thang Pham, Sehoon Oh, Patrick Stetz, Seita Onishi, Christian Kisielowski, Marvin L. Cohen, and Alex Zettl. "Torsional instability in the single-chain limit of a transition metal trichalcogenide," Science 361, pp 263 - 266 (2018) doi: 10.1126/science.aat4749

12. Q. Li, M. Yang, A. T. N'Diaye, Q. Y. Dong, A. Scholl, A. T. Young, N. Gao, E. Arenholz, C. Hwang, J. Li, and Z. Q. Qiu. "Ni and CoO spin cantings induced by Fe layer in Ni/CoO/Fe/vicinal MgO(001)," Phys. Rev. B 96, 214405 (2017).

13. M. Yang, Q. Li, A. T. N'Diaye, Q. Y. Dong, N. Gao, E. Arenholz, C. Hwang, Y. Z. Wu, and Z. Q. Qiu. "The effect of spin reorientation transition of antiferromagnetic NiO on the Py magnetic anisotropy in Py/NiO/CoO/MgO(001)," J. of Mag. Magn. Mat. 460, 6 (2018)

14. Z. H. Chen, Z. Chen, C. Y. Kuo, Y. Tang, L. R. Dedon, Q. Li, L. Zhang, C. Klewe, Y-L. Huang, B. Prasad, A. Farhan, M. Yang, J.D. Clarkson, S. Das, S. Manipatruni, A. Tanaka, P Shafer, E. Arenholz, A. Scholl, Y. H. Chu, Z.Q. Qiu, Z. W. Hu, L. H. Tjeng, R. Ramesh, L. W. Wang, L. W. Martin. "Complex strain evolution of polar and magnetic order in multiferroic BiFeO3 thin films," Nat. Commun. 9, 3764 (2018)

15. Jin, C., Ma, E. Y., Karni, O., Regan, E. C., Wang, F., and Heinz, T. "Ultrafast dynamics in van der Waals heterostructures," Nature Nanotechnology 13, 994–1003 (2018) DOI: 10.1038/s41565-018-0298-5

16. Chittari, B. L., Chen, G., Zhang, Y., Wang, F., Jung, J. "Gate-Tunable Topological Flat Bands in Trilayer Graphene Boron-Nitride Moire Superlattices," Phys. Rev. Lett. 122, 016401 (2019). DOI: 10.1103/PhysRevLett.122.016401

Project Title: Cold Exciton Gases in Semiconductor Heterostructures

PI: Leonid Butov, University of California San Diego

Program Scope

An indirect exciton (IX) is a bound pair of an electron and a hole confined in spatially separated quantum well layers in a semiconductor heterostructure. IXs are characterized by a set of properties:

- Long lifetimes of IXs allow them to cool below the temperature of quantum degeneracy. This gives an opportunity to realize cold excitons.

- Due to IX built-in dipole moment, IX energy is effectively controlled by voltage. This gives an opportunity to create tailored potential landscapes for IXs by voltage.

- Due to their built-in dipoles, IXs interact repulsively and form a dipolar system with correlations.

- Long IX lifetimes allow them to travel over large distances before recombination. This gives an opportunity to study exciton transport by imaging spectroscopy.

- The electron-hole separation in IX and the suppression of exciton scattering in IX condensate result to the suppression of spin relaxation. This allows the realization of long-range coherent spin transport.

Due to these properties, IXs are explored as a platform for basic studies of cold excitons - cold bosons in semiconductor materials and for the development of excitonic devices. The goal of this project is to explore IXs in GaAs heterostructures, which form the lowest-disorder platform for studying IXs, and in van der Waals transition-metal dichalcogenides (TMD) heterostructures, which are characterized by high IX binding energies and can bring the quantum IX phenomena studied in GaAs heterostructures at low temperatures to high temperatures.

Recent Progress

1. The phase singularities in IX condensate in GaAs heterostructures. We observed fork-like phase singularities (dislocations) in IX condensate interference patterns [1] (Fig. 1).

The fork-like defects in interference patters are commonly associated with vortices in quantum systems. In a quantized vortex, the phase of the wavefunction winds by 2π around the singularity point that can be revealed as a fork-like defect in a phase pattern. Fork-like defects in interference patterns are explored for vortices in atom condensates, optical vortices, and polariton vortices.

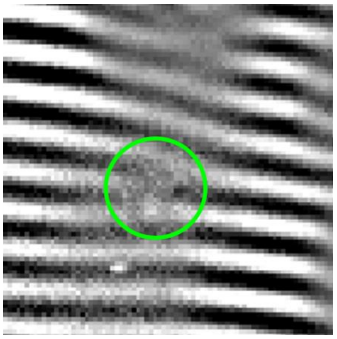

Fig. 1. Singularity in IX interference pattern.

Our simulations show that the observed phase singularities are not conventional topological defects such as vortices, half-vortices, or skyrmions. We found the origin of the observed new phase singularities in condensates. Our simulations reproduce the observed dislocations in interference patterns.

2. The Pancharatnam-Berry phase in IX condensate in GaAs heterostructures.

We also observed the Pancharatnam-Berry phase in condensate of IXs [2] (Fig. 2). The Pancharatnam-Berry phase is a geometric phase acquired over a cycle of parameters in the Hamiltonian governing the evolution of the system. We directly measured the Pancharatnam-Berry phase by detecting phase shifts of interference fringes in IX interference patterns. The correlation between the phase shift and the polarization change identifies the phase as the Pancharatnam-Berry phase acquired in a condensate of IXs. Evolving Pancharatnam-Berry phase is acquired due to coherent spin precession in IX condensate and is observed with no decay over lengths exceeding 10 μm indicating long-range coherent spin transport.

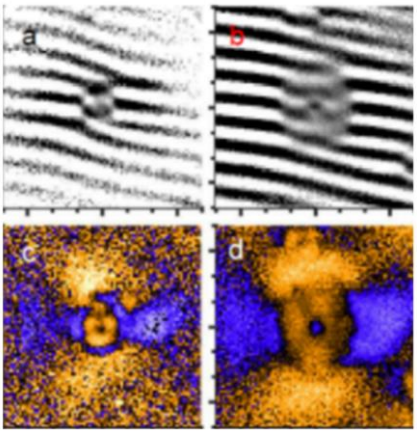

Fig. 2. Correlation between the phase shift and the polarization change identifies the phase as the Pancharatnam-Berry phase acquired in IX condensate.

3. Indirect trions in TMD heterostructures

In $MoSe_2/WSe_2$ heterostructures, we observed two IX luminescence lines whose energy splitting and temperature dependence identify them as neutral and charged IXs [4] (Fig. 3). The experimentally found binding energy of the indirect charged excitons, i.e. indirect trions, is close to the calculated binding energy of 28 meV for negative indirect trions in TMD heterostructures [Deilmann, Thygesen, Nano Lett. 18, 1460 (2018)]. The trion to exciton ratio decreases with

increasing temperature in agreement with the mass action law for the indirect trions, with the saturation of trion to exciton ratio at low temperatures.

We also realized indirect excitons with a luminescence linewidth reaching 4 meV at low temperatures. An enhancement of IX luminescence intensity and the narrowest linewidth are observed in localized spots.

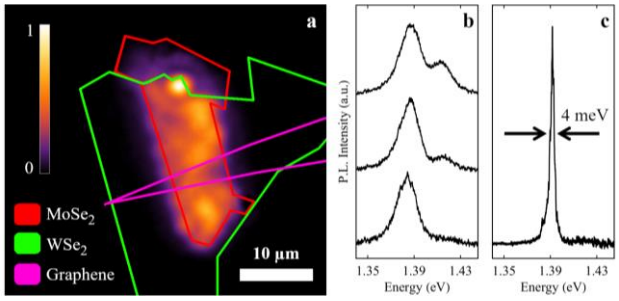

Fig. 3. (a) Indirect luminescence in $MoSe_2/WSe_2$ heterostructure. (b) Indirect exciton and indirect trion luminescence lines. (c) The narrowest linewidth of indirect luminescence.

4. Indirect excitons at room temperature in TMD heterostructures

We demonstrated IXs at room temperature both in type I MoS_2/hBN heterostructures [5] and in type II $MoSe_2/WSe_2$ heterostructures [4]. The IXs have lifetimes orders of magnitude longer than lifetimes of direct excitons in single-layer TMD and their energy is gate controlled (Fig. 4). TMD heterostructures can form a material platform for exploring high-temperature quantum Bose gases of IXs.

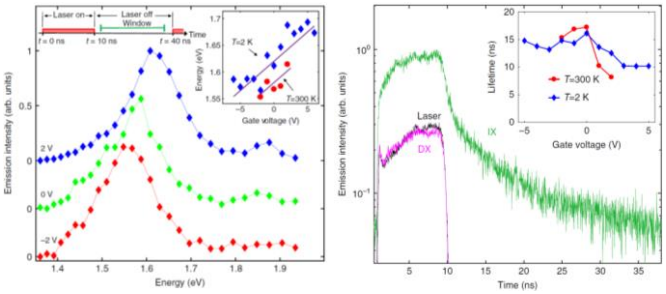

Fig. 4. (left) Control of IX energy by voltage in MoS_2/hBN heterostructure. (right) IX emission kinetics (green) shows long IX lifetime.

Future Plans

GaAs heterostructures form the lowest-disorder platform for studying IXs. We plan to explore the opportunity to realize long-range coherent spin transport with IXs and study spin-related phenomena in IXs in GaAs heterostructures. IXs in van der Waals heterostructures based on single-atomic-layers of TMD are characterized by high binding energies, significantly higher than in GaAs heterostructures. Due to this property, theoretical predictions indicate that TMD heterostructures can bring the quantum IX phenomena studied in GaAs heterostructures at low temperatures, such as condensation and long-range coherent spin transport, to high temperatures. We plan to explore quantum IX phenomena in TMD van der Waals heterostructures.

Publications

1. J.R. Leonard, Lunhui Hu, A.A. High, A.T. Hammack, Congjun Wu, L.V. Butov, K.L. Campman, A.C. Gossard, Phase singularities in condensate of indirect excitons, in preparation.

2. J.R. Leonard, A.A. High, A.T. Hammack, M.M. Fogler, L.V. Butov, K.L. Campman, A.C. Gossard, Pancharatnam–Berry phase in condensate of indirect excitons, Nature Commun. 9, 2158 (2018).

3. C.J. Dorow, M.W. Hasling, D.J. Choksy, J.R. Leonard, L.V. Butov, K.W. West, L.N. Pfeiffer, High-mobility indirect excitons in wide single quantum well, Appl. Phys. Lett. 113, 212102 (2018).

4. E.V. Calman, L.H. Fowler-Gerace, L.V. Butov, D.E. Nikonov, I.A. Young, S. Hu, A. Mishchenko, A.K. Geim, Indirect excitons and trions in $MoSe_2/WSe_2$ van der Waals heterostructures, arxiv1901.08664 and in preparation.

5. E.V. Calman, M.M. Fogler, L.V. Butov, S. Hu, A. Mishchenko, A.K. Geim, Indirect excitons in van der Waals heterostructures at room temperature, Nature Commun. 9, 1895 (2018).

Electronic and photonic phenomena of graphene-based heterostructures

D.N. Basov, Columbia University

Program Scope

The proposed research focuses on electronic, optical and plasmonic phenomena in the new generation of graphene-based heterostructures with high electronic mobility. The proposed program is comprised of three complementary research directions:

i) Intrinsic electrodynamics of two-dimensional electron liquid in graphene that has remained elusive but is now within the experimental reach, due to the availability of high mobility graphene/hBN samples and the advent of technology allowing nano-optical experimentation at cryogenic temperatures;

ii) Topological phenomena in bilayer graphene. Using plasmonic nano-imaging, the PI will investigate the electronic response associated with nano-scale stacking domains in bilayer samples, which are expected to show a rich variety of novel electronic properties governed by non-trivial topology and the electronic structure associated with the domain walls;

iii) Properties of graphene/hBN interfaces that will be continuously tuned in reconfigurable devices thus enabling in-operando modification of the electronic and photonic phenomena by moire superlattice patterns

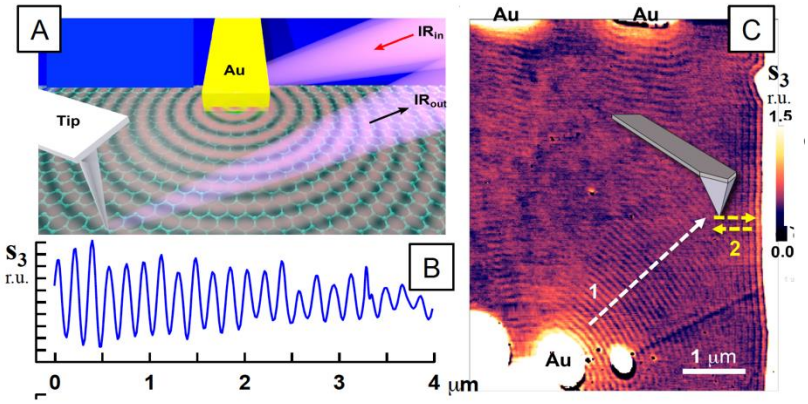

Figure 1. Plasmonic imaging at cryogenic temperatures. Panel A: the PI will investigate plasmonic waves launched by Au antennas and also tip-launched plasmon polaritons. Panel B and C: preliminary results for plasmonic imaging at T = 60 K carried out by the PI using a home-built apparatus in Fig.3. Large-area raster-scanned plasmonic image (Panel C) reveals plasmons launched by Au antennas (white arrow 1 and also panel B) as well as "round-trip" plasmons launched by the tip and reflected by the edge of the sample on the right of the frame (yellow arrows 2). Plasmonic imaging data are presented in the form of the scattering amplitude *s* normalized by that of Au. The probing frequency ω_0 = 886 cm^{-1} and the gate voltage V_G=97 V. Adapted from Publication 1.

Recent Progress

Plasmon polaritons may enable many enigmatic quantum effects, including lasing, topological protection and dipole-forbidden absorption. A necessary condition for realizing such

phenomena is a long plasmonic lifetime, which is notoriously difficult to achieve for highly confined modes. Plasmon polaritons \in graphene—hybrids of Dirac quasiparticles and infrared photons—provide a platform for exploring light–matter interaction at the nanoscale. However, plasmonic dissipation in graphene is substantial and its fundamental limits remain undetermined. Here we use nanometer-scale infrared imaging to investigate propagating plasmon polaritons in high-mobility encapsulated graphene at cryogenic temperatures. In this regime, the propagation of plasmon polaritons is primarily restricted by the dielectric losses of the encapsulated layers, with a minor contribution from electron–phonon interactions. At liquid-nitrogen temperatures, the intrinsic plasmonic propagation length can exceed 10 micrometres, or 50 plasmonic wavelengths, thus setting a record for highly confined and tunable polariton modes. Our nanoscale imaging results reveal the physics of plasmonic dissipation and will be instrumental in mitigating such losses in heterostructure engineering applications**.** Publication [1].

Future Plans

Empowered by new experimental capabilities for low-temperature spectroscopy and imaging of plasmon polaritons (Fig.1) we plan to investigate infrared and THz signatures of hydrodynamic transport in high mobility graphene.

References

N/A

Publications

[1] G. X. Ni, A. S. McLeod, Z. Sun, L. Wang, L. Xiong, K. W. Post, S. S. Sunku, B.-Y. Jiang, J. Hone, C. R. Dean, M. M. Fogler & D. N. Basov "*Fundamental limits to graphene plasmonics*" Nature 557, 530 (2018).

[2] S. S. Sunku, G. X. Ni, B. Y. Jiang, H. Yoo, A. Sternbach, A. S. McLeod, T. Stauber, L. Xiong, T. Taniguchi, K. Watanabe, P. Kim, M. M. Fogler, D. N. Basov, "*Photonic crystals for nano-light in moiré graphene superlattices* " Science 362, 1153–1156 (2018).

[3] A. Pustogow, A. S. McLeod, Y. Saito, D. N. Basov, M. Dressel, "*Internal strain tunes electronic correlations on the nanoscale*" Science Advances 4, eaau9123 (2018).

[4] Siyuan Dai, Jiawei Zhang, Qiong Ma, Salinporn Kittiwatanakul, Alex McLeod, Xinzhong Chen, Stephanie Gilbert Corder, Kenji Watanabe, Takashi Taniguchi, Jiwei Lu, Qing Dai, Pablo Jarillo-Herrero, Mengkun Liu, and D. N. Basov, "*Phase-Change Hyperbolic Heterostructures for Nanopolaritonics: A Case Study of hBN/VO_2*," Adv. Mat. 31 (18), 1900251 (2019)

[5] D.N. Basov, R.D. Averitt and D. Hsieh, "*Towards properties on demand in quantum materials*" Nature Materials 16, 1077 (2017).

[6] Z. Fei, G. X. Ni, B. Y. Jiang, M. M. Fogler, and D. N. Basov, "*Nanoplasmonic Phenomena at Electronic Boundaries in Graphene*," ACS Photonics 4, 12, 2971-2977 (2017).

Understanding and Manipulating Quantum Spin Exchange Interactions in Colloidal Magnet Based Nanostructures by Ultrafast Light

Min Ouyang, University of Maryland – College Park

Program Scope

Controlling spin interactions and magnetic ordering in a crystalline solid is the cornerstone of modern information storage and processing technology. The availability of ultrafast lasers has opened up a new avenue to achieve related control in an extremely fast time scale with potential for achieving opto-quantum technology. The overall scope of this program is to combine femtosecond optical spectroscopy and magnetism with recent materials advances on precisely tailored colloidal quantum structures to gain an improved understanding and control of nanoscale magnetism with particular emphasis on spin quantum exchange interactions. In particular, when the size of a magnet is reduced to be in the regime of its domain size and/or spin exchange length scale (below tens of nanometers), novel spin interactions, magnetic ordering and nanoscaling law appear, and corresponding spin-dependent processes should respond differently to the external stimuli, including photons. This program has adopted a two-pronged experimental approach to achieve our goals by combining novel ultrafast all optical spectroscopy for spin exchange measurement with chemically synthesized pure and hybrid quantum structures possessing precisely tailored structural and spin properties. Knowledge as well as materials advancement of zero-dimensional colloidal quantum structures from this program may enable new technology of such as next generation ultrahigh speed magnetic storage and quantum information processing by using colloidal quantum structures as functional building blocks.

Recent Progress

During the grant period (2017-2019), we have achieved substantial progresses in both materials development of colloidal quantum structures and their assembly and ultrafast optical control and measurement at the nanoscale, with a few selected results highlighted below:

- Development of emerging class of spin-based hybrid colloidal quantum structures

We have developed various colloidal quantum structures with precise structural tailoring and spin control. This includes both pure magnetic nanoparticles with controllable doping and their hybrid nanostructures to integrate with other functional units (such as nitrogen-vacancy centers and semiconductor quantum dots) to form intra-particle synergistic coupling with tunable structural parameters. Our goal is to provide new nanoscale condensed matter platform to allow study of

different magnetisms and spin coupling. Figure 1A shows one example of a 2% Gd doped iron oxide nanocrystals with uniform size distribution. It is generally believed that the exchange interactions in the ground state are mediated by the spins of oxygen ions. Controllable magnetic doping can provide a way to manipulate spin exchange interactions in oxide nanocrystals and further probed by the optical techniques. Figure 1B shows another example of controlled magnetic doping to the colloidal semiconductor quantum shells in a hybrid nanostructures, $(Au_{0.25}Ag_{0.75})$-CdS/Mn^{2+}-ZnS/CdSe, which was achieved by a rational step-wise solution-phase growth method. In this structure, a metallic plasmonic core ($Au_{0.25}Ag_{0.75}$) is coupled to a multiple monocrystalline semiconductor shells (CdS/ZnS/CdSe) in a centrosymmetric configuration to allow plasmons-spin coupling. More importantly, magnetic impurities (Mn^{2+}) can be selectively introduced with precise control of location and dopant quantity to mediate spin coupling. Our growth method can allow introduction of magnetic impurities with precise doping concentration and spatial location with precision of single atomic layer level. Our achievement of materials control of colloidal quantum structures offers a unique nanoscale condensed matter system to interface with photons and to allow study of spin-dependent phenomena at the nanoscale.

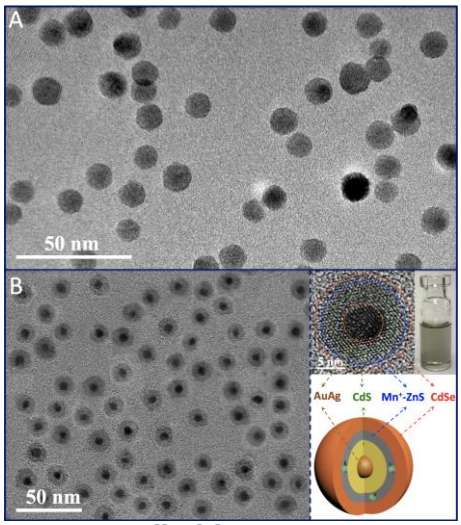

Figure 1. Colloidal quantum structures. (A) Typical TEM image of Gd^{+}-doped Fe_3O_4 nanocrystals. (B) Typical large-scale TEM image (left), high-resolution TEM image (top right) and structural model (bottom right) of complex hybrid colloidal quantum structures with controllable Mn^{+} doping.

• Bottom-up assembly of nanoscale supracrystals with collective magnet-plasmonic coupling

The colloidal quantum structures as highlighted in Figure 1 can be further utilized as building blocks for large-scale assembly to introduce collective interactions with long-range lattice order. One example is our recent development of artificial binary supracrystals in the range of nano- and micro- meter scale. As compared with thin film assembled superstructures, colloidal binary supracrystals are free-standing, and can offer a unique test bed for understanding nucleation and growth process of binary ordered state in bulk solution without external constraints from a substrate. We have developed an oil-in-water based assembly approach to achieve a high

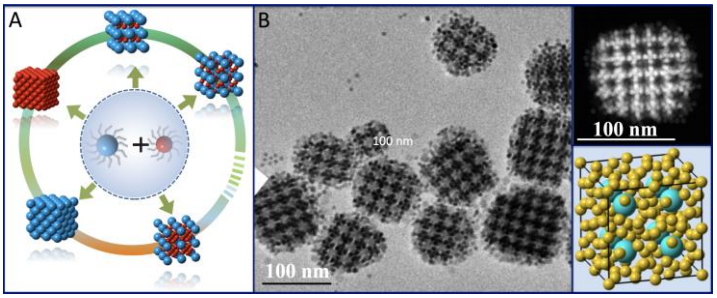

Figure 2. Bottom-up binary supracrystal assembly. (A) Schematics of lattice evolution of binary Fe_3O_4 (blue sphere)-Au (red sphere) supracrystals by oil-in-water emulsion growth method. (B) Typical large-scale TEM image (left), high-resolution TEM image (top right) and structural model (bottom right) of Fe_3O_4 -Au supracrystals possessing *ico*-$NaZn_{13}$ lattice.

degree control of colloidal binary supracrystals as shown in Figure 2, consisting of two different types of nanoparticles. This method can allow control of size, lattice structure and stoichiometry of the supracrystals (Figure 2A), with one example of the *ico*-$NaZn_{12}$ lattice-type supracrystal consisting of 10nm Fe_3O_4 and 5nm Au presented in Figure 2B. This new bottom-up assembly method is a general technique for colloidal binary supracrystals and can be readily extended to other nanoparticle building blocks. This progress can therefore allow us to design from the bottom-up and to achieve various artificial materials whose property and functionality are determined by different coupling physics such as nanoscale magneto-plasmonic couplings.

• Understanding intrinsic spin dynamics and many-body spin physics at the nanoscale

In addition to nanoscale materials development, we have also made significant progress in grant periods to develop different ultrafast optical spectroscopy to interface with colloidal quantum structures and to probe and control related spin physics within such nanoscale condensed matter system. One example highlighted in Figure 3 is our newly development of localized plasmon-assisted all-optical spin echo technique. Enabled by our materials achievement summarized above, we have demonstrated that in a Au-CdSe core-shell quantum structures, localized surface plasmon resonance from metallic core can enhance photon coupling to the semiconductor and further enable coherent spin manipulation by light based on underlying momentum-dependent optical Stark effect. This can allow to remove constraint of sample inhomogeneity in an ensemble spin measurement and to reveal intrinsic spin dynamics with microsecond long lifetime in colloidal semiconductor by using all-optical $(CPMG)_N$ spin echo scheme (Figure 3A). The long spin lifetime of colloidal semiconductor can therefore be useful for many applications, including central spin. By combining with our materials development in Figure 1B, we have shown that spin coherence of semiconductor quantum

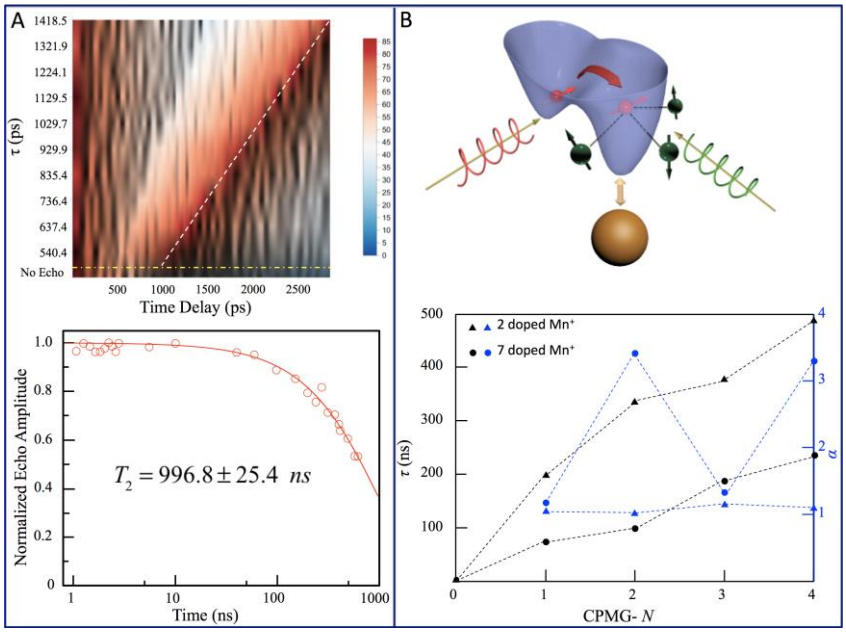

Figure 3. Plasmon-assisted all optical spin echo for uncovering nanoscale spin physics. (A) Spin echo dynamics in Au-CdSe by $(CPMG)_N$ sequence (top). Spin coherence lifetime of CdSe can be acquired by varying echo time (bottom). (B) Realization of colloidal central spin star system in colloidal quantum structures to reveal many-body interactions of magnetic impurities embedded in a spin bath by $(CPMG)_N$ spin echo. Top, schematic of structure. Bottom, dependence of spin lifetime and its stretching factor on the quantity of embedded magnetic impurities (Mn).

shell can be used to sense its environmental magnetic impurities. When the amount of magnetic impurities is increased, their many-body coupling effect starts manifesting by monitoring central spin, as shown in Figure 3B.

Future Plans

We will continue our achievements in both nanoscale materials development and ultrafast optical spectroscopy and control, with particular focus on understanding spin based fundamental interactions in the emerging organic-inorganic hybrid perovskite semiconductor quantum structures. A perovskite semiconductor possesses a generic $\mathbf{ABX_3}$ type cubic unit cell, where **A** and **B** are monovalent and divalent cations, respectively and **X** is a halogen anion. Particularly, **A** can be replaced with organic cation to form hybrid organic-inorganic perovskites. Such hybrid organic-inorganic perovskite quantum structures can provide unique dimensional tailoring as quantum test-beds for exploring many exotic physics beyond traditional *III-V* and *II-IV* semiconductors, and the structural flexibility in terms of wide selection of organic cations **A** offers a substantial scope for the emergent properties and functionalities through materials by-design from the bottom-up. Many exceptional electrical and optical properties have been predicted in hybrid perovskite semiconductors, including strong and tunable spin-orbit coupling. We will employ our developed ultrafast optical tools in prior grant periods to understand spin-structure relationship and their controls in low-dimensional hybrid organic-inorganic perovskite nanostructures. The outcomes of this new study should enable unexplored nanoscale spin physics and open up new horizons of spin measurement and control beyond the conventional semiconductors.

Publications (that acknowledged DOE support)

1. Jindong Ren *et al.* Interatomic Spin Coupling in Manganese Clusters Registered on Graphene, *Phys. Rev. Lett.* 119, 176806 (2017).

2. Pengpeng Wang *et al.* Colloidal Binary Supracrystals with Tunable Structural Lattices, *J.Am.Chem.Soc.* **140**, 9095 (2018).

3. Kwan Lee *et al.* Injective Morphology Imprinting Synthesis of Anisotropic Hybrid Nanostructures and Enabled Applications, *Nat. Mater.* (under peer-review, 2019).

4. Pengpeng Wang *et al.* Colloidal Spin with Robust Coherence and Many-Body Correlation Uncovered by Nanoscale Echo, *Science* (under peer-review, 2019).

5. Nat Steinsultz *et al.* Inherent Plasmonic and Excitonic Couplings in Emerging Nitrogen-Vacancy Centers Based Hybrid Nanostructures, *Nano Lett.* (submitted, 2019).

Session 2

Program Title: Magneto-transport in GaAs and AlAs Two-dimensional Systems

Principal Investigator: M. Shayegan

Mailing Address: Department of Electrical Engineering, Princeton University, Princeton, NJ, 08544

E-mail: shayegan@princeton.edu

Program Scope

Two-dimensional (2D) carrier systems confined to modulation-doped semiconductor hetero-structures provide a nearly ideal testing ground for exploring new physical phenomena. At low temperatures and in the presence of a strong magnetic field, these systems exhibit fascinating, often unexpected, many-body states, arising from the strong electron-electron interaction. Examples include the fractional quantum Hall liquid, the Wigner solid, and the newly discovered striped and bubble phases in the higher Landau levels.

The goal of this project is to study the materials science and physics of 2D carrier systems in the GaAs/AlGaAs system, with an emphasis on new phenomena in novel structures. Our work includes studies of 2D *electrons* or *holes* confined to GaAs wells, and also 2D electrons confined to *AlAs* quantum wells. Compared to the 2D electrons in GaAs, the 2D holes possess a more complex energy band structure which not only depends on the quantum well width and 2D hole density, but it can also be tuned via perpendicular electric field (gate bias), parallel magnetic field, and strain. AlAs 2D electron systems, on the other hand, occupy multiple conduction-band energies with anisotropic effective mass, and have a much larger effective g-factor compared to GaAs electrons. These characteristics add new twists and allow for insight into fundamental phenomena in confined, low-disorder carrier systems.

In our project we study structures which are grown via state-of-the-art molecular beam epitaxy, and use low-temperature magneto-transport measurements to explore their novel physics. Among the problems we are addressing are the different phases of 2D carrier systems at high magnetic fields and low temperatures, and the shapes of Fermi contours of composite fermions as a function of parameters such as parallel magnetic field and/or strain. Also of interest are the fractional quantum Hall states, including those at the even-denominator fillings. In our work, we collaborate closely with Dr. Loren Pfeiffer at Princeton University who is a world expert in molecular beam epitaxy, and Prof. Roland Winkler at the Univ. of Northern Illinois, who has expertise in calculating the energy band structure and Landau levels in various 2D systems. We also have a strong collaboration with Dr. Lloyd Engel at the National High Magnetic Laboratory in Tallahassee, FL, on high-frequency (microwave) measurements on 2D carrier systems at high magnetic fields.

Recent Progress

We briefly describe here two of our major, recent accomplishments:

A. Observation of an Unconventional Anisotropic Even-denominator Fractional Quantum Hall State in a System with Mass Anisotropy [13]:

The even-denominator fractional quantum Hall state (FQHS) observed at a half-filled Landau level in an interacting 2D electron system is among the most exotic states of matter as its quasi-particles are expected to be Majorana excitations with non-Abelian statistics. Also, there has

been a surge of recent interest in the role of anisotropy in interaction-induced phenomena in 2D charged carrier systems. We demonstrated in our work the unexpected presence of a FQHS at half-filling in a novel 2D electron system with a strong (factor of five) band-mass anisotropy, namely electrons confined to an AlAs quantum well (Fig. 1). The FQHS we observe occurs in the excited Landau level and has unusual characteristics. While its Hall resistance is well quantized at low temperatures, it exhibits highly anisotropic in-plane transport resembling compressible stripe or nematic charge-density-wave phases. The anisotropy is opposite in its direction compared to the transport anisotropy (related to the effective mass anisotropy) observed at zero magnetic field. More striking, the anisotropy sets in suddenly below a critical temperature, suggesting a finite-temperature phase transition. Our observations highlight how anisotropy modifies the many-body phases of a 2D electron system, and should further fuel the discussion surrounding the enigmatic even-denominator FQHSs.

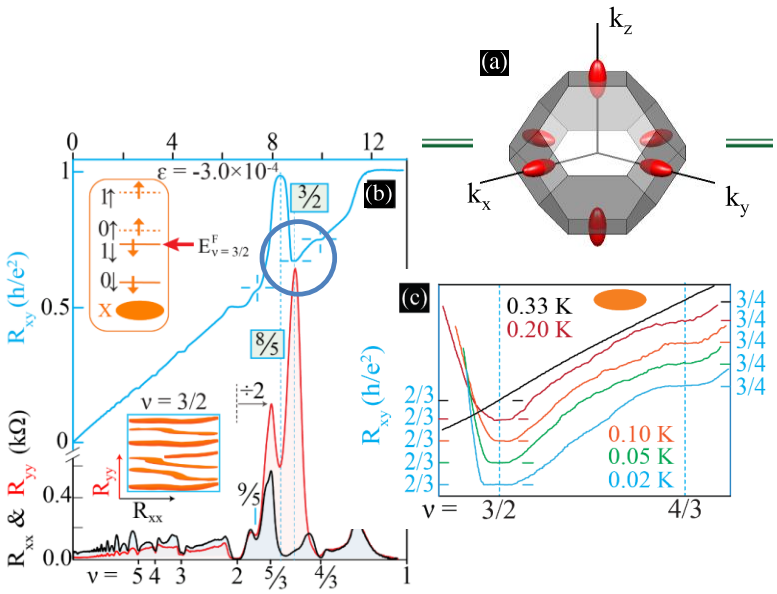

Fig. 1 (a) Brillouin zone showing ellipsoidal Fermi surfaces for AlAs electrons. (b) Magneto-transport traces showing a highly anisotropic fractional quantum Hall state at filling factor 3/2. (c) Despite the transport anisotropy, the Hall resistance is well quantized. (After Ref. 13)

B. Probing the Melting of a Two-dimensional Quantum Wigner Crystal via its Screening Efficiency [17]:

One of the most fundamental and yet elusive collective phases of an interacting 2D electron system is the quantum Wigner crystal (WC), an ordered array of electrons expected to form when the electrons' Coulomb repulsion energy eclipses their kinetic (Fermi) energy. In low-disorder, 2D electron systems, the quantum WC is known to be favored at very low temperatures and small Landau level filling factors (ν), near the termination of the FQHSs. This WC phase exhibits an insulating behavior, reflecting its pinning by the small but finite disorder potential. An experimental determination of a temperature vs. ν phase diagram for the melting of the WC, however, has proved to be challenging. In our work, we used capacitance measurements (Fig. 2) to probe the 2D WC through its effective screening as a function of temperature and ν. We find that, as expected, the screening efficiency of the pinned WC is very poor at very low temperature and improves at higher temperature once the WC melts. Surprisingly, however, rather than monotonically changing with increasing temperature, the screening efficiency shows a well-defined maximum at a temperature that is close to the previously reported melting temperature of the WC. Our experimental results suggest a new method to map out a temperature vs. ν phase diagram of the magnetic-field-induced WC precisely [17].

Future plans

We plan to continue our studies of 2D electrons in AlAs quantum wells and 2D holes in GaAs quantum wells. We have had a major breakthrough in fabricating ultra-high-quality, modulation-doped AlAs quantum wells [8]. The samples have an unprecedentedly high electron mobilities peaking at 2.4×10^6 cm^{2}V^{-1}s^{-1} at a density of 2.2×10^{11} cm^{-2}. This is about an order of magnitude improvement in mobility over previous results. The unprecedented quality of these samples has already enabled us to observe new phenomena and electronic states such as an unusual, even-denominator FQHS. We plan to further study the physics of these samples and explore their new properties with an emphasis on tuning the valley occupancy through the application of uniaxial strain.

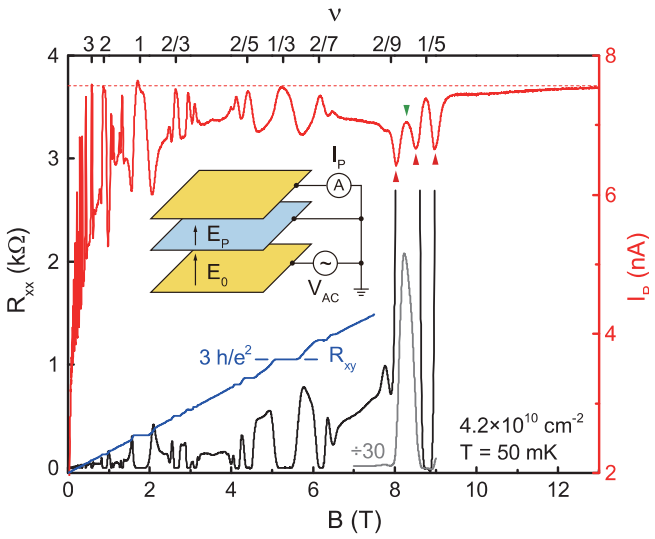

Fig. 2 Overview of transport and penetration current (I_P) results. The inset shows a schematic of measurement configuration. The yellow layers are the top and bottom gates, and the blue layer is the 2D electron system. An ac voltage (V_{ac}) applied to the bottom gate generates the source electric field E_0 between this gate and the 2D electron system. The penetration electric field E_P reaches the top gate and induces I_P, which is measured by a lock-in amplifier in ammeter mode (A). The black trace is the longitudinal magnetoresistance (R_{xx}); the gray trace shows R_{xx} reduced by a factor of 30 at high fields. The blue trace is the Hall resistance (R_{xy}). The red trace is the penetration current (I_P). (After [17])

We also plan to study the magnetic-field-induced WC state in dilute GaAs 2D *hole* systems. In low-disorder, GaAs 2D *electron* systems signatures of a field-induced WC appear at very low temperatures and small Landau level filling factors (near $\nu = 1/5$). In dilute GaAs 2D hole systems, on the other hand, thanks to the larger effective mass of 2D holes and the ensuing Landau level mixing, the WC forms at higher fillings (near $\nu = 1/3$). Although the 2D hole WC phase has been studied over the years using various experimental techniques, a temperature vs. filling factor phase diagram has been missing so far. We plan to measure such a phase diagram, using our recently developed technique which monitors the screening efficiency of the WC as a function of temperature and filling factor.

Publications acknowledging DOE support; since 2017:

1. Insun Jo, Yang Liu, L.N. Pfeiffer, K.W. West, K.W. Baldwin, M. Shayegan, and R. Winkler, "Signatures of an Annular Fermi Sea," Phys. Rev. B **95**, 035103 (2017).
2. M.A. Mueed, D. Kamburov, Md. Shafayat Hossain, L.N. Pfeiffer, K.W. West, K.W. Baldwin, and M. Shayegan, "Search for Composite Fermions at Filling Factor 5/2: Role of Landau Level and Subband Index," Phys. Rev. B **95**, 165438 (2017).
3. Insun Jo, K. A. Villegas Rosales, M. A. Mueed, L. N. Pfeiffer, K. W. West, K. W. Baldwin, R. Winkler, Medini Padmanabhan, and M. Shayegan, "Transference of Fermi Contour Anisotropy to Composite Fermions," Phys. Rev. Lett. **119**, 016402 (2017).

4. Insun Jo, M. A. Mueed, L. N. Pfeiffer, K. W. West, K. W. Baldwin, R. Winkler, Medini Padmanabhan, and M. Shayegan, "Tuning of Fermi Contour Anisotropy in GaAs (001) 2D Holes via Strain," Appl. Phys. Lett. **110**, 252103 (2017).
5. H. Deng, Y. Liu, I. Jo, L.N. Pfeiffer, K.W. West, K.W. Baldwin, and M. Shayegan, "Interaction-induced Interlayer Charge Transfer in the Extreme Quantum Limit," Phys. Rev. B (Rapid Communications) **96**, 081102(R) (2017).
6. Insun Jo, Hao Deng, Yang Liu, L. N. Pfeiffer, K. W. West, K. W. Baldwin, and M. Shayegan, "Cyclotron Orbits of Composite Fermions in the Fractional Quantum Hall Regime," Phys. Rev. Lett. **120**, 016802 (2018). **[Editor's Suggestion]**
7. Md. Shafayat Hossain, Meng K. Ma, M. A. Mueed, L. N. Pfeiffer, K. W. West, K. W. Baldwin, and M. Shayegan, "Direct Observation of Composite Fermions and Their Fully Spin Polarized Fermi Sea near $\nu = 5/2$," Phys. Rev. Lett. **120**, 256601 (2018). **[Editor's Suggestion]**
8. Yoon Jang Chung, K.A. Villegas Rosales, H. Deng, K.W. Baldwin, K.W. West, M. Shayegan, and L.N. Pfeiffer, "Multivalley Two-dimensional Electron System with Mobility Exceeding 10^6 $cm^2V^{-1}s^{-1}$," Phys. Rev. Materials (Rapid Communications) **2**, 071001(R) (2018).
9. M.A. Mueed, Md. Shafayat Hossain, I. Jo, L.N. Pfeiffer, K.W. West, K.W. Baldwin, M. Shayegan, "Realization of a Valley Superlattice." Phys. Rev. Lett. **121**, 036802 (2018). **[Editor's Suggestion]**
10. H. Deng, L.N. Pfeiffer, K.W. West, K.W. Baldwin, and M. Shayegan, "Critical Filling Factor for the Formation of a Quantum Wigner Crystal Screened by a Nearby Layer," Phys. Rev. B (Rapid Communications) **98**, 081111(R) (2018).
11. Md. Shafayat Hossain, M.A. Mueed, Meng K. Ma, Y.J. Chung, L.N. Pfeiffer, K.W. West, K.W. Baldwin, M. Shayegan, "Anomalous Coupling between Magnetic and Nematic Orders in Quantum Hall Systems," Phys. Rev. B (Rapid Communications) **98**, 081109(R) (2018). **[Editor's Suggestion]**
12. A. T. Hatke, Yang Liu, L. W. Engel, L. N. Pfeiffer, K. W. West, K. W. Baldwin, and M. Shayegan, "Wigner Solids of Wide Quantum Wells near Landau Filling $\nu=1$," Phys. Rev. B **98**, 195309 (2018).
13. Md. Shafayat Hossain, Meng K. Ma, Y. J. Chung, L. N. Pfeiffer, K. W. West, K. W. Baldwin, and M. Shayegan, "Unconventional Anisotropic Even-denominator Fractional Quantum Hall State in a System with Mass Anisotropy," Phys. Rev. Lett. **121**, 256601 (2018). **[Editor's Suggestion.]**
14. Jing Xu, Meng K. Ma, Maksim Sultanov, Zhi-Li Xiao, Yong-Lei Wang, Dafei Jin, Yang-Yang Lyu, Wei Zhang, Loren N. Pfeiffer, Ken W. West, Kirk W. Baldwin, Mansour Shayegan, and Wai-Kwong Kwok, "Negative Longitudinal Magnetoresistance in GaAs Quantum Wells," Nature Communications **10**, 287 (2019).
15. Yoon Jang Chung, K. W. Baldwin, K. W. West, N. Haug, J. van de Wetering, M. Shayegan, and L. N. Pfeiffer, "Spatial Mapping of Local Density Variations in GaAs Two-dimensional Electron Systems Using Photoluminescence," Nano Letters **19**, 1908 (2019).
16. A. T. Hatke, H. Deng, Yang Liu, L. W. Engel, L. N. Pfeiffer, K. W. West, K. W. Baldwin, M. Shayegan, "Wigner Solid Pinning Modes Tuned by Fractional Quantum Hall States of a Nearby Layer," Science Advances **5**, eaao2848 (2019).
17. H. Deng, L.N. Pfeiffer, K.W. West, K.W. Baldwin, and M. Shayegan, "Probing the Melting of a Two-dimensional Quantum Wigner Crystal via its Screening Efficiency," Phys. Rev. Lett. **122**, 116601 (2019). **[Editor's Suggestion]**
18. Md. Shafayat Hossain, Meng K. Ma, M. A. Mueed, D. Kamburov, L. N. Pfeiffer, K. W. West, K. W. Baldwin, R. Winkler, and M. Shayegan, "Geometric Resonance of Four-flux Composite Fermions," Phys. Rev. B (Rapid Communications) **100**, 041112(R) (2019).

Correlated Quasiparticles in Graphene

Philip Kim, Department of Physics, Harvard University

Program Scope

Interactions between particles in quantum many-body systems can lead to a collective behavior. In graphene, the highly symmetric honeycomb lattice structure yields the linear carrier dispersion analogous to the relativistic dispersion relation in the usual Dirac Fermion spectrum. Combining this quasi-relativistic spectrum with Coulomb interactions between charge carriers in graphene often lead to exotic electronic states. A notable example of such systems is the Dirac fluid, which can be realized near the neutrality point where strong electron-electron interactions and electron-hole symmetry can decouple heat current from charge flow, blurring the existence of quasiparticles. Here, the thermally excited electron-hole plasma reveals hydrodynamics of quasi-relativistic fermions, which is an ideal candidate to show this exciting and exotic phenomenon. Under quantizing magnetic fields, strong Coulomb interaction can also lead to spontaneous symmetry breaking in the internal quantum degrees of freedom of correlated quasiparticles. Finally, creating a hybrid system of a superconductor and quantum Hall states can also create strongly correlated quasiparticles in the mesoscopic sized graphene samples by proximity-induced superconductivity near the superconducting electrodes. In this project, we investigate the fundamental physics of correlated electronic systems realized in these three different ways. Our research goals are to probe the emergent phenomena in the Dirac fermionic system. More specifically we performed tasks (i) engineering graphene edge depletion and gate geometry to improve controlled quantum Hall edge state formation; (ii) investigating electronic thermal transport and measurement of magnetic hydrodynamics; (iii) developing experimental technique for measuring entropy and thermal conductance in quantum Hall ferromagnetism in bilayer graphene; (iv) exploring superfluid magneto-exciton condensation in graphene double layers; (v) investigation of proximitized quantum Hall edges to create and control non-Abelian quasiparticles; (vi) studying proximitized superconducting orders competing with the quantum Hall states for the creation of topological superconductivity.

Recent Progress

Engineering Quantum Hall Edge States in Bilayer Graphene to form PN Networks: The capability of probing and engineering the spatial and energy configurations of topological states holds the key in understanding exotic electronic excitations in solid state systems and towards realizing topological quantum computing. Conventional transport studies on quantum Hall (QH) effect have been focused on demonstrating topologically protected physical observables such as quantized Hall plateaus. While it is helpful in discovering new QH excitations, these experiments are insensitive to edge state wavefunctions and local configuration of the Hamiltonian. Conventional spectroscopy tools such as scanning tunneling microscopy have been implemented, each attempted at probing a specific selection of these physical properties. In these studies, device

geometry and experimental configuration prevent direct and comprehensive characterization of edge states with high spatial and energy resolutions. Utilizing electron-hole symmetry and tunable bandgap in extremely clean bilayer graphene sample, we create a unique platform allowing arbitrary placement and separation of QH edge states both in real and energy space. This allows unprecedented versatility in quantum manipulation as well as comprehensive probe of all fundamental details of QH states within the same context defined by tunable experimental conditions, providing a powerful tool and a new approach in both understanding and utilizing QH states (Fig. 1).

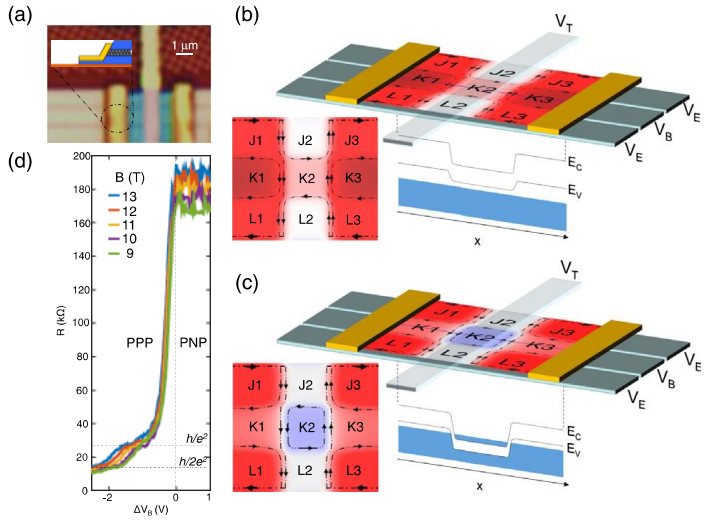

Fig.1. **Gate-defined p-n-p networks in bilayer graphene**. **(a)** image of the device **(b)** Simulated carrier density and edge state configuration at for p-p-p junctions. **(c)** Simulated carrier density and edge state configuration at for p-n-p junctions. Magneto-transport across the sample is dominated by quantum tunneling and the device enters the nonequilibrium regime. **(d)** While quantized plateaus are clearly visible in the p-p-p regime, a steep change in measured magnetoresistance occurs when transitioning to the p-n-p regime.

The significance of our work is: (i) We demonstrate a unique electrostatically engineered system for the first time where all fundamental physical properties of the QH states are probed simultaneously in the same experimental condition, with unprecedented spatial and energy resolution; (ii) In this system, we demonstrate high degree of freedom in tailoring the spatial and energy configuration of QH states as well as equilibration between them, providing key components towards quantum manipulation, controlled braiding and advanced interferometry.

Interlayer fractional quantum Hall effect in a coupled graphene double-layer: When a strong magnetic field is applied to a two-dimensional electron system, interactions between the electrons can cause fractional quantum Hall (FQH) effects [1,2]. Bringing two two-dimensional conductors close to each other, a new set of correlated states can emerge due to interactions between electrons in the same and opposite layers. We discovered novel emergent many-body quantum states enabled by interlayer Coulomb interactions in graphene double-layers separated by an atomically thin hexagonal-boron nitride (hBN). Fractional quantum Hall (FQH) effect is one of the most notable examples demonstrating strongly correlated quantum phenomena. These effects arise from electron-electron interactions in two-dimensional (2D) systems and enable prominent topological properties and anyonic quasi-particles, which can be utilized for topological quantum computing. In our work, we extend this exotic phenomenon even further by coupling two 2D layers with Coulomb interactions, resulting in new emergent correlated states of matter. Previously, interlayer coupled integer quantum Hall effect has been observed in coupled GaAs quantum wells and more

recently in coupled graphene double-layers under strong magnetic fields. This interlayer integer quantum Hall effect can also be viewed as exciton Bose-Einstein condensate phase (BEC). In this work, exploiting the strong Coulomb interaction across atomic thin hBN layers and drastically enhanced sample quality by dual graphite gates, we discover surprising and unexpected interlayer coupled FQH effects (Fig.2). We found that the observed interlayer FQH states can be explained by coupled composite fermions (CF). Remarkably, we also discover a BEC of CF excitonic pairs and a 'semi-quantized' quantum Hall state due to the pairing of anyonic quasiparticles in two layers. The newly discovered interlayer FQH in a double-layer system will open an entirely new research direction of FQH study. The properties of the discovered states await further investigation. The rich phase diagram of double-layer quantum Hall systems invites further pursuits of new topological states.

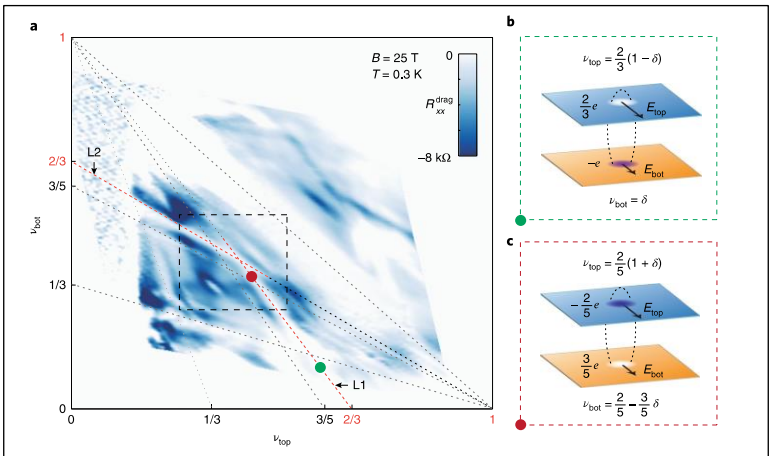

Fig. 2. **Interlayer correlation through quasiparticle pairing**. **a.** Longitudinal drag resistance as a function of filling factors in the top and bottom layers. Dotted lines show locations of semiquantized states where longitudinal drag resistance vanishes. **b,c**, Illustrations of quasiparticle pairing for two filling-factor configurations (green and red dots in a). The circles on the two graphene layers represent quasiparticle excitations with marked electrical charges.

<u>Spin-polarized Correlated Insulator and Superconductor in Twisted Double Bilayer Graphene</u>: Employing van der Waals heterostructures of twisted double bilayer graphene (TDBG), we realize a flat electron band that is tunable by perpendicular electric fields. Similar to the magic angle twisted bilayer graphene, TDBG exhibits energy gaps at the half and quarter filled flat bands, indicating the emergence of correlated insulating states. We find that the gaps of these insulating states increase with in-plane magnetic field, suggesting a ferromagnetic order. Upon doping the ferromagnetic half-filled insulator, superconductivity emerges with a critical temperature controlled by both

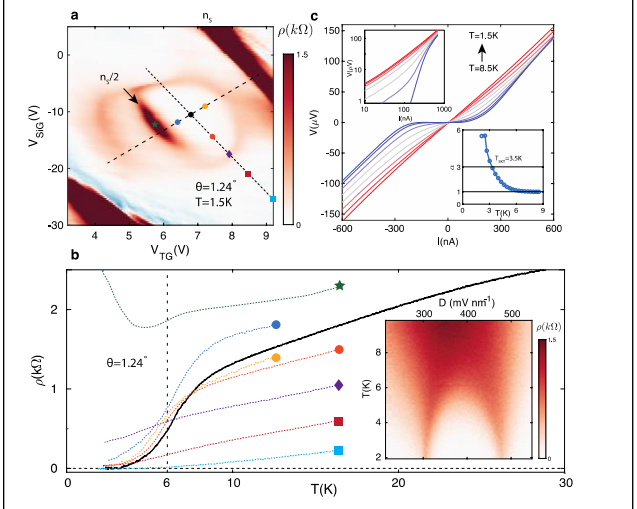

Fig. 3. **Superconductivity in 1.24◦ TDBG. a,** Resistivity map around the half-filled insulator and superconductor. **b,** Resistivity as a function of temperature at different spot marked by colored symbols in a using the corresponding colors and shapes. Inset, temperature dependence along the constant density line-cut marked by dotted line in a. **c,** I–V curves at optimal doping nm and displacement field.

density and electric fields (Fig. 3). We observe that the in-plane magnetic field enhances the superconductivity in the low field regime, suggesting spin-polarized electron pairing. Spin-polarized superconducting states discovered in TDBG provide a new route to engineering interaction-driven topological superconductivity.

Future Plans

To extend our success beyond our ongoing work, we propose a set of research aims to explore novel physical phenomena stemming from the Correlated Quasiparticles in Graphene. The near future plans include:

- Investigation of unusual spin triplet superconductivity appeared in twisted multiple graphene layers
- Investigation of the proximity induced superconductivity in graphene under magnetic fields.
- Investigation of magneto hydrodynamic thermal transport phenomena in momolayer and bilayer graphene.

References

[1] Tsui, D. C., Stormer, H. L. & Gossard, A. C. Two-dimensional magnetotransport in the extreme quantum limit. Phys. Rev. Lett. **48**, 1559–1562 (1982).
[2] Laughlin, R. B. Anomalous quantum Hall effect: an incompressible quantum fluid with fractionally charged excitations. Phys. Rev. Lett. **50**, 1395–1398 (1983).

Publications

K. Wang, A. Harzheim, J. U. Lee, T. Taniguchi, K. Watanabe, P. Kim, "Tunneling Spectroscopy of Quantum Hall States in Bilayer Graphene PN Networks," Phys. Rev. Lett. **122**, 146801 (2019).

X. Liu, Z. Hao, K. Watanabe, T. Taniguchi, B. Halperin, P. Kim, "Interlayer fractional quantum Hall effect in a coupled graphene double-layer," Nature Physics **15**, 893–897 (2019).

X. Liu, Z. Hao, E. Khalaf, J. Y. Lee, K. Watanabe, T. Taniguchi, A. Vishwanath, P. Kim, "Spin-polarized Correlated Insulator and Superconductor in Twisted Double Bilayer Graphene," arXiv:1903.08130, under review.

X. Liu, J.I.A Li, K. Watanabe, T. Taniguchi, J. Hone, B. I. Halperin, C.R. Dean, and P. Kim, "Crossover between Strongly-coupled and Weakly-coupled Exciton Superfluids," in preparation.

Symmetry Breaking in Two-Dimensional Flat-band Systems for Spin and Charge Transport

PI: Chun Ning (Jeanie) Lau
co-PI: Marc Bockrath
Department of Physics, The Ohio State University, Columbus, OH 43210

Program Scope

In a flat band system, the charge carriers' energy-momentum relation is very weakly dispersive. The resultant large density of states and the dominance of Coulomb potential energy relative to the kinetic energy often favor the formation of strongly correlated electron states. Such strong electronic correlations and competition between different degrees of freedom give rise to the formation of many interesting many-body phases, such as ferromagnetism, nematicity, antiferromagnetism, superconductivity, and charge density waves.

The advent of 2D materials has enabled unprecedented engineering and exploration of flat bands via control of layer thickness, magnetic field, and twisting. Building on past accomplishments, in this program and seek to create, engineer, and control the correlated states in flat band systems in 2D materials and heterostructures, and to exploit these states for transport of spins, charges and Cooper pairs. In the first thrust, we will focus on flat bands generated by magnetic fields that quench the charge carriers' kinetic energy. We plan to investigate the transport of spin degrees of freedom through the antiferromagnetic insulating states in monolayer and bilayer graphene[1, 2], with the goal of achieving electrical control of magnetic switching. By coupling trilayer graphene to superconductors, we will also engineer devices that host the much sought-after Majorana fermions[3] and may enable fault tolerant quantum computation.

The second thrust aims at investigating the correlated insulating states in few-layer graphene and superlattices. In the single particle picture, these systems are predicted to be metals, yet they are electrical insulators due to the strong electronic interactions. Here we will investigate the quantum Hall insulator and insulator-metal transition in tetralayer graphene, and the correlated insulator state in twisted bilayer graphene[4-7]. The latter system is particularly intriguing, since, by stacking two pieces of graphene at slightly different orientation, it becomes both a superconductor and an insulator, where the transition is tunable by charge density.

We will study these systems by transport measurements of high quality devices and varying temperatures, magnetic field, electric field, bias, charge density and disorder. These experiments will provide a comprehensive investigation of the many novel phenomena produced by electron-electron interactions in these exciting materials, and harness their unique properties for quantum information applications. Successful implementation of the project will be a major step forward in our fundamental knowledge of electron correlation and many-body physics in materials, which is important for physics, material science, engineering and energy science.

Recent Progress

In the past two years, we have made significant progress in our studies of ultra-clean ultra-clean graphene devices that are either suspended or supported on hexagonal BN substrates. Some of the works are highlighted below.

<u>Long Distance Spin Transport in a Graphene Quantum Hall Antiferromagnet</u>

Spin currents in magnetic insulators can be carried with dissipation by magnon quasiparticles, or collectively and without dissipation by spin supercurrents in systems with easy

plane magnetic order. Whereas magnon transport is less efficient in an ideal antiferromagnetic insulator (AFMI) than in a ferromagnetic insulator, superfluidity is theoretically possible in both cases. Because of their ultrafast intrinsic dynamics and robustness against stray fields, antiferromagnetic insulators are promising candidates for spintronic components. Therefore, long-distance, low-dissipation spin transport and electrical manipulation of antiferromagnetic order are key research goals in antiferromagnetic spintronics. In this work, following proposal in ref. [1] we report the first experimental evidence of robust spin transport through an antiferromagnetic insulator, in our case the gate-controlled state that appears in charge-neutral graphene in a magnetic field. Utilizing quantum Hall edge states as spin-dependent injectors and detectors, we observe large, non-local electrical signals across charge-neutral channels that are up to 5 μm long (Fig. 1). The dependence of the signal on magnetic field, temperature, and filling factor is consistent with spin superfluidity as the spin-transport mechanism. This work demonstrates the utility of graphene in the quantum Hall regime as a powerful model system for fundamental studies in antiferromagnetic spintronics. This work appeared in *Nature Physics*[2].

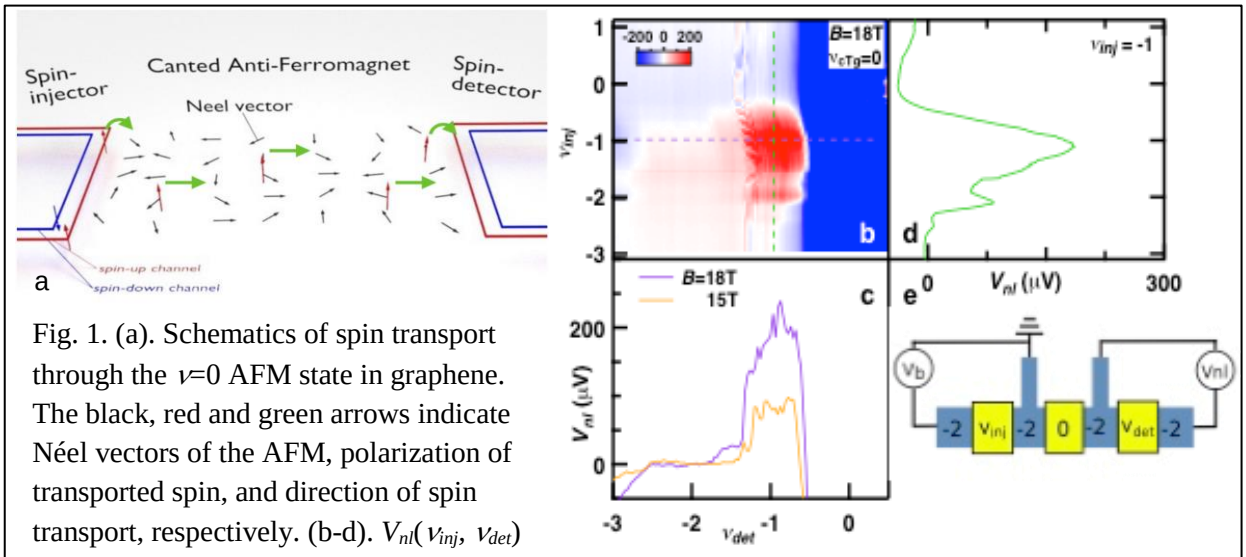

Fig. 1. (a). Schematics of spin transport through the ν=0 AFM state in graphene. The black, red and green arrows indicate Néel vectors of the AFM, polarization of transported spin, and direction of spin transport, respectively. (b-d). $V_{nl}(\nu_{inj}, \nu_{det})$ from Device 1 at V_{bias}=0.4V and B=18 T using the device configuration in (e), and line traces **b.**

<u>Large tunable intrinsic gap in rhombohedral-stacked tetralayer graphene at half filling</u>

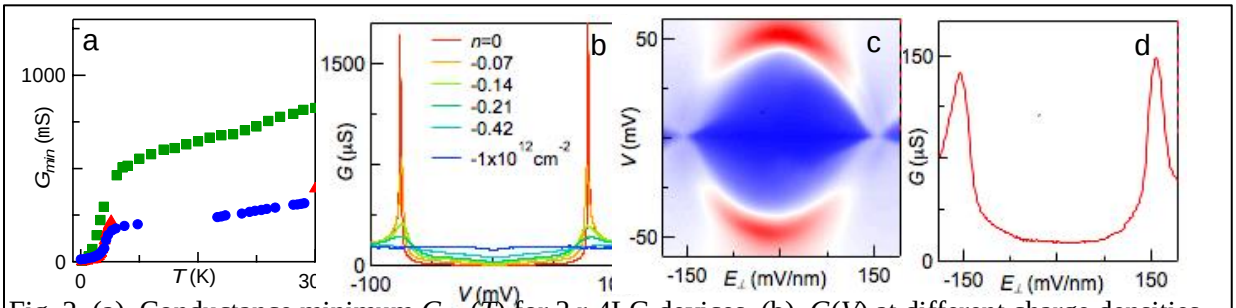

Fig. 2. (a). Conductance minimum $G_{min}(T)$ for 3 r-4LG devices. (b). $G(V)$ at different charge densities. (c-d). G *vs.* bias and out-of-plane electric field $E_\perp$ at n=0. (d). $G(E_\perp)$ at V=0.

The band structure of rhombohedral-stacked few-layer graphene (r-FLG) can be approximated as $E = \frac{(\hbar k v_F)^M}{\gamma_1^{M-1}}$, where γ_1~0.3 eV is the interlayer hopping energy, and $v_F \sim 10^6$ m/s the Fermi velocity of MLG. Thus r-FLG is highly unusual in the very flat bands near the charge

neutrality, which host large and even diverging (for $M>2$) density of states and extremely large electronic interactions. In the ultra-low density regime, these FLG systems host exceedingly strong electron-electron interactions, leading to phases with spontaneous broken symmetries. Using transport measurements on suspended dual-gated r-4LG, we observe an insulating ground state with an exceedingly large interaction-induced gap, up to 80 meV (Fig. 2). This gapped state can be enhanced by a perpendicular magnetic field, and suppressed by an interlayer potential, carrier density, or a critical temperature of ~40 K. We identify this insulating state at half filling to be a layer antiferromagnetic state with broken time reversal symmetry. This work was published by *2D Materials*[8].

Quantum Parity Hall and Topological Phases in ABA Trilayer Graphene

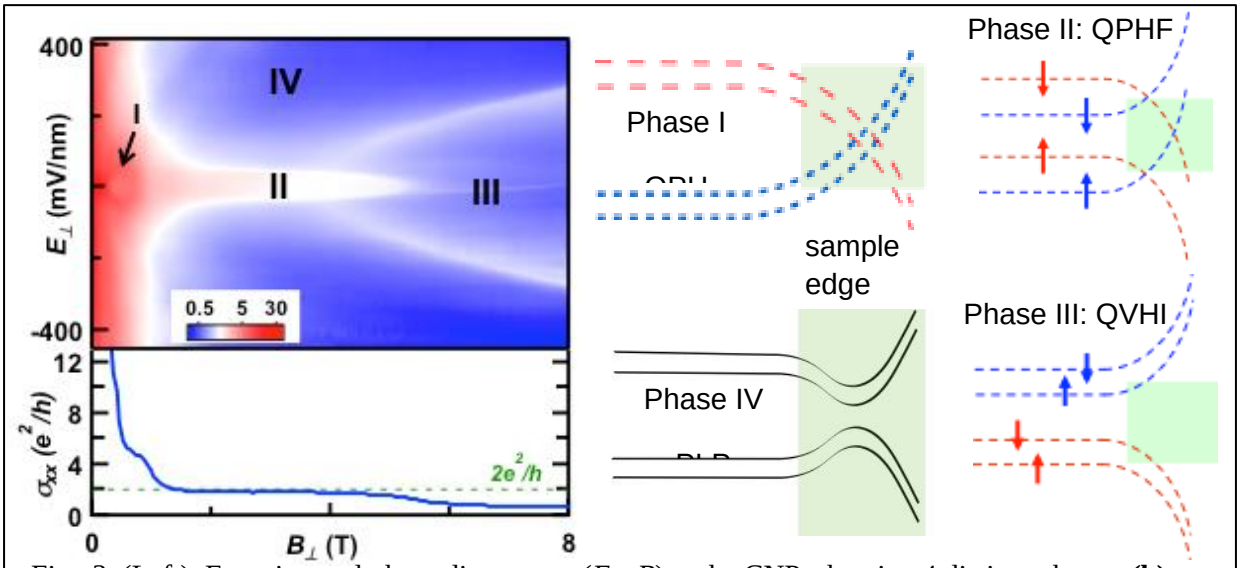

Fig. 3. (Left). Experimental phase diagram $\sigma_{xx}(E_\perp, B)$ at the CNP, showing 4 distinct phases. **(b).** Line trace $\sigma_{xx}(B)$ at $E_\perp=0$. (Right). Schematics of edge states for the different phases. The blue and red dashed lines indicate Landau levels from even- and odd- parity bands, respectively. QPH: Quantum parity Hall. QPHF: Quantum parity Hall ferromagnet. QVHI: Quantum valley Hall insulator. PLP: Partial layer polarization. Phases I and II have spin-degenerate and spin-polarized counter-propagating edge states, respectively, giving rise to quantized conductances $4e^2/h$ and $2e^2/h$.

The celebrated phenomenon of quantum Hall effect has recently been generalized from transport of conserved charges to that of other approximately conserved state variables, including spin and valley, which are characterized by spin- or valley-polarized boundary states with different chiralities. Here, we report a new class of quantum Hall effect in ABA-stacked graphene trilayers (TLG), the quantum parity Hall (QPH) effect, in which boundary channels are distinguished by even or odd parity under the system's mirror reflection symmetry. At the charge neutrality point and a small perpendicular magnetic field $B_\perp$, the even- and odd-parity Landau levels segregated to opposite sides of the sample, leading to counter-propagating edge states with longitudinal conductance σ_{xx} that are spin-degenerate at low field, and spin-polarized at intermediate fields, giving rise to $4e^2/h$ and $2e^2/h$ quantized conductances, respectively (Fig. 3). Exchange interaction in the strong B limit drives TLG to be an ordinary insulator. Our findings demonstrate a topological phase that is protected by a gate-controllable symmetry and sensitive to Coulomb interactions, and provides a stable, readily accessible system for realization of

topological superconductivity. This work was published by *Proc. Nat. Acad. Sci*.[9].

Future Plans

Apart from the general direction outlined in the first section, our immediate plans for the next year include investigation of

- spin transport mechanism in graphene quantum Hall antiferromagnet
- Josephson junctions based on trilayer graphene
- phase diagram of tetralayer graphene at the charge neutrality point

References

[1] S. Takei *et al.*, Phys. Rev. Lett. **116**, 216801 (2016).
[2] P. Stepanov *et al.*, Nat. Phys. **14**, 907 (2018).
[3] P. San-Jose *et al.*, Phys. Rev. X **5**, 041042 (2015).
[4] Y. Cao *et al.*, Nature **556**, 80 (2018).
[5] Y. Cao *et al.*, Nature **556**, 43 (2018).
[6] R. Bistritzer, and A. H. MacDonald, Proc. Nat. Acad. Sci. **108**, 12233 (2011).
[7] J. M. B. Lopes dos Santos *et al.*, Phys. Rev. Lett. **99**, 256802 (2007).
[8] K. Myhro *et al.*, 2D Mater. **5**, 045013 (2018).
[9] P. Stepanov *et al.*, Proc. Natl. Acad. Sci. **116**, 10286 (2019).

Two-year Publications Supported by BES

1. E. Codecido, Q. Wang, R. Koester, S. Che, H. Tian, R. Lv, S. Tran, K. Watanabe, T. Taniguchi, F. Zhang, M. Bockrath, and C. N. Lau, Correlated Insulating and Superconducting States in Twisted Bilayer Graphene Below the Magic Angle, *Science Advances*, accepted (2019).
2. P. Stepanov, Y. Barlas, S. Che, K. Myhro, G. Voigt, Z. Pi, K. Watanabe, T. Taniguchi, D. Smirnov, F. Zhang, R. Lake, A. H. MacDonald, C.N. Lau, "Quantum Parity Hall effect in ABA Graphene", *Proceedings of National Academy of Sciences*, **116**, 10286 (2019).
3. P. Stepanov, S. Che, D. Shcherbakov, K. Thilahar, G. Voigt, M. W. Bockrath, D. Smirnov, K. Watanabe, T. Taniguchi, R. Lake, Y. Barlas, A. H. MacDonald, C. N. Lau, "Long Distance Spin Transport Through a Graphene Quantum Hall Antiferromagnet", *Nature Physics*, **14**, 907 (2018).
4. K. Myhro, S. Che, Y. Shi, Y. Lee, K. Thilahar, K. Bleich, Dmitry Smirnov, C. N. Lau, "Large tunable intrinsic gap in rhombohedral-stacked tetralayer graphene at half filling", *2D Materials*, 045013 (2018).
5. Y. Wu, D. Zhai, C. Pan, B. Cheng, T. Taniguchi, K. Watanabe, N. Sandler, and M. Bockrath, "Quantum Wires and Waveguides Formed in Graphene by Strain," *Nano Letters* **18**, 64-69 (2018).
6. Y. Shi, S. Che, K. Zhou, S. Ge, Z. Pi, T. Espiritu, T. Taniguchi, K. Watanabe, R. Lake, and C.N. Lau, "Tunable Lifshitz Transitions and Multiband Transport in Tetralayer Graphene", *Physical Review Letters* **120**, 096802 (2018).
7. J. Y. Liu, J. Hu, D. Graf, T. Zou, M. Zhu, Y. Shi, S. Che, S. M. A. Radmanesh, **C. N. Lau**, L. Spinu, H. B. Cao, X. Ke, and Z. Q. Mao, Unusual interlayer quantum transport behavior caused by the zeroth Landau level in $YbMnBi_2$, *Nature Communications* **8,** 646 (2017).
8. B. Cheng, C. Pan, S. Che, P. Wang, Y. Wu, K. Watanabe, T. Taniguchi, S. Ge, R. Lake, D. Smirnov, C. N. Lau, and M. Bockrath, Fractional and Symmetry-Broken Chern Insulators in Tunable Moiré Superlattices, *Nano Letters*, **19**, 4321 (2019).

Quantum Transport in 2D Semiconductors

James Hone, Columbia University, Dept. of Mechanical Engineering
Cory Dean, Columbia University, Dept. of Physics

Program Scope

This project focuses on fundamental studies of quantum transport in two-dimensional transition metal dichalcogenides and their related heterostructures. Areas of study include: understand fundamental limits of quantum device characteristics, including scattering mechanisms, material and interfacial impurities, and electrical contacts; determining intrinsic properties of the 2D semiconductor TMDs such as the effective band mass, spin orbit coupling, and electron-phonon coupling; and measurement of novel quantum transport properties unique to the TMDs including the hierarchy of quantum Hall states and valley Hall effects.

Recent Progress

Direct measurement of quantum transport in 2D semiconductors has proven difficult due to low material quality and difficulties in making Ohmic contacts at low temperature. Toward the first challenge, we have utilized WSe_2 grown by techniques developed in the lab of Luis Balicas (Nat. High Magnetic Field Lab / FSU), which has defect density below $10^{11}/cm^2$. Toward the second challenge, we have partially circumvented the contact issue by using a single electron transistor (SET) fabricated directly on top of a hBN / WSe_2 / hBN heterostructure to measure the electronic compressibility of the WSe_2. In this measurement, the electrical contact to the WSe_2 only has to be sufficient to allow slow charging in response to an applied gate voltage. Such SET-based techniques have previously been employed with GaAs-based systems but not with 2D semiconductors. We performed measurements of monolayer WSe_2 at the National High Magnetic Field Laboratory, at fields up to 35 T.

Together, these improvements allow us to provide a near-complete map of the Landau Level spectrum of monolayer WSe_2, as shown in Figure 1, which shows the inverse compressibility ($d\mu/dn$) as a function of gate voltage and applied field. Well-developed Landau 'fans' are seen for both the valence (VB) and conduction (CB) bands, which are well fit by the general relation $B = nh/ve$, with the filling factor ν shown. By extrapolating the slopes of the LL gaps to B = 0, we find a separation in gate voltage of 2.7 V between the two bands, arising from the band gap of the material. Because the higher spin-split bands in WSe_2 are expected to be ~ 500 meV and ~ 30 meV removed from the lowest-energy VB and CB, respectively, this data reflects only the lowest spin-split bands.

A striking aspect of these LL maps is a clear alternation between large and small gaps, for all observed states in the CB and beginning at ν=-6 for the VB. In the CB, gaps at odd-valued ν are more pronounced than those at even-valued ν throughout the accessible range of electron density. In contrast, the VB the dominant parity in ν changes from odd to even as the hole

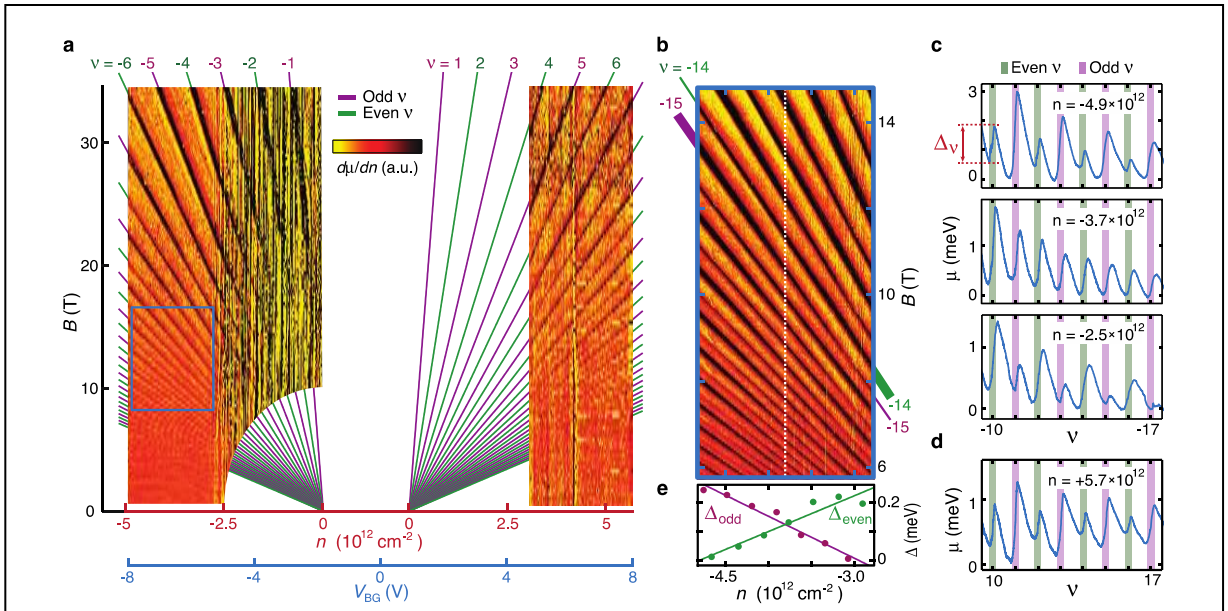

Figure 1. Ambipolar Landau level dispersion. **a**, The inverse compressibility dμ/dn of the WSe_2 produces a characteristic Landau fan as a function of carrier density n and magnetic field B. **b**, Zooming in on the valence band (blue outline in a) reveals that the gap magnitude alternates, and that the dominant gaps occur at odd ν for high hole density and for even ν at low density. The crossover occurs at $n \approx -3.8\times10^{12}$ cm^{-2} (dashed white line), and has no discernible dependence on B. **c**, The chemical potential μ acquired along three vertical cuts in the VB fan confirms the density-dependence of the LL gap sequence. At high hole density (top), gaps at odd filling dominate, whereas the ones as even filling dominate at low density (bottom). At the cross-over density (middle), consecutive gaps are equal.

density is reduced (Fig. 1c), with a cross-over point at $n \approx -3.8\times10^{12}$ cm^{-2}, independent of B (white dotted line in Fig. 1b).

Figure 2d shows the proposed structure of the Landau levels derived from the data shown in Figure 1. The alternating pattern of gaps arises from breaking of the degeneracy between the K and K' valleys, which are spin-polarized. Within a given valley, the LL spacing is given by the cyclotron energy, whereas the Zeeman splitting between valleys is given by an effective Lande g-factor g*. Since both are proportional to applied field, the number of valley-polarized bands is independent of field, and provides a measure of the ratio between the Zeeman and cyclotron energies. In the CB, g* is below 2, the Zeeman energy is smaller than the cyclotron energy, and the pattern of alternating gaps appears for all LLs. In contrast, for the VB we find that g* is above 10, and there are 6 'valley-polarized' LLs before the alternating sequence begins. In addition, the reduction in g* with increased carrier density causes the shift in gap pattern from even-odd to odd-even. The values of m* and g* derived fom the data are shown in Fig. 2a,b. The large value of g* indicates strong electron-electron interactions

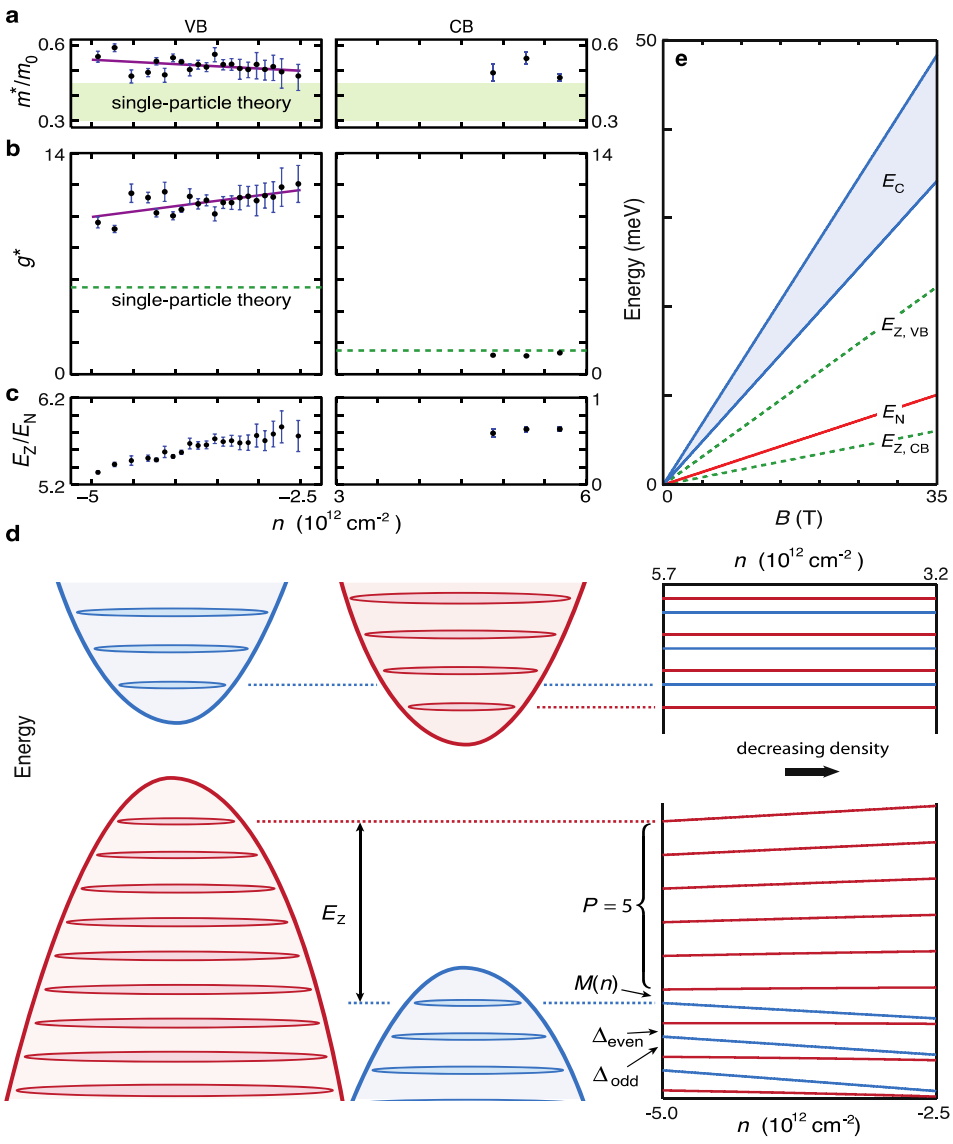

Figure 2. Extracted parameters and effects of interactions. **a**, Effective carrier mass and **b**, Landé g-factor for each accessible density for the VB and CB (black dots), and best-fit lines (purple). The green area/dotted line represent typical theoretical predictions from a single-particle model. Both m* and g* are enhanced in the VB compared to such predictions. The extraction of g* in the CB assumes P = 0 (see text and Supplementary Information). **c**, The ratio of Zeeman to cyclotron energy ($E_Z/E_N = m^*g^*/m_0$) is less than 1 in the CB but between 5-6 in the VB. **d**, Schematic of LL structure versus carrier density, assuming the m* and g* shown by solid purple lines in a and b for the VB, and average values of the three points in the CB. The offset between the spin-locked valleys in the VB is given by the fixed integral polarization P = 5 and the residual density-dependent contribution M(n). In the CB, we observe an odd-dominant sequence of gaps at all accessible electron densities, but our experiment cannot distinguish between the plotted sequence and one with the opposite shift between valleys. **e**, Energy scales in WSe_2 in the absence of carrier interactions. The cyclotron energy (red line) and total Zeeman energies in the VB and CB (green dotted lines) all scale linearly with B. The Coulomb energy (blue shaded region) is the largest energy in the system even at high density (plotted here for $2.5 \times 10^{12}\ cm^{-2} \leq n \leq 5 \times 10^{12}\ cm^{-2}$). As a result, many-body interactions are expected to significantly enhance the Zeeman effect.

The combination of a large single-particle Zeeman scale and high effective mass leads to a large Zeeman-to-cyclotron ratio, which is further enhanced by interactions even at high carrier densities. Our observed E_Z/E_N goes up to 5.8 in the VB (Fig. 2c), which is a factor of 2.6 higher than expected from a single-particle model, a factor of 2 higher than measured in multi-layer WSe_2 [1], and a factor of ~ 6 higher than in ZnO, which has the largest intrinsic E_Z/E_N reported in an engineered quantum well [2].

Future Plans

In the upcoming year, we will extend these measurements to other 2D semiconductors and improve contact techniques to improve the data near the band edges. In addition, the large measured value of E_Z/E_N, in conjunction with the high density of states, suggests the possibility that exchange interactions are strong enough to satisfy the Stoner criterion, implying potential itinerant ferromagnetism at zero magnetic field. This property, which has only recently been observed in a select few 2D materials [3, 4], would additionally be field effect tunable in the case of ML WSe2. We will search for magnetism in these materials by fabricating SQUID loops directly onto the heterostructures.

References

1. S. Xu, J. Shen, G. Long, Z. Wu, Z.-q. Bao, C.-C. Liu, X. Xiao, T. Han, J. Lin, Y. Wu, H. Lu, J. Hou, L. An, Y. Wang, Y. Cai, K. M. Ho, Y. He, R. Lortz, F. Zhang, and N. Wang, *Physical Review Letters* 118, 067702 (2017).

2. A.Tsukazaki,A.Ohtomo,M.Kawasaki,S.Akasaka,H.Yuji,K.Tamura,K.Nakahara,T.Tan- abe, A. Kamisawa, T. Gokmen, J. Shabani, and M. Shayegan, *Physical Review B* 78, 233308 (2008).

3. C. Cong, L. Li, Z. Li, H. Ji, A. Stern, Y. Xia, T. Cao, W. Bao, C. Wang, Y. Wang, Z. Q. Qui, R. J. Cava, S. G. Louie, J. Xia, and X. Zhang, *Nature* 546, 265 (2017).

4. B. Huang, G. Clark, E. Navarro-Moratalla, D. R. Klein, R. Cheng, K. L. Seyler, D. Zhong, E. Schmidgall, M. A. McGuire, D. H. Cobden, W. Yao, D. Xiao, P. Jarillo-Herrero, and X. Xu, *Nature* 546, 270 (2017).

Publications

Martin V. Gustafsson, Matthew Yankowitz, Carlos Forsythe, Daniel Rhodes, Kenji Watanabe, Takashi Taniguchi, James Hone, Xiaoyang Zhu, and Cory R. Dean, "Ambipolar Landau levels and strong band-selective carrier interactions in monolayer WSe_2", submitted.

Understanding and controlling phases with topological and charge order in the two-dimensional electron gas

Principal Investigator: Gabor Csathy
Institution: Purdue University
Address: 525 Northwestern Ave., West Lafayette, IN 47907
E-mail of PI: gcsathy@purdue.edu

Program Scope

The two-dimensional electron gas is a model system that supports a wealth of unusual ground states. Perhaps the most widely known ground states of this system are the fractional quantum Hall states. Interest in the fractional quantum Hall states is driven by their unusual property to host emergent quasiparticles, such as composite fermions. These states are under active scrutiny not only in traditional semiconductor systems, such as GaAs, but also in novel high quality electron gases hosted in graphene, ZnO, AlAs, and several other substrates.

In contrast to fractional quantum Hall states described by the free composite fermions, a small set of states harbors exotic particles with special topological properties. It is thought that certain fractional quantum Hall states have non-Abelian properties of various kinds, supporting excitations such as the Majorana particles or Fibonacci anions [a]. The study of such ground states has strongly impacted our understanding of topological physics and continues to be an active and a vibrant field of study.

Examples for non-Abelian fractional quantum Hall states are the ones at quantum numbers ν=5/2, 7/2, and 12/5. These ground states are not only of fundamental interest as they may manifest behavior not seen in any other physical system, but also may find technological utility in fault-tolerant schemes for quantum computation [b]. Many of the non-Abelian fractional quantum Hall states form in the region of the phase space commonly referred to as the second Landau level.

These exotic non-Abelian states are, however, fragile and hence they develop only under special conditions. In my labortory we pursue an experimental program targeting outstanding questions concerning the collective behavior of the correlated electronic ground states of the two-dimensional electron gas. Our primary focus is the study of the fractional quantum Hall states and exotic electronic solids. The goal of our program is to use state-of-the-art samples and incisive experimental measurement techniques to generate new insight into the nature of the exotic non-Abelian fractional quantum Hall states.

Recent Progress

Observation of a phase transition from a fractional quantum Hall state to the nematic. One current focus of our effort is the development of novel, incisive techniques probing the two-dimensional electron gas. Historically the most popular measurement technique used in investigations of this system is electronic transport. However, over the last decade or so it became increasingly clear that the probing of the new topologically ordered states requires more sophisticated techniques. Measurement of these systems at high hydrostatic pressures is one such techniques currently being used in our lab. At pressures of the order of 10,000 atmospheres one can tune many relevant quantities which are expected to impact numerous ground states.

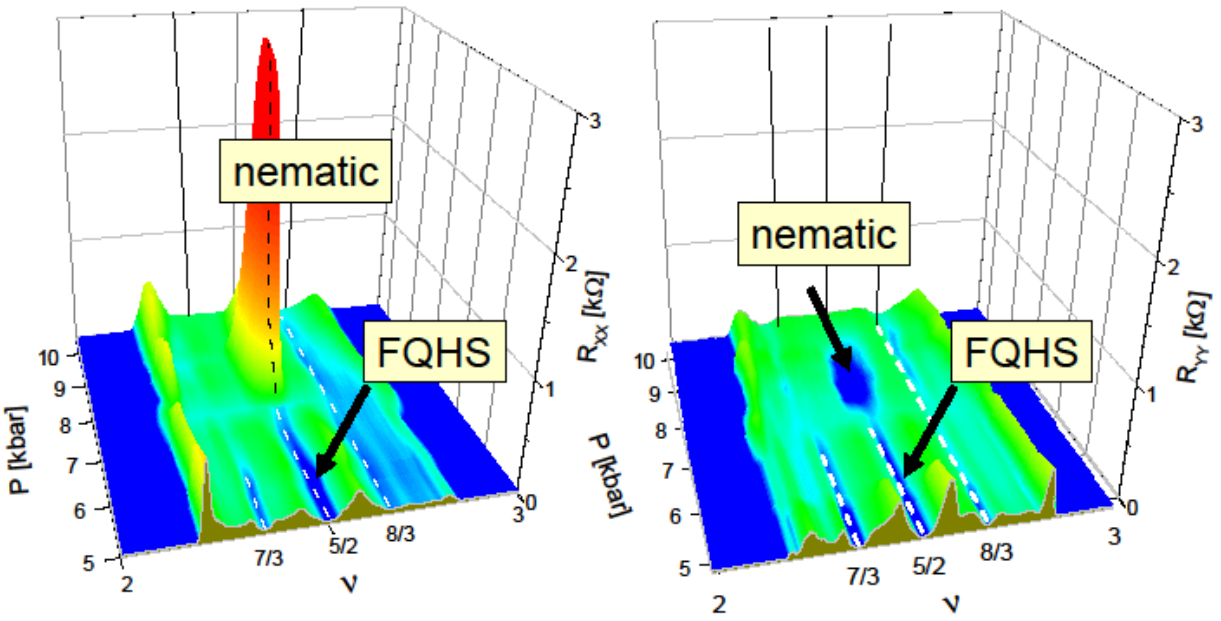

Figure 1. Magnetotransport data collected at T = 12 mK demonstrating a pressure-induced phase transition from a fractional quantum Hall state to a nematic phase in the second Landau level at ν=5/2.

As seen in Fig.1, our recent magnetotransport data revealed an unexpected phase transition from the ν=5/2 fractional quantum Hall state to the electronic nematic phase [1]. While both of these ground states were known to develop in our system, the nematic phase so far has only developed at the quantum number ν=9/2 and other higher values. Thus the stabilization of the nematic phase we observed at ν=5/2 came as a surprise. The most interesting feature of this transition from the fractional state to the nematic phase is that these two phases belong to fundamentally distinct classes of phases: the former is a topologically ordered phase while the latter is a traditional broken symmetry phase. The phase transition we found is thus a very interesting example of a rare phase transition between a topological and traditional broken symmetry phase.

We recently highlighted the importance of pairing in the phase transition from a fractional quantum Hall state to the nematic. Indeed, in our system there are about 100 known fractional quantum Hall states, but only two of these involve pairing, the ones at quantum numbers ν=5/2 and 7/2. In our recent work we showed that the fractional states involved in the phase transition towards the nematic cannot be of any kind, but they necessarily have to be paired [4]. As seen in Fig.2, pairing occurs between two composite fermions and the Cooper-pairs formed have a *p*-wave in nature [c]. Specifically, we have shown that the spontaneous pressure induced phase transition towards the nematic occurs only at ν=5/2 and ν=7/2, and not at any other quantum numbers [4].

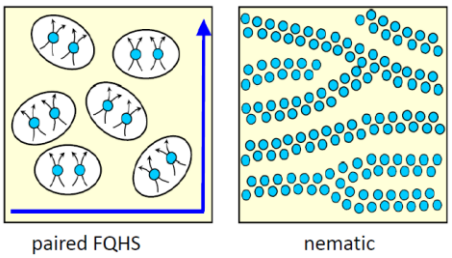

Figure 2. A representation of a paired fractional quantum Hall state (left) and of the electronic nematic phase (right panel).

Our conclusion is that pairing and nematicity are intimately linked. We found that where pairing ends, nematicity begins. This finding, we suggest, cannot be accidental, but it exposes a deep connection between the two orders. We believe that this finding is expected to have a strong impact in other strongly correlated systems in which superconductivity and nematicity strive, such as high Tc superconductors, heavy fermion systems, and certain transition metal dichalcogenides [5]. In contrast to other strongly correlated systems, the electron gas exhibits

single band physics, spin typically does not play a role, it is a very well understood system with a known Hamiltonian, and it is amenable to numerical experiments.

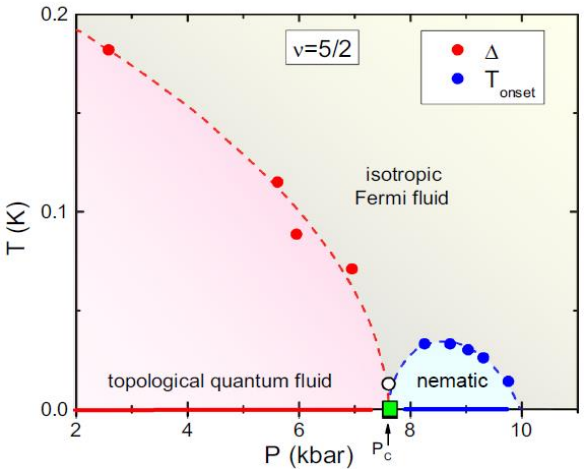

Figure 3. Stability diagram at ν=5/2 in the *P*-*T* space. The green square is a quantum critical point separating the fractional quantum Hall and nematic phases.

<u>We demonstrated that the paired-to-nematic transition is driven by the Coulomb interaction.</u> A puzzling aspect of our work is that in the three decade long history of the 5/2 fractional quantum Hall state, during which experiments were performed at ambient pressure, a transition to the nematic was not seen prior to our experiments. This leaves one with the question what is the role of the pressure in inducing the observed phase transition? We were able to specifically show that pressure in fact does not play any special role, but through its density changing effect, pressure tunes the effective electron-electron interaction away from its exact Coulomb expression.

A sustained effort in numerical simulations has shown that there are two notable parameters of the electron gas which tune the Coulomb interaction: the finite width of the quantum well *w* and the Landau level mixing parameter κ. The latter is the ratio of the Coulomb and cyclotron energies; the former is given in its dimensionless form in units of magnetic lengths l_B. If instead of plotting our data in the *P*-*T* space, shown in Fig3, we will switch to κ-w/l_B space. The information obtained from such a plot, shown in Fig.4, is particularly revealing. First, the nematic is stabilized in a region of the κ-w/l_B space that was never accessed before in samples measured at ambient pressures [4]. Second, the critical point of the transition to the nematic occurs at different pressures but at the same values of κ and w/l_B parameters for both ν=5/2 and ν=7/2. The common feature of the ν=5/2 and ν=7/2 fractional states is that they are both paired, highlighting therefore the importance of pairing and demonstrating that tuning of the electron-electron interaction is inducing the nematic [4].

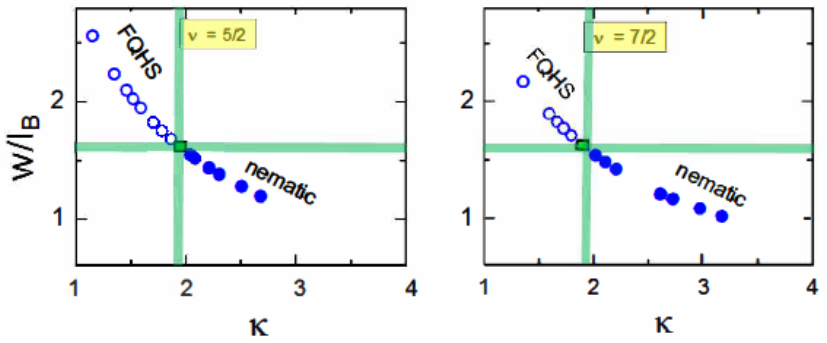

Figure 4. The evolution of the ground state at ν=5/2 (left panel) and at ν=7/2 (right panel) in the κ-w/l_B space. The transition from a fractional quantum Hall state to the nematic occurs at the same κ and w/l_B parameters, but very different pressures.

The last, most convincing evidence for the role of electron-electron interaction came from the measurement of a sample in ambient pressure, but which was engineered to have its parameters in the range for the nematic [4]. Transport measurements clearly found a nematic phase at the expected quantum number. We thus have shown that pressure is not necessary to induce the nematic. Instead, the quantity of relevance is the electron-electron interaction [4].

A particularly interesting aspect of our work is that the ν=5/2 fractional quantum Hall state can be thought of as a topological superconductor. This is because the state forms as a result of the Cooper-like pairing of the composite fermions and the edge of the sample supports topological

edge states. Owing to the spin-polarized nature of the ν=5/2 fractional quantum Hall state, the superconducting pairing symmetry is thought to be of *p*-type. Our observations can therefore be interpreted as a result of a **competition of topological superconductivity and nematicity**. We are hopeful that, due to the simplicity and cleanliness of our system we can learn new physics with potential insight on the competition of superconductivity and nematicity in other systems, such as the high temperature superconductors, transition metal dichalcogenides, and He-3 [5].

Future Plans

The existence of the quantum critical point in the paired-to-nematic transition opens up numerous questions relevant not just for the electron gas, but also in other strongly correlated materials. The Fermi sea near the critical point is likely not trivial, but a strange metal. Indeed, below the critical pressure the Fermi sea is formed of composite fermions, whereas above it by electrons. It thus will be interesting to investigate details of this Fermi sea, currently also under intense theoretical scrutiny. Furthermore, the enhanced critical fluctuations of the order parameter and gauge field near the critical point are expected to induce novel effects. We will look for such effects associated with fluctuations. We also plan thermodynamic measurements of the paired fractional quantum Hall state. Such investigations are part of our long term effort aimed at exploring unconventional collective behavior in topological systems and may lead to new insight of the behavior of related strongly correlated materials.

References

a. A. Stern, "Non-Abelian States of Matter", Nature (London) **464**, 187 (2010)

b. C. Nayak, S. Simon, A. Stern, M. Freedman, and S. Das Sarma, "Non-Abelian Anyons and Topological Quantum Computing", Review of Modern Physics. **80**, 1083 (2008)

c. G. Moore and N. Read, "Nonabelions in the Fractional Quantum Hall Effect", Nucl. Phys. B **360**, 362 (1991)

Publications

1. N. Samkharadze, K.A. Schreiber, G.C. Gardner, M.J. Manfra, E. Fradkin, and G.A. Csathy, "Observation of a Transition from a Topologically Ordered to a Spontaneously Broken Symmetry State", Nature Physics **12**, 191 (2016)

2. K.A. Schreiber, N. Samkharadze, G.C. Gardner, R.R. Biswas, M.J. Manfra, and G.A. Csathy, "Onset of Quantum Criticality in the Topological-to-Nematic Transition in a Two-dimensional Electron Gas at Filling Factor ν=5/2", Physical Review B Rapid Communication **96**, 041107 (2017)

3. Q. Qian, J. Nakamura, S. Fallahi, G.C. Gardner, J.D. Watson, S. Luscher, J.A. Folk, G.A. Csathy, and M.J. Manfra, "Quantum lifetime in ultrahigh quality GaAs quantum wells: Relationship to $\Delta_{5/2}$ and impact of density fluctuations", Physical Review B **96**, 035309 (2017)

4. K.A. Schreiber, N. Samkharadze, G.C. Gardner, Y. Lyanda-Geller, M.J. Manfra, L.N. Pfeiffer, K.W. West, and G.A. Csathy, "Electron-electron Interactions and the Paired-to-Nematic Quantum Phase Transition in the Second Landau Level", Nature Communications **9**, 2400 (2018)

5. K.A. Schreiber and G.A. Csathy, "Competition of Pairing and Nematicity in the Two-dimensional Electron Gas", editorially accepted in Annual Review of Condensed Matter Physics (2019)

6. Dohyung Ro, N. Deng, J.D. Watson, M.J. Manfra, L.N Pfeiffer, K.W. West, and G.A. Csathy, "Electron Bubbles and the Structure of the Orbital Wave Function", Physical Review B Rapid Communication **99**, 201111 (2019)

7. G.A. Csathy and J.K. Jain, "Next Level Composite Fermions", Nature Physics, News and Views Article, June (2019)

Session 3

LaCNS: Building Neutron Scattering Infrastructure in Louisiana for Advanced Materials

J. F. DiTusa[1], D. Zhang[2], R. Jin[1], J. Zhang[1], W. A. Shelton[3], V. T. John[4], R. Kumar[2], Z. Q. Mao[5], E. Nesterov[2], E. W. Plummer[1], S. W. Rick[6], G. J. Schneider[2], D. P. Young[1], I. Vekhter[1], J.W. Sun[5], W. Xei[2], J. A. Dorman[3], B. Bharti[3], M. Khonsari[7]

[1]Department of Physics and Astronomy, Louisiana State University, Baton Rouge, LA 70803
[2]Department of Chemistry, Louisiana State University, Baton Rouge, LA 70803
[3]Department of Chemical Engineering, Louisiana State University, Baton Rouge, LA 70803
[4]Dept. of Chem. and Biolmolecular Engineering, Tulane University, New Orleans, LA 70118
[5]Department of Physics and Engineering Physics, Tulane University, New Orleans, LA 70118
[6]Department of Chemistry, University of New Orleans, New Orleans, LA 70148
[7]Louisiana Board of Regents, Baton Rouge, LA 70821

Program Scope: This DOE EPSCoR / LA Board of Regents program aims to build neutron scattering infrastructure capable of treating both soft and hard materials. Our objectives include: discovery of the coupling of degrees of freedom that determine the emergent properties of complex materials, training of talented students in synthesis and neutron scattering techniques who will become the next generation of neutron users; and building a base of users of SNS and HFIR.

The scientific focus of this program is to explore emergent complex materials with guided-design of materials in mind. Our goal is to tune dominant couplings to enhance critical properties in order to derive new functionality. In the hard materials, we focus on topological magnetic and electronic materials and transition metal oxides where the coupling of electronic, magnetic, phononic, and orbital degrees of freedom lead to novel behaviors. In the soft materials we explore the role of secondary interactions in determining the structural and dynamic properties of polymeric systems.

Recent Progress

I include examples of projects that demonstrate the progress we have recently achieved that are most relevant to the ECMP research program.

According to electronic structure calculations [1], $PdSb_2$ is a candidate for hosting 6-fold-degenerate exotic fermions stabilized by a non-symmorphic symmetry. Unlike linearly dispersing Dirac and Weyl bands, the electronic structure of $PdSb_2$ displays a quadratic dispersion at the 6-fold degenerate R-point [Fig. 1b]. We have characterized the physical properties of crystalline $PdSb_2$ finding metallic behavior with indications of a Fermi-liquid ground state. Surprisingly, an unusually large transverse magneto-resistance is found that obeys Kohler's law indicating the dominance of a single band. To probe the electronic structure, we have measured the de Haas-van Alphen (dHvA) effect [Fig. 1a].

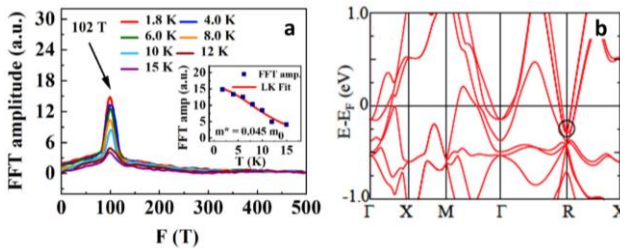

Fig. 1: $PdSb_2$ a) FFT of oscillatory Magnetization, *M*, with *H*//[111]. Inset: Mass determination. b) Electronic structure.

We identify a single band with a dHvA frequency of 102 T, and a mass of $m^* = 0.045m_0$ (m_0 is free electron mass). A Landau fan diagram yields a non-trivial Berry phase of $\Phi_{Berry} \sim 1.16\pi$, suggesting a topological nontrivial electronic structure. Remarkably, we discovered a superconducting transition for pressures, p>41 GPa. Our discovery of nearly massless electrons with nontrivial Berry phase and superconductivity identify $PdSb_2$ as unique for investigating metals with unusual topology [2].

Weyl semimetals (WSMs) evolve from Dirac semimetals in the presence of broken time-reversal symmetry (TRS) or space-inversion symmetry. Few examples of TRS-breaking WSMs have been reported. Previously, we have demonstrated a new type of magnetic semimetal $Sr_{1-y}Mn_{1-z}Sb_2$ (y; z < 0:1) with nearly massless relativistic fermion behavior (m^*=0.04-0.05m_0) and a π Berry phase [3]. This material exhibits a FM order for 304<T<565 K and a canted AFM order with a FM component for T<304 K [Fig. 2]. The combination of relativistic fermion behavior and FM in $Sr_{1-y}Mn_{1-z}Sb_2$ offers a rare interplay between relativistic fermions and spontaneous TRS breaking. Following up on this discovery, we have performed inelastic neutron scattering analyses of the spin dynamics and density functional theory (DFT) investigations of $Sr_{1-y}Mn_{1-z}Sb_2$. We observe a relatively large spin excitation gap ~8.5 meV and an interlayer magnetic exchange constant that is only 2.8% of the dominant intra-layer magnetic interaction [Fig. 2], indicating quasi-2D magnetism. DFT reveals a strong influence of the magnetic order on the electronic band structure, particularly the Dirac dispersions near the Fermi level in the presence of a FM ordering. Furthermore, Weyl dispersions coexists with the Dirac dispersions for small ferromagnetically ordered magnetic moments while they are not present for larger moment sizes. This indicates a novel interplay between the magnetic order and the electronic properties of $Sr_{1-y}Mn_{1-z}Sb_2$, and a new way to control relativistic behavior through magnetism.

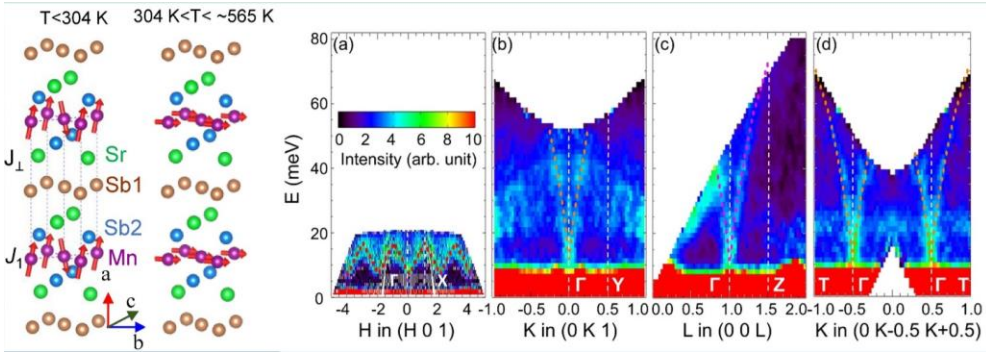

Fig. 2: Magnetic structures of $Sr_{1-y}Mn_{1-z}Sb_2$: canted AFM order T<304 K and FM order 304<T<565 K. (a) - (d) Magnetic excitations near the AFM zone center (001) at 5 K along high-symmetry directions.

Through small angle neutron scattering (SANS) measurements, we have investigated the skyrmion lattice (SKL) and helical order in $MnSi_{0.992}Ga_{0.008}$ [4]. We find that the order of the SKL is sensitive to the orientation of H with respect to the crystal lattice and to variations in the sequence of small T and H changes. The substitutional disorder is sufficient to reduce the pinning of the SKL to the underlying crystalline lattice, reducing the propensity for the SKL to be aligned with the crystal

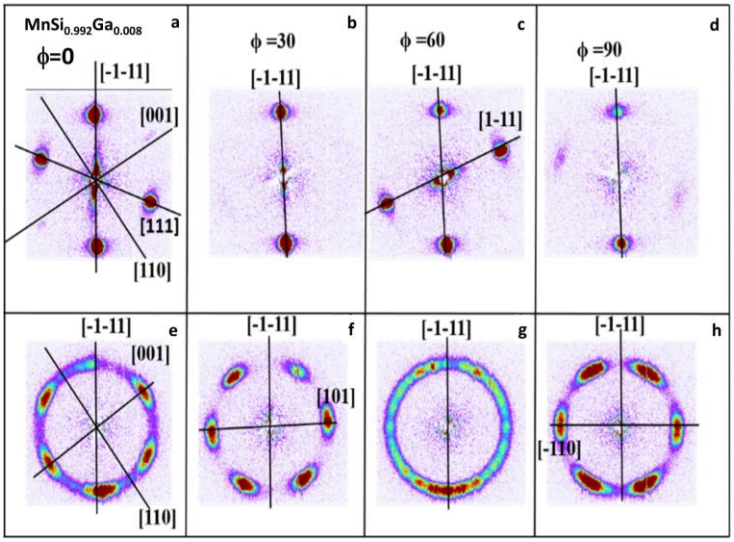

Fig. 3: Field orientation dependence of the skyrmion lattice. SANS data with $MnSi_{0.992}Ga_{0.008}$ crystal rotated about the [-1-11] axis at 32.2 K. (a) – (d) data taken at H=0. (e) – (h) Data at H=1.4 kOe, within the A-phase. In all cases H was parallel to the incident beam and the [-1-11] direction of the crystal was vertical.

lattice. This tendency is most evident when H is not well oriented with respect to the high symmetry axes of the crystal resulting in disorder in the long range SKL while maintaining sharp short-range order [Fig.3]. We have also investigated the effect of substituting heavier elements into MnSi on the reorientation process of the helical domains with field cycling in $MnSi_{0.992}Ga_{0.008}$ and $Mn_{0.985}Ir_{0.015}Si$. A comparison of the reorientation process with field reduction indicates that the presence of heavier elements creates an energy barrier for the reorientation of the helical order and for the formation of domains.

Motivated by the recent discovery of a magnetic soliton lattice in chiral and hexagonal $Cr_{1/3}NbS_2$ [5], we have explored the magnetic, thermodynamic, and charge transport properties of isostructural $Mn_{1/3}NbS_2$ [Fig. 4d]. $Mn_{1/3}NbS_2$ displays a magnetic transition at T_C=45 K with an anisotropic magnetization and a significant magnetic entropy surviving to $T << T_C$. SANS [Fig. 4a] and neutron diffraction revealed a disordered helical state with a small wave-vector parallel to the c-axis with magnetic moments lying in the ab-plane. This long period helical state is confirmed by preliminary Lorentz Force TEM at 12 K [Fig. 4c], which also displays variations in the period. The ac magnetic susceptibility [Fig. 4b and d] shows low field structure for $T<T_C$, including a sharply peaked imaginary component which subsides at low T. We observe significant temperature variation in the SANS data over the same T range. These data reveal a much richer and more dynamic magnetic behavior in $Mn_{1/3}NbS_2$ than in $Cr_{1/3}NbS_2$.

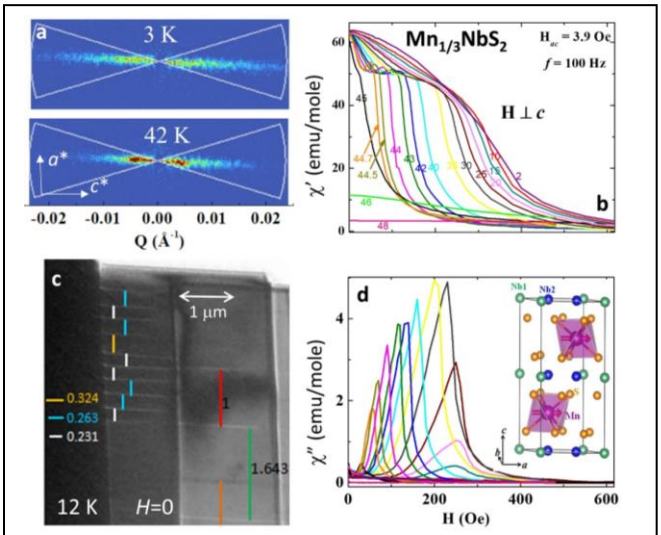

Fig. 4: $Mn_{1/3}NbS_2$: a) SANS data. b) Real part of the ac susceptibility at temperatures identified in the figure. c) LTEM image. d) Imaginary part of the ac susceptibility.

Future Plans

We will continue to develop a neutron-centric program in hard and soft materials. Several seed projects headed by assistant professors

are funded and we continue to hire young scientists that make use of neutrons in their research. The hard matter program now focuses on quantum materials including topological electronic and magnetic systems. Areas of emphasis include the synthesis and exploration of materials that are thought to host free fermionic excitations with no high-energy counterparts due to the symmetry of their crystal structures. We will explore the consequences of these particle types on the electronic structure and physical properties. Our effort to identify and characterize magnetic Weyl systems will be expanded to make use of chemical substitutions to stimulate magnetic ordering. In addition, the exploration of chiral and non-centrosymmetric magnetic materials will be extended to materials from other crystal families to explore the variety of spin textures that can be discovered and controlled. For the soft matter research, we will explore the structural and dynamic evolution of hierarchical self-assembly resulting from the complex interplay between secondary (non-covalent) interactions and primary (covalent) interactions in a reactive system.

References

[1] B. Bradlyn, J. Cano, Z. Wang, M. G. Vergniory, C. Felser, R. J. Cava, and B. A. Bernevig, *Science* **353**, aaf5037 (2016).
[2] R. Chapai, Y. Jia, W. A. Shelton, R. Nepal, M. Saghayezhian, J. F. DiTusa, E. W. Plummer, and R. Jin, *Phys. Rev. B* (*Rapid Comm*.) **99**, 161110 (2019).
[3] J. Y. Liu, J. Hu, Q. Zhang, D. Graf, H. B. Cao, S. M. A. Radmanesh, D. J. Adams, Y. L. Zhu, G. F. Cheng, X. Liu, W. A. Phelan, J. Wei, M. Jaime, F. Balakirev, D. A. Tennant, J. F. DiTusa, I. Chiorescu, L. Spinu, Z. Q. Mao. *Nature Materials* **16**, 905-910 (2017).
[4] C. Dhital, L. DeBeer-Schmitt, D. P. Young, J. F. DiTusa, *Phys. Rev. B* **99**, 024428 (2019).
[5] Y. Togawa, T. Koyama, K. Takayanagi, S. Mori, Y. Kousaka, J. Akimitsu, S. Nishihara, K. Inoue, A. S. Ovchinnikov, and J. Kishine, *Phys. Rev. Lett.* **108**, 107202 (2012).

Publications: The LaCNS program has produced 61 publications and over a dozen recent submissions since August 2017. I list five representative articles.

[1] Dhital C, DeBeer-Schmitt L, Zhang Q, Xie W, Young DP, DiTusa JF. Exploring the origins of the Dzyaloshinskii-Moriya interaction in MnSi. *Phys Rev B* **96**, 214425 (2017).
[2] Sternhagen GL, Gupta S, Zhang Y, John V, Schneider GH, Zhang D. Solution Self-Assemblies of Sequence-Defined Ionic Peptoid Block Copolymers. *J Am Chem Soc* **140**(11), 4100-4109 (2018).
[3] Chapai R, Jia Y, Shelton WA, Nepal R, Saghayezhian M, DiTusa JF, Plummer EW, Jin C, Jin R. Fermions and bosons in nonsymmorphic $PdSb_2$ with sixfold degeneracy. *Phys Rev B* **99**, 161110(R) (2019).
[4] Dhital C, DeBeer-Schmitt L, Young DP, DiTusa JF. Unpinning the skyrmion lattice in MnSi: Effect of substitutional disorder. *Phys Rev B* **99**, 024428 (2019).
[4] J. Lee, A. M. Brooks, W. A. Shelton, K. M. Bishop, B. Bharti, "Directed Propulsion of Spherical Particles Along Three Dimensional Helical Trajectories", *Nat. Commun.***10**, 2575 (2019).

Room-Temperature Topological Insulator α-Sn Thin Films - From Fundamental Physics to Applications

Mingzhong Wu, Colorado State University

Program Scope

There has been a rapidly growing interest in topological insulators (TIs) in recent years. The focus so far has been on bismuth-based compounds such as Bi_2Se_3 and Bi_2Te_3 as well as on Kondo insulators such as SmB_6, but these "conventional" TIs do not host *bona fide* topological surface states (TSS) at room temperature (RT). In this program, we will study a new TI – "α-Sn thin films" that can host TSS at RT. We will explore the spin-momentum locking and thickness dependence of the TSS, manipulation of the TSS via doping and voltage gating, sub-surface topological states, and damping enhancement in magnetic thin films interfacing with α-Sn. Following those fundamental physics studies, we will demonstrate highly efficient, RT magnetization switching using TSS in α -Sn thin films, exploring the potential applications of α-Sn. We will study (1) spin-momentum locking of TSS in α-Sn thin films, (2) thickness dependences of TSS, (3) manipulation of TSS via doping and voltage gating, (4) sub-surface topological states, (5) damping enhancement in α-Sn/magnetic insulator bilayers, and (6) TSS-driven, RT magnetization switching, among others. Under topic (1), we will investigate the helicity and strength of the spin-momentum locking in α-Sn through two different approaches – electrical transport measurements and spin-pumping measurements. The two approaches are complementary, with the first one exploring charge-to-spin conversion while the second examining the spin-to-charge conversion. Here "charge-to-spin" refers to charge current-to-spin current (conversion), while "spin-to-charge" refers to spin current-to-charge current. Under topic (2), we will study the thickness dependence of the TSS by fabricating α-Sn thin films with different thicknesses and examining how the efficiencies of charge-to-spin and spin-to-charge conversions vary with the thickness, using the above-mentioned approaches as well as spin transport measurements. This study will allow us to determine the penetration depth of the TSS. For (3), we will use two different approaches, doping and voltage gating, to tune the position of the Fermi level relative to the Dirac point and study how the Fermi level affects the properties of the TSS, including the efficiencies of the charge-to-spin and spin-to-charge conversions. For topic (4), we will study the helical spin texture of the sub-surface topological states (SSTS) and thereby confirm its non-trivial nature, determine the spin-to-charge and charge-to-spin conversion efficiencies and compare with those of the TSS, and explore the tuning of the SSTS properties via voltage gating. Under topic (5), we will examine the effects of the extension of TSS in α-Sn to an adjacent magnetic insulator (MI) thin film on the properties of the MI, including the damping and the anisotropy, through field angle- and temperature-dependent

ferromagnetic resonance measurements. Under Topic (6), we will demonstrate highly efficient, RT magnetization switching induced by bona fide TSS using α-Sn/ferromagnet layered structures. The ferromagnets to be studied will include both ferromagnetic metal and magnetic insulator thin films with perpendicular magnetic anisotropy.

Recent Progress

1. α-Sn thin films with compressive strain – sputtering growth and spin pumping

Previous work has shown that a (111)- or (001)-oriented α-Sn film is a topological insulator if it has compressive strain in the film normal direction; If the film has tensile strain, it is a material with topological surface states (TSS) on the surfaces and topological Dirac semimetal states in the bulk. We grew α-Sn films on (001) InSb substrates, and such films are expected to have compressive strain along the film normal and therefore be topological insulators. Our spin pumping measurements show that such films can cause substantial damping enhancement in a neighboring ferromagnetic film, which supports the presence of the TTS.

2. α-Sn thin films with tensile strain – sputtering growth, transport properties, and SOT switching

We also grew Sn thin films on (111)-oriented single-crystal Si substrates via sputtering. It is expected that the lattice mis-matching at the interface gives rise to tensile strain in the film normal direction, so the films are expected to host Dirac semimetal states in the bulk and TSS on the surfaces. We examined the phase of the Sn films through X-ray diffraction (XRD) measurements. Very thin films do not show any peaks for Sn, while thicker films show α-Sn (111) peaks and no β-Sn peaks, or the mixture of α-Sn and β-Sn phases. The temperature-dependent resistance measurements indicated the metallic nature of the films near the room temperature. The field-dependent longitudinal resistance and Hall resistance measurements indicated the co-existence of the bulk and surface states. Current-induced magnetization switching was demonstrated using Sn(6 nm)/Ag(2 nm)/CoFeB(2 nm) tri-layered structures.

3. Magnetization switching utilizing topological surface states

One of our goals of this project is to use topological surface states (TSS) in α-Sn topological insulators to induce magnetization switching in ferromagnets. We were not able to demonstrate this in Year 1; instead, we tried to demonstrate such switching using Bi_2Se_3 topological insulators in Year 1, which is summarized below. For the switching work described above, most likely the α-Sn thin films are topological Dirac semimetals, rather than topological insulators; this will be further explored in Year 2. Topological surface states (TSS) in a topological insulator is expected to be able to produce a spin-orbit torque that can switch a neighboring ferromagnet. This effect may be absent if the ferromagnet is conductive because it can completely suppress the TSS, but it should be present if the ferromagnet is insulating. We demonstrated TSS-induced switching in a bi-layer consisting of a topological insulator Bi_2Se_3

and an insulating ferromagnet $BaFe_{12}O_{19}$. A charge current in Bi_2Se_3 can switch the magnetization in $BaFe_{12}O_{19}$ up and down. When the magnetization is switched by a field, a current in Bi_2Se_3 can reduce the switching field by ~4000 Oe. The switching efficiency at 3 K is 300 times higher than at room temperature; it is ~30 times higher than in Pt/$BaFe_{12}O_{19}$. Such strong effects originate from the presence of more pronounced TSS at low temperatures due to enhanced surface conductivity and reduced bulk conductivity. The details about this work are provided in a manuscript which has been recently accepted for publication by Science Advances.

Future Plans

In year 2, we will modify our sample preparation processes for the realization of Sn thin films on Si substrates with pure α phase. Specifically, we will reduce the substrate temperature during the sputtering through tuning the temperature of the cooling water, reduce sputtering growth rate, and carry out lithography processes at relatively low temperatures. We will measure and compare the XRD spectra on Sn films of different thicknesses, as well as on bare Si substrates, to confirm the α phase. We expect that α-Sn films grown on Si substrates will have tensile strain along the film normal direction and will therefore be Dirac semimetals. For Sn films with α phase, we will perform extensive electrical transport measurements and explore quantum oscillation and negative magnetic resistance phenomena which have been predicted theoretically for α-Sn Dirac semimetals. We will also carry out Hall measurements and thereby analyze the properties of the carriers in α-Sn films. If time permits, we also plan to measure the band structures of α-Sn films through collaborations with Professor Andrew Wray in New York University and utilize spin-orbit coupling in α-Sn films to switch the magnetization in neighboring ferromagnetic thin films.

Publications

In Year 1, our publications on the works supported by this grant include the following:

1. "Magnetization switching utilizing topological surface states," Peng Li, James Kally, Steven S.-L. Zhang, Timothy Pillsbury, Jinjun Ding, Gyorgy Csaba, Junjia Ding, Sam Jiang, Yunzhi Liu, Robert Sinclair, Chong Bi, August DeMann, Gaurab Rimal, Wei Zhang, Stuart B. Field, Jinke Tang, Weigang Wang, Olle G. Heinonen, Valentine Novosad, Axel Hoffmann, Nitin Samarth, and Mingzhong Wu, Science Advances, accepted (2019).

2. "Effects of growth order on perpendicular magnetic anisotropy of heavy metal/ferromagnet /MgO tri-layered structures," Yuejie Zhang, Xiaofei Yang, Peng Li, Jun Ouyang, and Mingzhong Wu, IEEE Magn. Lett. 7, 1 (2019). DOI 10.1109/LMAG.2019.2914007.

3. "Room-temperature spin-to-charge conversion in sputtered bismuth selenide thin films via spin pumping from yttrium iron garnet," Mahendra DC, Tao Liu, Jun-Yang Chen, Thomas Peterson, Protyush Sahu, Hongshi Li, Zhengyang Zhao, Mingzhong Wu, and Jian-Ping Wang, Appl. Phys. Lett. 114, 102401 (2019).

Interplay of Magnetism and Superconductivity in van der Waals Heterostructures

Pablo Jarillo-Herrero, MIT

Program Scope

Magnetic phenomena are often dominated by interfaces. From magnetic tunnel junctions to magnetically-enhanced topological states, the behavior of nanoelectronic devices can be determined by just a few atomic layers. For this reason, the advent of magnetic van der Waals materials promises a revolution in our understanding of fundamental and applied magnetism. With these materials, we can stack atomically thin magnets with any other layered material, with disorder-free interfaces. This opens the way to previously impossible experiments involving coexistence of magnetism and superconductivity without disorder.

In this proposal, we will investigate how layered magnetic insulators (primarily CrI_3, $CrBr_3$, $CrCl_3$ and $RuCl_3$) can shed new light on the interplay between superconductivity and magnetism, a rich area for fundamental and applied physics. Our proposal is divided into three areas: to identify the magnetic ground states of ultrathin transition-metal halides, to study the competition between magnetism and superconductivity across the van der Waals gap, and to create new spintronic devices incorporating unconventional superconductivity.

Recent Progress

4.1 Tunneling through $CrCl_3$ tunnel barriers – Nature Physics (in press, 2019)

An urgent question in the field of 2D materials is how exfoliating van der Waals magnets to the 2D limit affects their magnetic ground state. Ultrathin magnets will be influenced by doping, local electric fields, strain, and quantum confinement effects -- a central goal of 2D magnet research is to harness these influences to stabilize new electronic states such as quantum spin liquids. An early result in this direction was the realization that ultrathin CrI_3 is an antiferromagnet (AFM) whereas bulk crystals are ferromagnetic (FM), and that this behavior can be toggled via doping in ultrathin films. However, the origin of this behavior has remained mysterious for several years.

Recently, we have developed electron tunneling as a probe of magnetism in the ultrathin limit. By tunneling through ultrathin $CrCl_3$ crystals using graphite electrodes (Fig. 1a) we can probe the magnetic state of 2D $CrCl_3$ as a function of magnetic field and temperature (Fig. 1b). To our surprise, we find that the antiferromagnetic coupling between adjacent layers of ultrathin $CrCl_3$ is 10X stronger than in bulk, reminiscent of the AFM to FM transition in CrI_3. Using polarization dependent Raman scattering, we demonstrated that the stacking structure of exfoliated films differs from the bulk crystals (Fig. 1c). Furthermore, our first principles calculations show that this different stacking structure shows much larger AFM exchange due to the different

coordination of Cr atoms along the stacking direction (Fig. 1d). We reached a similar conclusion for the stacking structure of exfoliated CrI_3. Our results have therefore solved a major open question in the burgeoning field of 2D magnetism and opened the way for strain or stacking order as a knob to control magnetic states.

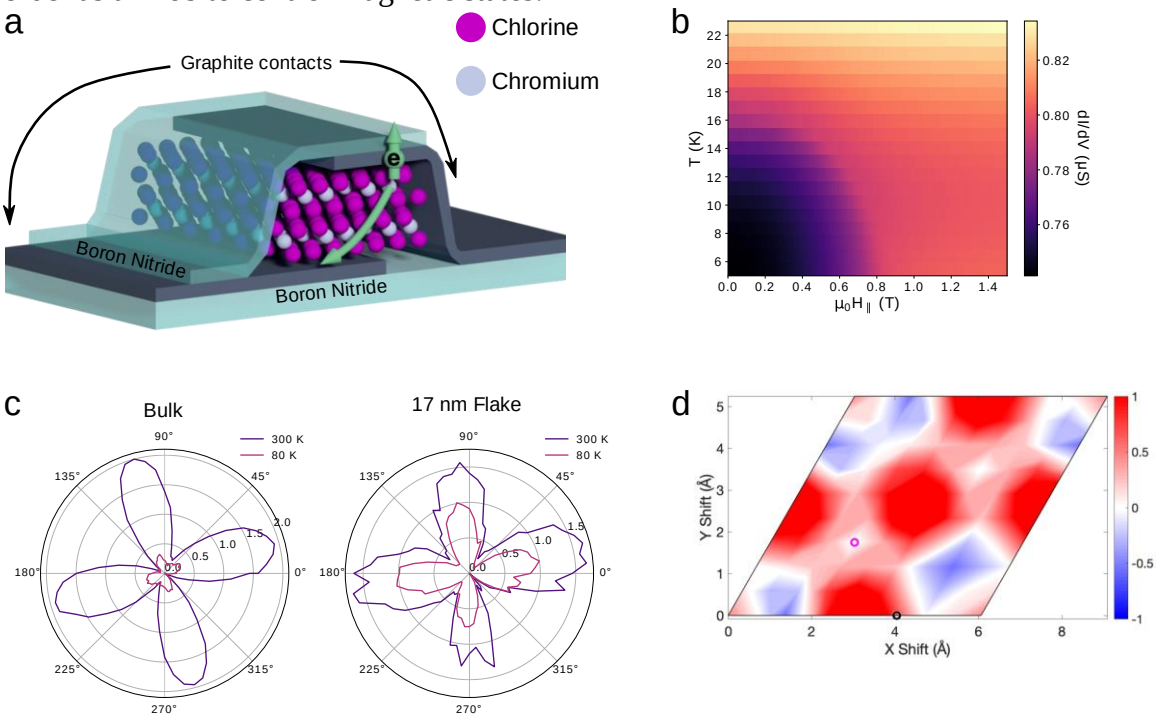

Figure 1. Tunneling through $CrCl_3$ barriers

4.2 Antiferromagnetic resonance in bulk $CrCl_3$ – Under review in PRL

Another promising feature of 2D magnets is the ability to integrate collective magnetic excitations (magnons) with nanoelectronic devices in a substrate independent way. The highly anisotropic magnetic interactions of these materials mean that bulk and ultrathin crystals have a non-trivial magnon band structure. To explore this direction, we have measured antiferromagnetic resonance (AFMR) of bulk $CrCl_3$ single crystals (Fig. 2a, b), finding that the weak interlayer coupling brings both the optical and acoustic magnon modes into the gigahertz frequency range, rather than the terahertz range for typical antiferromagnets.

By studying the magnetic field dependence of the AFMR, we have uncovered a fascinating evolution of the mode structure, where the optical and acoustic mode frequencies cross at a modest magnetic field <0.2 T (Fig. 2c). When the field is applied in the plane of the crystal this crossing is protected by symmetry leading to an accidental degeneracy. On the other hand, when there is an out-of-plane component of the applied field, the symmetry is broken and magnon-magnon coupling is induced. The hybridization gap can become larger than the dissipation rates, so that we reach the strong coupling regime. This highly tunable mode spectrum combined with device integration via mechanical exfoliation provides a unique platform to study

antiferromagnetic dynamics, including on chip cavity magnonics experiments and multi-magnon processes.

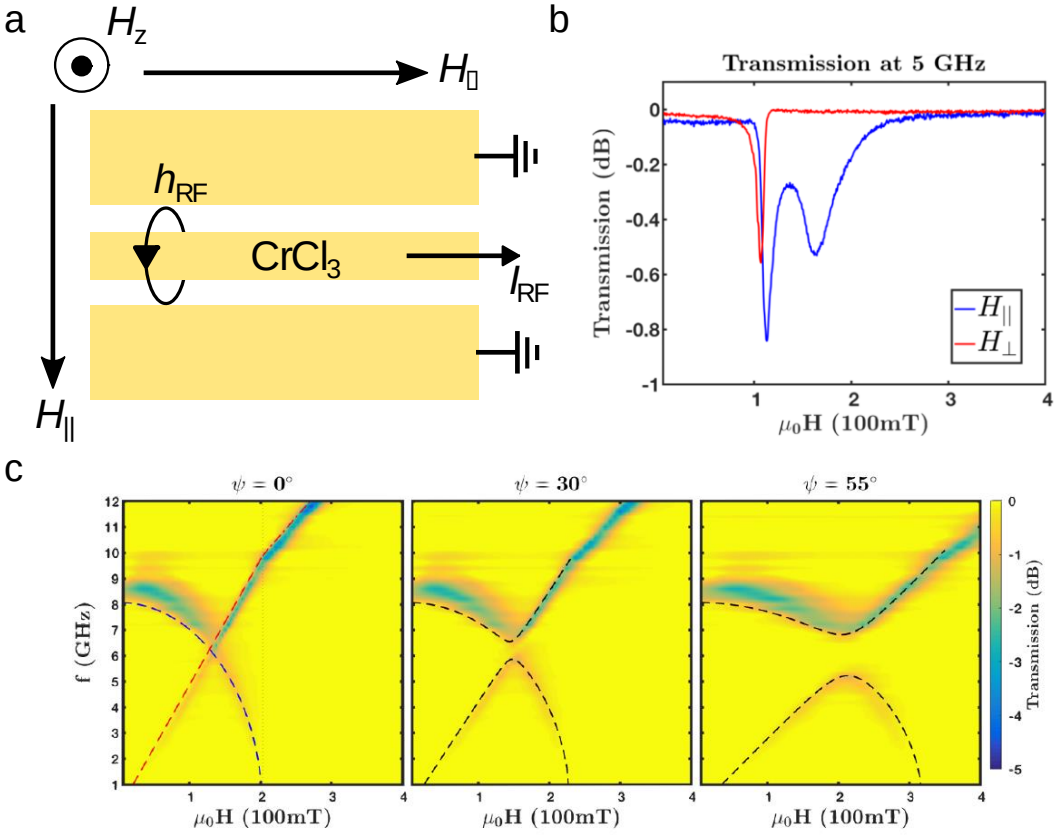

Figure 2. Antiferromagnetic resonance and mode coupling of bulk $CrCl_3$ crystals

Future Plans

Over the next two years we plan to investigate both novel 2D magnets as well as the coupling between 2D magnets and 2D superconductors. In particular, we will focus on:

1. Unconventional superconducting states induced by proximity magnetism in van der Waals heterostructures.
2. Using ultrathin ferromagnetic insulators as Josephson barriers to filter triplet Cooper pairs from spin-orbit coupled superconductors.
3. Using ultrathin ferromagnetic insulators as Josephson barriers to realize π Josephson junctions and SQUIDs.

References

Publications

1) Dahlia R. Klein*, David MacNeill*, Qian Song, Daniel T. Larson, Shiang Fang, Mingyu Xu, R. A. Ribeiro, Paul C. Canfield, Efthimios Kaxiras, Riccardo Comin, and Pablo Jarillo-Herrero, *"Giant enhancement of*

interlayer exchange in an ultrathin 2D magnet"
Nature Physics (in press, 2019); arXiv:1903.00002 (2019)

2) David MacNeill, Justin T. Hou, Dahlia R. Klein, Pengxiang Zhang, Pablo Jarillo-Herrero, Luqiao Liu, *"Gigahertz frequency antiferromagnetic resonance and strong magnon-magnon coupling in the layered crystal CrCl3"*
Phys. Rev. Lett. **123**, 047204 (2019)

Project Title: **Spin Dynamics and Magnonic Spin Transport in Antiferromagnetic Heterostructures at High Frequencies up to 360 GHz**

Principle Investigator: **Fengyuan Yang**
Mailing Address: Department of Physics, The Ohio State University, Columbus, OH 43210

Project Scope:

This goal of this DOE project is to generate, detect, and understand antiferromagnetic (AF) excitations and dynamic spin transport in heterostructures that comprise AFs, ferromagnets (FM), and nonmagnetic (NM) materials within a broad range of microwave frequencies. The ability to drive and manipulate spin currents in these heterostructures is critical for the spintronics field, where the spin currents can be carried either by spin-polarized electrons in conducting materials or by magnons in magnetic conductors and insulators. The transfer and manipulation of spin angular momentum in heterostructures offer the promises of energy efficient, high frequency, and new paradigms of spin-electronic devices. Recently, AFs have become a new focus of the spintronics field where the AFs are the active components in spin transport. AF insulators (AFI) are especially desirable for dynamic spin transport because of their abundance with a broad range of properties, their high resonance frequencies up to THz for high speed operations, and efficient spin conversion at interfaces between AFs and other materials. This DOE project has the following goals: 1) achieve high efficiency spin pumping in $Y_3Fe_5O_{12}$ (YIG)/Pt bilayers up to 360 GHz; 2) characterize AF resonance in AF insulator films at high frequencies at various temperatures; and 3) investigate dynamic spin transport in YIG/AF/Pt trilayers to understand spin conduction in AF films as a function of excitation frequency, temperature, and AF film thickness.

In the past several months, under primary support of this DOE project, the PI's group has made several exciting discoveries in spin dynamics and spin manipulation in AF heterostructures, including magnetic proximity effect induced in Pt on AF insulator α-Fe_2O_3 epitaxial films [1], electrical switching of tri-state AF Néel Order in Pt/α-Fe_2O_3 bilayers [2], and spin-textures detected by topological Hall effect in Pt/Cr_2O_3 bilayers where Cr_2O_3 is an AF insulator [3]. This abstract will focus on the AF proximity effect and electrical switching in Pt/α-Fe_2O_3 bilayers.

Recent Progress

1. AF-Induced Magnetization in Pt/α-Fe_2O_3 Bilayers: Antiferromagnetic Proximity Effect

Magnetic proximity effect is a fundamentally important phenomenon with potential for spintronic applications. However, to date, MPE has only been conclusively observed in nonmagnetic materials on FMs. We grow epitaxial α-Fe_2O_3 films on Al_2O_3 substrates, both with hexagonal structure (Fig. 1a), using off-axis sputtering. The α-Fe_2O_3 films exhibit high crystal quality (Figs. 1b and 1c) as verified by scanning transmission electron microscopy (STEM). Transport measurement on a Pt(2 nm)/α-Fe_2O_3(30 nm) bilayer reveal anomalous Hall effect (AHE) at 10 K, which disappears above 100 K, suggesting magnetization in Pt. To further confirm the MPE and understand its mechanism, we measure the angular dependent magnetoresistance (ADMR) in Pt/α-Fe_2O_3 bilayers by performing the complete set of ADMR

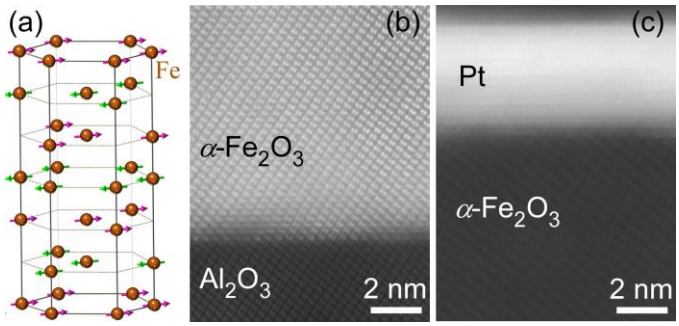

Fig. 1. (a) Schematic of the α-Fe_2O_3 lattice with FM-aligned Fe moment in the *ab*-plane and AF coupling between adjacent *ab*-planes. STEM images of a Pt(2 nm)/α-Fe_2O_3(30 nm) bilayer on Al_2O_3(0001) showing the (b) Fe_2O_3/Al_2O_3 and (c) Pt/Fe_2O_3 interface.

measurements in the *xy* (α-scan), *yz* (β-scan), and *zx* (γ-scan) planes. The ADMR measurements from all three principal planes can clearly distinguish various contributions, including spin Hall magnetoresistance (SMR), anisotropic magnetoresistance (AMR), and ordinary magnetoresistance. Our ADMR results provide strong evidence for the existence of MPE in Pt/α-Fe_2O_3 bilayers. In addition, we use a macrospin response model to describe AF spins in α-Fe_2O_3 by modeling the Néel order in α-Fe_2O_3 and MPE-induced moment in Pt, and the competition between the spin-flop transition and the anisotropies in α-Fe_2O_3, which successfully reproduces the main features arising from the MPE and SMR. A manuscript about this work is currently under review [1].

2. Reliable Electrical Switching of Tri-State AF Néel Order in α-Fe_2O_3 Epitaxial Films

The ability to manipulate AF spins is a key requirement for the field of AF spintronics. Spin-orbit torque (SOT) induced switching of FMs by an adjacent heavy metal (HM) has raised wide interests in recent years where a charge current in the HM generates spins at the HM/FM interface via the spin Hall effect (SHE). It has been predicted that Néel SOT can be utilized to switch AF spins, paving the way for THz oscillators and other devices. For AFIs, the switching of Néel order can be achieved in HM/AFI bilayers by damping-like SOT. Electrical switching of bi-state AF spins has been demonstrated in metallic AFs. Recently, current-induced "saw-tooth"-shaped Hall resistance was reported in Pt/NiO bilayers [4], while its mechanism is under debate.

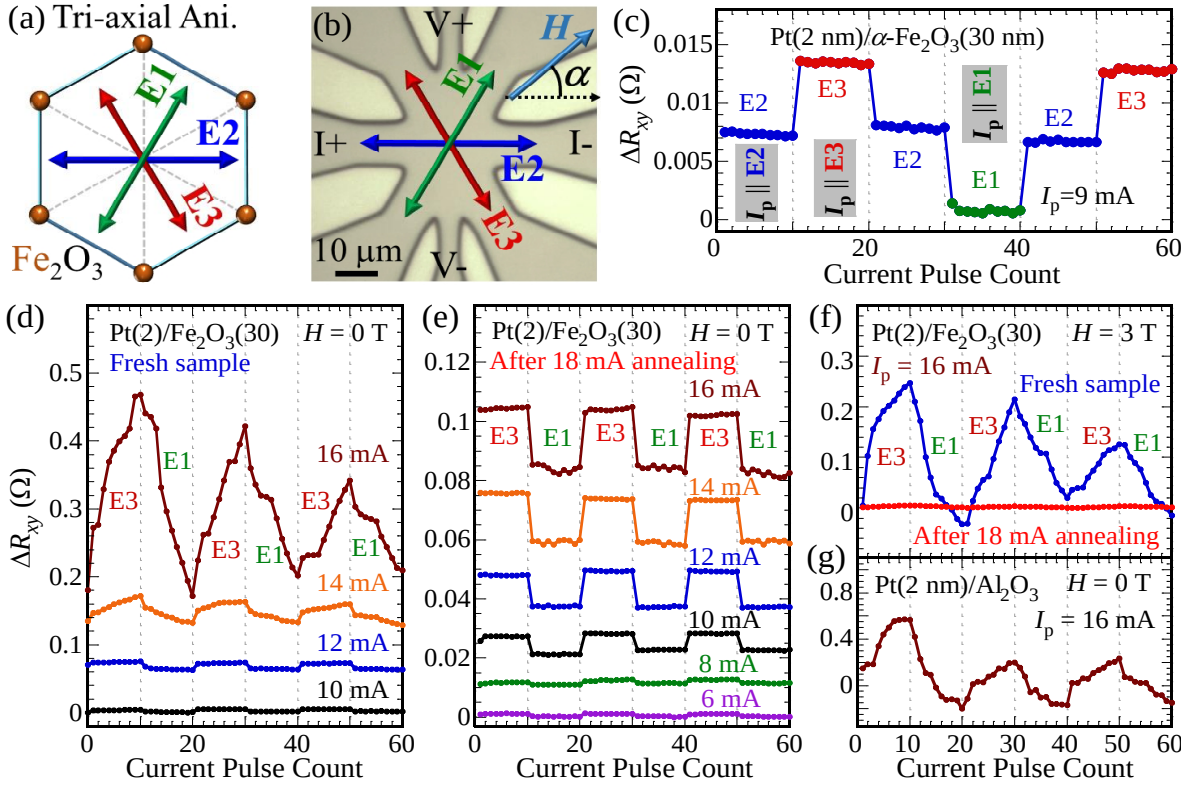

Fig. 2. (a) The *ab*-plane of α-Fe_2O_3 lattice with three in-plane easy axes, E1, E2 and E3, resulting in a tri-axial anisotropy. (b) Optical image of an eight-leg Hall cross of a Pt(2 nm)/α-Fe_2O_3(30 nm) bilayer. (c) A sequential pulse current of I_p = 9 mA is applied along one of the three easy axes (10 pulses for each segment) at 300 K and a reversible control of tri-state Hall resistance $\triangle R_{xy}$ is detected by applying a 0.1 mA sensing current along E2. (d) Evolution of $\triangle R_{xy}$ when $\boldsymbol{I_p}$ is switched between E3 and E1 at H = 0 T for a fresh Pt/α-Fe_2O_3 bilayer at 300 K. (e) Pulse current dependence of $\triangle R_{xy}$ for a Pt/α-Fe_2O_3 bilayer at 300 K after 18 mA annealing. (f) $\triangle R_{xy}$ for a fresh bilayer and the same sample after 18 mA annealing at I_p = 16 mA in a 3 T in-plane field. (g) $\triangle R_{xy}$ for a 2 nm Pt layer directly grown on Al_2O_3(001).

We show the first demonstration of step-like electrical switching of tri-state Néel order in Pt/α-Fe_2O_3 bilayers, which is explained by Monte-Carlo simulations. Figure 2a shows the *ab*-plane of α-Fe_2O_3 hexagonal lattice with three in-plane easy axes. We pattern our Pt(2 nm)/α-Fe_2O_3(30nm) bilayers into 8-leg Hall crosses (Fig. 2b) for electrical switching and Hall detection.

Figure 2c shows ΔR_{xy} as a pulse current $\boldsymbol{I}_p$ = 9 mA is switched from **E2**→**E3**→**E2**→**E1**→**E2** at zero field, which exhibits clean, step-like, tri-state ΔR_{xy} at $\boldsymbol{I}_p \parallel$ **E1** (low), $\boldsymbol{I}_p \parallel$ **E2** (intermediate), and $\boldsymbol{I}_p \parallel$ **E3** (high). This switching behavior can be understood as follows: 1) when $\boldsymbol{I}_p$ is applied along an easy axes, the SOT rotates the Néel order $\boldsymbol{n}$ to align with $\boldsymbol{I}_p$, 2) a small sensing current is sent along **E2** and a spin-Hall induced anomalous Hall effect (SH-AHE) voltage is measured, which reflects the orientation of $\boldsymbol{n}$, 3) after the first pulse, the subsequent 9 pulses cause essentially no change in $\boldsymbol{n}$, resulting in a plateau, indicating single-pulse saturation of $\boldsymbol{n}$, which is distinct from previous reports in Pt/NiO bilayers with "saw-tooth"-shaped ΔR_{xy}, 4) as $\boldsymbol{I}_p$ is changed to a new easy axis, $\boldsymbol{n}$ aligns with the new direction of $\boldsymbol{I}_p$, leading to a step-jump of ΔR_{xy} to a new value.

Figure 2d shows the I_p dependence of Pt(2 nm)/α-Fe_2O_3(30 nm) bilayers by applying $\boldsymbol{I}_p$ along E1 and E3 at zero field. As I_p increases, ΔR_{xy} changes from step-like switching to "saw-tooth"-shaped switching. At I_p = 16 mA, there is a clear decay of ΔR_{xy} after several cycles of pulses, which has been observed in other HM/AFI systems and attributed to the decrease of switching efficiency. Next, we apply a high pulse current of 18 mA to anneal the Pt layer and then redo the measurement at I_p = 6 to 16 mA (Fig. 2e). For the whole current range, ΔR_{xy} exhibits step-like switching with high stability and no detectable decay. The onset of switching occurs at I_p = 6 mA or $j = 3.0 \times 10^7$ A/cm^2, comparable to the values for typical HM/FM systems. From Fig. 2e, we extract a linear dependence of ΔR_{xy} vs. I_p, indicating that the SOT responsible for the AF switching is linearly proportional to the SHE-generated spin accumulation at the Pt/α-Fe_2O_3 interface.

Since an in-plane magnetic field can induce spin-flop transition and align $\boldsymbol{n}$ along $\boldsymbol{n} \perp \boldsymbol{H}$, the application of $\boldsymbol{H}$ should be able to "freeze" the AF spins. Figure 2f shows the comparison of ΔR_{xy} between H = 0 and 3 T at I_p = 16 mA. For I_p = 16 mA, there is essentially no difference between the 0 and 3 T curves, while the 3 T field turns the step-like ΔR_{xy} at 0 T into a flat line. This suggests that only the step-like switching is the real SOT-induced switching while the "saw-tooth" feature has a different origin. To reveal the origin of the "saw-tooth" feature, we show in Fig. 2g the switching measurement for a Pt(2 nm) film directly deposited on Al_2O_3, which displays the "saw-tooth"-shaped $\triangle R_{xy}$. This indicates that the "saw-tooth" feature of $\triangle R_{xy}$ is due to the current-driven migration of grain boundaries in thin Pt layers. This indisputably proves that the "saw-tooth" feature is indeed an artifact due to Pt and not related to the AF switching, while the actual AF switching can be confirmed through the detection of single-pulse saturation, step-like Hall resistance. Our results point to a promising path toward controlling the AF spins in insulating AFs using spin-orbit torque. A manuscript about this work is currently under review [2].

Future Plans

For the coming year, this DOE project will focus on two related sub-projects: 1) high frequency spin dynamics and spin transport studies of YIG/AF/NM systems with various AF insulators using the OSU magnetic resonance spectrometer with frequencies up to 360 GHz, which is expected to be commissioned in August, 2019; and 2) electrical manipulation and detection of AF spins in AF insulator based heterostructures. The goal is to reveal magnonic spin transport and spin-torque control of AF spins in various AF insulator systems.

References:

1. Y. Cheng, S. S. Yu, A. S. Ahmed, M. L. Zhu, J. Hwang and F. Y. Yang, "Anisotropic Magnetoresistance and Nontrivial Spin Magnetoresistance in Pt/α-Fe_2O_3 Bilayers: Evidence

for Antiferromagnetic Proximity Effect," *arXiv:1906.04395* (2019).
2. Y. Cheng, S.S. Yu, M.L. Zhu, J. Hwang and F.Y. Yang, "Reliable Electrical Switching of Tri-State Antiferromagnetic Néel Order in α-Fe_2O_3 Epitaxial Films," *arXiv:1906.04694* (2019).
3. Y. Cheng, S. S. Yu, M. L. Zhu, J. Hwang and F. Y. Yang, "Topological Hall Effect in Pt/Antiferromagnetic-Insulator Bilayers," *Submitted* (2019).
4. X. Z. Chen, R. Zarzuela, J. Zhang, C. Song, X. F. Zhou, G. Y. Shi, F. Li, H. A. Zhou, W. J. Jiang, F. Pan and Y. Tserkovnyak, "Antidamping-Torque-Induced Switching in Biaxial Antiferromagnetic Insulators," *Phys. Rev. Lett.* **120**, 207204 (2018).

Publications supported by this DOE grant (2017 – 2019)

1. Y. Cheng, S. S. Yu, A. S. Ahmed, M. L. Zhu, J. Hwang and F. Y. Yang, "Anisotropic Magnetoresistance and Nontrivial Spin Magnetoresistance in Pt/α-Fe_2O_3 Bilayers: Evidence for Antiferromagnetic Proximity Effect," *arXiv:1906.04395* (2019).
2. Y. Cheng, S.S. Yu, M.L. Zhu, J. Hwang and F.Y. Yang, "Reliable Electrical Switching of Tri-State Antiferromagnetic Néel Order in α-Fe_2O_3 Epitaxial Films," *arXiv:1906.04694* (2019).
3. Y. Cheng, S. S. Yu, M. L. Zhu, J. Hwang and F. Y. Yang, "Topological Hall Effect in Pt/Antiferromagnetic-Insulator Bilayers," *Submitted* (2019).
4. H.L. Wang, K.Y. Meng, P.X. Zhang, J.T. Hou, J. Finley, J.H. Han, F.Y. Yang, L.Q. Liu, "Large spin-orbit torque observed in epitaxial $SrIrO_3$ thin films," *Appl. Phys. Lett.* **114**, 232406 (2019).
5. A. J. Lee, A. S. Ahmed, S. D. Guo, B. D. Esser, D. W. McComb, F. Y. Yang, "Epitaxial $Co_{50}Fe_{50}$(110)/Pt(111) Films on $MgAl_2O_4$(001) and its Enhancement of Perpendicular Magnetic Anisotropy," *J. Appl. Phys.* **125**, 183903 (2019).
6. K.-Y. Meng, A. S. Ahmed, M. Baćani, A.-O. Mandru, X. Zhao, N. Bagués, B. D. Esser, J. Flores, D. W. McComb, H. J. Hug, and F. Y. Yang, "Observation of Nanoscale Skyrmions in $SrIrO_3$/$SrRuO_3$ Bilayers," *Nano Lett.* **19**, 3169 (2019).
7. Y. Cheng, R. Zarzuela, J.T. Brangham, A.J. Lee, S. White, P.C. Hammel, Y. Tserkovnyak, F. Y. Yang, "Non-sinusoidal angular dependence of FMR-driven spin current across an antiferromagnet in $Y_3Fe_5O_{12}$/NiO/Pt trilayers," *Phys. Rev. B Rapid Comm* **99**, 060405 (2019).
8. F. Y. Yang and P. C. Hammel, "Topical review: FMR-Driven Spin Pumping in $Y_3Fe_5O_{12}$-Based Structures," *J. Phys. D: Appl. Phys*. **51**, 253001 (2018).
9. W. T. Ruane, S. P. White, J. T. Brangham, K. Y. Meng, D. V. Pelekhov, F. Y. Yang, P. C. Hammel, "Controlling and patterning the effective magnetization in $Y_3Fe_5O_{12}$ thin films using ion irradiation," *AIP Adv*. **8**, 056007 (2018).
10. A. Prakash, B. Flebus, J. Brangham, F. Y. Yang, Y. Tserkovnyak, and J. P. Heremans, "Evidence for the role of the magnon energy relaxation length in the spin Seebeck effect," *Phys. Rev. B* **97**, 020408(R) (2018).
11. S. Singh, J. Katoch, T. C. Zhu, K. Y. Meng, T. Y. Liu, J. T. Brangham, F. Y. Yang, M. Flatté, R. Kawakami. "Strong modulation of spin currents in bilayer graphene by static and fluctuating proximity exchange fields," *Phys. Rev. Lett.* **118**, 187201 (2017).
12. H. L. Wang, C. H. Du, P. C. Hammel and F. Y. Yang, "Comparative determination of $Y_3Fe_5O_{12}$/Pt interfacial spin mixing conductance by spin-Hall magnetoresistance and spin pumping," *Appl. Phys. Lett.* **110**, 062402 (2017).
13. J. Kimling, G.-M. Choi, J. T. Brangham, T. Matalla-Wagner, T. Huebner, T. Kuschel, F. Y. Yang, and D. G. Cahill, "Picosecond spin Seebeck effect," *Phys. Rev. Lett.* **118**, 057201 (2017).
14. J.C. Gallagher, K.Y. Meng, J. Brangham, H.L. Wang, B.D. Esser, D.W. McComb, and F.Y. Yang, "Robust Zero-Field Skyrmion Formation in FeGe Epitaxial Thin Films," *Phys. Rev. Lett.* **118**, 027201 (2017).

Effects of Lateral Broken Crystal Symmetries on Spin-Orbit Torques and Magnetic Anisotropy

Daniel C. Ralph, Cornell University

Program Scope

The goals of this program are to investigate new physical effects that can be enabled in multilayer magnetic structures by introducing forms of broken structural symmetry beyond that provided by a planar interface. By coupling a magnetic layer to a low-symmetry crystalline material possessing strong spin-orbit coupling it is possible to realize qualitatively-new strategies for controlling both the static magnetic orientation and the direction of current-induced spin-orbit torques. We are working to achieve a fundamental understanding of the mechanisms for these effects and to learn what materials and structures can be used to make them as strong as possible. The project consists of three lines of research:

(A) To investigate the use of lateral broken symmetries to control the direction and strength of current-induced spin-orbit torques.

(B) To investigate the use of lateral broken symmetries to generate strong in-plane uniaxial magnetic anisotropy to stabilize in-plane-oriented magnetic configurations.

(C) To investigate whether ferroelectric switching can be used to dynamically change the orientation of lateral broken symmetries in magnetic multilayers.

Recent Progress

Background: This program aims to investigate fundamental physics questions related to a practical application: What is the most efficient mechanism to achieve electrical control over the orientation of ferromagnetism, for example in magnetic random access memory (MRAM) devices? The mechanism currently in use is spin-transfer torque from a spin-polarized current. "STT-MRAM" devices using this mechanism are attractive for their non-volatility, infinite endurance, and good speed. They have been commercialized successfully and recently began to be offered as an option by several major semiconductor foundries. However, the efficiency of STT-MRAM has a fundamental quantum limit – the torque cannot be more efficient than 1 unit of $\hbar/2$ angular momentum transferred per unit charge in the current, requiring relatively large costs in current and energy. A possible alternative, current-induced spin-orbit torques, offer the promise of much more efficient magnetic manipulation because each electron can transfer angular momentum to the magnet many times, not just once. But there is a challenge in using spin-orbit torques in applications. To achieve thermally-stable high-spatial-density MRAM it is

necessary to use magnetic materials with a strong magnetic anisotropy perpendicular to the sample plane, and to switch such materials efficiently using spin-transfer torque requires that the spins also have a strong component perpendicular to the plane. (Technically, an out-of-plane antidamping spin torque is needed.) Unfortunately, most of the materials that have been used to study spin-orbit torques previously have crystal structures for which symmetry arguments require that the generated spins must be rigorously in the sample plane. The main goal of this research program is to understand physics that might provide a solution to this problem -- by studying low-symmetry spin-orbit materials that might be able to generate a strong spin current with out-of-plane spins or/and to provide a strong enough in-plane magnetic anisotropy to stabilize nanoscale magnets against thermal fluctuations.

In the two years of this program we have completed a study of the symmetries of spin-orbit torques and magnetic anisotropies generated by four different low-symmetry transition-metal dichalcogenide (TMD) materials: WTe_2, strained $NbSe_2$, $TaTe_2$, and $MoTe_2$. (Measurements on the first two materials were begun before the start of the DOE grant; the experiments under the latter two were done entirely under this DOE funding with additional comparisons to the first two.) These materials all have distinct low-symmetry bulk crystal structures, and exfoliation allows the preparation of flat single crystals.

The project required the optimization of ways to integrate a magnetic layer (we use the magnetic alloy $Ni_{80}Fe_{20}$ = Permalloy) with the air-sensitive TMD materials without damaging the crystal symmetry of the interface. We do this by exfoliating the TMD materials within the load-lock of our sputter system, and then depositing the Permalloy at a glancing angle onto the newly-exposed interface without breaking vacuum. Figure 1 shows that when this is done carefully, the TMD layer at the interface can remain well-ordered.

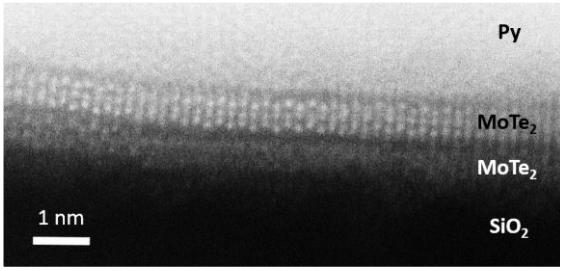

Fig. 1. Cross-section STEM image of a clean interface between bilayer $MoTe_2$ and Permalloy.

The deposition of the Permalloy protects the TMD layers from further air exposure, so that the samples can then be removed from the vacuum system and processed by optical lithography and ion milling to make samples for measurement. To measure spin-orbit torques we used two independent techniques to guard against artifacts: spin-torque ferromagnetic resonance (ST-FMR) and 2nd-harmonic Hall measurements. By measuring the resulting signals as a function of the angle of an applied magnetic field, we can reliably determine all possible components of torque and also measure the magnetic anisotropy. Measurements are performed for a dozen or more samples for each TMD material, with different TMD thicknesses and different angles between the applied current at the crystal lattice. Figure 2 shows results from ST-FMR measurements on a low-crystal-symmetry $MoTe_2$/Permalloy sample, with a comparison to a high-symmetry Pt/Permalloy sample. The antisymmetric ST-FMR component, V_A, for the

$MoTe_2$/Permalloy sample has a dependence on magnetic-field angle that is distinctly different from all of the other components shown in Fig. 2. This difference provides a quantitative measurement of a non-zero out-of-plane antidamping torque.

The primary results of our comparisons between WTe_2, strained $NbSe_2$, $TaTe_2$, and $MoTe_2$ are the following:

- The out-of-plane antidamping torques desired for applications are present for WTe_2 and β-$MoTe_2$,[1] but not $TaTe_2$ or strained $NbSe_2$. These torques go to zero when the current is applied parallel to a mirror plane, as required by symmetry. They persist down to monolayer TMD thickness, and have a weak thickness dependence suggestive of an interfacial mechanism for the torque, except that the torque can be much weaker for bilayer-TMD samples than for other thicknesses for reasons not understood.[1] The strength of the out-of-plane antidamping torque is about 50% of conventional spin-orbit torque in WTe_2 and about 15% in $MoTe_2$, with a maximum spin-torque ratio of 0.013. So far, this is about 5x too weak to be useful for switching 3D magnetic materials in practical applications.
- In addition, there are "field-like" torque components originating from current-induced out-of-plane spins in $MoTe_2$ and strained $NbSe_2$, but not WTe_2 or $TaTe_2$.[1] The same symmetry constraints apply to both these field-like torques and the out-of-plane antidamping torques, so it is puzzling why one torque component is present and not the other in WTe_2 and strained $NbSe_2$, with the two materials exhibiting opposite behaviors.
- Finally, a third component of unusual current-induced torque, with Dresselhaus symmetry, is present in all of the materials with a strong resistance anisotropy (WTe_2, $TaTe_2$, and $MoTe_2$).[2] We have proposed that this is not due to a spin-orbit torque, but arises from transverse current loops associated with the resistance anisotropy.

These results represent an extensive data set with a number of surprising and clearly-defined puzzles. We do not yet have a microscopic model to understand the different components of spin-orbit torque measured in the different materials, and why the out-of-plane antidamping torque is suppressed in two-layer samples of WTe_2 and $MoTe_2$. The differences must be due to microscopic factors like the nature of the

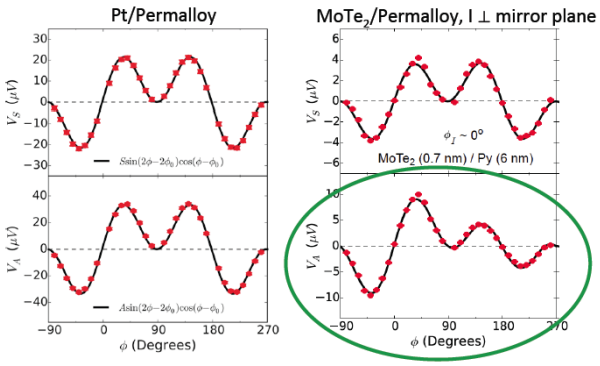

Fig. 2. Comparison of the magnitude of the symmetric (V_S) and antisymmetric (V_A) components of ST-FMR resonances as a function of magnetic field angle for high-symmetry Pt/Permalloy and low-symmetry $MoTe_2$/Permalloy. The distorted field dependence at the bottom right is due to a non-zero out-of-plane antidamping torque.

atomic orbitals that contribute to charge and spin transport, local atomic point-group symmetries, or perhaps the interface transparency between the spin-orbit material and the ferromagnet. We have begun collaborations with the group of Craig Fennie (Cornell) and Paul Haney (NIST) to try to understand these data sets using first-principles techniques.

As a side project, in the last year we have also experimented with using the same vacuum-exfoliation + sputter coating techniques we developed for TMD/Permalloy samples in order to make samples incorporating recently-discovered 2D van der Waals magnets. We have been able to deposit the spin-orbit metals Ta and Pt onto the 2D magnet $Cr_2Ge_2Te_6$ with no visible damage to the 2D layer, and have demonstrated that the magnetic state of the 2D magnet can be read out both electrically using anomalous Hall effect measurements and optically using magnetic circular dichroism (with good consistency). Furthermore, we have measured that spin-orbit torque from the heavy metals can generate magnetic switching of the $Cr_2Ge_2Te_6$ with world-record low current densities for current-controlled switching.

Future Plans

The TMD materials we have reported so far exhibit the desired out-of-plane antidamping torques (in WTe_2 and $MoTe_2$), but these torques are not yet strong enough to be interesting for applications. The lateral symmetry breaking that gives rise to this torque is also relatively weak in these materials, though. To investigate strategies that might allow stronger torques, we have begun experimenting with the incorporation of ferroelectric materials into magnetic multilayers, to make use of the strong ferroelectric polarization vector as the source of lateral symmetry breaking. We have measurements underway on samples made on $BaTiO_3$ substrates with a fixed in-plane polarization vector and $BiFeO_3$ thin films (provided by the group of Ramamoorthy Ramesh, UC Berkeley) in which the lateral component of the polarization should be switchable by applying an out-of-plane electric field.

We also plan in the next year to perform additional experiments on the recently discovered 2D magnets, with a focus on studying spin-orbit switching in these materials using spin-orbit torque from the TMD materials studied previously under this grant.

Publications/References

1. Gregory M. Stiehl, David MacNeill, Nikhil Sivadas, Ismail El Baggari, Marcos H. D. Guimaraes, Neal D. Reynolds, Lena F. Kourkoutis, Craig Fennie, Robert A. Buhrman, and Daniel C. Ralph, “Current-Induced Torques with Dresselhaus Symmetry Due to Resistance Anisotropy," *ACS Nano* **13**, 2599–2605 (2019).

2. Gregory M. Stiehl, Ruofan Li, Vishakha Gupta, Ismail El Baggari, Shengwei Jiang, Hongchao Xie, Lena F. Kourkoutis, Kin Fai Mak, Jie Shan, Robert A. Buhrman, and Daniel C. Ralph, “Layer-dependent spin-orbit torques generated by the centrosymmetric transition metal dichalcogenide β-$MoTe_2$,” arXiv:1906.01068 (in review).

Oxide Quantum Heterostructures

PI: Ho Nyung Lee
Co-PIs: Matthew Brahlek, Gyula Eres, Christopher Rouleau, T. Zac Ward,

Oak Ridge National Laboratory

Program Scope

The overarching goal of this project is to understand, control, and exploit the electronic, magnetic, and structural interactions of oxide quantum heterostructures through interfacial coupling. To address this goal, we will focus on the following specific aims: (1) Exploit spin orbit coupling and lattice symmetry to develop oxide heterostructures with novel quantum phenomena, (2) Create novel electronic ground states by interfacial charge transfer and orbital coupling, and (3) Understand strain coupling to develop novel ferroic quantum materials. Particular topical emphasis will be on studying the spin orbit coupling, Dzyaloshinskii-Moriya interaction, anomalous Hall states, topologically non-trivial states, and spin and charge transport. Underpinning this work is a unique combination of experimental expertise, in particular, in the growth of epitaxial oxides using pulsed-laser epitaxy and detailed characterization of the physical properties by in-house equipment, neutron scattering, and optical and x-ray spectroscopy. Ultimately, the outcome of this work will result in enhanced understanding of interfacial behaviors and functionalities in oxide quantum heterostructures.

Recent Progress

The research has been focused on the discovery of new materials and phenomena arising from well-controlled, functionally cross-coupled interfaces. In particular, we have focused on the development of 5*d* based heterostructures to explore strong spin-orbit coupling (SOC) and interfacial charge transfer. Understanding interfacial coupling in oxide heterostructures using neutron scattering has been also one of the main focus areas. Selected research highlights are listed as follows:

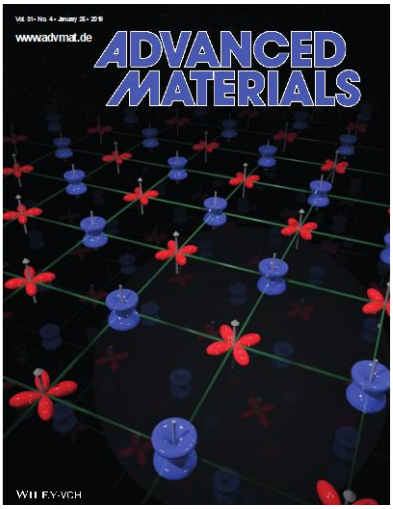

Figure 1. Illustration of spin and orbital structures of the Sr_2FeReO_6 double perovskite composed of localized 3d orbitals (red) and spin-orbit coupled 5d orbitals (blue).

Room-temperature ferromagnetic insulating state in cation-ordered double-perovskite $Sr_2Fe_{1+x}Re_{1-x}O_6$ films: A hidden ferromagnetic insulating (FMI) state emerged in $Sr_2Fe_{1+x}Re_{1-x}O_6$ (SFRO) films when the material's local ionic order was disturbed by a small modification in cation ratio. This work provides a promising new route to developing oxide quantum devices, as the high Curie temperature (T_c) FMI state is rare in nature but critical for realizing quantum electronic and computing devices that may operate at room temperature

without dissipating energy. We used pulsed laser epitaxy to grow highly cation-ordered SFRO thin films and further control the ratio between iron (Fe) and rhenium (Re) ions. Compared to the ferromagnetic metallic ground state found in stoichiometric SFRO, the change in 3d and 5d transition metal ratio created by Fe surplus and Re deficit in SFRO was found to play an important role in inducing the novel FMI state with a high Tc of approximately 400 K. Soft X-ray and optical spectroscopies as well as scanning transmission electron microscopy were employed to understand the metal-insulator transition (MIT) with robust ferromagnetism. Excess Fe^{3+} ions and emergent Re^{6+} ions contributed to the MIT. This work demonstrates the versatile functionality of 3*d*-5*d* double perovskites, in which strong electron correlation from 3d orbitals and large spin-orbit coupling from 5d orbitals cooperate to change local magnetic states.

Large orbital polarization in nickelate-cuprate heterostructures by dimensional control of oxygen coordination: The deliberate control of oxygen coordination in perovskite oxides permits never-before-possible manipulation of orbital configuration and electronic properties. We found that the orbital polarization in the correlated oxide $LaNiO_3$ can be drastically increased when the octahedral NiO_6 sublattice is transformed into pyramidal NiO_5 by precise interfacing with $SrCuO_2$. This work utilized pulsed laser epitaxy and grew $LaNiO_3$ and $SrCuO_2$ ultrathin layers atom-by-atom to exert control over the orbital configuration across the interfaces, which enabled the design of heterostructures with plane-like or chain-like oxygen sublattices. Soft X-ray spectroscopy demonstrated that bulk octahedral NiO_6 with chain-like oxygen sublattices has no preferential direction for the orbital occupancy (as in bulk $LaNiO_3$), but the introduction of a plane-like interface (by forming pyramidal NiO_5) induces a large degree of Ni-orbital polarization. Such extreme levels of orbital control open previously inaccessible phase spaces necessary to the discovery and design of unconventional functional properties in correlated quantum materials.

Future Plans

Exploit spin orbit coupling and lattice symmetry to develop oxide heterostructures with novel quantum phenomena: We will investigate symmetry breaking and interfacial charge transfer in 3*d*-5*d* TMO superlattices and examine their role in controlling the interfacial DM interactions to generate and stabilize skyrmions. $[(SrIrO_3)_n/(LaMnO_3)_n]_m$ superlattices with compositional inversion symmetry breaking originating from the dissimilar A- and B-site cations (Sr and La) will be studied. The ability of multilayers within the superlattices to enhance skyrmion stabilization will also be examined through the control of layer thickness and interfacial symmetry. The proposed work will be conducted by combining various experimental techniques to investigate the interplay of symmetry, interface charge transfer, and magnetism originating from 3*d*-5*d* transition metal oxide superlattices. We will investigate superlattices with various interfacial symmetries induced by different terminations of interfacial layers, layer repetitions, and layer separations. This approach will enable us to determine separately the influence of cumulative interfacial DM interactions (e.g., cooperative or opposing effects from top and bottom interfaces of the FM) and interlayer coupling that affect the creation of chiral magnetism.

We plan to determine the magnetic spin configuration of the bulk of the superlattice using GP-SANS measurements at High-Flux Isotope Reactor (HFIR, beam line CG-2). We will also measure the surface magnetization with nm-scale resolution to visualize skyrmions at the superlattice surface using scanning-tunneling microscopy (STM) combined with XMCD, which will be available at the Advanced Photon Source. PEEM measurements will be also conducted at the ALS (Beamline 11.0.1). Therefore, our work will ultimately lead to an improved quantitative and systematic understanding of the various materials and symmetry characteristics responsible for skyrmion formation in multi-layered systems.

Search for quantum anomalous Hall states in buckled honeycomb lattices of 3d-5d double perovskites*:* The large spin-orbit coupling of 5*d* TMs combined with buckled honeycomb lattices in symmetry-controlled (111) heterostructures (see Fig. 2) provides an ideal platform to stabilize inverted band structures as recent theoretical calculations predicted in Ba_2FeReO_6 [S. Baidy et al., *Phys. Rev. B* **94** (2016)]. We will study (111) double perovskites, including A_2FeReO_6 (A =Ba, Sr, and Ca), to check the viability of the high temperature quantum anomalous Hall (QAH) effect. To precisely tune the Hamiltonian, we will control not only the strain and dimensionality to modulate the trigonal crystal field and hopping integrals, but also the B-site cation ratio and their ordering to directly change the density of states near the Fermi level and, thereby, to subsequently open the band gap. We note that our preliminary growth testing indicated that the degree of B-site cation ordering depends sensitively on the growth condition, in particular, on the oxygen background pressure. The choice of double perovskites will be further extended to other 5*d* TMOs, including W and Re to vary the valence electron in the 5*d* constituent and the T_c. This will allow us to study further the lattice instability and competing spin states via investigations of the spin structure, electric structure, and magnetic and transport properties. The inverted band gap in QAH insulators will be studied by *in-situ* ARPES available now at ORNL.

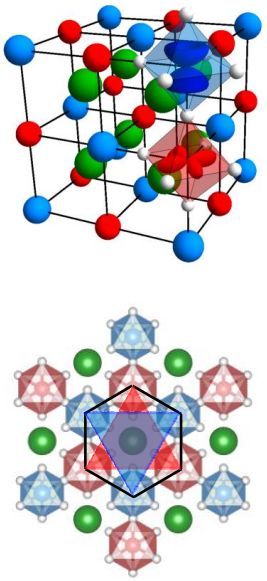

Fig. 2 (top) 3*d*-5*d* double perovskite and (bottom) its buckled honeycomb lattice formed on the (111) plane. Red, blue, and green spheres represent 3*d* and 5*d* TMs and oxygen, respectively.

Publications (selected from over 30 publications)

1. E.J. Guo, R. Desautels, D. Lee, M. Roldan, Z. Liao, T. Charlton, H.A. Ambaye, J.J. Molaison, R. Boehler, D. Keavney, A. Herklotz, T.Z. Ward, H.N. Lee, M.R. Fitzsimmons, Exploiting symmetry mismatch to control magnetism in a ferroelastic heterostructure, *Phys. Rev. Lett*. **122**, 187202 (2019).
2. E.J. Guo, R. Desautels, D. Keavney, M.A. Roldan, B.J. Kirby, D. Lee, Z. Liao, T. Charlton, A. Herklotz, T.Z. Ward, M.R. Fitzsimmons, H.N. Lee, Nanoscale ferroelastic twins formed in strained $LaCoO_3$ films, *Science Adv*. **5**, eaav5050 (2019).

3. Z. Liao, E. Skoropata, J. W. Freeland, E.-J. Guo, R. Desautels, X. Gao, C. Sohn, A. Rastogi, T. Z. Ward, T. Zhou, T. Charlton, M. R. Fitzsimmons, and H. N. Lee, Large orbital polarization in nickelate-cuprate heterostructures by dimensional control of oxygen coordination, *Nature Commun.* **10**, 589 (2019).
4. Z. Liao, M. Brahlek, J. M. Ok, L. Nuckols, Y. Sharma, Q. Lu, Y. Zhang, and H. N. Lee, Pulsed-laser epitaxy of topological insulator Bi_2Te_3 thin films, *APL Mater*. **7**, 041101 (2019).
5. E.-J. Guo, R. D. Desautels, D. Keavney, A. Herklotz, T. Z. Ward, M. R. Fitzsimmons, and H. N. Lee, Switchable orbital polarization and magnetization in strained $LaCoO_3$ films, *Phys. Rev. Mater*. **3**, 014407 (2019).
6. Y. Sharma, A. T. Wong, A. Herklotz, D. Lee, A. V. Ievlov, L. Collins, H. N. Lee, S. Dai, N. Balke, P. D. Rack, and T. Z. Ward, *Adv. Mater. Interfaces*, **6**, 1801723 (2019).
7. E.-J. Guo, R. D. Desautels, D. Keavney, M. A. Roldan, B. J. Kirby, D. Lee, Z. Liao, T. Charlton, A. Herklotz, T. Z. Ward, M. R. Fitzsimmons, and H. N. Lee, Nanoscale ferroelastic twins formed in strained $LaCoO_3$ films, *Sci. Adv*. **5**, eaav5050 (2019).
8. C. Sohn, E. Skoropata, Y. Choi, X. Gao, A. Rastogi, A. Huon, M. A. McGuire, L. Nuckols, Y. Zhang, J. Freeland, D. Haskel, and H. N. Lee, Room-temperature ferromagnetic insulating state in highly cation-ordered double perovskite $Sr_2Fe_{1+x}Re_{1-x}O_6$ films, *Adv. Mater*. 1805389. (2019).
9. E.-J. Guo, M. A. Roldan, X. Sang, S. Okamoto, T. Charlton, H. Ambaye, H. N. Lee, and M. R. Fitzsimmons, Influence of chemical composition and crystallographic orientation on the interfacial magnetism in $BiFeO_3/La_{1-x}Sr_xMnO_3$ superlattices, *Phys. Rev. Mater*. **2**, 114404 (2018).
10. T. Meyer, R. Jacobs, D. Lee, L. Jiang, J. W. Freeland, C. Sohn, T. Egami, D. Morgan, and H. N. Lee, Strain control of oxygen kinetics in the Ruddlesden–Popper oxide $La_{1.85}Sr_{0.15}CuO_4$, *Nature Commun*. **9**, 92 (2018). *Editor's Choice article.*
11. E.-J Guo, Y. Liu, C. Sohn, R. D. Desautels, A. Herklotz, Z, Liao, J. Nichols, J. W. Freeland, M. R. Fitzsimmons, and H. N. Lee, Oxygen diode formed in nickelate heterostructures by chemical potential mismatch, *Adv. Mater.* 1705904 (2018).
12. E. -J. Guo, M. A. Roldan, T. Charlton, Z. Liao, Q. Zheng, H. Ambaye, A. Herklotz, Z. Gai, T. Z. Ward, H. N. Lee, and M. R. Fitzsimmons, Removal of the magnetic dead layer by geometric design, *Adv. Funct. Mater.* 1800922 (2018).
13. Y. Sharma, J. Balachandran, C. Sohn, J. T. Krogel, P. Ganesh, L. Collins, Q. Li, N. Balke, S. Kalinin, O. Heinonen, and H. N. Lee, Nanoscale control of metal-insulator transition in epitaxial vanadium dioxides, *ACS Nano* **12**, 7159 (2018).
14. Z.Q. Liu, J. Liu,i, M. Biegalski, J. Hu, S. Shang, Y. Ji, J. Wang, S. Hsu, A.T. Wong, M. Cordill, B. Gludovatz, C. Marker, H. Yan, Z. Feng, L. You, M. Lin, T.Z. Ward, Z. Liu, C. Jiang, L. Chen, R. Ritchie, H.M. Christen, R. Ramesh, Electrically Reversible Cracks in an Intermetallic Film Controlled by an Electric Field, *Nature Commun*. **9**, 41 (2018).
15. Y. Sharma, B. L. Musico, X. Gao, C. Hua, A. F. May, A. Herklotz, A. Rastogi, D. Mandrus, J. Yan, H. N. Lee, M. F. Chisholm, V. Keppens, and T. Z. Ward (ECA), Single-crystal high entropy perovskite oxide epitaxial films, *Phys. Rev. Materials* **2**, 060404(R) (2018).
16. Q. Lu, S. R. Bishop, D. Lee, S. Lee, H. Bluhm, H. L. Tuller, H. N. Lee, and B. Yildiz, Electrochemically triggered metal-insulator transition between VO_2 and V_2O_5, *Adv. Funct. Mater*. 1803024 (2018).

Session 4

Experiments on Nonsymmorphic Topological and Weyl Semimetals

N. Phuan Ong, Princeton University

Program Scope

The goals are the investigation of quantum properties of topological quantum materials (including spin liquids) to explore novel excitations ranging from Weyl fermions to possible Majorana particles. We have broadened the experimental approach (with the consent of the Project Monitor) to include thermal Hall conductivity experiments on quantum spin liquids which are platforms for exploring novel topological excitations.

Recent Progress

In experiments on the topological Weyl superconductor $MoTe_2$, we have uncovered evidence for the existence of an edge supercurrent encircling the edge of the crystal in its superconducting state at 20 mK. Figure 1 shows a color map of the differential resistivity vs. current *I* and field *B*. Fluxoid quantization produces a scalloped boundary for the dissipationless region.

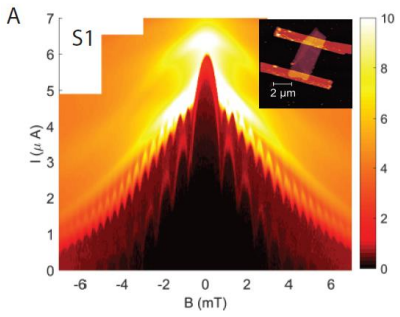

Color map of dV/dI in superconducting state of $MoTe_2$, showing oscillations arising from the edge supercurrent.

In a second experiment, we have investigated in detail the thermal Hall conductivity Kxy of the candidate Kitaev spin liquid α-$RuCl_3$ to test claims that Kxy is quantized. Our experiments have uncovered a rich variety of novel features in Kxy at 0.4 K.

Future Plans

We plan to investigate ramifications of the edge supercurrent in $MoTe_2$ and Kxy in α-$RuCl_3$.

Publications

1) Sihang Liang, Satya Kushwaha, Tong Gao, Max Hirschberger, Jian Li, Zhijun Wang, Karoline Stolze, Brian Skinner, B. A. Bernevig, R. J. Cava and N. P. Ong, "A gap-protected zero-Hall effect state in the quantum limit of the non-symmorphic metal KHgSb," *Nature Materials* **18**, 443 (2019); doi.org/10.1038/s41563-019-0303-x

2) Wudi Wang, Stephan Kim, Minhao Liu, F. A. Cevallos, R. J. Cava, and N. P. Ong, "Observation of an edge supercurrent in the Weyl superconductor $MoTe_2$," *under review* at *Science*.

Quantum Fluctuations in Narrow Band Systems

Filip Ronning, Eric Bauer, Roman Movshovich, Priscila Rosa, and Sean Thomas (Los Alamos National Lab)

Program Scope

Coherence and topologically protected modes in quantum matter arise from highly entangled spin, charge, lattice, and orbital degrees of freedom. Narrow band systems, whose renormalized electronic bandwidth is comparable to other relevant energy scales in the material, inherently have stronger interactions and a proliferation of quantum fluctuations. 5*f*-materials possess strong Coulomb repulsion, large spin-orbit coupling, and multiple competing energy scales, which generate coherent narrow bands and topologically non-trivial states of matter. This complexity provides a rich environment for discovering new states of matter, as well as providing representatives that will enable the understanding of quantum matter that also arises in 3*d*- to 4*f*-materials more generally. Using principally 5*f*-materials, we will address how quantum fluctuations renormalize excitations in topologically trivial and non-trivial matter and will develop conceptual frameworks for understanding and controlling the consequences of quantum fluctuations in classes of electronically correlated systems.

Recent Progress

To investigate how quantum fluctuations generate narrow band systems, we have performed resonant inelastic X-ray scattering (RIXS) of $CePd_3$. Our work is in good agreement with previous neutron scattering data, which illustrates that DMFT, with a purely local self energy, accurately captures the low energy excitation spectrum. However, our work also illustrates that the same DMFT calculations fail to capture the high energy excitations to excited *f*-states, revealing that a complete understanding of the narrow band formation in $CePd_3$ has yet to be achieved [R1].

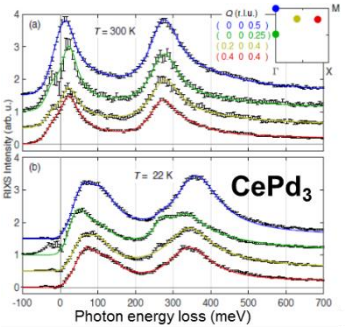

RIXS spectra of $CePd_3$ at 4 different momenta at 300K (top) and 22K (bottom).

Previous work on $CeRhIn_5$ has shown that the high field state possesses a strong electronic nematic character. In the past year, we have investigated this state with magnetostriction measurements, and suggest that the role of the evolving crystal field excitations play an important role in stabilizing a state with strong nematic character [P2]. In collaboration with Andrea Severing we established the ground state orbital character of $CeRhIn_5$ [P5]. With Hiuqui Yuan we used specific heat measurements to examine the mass enhancement of the high field state [P6], and finally with Philip Moll we showed the pressure evolution of the high field state, which appears to suggest it has no direct connection with the superconducting state found under pressure [R2]. This latter work also established that at high pressures a previously unidentified

novel field induced state, likely of magnetic origin, exists. Work on $CeAuSb_2$ also demonstrates an electronic nematic state [R3]. Under pressure a complex evolution with various magnetic states is found.

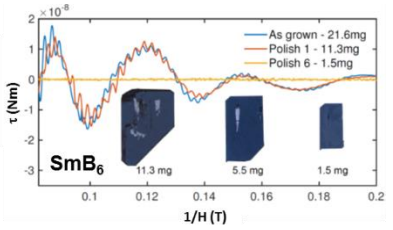

Torque magnetization revealing quantum oscillations in SmB_6 only when Al inclusions are present.

Due to the combination of strong spin-orbit coupling and strong Coulomb interactions, *f*-electron materials are ripe to explore the intersection between electronic correlations and non-trivial topology. We have made progress on three systems. SmB_6 is possibly the most strongly correlated topological material. Two prior reports on quantum oscillations in SmB_6 claimed vastly different origins for the oscillations: one from the topological surface states and the other from insulating bulk states. Both are highly interesting, but controversial, claims. Our results demonstrate that quantum oscillations mimicking a surface state can be caused by aluminum inclusions created during the flux growth process [P1]. This can explain one of the two previous claims. The high purity of our flux grown crystals, established by our heat capacity measurements, further illustrate that disorder must play a role in creating quantum oscillations observed in floating zone samples by the Cambridge group. $Eu_5In_2Sb_6$ is a magnetic analog of $Ba_5In_2Sb_6$ – a predicted topological insulator. In $Eu_5In_2Sb_6$ we have found evidence for a colossal negative magnetoresistance, which may be a consequence of magnetic polarons while experimental evidence for a topological state is still lacking [R4]. In the non-collinear magnetic metal $U_3Ru_4Al_{12}$ we demonstrate that the anomalous Hall effect is dramatically enhanced in small magnetic fields, and is consequently highly tunable with the magnetic field orientation. Comparison with theoretical calculations at LANL suggest this is a consequence of the small energy scale in this narrow band system [R5].

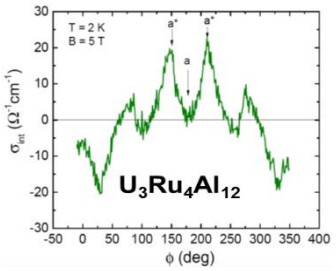

Example of the tunable intrinsic anomalous Hall effect of $U_3Ru_4Al_{12}$, here as a function of field angle

Future Plans

Continuing on our recent progress, we will perform RIXS on UAl_3 and ARPES measurements on $CePd_3$ to understand how quantum fluctuations renormalize the electronic structure. We will continue to investigate the high field state of $CeRhIn_5$ with doping studies to bring down the critical field, and with elastoresistance measurements to understand what degrees of freedom couple best to the nematic response. The origin of this intriguing state currently is still unknown.

In trying to understand how correlations interact with topological properties, we will perform thermopower measurements as a function of pressure on SmB_6. These measurements will allow us to determine the effective mass of the surface state as the hybridization to the *f*-electrons is increased. We will also tune magnetism, which produces a non-trivial Berry curvature, in 5*f* based systems, through a quantum phase transition, to understand the effects that the Berry curvature may play on the critical phenomena of the phase transition. We will do this with

doping and pressure studies, such as Sm and La doping of the candidate topological insulator PuB_4. Resonant X-ray, neutron scattering and NMR measurements are underway on $Eu_5In_2Sb_6$ to determine the magnetic structure, which is important input for assessing theoretically whether the system is a viable candidate to be a magnetic topological insulator.

Finally, we hypothesize that the small energy scales and complex order parameters of strongly spin-orbit coupled superconductors (SC) will enable us to create novel tunable devices from which we will gain the understanding that will enable control of the amplitude and phase of the SC wavefunction. We will demonstrate how to control the amplitude of the SC wave function through novel strain engineering in focused ion-beam (FIB) microstructured devices of *f*-electron SCs such as $CeIrIn_5$ [R6]. We will identify new SC materials with enhanced strain sensitivity using thermal expansion and the Ehrenfest relations. Thermal transport measurements to mK temperatures will be used to determine the complex and possibly topological order parameter of these materials. We will demonstrate the transparency of *f*-electron SCs through grain boundaries created in polycrystalline samples using scanning SQUID microscopy, which will be a foundational step for demonstrating that we can eventually control the response of these novel superconducting order parameters.

References

[R1] "Anderson lattice dynamics observed by resonant x-ray scattering," M. C. Rahn, K. Kummer, A. Amorese, D. D. Byler, K. J. McClellan, E. D. Bauer, C. H. Booth, J. Lawrence, F. Ronning, and M. Janoschek, *Unpublished.*

[R2] "Pressure-induced critical suppression of high-field nematicity in $CeRhIn_5$," T. Helm, A. Grockowiak, F.F. Balakirev, J. Singleton, K.R. Shirer, M. König, E.D. Bauer, F. Ronning, S.W. Tozer, P.J.W. Moll, Submitted to PRX; *ArXiv*:1902.00970.

[R3] "Putative nematic state in $CeAuSb_2$," S. Seo, X. Wang, S.M. Thomas, M.C. Rahn, D. Carmo, F. Ronning, E.D. Bauer, R.D. dos Reis, M. Janoschek, J.D. Thompson, R.M. Fernandes and P.F.S. Rosa, Submitted to PRX; *Unpublished.*

[R4] "Colossal magnetoresistance in a nonsymmorphic antiferromagnetic insulator," P. F. S. Rosa, S. K. Kushwaha, J. C. Souza, M. C. Rahn, L. S. I. Veiga, S. M. Thomas, M. Janoschek, E. D. Bauer, M. K. Chan, J. D. Thompson, P. G. Pagliuso, N. Harrison, F. Ronning, *Unpublished.*

[R5] "Large tunable anomalous Hall effect in Kagome antiferromagnet $U_3Ru_4Al_{12}$," T. Asaba, Y. Su, M. Janoschek, J. D. Thompson, S. M. Thomas, E. D. Bauer, S.-Z. Lin, F. Ronning, Submitted to PRL (2019), *Unpublished.*

[R6] "Spatially modulated heavy-fermion superconductivity in $CeIrIn_5$," M. D. Bachmann, G. M. Ferguson, F. Theuss, T. Meng, C. Putzke, T. Helm, K. R. Shirer, Y.-S. Li, K. A. Modic, M. Nicklas, M. Koenig, D. Low, S. Ghosh, A.P. Mackenzie, F. Arnold, E. Hassinger, R.D. McDonald, L.E. Winter, E.D. Bauer, F. Ronning, B. J. Ramshaw, K. C. Nowack, P. J. W. Moll, Submitted to Science (2018); *ArXiv*:1807.05079.

Publications (as of Jan. 2019; P1, P2, and P9 are led by this FWP)

[P1] "Quantum oscillations in flux-grown SmB_6 with embedded aluminum," S.M. Thomas, X. Ding, F. Ronning, V. Zapf, J.D. Thompson, Z. Fisk, J. Xia, P.F.S. Rosa. *Physical Review Letters* **122**, 166401 (2019).

[P2] "Enhanced Hybridization Sets the Stage for Electronic Nematicity in $CeRhIn_5$," P.F.S. Rosa, S.M. Thomas, F.F. Balakirev, E.D. Bauer, R.M. Fernandes, J.D. Thompson, F. Ronning, and M. Jaime, *Physical Review Letters* **122**, 016402 (2019).

[P3] "Magnetoelastic coupling in URu_2Si_2: Probing multipolar correlations in the hidden order state," M. Wartenbe, R.E. Baumbach, A. Shekhter, G.S. Boebinger, E.D. Bauer, C.C. Moya, N. Harrison, R.D. McDonald, M.B. Salmon, and M. Jaime, *Physical Review B* **99**, 235101 (2019).

[P4] "Anomalous connection between antiferromagnetic and superconducting phases in the pressurized noncentrosymmetric heavy-fermion compound $CeRhGe_3$," H. Wang, J. Guo, E.D. Bauer, V.A. Sidorov, H. Zhao, J. Zhang, Y. Zhou, Z. Wang, S. Cai, K. Yang, A. Li, P. Sun, Y.-f. Yang, Q. Wu, T. Xiang, J.D. Thompson, and L. Sun, *Physical Review B* **99**, 024504 (2019).

[P5] "Orientation of the ground-state orbital in $CeCoIn_5$ and $CeRhIn_5$," M. Sundermann, A. Amorese, F. Strigari, B. Leedahl, L.H. Tjeng, M.W. Haverkort, H. Gretarsson, H. Yavas, M.M. Sala, E.D. Bauer, P.F.S. Rosa, J.D. Thompson, and A. Severing, *Physical Review B* **99**, 235143 (2019).

[P6] "Enhancement of the effective mass at high magnetic fields in $CeRhIn_5$," L. Jiao, M. Smidman, Y. Kohama, Z.S. Wang, D. Graf, Z.F. Weng, Y.J. Zhang, A. Matsuo, E.D. Bauer, H. Lee, S. Kirchner, J. Singleton, K. Kindo, J. Wosnitza, F. Steglich, J.D. Thompson, and H.Q. Yuan, *Physical Review B* **99**, 045127 (2019).

[P7] "Putative hybridization gap in $CaMn_2Bi_2$ under applied pressure," M. M. Piva, S. M. Thomas, Z. Fisk, J.-X. Zhu, J. D. Thompson, P. G. Pagliuso, and P. F. S. Rosa. *Physical Review B* **100**, 045108 (2019).

[P8] "Raman spectroscopy of f-electron metals: An example of CeB_6," M. Ye, H.H. Kung, P.F.S. Rosa, E.D. Bauer, Z. Fisk, and G. Blumberg, *Physical Review Materials* **3**, 065003 (2019).

[P9] "$CeAu_2Bi$: A new nonsymmorphic antiferromagnetic compound," M. M. Piva, W. Zhu, F. Ronning, J. D. Thompson, P. G. Pagliuso, and P. F. S. Rosa. *Physical Review Materials* **3**, 071202(R) (2019).

[P10] "Separate measurement of the $5f_{5/2}$ and $5f_{7/2}$ unoccupied density of states of UO_2," J.G. Tobin, S. Nowak, C.H. Booth, E.D. Bauer, S.W. Yu, R. Alonso-Mori, T. Kroll, D. Nordlund, T.C. Weng, and D. Sokaras, *Journal of Electron Spectroscopy and Related Phenomena* **232**, 100 (2019).

Symmetries, Interactions and Correlation Effects in Carbon Nanostructures

Gleb Finkelstein, Physics Department, Duke University, Durham, NC 27708

Program Scope

1) In 2016, the PI's group had detected supercurrent through a quantum Hall (QH) region contacted by superconducting electrodes [F. Amet et al., Science 2016, publication supported by DOE]. We worked with graphene encapsulated in boron nitride and contacted by superconducting molybdenum-rhenium leads (Figure 1). This was the first observation of a quantum Hall supercurrent in any material system.

We continue studying this material platform, aiming to better understand the microscopic origin of the superconducting coupling with the QH edge states, and also aiming to utilize this phenomenon for engineering novel states at the QH-SC interface. Specifically, one can expect to form topological superconducting states and Majorana modes, which may be then used for quantum information processing.

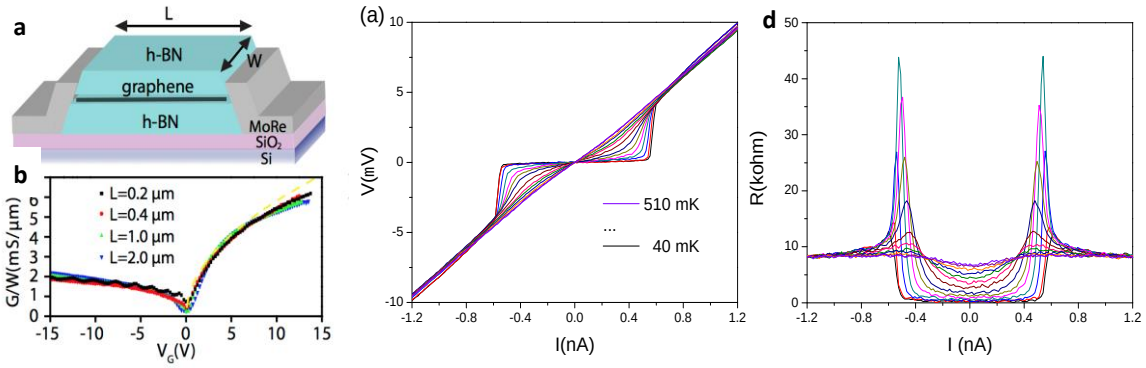

Figure 1. a) Schematic of a Josephson junction made of graphene encapsulated in h-BN, contacted by superconducting molybdenum-rhenium leads. (b) Gate dependence of the normal state conductance G for several channel lengths, demonstrating the length independent (ballistic) sample conductance. (c) V-I curves measured at B = 1 T and ν = 2 in the temperature range 40-500 mK. The supercurrent branch is clearly visible at the lowest temperature (40 mK) for I < 0.5 nA. d) The temperature dependence of the dV/dI curves. The differential resistance is suppressed at zero bias and peaks at ~0.5 nA where the junction switches from the superconducting to the normal branch.

2) The second research direction is the study of dissipation and interactions in "quantum impurity" systems, which is based on carbon nanotube quantum dots with dissipative leads. Here, a quantum dot plays the role of the quantum impurity, while the leads provide interactive environment in which it is embedded. Our earlier works identifier a quantum critical point (QCP) in this system, which is enabled by dissipation / interactions in the leads. We are now particularly interested in probing non-equilibrium physics at the QCP. Non-equilibrium phenomena in interacting quantum systems are notoriously difficult, and we are exploring them in collaboration with the theory group of Harold Baranger (supported by DOE CMT program).

Recent Progress – main results

1. Quantum Hall – based SQUID

In order to control the propagation of the QH edge states we worked with Josephson junctions which had dedicated side gates carved from the same sheet of graphene as the junction itself. These side gates are highly efficient, and allow us to modulate carrier density along either edge of the junction in a wide range. In particular, in magnetic fields in the 1 − 2 Tesla range, we are able to populate the next Landau level, resulting in Hall plateaus with conductance that differs from the bulk filling factor (Figure 2).

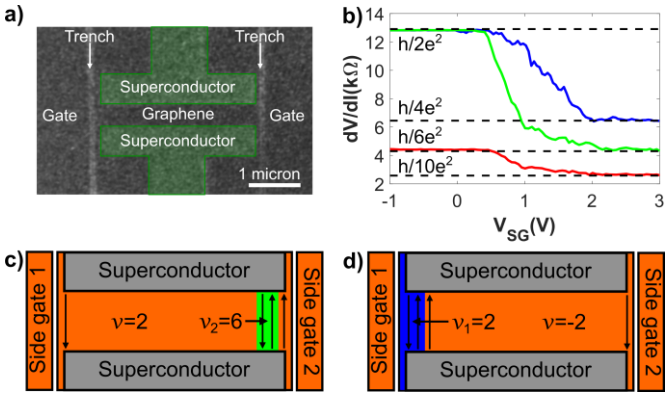

Figure 2: (a) SEM image of a side gated graphene Josephson junction. (b) Resistance plotted vs. SG voltage in 3 cases: Green: bulk filling factor ν= 2, SG2 induces change in the local filling from ν_2 = 2 to 6 (schematic in panel c). Red: similar to green, but SG1 is set at ν_1 = 6 providing 4 additional channels. Blue: bulk filling ν= –2, SG1 induces change in the local filling from ν_1 = –2 to +2 (schematic in panel d).

When counter-propagating quantum Hall edge states are introduced along either edge, we observe supercurrent localized along that edge of the junction. We studied these supercurrents as a function of magnetic field and carrier density. When both side gates are activated, supercurrents flow on both sides of the junction, thus turning it into a SQUID. We observed and studied interference fringes, which have periodicity of less than 1 mT (on top of the quantizing field of ~ 2 T). The fringes are very sensitive to the back- and side-gate voltages, which control the location of the QH edge channels. Our results open the road for manipulation of the QH edge states carrying superconducting correlations by electrostatic gating. **Science Advances**, Accepted, https://arxiv.org/abs/1901.05928

2. Supercurrent Flow in Multi-Terminal Graphene Josephson Junctions,

Recent theories points to the exciting possibility to emulate complex band structures of bulk topological materials in multi-terminal Josephson junctions [69, 70, 73]. Namely, the energy of Andreev bound states in a four-terminal junction depends on phase differences between the pairs of leads (three in total; the overall phase drops out) with a periodicity of 2π. This is formally similar to the periodic dependence of the energy bands in a Brillouin zone of a crystal on three quasi-momenta. The similarity should allow one to produce complex topological objects, e.g. Weyl points, in multiterminal junctions.

We have fabricated and investigated the electronic properties of multi-terminal graphene Josephson junctions. These are the first multi-terminal Josephson junctions made in any ballistic material; the ballistic nature of graphene allows one to efficiently couple more than 2 electrodes. (This work was performed at zero

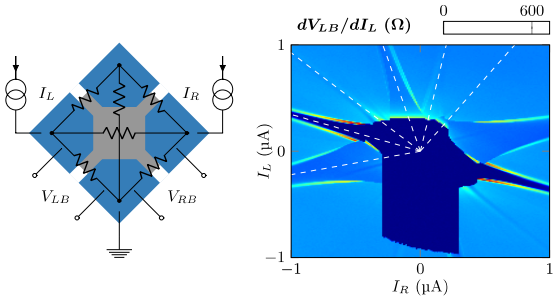

Figure 3: (a) Schematic of a 4-terminal graphene Josephson junction. (b) Resistance map between the left and bottom contacts, plotted vs. two bias currents. Multiple resonances are visible.

magnetic field, not in the QH regime.) We have measured differential resistance between different pairs of contacts. These measurements yield multiple resonant features, which are attributed to supercurrent flow among adjacent and nonadjacent Josephson junctions. Surprisingly, we find that superconducting and dissipative currents coexist within the same region of graphene. These measurements open the road for attempting to emulate and artificial a Brillouin zone as proposed by theory.

Nano Letters 19, p. 1039 (2019), https://arxiv.org/abs/1810.11632

Minor results and preprints:

3. Investigation of Supercurrent in the QH Regime in Graphene Josephson Junctions. We examined multiple graphene Josephson junctions of different shapes and dimensions to determine which mechanisms may be responsible for the supercurrent observed in the quantum Hall (QH) regime. **Journal of Low Temperature Physics 191**, p. 288 (2018). https://doi.org/10.1007/s10909-018-1872-9

4. Sub-Kelvin Lateral Thermal Transport in Diffusive Graphene. We reported on hot carrier diffusion in graphene across large enough length scales that the carriers are not thermalized across the crystal. **PRB** 99, 125427 (2019), https://arxiv.org/abs/1812.11711

5. Supercurrent in Graphene Josephson Junctions with Narrow Trenches in the QH Regime. We studied supercurrent in the regime of the quantum Hall effect in graphene Josephson junctions, in which the active material was cut by a narrow trench, intended to induce counter-propagating edge states. **MRS Advances** 3 (2018), https://arxiv.org/abs/1807.11923

6. Interference of Chiral Andreev Edge States. We explored the interface between the quantum Hall the superconductor. We find clear signatures of chiral Andreev edge states: hybridized electron-hole states similar to chiral Majorana fermions. Preprint at https://arxiv.org/abs/1907.01722

7. Chiral Quasiparticle Tunneling Between QH Edges in Proximity with a Superconductor. We studied a graphene Josephson junctions with contacts shaped to form a narrow constriction. The device conductance is determined by QH edge states, which come close together and can support tunneling supercurrents up to fields of ~2.5T. Preprint at https://arxiv.org/abs/1904.11689

8. $2\Phi_0$-periodic magnetic interference in ballistic graphene Josephson junctions. We investigate supercurrent interference patterns measured as a function of magnetic field in ballistic graphene Josephson junctions. Close to the Dirac point, we find anomalous interference patterns with an apparent $2\Phi_0$ periodicity, similar to that predicted for topological Andreev bound states carrying a charge of e instead of 2e. Preprint at https://arxiv.org/abs/1906.07935

Future Plans

Building on our existing momentum in graphene-based Josephson junctions, I plan to concentrate on the following directions:

1) To further develop the QH-based SQUID, in particular to make SQUIDS with multiple terminals. Their coupling will be enabled by the QH edge states, which could be redirected on-demand by top gates.

2) To extend these measurements to the fractional QH regime and to independently gate-able bilayers, in both of which non-abelian excitations are expected to form upon contact with a superconductor.

3) To explore the phase space of the multiterminal Josephson junctions at zero magnetic field, in particular to look for the theoretically predicted regime in which the spectrum of Andreev bound states emulates the Brillouin zone of a topological material.

I further plan to continue exploring the quantum critical point we observed in a nanotube quantum dot subject to dissipative environment. In particular, we will create tunnel probe which provide information analogous to the density of states, but in a highly correlated and non-equilibrium regime. In addition to the more ambitious project we are continuing to work on a topic outlined in the original proposal: spinful resonant level with dissipation, including the Kondo effect with dissipation.

Publications in 2018-2019

[1] A.W. Draelos, M.-T. Wei, A. Seredinski, C.T. Ke, K. Watanabe, T. Taniguchi, M. Yamamoto, S. Tarucha, I.V. Borzenets, F. Amet, and G. Finkelstein, "*Investigation of Supercurrent in the Quantum Hall Regime in Graphene Josephson Junctions*." **Journal of Low Temperature Physics 191**, p. 288 (2018).
https://doi.org/10.1007/s10909-018-1872-9

[2] A. Seredinski, A.W. Draelos, M-T. Wei, C.T. Ke, T. Fleming, Y. Mehta, E. Mancil, H.M. Li, T. Taniguchi, K. Watanabe, S. Tarucha, M. Yamamoto, I.V. Borzenets, F. Amet, and G. Finkelstein, "*Supercurrent in Graphene Josephson Junctions with Narrow Trenches in the Quantum Hall Regime*." **MRS Advances 3**, (2018).
https://doi.org/10.1557/adv.2018.469

[3] A. Draelos, M. T. Wei, A. Seredinski, H. Li, Y. Mehta, K. Watanabe, T. Taniguchi, F. Amet, and G. Finkelstein. "*Supercurrent Flow in Multiterminal Graphene Josephson Junctions."* **Nano Letters 19** (2), p. 1039 (2019).
https://doi.org/10.1021/acs.nanolett.8b04330

[4] A. W. Draelos, A. Silverman, B. Eniwaye, E. Arnault, C. T. Ke, M. T. Wei, I. Vlassiouk, I. V. Borzenets, F. Amet and G. Finkelstein. "*Sub-Kelvin Lateral Thermal Transport in Diffusive Graphene*." **Physical Review B** 99, 125427 (2019),
https://doi.org/10.1103/PhysRevB.99.125427

[5] A. Seredinski, A.W. Draelos, E. Arnault, M.-T. Wei, H. Li, K. Watanabe, T. Taniguchi, F. Amet, and G. Finkelstein, "*Full control of quantum Hall supercurrent in a side gated graphene Josephson junction*." **Accepted to Science Advances**, available at: arXiv:1901.05928.

Preprints

[6] C. T. Ke, A. W. Draelos, A. Seredinski, M. T. Wei,1 H. Li, M. Hernandez-Rivera, K. Watanabe, T. Taniguchi, M. Yamamoto, S. Tarucha, Y. Bomze, I. V. Borzenets, F. Amet, and G. Finkelstein, *"Robust anomalous $2\Phi_0$-periodic magnetic interference in ballistic graphene Josephson junctions."* https://arxiv.org/abs/1906.07935

[7] L. Zhao, E. G. Arnault, A. Seredinski, A. Bondarev, A. W. Draelos, H. Li, K. Watanabe, T. Taniguchi, H. Baranger, F. Amet and G. Finkelstein, "*Andreev Edge States at the Quantum Hall – Superconductor Interface*." https://arxiv.org/abs/1907.01722

[8] M.-T. Wei, A.W. Draelos, A. Seredinski, C.T. Ke, K. Watanabe, T. Taniguchi, M. Yamamoto, S. Tarucha, I.V. Borzenets, F. Amet, and G. Finkelstein, *"Chiral Quasiparticle Tunneling Between QH Edges in Proximity with a Superconductor."* https://arxiv.org/abs/1904.11689

Project Title: Topological Superconductivity in Strong Spin-Orbit Materials
Principal Investigator: Johnpierre Paglione
Institution: University of Maryland
Email address: paglione@umd.edu

Project Scope

A non-trivial band structure that exhibits band ordering analogous to that of the known 2D and 3D topological insulator [1,2] TI materials was predicted in a variety of 18-electron half-Heusler compounds using first principles calculations [3–7]. A subset of these compounds possess an inverted band structure, with the top of an *s*-type orbital-derived valence band lying below a *p*-type conduction band, with both centered at the high-symmetry Γ point and with no other bands crossing the Fermi level elsewhere in the Brillouin zone. Because such a band inversion changes the parity of the wavefunction, it provides the proper condition for the TI state, yielding a handy indicator of the potential for specific compounds to be TIs. This can be quantified by calculating the band structure and measuring the degree of band inversion; in the half-Heuslers, a sensitive tuning of band inversion is possible due to the tunable lattice constants [3–7]. With the ability to tune the energy gap and set the desired band inversion by appropriate choice of compound with appropriate hybridization strength (i.e., lattice constant) and magnitude of spin-orbit coupling (i.e., nuclear charge), the half Heusler family shows much promise for realizing the next generation of TI materials.

Superconductors are among the most fascinating systems for realizing topological states, either via a proximity effect, or intrinsically via an odd-parity, time-reversal-invariant pairing state. Alongside the usual signature supercurrents arising from Cooper pair coherence, a direct analogy exists between superconductors and insulators: since the Bogoliubov-de Gennes (BdG) Hamiltonian for the quasiparticles of a superconductor is essentially analogous to that of a band insulator, one can consider the interesting possibility of TI surface states arising due to a superconducting "band gap". Similar to TI systems, a topological superconductor (TSC) thus has a fully gapped bulk band structure and gapless surface Andreev bound states. Thus the search for TSCs in materials with strong band inversion is a promising direction. In the case of time-reversal-invariant (centrosymmetric) systems, a material is a TSC if it is an odd-parity, fully gapped superconductor and its Fermi surface encloses an odd number of time-reversal-invariant momenta in the Brillouin zone [8].

Recent Progress

Beyond band inversion, strong SOC has significant consequences for other physical properties both in the normal and superconducting states. SOC in the XYZ compounds separates the *p*-orbital derived 6-fold degenerate valence band into 2-fold and 4-fold degenerate bands with the latter being higher in energy. In RPtBi (R=rare earth), SOC is big enough to push the 4-fold band above the *s*-orbital derived conduction bands, i.e., band inversion of Γ_6 and Γ_8. This band structure is identical to the first experimentally identified topological materials HgTe. In our prototypical YPtBi, the chemical potential is located in the Γ_8 band which implies *p*-like Bloch electrons occupy the low energy quasiparticle states. With a lack of inversion symmetry causing a Rasha-type splitting of the spin-degeneracy, YPtBi exhibits phenomenal behavior such as an apparent beating of Shubnikov-de Haas (SdH) quantum oscillations from two different spin species and exotic pairing as discussed below. Generally, strong SOC introduces an extra phase factor in the Bloch wavefunction as well as Landau levels. In YPtBi, extreme SOC manifests a phase quadrature to

the periodic pseudopotential of lattice, which results in the total phase difference of π. This π-phase difference causes an abrupt disappearance of SdH effect when a magnetic field is applied along crystallographic [110] direction where two quantum oscillations with the same frequency and π-phase difference. This phenomena is extremely unusual, and should be manifest in a host of XYZ compounds of interest to this project.

HoPtBi is a magnetic analogue to the band-inverted semimetal YPtBi. By analogue to the similarly magnetic GdPtBi we expect to see a mean-field magnetic interaction from the localized f-state electrons on the Ho site. In the presence of a strong applied magnetic field this interaction can lift the high-symmetry of the Γ-point, introducing novel structure to the fermi surface including the potential for Weyl points. Unlike GdPtBi, HoPtBi is paramagnetic above 1.25K so it is possible to continuously explore this behavior without crossing into the antiferromagnetically ordered regime present in the Gd analogue. We have characterized the temperature-field dependence of magnetic order using neutron scattering in collaboration with Jeff Lynn at NIST Gaithersburg, as shown in **Figure 1**.

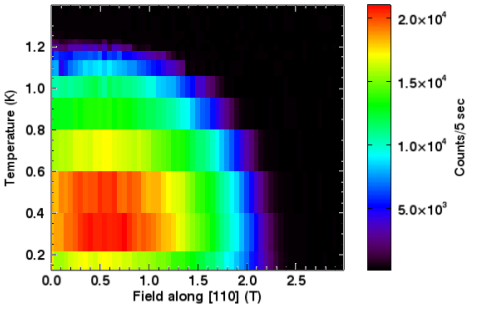

Figure 1: (top) Neutron scattering investigation of Q = (½ ½ ½) magnetic Bragg peak in HoPtBi as a function of magnetic field aligned along (110), showing ordered state in high intensity region. (bottom) Hall effect study of HoPtBi crystal, showing anomalous Hall angle effect at low temperatures.

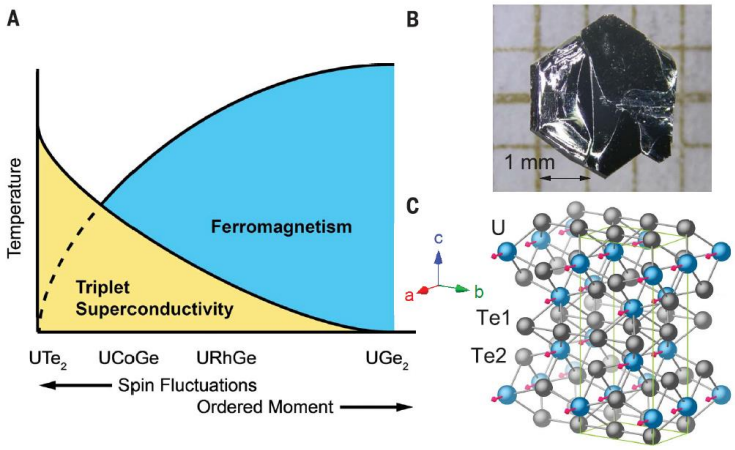

Figure 2: Structure of UTe2. (A) Global phase diagram of ferromagnetic superconductors; UTe2 is located at the paramagnetic end of the series. (B) A photo of a single crystal of UTe2 grown using chemical vapor transport method on the millimeter scale. (C) Crystal structure of UTe2, with U atoms in blue and Te atoms in gray. The U atoms sit on chains parallel to the [100] a axis, which coincides with the magnetic easy axis.

Finally, a new discovery in collaboration with N. Butch at NIST Center for Neutron Research has uncovered a new spin-triplet superconductor that exhibits properties that make it promising to be an intrinsic topological superconductor. We recently reported [9] the discovery of spin-triplet superconductivity in UTe_2, featuring a transition temperature of 1.6 kelvin and a very large and anisotropic upper critical field exceeding 40 T and re-entrant superconducting phases at even higher fields [10]. This superconducting phase stability suggests that UTe_2 is related to ferromagnetic superconductors such as UGe_2, URhGe, and UCoGe, but remains paramagnetic down to the lowest measured temperatures [11]. However, the lack of magnetic order and the observation of quantum critical scaling place UTe_2 at the paramagnetic end of this ferromagnetic superconductor series. A large intrinsic zero-temperature reservoir of ungapped fermions indicates a highly unconventional type of superconducting pairing, which our thermodynamic experiments suggest forms a superconducting order parameter with a point node gap structure [12].

Future Plans

We continue to explore the exotic normal and superconducting state properties of this family of compounds to understand the nature of the normal and superconducting states, using our full arsenal of probes in combination with a systematic growth program aimed at comparing properties of the RPtBi and RPdBi series, as well as the newly discovered superconductor UTe_2. Most interesting, tuning spin orbit coupling via elemental substitution may be a powerful method of both studying and controlling the parity of the superconducting state and the topology of the half-Heusler series.

References

[1] C. L. Kane et al., "Z2 Topological Order and the Quantum Spin Hall Effect", *Phys. Rev. Lett.* **95**, 146802 (2005).

[2] L. Fu et al., "Topological insulators with inversion symmetry", *Phys. Rev. B* **76**, 45302 (2007).

[3] S. Chadov et al., "Tunable multifunctional topological insulators in ternary Heusler compounds", *Nat. Mater.* **9**, 541–545 (2010).

[4] H. Lin et al., "Half-Heusler ternary compounds as new multifunctional experimental platforms for topological quantum phenomena.", *Nat. Mater.* **9**, 546–9 (2010).

[5] D. Xiao et al., "Half-Heusler Compounds as a New Class of Three-Dimensional Topological Insulators", *Phys. Rev. Lett.* **105**, 96404 (2010).

[6] W. Feng et al., "Half-Heusler topological insulators: A first-principles study with the Tran-Blaha modified Becke-Johnson density functional", *Phys. Rev. B* **82**, 235121 (2010).

[7] W. Al-Sawai et al., "Topological electronic structure in half-Heusler topological insulators", *Phys. Rev. B* **82**, 125208 (n.d.).

[8] L. Fu et al., "Odd-Parity Topological Superconductors: Theory and Application to $CuxBi_2Se_3$", *Phys. Rev. Lett.* **105**, 97001 (2010).

[9] S. Ran et al., "Nearly ferromagnetic spin-triplet superconductivity", *Science* **365**, 684–687 (2019).

[10] S. Ran et al., "Extreme magnetic field-boosted superconductivity", *unpublished* (2019).

[11] S. Sundar et al., "Coexistence of ferromagnetic fluctuations and superconductivity in the actinide superconductor UTe_2", *under Review* (2019).

[12] T. Metz et al., "Point Node Gap Structure of Spin-Triplet Superconductor UTe_2", *under Rev.* (2019).

Publications

S. Ran, C. Eckberg, Q.-P. Ding, Y. Furukawa, T. Metz, S. R. Saha, I.-L. Liu, M. Zic, H. Kim, J. Paglione, and N. P. Butch, "Nearly ferromagnetic spin-triplet superconductivity," *Science* **365**, 684–687 (2019). [http://dx.doi.org/10.1126/science.aav8645].

S. Sundar, S. Gheidi, K. Akintola, A. M. Cote, S. R. Dunsiger, S. Ran, N. P. Butch, S. R. Saha, J. Paglione, and J. E. Sonier, "Coexistence of ferromagnetic fluctuations and superconductivity in the actinide superconductor UTe2," *under Review* (2019). [http://arxiv.org/abs/1905.06901].

S. Ran, I.-L. Liu, Y. S. Eo, D. J. Campbell, P. Neves, W. T. Fuhrman, S. R. Saha, C. Eckberg, H. Kim, J. Paglione, D. Graf, J. Singleton, and N. P. Butch, “Extreme magnetic field-boosted superconductivity,” *unpublished* (2019). [http://arxiv.org/abs/1905.04343].

I.-L. Liu, C. Heikes, T. Yildirim, C. Eckberg, T. Metz, S. Ran, W. Ratcliff, J. Paglione, and N. P. Butch, “Quantum oscillations from networked topological interfaces in a Weyl semimetal,” *unpublished* (2019). [http://arxiv.org/abs/1905.02277].

H. Hodovanets, C. J. Eckberg, P. Y. Zavalij, H. Kim, W.-C. Lin, M. Zic, D. J. Campbe, J. S. Higgins, and J. Paglione, “Single-crystal investigation of the proposed type-II Weyl semimetal CeAlGe,” *Phys. Rev. B* **98**, 245132 (2018). [http://dx.doi.org/10.1103/PhysRevB.98.245132].

Proximity effects and topological spin currents in van der Waals heterostructures

Benjamin Hunt, Carnegie Mellon University

Program Scope

The major goals of this project are to study spin-polarized topological edge states, specifically those of the quantum anomalous Hall (QAH) effect, which has been proposed to be realizable via a (simultaneous) magnetic and spin-orbit proximity effect in graphene[1]. En route to realizing the QAH effect, the goal was also to study the newly-discovered 2D van der Waals magnetic insulators, and the extent to which magnetic effects could be seen in graphene via proximity coupling. The QAH effect was initially observed in magnetic topological insulators, and since the beginning of this project has been subsequently observed in "magic-angle" twisted bilayer graphene aligned to boron nitride[2]. Observation of the QAHE as a consequence of proximity effects is still outstanding and would mark a significant step in our understanding of the emergence of topological states in heterostructures.

The broader scientific context of the experiments in this proposal is to understand the physical mechanisms behind proximity effects in van der Waals heterostructures. Perhaps the ultimate scientific and technological goal of realizing topological states through proximity effects is the creation of Majorana zero modes in solid-state devices, which has been identified as a major priority in condensed-matter physics because of the potential use of Majorana zero modes in topological quantum computing[3]. Van der Waals materials offer advantages in this area because of the diversity of materials that can potentially be used and the unique device architectures that are possible using the van der Waals assembly techniques. There are several possible routes to Majorana modes using topological edge states: one involves proximity-coupling the QAH edge state to a superconductor; another involves proximity-coupling the quantum spin Hall (QSH) edge state to a superconductor and interrupting it with a magnetic insulator[3]. We have expanded our investigation of spin-polarized topological states by investigating the nature of the QSH in the only 2D van der Waals material in which it is known to occur, monolayer 1T'-WTe_2[4]. We have studied its energy gaps using quantum capacitance and we have coupled it to a van der Waals superconductor, $NbSe_2$. The goals of this related effort are (1) to understand the magnitude and mechanism of the energy gaps in WTe_2 and (2) to understand the nature of the proximity-induced superconducting gap in the QSH edge state, measured directly for the first time and presented in our new manuscript[5].

Recent Progress

In the past year, we have continued our transport and capacitance studies of monolayer graphene-magnetic insulator (MI) heterostructures, particularly with the MIs CrI_3, $CrSiTe_3$ (CST), and $RuCl_3$ with the goal of measuring an electronic transport signature of the magnetic proximity effect. In a new effort, we have begun to study the QSH insulator monolayer 1T'-WTe_2, the only 2D material

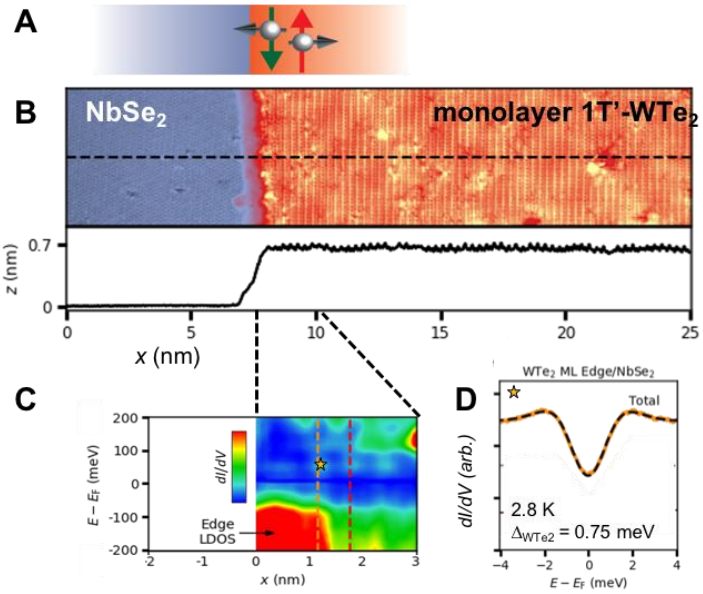

Fig. 1 A. Schematic of spin-momentum coupled (helical) edge states of the 2D topological insulator (aka quantum spin Hall – QSH - insulator). **B.** Scanning tunneling microscopy (topograph) near WTe_2 edge on top of $NbSe_2$. **C**. Scanning tunneling spectroscopy near WTe_2 edge, showing signature of QSH edge state. **D.** Spectrum in lower energy range, at location indicated in panel C, showing induced superconducting gap of 0.75 meV in the QSH edge state

known to have intrinsic topological edge states, and have succeeded in inducing a superconducting gap into these edge states by proximity-coupling to the van der Waals superconductor $NbSe_2$.

Scanning Tunneling Microscopy of 1T'-WTe_2-$NbSe_2$. We demonstrate a novel fabrication technique which is used to assemble a WTe_2/ $NbSe_2$ van der Waals heterostructure in an inert environment and without contaminating the heterostructure surface. Using scanning tunnelling microscopy (STM), we demonstrate that the resulting heterostructure surface is atomically clean despite both $NbSe_2$ and WTe_2 being extremely air-sensitive. As a result, we are the first to report the study of exfoliated monolayer WTe_2 flakes using scanning tunnelling microscopy. By studying the electronic properties of the heterostructure with scanning tunnelling spectroscopy (STS), we demonstrate the existence of the QSH edge state at the WTe_2 monolayer boundary along with a superconducting gap, induced by the proximity effect. We characterize the induced super-conductivity in detail, as function of magnetic field, temperature and WTe_2 layer thickness. This represents the first study on topological superconductivity at the surface of an assembled van der Waals heterostructure.

Capacitance Measurements of QSH Insulator 1T'-WTe_2. Monolayer 1T'-WTe_2 is of great interest because it is the only known van der Waals material to exhibit topological edge states. We

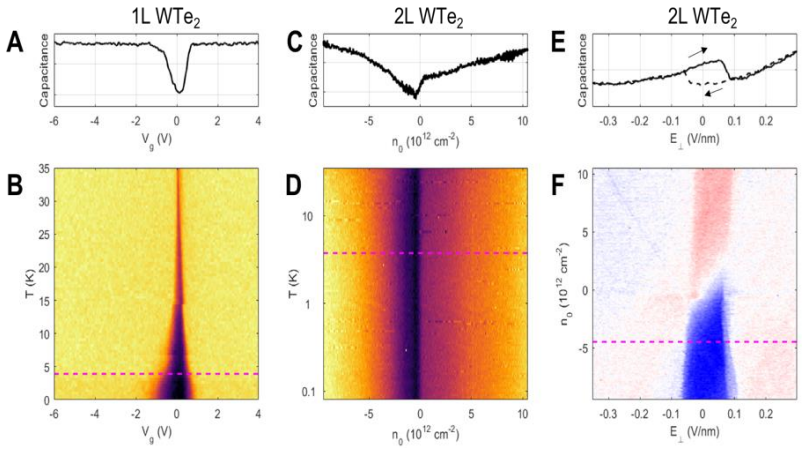

Fig. 2 Capacitance measurement of gaps and of ferroelectric polarization in 1T'-WTe_2. **(A)** and **(B)**. Monolayer WTe_2 (QSH insulator). The gap appears to get larger at low temperatures, perhaps pointing to many-body effects. **(C)** and **(D)** Bilayer WTe_2. **(E)** Capacitance vs. electric field of bilayer WTe_2, showing hysteretic behavior indicative of ferroelectric polarization. Arrows indicate direction of sweep. (F) Colormap showing the *difference* of the solid and dashed curves in (E).

have used sensitive quantum capacitance techniques to measure and compare the gaps of monolayer and bilayer WTe_2. We identified a strong and unanticipated temperature dependence in the gap of monolayer WTe_2, which may point to many-body (i.e. excitonic) effects. We have also measured a smaller, electric-field induced minimum in the (non-topological) bilayer system, which may be indicative of a gap opening but may also be representative of the electron-hole compensation point (Fig. 2). Serendipitously, we affirmed that the capacitance technique is especially good at measuring layer polarization effects in the bilayer system[6] and measured *ferroelectric* behavior in bilayer WTe_2 that was consistent with the only other experimental paper about bilayer WTe_2 ferroelectricity[7]. We studied its density dependence and compared the capacitance to a model derived from the "tilted Dirac fermion" model of the electronic structure.

Graphene on Antiferromagnetic (Mott) Insulator $RuCl_3$. We have recently studied graphene coupled to the magnetic insulator $RuCl_3$, which is an antiferromagnet below 7K. It has the interesting additional property that it is thought to be a "Kitaev quantum spin liquid" between about 80K and 7K, which may host exotic excitations such as chiral edge Majorana modes[8]. Our preliminary data on a back-gated BN/ $RuCl_3$,/graphene/BN (bottom to top) show some interesting results (Fig. 2). First of all, the graphene remains relatively high quality compared to the G-CrI_3 and G-CST, such that we can start to see the emergence of broken-symmetry quantum Hall states (ν=1) at B<9T. Second, the transport data show an interesting feature when the graphene is hole-doped: there is a peak in R_{xx} vs. temperature at a (gate-dependent) temperature of around 40 K (Fig. 2C,D). Investigation of this phenomenon is ongoing.

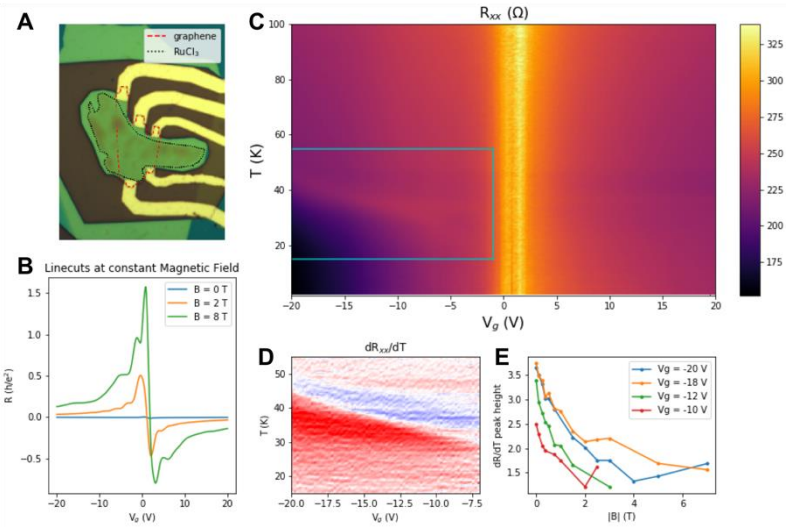

Fig. 3. Transport data on a graphene-$RuCl_3$ device. **(A)** Optical micrograph of device. **(B)** Quantum Hall indicates good quality of graphene preserved. **(C)** Longitudinal resistance R_{xx} and **(D)** dR_{xx}/dT of graphene vs. temperature and gate voltage. The interesting feature, enclosed by the blue box, shows a peak that emerges around 20-40 K (depending on gate voltage). This feature may be indicative of a new magnetic transition. **(E)** The peak height is diminished with increasing perpendicular magnetic field.

Future Plans

In the upcoming year, we plan to focus more effort on scanning tunneling microscopy (STM) studies of the graphene-vdW magnetic insulator structures. Transport studies of G-CST and G-CrI_3 in my own group, and of G-CGT, G-CrI_3, and G-$CrCl_3$ by groups at Stanford, Columbia, and other physics departments, have not yielded convincing evidence of induced magnetism in the graphene in these bulk measurements. At the same time, our efforts at Carnegie Mellon towards measuring air-sensitive van der Waals heterostructures using STM have been immediately successful. There is great potential for answering many questions about the nature

of the magnetic proximity effect in graphene-vdW MI structures -- if one even exists -- by using a local, atomically-precise spectroscopic probe. We also plan to study the QAHE edge states in twisted bilayer graphene[2] using STM/STS.

References

1. Zhang, J., Zhao, B., Yao, Y. & Yang, Z. Robust quantum anomalous Hall effect in graphene-based van der Waals heterostructures. *Phys. Rev. B* **92**, 165418 (2015).
2. Serlin, M. *et al.* Intrinsic quantized anomalous Hall effect in a moir\'e heterostructure. *ArXiv190700261 Cond-Mat* (2019).
3. Alicea, J. New directions in the pursuit of Majorana fermions in solid state systems. *Rep. Prog. Phys.* **75**, 076501 (2012).
4. Tang, S. *et al.* Quantum spin Hall state in monolayer 1T'-WTe_2. *Nat. Phys.* **13**, 683–687 (2017).
5. Lüpke, F. *et al.* Proximity-induced superconducting gap in the quantum spin Hall edge state of monolayer WTe$_2$. *ArXiv190300493 Cond-Mat* (2019).
6. Hunt, B. M. *et al.* Direct measurement of discrete valley and orbital quantum numbers in bilayer graphene. *Nat. Commun.* **8**, 948 (2017).
7. Fei, Z. *et al.* Ferroelectric switching of a two-dimensional metal. *Nature* **560**, 336 (2018).
8. Kasahara, Y. *et al.* Majorana quantization and half-integer thermal quantum Hall effect in a Kitaev spin liquid. *Nature* **559**, 227–231 (2018).

Publications

"Tuning Ising superconductivity with layer and spin–orbit coupling in two-dimensional transition-metal dichalcogenides", Sergio C. Barrera, Michael R. Sinko, Devashish P. Gopalan, Nikhil Sivadas, Kyle L. Seyler, Kenji Watanabe, Takashi Taniguchi, Adam W. Tsen, Xiaodong Xu, Di Xiao, Benjamin M. Hunt. *Nat. Comm.* **9**, 1427 (2018)

"Electron transport in multi-dimensional fuzzy graphene nanostructures", Raghav Garg, Devashish P. Gopalan, Sergio C. de la Barrera, Noel T. Nuhfer, Benjamin M. Hunt, Tzahi Cohen-Karni. *Nano Letters* **19**, 5335 (2019).

"Proximity-induced superconducting gap in the quantum spin Hall edge state of monolayer WTe_2", Felix Lüpke, Dacen Waters, Sergio C. de la Barrera, Michael Widom, David G. Mandrus, Jiaqiang Yan, Randall M. Feenstra, Benjamin M. Hunt. *arXiv*:1903.00493 (2019); *in review.*

"Towards a magnetic proximity effect in a van der Waals heterostructure", Devashish P. Gopalan. Ph.D. thesis, Carnegie Mellon University (2019).

Tuning from Quantum Anomalous Hall to Topological Hall Effect in a Magnetic Topological Insulator sandwich device

Moses H. W. Chan (PI), Cui-Zu Chang and Chaoxing Liu

Department of Physics, The Pennsylvania State University

Program Scope

The major goals of this project are to explore the topological magnetoelectric effect, as well as other topological phenomena, including topological Hall effect, in the magnetic topological insulator-based sandwich heterostructures and to develop high Chern number quantum anomalous Hall state in the magnetic topological insulator and normal insulator superlattices.

The goal of the theoretical part of this project is to understand topological electronic band structures and explore topological transport and optical phenomena in magnetically doped topological insulator heterostructures.

Recent Progress

We fabricated a TI-based sandwich structure with an undoped TI layer (5 QL (Bi, Sb)$_2$Te$_3$ layers) inserted between two magnetic TI layers (two 3QL Cr-doped (Bi,Sb)$_2$Te$_3$ layers with the same Cr concentration). Such a 3-5-3 sandwich heterostructure has the following advantages: (*i*) The nonmagnetic TI layer can serve as a spacer to separate the magnetic exchange interaction between the two magnetic TI layers. As a result, the influence of the Dzyaloshinskii-Moriya (DM) interaction can be maximized since the magnetic moments in each magnetic TI layer interacts only with their own surface state (SS). (*ii*) Both the top and bottom SSs are separately gapped by the magnetization in the two magnetic TI layers, thus making the QAH effect possible.

When the bottom gate $V_g = V_g^0 =$

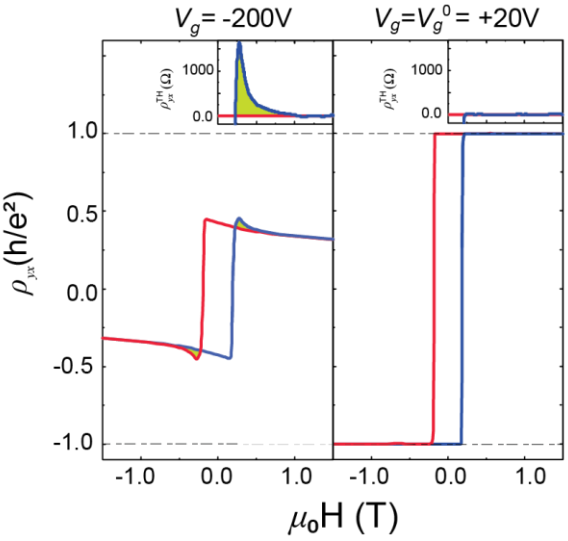

Fig.1. Gate-induced crossover from the QAH to TH effect. Magnetic field $\mu_0 H$ dependence of the Hall resistance ρ_{yx} at V_g = -200 V (left) and $V_g = V_g^0$ = +20 V (right). When V_g is tuned away from V_g^0, ρ_{yx} deviates from the quantized value (i.e., h/e^2) and a "hump" feature shaded in green which is known as the TH effect appears. Insets show the TH resistance ρ_{yx}^{TH}, which is subtracted using the following method: the offset resistance of ρ_{yx} when the external $\mu_0 H$ is swept upward and downward. Blue (red) curve represents the process for increasing (decreasing) $\mu_0 H$.

+20 V, the sample displays a perfect QAH state: at zero magnetic field, $\rho_{yx}(0) = \pm h/e^2$ and $\rho_{xx}(0) < 1\ \Omega$ (Fig. 1, right). The Hall curves under upward and downward magnetic field ($\mu_0 H$) sweeps completely overlap when $\mu_0 H > \mu_0 H_c$ ($\mu_0 H_c$ is the coercive field). When V_g is tuned to -200 V, a number of hole carriers are injected into the sample and dissipative channels are introduced. $\rho_{yx}(0)$ thus deviates from h/e^2(Fig. 1, left). Intriguingly and a "hump" feature within a range of a fraction of a Tesla above $\mu_0 H_c$ appears in ρ_{yx} curves (green shadow area). In other words, the Hall curve under downward $\mu_0 H$ sweep does not overlap with that under upward $\mu_0 H$ sweep when $\mu_0 H > \mu_0 H_c$. The "hump" feature observed here is usually interpreted as a signature of the TH effect and considered as strong evidence for the existence of chiral magnetic textures in the real-space [1, 2, 3]. Therefore, by utilizing the bottom electrostatic gating effect on such magnetic/nonmagnetic/magnetic TI sandwich heterostructures, our experiment demonstrated a clear crossover between the QAH and TH effect.

In order to understand the experimental observations, we propose a physical picture based on the emergence of chiral spin textures around the $\mu_0 H_c$ regime. The observed "hump" structure in the ρ_{yx} has been observed in a variety of noncollinear magnetic systems, particularly magnetic skyrmion systems [1, 2, 3]. Therefore, we theoretically study the off-diagonal components of spin susceptibility, which directly determine the strength of the DM interaction in our system, based on a model consisting of both surface states and bulk states [4]. Interestingly, our results on the off-diagonal spin susceptibility reveal a similar dependence on the Fermi energy as found in the TH resistance extracted from the experiment data. Our results also suggest that the system is still in the ferromagnetic ground state, but chiral spin texture can appear at the domain walls during the magnetization reverse process at the coercive field. Thus, our transport experiment and theoretical modeling together imply that the chiral edge state of the QAH effect may coexist with the chiral magnetic domain walls in magnetic TI-based heterostructures.

Future Plans

(*i*) Optimize the growth parameters for the magnetic TI/normal insulator superlattice and realize the high Chern number QAH state.

(*ii*) Explore the axion insulator state in antiferromagnetic topological insulator $MnBi_2Te_4$ with odd number layers.

(*iii*) Optimize the growth parameters for MnBi2Te4 and realize the QAH and axion insulator state.

On the theoretical side, our recent theoretical calculations suggest that magnetic resonance can induce a "pseudo-electric field" in our TI-based sandwich structure and give rise to a giant current response with its magnitude several orders of magnitude larger than that of the topological magnetoelectric effect in the axion insulator phase. This provides a new method to demonstrate the axion insulator phase through magnetic resonance. We will continue the study of

electromagnetic response in magnetic TIs for both the cases of anti-ferromagnetism and ferromagnetism and extend our theory to the nonlinear response regime.

References

1. K. Yasuda, R. Wakatsuki, T. Morimoto, R. Yoshimi, A. Tsukazaki, K. S. Takahashi, M. Ezawa, M. Kawasaki, N. Nagaosa, and Y. Tokura, *Nat. Phys.* **12**, 555 (2016).
2. N. Nagaosa and Y. Tokura, *Nat. Nanotechnol.* **8**, 899 (2013).
3. C. Liu, Y. Y. Zang, W. Ruan, Y. Gong, K. He, X. C. Ma, Q. K. Xue, and Y. Y. Wang, Dimensional crossover-induced topological Hall effect in a magnetic topological insulator. *Phys. Rev. Lett. 119, 176809 (2017).*
4. C. X. Liu, H. Zhang, B. H. Yan, X. L. Qi, T. Frauenheim, X. Dai, Z. Fang, and S. C. Zhang, *Phys. Rev. B* **81**, 041307 (2010).

Publications

1. F. Wang, D. Xiao, W. Yuan, J. Jiang, Y.-F. Zhao, L. Zhang, Y. Yao, B. Dong, W. Liu, Z. Zhang, **C. Liu**, J. Shi, W. Han, **M. H. W. Chan**, N. Samarth, and **C.-Z. Chang**, "Observation of Interfacial Antiferromagnetic Coupling between Magnetic Topological Insulator and Antiferromagnetic Insulator" ***Nano Lett.*** 19, 2945-2952 (2019)
2. S. H. Lee, Y. Zhu, Y. Wang, L. Miao, H. Yi, T. Pillsbury, S. Kempinger, J. Hu, C. A. Heikes, P. A. Quarterman, W. Ratcliff, J. A. Borchers, H. Zhang, X. Ke, D. Graf, N. Alem, **C.-Z. Chang**, N. Samarth, and Z. Mao, "Spin scattering and noncollinear spin structure-induced intrinsic anomalous Hall effect in antiferromagnetic topological insulator $MnBi_2Te_4$" ***Phys. Rev. Research*** 1, 012011(R) (2019).
3. J. Yu, J. Zang, **C.-X. Liu, "**Magnetic-Resonance-Induced Current Response in Axion Insulators" ***Phys. Rev. B*** 100, 075303 (2019).
4. J. Yu, **C.-X. Liu** , **"**Interaction and Impurity Effect on Surface Majorana Flat Bands in j=3/2 Superconductors with Singlet-Quintet Mixing" ***Phys. Rev. B*** 98, 104514 (2019).
5. J. Yu, R. Roiban, **C.-X. Liu**, "2+1D Emergent Supersymmetry at First-Order Quantum Phase Transition" ***Phys. Rev. B*** 100, 075153 (2019)
6. J. Jiang, D. Xiao, F. Wang, J.-H. Shin, D. Andreoli, J. Zhang, R. Xiao, Y.-F. Zhao, M. Kayyalha, L. Zhang, K. Wang, J. Zang, **C. Liu**, N. Samarth, **M. H. W. Chan**, and **C.-Z. Chang**, "Crossover of Quantum Anomalous Hall to Topological Hall Effect in Magnetic Topological Insulator Sandwich Heterostructures" *under review by **Nat. Mater***. (Primary support)
7. M. Kayyalha, D. Xiao, R. Zhang, J. Shin, J. Jiang, F. Wang, Y.-F. Zhao, L. Zhang, K. M. Fijalkowski, P. Mandal, M. Winnerlein, C. Gould, Q. Li, L. W. Molenkamp, **M. H. W. Chan**, N. Samarth, and **C.-Z. Chang, "**Non-Majorana Origin of the Half-Quantized Conductance

Plateau in Quantum Anomalous Hall Insulator and Superconductor Hybrid Structures" Under review by ***Science***.

8. J.-X. Zhang, D. Andreoli, J. Zang, **C.-X. Liu, "**Topological Hall Effect in Magnetic Topological Insulator Films" Under review of ***Phys. Rev. B*** (2019). (Primary support)
9. J.Y. Liu, J. Yu, J.L. Ning, L. Miao, L.J. Min, K.A. Lopez, Y.L. Zhu, H.M. Yi, T. Pillsbury, Y. B. Zhang, Y. Wang, J. Hu, H.B. Cao, F. Balakirev, F. Weickert, M. Jaime, K. Yang, J.W. Sun, N. Alem, V. Gopalan, **C.Z. Chang**, N. Samarth, **C.X. Liu**, R.D. McDonald, and Z.Q. Mao, "Surface chiral metal in a bulk half-integer quantum Hall insulator" Under review by ***Sci. Adv.***
10. X. Wu, D. Xiao, C.-Z. Chen, J. Sun, L. Zhang, **M. H. W. Chan**, N. Samarth, X. C. Xie, X. Lin, and **C.-Z. Chang**, "Scaling Behavior of the Quantum Phase Transition from a Quantum Anomalous Hall Insulator to an Axion Insulator", Under review by ***Phys. Rev. Lett.***
11. H. Fu, **C.-X. Liu**, B. Yan, "Exchange Bias and Quantum Anomalous Hall Effect in the $MnBi_2Te_4$-CrI_3 Heterostructure", Under review by ***Sci. Adv.***
12. X. Wu, X. Liu, R. Thomale, **C.-X. Liu**, "High-Tc Superconductor Fe(Se,Te) Monolayer: an Intrinsic, Scalable and Electrically-tunable Majorana Platform", Under review by ***Phys. Rev. Lett.***
13. J.-X. Zhang, **C.-X. Liu**, "Disordered Quantum Transport in Quantum Anomalous Hall Insulator-Superconductor Junctions", Under review by ***Phys. Rev. B (Rapid).***

Session 5

Revealing Collective Spin Dynamics Under Device-Operating Conditions to Enhance Tomorrow's Electronics

Valentina Bisogni, National Synchrotron Light Source II, Brookhaven National Laboratory, USA, bisogni@bnl.gov

Program Scope

Collective spin excitations (CSE) in quantum materials provide a revolutionary alternative for devices with improved performances and energy-efficiency, as they permit the transfer of information without any movement of charge, thus eliminating the dominant source of energy dissipation. Understanding how to manipulate CSE would provide a foundation for the next generation of energy-efficient electronic devices. A promising direction is to undertake the study of the microscopic spin dynamics in technologically relevant quantum materials under device-operating conditions. This FWP focuses on utilizing soft X-ray Resonant Inelastic Scattering (RIXS) and achieve an unprecedented insight into the material properties and the behavior of the CSE when subject to device-relevant perturbations of applied current, electric-field, and temperature gradient.

Recent Progress

The first year of the project focused on the study of fundamental electronic properties and CSE in systems with potential impact for magnonic-applications such as Cu_2OSeO_3, Fe thin films and $LiCuVO_4$ by using RIXS.

Understanding the quantum nature behind the skyrmion material Cu_2OSeO_3: Skyrmions - nano-sized, topological spin objects - are raising a large interest in the context of novel technologies thanks to their mobility in response to low current and electric fields, making them very appealing for energy-efficient applications. In this respect, generating skyrmions in insulators is particularly attractive because of the reduced heat dissipation and fast switching responses. The first observation of skyrmions in an insulating antiferromagnet was in Cu_2OSeO_3 (CSO) [1] (see

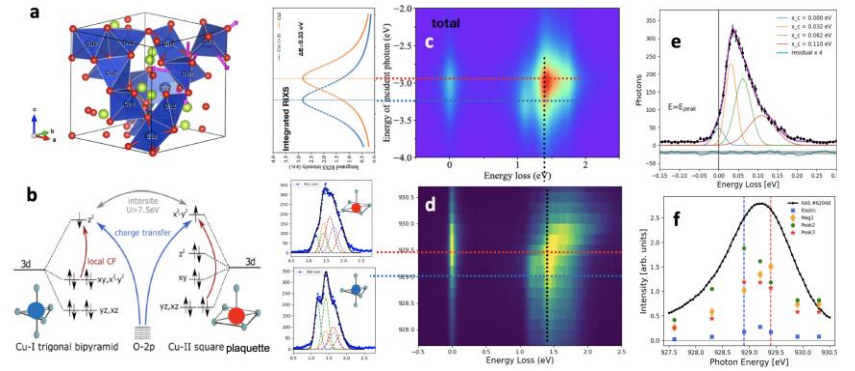

Figure 1: **a**. Crystal structure of CSO. **b**. Sketch of the 3d energy levels for the two differently coordinated Cu sites, the bipyramid Cu-I, and the plaquette Cu-II [5]. **c**. RIXS calculation as a function of the excitation energies **d**. Measured RIXS energy map at Cu L_3 edge and example of two decomposed RIXS spectra (left) corresponding to the resonant excitation energies for Cu-I (blue line) and Cu-II (red line). **e**. Decomposition of high-resolution RIXS spectrum into four low-energy gaussians. **f.** Peak intensity of the individual gaussian contribution as a function of excitations energy.

Fig. 1a). Despite their "macroscopic" dimensions (stretching over several atomic units), the formation of skyrmions in CSO stems from a delicate balance between different quantum interactions, i.e. the magnetic interactions in terms of super-exchange coupling constants and the Dzyaloshinskii-Moriya interaction. Understanding such interactions at a fundamental level is thus of crucial importance to unravel the quantum nature of the skyrmion formation process.

To address this need, we proposed using RIXS to resolve the fine structure of the magnetic exchange interactions behind the magnetic building blocks leading to the skyrmion lattice. Specifically, our goal was to exploit the resonant character of RIXS to disentangle the contribution of the two inequivalent Cu sites present in the CSO unit cell – Cu-I and Cu-II (Fig. 2a) - to the magnetic spectrum and thus understand their role in the short-range magnetic interactions. This would take the field beyond the model extracted by inelastic neutron scattering studies [2], which cannot distinguish the two sites. Combining RIXS energy maps with DFT+LDA calculations for the system eigenstates and eigenvalues and a RIXS cross section calculation for our specific geometries (all calculations performed by Yilin Wang, BNL), we succeeded in identifying the direct fingerprints of the Cu-I (pyramid) and Cu-II (plaquette) resonant energies for the first time. This was possible by interpreting from the RIXS spectra the intra-band *d-d* orbital excitations associated with each Cu site (Fig. 1c-d). The outcome of this part of the study reveals a splitting of ~ 0.5 eV between the Cu-I and Cu-II resonant energies.

With this information at hand, we moved onto the second part of our RIXS study looking at low-energy magnetic excitations as a function of the incident energy. Below 100 meV, we successfully detected with RIXS multiple low energy excitations in CSO [3,4]. Due to overlapping character of such excitations, it is necessary to perform a decomposition analysis using four gaussian peaks (Fig. 1e). From this analysis, we find a strong variation in the peak intensity while tuning the incident energies across the Cu-I and the Cu-II resonances (Fig. 1f). Also, different trends have been found for different peaks. In collaboration with the theory group headed by Jeroen van den Brink from IFW Dresden, we are currently working on understanding the exact nature of these excitations.

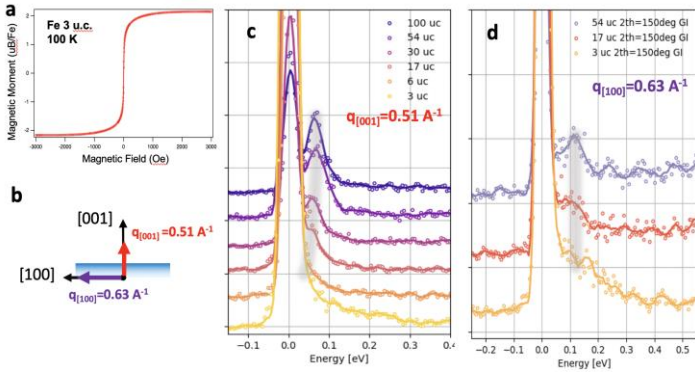

Figure 2: Magnetization curve of 3uc Fe thin film. b. Experimental configurations of ***q*** transferred. c. RIXS spectra versus Fe thickness for q=0.51 Å^{-1} along [001] (⊥ to film surface). c. RIXS spectra versus Fe thickness for q=0.63 Å^{-1} along [100] (// to film surface).

<u>Spin excitations in ultra thin films of Fe</u>***:*** In order to effectively use collective spin excitation in magnonic applications, it is essential to gain control over these modes and ultimately realize all the functionality required for a device utilizing spin waves. Electric field control is the preferred route to manipulate spin waves in miniaturized devices, as it can be integrated in a much easier way than magnetic field. A recently published work predicts a

dramatic suppression of the spin-wave energy by reducing the exchange stiffness parameter down to 80% when the electric field is applied across few unit cells of Fe metal [6]. Spin excitations in single crystal of Fe have been reported by inelastic neutron scattering roughly fifty years ago [7]. The proposed study instead requires Fe metal in the ultra-thin form.

In collaboration with the group headed by Fred Walker from Yale University, we worked on several Fe thin films with thicknesses of 100, 54, 30, 17, 6 and 3uc (uc=unit cell). Metallic films have been synthetized with the targeted thicknesses showing a magnetization comparable to the bulk (Fig. 2a). RIXS measurements on Fe thin films revealed a considerable sensitivity to the spin excitations and confirmed their presence in all the films. Interestingly, our measurements performed with a momentum along [001] (Fig. 2b) display a strong softening of the spin-excitation versus thickness, as a possible effect of confinement (Fig. 2c). Instead, our measurements performed with a momentum along [100] display a bulk-like behaviour for all thicknesses (Fig. 2d). This finding represents a very intriguing and exciting result for magnons behaviour in confined thin films in general.

Evidence of exotic quadrupolar spin excitations in $LiCuVO_4$: Transport properties of low-dimensional magnetic materials can potentially be employed in magnonic applications with enhanced performances. A particularly interesting case is the spin nematic phase of frustrated spin-1/2 J_1-J_2 Heisenberg chains, which is dominated in the ground state by bound pairs of magnons intermediated by quadrupolar correlations [8]. Such bound-magnons, or quadrupolar modes, could contribute to the spin transport, according to recent theoretical studies [9], and enhance the process efficiency owing to the fact that bound-magnons carry S=2.

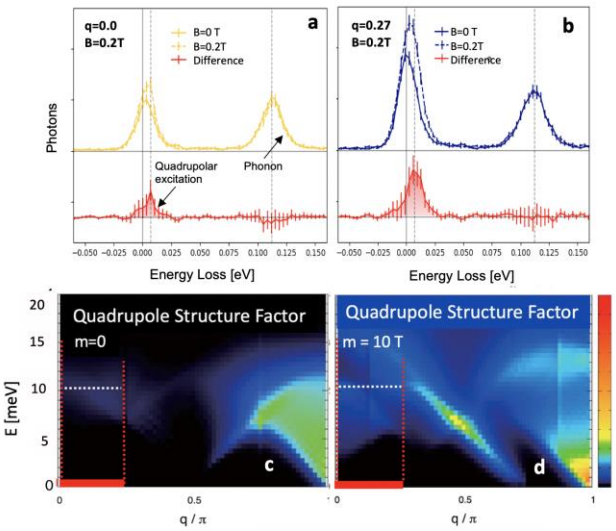

Figure 3: **a-b**. O K RIXS data at B=0.2T (dashed line) compared with spectra measured at B=0 (solid line), for q=0 (**a**) and q=0.27 (**b**) r.l.u. Shaded red area represent the spectral weight enhanced by the application of B. **c**. Quadrupolar structure factor calculated for a frustrated spin-1/2 Heisenberg chain at zero magnetic field m=0, and **d.** at the presence of magnetic field m>0 [12]. The red box identifies the ***q*** region explored with RIXS.

Under the application of magnetic field, $LiCuVO_4$ is one of the main candidates for the realization of spin nematicity. However, the mechanism that drives the system into such a phase, possibly based on quadrupolar excitations, is hard to be detected given that multipolar *hidden* orders and excitations are not accessible with 'conventional' dipolar techniques, such as x-ray diffraction and inelastic neutron scattering. Moreover, at zero field the system is expected to still hold quadrupolar fluctuations (Fig. 3a), competing with spinon and multispinon excitations [10], despite the fact that the nematic phase is only stabilised at high magnetic field.

It has been recently proposed that RIXS is sensitive to *hidden* orders and to multipolar excitations [11]. We planned therefore to use RIXS to investigate $LiCuVO_4$, looking for the first evidence of quadrupolar excitations. O K RIXS measurements with unprecedented energy resolution displays a residual, non-dispersive component at an energy loss of ~ 10 meV (Fig. 3a-b), consistently with calculated behaviour for the quadrupolar structure factor (Fig.3c). Such a mode gets enhanced while applying a magnetic field of 0.2T, while the phonon contributions at higher energies remain unperturbed. This result is in line with the enhanced spectral weight obtained in the quadrupolar structure factor at the presence of B (Fig. 3d), thus supporting the interpretation of our result as quadrupolar spin excitations.

Future Plans

We plan to expand the investigation of spin excitations in Fe thin films under electric field through our unique sample environment *Opera*, and verify the possibility of manipulating the exchange interactions in this system. Building on our successful detection of spin-waves in Fe as a function of thickness, we will extend our study of magnons to yttrium iron garnet and follow their changes as a function of strain and thickness. Such material is in fact widely used for magnonics application, thus it is fundamental to understand its magnetic structure in detail. Finally, we plan to investigate the 1D spin chain Sr_2CuO_3 and study with RIXS the dispersion of magnetic excitation during the spinon mediated transport under spin Seebeck effect, i.e. under the presence of thermal gradient, as demonstrated in [13].

References: [1] Seki et al., Science 336, 198-201 (2012); [2] Portnichenko et al., Nat. Comm. 7, 10725 (2016); [3] Janson et al., Nat. Comm. 5, 5376 (2014); [4] Versteeg et al., arXiv:1908.10279; [5] Versteeg et al., Phys. Rev. B 94, 094409 (2016); [6] Wang et al., Sci. Rep. 6, 31783 (2016); [7] Collins et al., Phys. Rev. 179, 417 (1969); [8] Hikihara et al. Phys. Rev. B 78, 144404 (2008); [9] Onishi, J. Mag. and Mag. Mat., 479, 88 (2019); [10] Enderle et al., Phys. Rev. Lett. 104, 237207 (2010); [11] L. Savary et al, arXiv 1506.04752 (2015); [12] Onishi, J. Phys. Soc. Jpn. 84, 083702 (2015). [13] Hirobe et al., Nat. Phys. 13, 30 (2017).

Publications

No paper has been published during the first year of the funded research project. Manuscripts on the quadrupolar spin excitations in $LiCuVO_4$ and on the spin-wave excitation in Fe versus thickness are under preparation.

Non-volatile active control of spin transport using interfaces with molecular ferroelectrics

Xiaoshan Xu

Department of Physics and Astronomy, University of Nebraska Lincoln

Program Scope

Generation, detection, and manipulation of spin current, as key aspect of spintronics, are essential for the next-generation technology for information storage and computing. While the generation and detection of spin current have been established, active control of spin current, particularly using non-magnetic means, which is much desired for device applications, is far from being fully investigated. Recent development of ferroelectric control of magnetoresistance of spin valves, suggests a route for electric-field control of spin current, with additional advantage of non-volatility [1–4]. The overarching goal of this project is to realize the non-volatile electric-field control of spin transport across interfaces and in spin-orbit coupled materials, which is crucial for the operations in spin-based circuitry. Particularly, this project exploits non-volatile control using interfaces with ferroelectrics in both spin-polarized charge current and in non-magnetic spin-orbit coupled materials, especially the recently discovered molecular ferroelectrics that have large polarizations and small switching fields[5]. The specific aims are 1: elucidate the effect of polarization on the spin transport through the ferromagnet/molecular ferroelectrics interfaces; 2: gain fundamental understanding on the effect of polarization on the charge/spin conversion in spin-orbit coupled materials at the interfaces with molecular ferroelectrics. 3: characterize spin transport in crystalline molecular ferroelectrics.

Recent Progress

A. Voltage controlled spin transport in multiferroic tunnel junction

The effect of ferroelectric polarization reversal could significantly impact the spin transport by altering the interfacial crystal and electronic structures due to the atomic displacement during the polarization reversal, or by changing the energy landscape of the multilayer structure due to the electrostatic effect of the polarization. The ferroelectric control of spin transport employing the change of interfacial crystal and electronic structures, has been demonstrated experimentally[1,2,6]. On the other hand, ferroelectric control of spin transport employing the electrostatic effect (energy landscape change) due to the polarization reversal, has been more difficult to demonstrate since the ferroelectric polarization reversal always involves displacement of atoms which roughly scales with the polarization. Organic ferroelectric materials appear more suitable for studying this effect because of the weak structural coupling at the organic/inorganic interfaces and the small dielectric constant of organic materials that enable a large depolarization field and large electric potential shift and maximize the electrostatic effect. Compared with inorganic materials, organic semiconductors in general are also appealing for spintronics because of the weak spin-orbit coupling and hence the long spin lifetime of charge carriers[7,8], as well as the flexibility and low cost.

Recently discovered molecular ferroelectric materials offer a great opportunity in studying electrostatic mechanism for the ferroelectric control of spin transport in organic spin valves.[5,9–11] In particular, croconic acid, with a chemical formula $C_5O_5H_2$, exhibits a large polarization 25 $\mu C/cm^2$, which is comparable with that of $BaTiO_3$.[5] The unique origin of spontaneous polarization, i.e., the ordered hydrogen bonds and the distorted π electron cloud[12], suggests a minimal change to interfacial crystal structure upon polarization reversal.

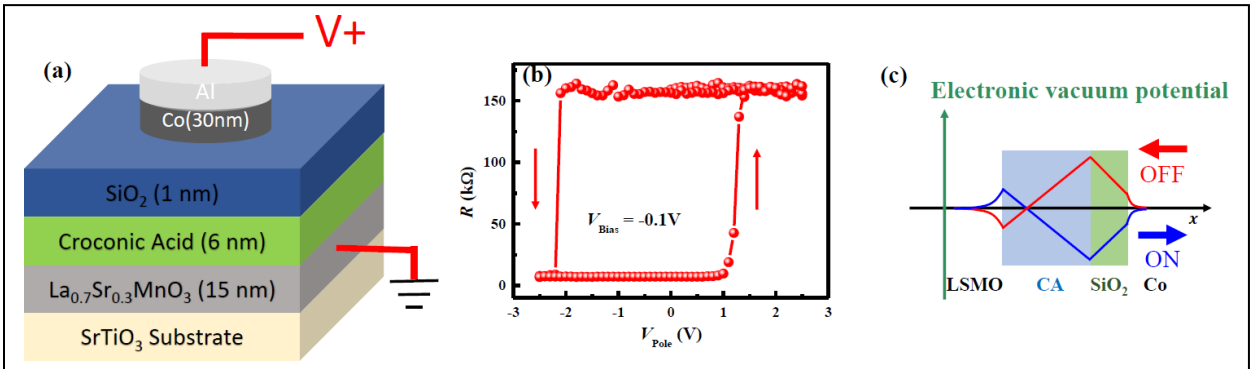

Figure 1 (**a**) Schematic device structure. (**b**) Resistances as a function of V_{Pole} measured at V_{Bias} = -0.1 V. **(c)** Schematics of the vacuum potential across the junction for electrons for both the ON and OFF states of the junction; the arrows indicate polarization directions of CA.

As shown in Fig. 1(a), LSMO/CA/SiO_2/Co junctions have been constructed to study the transport of spin polarized current, where LSMO stands for $La_{0.7}Sr_{0.3}MnO_3$ and croconic acid (CA) is the molecular ferroelectric layer. The resistance measured at a small bias voltage (V_{Bias}) can be controlled by applying a poling voltage (V_{Pole}) before the measurement. Figure 1(b) shows that the resistance of the junction can be switched between a high resistance (OFF) state and a low resistance (ON) state using a +2.5 V and a -2.5 V poling voltage respectively, where the OFF/ON ratio is about 4000%. These observations are consistent with the scenario of tunneling resistance that can be controlled by the polarization of the ferroelectric barrier. In general, a ferroelectric material shifts the vacuum potential due to its polarization and the corresponding electric field. However, when a ferroelectric layer is sandwiched by metal electrodes, the vacuum potential change is minimized due to the screening effect of the charge carriers in the electrodes. On the other hand, as shown in Fig. 1(c), because of the insertion of the SiO_2 layer, the screening effect of the Co electrode is greatly reduced. Hence, the electric polarization of CA generates an uneven vacuum potential profile which affects the energy barrier for the electron tunneling across the junction. By switching the electric polarization, the vacuum potential profile and the tunnel barrier can be switched. In particular, Fig. 3(a) shows that when the polarization of the CA layer is pointing toward LSMO, the tunnel barrier is significantly higher, consistent with the observed OFF state when a positive 2.5 V poling voltage is applied.

Besides tunnel electroresistane (TER), tunnel magnetoresistance (TMR) is expected in these junctions due to the two ferromagnetic electrodes, i.e., the resistance of the junction is expected to be different when the alignment of the magnetization of the two ferromagnetic electrodes are different. As shown in Fig. 2(a) and (b), the resistance of the junction changes with magnetic field with a clear hysteresis. The two magnetic fields where the resistance show rapid changes are consistent with the magnetic coercive fields of Co and LSMO. The observation of both TER (on the order of 1000%) and TMR (on the order of 10%) makes the LSMO/CA/SiO_2/Co structure a multiferroic tunneling junction (MFTJ).

What's more interesting is that TMR of the MFTJ differ dramatically when the MFTJs are in the ON from that of the OFF states. For example, for measurement voltage V_{Bias} =1 V, both the ON and OFF states show negative TMR, which is typical for the LSMO/organic space/Co type spin valves. For V_{Bias} =-1 V, however, while the TMR of the ON state remains negative, the TMR of the OFF state becomes positive, which is unusual for similar spin valves with LSMO

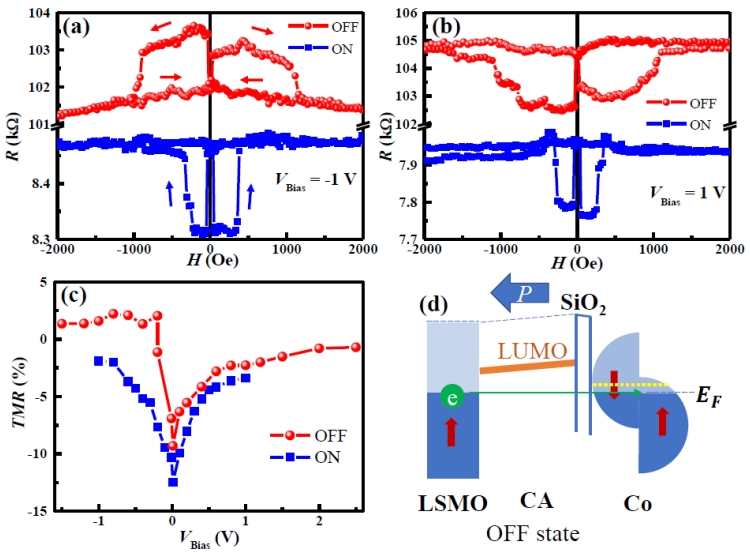

Figure 2 TMR under (**a**) V_{Bias} = -1 V and (**b**) V_{Bias} = +1V after applying V_{Pole} = +2.5 V and V_{Pole} = –2.5 V respectively. The arrows indicate the measurement sequence. (**c**) TMR as a function of V_{Bias} for both ON and OFF states of the junction. **(d)** energy diagram illustrating the shift of Fermi energy in the OFF states. The thin arrows indicate the tunneling process.

and CO electrodes. The dependence of TMR on V_{Bias} is displayed in Fig. 2(c) for both the ON and OFF states. Again, for the ON state, the TMR(V_{Bias}) relation resembles that of typical LSMO/organic space/Co spin valves. On the other hand, for the OFF state, the TMR(V_{Bias}) relation basically changes sign at when V_{Bias} changes sign.

The dramatic change of TMR(V_{Bias}) relation between the ON and the OFF states can be understood as the change of energy landscape that shifts the Fermi energy of interfacial Co relative to its density of states. Since the spin polarization of Co changes with the energy level, it has been observed that the TMR of LSMO/$SrTiO_3$/Co junction changes sign at high V_{Bias} due to the access to the density of states below the Fermi level[13]. In other words, if the Fermi level shifts down, the TMR may change sign at much lower V_{Bias}, as observed in Fig. 2(c).

The shift of Co Fermi level could come from two different effects: electrostatic effect of the CA polarization, or the redox effect of the interfacial Co. In both cases, when a positive V_{Pole} is applied on the MFTJ, a charge depletion that may even turn Co into Co^{2+} occurs in the interfacial Co, which shifts the Fermi energy down and causes the change of spin polarization at the down-shifted Fermi energy. The electron depletion or oxidation has been corroborated by the x-ray absorption spectroscopy study on the Co L_3 edge for the ON and OFF states of the MFTJ.

Besides the realization of non-volatile control of spin transport using molecular ferroelectrics, one intriguing observation in this work is the “spin diode” behavior: in the high resistance state, when the charge current of a certain spin polarization prefers flowing in one direction. Similar to the traditional p/n junction diodes, the turn-on voltage is nonzero but very small (~0.1 V).

B. Ferroelectric switching kinetics of large area croconic acid thin films

Owing to the proton-transfer mechanism, molecular ferroelectric materials have small switching field (20 kV/cm), which is 1-2 orders of magnitude smaller than the oxide ferroelectrics. However, previous work indicates that the switching field is much larger for the thin films compared with that of the bulk[14]. To resolve this controversy and to study the switching mechanism of molecular ferroelectrics, we have studied the ferroelectric switching kinetics of croconic acid films using piezoresponse force microscopy (PFM).

As shown in Fig. 3(a), CA films of 50 nm thickness have been deposited on indium tin oxide (ITO) using physical vapor deposition. Grazing incident x-ray diffraction shows that the films crystalize in the same structure as that of the powder. Hysteresis loops of ferroelectric switching has been measured using PFM to confirm ferroelectricity [Fig. 3(b)].

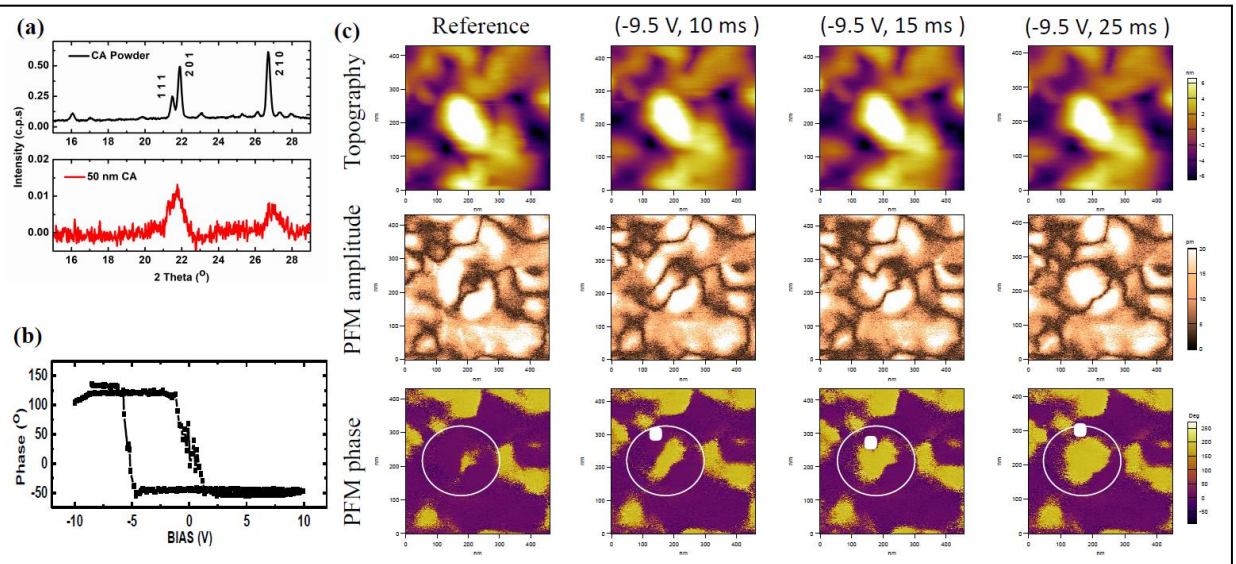

Figure 3 (**a**) X-ray diffraction of CA powder and films. (b) Phase hysteresis of the piezoresponse force microscopy (PFM). (c) Domain witching process of the CA film.

For smaller crystallites (<50 nm) the reversal occurs on the crystallite level, i.e. the whole crystallite reverses the polarization collectively. Therefore, the domain motion was not involved, this type of ferroelectric switching is expected to have large coercivity directly related to the anisotropy energy. For larger crystallites (>100 nm), the polarization reversal is realized through nucleation of opposite domains and the motion of the domain walls. The time scale is on the order of 10-100 ms under the inhomogeneous field generated by a PFM tip, as shown in Fig. 3(a).

These results explain the previously observed much larger coercive field on small croconic acid crystallite, in comparison with that of the bulk.

Future Plans

We will continue studying the charge and spin transport across the molecular ferroelectric/ferromagnetic interfaces, for spacer and electrode parameters. In addition, we will study the transport properties in spin-orbit coupled metals interfaced with molecular ferroelectric materials and the voltage control of the spin transport. We will continue studying the mechanism of growth of the ferroelectric thin films as well as the mechanism of ferroelectric switching, expanding the study to molecular ferroelectric materials other than croconic acid.

Publications

None to report.

References

1. Garcia, V. *et al.* Ferroelectric Control of Spin Polarization. *Science (80-.).* **327**, 1106–1110 (2010).
2. Pantel, D., Goetze, S., Hesse, D. & Alexe, M. Reversible electrical switching of spin polarization in multiferroic tunnel junctions. *Nat. Mater.* **11**, 289–293 (2012).
3. Valencia, S. *et al.* Interface-induced room-temperature multiferroicity in BaTiO3. *Nat. Mater.* **10**, 753–758 (2011).
4. Xu, X. A brief review of ferroelectric control of magnetoresistance in organic spin valves. *J. Mater.* **4**, 1 (2018).
5. Horiuchi, S. *et al.* Above-room-temperature ferroelectricity in a single-component molecular crystal. *Nature* **463**, 789–792 (2010).
6. Zhuravlev, M. Y., Jaswal, S. S., Tsymbal, E. Y. & Sabirianov, R. F. Ferroelectric switch for spin injection. *Appl. Phys. Lett.* **87**, 222114 (2005).
7. McCamey, D. R. *et al.* Spin Rabi flopping in the photocurrent of a polymer light-emitting diode. *Nat. Mater.* **7**, 723–728 (2008).
8. Pramanik S. *et al.* Observation of extremely long spin relaxation times in an organic nanowire spin valve. *Nat. Nanotechnol.* **2**, 216–219 (2007).
9. Horiuchi, S. *et al.* Above-room-temperature ferroelectricity and antiferroelectricity in benzimidazoles. *Nat. Commun.* **3**, 1308 (2012).
10. Noda, Y. *et al.* Few-Volt Operation of Printed Organic Ferroelectric Capacitor. *Adv. Mater.* **27**, 6475–6481 (2015).
11. Horiuchi, S., Kumai, R. & Tokura, Y. Hydrogen-Bonding Molecular Chains for High-Temperature Ferroelectricity. *Adv. Mater.* **23**, 2098–2103 (2011).
12. Seliger, J., Plavec, J., Sket, P., Zagar, V. & Blinc, R. 17O NQR and 13C NMR study of hydrogen-bonded organic ferroelectric croconic acid. *Phys. status solidi B* **248**, 2091–2096 (2011).
13. De Teresa, J. *et al.* Inverse Tunnel Magnetoresistance in Co/$SrTiO_3$/$La_{0.7}Sr_{0.3}MnO_3$: New Ideas on Spin-Polarized Tunneling. *Phys. Rev. Lett.* **82**, 4288–4291 (1999).
14. Jiang, X. *et al.* Room temperature ferroelectricity in continuous croconic acid thin films. *Appl. Phys. Lett.* **109**, 102902 (2016).

Exotic frustration-induced phenomena in artificial spin ice

Principal Investigator: Peter Schiffer, Yale University, New Haven, CT.

Program Scope: This program encompasses studies of lithographically fabricated "artificial spin ice" arrays of nanometer-scale single-domain ferromagnetic islands in which the array geometry results in frustration of the magnetostatic interactions between the islands. Artificial spin ice offers a wide range of opportunities for studying the mechanism by which nature accommodates frustration and accesses physics associated with frustration in ferromagnetic nanostructures. Since the arrays are created lithographically, we can easily vary the array characteristics, including the geometry of the lattice and the level and type of lattice disorder. We can probe both the local properties of the arrays by imaging individual moments, and we can also probe thousands of moments simultaneously, allowing us to gain insight into the collective properties of the system.

In previous work, we have designed frustrated lattices, including those with types of frustration that are inaccessible in natural materials [1]. We have also explored electrical transport through these structures [2-4] and field-induced switching [5]. Current work is focusing on probing and understanding the properties of these new manifestations of frustration [6,7]. We are also studying the process by which the magnetic moments are brought into a low energy collective state through fluctuations of their moments and exploring arrays of more complex nanomagnet shapes in artificial spin ice systems.

Recent Progress: The past two years of this program have focused on several projects within the scope described above, and also included a move with the principal investigator from the University of Illinois at Urbana-Champaign to Yale University. All work has been done in close collaboration with the groups of Chris Leighton at the University of Minnesota and Cristiano Nisoli at Los Alamos National Laboratory, and the work has also included a long-standing collaboration with the group of Nitin Samarth at Penn State University. Dr. Samarth will no longer be a co-investigator on the grant in the newest funding period, although the collaboration is continuing. In this abstract, we focus on two different research thrusts, one in vertex-frustrated systems and one in systems consisting of more complex moment structures.

Vertex-frustrated artificial spin ice

One of the most exciting aspects of artificial spin ice is that we can design the lattice to better understand the nature of frustration and its accommodation. An important focus of our work has leveraged this aspect, to enable the examination of 'vertex-frustrated' systems [1]. In these lattices, the moments of the magnetic islands at every vertex of the lattice have a local magnetic

ground state, but the lattice does not allow the moments in all its vertices to be in a ground state. In other words, the topology of vertex-vertex connectivity prevents all vertices from simultaneously occupying a locally favored state, so that the placement of excited-state vertices is frustrated rather than the orientation of the magnetic moments. For example, the local island geometry of the Shakti lattice has three-fold and four-fold vertices. In the ground state of the system, the four-fold vertices all are in their lowest energy state, but the loop of three-fold vertices circuiting a plaquette cannot close on itself without two of the four such vertices having their moments configured in the first excited state. This is a rather new form of frustration, only conceived and implemented in the context of artificial spin ice, and quite different from that seen in geometrically frustrated magnetic materials.

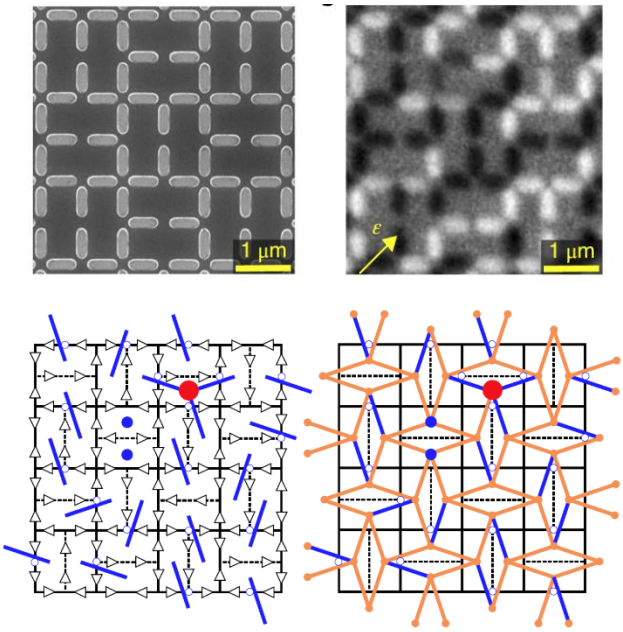

Figure 1. The Shakti lattice, an example of a vertex-frustrated artificial spin ice system. Top row: scanning electron microscope image that shows lattice structure and photoemission electron microscope (PEEM) image that shows moment orientations. Bottom row: schematic of moments including excitations above ground state and mapping of moments and excitations onto a dimer cover model. After reference 6.

We have previously demonstrated that the Shakti system achieves a physical realization of the classic six-vertex model ground state among the vertex states. Furthermore, the mixed coordination of the Shakti lattice leads to effective charges on the three-island vertices, and we also found crystallization of these effective magnetic charges after thermalization [1]. Most recently, we showed that the dynamics of the system, as observed through sequential PEEM imaging, can be characterized as a rare physical realization of a classical thermal topological state [6]. We show that its disordered moment configuration is a topological phase described by an emergent dimer-cover model. Excitations in the system can be characterized as effective topological charges have long lifetimes associated with their topological protection, that is, they

can be created and annihilated only as charge pairs with opposite sign and are kinetically constrained. This manifestation of classical topological order demonstrates that geometrical design in nanomagnetic systems can lead to emergent, topologically protected kinetics.

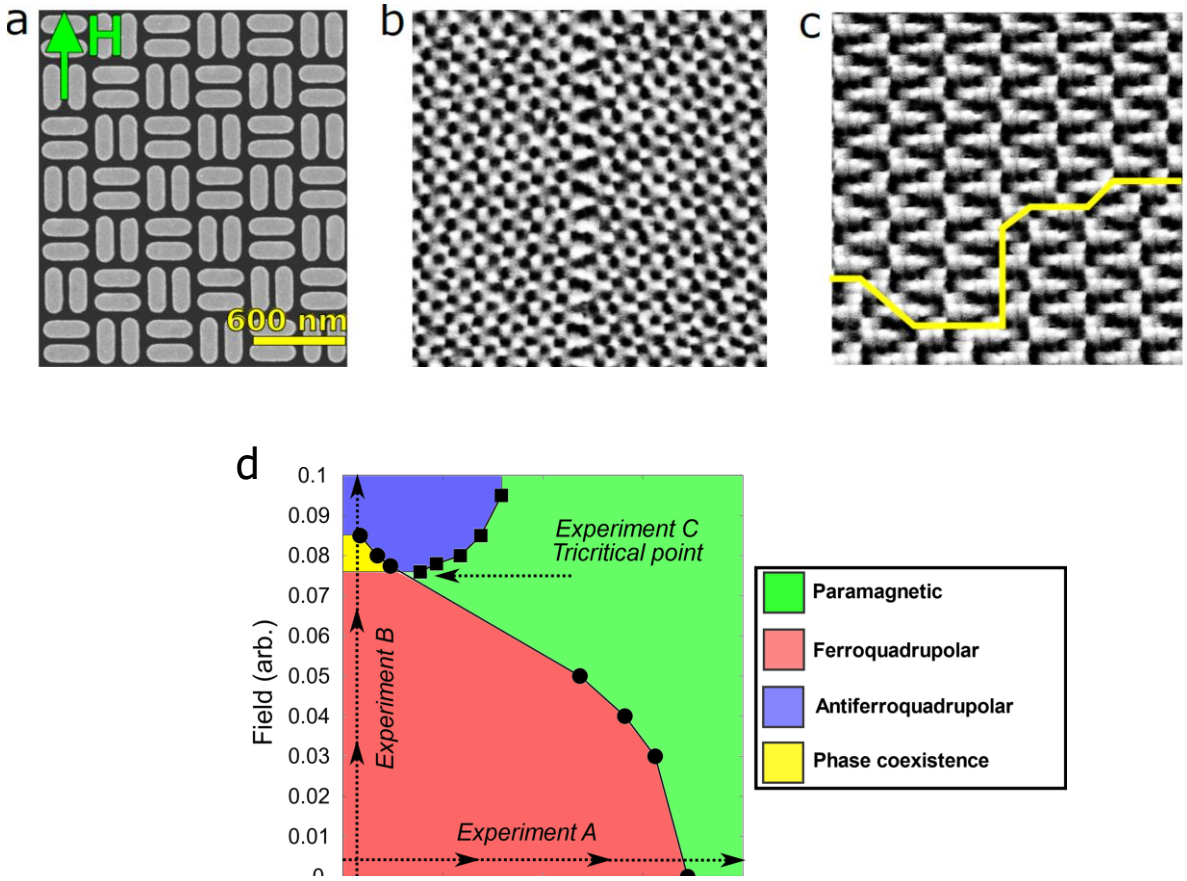

Figure 2. (a) A scanning electron micrograph image of the quadrupole lattice geometry. The system is made up of alternating vertical and horizontal pairs of permalloy nanoislands and a field can be applied in-plane as shown. (b) A magnetic force microscopy image of the long-range ordered ferroquadrupolar phase in this structure, with a central grain boundary separating two ordered regions. (c) A magnetic force microscope image of the long-range ordered antiferroquadrupolar phase in this structure with grain boundary marked in yellow between two equivalent orderings of the moments. (d). Phase diagram of system, with possible future experimental studies indicated with dashed lines. After reference 7.

Lattices of non-bimodal moments

Artificial spin ice research to date has almost entirely focused on bimodal, Ising-like, moments. This focus has arisen primarily because such systems are good representations of simple theoretical models of frustration and because such systems are easy to fabricate and study experimentally. Extending beyond this paradigm, our group has recently demonstrated the

possibilities inherent in a system of a more complex fundamental building block consisting of pairs of stadium-shaped islands shown in figure 2, which can be considered as effective quadrupoles. That system can be described with a Potts model, and we demonstrated it to have a field-dependent phase diagram, analogous to that expected from a Blume-Emery-Griffiths model developed originally for liquid helium, consisting of a ferroquadrupolar state in low field and an antiferroquadrupolar state in high field and a region of mixed phase in between. Such non-bimodal moment systems offer a wide-range of possible physics to explore, again quite separate from that accessible in natural frustrated systems.

Future Plans: Future plans for this research program include the vertex frustrated systems and complex moment systems that are discussed above, especially exploration of new lattice geometries. We are also exploring electrical transport in these systems, as well as the nature of thermalization of the moments near the Curie temperature of the ferromagnetic material.

References and Publications

1. "Deliberate exotic magnetism via frustration and topology", Cristiano Nisoli, Vassilios Kapaklis, and Peter Schiffer, Nature Physics **13**, 200-203 (2017).

2. "Understanding magnetotransport signatures in networks of connected permalloy nanowires" B. L. Le, J.-S. Park, J. Sklenar, G.-W. Chern, C. Nisoli, J. Watts, M. Manno, D. W. Rench, N. Samarth, C. Leighton, P. Schiffer, Physical Review B **95**, 060405(R) – 1-5 (2017).

3. "Magnetic response of brickwork artificial spin ice," Jungsik Park, Brian L. Le, Joseph Sklenar, Gia-Wei Chern, Justin D. Watts, and Peter Schiffer Physical Review B **96**, 024436 – 1-7 (2017).

4. "High-Frequency Dynamics Modulated by Collective Magnetization Reversal in Artificial Spin Ice," Matthias B. Jungfleisch, Joseph Sklenar, Junjia Ding, Jungsik Park, John E. Pearson, Valentine Novosad, Peter Schiffer, and Axel Hoffmann Physical Review Applied **8**, 064026 – 1-7 (2017).

5. "Characterization of switching field distributions in Ising-like magnetic arrays," Robert D. Fraleigh, Susan Kempinger, Paul E. Lammert, Sheng Zhang, Vincent H. Crespi, Peter Schiffer, and Nitin Samarth Physical Review B **95**, 144416 – 1- 4 (2017).

6. "Classical topological order in the kinetics of artificial spin ice," Yuyang Lao, Francesco Caravelli, Mohammed Sheikh, Joseph Sklenar, Daniel Gardeazabal, Justin D. Watts, Alan M. Albrecht, Andreas Scholl, Karin Dahmen, Cristiano Nisoli and Peter Schiffer Nature Physics **14**, 723–727 (2018).

7. "Field-induced phase coexistence in an artificial spin ice", Joseph Sklenar, Yuyang Lao, Alan Albrecht, Justin D. Watts, Cristiano Nisoli, Gia-Wei Chern, and Peter Schiffer Nature Physics **15**, 191–195 (2019).

Program Title: Atomic Engineering Oxide Heterostructures: Materials by Design

PI: H. Y. Hwang[1,2*]; Co-PI: S. Raghu[1,3]

[1]Stanford Institute for Materials & Energy Sciences, SLAC National Accelerator Laboratory, Menlo Park, CA 94025

[2]Department of Applied Physics, Stanford University, Stanford, CA 94305

[3]Department of Physics, Stanford University, Stanford, CA 94305

**hyhwang@slac.stanford.edu*

Program Scope

A central aim of modern materials research is the control of materials and their interfaces to atomic dimensions. In the search for emergent phenomena and ever-greater functionality in devices, transition metal oxides have enormous potential. They host a vast array of properties, such as orbital ordering, unconventional superconductivity, magnetism, and ferroelectricity, as well as quantum phase transitions and couplings between these states. Our broad objective is to develop the science and technology arising in heterostructures of these novel materials. Using atomic scale growth techniques we explore the synthesis and properties of novel interface phases, metastable films, and freestanding crystalline membranes. Magnetotransport, x-ray, and optical probes are used to determine the static and dynamic electronic and magnetic structure. The experimental efforts are guided and analyzed theoretically, particularly with respect to superconductivity and new states of emergent order. A wide set of tools, ranging from analytic field theory methods to exact computational treatments, are applied towards the understanding and design of heterostructures.

Recent Progress

Phase transitions using extreme tensile strain in oxide membranes [1]:

A defining feature of emergent phenomena in complex oxides is the competition and cooperation between ground states, which can be sensitively tuned by the lattice. This has been explored using hydrostatic pressure, epitaxial lattice-mismatch in films, and uniaxial strain. Manganites provide canonical examples where various metallic and insulating phases, and associated magnetic and orbital ordering, are delicately balanced. Extending the range of lattice control would enhance the ability to access and investigate new phases. Here we stabilize extreme tensile strain in nanoscale $La_{0.7}Ca_{0.3}MnO_3$ membranes, which we have recently developed [2], exceeding 8% uniaxially and 5% biaxially (Fig. 1). Biaxial strain suppresses the ferromagnetic metal, inducing an insulating ground state that can be extinguished by magnetic field.

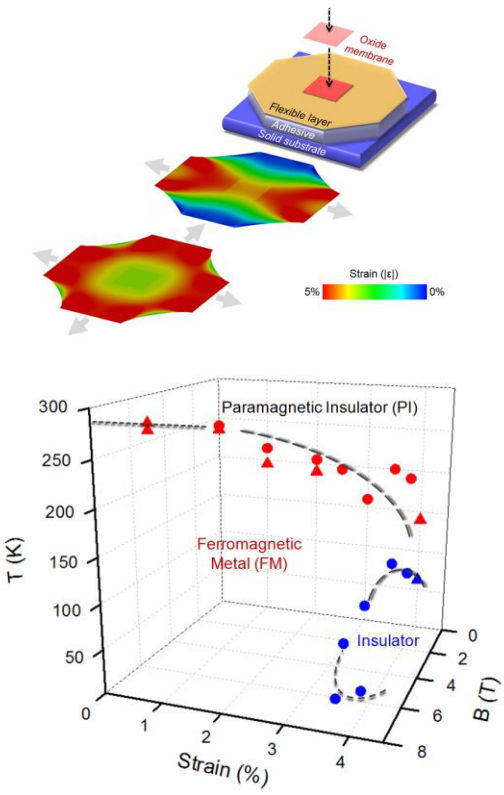

Fig. 1. (Top) Schematic assembly of the strain platform and calculated strain profile maps. (Bottom) Phase diagram of $La_{0.7}Ca_{0.3}MnO_3$ under varying biaxial strain.

Electronic structure calculations indicate that the insulator consists of charge-ordered Mn^{4+} and Mn^{3+} with staggered strain-enhanced Jahn-Teller distortions within the membrane plane. This highly-tunable strained membrane approach provides a broad opportunity to design and manipulate correlated states in transition metal compounds.

Low-density superconductivity in $SrTiO_3$ bounded by the adiabatic condition:

The oxide semiconductor $SrTiO_3$ exhibits a superconducting ground state when electron doped over a wide range of carrier densities (10^{19}-10^{21} cm^{-3}). Across this range, the Fermi level traverses a variety of vibrational modes in the system, making it an ideal choice to study the physics of dilute superconductivity. We use planar tunneling spectroscopy to examine bulk Nb and La doped $SrTiO_3$ across the superconducting dome, using atomically designed polar tunnel barriers that enable very high-resolution measurements. We find that the overdoped side of the dome is precisely bounded by the adiabatic condition, i.e. where the Fermi energy (E_F) is equal to the Debye energy. Thus the entirety of the superconducting dome is in the anti-adiabatic regime, extending down to low densities for which E_F is below all phonon van Hove singularities, except for the soft transverse optic (TO) mode corresponding to the ferroelectric instability. Despite this unusual regime, the thermodynamic relationship of BCS weak-coupling theory ($2\Delta_0/k_BT_c = 3.53$) is observed for all superconducting samples. These results suggest the possibility of unconventional pairing via TO phonons, for which there is usually no first order coupling in inversion symmetric materials.

Future Plans

- Extension of the current work to strain-tune ferroelectric and superconducting membranes, focusing on titanates and cuprates.
- Investigation of mesoscopic structures fabricated by integrating soluble buffer layers with e-beam lithography of oxide heterostructures. Initial focus will be on $SrTiO_3$-based heterostructures.
- Development of hot-electron spectroscopy in correlated electron systems using perpendicular transport in oxide heterostructures.
- Investigation of the superconducting and normal state properties of the newly discovered infinite-layer nickelates.

References

1. S. S. Hong, M. Q. Gu, M. Verma, D. Lu, V. Harbola, A. Vailionis, Y. Hikita, R. Pentcheva, J. M. Rondinelli, and H. Y. Hwang, "Extreme Tensile Strain States in $La_{0.7}Ca_{0.3}MnO_3$ Membranes," *Science*, in revision (2019).
2. D. Lu, D. J. Baek, S. S. Hong, L. F. Kourkoutis, Y. Hikita, and H. Y. Hwang. "A New Synthetic Route to Freestanding Single Crystal Perovskite Films and Heterostructures," *Nature Materials* **15**, 1255 (2016).

Publications

1. Y. Frenkel, N. Haham, Y. Shperber, C. Bell, Y. W. Xie, Z. Y. Chen, Y. Hikita, H. Y. Hwang, E. K. H. Salje, and B. Kalisky, "Imaging and Tuning Polarity at $SrTiO_3$ Domain Walls," *Nature Materials* **16**, 1203 (2017).
2. H. Goldman, M. Mulligan, S. Raghu, G. Torroba, and M. Zimet, "Two-Dimensional

Conductors with Interactions and Disorder from Particle-Vortex Duality," *Physical Review B* **96**, 245140 (2017).
3. Y. J. Fu, E. F. Liu, H. T. Yuan, P. Z. Tang, B. Lian, G. Xu, J. W. Zeng, Z. Y. Chen, Y. J. Wang, W. Zhou, K. Xu, A. Y. Gao, C. Pan, M. Wang, B. G. Wang, S.-C. Zhang, Y. Cui, H. Y. Hwang, and Feng Miao, "Gated Tuned Superconductivity and Phonon Softening in Monolayer and Bilayer MoS_2", *npj Quantum Materials* **2**, 52 (2017).
4. S. S. Hong, J. H. Yu, D. Lu, A. F. Marshall, Y. Hikita, Y. Cui, and H. Y. Hwang, "Two-Dimensional Limit of Crystalline Order in Perovskite Membrane Films," *Science Advances* **3**, eaao5173 (2017).
5. D. J. Baek, D. Lu, Y. Hikita, H. Y. Hwang, and L. F. Kourkoutis, "Mapping Cation Diffusion through Lattice Defects in Epitaxial Oxide Thin Films on the Water-soluble Buffer Layer $Sr_3Al_2O_6$ using Atomic Resolution Electron Microscopy", *APL Materials* **5**, 096108 (2017).
6. J.-Y. Chen, J H Son, C. Wang, and S. Raghu, "Exact Boson-Fermion Duality on a 3D Euclidean Lattice," *Physical Review Lett*ers **120**, 016602 (2018).
7. D. Lu, Y. Hikita, D. J. Baek, T. A. Merz, H. K. Sato, B. Kim, T. Yajima, C. Bell, A. Vailionis, L. F. Kourkoutis, and H. Y. Hwang, "Strain Tuning in Complex Oxide Epitaxial Films Using an Ultrathin Strontium Aluminate Buffer Layer," *Phys. Stat. Solidi RRL* **12**, 1700339 (2018).
8. A. G. Swartz, H. Inoue, T. A. Merz, Y. Hikita, S. Raghu, T. P. Devereaux, S. Johnston, and H. Y. Hwang, "Polaronic Behavior in a Weak Coupling Superconductor," *Proceedings of the National Academy of Sciences* **115**, 1475 (2018).
9. B. S. Y. Kim, M. Minohara, Y. Hikita, C. Bell, and H. Y. Hwang, "Atomically Engineered Epitaxial Anatase TiO_2 Metal-Semiconductor Field-Effect Transistors," *Applied Physics Letters* **112**, 133506 (2018).
10. X. G. Liu, J. H. Kang, H. T. Yuan, J. H. Park, Y. Cui, H. Y. Hwang, and M. L. Brongersma, "Tuning of Plasmons in Transparent Conductive Oxides By Carrier Accumulation", *ACS Photonics* **5**, 1493 (2018).
11. M. Osada, K. Nishio, H. Y. Hwang, and Y. Hikita, "Synthesis and Electronic Properties of Fe_2TiO_5 Epitaxial Thin Films," *APL Materials* **6**, 056101 (2018).
12. S. Emori, D. Yi, S. Crossley, J. J. Wisser, P. Balakrishnan, P. Shafer, C. Klewe, A. T. N'Diaye, B. T. Urwin, K. Mahalingam, B. M. Howe, H. Y. Hwang, E. Arenholz, and Y. Suzuki, "Ultralow Damping in Epitaxial Spinel Ferrite Thin Films," *Nano Letters* **18**, 4273 (2018).
13. H. Noad, C. A. Watson, H. Inoue, M. Kim, H. K. Sato, M. Hosoda, C. Bell, H. Y. Hwang, J. R. Kirtley, and K. A. Moler, "Imaging Sub-Resolution Defects in Two-Dimensional Superconductors with Scanning SQUID," *Physical Review B* **98**, 064510 (2018).
14. P. Kumar, M. Mulligan, and S. Raghu, "Topological Phase Transition Underpinning Particle-Hole Symmetry in the Halperin-Lee-Read Theory," *Physical Review B* **98**, 115105 (2018).
15. Z. Y. Chen, A. G. Swartz, H. Yoon, H. Inoue, T. A. Merz, D. Lu, Y. W. Xie, H. T. Yuan, Y. Hikita, S. Raghu, and H. Y. Hwang, "The Density and Disorder Tuned Superconductor-Metal Transition in Two Dimensions," *Nature Communications* **9**, 4008 (2018).
16. A. T. Hristov, J. C. Palmstrom, J. A. W. Straquadine, T. A. Merz, H. Y. Hwang, and I. R. Fisher, "Measurement of Elastoresistivity at Finite Frequency by Amplitude Demodulation," *Review of Scientific Instruments* **89**, 103901 (2018).
17. Y. Yu, A. K. C. Cheung, S. Raghu, and D. Agterberg, "Residual Spin Susceptibility in the Spin-Triplet Orbital-Singlet Model," *Physical Review B* **98**, 184507 (2018).
18. A. G. Swartz, A. K. C. Cheung, H. Yoon, Z. Y. Chen, Y. Hikita, S. Raghu, and H. Y. Hwang, "Superconducting Tunneling Spectroscopy of Spin-Orbit Coupling and Orbital Depairing in Nb:$SrTiO_3$," *Physical Review Letters* **121**, 167003 (2018).

19. D. V. Christensen, Y. Frenkel, Y. Z. Chen, Y. W. Xie, Z. Y. Chen, Y. Hikita, A. Smith, L. Klein, H. Y. Hwang, N. Pryds, and B. Kalisky, "Strain-Tunable Magnetism at Oxide Domain Walls," *Nature Physics* **15**, 269 (2019).
20. T. Yajima, M. Minohara, C. Bell, H. Y. Hwang, and Y. Hikita, "Inhomogeneous Barrier Heights at Dipole-Controlled $SrRuO_3$/Nb:$SrTiO_3$ Schottky Junctions," *Applied Physics Letters* **113**, 221603 (2018).
21. B. S. Y. Kim, Y. A. Birkhölzer, X. Feng, Y. Hikita, and H. Y. Hwang, "Probing the Band Alignment in Rectifying $SrIrO_3$/Nb:$SrTiO_3$ Heterostructures," *Applied Physics Letters* **114**, 133504 (2019).
22. D. Lu, S. Crossley, R. Xu, Y. Hikita, and H. Y. Hwang, "Freestanding Oxide Ferroelectric Tunnel Junction Memories Transferred onto Silicon," *Nano Letters* **19**, 3999 (2019).
23. H. Inoue, H. Yoon, T. A. Merz, A. G. Swartz, S. S. Hong, Y. Hikita, and H. Y. Hwang, "Delta-Doped $SrTiO_3$ Top-Gated Field Effect Transistor, *Applied Physics Letters* **114**, 231605 (2019).
24. Z. Y. Chen, B. Y. Wang, B. H. Goodge, D. Lu, S. S. Hong, D. F. Li, L. F. Kourkoutis, Y. Hikita, and H. Y. Hwang, "Freestanding Crystalline $YBa_2Cu_3O_{7-x}$ Heterostructure Membranes," *Physical Review Materials (Rapid Communications)* **3**, 060801 (2019).
25. P. Singh, A. G. Swartz, D. Lu, S. S. Hong, K. Lee, K. Nishio, Y. Hikita, and H. Y. Hwang, "Large-Area Crystalline $BaSnO_3$ Membranes with High Electron Mobilities," *ACS Applied Electronic Materials* **1**, 1269-1274 (2019).
26. J. H. Son, J.-Y. Chen, and S. Raghu, "Duality Web on a 3D Euclidean Lattice and Manifestation of Hidden Symmetries," *Journal of High Energy Physics* **2019**, 38 (2019).
27. P. Kumar, M. Mulligan, and S. Raghu, "Emergent Reflection Symmetry from Non-Relativistic Composite Fermions," *Physical Review B* **99**, 205151 (2019).
28. D. F. Li, K. Lee, B. Y. Wang, M. Osada, S. Crossley, H. R. Lee, Y. Cui, Y. Hikita, and H. Y. Hwang, "Superconductivity in an Infinite-Layer Nickelate," *Nature,* DOI: 10.1038/s41586-019-1496-5 (2019)
29. A. Pustogow, Yongkang Luo, A. Chronister, Y.-S. Su, D. A. Sokolov, F. Jerzembeck, A. P. Mackenzie, C. W. Hicks, N. Kikugawa, S. Raghu, E. D. Bauer, and S. E. Brown, "Constraints on the Superconducting Order Parameter in Sr_2RuO_4 from ^{17}O NMR," *Nature*, in press.
30. M. Zhang, K. Du, T. S. Ren, H. Tian, Z. Zhang, H. Y. Hwang, and Y. W. Xie, "A Termination-Insensitive and Robust Electron Gas at the $CaHfO_3$/$SrTiO_3$ Heterointerface," *Nature Communications*, in press.
31. J. A. Damia, S. Kachru, S. Raghu, and G. Torroba, "Two Dimensional Non-Fermi Liquid Metals: a Solvable Large N Limit," *Physical Review Letters*, in press.
32. S. Crossley, A. G. Swartz, K. Nishio, Y. Hikita, and H. Y. Hwang, "All-Oxide Ferromagnetic Resonance and Spin Pumping with $SrIrO_3$," *Physical Review B*, in press.

Nanostructured Materials: From Superlattices to Quantum Dots

Ivan K. Schuller
Physics Department
University of California, San Diego
La Jolla, Ca. 92093

i) Program Scope

This project is dedicated to dimensionality and disorder issues in modern magnetic materials. The comprehensive approach combines preparation of nanostructures using thin film (Sputtering and MBE) and lithography (electron beam and self assembly) techniques, characterization using surface analytical, scanning probe microscopy, high-resolution scattering (light, X-ray, synchrotron and neutron) and microscopy techniques, measurement of physical properties (magneto-transport, magnetic and magneto-optical) and modeling. All preparation of unique materials and devices and most structural and physical characterization are performed in the PI's laboratory at UCSD. More sophisticated structural and magnetic studies at the nanoscale are performed in collaboration at several at major facilities of DOE funded national labs.

We aim to investigate mostly magnetic physical phenomena, including exchange bias, effects of confinement, disorder, proximity effects in hybrids, and induced phenomena by the application of external driving forces such as time varying electric and magnetic fields, light and other types of radiation. In all cases, a crucial ingredient is the reduction of complex or highly correlated materials to the nanoscale, where fundamental changes may occur in their physical properties. Our studies to date have included fluorides, oxides, borides and organics in addition to many combinations of transition metal elements. In some form or another these include magnetic components. We have established a battery of state of the art instrumentation and continue expanding our unique experimental capabilities at UCSD. These facilities have also been used by other researchers funded by DOE.

ii) Recent Progress

The extensive work done during the last period cannot be summarized in a brief review, so below I summarize a few highlights during the last funding period:

1) One dimensional (1D)

We discovered an unexpected increase of coercivity related to chiral ferromagnetic order in 1D ferromagnetic (1D FM) chains. The 1D iron incorporated into a superlattice were fabricated using organic molecular beam epitaxy, which allows for precise control of chain length, only a few atoms long (7 to 150 atoms), subject to controlled boundary conditions. The observed electronic hybridization of the Fe atoms with the H at the chain ends, determines the chiral magnetic response. The coercivity increases with chain length in 1D FM chains with hybridized boundaries, but not for chains with free ends. This implies that the electronic environment of the end atoms controls the spin structure of these 1D chains. A semi-classical model, which includes short-range exchange and Dzyaloshinsky-Moriya interactions, explains quantitatively these results.

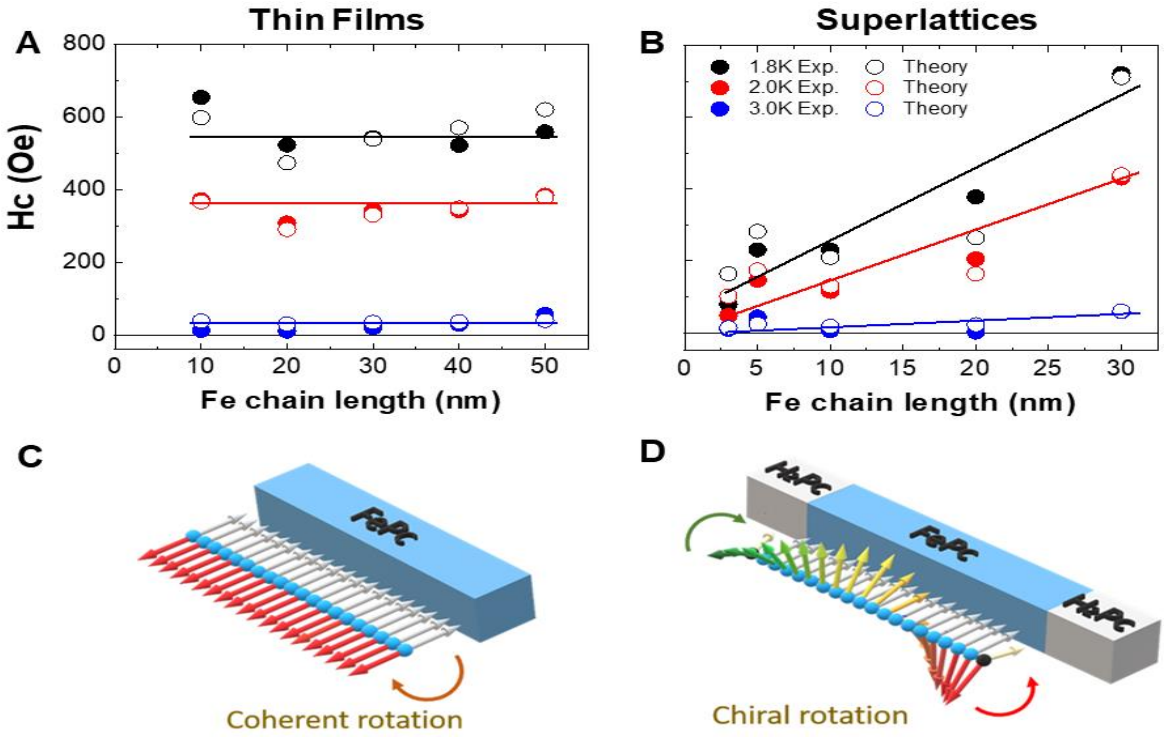

Figure: Coercivity Hc as function Fe chain length (**A**) is constant in FePc thin films and (**B**) increases in FePc/H_2Pc superlattices (SLs). Excellent agreement with theoretical calculation based on: (**C**) coherent reversal in free Fe spin chain and (**D**) chiral symmetry breaking in Fe spin chain subject to DMI at the chain boundary.

2) Two dimensional (2D)

We discovered a dipole-induced exchange bias (EB), switching from negative to positive sign, in systems where the antiferromagnet and the ferromagnet were separated by a paramagnetic spacer (AFM–PM–FM). The EB as a function of the spacer thickness and its change of sign, can be understood quantitatively without the need to invoke short range interfacial exchange interactions used in usual EB theories. The long-range dipole field provides the coupling of the FM and AFM across the PM spacer. The experiments allow for novel switching capabilities of long-range EB systems, while the theory allows description of the structures where the FM and AFM are not in atomic contact. The results provide a new approach to design novel interacting heterostructures.

3) Three dimensional (3D)

Despite decades of efforts, the origin of metal-insulator transition (MIT) in strongly correlated materials remains a longstanding problem in condensed-matter physics. An archetypal example is V_2O_3, which undergoes simultaneous electronic, structural and magnetic phase transitions. This remarkable feature highlights the many degrees of freedom at play in this material. Acting solely on the magnetic degree of freedom, we discovered an anomalous feature in the electronic transport of V_2O_3: on cooling, the magnetoresistance (MR) changes from positive to negative well above the MIT temperature, and diverges at the transition. The effects are produced by the magnetic field

quenching antiferromagnetic fluctuations above the Néel temperature, T_N, and preventing long-range antiferromagnetic ordering below T_N. In both cases, suppressing the antiferromagnetic order prevents the opening of the incipient electronic gap. This interpretation is supported by Hubbard model calculations and reproduces the experimental behavior.

iii) Future Plans

The future plans include clarification and firming up some of the conclusions obtained in the past period, and developing interesting scientific directions, which have direct relevance to the research done under this project.

1) One Dimensional (1D)

The possibility of fabricating well-controlled 1D magnetic chains provides a tool for the exploration of fundamental kinetics of magnetism with slow relaxation (not accessible in conventional magnets). These slow relaxation times can be extracted from the magnetic remanence evolution with time at different freezing temperatures and interpreted within the theoretical framework of the Glauber-Ising kinetic model. The understanding of magnetic dynamics in one-dimensional chiral magnetic order is a fundamental research problem revealing the importance of dimensionality and boundary conditions in reduced dimension.

2) Two Dimensional (2D)

Effect of MIT on Magnetism Proximity effects and exchange coupling across interfaces of hybrid magnetic heterostructures present unique opportunities for functional material design. Recently we found that V_2O_3 proximity coupled to ferromagnetic (FM) layers strongly affect the magnetization and coercivity of the FM at temperatures at which the V_2O_3 MIT occurs. Indirect measurements imply that phase separation in the oxide plays a major role. We will examine directly the effect of phase separation on magnetic domains in FM, using X-ray magnetic circular dichroism (XMCD) to image Ni magnetic domains in a Ni/V_2O_3 bilayer in the phase coexistence state.

Effect of Magnetism on the MIT This part of the project is dedicate to investigating the reverse of the effect mentioned above: is it possible to control the phase transitions of metal oxides by using magnetostriction ? We will use Terfenol-D, which is one of the most magnetostrictive materials with over 2000 ppm magnetostrictive strain (compared to ~30 for Nickel). Various combinations of Terfenol-D/Vanadium Oxide bilayers will be used to control structural and electronic phase transitions of the oxide layer by applying magnetic field.

3) Three Dimensional (3D)

Insulating antiferromagnets (AFM) attract a lot of attention due to their applications in magnetic phenomena such as exchange bias and application in ultrafast low-power spintronics devices. Pinned uncompensated moments (UM) at the surface of an insulating AFM play a key role when these materials are incorporated into 3D heterostructures. We will fabricate heterostructures composed of layers of an AFM (FeF_2) and a FM (Co) separated by a normal thin Cu separator. Scattering of electrons polarized by the Co layer

may produce a giant magnetoresistance effect when scattered by the pinned UM at the FeF_2/Cu interface. A measurement of the angular dependence of the spin valves resistance enables determining of the behavior of the pinned UM at different temperatures and magnetic fields, which is nearly impossible to achieve by any other technique. These measurements will provide the orientation of the pinned UM an important ingredient in the understanding of AFM spintronics.

4) Disorder

The investigation of the effect of disorder in solids is important for fundamental understanding and technological developments. Studies of disorder reveal key information regarding the fundamental nature of the behavior of materials. Disorder can be used to investigate and mitigate the effects of damage in hostile environments, and also as a tool for the creation of new functional concepts and devices.

We will extend our earlier studies in the vanadates to FeRh, which exhibits a first order antiferromagnetic to ferromagnetic phase transition. Combining into a heterostructure FeRh with vanadium oxide may prove to be particularly interesting. Strain mediated effects produced by the vanadium oxide may substantially modify the FeRh antiferro- to ferromagnetic transition. Moreover, the prospect of an electrically triggered vanadium oxide transition leads to an alternative method for electrical control of the magnetism, an important prospect for low power spintronic devices.

iv) Publications

1. *Interface-Induced Phenomena in Magnetism,* Frances Hellman, et al, Rev. Mod. Phys. 89, 025006 (2017). doi: 10.1103/RevModPhys.89.025006
2. *Magnetic Anistropy in Fe Phthalocyanine Film Deposited on Si(110) Substrate: Standing Configuration*, J. Bartolome, et al, Fizika Nizkizh Temperatur, 43, 1189 (2017). doi: 10.1063/1.5001295
3. *Dipole-Induced Exchange Bias*, Felipe Torres, et al, Nanoscale, 9, 17074 (2017). doi: 10.1039/C7NR05491B
4. *Growth-Induced In-Plane Uniaxial Anisotropy in V_2O_3/Ni Films*, Dustin A. Gilbert, et al, Sci. Rep. 7, Article number: 13471 (2017). doi: 10.1038/s41598-017-12690-z
5. *Nonequilibrium Phase Precursors during a Photoexcited Insulator-to-Metal Transition in V_2O_3,* Andrej Singer, et al, Phys. Rev. Lett. 120, 207601 (2018). doi: 10.1103/PhysRevLett.120.207601
6. *New Magnetic States in Nanorings Created by Anisotropy Gradients*, Mario A. Castro, et al, J. Magn. Magn. Mater. 484, 55 (2019). doi: 10.1016/j.jmmm.2019.03.118
7. *Coercivity Increase Due to Chiral Magnetic Order in 1D Iron Chains,* Nicolas M. Vargas, et al, *Submitted* (2019). doi: pending
8. *Magnetic-Field Frustration Reveals the Nature of the Metal-Insulator Transition in V_2O_3*, J. Trastoy, et al, *Submitted* (2019). doi: pending
9. *Quantifying Inactive Lithium in Lithium Metal Batteries*, Chengcheng Fang, et al, Nature 572, 511 (2019). doi: 10.1038/s41586-019-1481-z

Session 6

Electron Spectroscopy of Novel Materials

Tonica Valla, Christopher C. Homes and Peter D. Johnson

valla@bnl.gov, homes@bnl.gov, pdj@bnl.gov

Condensed Matter Physics & Materials Science Department

Brookhaven National Laboratory, Upton, NY 11973-5000

Program Scope

The focus of this program is the exploration of the electronic structure and electrodynamics of strongly correlated electron systems, with particular attention to emergent phenomena, such as superconductivity and magnetism, using angle-resolved photoemission (ARPES) and optical spectroscopy. A central goal of the program is to discover the mechanism of superconductivity in the high-temperature superconductors and iron-based superconductors and to better understand the role of spin- and charge-orders and nematicity that shape the phase diagrams of these materials. The studies also include other quantum materials such as topological insulators, 3D Dirac and Weyl semimetals and materials with extremely large magnetoresistance. Interactions of topological insulators with materials displaying magnetism and superconductivity, have been also studied, as the proximity of these two distinct types of matter is expected to produce exotic new phenomena, some of which could be applied in devices.

Recent Progress

Cuprate phase diagram revisited. In high-temperature cuprate superconductors, doping of carriers into the parent Mott insulator induces superconductivity and various other phases whose characteristic temperatures are in phase diagrams typically plotted versus the doping level *p*, or concentration of additional holes (or electrons) away from the half-filled Mott insulator. In most materials, including $Bi_2Sr_2CaCu_2O_{8+\delta}$ *p* cannot be determined from the chemical composition, but it is instead back-derived from the superconducting transition temperature, T_c, using the assumption that T_c dependence on doping is universal in all cuprates [1]. In our ARPES studies of $Bi_2Sr_2CaCu_2O_{8+\delta}$ single crystals cleaved and annealed in vacuum or in ozone to reduce or increase the doping from the initial value, we show that *p* can be precisely determined from the measured Fermi surfaces and that the *in-situ* annealing allows mapping of a wide doping regime, covering not only superconducting dome, but also

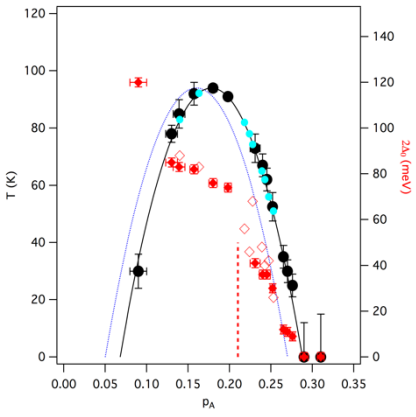

Figure 1. Phase diagram of $Bi_2Sr_2CaCu_2O_{8+\delta}$. Experimentally obtained T_c (black circles) and the antinodal gap, $2\Delta_0$ (red diamonds) are plotted versus experimentally determined doping parameter, p_A. The "universal" superconducting dome is shown as blue dashed line, while the corrected dome is represented by black solid line.

the metallic, non-superconducting phase on the overdoped side (Fig. 1) [2]. Our results show a smooth doping dependence, lacking the evidence for the elusive symmetry breaking transitions and the related reconstruction of the Fermi surface. In the highly overdoped regime ($p > 0.25$), superconducting gap approaches the mean-field value of $2\Delta_0 = 4.3 k_B T_c$.

Disappearance of superconductivity due to vanishing coupling in the overdoped cuprates. More than 30 years after the discovery of cuprate superconductors, the pairing mechanism in these materials still remains unknown. The observation of renormalization effects in the low energy electronic excitations in ARPES has re-ignited the hope that a bosonic mode playing a role in pairing in cuprates could finally be identified, in analogy with how tunneling experiments provided the smoking gun evidence for phononic mechanism in conventional superconductors. However, after decades of intense research, the debate about the coupling mechanism is still open. One problem was that early studies were focused on the nodal "kink" that did not show any significant correlations with superconductivity when the latter was altered by doping or when different cuprate families were compared. Another problem is that cuprates are fundamentally different from simple metals – their parent compounds are antiferromagnetically ordered Mott insulators wherein conduction and superconductivity are induced by doping holes or electrons away from the half filled case. The effects of strong correlations extend far away from half filling, deep into the regime that overlaps with superconductivity, where their presence and intertwining with superconductivity complicates the identification of the superconducting mechanism. To avoid those complications, it is desirable to study superconducting properties in the highly overdoped regime. Recently, we have succeded in extending the overdoped range beyond the point at which superconductivity vanishes by annealing the *in-situ* cleaved samples in ozone. That enabled monitoring of the development of electronic excitations as superconductivity weakens and finally completely disappears, allowing a closer look at its origins. Our ARPES studies of $Bi_2Sr_2CaCu_2O_{8+\delta}$ in the overdoped regime show that the mass renormalization in the antinodal region of the Fermi surface, associated with the structure in the quasiparticle self-energy, that possibly reflects the pairing interaction, monotonically weakens with increasing doping and completely disappears precisely where superconductivity disappears (Fig. 2) [3]. This is the direct evidence that in the overdoped regime, superconductivity is determined by the coupling strength. A strong doping dependence and an abrupt disappearance above the transition temperature (T_c) eliminate the conventional phononic mechanism of the observed mass renormalization and identify the onset of spin-fuctuations as its likely origin.

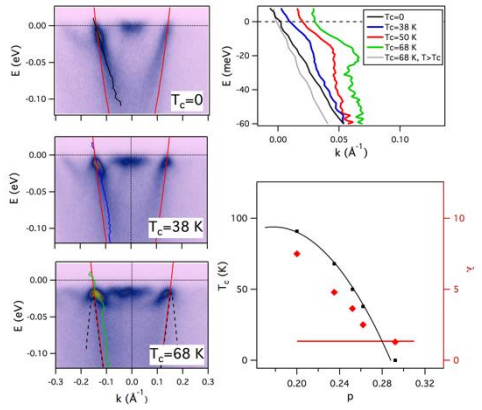

Figure 1. Left: ARPES spectra of $Bi_2Sr_2CaCu_2O_{8+\delta}$ near the antinode for three highly overdoped samples. Right: experimental dispersions, for several overdoped samples (top). A kink in dispersion, indicating a coupling to a bosonic mode, is seen only for superconducting samples and only below T_c. Both the coupling strength (bottom) and the energy of the involved mode scale with T_c.

Future Plans

The group is leading the OASIS project – the integration of precise Oxide Molecular Beam

Epitaxy (OMBE) synthesis of correlated oxides with ARPES and state-of-the-art SI-STM in a single instrument. OASIS is now fully operational science-driven facility, enabling in-situ SI-STM and ARPES studies of single-crystal films of a wide variety of correlated oxides, oxide heterostructures and topological materials [4]. The two studies presented here were only possible due to this new facility. The forthcoming addition of a non-oxide MBE to the system will expand our capabilities in synthesis and characterization of more complex heterostructures involving interfaces of correlated oxides with chachogenides and other quantum materials. The group is also developing a laser-based time-of-flight ARPES facility that will enable studies of transient phenomena and the dynamics of carriers in correlated materials. The group is also involved in developing the optical instrumentation at the NSLS II infrared MET beamline that will allow reflectance studies of small samples at long wavelengths (diffraction limit), with a new high-temperature stage that will allow optical studies to be performed up to 800 K; this will be applied to studies of both the under- and over-doped cuprates.

References

[1] S. D. Obertelli, J. R. Cooper, and J. L. Tallon, Physical Review B, **46**, 14928 (1992).
[2] I. K. Drozdov, I. Pletikosić, C.-K. Kim, K. Fujita, G. D. Gu, J. C. Séamus Davis, P. D. Johnson, I. Božović, and T. Valla, Nature Communications **9**, 5210 (2018).
[3] T. Valla, I. K. Drozdov and G. D. Gu, in review in Nature Communications, arXiv:1905.01370.
[4] C.-K Kim, I. K. Drozdov, K. Fujita, J. C. Séamus Davis, I. Božović and T. Valla, in print in JESRP, https://doi.org/10.1016/j.elspec.2018.07.003.

Publications

[5] S. Vig, A. Kogar, V. Mishra, L. Venema, M. S. Rak, A. A. Husain, P. D. Johnson, G. D. Gu, E. Fradkin, M. R. Norman, P. Abbamonte, SciPost **3**, 026 (2017).
[6] R. Yang, Z. Yin, Y. Wang, Y. Dai, H. Miao, B. Xu, X. Qiu, and C. C. Homes, Phys. Rev. B **96**, 201108 (2017).
[7] N. Zaki, H.-B. Yang, J. D. Rameau, P. D. Johnson, H. Claus, and D. G. Hinks, Phys. Rev. B **96**, 195163 (2017).
[8] I. Crassee, E. Martino, C. C. Homes, O. Caha, J. Novak, P. Tueckmantel, M. Hakl, A. Nateprov, E. Arushanov, Q. D. Gibson, R. J. Cava, S. M. Koohpayeh, K. E. Arpino, T. M. McQueen, M. Orlita, and A. Akrap, Phys. Rev. B **97**, 125204 (2018).
[9] T. Konstantinova, J. D. Rameau, A. H. Reid, O. Abdurazakov, L. Wu, R. Li, X. Shen, G. Gu, Y. Huang, L. Rettig, I. Avigo, M. Ligges, J. K. Freericks, A. F. Kemper, H. A. Duerr, U. Bovensiepen, P. D. Johnson, X. Wang, and Y. Zhu, Sci. Adv. **4**, eaap7427 (2018).
[10] *"Photoelectron Spectroscopies applied to Condensed Matter Systems"*, P. D. Johnson, in "Physics of Solid Surfaces", edited by Prof. G. Chiarotti and Prof. P. Chiaradia, (Landolt-Börnstein, Springer-Verlag, GMBH Germany) 2018.
[11] I. Pletikosic, F. von Rohr, P. Pervan, P. K. Das, I. Vobornik, R. J. Cava, and T. Valla, Phys. Rev. Lett. **120**, 156403 (2018).
[12] C. C. Homes, Y. M. Dai, A. Akrap, S. L. Bud'ko, and P. C. Canfield, Phys. Rev. B **98**, 035103 (2018).

[13] H. Miao, W. H. Brito, Z. P. Yin, R. D. Zhong, G. D. Gu, P. D. Johnson, M. P. M. Dean, S. Choi, G. Kotliar, W. Ku, X. C. Wang, C. Q. Jin, S.-F. Wu, T. Qian, and H. Ding, Phys. Rev. B **98**, 020502 (2018).
[14] C. C. Homes, Q. Du, C. Petrovic, W. H. Brito, S. Choi, and G. Kotliar, Sci. Rep. **8**, 11692 (2018).
[15] Y. Tian, G. Gu, P. Johnson, T. Rao, T. Tsang, and E. Wang, Applied Physics Letters **113**, 233504 (2018).
[16] T.-R. Chang, I. Pletikosic, T. Kong, G. Bian, A. Huang, J. Denlinger, S. K. Kushwaha, B. Sinkovic, H.-T. Jeng, T. Valla, W. Xie, and R. J. Cava, Adv. Sci. **6**, 1800897 (2019).
[17] S. Freutel, J. D. Rameau, L. Rettig, I. Avigo, M. Ligges, Y. Yoshida, H. Eisaki, J. Schneeloch, R. D. Zhong, Z. J. Xu, G. D. Gu, U. Bovensiepen, and P. D. Johnson, Phys. Rev. B **99**, 081116 (2019).
[18] R. Yang, Y. Dai, J. Yu, Q. Sui, Y. Cai, Z. Ren, J. Hwang, H. Xiao, X. Zhou, X. Qiu, and C. C. Homes, Phys. Rev. B **99**, 144520 (2019).
[19] J. D. Rameau, N. Zaki, G. D. Gu, P. D. Johnson, and M. Weinert, Phys. Rev. B **99**, 205117 (2019).
[20] C. C. Homes, S. Khim, and A. P. Mackenzie, Phys. Rev. B **99**, 195127 (2019).
[21] X. Gui, I. Pletikosic, H. Cao, H.-J. Tien, X. Xu, R. Zhong, G. Wang, T.-R. Chang, S. Jia, T. Valla, W. Xie, and R. J. Cava, ACS Cent. Sci. **5**, 900 (2019).
[22] E. Martino, I. Crassee, G. Eguchi, D. Santos-Cottin, R. D. Zhong, G. D. Gu, H. Berger, Z. Rukelj, M. Orlita, C. C. Homes, and A. Akrap, Phys. Rev. Lett. **122**, 217402 (2019).
[23] G. D. Samolyuk, C. C. Homes, A. F. May, S. Mu, K. Jin, H. Bei, G. M. Stocks, and B. C. Sales, Phys. Rev. B **100**, 075128 (2019).

Program Title: Complex States, Emergent Phenomena, and Superconductivity in Intermetallic and Metal-Like Compounds

Principle Investigators: Paul Canfield (FWP leader), Sergey Bud'ko, Yuji Furukawa, David Johnston, Adam Kaminski, Vladimir Kogan, Makariy Tanatar, Ruslan Prozorov. Linlin Wang, Division of Materials Science and Engineering, Ames Laboratory, Iowa State University, Ames, IA 50011

Program Scope

Our FWP focuses on discovering, understanding and ultimately controlling new and extreme examples of complex states, emergent phenomena, and superconductivity. Materials manifesting specifically clear or compelling examples (or combinations) of superconductivity, strongly correlated electrons, novel electronic topologies, quantum criticality, and exotic, bulk magnetism are of particular interest given their potential to lead to revolutionary steps forward in our understanding of their complex, and potentially energy relevant, properties. The experimental work consists of new materials development and crystal growth, combined with detailed and advanced measurements of microscopic, thermodynamic, transport and electronic properties, at extremes of pressure, temperature, magnetic field, and resolution. The theoretical work focuses on understanding and modeling transport, thermodynamic and spectroscopic properties using world-leading and advanced phenomenological approaches to superconductors and electronic band structures.

The priority of this FWP is the development and understanding of model systems combined with agile and flexible response to, and leadership in, a rapidly-changing materials landscape. To accomplish this goal, our combined synthetic, characterization and theory efforts operate both in series and in parallel. This work supports the DOE mission by directly addressing the Grand Challenge of understanding the Emergence of Collective Phenomena: Strongly Correlated Multiparticle Systems and is a key contributor to fulfilling the Ames Laboratory Scientific Strategic Plan for preeminence in solid-state materials discovery, synthesis, and design; this FWP designs, discovers, characterizes and understands systems that shed light on how remarkable properties of matter emerge from complex correlations of the atomic or electronic constituents and, as a result, provides better control of these properties. These efforts directly address research priorities identified in the Basic Research Needs Workshops on *Quantum Materials for Energy Relevant Technology* and *Synthesis Science for Energy Relevant Technology*.

Recent Progress

The Complex States FWP has diverse efforts on a number of systems and ground states. For example, we are currently studying the interaction between electronic, structural and magnetic degrees of freedom in Fe-based superconductors, fragile magnetic systems and systems that

manifest variants of collapsed tetragonal structural phase transitions. In parallel, we endeavor to design and discover new compounds and systems with exotic transitions and properties. We have also been developing new, in house, capabilities ranging from specific heat under pressures up to 2.5 GPa, to optical-NV-magnetometry, to laser-based ARPES with base temperatures as low as 3 K.

For this contractors meeting, we will primarily review our progress in manipulating, controlling and understanding $CaKFe_4As_4$-based materials. Over the past two years we have been able to substitute Ni and Co for Fe in $CaKFe_4As_4$. By growing and studying single crystals of these five component compounds we have been able to identify the $CaKFe_4As_4$-based materials as fragile magnetic systems with high temperature superconductivity emerging near a quantum critical point associated with hedgehog-type-spin-vortex-crystal antiferromagnetism. This form of antiferromagnetism has no associated structural phase transition and is not inherently nematic in nature. Detailed neutron scattering and Mossbauer spectroscopy measurements on $CaK(Fe_{1-x}Ni_x)_4As_4$ crystals reveal that there is a strong competition between the superconducting and spin-vortex-ordered states. NMR measurements on the same $CaK(Fe_{1-x}Ni_x)_4As_4$ samples suggest that, based on the fluctuations in the normal state, there should be a quantum critical point close to $x = 0$, i.e. for the pure $CaKFe_4As_4$ compound. Whereas this may be the case for the normal state, the competition between the superconducting and antiferromagnetically ordered states leads to a sudden loss of antiferromagnetic order for x-values that would have $T_N < T_c$; ^{57}Fe-Mossbauer spectroscopy data do not show any indication of any hyperfine field for x-values that would have $T_N < T_c$. These results strongly suggest a sharp decrease in $T_N(x)$ or even a back-bending.

In addition to superconductivity and antiferromagnetism, $CaFe_2As_2$ and $CaKFe_4As_4$ can also undergo a collapsed-tetragonal, or a series of half-collapsed-tetragonal, phase transitions under pressure or stress. We have extended our understanding of these transition by measuring the uniaxial stress-strain properties of these compounds. We have been able to identify the collapsed tetragonal phase transition as (i) a powerful mechanism for changing and controlling the electronic, magnetic, and structural properties of these compounds and (ii) a new route to super-elastic behavior, allowing for over 17% recoverable strain in $CaKFe_4As_4$ at room temperature.

Future Plans

Given that we have been able to successfully create and study electron doped $CaKFe_4As_4$ via substitution of Co or Ni for Fe, we now are studying the effects of hole doped $CaKFe_4As_4$ via Mn and Cr substitution. This will allow us to use transition metal substitution to study both sides of putative quantum critical point near $x = 0$ and also address the question of whether Mn, with its more local-moment-like behavior, is qualitatively or quantitatively different form other 3d-transition metal substitutions.

More widely, across the FWP we will be using uniaxial strain to study the response of a Fe-based superconductors as well as other compounds with NMR, ARPES, London Penetration, and resistivity measurements. Having both orthorhombic, stripe and spin-vortex-crystal,

tetragonal systems will allow us to further to investigate the interplay between electronic/magnetic and structure associated with the formation of the superconducting state

Beyond superconductivity, we will continue to develop new, fragile magnetic systems with the intent of discovering new quantum critical systems and mastering new emergent phases that may be in proximity to their quantum critical points. The discovery and development of these new systems will be accomplished by implementation of new algorithms for the discovery of low dimensional crystal structures as well as on the use of bandstructure theory to identify antiferromagnetic systems that respond strongly to pressure, stress, and/or substitution. (A detailed discussion of some of these can be found in "New Materials Physics" arXiv:1908.02369.)

References and Publications

The FWP published over 100 papers over the past two years and their list will not fit within allocated space. This includes papers spanning a wide range of materials, states and phase transitions published in Physical Review Letters, Physical Review B, and Nature and Science families of journals. Below we list the papers published during this period concerning the $CaKFe_4As_4$ materials.

1) Cui, J.; Ding, Q. -P.; Meier, W. R.; Bohmer, AE; Kong, T; Borisov, V; Lee, Y; Bud'ko, SL; Valenti, R; Canfield, PC; Furukawa, Y, "Magnetic fluctuations and superconducting properties of $CaKFe_4As_4$ studied by As-75 NMR" Phys. Rev. B 96, 2017, 104512.

2) Kaluarachchi, Udhara S.; Taufour, Valentin; Sapkota, Aashish; Borisov, V; Kong, T; Meier, WR; Kothapalli, K; Ueland, BG; Kreyssig, A; Valenti, R; McQueeney, RJ; Goldman, AI; Bud'ko, SL; Canfield, PC, "Pressure-induced half-collapsed-tetragonal phase in $CaKFe_4As_4$", Phys. Rev. B 96, 2017, 140501

3) Ding, Q. -P.; Meier, W. R.; Bohmer, A. E.; Bud'ko, SL; Canfield, PC; Furukawa, Y, "NMR study of the new magnetic superconductor $CaK(Fe_{0.951}Ni_{0.049})_4As_4$: Microscopic coexistence of the hedgehog spin-vortex crystal and superconductivity", Phys. Rev. B 96, 2017, 220510.

4) Sypek, John T.; Yu, Hang; Dusoe, Keith J.; Drachuck, G; Patel, H; Giroux, AM; Goldman, AI; Kreyssig, A; Canfield, PC; Bud'ko, SL; Weinberger, CR; Lee, SW, "Superelasticity and cryogenic linear shape memory effects of $CaFe_2As_2$" Nature Comm. 8, 2017, 1083.

5) Meier, William R.; Ding, Qing-Ping; Kreyssig, Andreas; Bud'ko, SL; Sapkota, A; Kothapalli, K; Borisov, V; Valenti, R; Batista, CD; Orth, PP; Fernandes, RM; Goldman, AI; Furukawa, Y; Bohmer, AE; Canfield, PC, "Hedgehog spin-vortex crystal stabilized in a hole-doped iron-based superconductor"NPJ QUANTUM MATERIALS 3 2018, Article Number: 5.

6) Fente, Anton; Meier, William R.; Kong, Tai; Kogan, VG; Bud'ko, SL; Canfield, PC; Guillamon, I; Suderow, H, "Influence of multiband sign-changing superconductivity on vortex cores and vortex pinning in stoichiometric high-T_c $CaKFe_4As_4$", Phys. Rev. B 97, 2018, 134501.

7) Khasanov, Rustem; Meier, William R.; Wu, Yun; Mou, DX; Bud'ko, SL; Eremin, I; Luetkens, H; Kaminski, A; Canfield, PC; Amato, A, "In-plane magnetic penetration depth of superconducting $CaKFe_4As_4$" Phys. Rev. B 97, 2018, 140503.
8) Teknowijoyo, S.; Cho, K.; Konczykowski, M.; Timmons, EI; Tanatar, MA; Meier, WR; Xu, M; Bud'ko, SL; Canfield, PC; Prozorov, R, "Robust s(+/-) pairing in $CaK(Fe_{1-x}Ni_x)_4As_4$ (x=0 and 0.05) from the response to electron irradiation", Phys. Rev. B 97, 2018, 140508.
9) Xiang, Li; Meier, William R.; Xu, Mingyu; Kaluarachchi, US; Bud'ko, SL; Canfield, PC, "Pressure-temperature phase diagrams of $CaK(Fe_{1-x}Ni_x)_4As_4$ superconductors", Phys. Rev. B 97, 2018, 174517.
10) A. Kreyssig, J. M. Wilde, A. E. Böhmer, W. Tian, W. R. Meier, Bing Li, B. G. Ueland, Mingyu Xu, S. L. Bud'ko, P. C. Canfield, R. J. McQueeney, and A. I. Goldman, "Antiferromagnetic order in $CaK(Fe_{1-x}Ni_x)_4As_4$ and its interplay with superconductivity", Phys. Rev. B 97, 2018, 224521.
11) Zhang, WL; Meier, WR; Kong, T; Canfield, PC; Blumberg, G, "High-T-c superconductivity in $CaKFe_4As_4$ in absence of nematic fluctuations", Phys. Rev. B 98, 2018, 140501.
12) Ding, QP ; Meier, WR; Cui, J; Xu, M; Bohmer, AE; Bud'ko, SL; Canfield, PC; Furukawa, Y, "Hedgehog Spin-Vortex Crystal Antiferromagnetic Quantum Criticality in $CaK(_{Fe1-x}Ni_x)_4As_4$ Revealed by NMR" Phys. Rev. Lett. 121, 2018, 137204.
13) Singh, SJ; Bristow, M; Meier, WR; Taylor, P; Blundell, SJ; Canfield, PC; Coldea, AI, "Ultrahigh critical current densities, the vortex phase diagram, and the effect of granularity of the stoichiometric high-T-c superconductor $CaKFe_4As_4$", Phys. Rev. Mat. 2, 2018, 074802.
14) Jost, D; Scholz, JR; Zweck, U; Meier, WR; Bohmer, AE; Canfield, PC; Lazarevic, N; Hackl, R, "Indication of subdominant d-wave interaction in superconducting $CaKFe_4As_4$" Phys. Rev. B 98, 2018, 020504.
15) Borisov, V; Canfield, PC; Valenti, R, "Trends in pressure-induced layer-selective half-collapsed tetragonal phases in the iron-based superconductor family $AeAFe_4As_4$", Phys. Rev. B 98, 2018, 064104.
16) Khasanov, R; Meier, WR; Bud'ko, SL; Luetkens, H; Canfield, PC; Amato, A, "Anisotropy induced vortex lattice rearrangement in $CaKFe_4As_4$", Phys. Rev. B 99, 2019, 140507.
17) Bud'ko, SL; Kogan, VG; Prozorov, R; Meier, WR; Xu, MY; Canfield, PC, "Coexistence of superconductivity and magnetism in $CaK(Fe_{1-x}Ni_x)_4As_4$ as probed by ^{57}Fe Mossbauer spectroscopy", Phys. Rev. B 98, 2019, 144520.
18) Gyuho Song, Vladislav Borisov, William R. Meier, Mingyu Xu, Keith J. Dusoe, John T. Sypek, Roser Valentí, Paul C. Canfield, and Seok-Woo Lee, "Ultrahigh elastically compressible and strain-engineerable intermetallic compounds under uniaxial mechanical loading", APL Materials 7, 2019, 061104.

Nanostructure Studies of Correlated Quantum Materials

Douglas Natelson, Dept. of Physics and Astronomy (joint with Electrical & Computer Engineering and Materials Science & Nanoengineering), Rice University

Program Scope

In strongly correlated quantum materials, the dynamics of the charge and spin degrees of freedom are particularly rich, thanks to strong interactions between the charge carriers as well as between the carriers and the lattice. One result is competition between multiple ordered states with broken symmetries, including superconductivity, magnetic order, and a variety of density wave states. Another implication is the emergence of collective degrees of freedom (e.g., the fractionally charged quasiparticles of the fractional quantum Hall state), and deviations from the expectations of Landau Fermi Liquid (FL) theory. The scope of this program has been to apply nanostructure-based tools and measurement techniques toward two ends: Assessing the effective charge of low-energy current-carrying excitations in archetypal non-Fermi liquids (NFLs) using shot noise; and attempting to understand the role of quantum coherent corrections to semiclassical conduction in NFLs ("strange metals" when quasiparticles may not be well-defined, and "bad metals" when the resistivity seems to violate the Mott-Ioffe-Regel limit expected for carriers that travel many wavelengths before scattering).

First, we have made considerable progress using shot noise measurements to examine the nature of charge carriers in underdoped $La_{2-x}Sr_xCuO_4$ (LSCO), an exemplar of the superconducting cuprates known to exhibit a pseudogap and a "strange metal" normal state. These experiments have been enabled by a collaboration with Dr. Ivan Božović of Brookhaven National Lab, through his group's growth of exquisitely clean LSCO/LCO/LSCO tunnel junctions. Shot noise is the fluctuation in current due to the discreteness of charge carriers. Independent (Poissonian) carriers of charge e are expected to lead to current fluctuations with a spectral density $S_{I,e} = 2eI \coth(eV/2k_BT)$ A^2/Hz, where I is the average current[1]. Present experiments measure the noise in cuprate tunnel junctions as a function of temperature and bias over a broad range, and compare the results with these independent-single-charge expectations.

Second, we are using transport measurements, including low frequency studies of temporal conductance fluctuations, to try to examine coherence and the nature of the metal-insulator phase transition in other correlated systems, most recently V_2O_3 films provided through a collaboration with the group of Prof. Ivan Schuller of UC San Diego.

Recent Progress

We have measured the shot noise in epitaxial c-axis cuprate tunnel junctions (LSCO/LCO/LSCO), where $x = 0.1$, 0.12, 0.14, and 0.15, spanning the underdoped to optimally doped range for LSCO. The tunnel barrier in these devices is 2 nm (1.5 unit cells) of the undoped parent Mott insulator, La_2CuO_4. This maximizes the structural perfection of the epitaxial structures, while also differing from the localized vacuum tunneling situation examined

in the large number of scanning tunneling microscopy/spectroscopy experiments in the literature. One expectation for such planar tunnel junctions is the conservation of carrier momentum in the *ab* plane. Unlike vaccum, the Mott state may support unconventional excitations relevant to the LSCO strange metal. These tunnel junctions, patterned to be 10-20 microns in diameter via photolithography and argon ion-milling, are tools that allow unique access to both the normal/pseudogap state, the superconducting state, and their excitations.

We use a low-frequency cross-correlation method to measure the voltage noise power, S_V, at a given bias voltage/current and temperature, and convert that to the current noise power $S_I = S_V/(dV/dI)^2$, using the measured differential resistance dV/dI at that bias, and correcting for the frequency-dependent effects of parasitic capacitance in the measurement setup. We have measured multiple junctions of each doping value, over a broad range of temperatures from room temperature down to 5 K, and over a broad range of biases from 0 V up to well over the scale of the superconducting gap Δ inferred from the tunneling dV/dI characteristics. We note that there is no sign of a coherent Josephson current in any of the junctions examined, even down to temperatures of 25 mK (via the laboratory of Prof. Ilya Sochnikov at the University of Connecticut) and pA scales. This is consistent with prior measurements on related structures[2], and implies that the coherence length for transport along the *c*-axis direction is well under 2 nm.

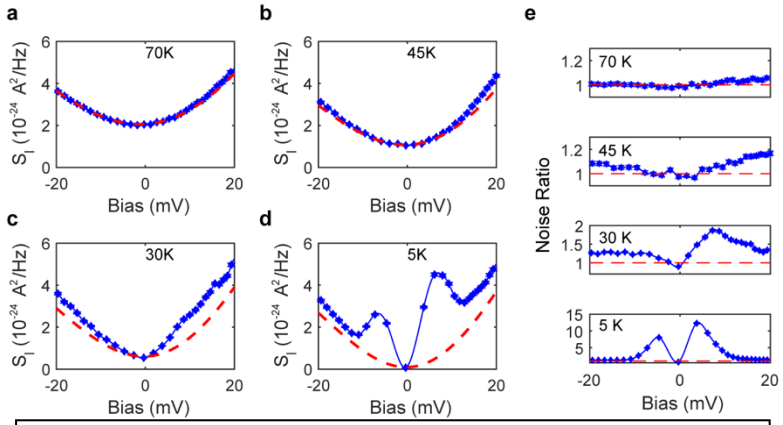

Figure 1. Noise as a function of bias in a x = 0.14 LSCO/LCO/LSCO tunnel junction. (a-d) Red dashed line is single-electron tunneling expectation. (e) Ratio of measured noise to single-charge tunneling expectation.

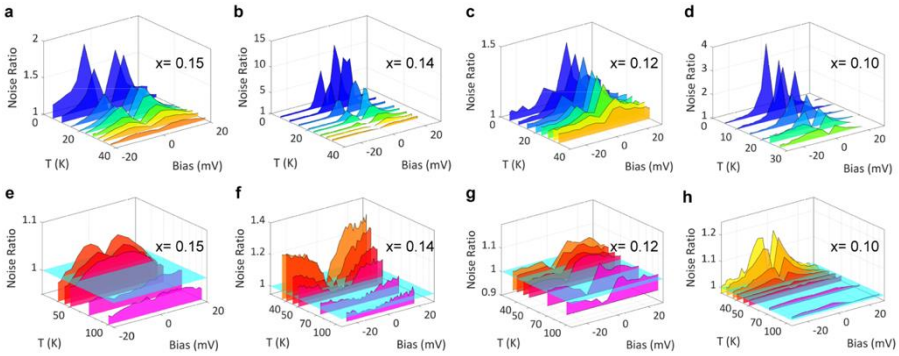

Figure 2. Noise ratio vs. temperature for devices at four doping levels. Upper row = below T_c, lower row = above T_c. Note that the noise ratio exceeds one both above T_c and at high biases.

Figures 1 and 2 show the essential, extremely exciting result of these studies so far, currently in press at *Nature*[3]. Fig. 1 shows data for one of the $x = 0.14$ devices ($T_c \sim 37$ K). The red dashed line shows the S_I expected for Poissonian single-charge tunneling for the

measured *I-V* characteristics at each temperature, while the blue points show the measured noise values. The *noise ratio*, $S_I/S_{I,e}$, is shown in panel (e), and clearly shows excess, super-Poissonian noise, both well above T_c, and also at biases well in excess of the superconducting gap scale (less than 10 mV on this plot). The large enhancements of S_I when the source and drain are superconducting are reminiscent of Andreev processes. Figure 2 shows a summary of the noise ratios for four of the measured devices, over the broad temperature and bias ranges.

The simplest interpretation of super-Poissonian shot noise is that some of the tunneling current results from the transport of some paired charges as well as individual charges. This is the interpretation applied in Andreev transport experiments, and below T_c multiple Andreev reflection can lead to transport of charge in units of 2*e*, 3*e*, etc. [4]. Note that for conventional low-T_c-based SIS tunnel junctions, Andreev charge enhancement is only seen for biases $eV < 2\Delta$, and for temperatures below T_c, in contrast to the results here. Assuming that the tunneling current is carried either by single charges or the transfer of pairs, from the noise ratio it is possible to infer the *fraction* of the current from pair transfer: $z = [(S_I/S_{I,e}) - 1]/[2\coth(eV/k_BT)/\coth(eV/2k_BT) - 1]$. (This analysis breaks down when $eV/k_BT \rightarrow 0$, because in the zero-bias/equilibrium limit, the only current fluctuations are the Johnson-Nyquist noise, which depends only on device impedance, regardless of the charge of the carriers.) Figure 3 shows the inferred pair fraction as a function of bias and temperature for the devices in Fig. 2. In a conventional SIS junction, there would be essentially no blue outside the red gap curve.

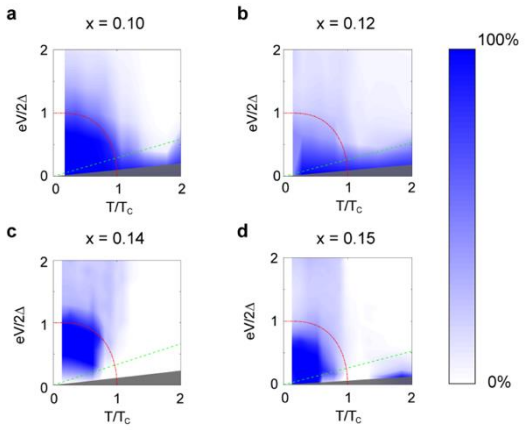

Figure 3. Inferred fraction *z* of tunneling current transferred by pairs as a function of *T* and *V*. Red line = BCS gap expectation based on T_c. Gray region indicates where uncertainty in *z* exceeds 0.5.

These data show the direct detection of the presence of pairs significantly above T_c, quantitatively consistent with prior, indirect measurements (Nernst effect[5], diamagnetism[6], THz optical conductivity[7]). Moreover, the high bias data demonstrate explicitly that the energy scale associated with pairing is larger than that associated with condensation into the superconducting state. The high bias tunneling data is expected[8] to be dominated by the antinodal parts of the band structure most affected by the pseudogap, and the bias/temperature region above T_c is also in the pseudogap.

Additional fine transport studies of the differential conductance and d^2I/dV^2 as a function of bias and temperature for these tunnel junctions have also been performed and are being prepared for publication. The essential observations are: (1) Coherence peaks in dI/dV spectra are severely smeared or absent, and the usual expectation that the product of critical current and normal-state resistance, I_cR_N should be approximately Δ is violated by more than five orders of

magnitude; (2) The residual zero-bias conductance as $T \rightarrow 0$ is ~ 0.2-0.3× the normal-state tunneling conductance, indicating many unpaired quasiparticles; (3) The gap inferred from fitting the dI/dV spectra does not close as $T \rightarrow T_c$, but rather the "Dynes parameter" grows in that limit, showing that the material is a "Dynes superconductor"[8]; and (4) There are inelastic features in the tunneling spectra near 80-100 mV that become suppressed above T_c. A manuscript on these observations is in preparation.

Separate from the cuprate work, we also have been measuring "flicker noise"/temporal conductance fluctuations in V_2O_3 film devices, both at low frequencies (Hz-100 kHz) and at radio frequencies (up to 800 MHz). These measurements show the presence of fluctuating domains in the mixed-phase regime of the metal-insulator transition up to GHz frequency scales. Analysis of these measurements is also underway, leading toward a manuscript.

Future Plans

The need is clear for additional cuprate junction measurements building on these important result. Both thicker and thinner barrier structures are needed to understand the apparent Andreev transport features in detail. It is also greatly desirable to attempt experiments toward the overdoped regime, if possible, given the surprising suppression of the superconducting condensate and lack of pseudogap in that parameter range. On the longer term, we will also pursue approaches to tuning or controlling coherence in these structures.

We will complete the V_2O_3 fluctuation measurements and will also pursue tunneling measurements of the density of states in that material as the Mott insulating state is approached. Still on the agenda, too, are shot noise measurements in other NFL systems, ideally including $YbRh_2Si_2$, which may be tuned between FL and NFL response via external magnetic field.

References

1. Y.M. Blanter and M. Buttiker, *Physics Reports* **336**(1-2), 1-166 (2000).
2. I. Bozovic *et al*., *Nature* **422**(6934), 873 (2003).
3. P. Zhou *et al*., *Nature*, in press (2019)
4. Y. Ronen *et al*., *Proc. Nat. Acad. Sci. US* **113**, 1743 (2016).
5. Y. Wang *et al*., *Phys. Rev. B* **73**, 024510 (2006).
6. L. Li *et al*., *Phys. Rev. B* **81**, 054510 (2010).
7. L. S. Bilbro *et al*., *Nat. Phys.* **7**, 298-302 (2011).
8. F. Herman and R. Hlubina, Phys. Rev. B **97**, 014517

Publications

1. P. Zhou *et al*., *Nature*, in press (2019), doi: 10.1038/s41586-019-1486-7
2. L. A. Stevens *et al*., *Appl. Phys. Lett*. **115**, 052107 (2019).
3. Shi Chen *et al*., *Phys. Rev. B* **96**, 125130 (2017).

Experimental study of novel relativistic Mott insulators in the 2-dimensional limit

PI: Claudia Ojeda-Aristizabal, Department of Physics and Astronomy, California State University Long Beach, CA 90840

Program Scope The Kitaev-Heisenberg model, a quantum compass model that describes a set of spin-1/2 moments in a honeycomb lattice, yields exciting of ground states, such as gapless spin liquids and a variety of spin ordered states. In real materials, the Kitaev-Heisenberg model comes to life assisted by electronic correlations, spin-orbit coupling, crystal field effects and a honeycomb arrangement of ions. Compounds with partially filled 4d and 5d orbitals present important spin-orbit coupling, giving rise to insulating Mott states with spin-orbit coupled moments. In materials like Sodium iridate (Na_2IrO_3) and Ruthenium Chloride ($RuCl_3$), the spin-orbit entangled moments present bond directional interactions thanks to their crystalline structure, where the geometric orientation of their IrO_6 and $RuCl_6$ octahedra is such that the exchange interaction between the moments is highly anisotropic. These features together with the Ir and Ru ions forming a honeycomb lattice, leads to an experimental incarnation of the celebrated Heisenberg-Kitaev model. This project aims to study these exciting compounds in the two dimensional limit, using two different experimental techniques: electronic transport measurements at low temperatures and angle resolved photoemission spectroscopy (ARPES). Both sodium iridate and ruthenium chloride have weakly bounded layers which allows the isolation of very thin crystals and the use of nanofabrication techniques to integrate them into an electronic device, allowing electronic transport measurements not explored before for their parent crystals. ARPES measurements will allow us to investigate the spin and orbital texture of electrons in these materials. High quality bulk crystals will be provided by the Analytis group at UC Berkeley through our ongoing collaboration. Sample fabrication and electronic transport measurements will be performed at California State University Long Beach and ARPES measurements will be conducted at the Advanced Light Source (ALS) at the Lawrence Berkeley National Lab (LBNL). Our collaboration with the Lanzara group at LBNL a world expert in ARPES, will give us access to additional state of the art capabilities.

Recent Progress

Electronic properties of thin crystals of Na_2IrO_3 :Magnetic ordered states predicted in the frame of the Kitaev-Heisenberg model have been gauged experimentally in materials like Na_2IrO_3 and $RuCl_3$ through experimental probes that require bulk crystals, such as x-ray resonant magnetic–scattering studies, magnetic susceptibility and heat capacity measurements, finding a transition temperature to a long ranged antiferromagnetically ordered state below 15K with a zig-zag pattern. Here, we have implemented a thin crystal of Na_2IrO_3 into an electronic device identifying a variable range hopping (VRH) mechanism mediated by a non-vanishing density of states at the Fermi level, observed through ARPES measurements. This VRH hopping behavior shows a clear change below 15K, identified as the magnetic ordering transition temperature. Following Mott's variable range hopping model and introducing a spin-spin exchange interaction between the carrier spins as in Shi-shen Yan et al (J. Phys.: Condens. Matter **18**, 10469 (2006)),

we have found that a spin-dependent variable range hopping explains qualitatively the change of the characteristic temperature T_0 below the magnetic ordering transition. This work provides insight about the way a Kitaev-Heisenberg model ground state (a zig-zag antiferromagnetic state) can impact the transport mechanism in an electronic device.

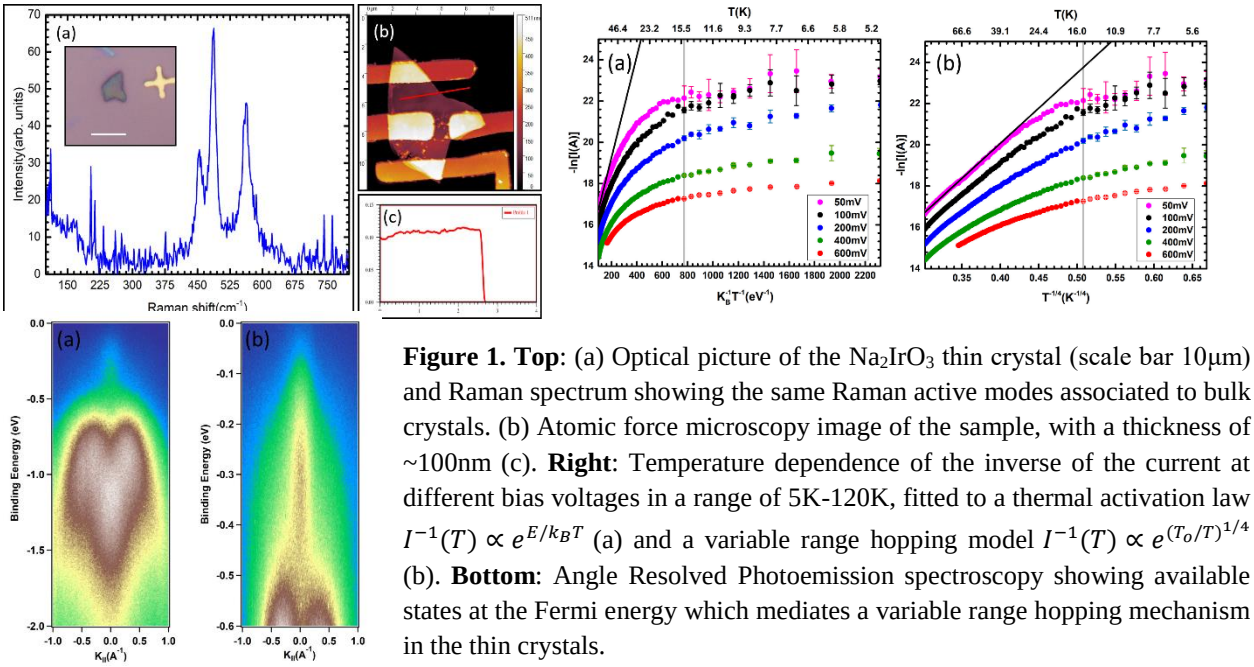

Figure 1. Top: (a) Optical picture of the Na_2IrO_3 thin crystal (scale bar 10μm) and Raman spectrum showing the same Raman active modes associated to bulk crystals. (b) Atomic force microscopy image of the sample, with a thickness of ~100nm (c). **Right**: Temperature dependence of the inverse of the current at different bias voltages in a range of 5K-120K, fitted to a thermal activation law $I^{-1}(T) \propto e^{E/k_BT}$ (a) and a variable range hopping model $I^{-1}(T) \propto e^{(T_o/T)^{1/4}}$ (b). **Bottom**: Angle Resolved Photoemission spectroscopy showing available states at the Fermi energy which mediates a variable range hopping mechanism in the thin crystals.

First observation of highly dispersive bands in thin film C_{60}: While studying Na_2IrO_3 through ARPES, we explored a C_{60} thin film. C_{60} has an unconventional zero-dimensional buckyball molecular structure that, when combined with its strong electron-electron and electron-phonon interactions in its bulk form, allow for unique properties not seen in ordinary (nonmolecular) crystalline materials. As an initial approximation, one would expect the electronic structure of a thin film C_{60} to be dominated by the electronic interactions within a single molecule—indeed the relative bond length between carbon atoms in a single molecule (~1 Å) is much smaller than the bond length between the closest carbon atoms in adjacent molecules (~3 Å) and the van der Waals bonds between adjacent C_{60} molecules (~10 Å). However, we have found through angle resolved photo emission spectroscopy (ARPES) measurements and density functional theory (DFT) calculations that long range interactions between the molecules in a thin film have a profound effect shaping the electronic structure of this material. We reported the observation for the first time of multiple highly dispersive bands within the highest occupied molecular orbitals (HOMO) in high quality C_{60} thin films grown on a novel substrate, Bi_2Se_3. The constraints that this substrate imposes on the orientation of the buckyballs and its excellent lattice matching, support a long range crystalline order in C_{60}, in contrast to previous works. By comparing our DFT calculations with our ARPES data, we concluded that not only interactions within a single molecule define the band structure of thin film C_{60} (as is the case in a molecular solid), long range interactions play an important role defining the electronic structure of the material. Our results solve the missing link between electronic dispersions, vibronic loss, and the

gas state spectra, reported through the long history of C_{60}, paving the way to the engineering of novel C_{60} heterostructures, of interest for photovoltaic and optoelectronic applications.

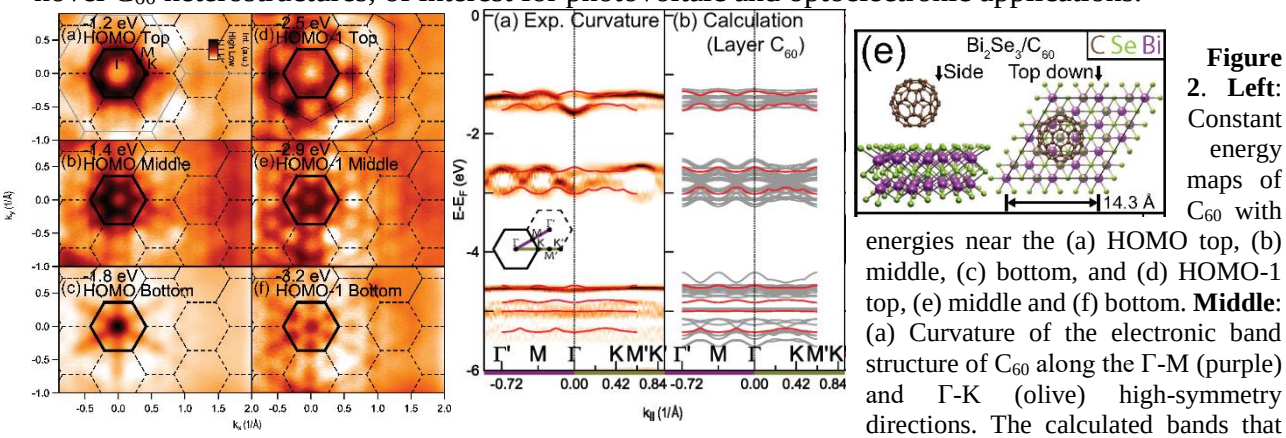

Figure 2. Left: Constant energy maps of C_{60} with energies near the (a) HOMO top, (b) middle, (c) bottom, and (d) HOMO-1 top, (e) middle and (f) bottom. **Middle**: (a) Curvature of the electronic band structure of C_{60} along the Γ-M (purple) and Γ-K (olive) high-symmetry directions. The calculated bands that best fit the HOMO, HOMO-1, and HOMO-2 experimental dispersions are plotted over the data as red lines. (b) Full DFT-calculated theory band structure of single layer C_{60} including the same bands plotted in (a) highlighted in red. **Right**: Configuration of the Bi_2Se_3/C_{60} structure.

Orbital character effects in pure C_{60} photoemission: Following our work above, we combined the excellent substrate for the growth of a C_{60} thin film (Bi_2Se_3) and high-resolution angle-resolved photoemission spectroscopy (ARPES), to explore the effects of incident light polarization and photon energy dependence of the multiple highly-dispersive valence bands of the C_{60} thin film. Our study showed specific polarization-dependent intensity enhancements and patterns of the valence bands, allowing to identify multiple bands within each band manifold and in some cases revealing band splitting. We found that the ensemble of these probes gives a clear picture of the orbital makeup of the C_{60} band manifolds and provides new insight to the electronic structure of C_{60}. The highly dispersive band clusters have a clear dependence on the linear polarization of incident light across a wide range of momenta including far beyond the first Brillouin zone. Additionally, by using circularly polarized light we have measured a strong circular dichroism effect, both observations suggesting the different orbital character of the valence band manifolds. Our photon-energy dependent study resolves strong photoemission intensity oscillations over a large range of momentum and photon energy. By performing Fourier analysis, we identified a dominant frequency, related to the C_{60}'s structural diameter and its corresponding phase, which varies significantly across the different band manifolds, suggesting signature of the different orbital character of each band manifold and giving additional information about the mixed orbital character of HOMO-2, which has been little investigated in the past. This work elucidates precise details of the C_{60} valence band manifolds through a careful analysis of the effect of linearly and circularly polarized light as well as the effect of light energy on the photoemission of C_{60}. It constitutes the first photon-dependent study of a C_{60} thin film that exhibits ARPES-level lateral order.

Future Plans

<u>$RuCl_3$/graphene/h-BN heterostructures:</u> We are currently building van der Waals heterostructures to gauge the electronic properties of RuCl3 through graphene/h-BN by proximity

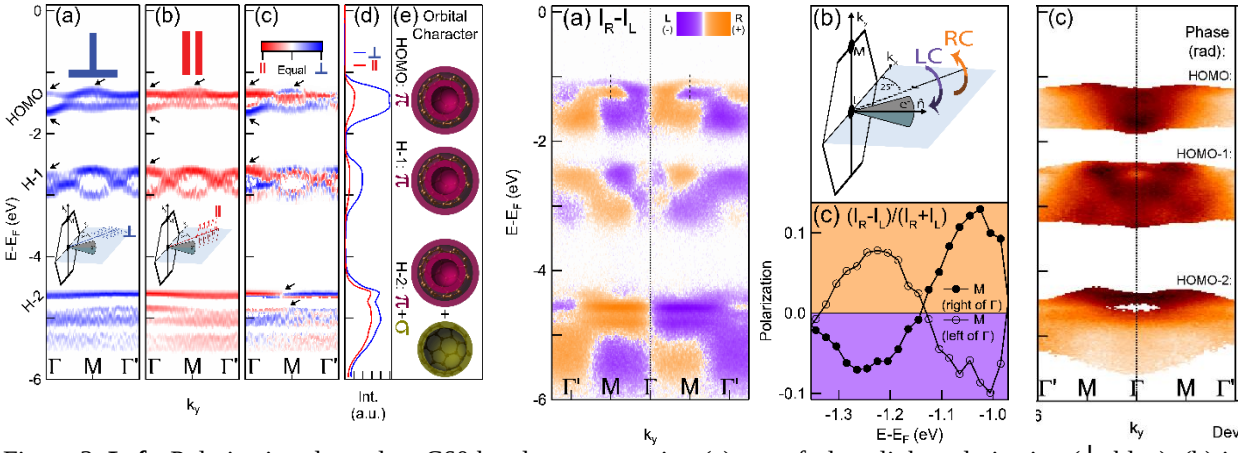

Figure 3. **Left**: Polarization-dependent C60 band structure using (a) out-of-plane light polarization (⊥, blue), (b) in-plane light polarization (∥, red) and (c) an image of their difference, which reveals different bands (see arrows) (d) Energy distribution curves (EDCs) for incident out-of-plane (blue) and in-plane (red) polarized light. It shows how photoemission signal is minimized from the π-like states (HOMO and HOMO-1) for the case of ∥ incident light, while the σ-like states (HOMO-2) are left mostly attenuated. (e) Cross section diagram illustrating a C60 molecule. Π-like states are localized to a surface inside and outside the C60 shell (HOMO, HOMO-1 and partially HOMO-2), while σ-like states are localized to the surface of the C60 shell (HOMO-2). **Middle**: (a) Circular dichroism intensity difference (I_R-I_L) of C60 band structure where orange (purple) indicates a stronger intensity from right-hand (left-hand) circularly polarized incident light. (b) Geometry of the experimental setup indicating incoming right-hand (RC, orange) or left-hand (LC, purple) circularly polarized light. (c) Circular dichroism polarization ([I_R-I_L]/[I_R+I_L]) versus energy near the top energy of the HOMO at the M points on either side of Γ (dashed lines in panel (a)). **Right**: Extracted relative phase of the k_Z dependent oscillations for each in-plane momentum k_y.

effect. This method will allow us to overcome the difficulty of the high resistance of $RuCl_3$ thin crystals at low temperatures.

High impedance measurements of $RuCl_3$ and $Na2IrO_3$ electronic devices: Additionally, by using a newly arrived triax probe in our lab, will be able to perform through guarded measurements further experiments in our Na_2IrO_3 and $RuCl_3$ samples such as magnetoresistance, which will give us a richer information about the magnetic ordering in our electronic devices.

Study of the electronic structure of endofullerenes through ARPES: following our previous results on ARPES on fullerenes, we plan to explore magnetic endofullerenes, and test the robustness of the topologically protected surface state of Bi_2Se_3.

Publications

1. D. W. Latzke*, C. Ojeda-Aristizabal*, S. M. Griffin, J. D. Denlinger, J. B. Neaton, A. Zettl and A. Lanzara, "Observation of highly dispersive bands in pure thin film C_{60} **Phys. Rev. B 99, 045425 (2019).**
2. D. W. Latzke*, C. Ojeda-Aristizabal*, J. D. Denlinger, R. Reno, A. Zettl and A. Lanzara, "Orbital character effects in the photon energy and polarization dependence of pure C_{60} photoemission" **Under review ACS Nano (2019)** ArXiv: 1905.00119 (2019).
3. Josue Rodriguez, Amirari Diego, Nicholas Breznay, Drew Latzke, Francisco Ramirez, Peter Santiago, Samantha Crouch, Robert Kellahoffer, Gilbert Arias, David Rosser, Christopher Kim, Sabrina Kaplan, Joseph Guzman, Hadi Tavassol, Alessandra Lanzara, James Analytis and Claudia Ojeda-Aristizabal. "Electronic transport in thin crystals of Na_2IrO_3" **Submitted to Applied Physics Letters (2019)**.

Project Title: Spectroscopy of Degenerate One-Dimensional Electrons in Carbon Nanotubes

Principal Investigator: Junichiro Kono
Mailing Address: Department of Electrical and Computer Engineering, Rice University, Houston, Texas 77005, U.S.A.
Email Address: kono@rice.edu

Program Scope

The goal of this research program is to understand the fundamental properties of degenerate one-dimensional (1-D) electrons in single-wall carbon nanotubes (SWCNTs). SWCNTs provide an ideal 1-D environment in which to study many-body physics. Semiconducting SWCNTs exhibit rich optical spectra dominated by extremely stable 1-D excitons, whereas metallic SWCNTs contain massless 1-D carriers with ultralong mean-free paths. Despite the large number of electrical, optical, and magnetic studies of SWCNTs during the last two decades, most of the predicted exotic properties of interacting 1-D electrons have yet to be observed, and some of the reported experimental results remain highly controversial.

Here, using an arsenal of spectroscopic methods from the terahertz to the visible spectral range, including ultrafast optical spectroscopy and ultrahigh magnetic fields, we aim to probe correlations and many-body effects in this prototypical 1-D nanostructure. These studies can provide a wealth of new insights into the nature of strongly correlated carriers in the ultimate 1-D limit that will lead to novel nanodevice concepts and implementations.

Specifically, the primary objective of this research program is to address the following key questions and issues, which are of critical importance in many-body physics:

- ‘Spinons’ and ‘holons’ in high magnetic fields: What will be the signatures of spin-charge separation in electron spin resonance? Will a magnetic field split spinon and holon peaks differently, as predicted?
- Optical conductivity of Tomonaga-Luttinger liquids: How will many-body effects modify the frequency, temperature, and magnetic field dependences of dynamic conductivity of metallic SWCNTs? Will there be any scaling laws indicative of quantum criticality?
- Light emission from high-density 1-D excitons: How will excitons in SWCNTs behave at quantum degenerate densities? How will the bosonic characters of 1-D excitons manifest themselves in emission spectra? Will they cooperate to emit superradiantly?

The overall theme of this research is based on one of the emergent concepts in condensed matter physics today. Namely, dynamical, non-equilibrium, and nonlinear aspects of many-body effects in quantum-confined systems have been poorly addressed to date despite the fact that one can expect a wide range of extraordinary phenomena that are not expected in bulk solids or atoms/molecules. In addition, they will undoubtedly become important when one wants to operate any electrical or photonic nanodevices. Particular emphasis is placed on the dynamic 1-D phenomena in the terahertz, infrared, and optical frequency ranges, which is a widely open research field that deserves more exploration both from basic and applied points of view. Because they are direct band gap materials, SWCNTs are one of the leading candidates to unify electronic and optical functions in nanoscale circuits and elucidate how electron correlations can affect and control finite-frequency phenomena in 1-D systems.

Recent Progress

Non-perturbative coupling of photons and excitons produces hybrid particles, exciton–polaritons, which have exhibited a variety of many-body phenomena in various microcavity systems. However, the vacuum Rabi splitting (VRS), which defines the strength of photon–exciton coupling, is usually a single constant for a given system. Here, we have developed a unique architecture in which excitons in an aligned single-chirality SWCNT film interact with cavity photons in polarization-dependent manners. The system reveals ultrastrong coupling (VRS up to 329 meV or a coupling-strength-to-transition-energy ratio of 13.3%) for polarization parallel to the nanotube axis, whereas VRS is absent for perpendicular polarization. Between these two extremes, VRS is continuously tunable through polarization rotation with exceptional points separating crossing and anticrossing. The points between exceptional points form equienergy arcs onto which the upper and lower polaritons coalesce. The demonstrated on-demand ultrastrong coupling provides ways to explore topological properties of polaritons and quantum technology applications.

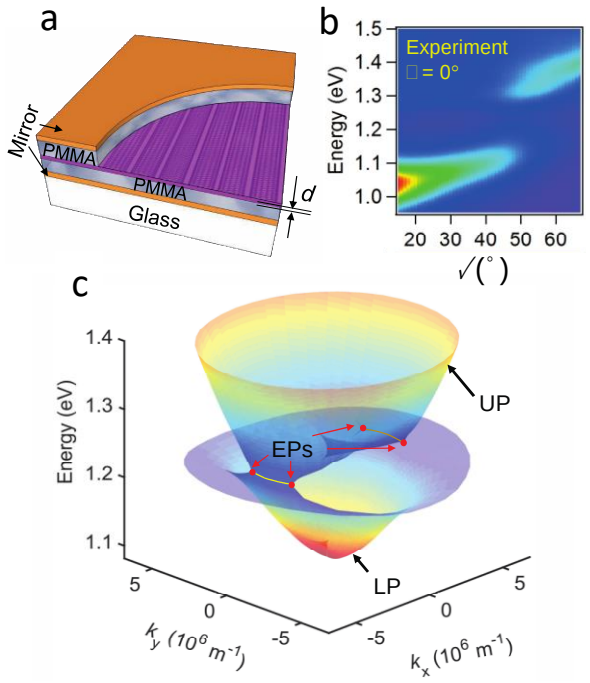

Figure 1: Continuous transition between weak and ultrastrong coupling through exceptional points in carbon nanotube microcavity exciton–polaritons [1]. **a.** Schematic of the fabricated aligned carbon nanotube exciton-polariton device. **b.** Dispersion for parallel polarization, exhibiting large vacuum Rabi splitting. **c.** Dispersion surfaces of the upper polartion (UP) and lower polartion (LP). There are four exceptional points (EPs) symmetrically located with respect to the origin.

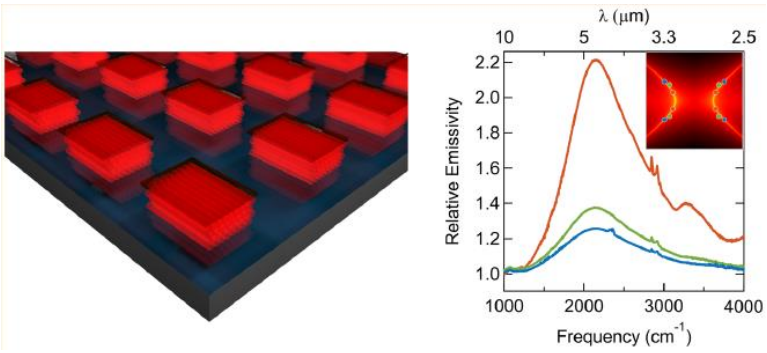

Figure 2: [2] (left) An array of indefinite cavities of SWCNTs optimized for selective thermal emission. (right) Measured emissivity of three cavities with different combinations of dimensions, mapping out the hyperbolic equifrequency lines.

Nanophotonic thermal emitters with large photonic density of states (PDOS) have the potential to significantly enhance the efficiency of radiative cooling and waste heat recovery. Because of their nearly infinite PDOS, refractory hyperbolic materials make a promising material platform for thermal emitters. However, it is challenging to achieve a prominent PDOS in existing refractory hyperbolic

materials, especially in a broad bandwidth. Here, we demonstrate macroscopically aligned SWCNTs as an excellent refractory material platform for hyperbolic nanophotonic devices. Aligned SWCNTs are thermally stable up to 1600 °C and exhibit extreme anisotropy: metallic in one direction and insulating in the other two directions. Such extreme anisotropy results in an exceptionally large PDOS over a broadband spectrum range (longer than 4.3 μm) in the mid-infrared, manifesting as strong resonances in deeply subwavelength-sized cavities. We demonstrate polarized, spectrally selective, thermal emission from aligned SWCNT films and indefinite cavities of volume as small as $\sim\lambda^3/700$ operating at 700 °C. These experiments suggest that aligned carbon nanotubes enhance PDOS and hence also thermal photon density by over 2 orders of magnitude, making them a promising refractory nanophotonics platform.

Future Plans

We will perform further gigahertz, terahertz, and infrared spectroscopy experiments on these aligned large-scale SWCNT films to understand their 1-D nature on a macroscopic scale. We will use modern nonlinear and ultrafast optical methods, combined with our unique capabilities of studying materials in ultrahigh magnetic fields using a 30 T table-top magnet [3,4]. Furthermore, using the developed method, we will be trying to fabricate single crystals of single-chirality SWCNTs (see Fig. 3). Such crystals are expected to exhibit new phenomena arising from the intrinsically one-dimensional nature of the interacting electrons in these systems in a chirality-specific manner.

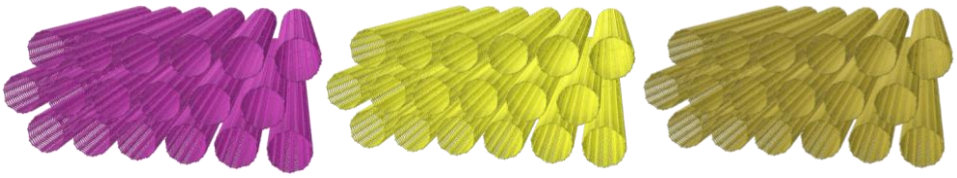

Figure 3: Single crystals of single-chirality single-wall carbon nanotubes with distinct optical, electronic, and magnetic properties.

References

1. W. Gao, X. Li, M. Bamba, and J. Kono, "Continuous Transition between Weak and Ultrastrong Coupling through Exceptional Points in Carbon Nanotube Microcavity Exciton–Polaritons," *Nature Photonics* **12**, 362 (2018).
2. W. Gao, C. F. Doiron, X. Li, J. Kono, and G. V. Naik, "Macroscopically Aligned Carbon Nanotubes as a Refractory Platform for Hyperbolic Thermal Emitters," *ACS Photonics* **6**, 1602 (2019).
3. G. T. Noe, H. Nojiri, J. Lee, G. L. Woods, J. Léotin, and J. Kono, "A Table-Top, Repetitive Pulsed Magnet for Nonlinear and Ultrafast Spectroscopy in High Magnetic Fields Up to 30 T," *Review of Scientific Instruments* **84**, 123906 (2013).
4. G. T. Noe, I. Katayama, F. Katsutani, J. J. Allred, J. A. Horowitz, D. M. Sullivan, Q. Zhang, F. Sekiguchi, G. L. Woods, M. C. Hoffmann, H. Nojiri, J. Takeda, and J. Kono, "Single-Shot Terahertz Time-Domain Spectrscopy in Pulsed High Magnetic Fields, *Optics Express* **24**, 30328 (2016).

Publications

1. W. Gao, C. F. Doiron, X. Li, J. Kono, and G. V. Naik, "Macroscopically Aligned Carbon Nanotubes as a Refractory Platform for Hyperbolic Thermal Emitters," *ACS Photonics* **6**, 1602 (2019).
2. W. Gao and J. Kono, "Science and Applications of Wafer-Scale Crystalline Carbon Nanotube Films Prepared through Controlled Vacuum Filtration," *Royal Society Open Science* **6**, 181605 (2019).
3. F. Katsutani, W. Gao, X. Li, Y. Ichinose, Y. Yomogida, K. Yanagi, and J. Kono, "Direct Observation of Cross-Polarized Excitons in Aligned Single-Chirality Single-Wall Carbon Nanotubes," *Physical Review B* **99**, 035426 (2019).
4. K. Fukuhara, Y. Ichinose, H. Nishidome, Y. Yomogida, F. Katsutani, N. Komatsu, W. Gao, J. Kono, and K. Yanagi, "Isotropic Seebeck Coefficient of Aligned Single-Wall Carbon Nanotube Films," *Applied Physics Letters* **113**, 243105 (2018).
5. X. Wang, W. Gao, X. Li, Q. Zhang, S. Nanot, E. H. Hároz, J. Kono, and W. D. Rice, "Magnetotransport in Type-Enriched Single-Wall Carbon Nanotube Networks," *Physical Review Materials* **2**, 116001 (2018).
6. W. Gao, X. Li, M. Bamba, and J. Kono, "Continuous Transition between Weak and Ultrastrong Coupling through Exceptional Points in Carbon Nanotube Microcavity Exciton–Polaritons," *Nature Photonics* **12**, 362 (2018).
7. K. Yanagi, R. Okada, Y. Ichinose, Y. Yomogida, F. Katsutani, W. Gao, and J. Kono, "Intersubband Plasmons in the Quantum Limit in Gated and Aligned Carbon Nanotubes," *Nature Communications* **9**, 1121 (2018).
8. A. Zubair, X. Wang, F. Mirri, D. E. Tsentalovich, N. Fujimura, D. Suzuki, K. P. Soundarapandian, Y. Kawano, M. Pasquali, and J. Kono, "Carbon Nanotube Woven Textile Photodetector," *Physical Review Materials* **2**, 015201 (2018).

Poster Sessions

Experimental Condensed Matter Physics Principal Investigators' Meeting

POSTER SESSION I
Monday Morning, September 16, 2019

1. *Visualizing orbital-selective spin polarization in picoscale designed chromates and molybdates by MBE and ARPES*
   Charles Ahn, Yale University

2. *Towards a universal description of vortex matter in superconductors*
   Leonardo Civale, Los Alamos National Laboratory

3. *Novel x-ray probes of electronically heterogeneous quantum materials*
   Matteo Mitrano, University of Illinois at Urbana-Champaign

4. *Designing metastability: Coercing materials to phase boundaries*
   Thomas Ward, Oak Ridge National Laboratory

5. *Exposing the electronic properties of topologically non-trivial and correlated compounds: A quest for topological superconductivity*
   Luis Balicas, Florida State University

6. *Dynamics of electronic interactions in superconductors and related materials*
   Dan Dessau, University of Colorado at Boulder

7. *One-dimensional topological nanomaterials and superconductivity*
   Jeeyoung Cha, Yale University

8. *Probing excitons in confined environments using photon-resolved methods*
   Moungi Bawendi, Massachusetts Institute of Technology

9. *Magnetoelectronic phenomena due to quantum magnetization fluctuations*
   Sergei Urazhdin, Emory University

10. *Spectroscopic investigations of novel electronic and magnetic materials*
    Janice Musfeldt, University of Tennessee

11. *Search for novel topological phases in superconductors using laser-based spectroscopy*
    David Hsieh, California Institute of Technology

12. *An experimental study of flat bands and correlated phases in twisted carbon layers*
    Eva Andrei, Rutgers University

13. *Quantum materials*
    Joseph Orenstein, Lawrence Berkeley National Laboratory

14. *Microwave spectroscopy of correlated 2d electron systems in semiconductors and graphene*
    Lloyd Engel, Florida State University

15. *Emerging materials*
    John Mitchell, Argonne National Laboratory

16. *THz plasmonics and topological optics of Weyl semimetals*
    Dennis Drew, University of Maryland

17. *Tuning phase transformations for designated functionality*
    Athena Sefat, Oak Ridge National Laboratory

POSTER SESSION II
Monday Afternoon, September 16, 2019

1. *Direct observation of fractional quantum Hall quasiparticle braiding statistics via interferometry*
   Michael Manfra, Purdue University

2. *Nanoscale electrical transfer and coherent transport between atomically-thin materials*
   Douglas Strachan, University of Kentucky

3. *Ultrasonic determination of electron viscosity and hydrodynamics in metals*
   Brad Ramshaw, Cornell University

4. *Correlated materials – synthesis and physical properties*
   Ian Fisher, SLAC National Accelerator Laboratory

5. *Heterostructures of quantum spin liquid and quantum electronic liquid for electrically sensing entangled excitations*
   Haidong Zhou, University of Tennessee

6. *Symmetry engineering of topological quantum states*
   Jin Hu, University of Arkansas–Fayetteville

7. *Influence of dimensional confinement at the metal-layered crystal interface*
   Timothy Kidd, University of Northern Iowa

8. *Investigation of topologically trivial and non-trivial spin textures and their relationships with the topological Hall effect*
   TeYu Chien, University of Wyoming

9. *Antiferromagnetism and superconductivity*
   William Halperin, Northwestern University

10. *Electronic and spin correlations in novel magnetic compounds*
    George Hadjipanayis, University of Delaware

11. *Time-resolved spectroscopy of insulator-metal transitions: Exploring low-energy dynamics in strongly correlated systems*
    Gunter Luepke, College of William and Mary

12. *Single molecule investigations and manipulation of magnetic and superconducting molecular systems on surfaces*
    Saw-Wai Hla, Ohio University

13. *Hybrid electro- and acousto-dynamical systems for quantum optical networks*
    Maria Spiropulu, Caltech

14. *Superconductivity and magnetism in d- and f-electron materials*
    Brian Maple, University of California, San Diego

POSTER SESSION III
Tuesday Morning, September 17, 2019

1. *Correlated and complex materials*
   Brian Sales, Oak Ridge National Laboratory

2. *Chiral materials and unconventional superconductivity*
   Qiang Li, Brookhaven National Laboratory

3. *Magnetometry studies of quantum correlated topological materials in intense magnetic fields*
   Lu Li, University of Michigan

4. *Study of topological and unconventional low-dimensional superconductors*
   Qi Li, Pennsylvania State University

5. *Charge inhomogeneity in correlated electronic systems*
   Barry Wells, University of Connecticut

6. *Imaging electrons in atomically layered materials*
   Robert Westervelt, Harvard University

7. *Understanding topological pseudospin transport in van der Waals' materials*
   Kin Fai Mak, Cornell University

8. *Creating and interfacing designer chemical qubits*
   Danna Freedman, Northwestern University

9. *Non-equilibrium magnetism: Materials and phenomena*
   Frances Hellman, Lawrence Berkeley National Laboratory

10. *Spin effects in low dimensional correlated systems*
    Philip Adams, Louisiana State University

11. *Magnetic interactions and excitations in quantum materials*
    Robert McQueeney, Ames Laboratory

12. *Exploring superconductivity at the edge of magnetic or structural instabilities*
    Ni Ni, University of California, Los Angeles

13. *QPress: Quantum press for next-generation quantum information platforms*
    Amir Yacoby, Harvard University

14. *Novel synthesis of epitaxial thin films of quantum materials*
    Chang-Beom Eom, University of Wisconsin, Madison

15. *The investigation of oxygen vacancies in magnetic-ferroelectric heterostructures*
    Mikel Holcomb, West Virginia University

16. *Engineering topologically protected superconducting states*
    Leonid Rokhinson, Purdue University

17. *Digital synthesis – A pathway to create and control novel states of condensed matter*
    Dillon Fong, Argonne National Laboratory

POSTER SESSION IV
Tuesday Afternoon, September 17, 2019

1. *Magneto-optical study of correlated electron materials in high magnetic fields*
   Dmitry Smirnov, Florida State University

2. *Quantum Hall systems in and out of equilibrium*
   Michael Zudov, University of Minnesota

3. *Transient studies of nonequilibrium transport in two-dimensional semiconductors*
   Jonathan Bird, University at Buffalo

4. *Tuning quantum fluctuations in low-dimensional and frustrated magnets*
   Arthur Ramirez, University of California, Santa Cruz

5. *Novel temperature limited tunneling spectroscopy of quantum Hall systems*
   Raymond Ashoori, Massachusetts Institute of Technology

6. *Synthesis and observation of emergent phenomena in Heusler compound heterostructures*
   Chris Palmstrøm, University of California, Santa Barbara

7. *Frustration as tuning parameter for quantum criticality*
   Emilia Morosan, Rice University

8. *Science of 100 Tesla*
   Neil Harrison, Los Alamos National Laboratory

9. *Correlated quasiparticles in graphene*
   John Ketterson, Northwestern University

10. *Superconductivity and magnetism*
    Wai-Kwong Kwok, Argonne National Laboratory

11. *Topological materials with complex long-range order*
    James Analytis, University of California, Berkeley

12. *Ultrafast spectroscopy of pnictides in high magnetic field: Strongly nonequilibrium physics in the 25 Tesla Split Florida-Helix magnet*
    David Hilton, The University of Alabama at Birmingham

13. *Novel sp2-bonded materials and related nanostructures*
    Alex Zettl, Lawrence Berkeley National Laboratory

14. *Quantum order and disorder in magnetic materials*
    Thomas Rosenbaum, California Institute of Technology

15. *Magnetothermal imaging of correlated electrons in moiré heterostructures*
    Andrea Young, University of California at Santa Barbara

16. *Spin-polarized scanning tunneling microscopy studies of magnetic, electronic, and spintronic phenomena in nitride systems*
    Arthur Smith, Ohio University

17. *Spin orbit torque in ferromagnet/topological-quantum-matter heterostructures*
    ***John Xiao**, University of Delaware*

Poster Abstracts

Program Title: **Spin Effects in Low Dimensional Correlated Systems**

Principle Investigator: **Philip W. Adams**
Mailing Address: **Department of Physics and Astronomy, Louisiana State University, Baton Rouge, LA 70803**
Email: **adams@phys.lsu.edu**

Program Scope

Our program focuses on the magneto-transport, non-equilibrium relaxation, and spin-resolved density-of-states properties of disordered two-dimensional paramagnetic, ferromagnetic, and superconducting systems. Specifically, we are currently investigating Zeeman-limited superconductivity in highly disordered Be/Al bilayer films, and in superconducting films having a non-trivial multiply connected geometries. In addition, we provide heat capacity measurements for Prof. Shane Stadler's studies of NiMnSi-based and Ni_2MnGa-based magnetocalorics.

Recently, we have been completed a study of the critical field behavior of thin Al films deposited onto multiply connected substrates. The substrates were fabricated via a standard electrochemical process that produced a triangular array of 66 nm diameter holes having a lattice constant of 100 nm. The critical field transition of the Al films was measured near T_c as a function of field orientation relative to the substrate normal. These measurements were compared with results from homogeneous films.

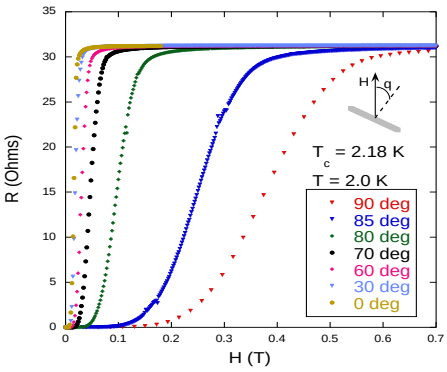

Fig 1. Plot of the critical field transition of a 9 nm-thick Al film on glass as a function of the angle between the applied field and the normal to the film surface.

As can be seen in Fig. 1 the critical field behavior of Al films on glass substrates is a monotonic function of the tilt angle. In contrast, see Fig. 2, the behavior on the multiply connected substrates is much more complex. With the field oriented along the normal ($\theta = 0$), we observe reentrant superconductivity at a characteristic matching field $H_m = 0.22$ T, corresponding to one flux quantum per substrate hole [1,2]. In tilted fields, the position H^* of the reentrance feature increases as sec(θ), but the resistivity traces exhibit crossings that are not seen in the uniform films. We show that when the tilt

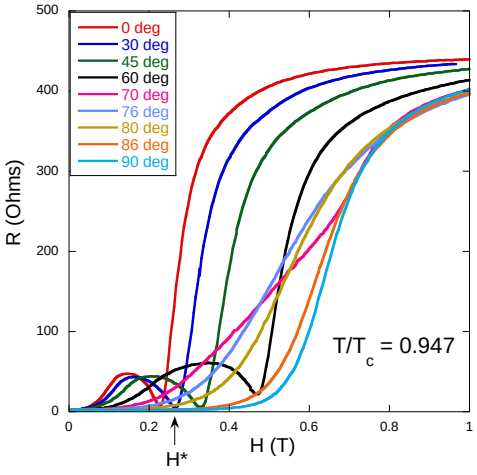

Fig 2. Resistive critical field transitions of a 9 nm-thick Al film on a nano-pore substrate near $T_C = 2.27$ K. The dips in the traces occur when the perpendicular component of the applied field equals the matching field $H_m = 0.22$ T.

angle is tuned such that H^* is of the order of the upper critical field H_c, the entire critical region is dominated by the enhanced dissipation associated with a sub-matching perpendicular component of the applied field. In addition, our data suggests that the maximum critical field is not obtained at parallel orientation but rather slightly off parallel such that the perpendicular component of the field is H*[3].

Recent Progress

Spin-imbalanced superconductivity is a historically important problem that remains at the forefront of condensed matter physics [4,5]. By the late 1960's it was known that a Zeeman field could induce a first-order transition from the superconducting phase to the normal phase in a low spin-orbit superconductor [6,7]. Moreover, Tedrow amd Meservey and coworkers showed that a large parallel magnetic field induces a Zeeman-splitting of the BCS density of states spectrum in ultra-thin Al films [8]. This Zeeman splitting can be used to probe the spin states of the system. We are currently working a project aimed at mapping out the Zeeman-limited superconductor-insulator phase diagram in highly disordered Be/Al bilayer films. The films are formed by first depositing a Be layer of varying thickness on glass followed by a 1 nm layer of Al. The Be serves to stabilize the resistance of the films by reducing their granularity. A planar tunnel junction is then formed on the bilayer using SiO_x as the tunnel barrier. The films are cooled to mK temperatures and a magnetic field is applied parallel to the film surface. Since the thickness of the films is roughly a factor of 5-10 smaller than the coherence length, orbital effects are suppressed and the parallel critical field is completely dominated by the Zeeman splitting.

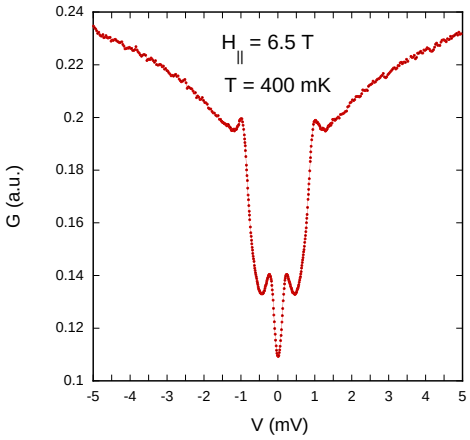

Fig 3. Planar tunneling conductance of a high resistance superconducting Be/Al film in a 6.5 T parallel magnetic field.

Shown in Fig. 3 is the tunneling conductance of a film with a low temperature sheet resistance that is of the order of the quantum resistance $R_Q=h/e^2$. This transition temperature of the film was $T_c \sim 1.8$ K and the parallel critical field was ~7 T. The film remained in the superconducting phase at 6.5 T. Note that the Zeeman-split coherence peaks are evident in the tunneling spectra but they are superimposed on a large Coulomb-mediated zero bias anomaly (ZBA) [9,10]. This anomaly represents a logarithmic depletion of states near the Fermi energy due to repulsive electron-electron correlations. In general these correlations are disruptive to the superconducting phase.

In Fig. 4 we show the normalized tunneling spectrum from the data in Fig. 3 for which the ZBA has been divided out. Now the Zeeman splitting of the BCS spectrum is clearly evident. We are currently analyzing spectra such as these in order to determine how the superconducting state accommodates the ZBA. In principle, the Coulomb effects will induce an energy dependence in the coupling parameter which will be manifest in the spectra.

Future Plans

In the near future we will begin a series of experiments aimed at exploring the Zeeman critical field transition and its associated dynamics in a multiply connected geometry. We have established the characteristics of the Zeeman-limited phase diagram in continuous, epitaxial films and we would like to extend these studies to the more complex case of a multiply connected geometry. This is a "high risk – high reward" project that is motivated by Jim Valles' pioneering studies of the S-I transition on nano-honeycombed substrates . Specifically, the Valles group observed field-induced oscillations in the normal state resistance of critically disordered films that were deposited on nano-pore substrates [11]. The oscillations are attributed to quantized flux through the substrate holes. Indeed, the oscillations are reminiscent of Little-Parks oscillations, but they occur in the insulating phase of the films. This surprising result indicated that near the critical field, the insulating phase of the films was populated by incoherent Cooper pairs.

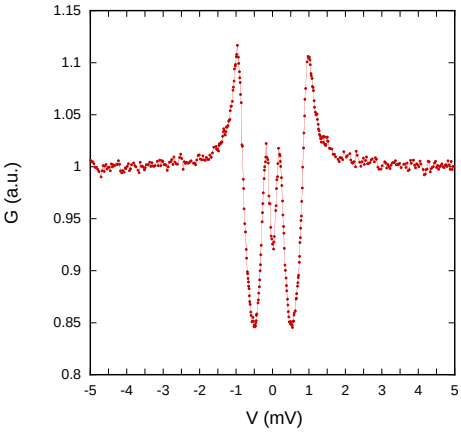

Fig 4. Normalized BCS spectrum obtained from data in Fig. 3.

References

1. M. L. Latimer, Z. L. Xiao, J. Hua, A. Joshi-Imre, Y. L. Wang, R. Divan, W. K. Kwok, and G. W. Crabtree, Phys. Rev. B 87, 020507(R) (2013).
2. M. D. Stewart, Jr., Zhenyi Long, James M. Valles, Jr., Aijun Yin, and J. M. Xu, Phys. Rev. B 73, 092509 (2006).
3. F.N. Womack, J.M. Valles, G. Catelani, and P.W. Adams, *submitted*
4. A. I. Larkin and Y. N. Ovchinnikov, Zh. Eksp. Teor. Fiz. **47** (1964).
5. P. Fulde and R. A. Ferrell, Phys. Rev. **135**, A550 (1964).
6. Clogston Phys. Rev. Lett. **9**, 266 (1962)
7. B.S. Chandrasekhar, Appl. Phys. Lett. **1**, 7 (1962)
8. P.M. Tedrow and R. Meservey, Phys. Rev. Lett. **43**, 384 (1979)
9. V. Yu. Butko, J.F. DiTusa, and P.W. Adams, Phys. Rev. Lett. **84**, 1543 (2000).
10. B.L.Altshuler,A.G.Aronov,M.E.Gershenson,andYu.V. Sharvin, Sov. Sci. Rev. A **9**, 223 (1987).
11. M. D. Stewart Jr., Aijun Yin, J. M. Xu,1, and J.M.Valles Jr., Science **318**, 1273 (2007).

Publications (2017 - 2019)

1. "The Effects of Hydrostatic Pressure on the Martensitic Transition, Magnetic, and Magnetocaloric Effects of $Ni_{45}Mn_{43}CoSn_{11}$", S. Pandey, A. Saleheen, A. Quetz, J.-H. Chen, A. Aryal, I. Doubenko, P. W. Adams, S. Stadler, and N. Ali, *MRS Comm.* **7**, 885 (2017).
2. "On Entropy Determination from Magnetic and Calorimeteric Experiments in Conventional Giant Magnetocaloric Materials", J.H. Chen, A.U. Saleheen, P.W. Adams, D.P. Young, N. Ali, and S. Stadler, *J. Appl. Phys*. **123**, 145101 (2018).
3. "Specific Heat and the Influence of Hydrostatic Pressure on the Phase Transitions in Ni50Mn35In14.25B0.75", S. Pandey, J.H. Chen, A.U. Saleheen, I. Dubenko, A. Aryal, P.W. Adams, S. Stadler, and N. Ali, *J. Magn. Magn. Mater*. ***463***, 19 (2018).
4. "Barocaloric and magnetocaloric effects in (MnNiSi)(1-x)(FeCoGe)(x)",T. Samanta, P. Lloveras, A.U. Saleheen, D.L. Lepkowski, E. Kramer, I. Dubenko, P.W. Adams, D.P. Young, M. Barrio, J.L. Tamarit, N. Ali, and S. Stadler, *Appl. Phys. Lett*. **112**, 021907 (2018).
5. "Atomic-scale Tailoring of Spin Susceptibility via Non-magnetic Spin-orbit Impurites", F.N. Womack, P.W. Adams, H. Nam, C.K. Shih, and G. Catelani, *Communication Physics* **1**, 72 (2018).
6. "Geometric Quenching of Orbital Pair Breaking in a Single Crystalline Superconducting Nanomesh Network", H. Nam, H. Chen, P.W. Adams, S.Y. Guan, T.M. Chauang, C.S. Chang, A.H. MacDonald, and C.K. Shih, *Nat. Commun.* **9**, 5431 (2018).
7. "Zeeman-limited Superconductivity in Crystalline Al Films", P.W. Adams, H. Nam, C.K. Shih, and G. Catelani, *Phys. Rev. B* **95**, 094520 (2017).
8. "Emergence of intrinsic superconductivity below 1.178 K in the topologically non-trivial semimetal state of $CaSn_3$", Y.L. Zhu, J. Hu, F.N. Womack, D. Graf, Y. Wang, P.W. Adams, and Z.Q. Mao, J. Phys. Condens. Matter **31**, 245703 (2019).
9. "Critical Behavior of a Multiply-connected Superconductor in a Tilted Magnetic Field", F.N. Womack, J.M. Valles, G. Catelani, and P.W. Adams, *submitted.*

Visualizing electronic structure of transition metal oxides

Charles H. Ahn and Fred J. Walker
Yale University

Program Scope

Understanding the electronic and magnetic properties of strongly correlated materials is a key challenge in condensed matter physics. Transition-metal oxides (TMO) with the perovskite-type structure have received intense interest because of their rich physical properties, which result from the interplay between orbital, charge, and spin degrees of freedom. These degrees of freedom can be tuned by changing the transition metal cation; moving vertically in the periodic table from the 3d transition metals to the 4d transition metals leads to a larger degree of covalency and spin-orbit coupling. By synthesizing thin films and heterostructures of these materials via molecular beam epitaxy (MBE), we aim to control the magnetic and electronic properties. To examine the resulting properties and visualize the electronic structure, we are using the Electron Spectro-Microscopy (ESM) beamline of the National Synchrotron Light Source II (NSLS II) at Brookhaven National Lab (BNL). To enhance the capabilities of this facility, we are constructing an oxygen plasma assisted MBE that will be tied in vacuo to the angle-resolved photoemission spectroscopy (ARPES) instrument on the beamline.

Recent Progress

During the first year of this project, we have synthesized and characterized epitaxial 4d rhodate films, and we are constructing and testing the MBE system at the NSLS II ESM beamline.

1. Synthesis and characterization of the $La_{1-x}Sr_xRhO_3$ thin films

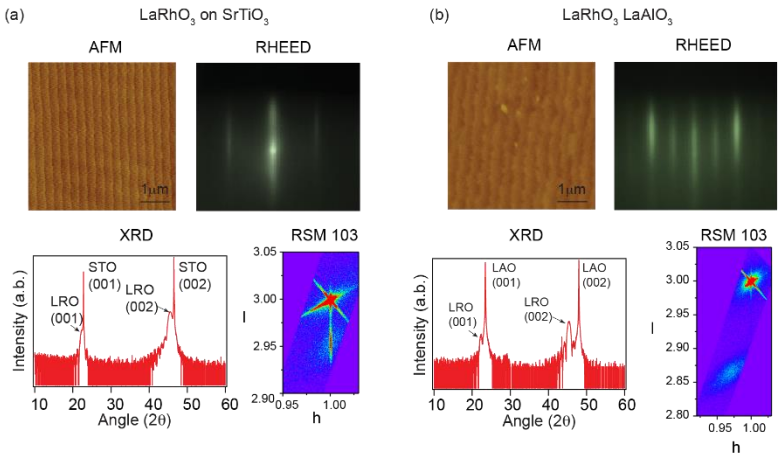

Figure 1. Properties of rhodate thin films. (a) Characterization of 30uc LRO on STO. (b) Characterization of 30uc LRO on LAO.

(1) We have grown high quality, epitaxial $La_{1-x}Sr_xRhO_3$ (x=0~0.5) (LSRO) thin films on $SrTiO_3$ (STO) and $LaAlO_3$ (LAO) substrates using MBE at Yale. The crystalline quality of the $LaRhO_3$ (LRO) thin films is confirmed by reflection high energy electron diffraction (RHEED), x-ray diffraction (XRD), and atomic force microscopy (AFM) (Fig.1). Large,

atomically flat terraces are observed using AFM, consistent with sharp RHEED patterns observed during growth and finite thickness oscillations observed in XRD. The (00l) reflections of the films are visible, and the positions of the peaks on both substrates indicate the relative degrees of compressive strain, with the c-axis being elongated (in the perovskite unit cell). Films grown on STO are coherently strained, while films grown on LAO are relaxed. We have also grown doped films over a Sr doping range from x=0 to x=0.5. The out-of-plane lattice parameter and crystal volume are observed to increase with increasing doping concentration x.

(2) We have also measured electrical transport for LSRO thin films, which are shown in Figs.2(a) and 2(b). Since the Rh in LRO has filled t_{2g} bands in the $4d^6$ electronic configuration, the undoped films are insulating (Fig. 2(a)). Doping with Sr removes an electron from the valence band, progressively making the films conducting as the Sr doping is increased. We observe from the transport data that an insulator to metal transition occurs at x=0.3 for films grown on both substrates. Hall measurements at room temperature are used to measure the 2D carrier densities and are plotted in Fig.2(c). Interestingly, there is a carrier type change from p-type to n-type as the Sr concentration increases, indicating a probable Lifshitz transition as the Fermi level in the oxide is tuned by doping. To visualize this transition, we will investigate the electronic structure via ARPES experiments using the MBE system at the NSLS II, which will provide direct measurements of the electronic structure as a function of doping.

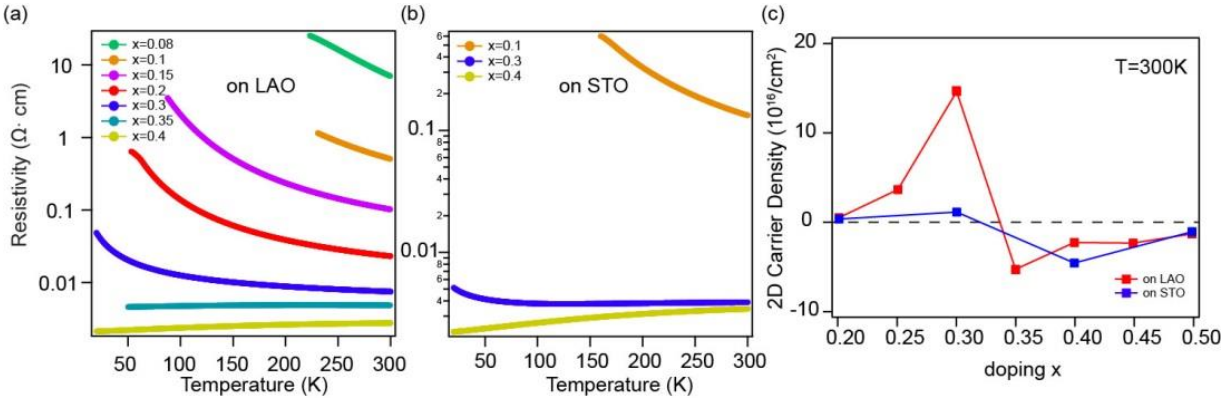

Figure 2. Transport properties of LSRO films. (a) Doping-dependent transport data on 30 uc-thick films of LSRO on LAO. (b) Doping dependent transport data on 30 uc-thick films of LSRO on STO. (c) Doping dependent 2D carrier densities on STO and LAO.

2. The MBE-ARPES system at NSLS II

To further explore the origin of the Lifshitz transition in the rhodate system, we will study the evolution of its electronic structure as a function of doping using ARPES. The ARPES system at the ESM beamline is a state-of-the-art ARPES beamline, with a photon energy range from 25 eV~1500 eV, a micrometer beam size, sample temperature control down to 10K, and a system energy resolution of 10 meV. During the commissioning phase of the ARPES instrument, we have measured single crystals that can be cleaved in situ to obtain a fresh surface. The two systems we have investigated to date are $Ir_{1-x}Pt_xTe_2$, a type-II Dirac semimetal, and $LaCoIn_5$, a reference compound for the heavy fermion superconductor $CeCoIn_5$.

(1) *Visualizing the 3D electronic structure of the type-II Dirac semimetal $Ir_{1-x}Pt_xTe_2$.*

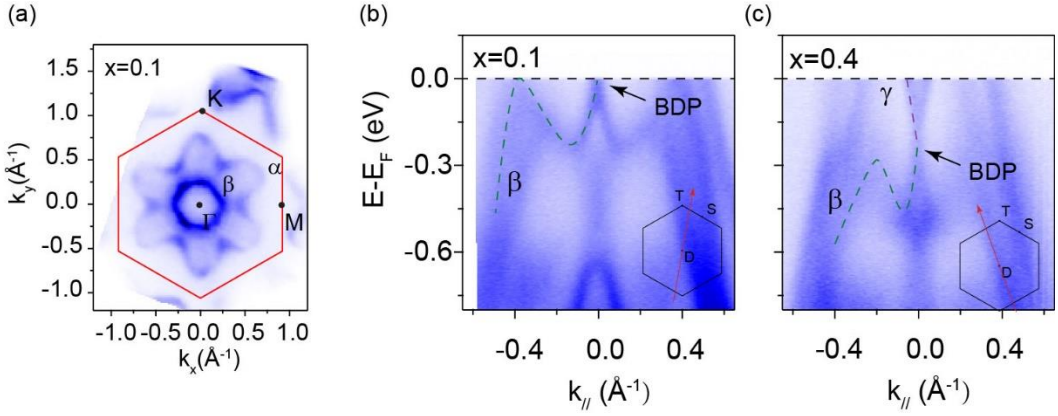

Figure 3. Electronic structure of $Ir_{1-x}Pt_xTe_2$. (a) Fermi surface of $Ir_{1-x}Pt_xTe_2$ with x=0.1 in the ΓMK plane. (b,c) Doping dependence of the band structure across the Dirac point for x=0.1 and x=0.4, showing the evolution of the energy position of the bulk Dirac point (BDP). The dispersion of the β band shows that for x=0.1, the system is close to a type II van Hove filling.

Searching for superconductivity among topological materials offers a new route to realize topological superconductivity; these systems are predicted to host exotic Majorana fermions that can be applied to quantum computing approaches [1]. One such material is $Ir_{1-x}Pt_xTe_2$, which is a superconductor that has a type-II Dirac semimetal electronic structure that can be tuned by varying the alloy composition. Using ARPES, we obtain a comprehensive understanding of the three-dimensional electronic structure of this material in the normal state for doping concentrations x=0.1 to 0.4, which tune the material from a superconducting to non-superconducting phase. Fig. 3(a) demonstrates an example of the Fermi surface map in the ΓMK plane for x=0.1. Many features of the electronic structure are attributed to strong Te-Te interactions between the layers of the parent structure. These strong interlayer interactions result in an electronic structure with a strong 3D character, which can be resolved by photon-energy dependent measurements at the synchrotron. We demonstrate that by Pt doping to x=0.1, where the superconducting transition temperature is a maximum, one can tune the Fermi level so that it lies close to the Dirac point (Fig.3 (b)). The ARPES measurements also reveal that in the superconducting samples, the β band is close a to type-II van Hove filling, where spin triplet paring symmetry has been predicted (Fig.3(b)) [2]. Our results provide a comprehensive understanding of the band structure of $Ir_{1-x}Pt_xTe_2$ and the possible existence of topological superconductivity in this system. A manuscript is currently in preparation.

(2) Electronic structure study of $LaCoIn_5$ and its comparison with $CeCoIn_5$.

A key to understanding heavy-fermion systems involves revealing how itinerant low-energy excitations emerge from local f moments [3]. An effective way to understand the f electron behavior is to compare the electronic structure with an isostructural reference compound with no f electrons. We conducted a systematic study of the electronic structure of $LaCoIn_5$, which has the same crystal structure as the heavy-fermion superconductor $CeCoIn_5$ but with no f electrons. Our ARPES study of the three-dimensional Fermi surface and band structure of $LaCoIn_5$

highlights the three-dimensional electronic character of this compound. The conduction bands of $LaCoIn_5$ are almost identical to those of $CeCoIn_5$ except that $CeCoIn_5$ displays flat 4f bands near the Fermi level. A quantitative comparison of the Fermi surfaces for $LaCoIn_5$ and $CeCoIn_5$ reveals how the d and f bands hybridize to address the "large" and "small" Fermi surface issue in heavy-fermion compounds. This result is published in Phys. Rev. B **100**, 035117 (2019).

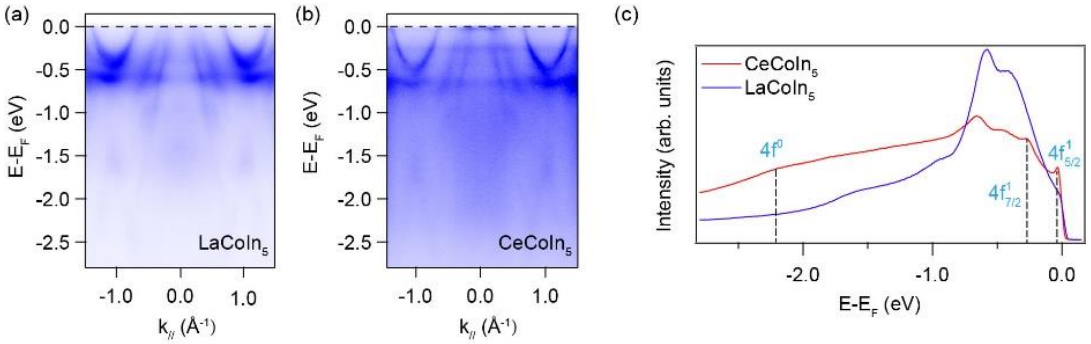

Figure 4. Comparison of the electronic structure of $LaCoIn_5$ and $CeCoIn_5$. (a) Strongly dispersing d bands are observed for $LaCoIn_5$. (b) Flat f bands are observed for $CeCoIn_5$ near the Fermi level, in addition to the dispersing d bands. These differences are highlighted in panel (c), where the 4f bands can be observed as sharp peaks for $CeCoIn_5$. This figure is adapted from ref. [4]; panel (b) data was taken by collaborator Q.Y. Chen.

Future Plans

1. Realize in vacuo connection between the MBE and ARPES system at NSLS II via a vacuum suitcase, which will enable electronic structure measurements of thin films grown in the MBE.
2. Visualize the origin of the Lifshitz transition in LSRO thin films using ARPES measurements. These electronic structure measurements will complement the transport measurements and be used to understand the origin of the Lifshitz transition.
3. Measure ARPES and transport for LSRO thin films as a function of film thickness.
4. Engineer the electronic and magnetic properties of rhodates by synthesizing $LaRhO_3/LaTiO_3$ superlattice structures, where strong charge transfer between Rh and Ti is expected based on electronegativity differences.

References

[1] Masatoshi Sato and Yoichi Ando, "Topological superconductors: a review", Rep. Prog. Phys, **80**, 076501 (2017).
[2] Z. Y. Meng, F. Yang, et. al., "Evidence for spin-triplet odd-parity superconductivity close to type-II can Hove singularities", Phys. Rev. B **91**, 184509 (2015).
[3] Q. Y. Chen, D. F. Xu, et. al., "Direct observations of how the heavy-fermion state develops in $CeCoIn_5$", Phys. Rev. B **96**, 045107 (2017).
[4] Q. Y. Chen, X. B. Luo, et. al., "Electronic structure study of $LaCoIn_5$ and its comparison with $CeCoIn_5$.", Phys. Rev. B **100**, 035117 (2019).

Publications to date

Q. Y. Chen, X. B. Luo, E. Vescovo, K. Kaznatcheev, F. J. Walker, C. H. Ahn, Z. F. Ding, Z. H. Zhu, L. Shu, Y. B. Huang, and J. Jiang, "Electronic structure study of $LaCoIn_5$ and its comparison with $CeCoIn_5$.", Phys. Rev. B **100**, 035117 (2019).

Topological materials with complex long-range order

James Analytis
Department of Physics, University of California, Berkeley, California 94720, USA

Program Scope

This program is focused on the study of strongly frustrated magnetic systems, particularly materials where Coulomb, kinetic and spin orbit energy scales conspire to give exotic exchange interactions. The current scope of the program can be summarized as follows.

- ***Using pressure and magnetic field to tune the ground state of Kitaev materials.*** Frustrated magnets have a rich array of possible ground states to choose from. A key question is whether we can couple to the appropriate energy scale to tune between these ground states. Magnetic field can be used to couple to the Zeeman response of local moments and take advantage of large *g*-factor anisotropies. Pressure can be used to tune the bond angles and distances between magnetic ions, with dramatic effects on the exchange energy.
- ***Using ultra-sensitive magnetic measurements to understand the nature of intertwined ground states.*** Many of the state in frustrated systems are extremely subtle, forming hidden orders that are intertwined with the known ones. By focusing on ultra-low noise magnetic measurements, we reveal the magnetic signatures of these hidden states.
- ***Using Resonant Inelastic X-ray Scattering techniques to understand magnon band structure.*** Resonant Inelastic X-ray techniques have come to the for as the preeminent tools for the determination of excitations in correlated systems. We utilize these tools to determine the magnon dispersion of Kitaev candidate materials.
- ***Understanding the symmetry and thermodynamic response of states borne from magnetic frustration.*** By developing symmetry-sensitive thermodynamic techniques, we determine the existence and symmetry of hidden ordered states, as well as their thermal conductivity properties.

Recent Progress

Background. In the honeycomb iridates A_2IrO_3 (A is the alkali), an exotic kind of anisotropic exchange emerges which maps these structures onto a remarkable theoretical model pioneered by Kitaev [1]. The layered honeycomb structure is composed of octahedrally coordinated Ir^{4+}, bonded together along O_2 edges. The exchange pathway between spin-1/2 Ir, across these bonds is predicted to be highly anisotropic due to the spin-orbit coupling [2]. This material has three known polytypes, identified for the first time in our recent work [3].

(1) Hidden spin-orbital order in β-Li_2IrO_3. We report the existence of a novel phase transition at high temperature in the 3D Kitaev candidate materials, β-Li_2IrO_3. The transition can only be observed at very low energy scales and has therefore remained hidden from previous studies. It is intrinsic and orders a tiny magnetic moment with strong spatial anisotropy. We show that even

though this transition is global, it does not order the local Ir moments. We suggest this puzzle could be resolved by the appearance of an emergent degree of freedom from the combined action of Kitaev and spin-orbit interactions.

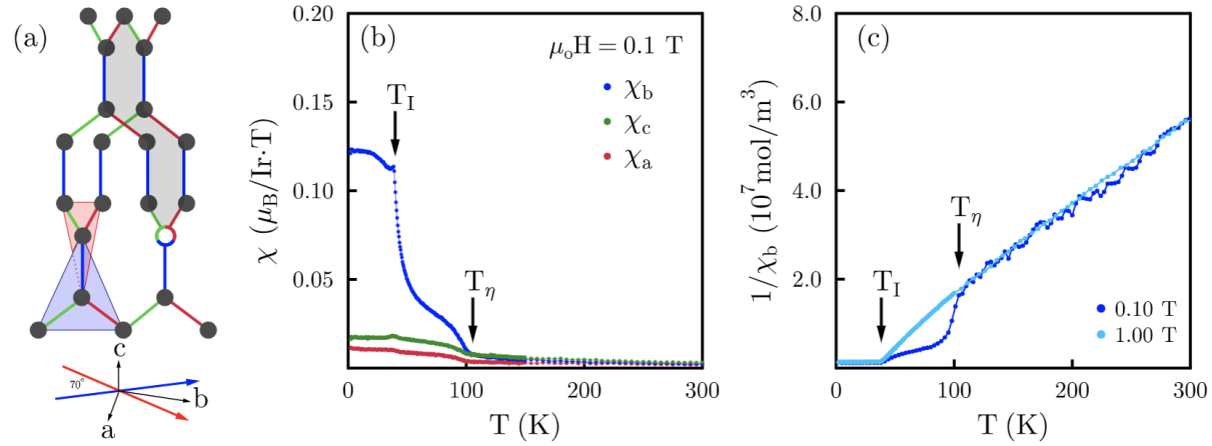

Figure 1: (a) Three dimensional structure of \blio, where the red, green and blue colors correspond to orthogonal compass directions of the Kitaev model. The two triangles, situated 70° apart, show the possible environments for a magnetic ion in \blio, and determine the g-factor anisotropy. Also shown is a site vacancy which can trap flux excitations in a Kitaev spin liquid, creating a large local moment. (b) The anisotropic magnetic susceptibility of \blio\ for an applied magnetic field of \unit[0.1]{T}. At $T_I=\unit[38]{K}$, the system transitions into an incommensurate spiral state with non-coplanar, counter-rotating moments. When a small magnetic field is applied ($H<\unit[0.5]{T}$), a separate transition is also observed at \unit[100]{K}. (c) Comparison of the inverse $\hat{b}$-axis susceptibility for \unit[1.0]{T} and \unit[0.1]{T}. The low-field data shows two distinct behaviors: a linear response above \unit[100]{K} and a strong deviation from Curie-Weiss behavior $100 >T> \unit[40]{K}$..

The thermodynamic and spectroscopic evidence unambiguously establishes the hidden order as an intrinsic thermodynamic phase in \blio; there exist sharp signatures in both susceptibility and heat capacity, and μSR shows the magnetic moment is static, existing throughout the volume of the sample. There are therefore two coexisting phases in this system: the incommensurate phase which onsets at \unit[38]{K}, and the hidden order at \unit[100]{K}. Strikingly, susceptibility and hysteresis fields of the hidden phase cross the incommensurate transition in both field and temperature with complete impunity, suggesting they each arise from a distinct magnetic species. The main question is what is the identity of this species and the associated hidden order parameter.

The existence of competing phases is widely known in these materials. In \blio\, for example, it is known that a zig-zag phase is close in energy and can be induced with the application of relatively small fields. However, the μSR data unambiguously rules this out, as the presence of such a phase would lead to oscillations in the muon relaxation, as seen in Na2IrO3. Another possibility is a valence-bond transition, similar to that seen in α-RuCl$_3$ under pressure. However the spin dimerization has an associated structural distortion that leads to strong hysteresis on warming and cooling, and this is absent in the current data. The μSR data is more consistent with a disordered magnet, like a spin glass. To explain our data, the moment of the disordered

species would have to be extremely weak as, according to our fits, the local field is of the order of a few Gauss (by contrast the local field in Na2IrO3 is an order of magnitude larger). Even supposing that the true moment is somehow screened from the muons (which itself would require an exotic explanation given the absence of itinerant electrons to Kondo screen), the smallness of the induced moment in our magnetic measurements would suggest a highly dilute magnetic species, which is difficult to reconcile with the high transition temperature, the sample-to-sample reproducibility, and the sharp heat capacity anomaly, all of which are rare in typical examples of dilute spin glasses. Moreover, the absence of relaxation effects, magnetic and thermal memory effects, and exchange bias is inconsistent with a spin glass scenario.

(2) Disorder dependence of Hidden spin-orbital order in β-Li_2IrO_3.

Preliminary studies of doping dependence have shown this transition becomes rapidly suppressed by small amounts of impurities, as shown in the figure below.

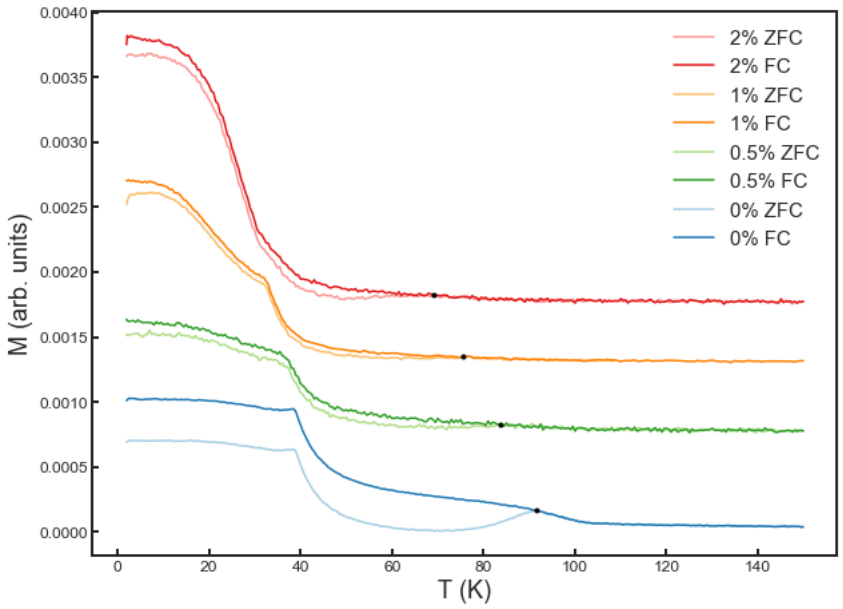

Figure 2: Figure shows magnetization taken at 100Oe in field cooled and zero-field cooled configurations. This shows directly the suppression of the hidden spin-orbital order with small disorder (in this case Ru substitution for Ir).

Future Plans

(1) Resonant Inelastic X-ray Scattering studies. Our recent measurement using state-of-the-art RIXS tools at the Advanced Photon Source have been able to resolve features in the magnon dispersion down to a few milli-electron Volts. In these tour de force experiments, we have shown that the incommensurate magnetic phases have extraordinarily large magnon group velocities.

(2) Doping studies. While carriers are difficult to dope into these systems in general, we have had recent success in Ru and Rh doping these systems, leading to a dramatic suppression of the incommensurate magnetic transition. However, a new transition arises in its wake, whose properties are highly unusual.

(3) Search for hidden spin-orbital order in $RuCl_3$. Preliminary studies have shown similar signatures of hidden order at high temperatures in RuCl3, seen in both muon and magnetization measurements. This may provide a unifying picture for Kitaev candidate materials.

(4) Inelastic Resonant X-ray Scattering studies in applied field. We have a preliminary characterization of the magnon dispersion of beta-Li2IrO3. In a tour de-force experiment, we have also applied small magnetic fields to observe the evolution of the magnon dispersion as the system is tuned toward the spin-liquid state.

Publications

I. Alejandro Ruiz, Alex Frano, Nicholas P. Breznay, Itamar Kimchi, Toni Helm, Iain Oswald, Julia Y. Chan, R. J. Birgeneau, Z. Islam, James G. Analytis, "Field-induced intertwined orders in 3D Mott-Kitaev honeycomb β-Li2IrO3", Nature Communications (in press) arXiv:1703.02531

II. K.A. Modic, B.J. Ramshaw, Nicholas P. Breznay, James G. Analytis, Ross D. McDonald, Arkady Shekhter, "Robust spin correlations at high magnetic fields in the honeycomb iridates", Nature Communications 8, Article number: 180 (2017)

III. Nicholas P. Breznay, Alejandro Ruiz, Alex Frano, Wenli Bi, Robert J. Birgeneau, Daniel Haskel, James G. Analytis, "Resonant x-ray scattering reveals possible disappearance of magnetic order under hydrostatic pressure in the Kitaev candidate γ-Li2IrO3", Phys. Rev. B 96, 020402 (2017)

IV. A. Biffin, R. D. Johnson, I. Kimchi, R. Morris, A. Bombardi, J. G. Analytis, A. Vishwanath, and R. Coldea, "Noncoplanar and Counterrotating Incommensurate Magnetic Order Stabilized by Kitaev Interactions in γ−Li2IrO3", Phys. Rev. Lett. 113, 197201 (2014)

V. J. P. Hinton, S. Patankar, E. Thewalt, J. D. Koralek, A. Ruiz, G. Lopez, N. Breznay, I. Kimchi, A. Vishwanath, J. G. Analytis, J. Orenstein, "Photoexcited states of the harmonic honeycomb iridate γ-Li2IrO3", Phys. Rev. B 92, 115154 (2015).

An experimental study of flat bands and correlated phases in twisted carbon layers.

Eva Y. Andrei, Department of Physics, Rutgers University, 136 Frelinghuysen Rd, Piscataway, NJ 08904

Program Scope

The discovery of atomic layers and their stacking into van-der Waals heterostructures has led to the emergence of new material properties that could not have been achieved by standard chemical synthesis. In particular, introducing a twist between overlaid 2D crystals, creates a moiré superstructure which alters the electronic properties. In the case of superposed graphene layers with small twist angles, the energy band flattens and the electrons slow-down until, at some "magic" twist-angle, they almost come to a complete halt facilitating the emergence of correlated phases. The recent reports of superconductivity and a nearby correlated insulating phase emerging in magic-angle twisted bilayer graphene (TBLG) spurred a torrent of ideas about the underlying mechanism. To make further progress, detailed experimental studies that constrain the theoretical models are needed. In this regard, our research is guided by the following questions:

i) What is the nature of the insulating phase? In this effort we focus on the twist-induced spectral reconstruction of the band structure, the symmetry of the electronic wave function, the energy gap and its dependence on doping, temperature and magnetic field.

ii) What is the nature of the superconducting state? In this effort we study the superconducting phase aiming to understand the pairing mechanism, the symmetry of the wave function and the low energy excitations.

iii) Can one achieve flat bands with non-twist induced superstructures? Our efforts are guided by our recent findings showing the formation of strong strain-induced periodic pseudo-magnetic fields observed by thermal cycling of overlaid layers with different expansion coefficients.

Our research utilizes a wide range of expertise and experimental techniques developed in our group. These include sample fabrication and characterization tools to access and probe the electronic properties of 2D systems and to follow their evolution with parameters such as distance from a point defect, strain, magnetic field, doping and local screening. The characterization techniques deployed in this program cover a range of local probes such as low temperature scanning tunneling microscopy (STM), scanning tunneling spectroscopy (STM), Landau level spectroscopy (LLS), atomic force microscopy, intermediate range probes such as Raman spectroscopy, and global probes such transport, magneto-transport and thermal measurements.

Recent Progress

Observation of nematic charge-order and broken rotational symmetry in magic angle twisted bilayer graphene[4]. Moiré-superstructures created by stacking two graphene layers with a twist between their crystallographic orientations can have a dramatic effect on the electronic properties of the material, as was first demonstrated by the pioneering STM/STS studies in my group[1]. In these studies we discovered that the moiré patterns in twisted bilayer graphene (TBLG) produced two van Hove singularities where the density-of-states (DOS) is dramatically enhanced, at the same time slowing down the electron velocity[2]. At a twist angle of $\sim 1.1^0$, later dubbed

"magic angle", these van-Hove-singularities merged producing an almost flat-band of electronic states, where a gap at partial filling of the band indicated the emergence of a correlated-electron phase[1]. With the recent discovery of superconductivity, uncommon insulating states and magnetism, magic angle TBLG has joined the realm of strongly correlated materials. Remarkably, the phenomenology of magic angle TBLGs is similar to that of high–T_c superconductors, a central mystery in condensed matter physics, but their behavior is richer. Transport measurements have shown that, similar to high–T_c superconductors, superconductivity in TBLG emerges near the insulting phases observed at integer fillings of the moiré unit cell and exhibits a dome-like doping dependence of T_c. Further similarities include the linear temperature dependence of the resistivity, and the large ratio of T_c to the Fermi energy. Because TBLG is cleaner and its properties easily tuned by electrical gating, as opposed to chemical doping in the case of the high–T_c superconductors, it could provide crucial insights into the underlying physics. Local spectroscopy, which is capable of accessing the symmetry and spatial distribution of the spectral function, may hold the key to unraveling this puzzle. Using STM and STS to visualize the local DOS, combined with a new method of analyzing spectroscopic data that provides a measure of the local charge, and together with dynamical mean field theory simulations, we discovered that the emergence of the low-temperature correlated phases in TBLG is preceded by a charge ordered precursor which breaks the global three-fold symmetry of the moiré lattice. Doping the sample to partially fill the flat band, where low temperature transport measurements revealed the emergence of correlated electronic phases, we discovered a pseudogap phase accompanied by global nematic charge-order which closely resemble observations of charge order in the pnictides and cuprates[3], where the superconductivity is believed to be intimately connected to the pseudogap phase and the stripe order is common. Our findings add a new piece to the puzzle connecting TBLG and high–T_c superconductors, and identify an important constraint towards unraveling the nature of their correlated electronic states.

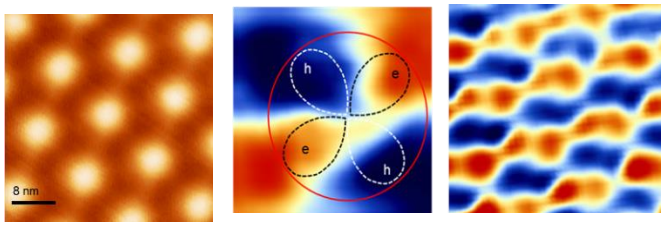

Figure 1. Charge order in magic TBLG. Left: STS map showing the moiré superlattice of crests (bright) and troughs (dark). Center: dipolar charge polarization within each crest consists of four lobes of alternating electron (e) and hole (h) doping. Right: global stripe charge order breaks the rotational C6 symmetry of the moiré structure.

Kondo Screening in Graphene[5]. We studied the emergence of magnetism in graphene resulting from the unpaired spins created by the removal of a carbon atom. In normal metals, the magnetic moment of impurity spins disappears below a characteristic "Kondo temperature", T_K, marking the formation of cloud of polarized conduction-band electrons which screen the local moment. In contrast, moments embedded in insulators remain unscreened at all temperatures. This raises the question about the fate of magnetic moments in intermediate pseudogap systems, such graphene, which are gapless but have a vanishing DOS at the Fermi energy, E_F. In these systems theory predicts a quantum phase-transition at a critical coupling strength which separates a magnetic phase from a Kondo-screened phase. Using STM/STS, and numerical renormalization group

calculations, we have shown that vacancies in graphene provide direct access to the physics of Kondo screening in a pseudogap system. Kondo screening in graphene has been considered controversial, following reports of contradictory results obtained from magnetometry and resistivity measurements. While magnetometry showed no evidence of Kondo screening, resistivity measurements found Kondo screening with unusually large values of $T_K \sim 90K$. We demonstrated that these inconsistencies stemmed from the global nature of these measurements, and from the fact that they are sensitive to complementary aspects of the problem. Magnetometry probes the magnetic moment and only sees the unscreened vacancies, while transport which is sensitive to the scattering from the Kondo cloud is only sensitive screened moments. Therefore, in the presence of a distribution in the local coupling-strengths, global measurement techniques necessarily lead to opposite conclusions. The local nature of our spectroscopy measurements resolved this ambiguity. We showed that Kondo screening is controlled by the local curvature and the chemical potential and identified the quantum phase transition between a screened and an unscreened spin. Highlights of our findings include:

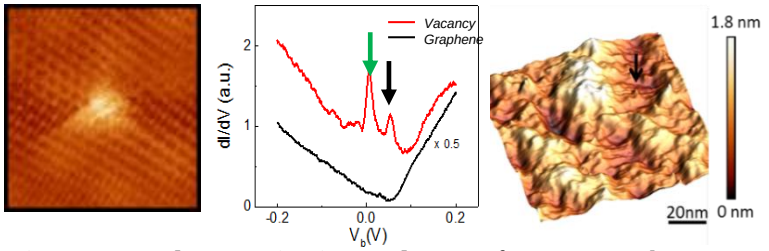

Figure 2. Kondo-screening in graphene. Left: atomic resolution topography of a vacancy shows the characteristic triangular interference pattern. Center: *dI/dV* spectra at the vacancy (top) and far from it (bottom). Green arrow shows the Kondo resonance; black arrow marks the zero-mode peak Right: STM topography of the G/G/SiO2 surface.

1) Using the spectroscopic signature of Kondo screening we extracted the T_K for each vacancy.
2) Demonstrated that Kondo screening can be controlled by a gate voltage.
3) Discovered that Kondo screening in this system strongly depends on the local curvature.
4) Mapped the hitherto elusive quantum phase transition separating magnetically screened from non-screened states in a pseudogap system.
5) The ability to control the magnetic moment by a gate voltage and by the local curvature demonstrated in our work paves the way to electrostatic and mechanical control of magnetism.

Flat bands through strain induced superstructures[6]. Periodic strain fields provide an alternative mechanism for the emergence of flat bands in graphene that does not involve magic angle TBLG. In the presence of a periodic strain field with periods of order 10nm, the theory predicts the formation of very flat bands. Adding a small attractive interaction between electrons is expected to produce a superconducting state with a periodic gap structure of amplitude comparable to room temperature. We have found that periodic strain structures readily form in graphene supported by certain substrates such as $NbSe_2$ due to a thermally driven buckling transition of the graphene membrane. An example is shown in the topography image (Figure3). This buckled structure with a period of 10nm was generated upon cooling the device from $200C^0$ to 4K. Its emergence is likely driven by the different thermal expansion coefficients of the two materials. STS measurements on

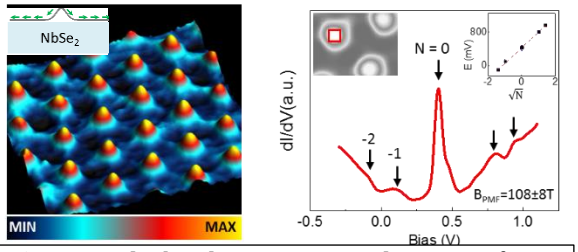

Figure 3. Flat bands in strain superlattice. Left: STM map of thermally cycled graphene on $NbSe_2$ shows a strain super-structure with period 10nm. Inset: schematic of buckled sample. Right: STS shows a pseudo-Landau level sequence corresponding to a pseudo-magnetic field of~180T.

this structure revealed a very large periodic pseudo-magnetic field which reaches 180T on the crests and changes sign in the troughs. In this part of the project we will measure the band structure of strain induced periodic structures in samples that allow gating. This will enable to bring the Fermi energy within the flat band where we will explore the emergence of correlated behavior and superconductivity.

Future Plans

Our research will pursue two experimental thrusts. (i) Elucidate the nature of the superconducting, insulating and magnetic states in TBLG. Using ultra-low temperature tunneling and transport measurements we will study the band structure reconstruction in the correlated electron states and their evolution with temperature, magnetic field, strain and carrier density. We will study the pseudogap phase in magic-angle TBLG and its relation to charge order and to the emergence of the superconducting phase, aiming to understand the pairing mechanism, the symmetry of the wave function and the low energy excitations. (ii) Devise new methods for creating flat bands and for inducing robust correlated electron states. This thrust will aim to create flat bands with non-twist induced superstructures such as strain-induced periodic pseudo-magnetic fields through thermal cycling of superposed layers with different expansion coefficients or by suspending atomic layers on nanometer-scale periodic structures.

References

1. Observation of Van Hove singularities in twisted graphene layers, G. Li, et al., Nature Physics, 6 (2010) 109-113.
2. Single-Layer Behavior and Its Breakdown in Twisted Graphene Layers, A. Luican, et. al.,Physical Review Letters, 106 (2011) 126802.
3. Ubiquitous Interplay Between Charge Ordering and High-Temperature Superconductivity in Cuprates, E.H. da Silva Neto et. al., Science, 343 (2014) 393.

Publications acknowledging DOE support

4. Charge-Order and Broken Rotational Symmetry in Magic Angle Twisted Bilayer Graphene , Y. Jiang, et al., **Nature** adv. on-line publication doi.org/10.1038/s41586-019-1460-4 (2019)
5. Visualizing Encapsulated Graphene, its Defects and its Charge Environment by Sub-Micron Resolution Electrical Imaging, M. A. Altvater, et al., **2D Materials** 2019 (accepted).
6. Flat Bands in Buckled Graphene Superlattices, Y. Jiang, et al., arXiv:1904.10147 (2019)
7. Inducing Kondo Screening of Vacancy Magnetic Moments in Graphene with Gating and Local Curvature, Y. Jiang, et al., **Nature Communications** 9, 2349 (2018)
8. Modeling of the gate-controlled Kondo effect at carbon point defects in graphene , D. May, et al., **Phys. Rev. B** 97, 155419 (2018)
9. Tuning a Circular p-n Junction in Graphene from Quantum Confinement to Optical Guiding , Y. Jiang, et al., **Nature Nanotechnology** 12, 1045 (2017)
10. Observing a Scale Anomaly in Graphene: A Universal Quantum Phase Transition, O. Ovdat, et al., **Nature Communications** 8, 507 (2017)

Novel Temperature Limited Spectroscopy of Quantum Hall Systems

Raymond Ashoori, MIT

Program Scope

Our project seeks to advance the use of two tunneling spectroscopies, time domain capacitance spectroscopy (TDCS), and momentum and energy resolved tunneling spectroscopy (MERTS) in semiconductor quantum Hall systems. We are specifically working to use TDCS, MERTS, and capacitance spectroscopy to examine phases of the 2D electronic system in high magnetic field (such as Wigner Crystal and stripe and bubble phases) and unusual fractional quantum Hall states. We are also looking to find spectral signatures of fractional quantum Hall states. Over the two years, after realizing that these measurements could also probe these states in a new and powerful way by determining the spin structure of the states described above, we focused our efforts on this new method (described in this report). This method and the results from it are described below. We are working to apply this new method to study the spin-polarizations of other phases – such as the Wigner Crystal and stripe and bubble phases. We have also used our capacitance measurements with single-electron sensitivity to probe a mini-2D electronic system and have made a remarkable discovery (see below) that may shed light on atypical fractional quantum Hall states such as the 5/2 state.

Recent Progress

Spin-Resolved Tunneling

Over the past two years, we have continued developing our pulsed tunneling methods and have extended them to give us a profound new capability - to measure spin. We can now measure the spin of tunneling electrons and, importantly, the spin polarizations of two-dimensional systems. These measurements allow us to make direct comparisons with fractional quantum Hall theory and particularly the theory of the unusual fractional quantum Hall states (e.g. the 5/2 state) that are frequently discussed as candidates for creating new quantum computers. These measurements have revealed a number of surprises. We find a strongly spin-polarized 5/2 state down to very low magnetic fields; the 8/3 state is, in contrast with prior results, spin-polarized and thence a candidate for non-Abelian quantum computing. We have also detected, unusually, skyrmions at filling factor 1/3.

After using our pulsed tunneling work to perform momentum resolved tunneling spectroscopy, we realized that the very same samples and tunneling measurements could be used for a novel and powerful method for measuring spins in 2D electronic system. This method particularly leverages our ability to make measurements of tunneling into insulators.

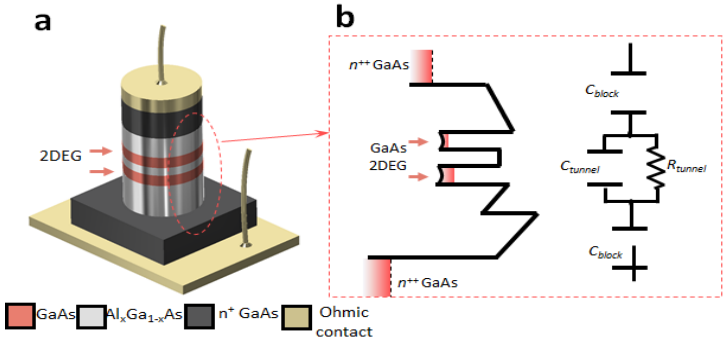

Figure 1. a, Schematic of a vertical tunneling device. **b,** the conduction band edge (left) and an equivalent circuit model (right) of the sample used in the study.

Our spin-resolved tunneling (SRT) method can precisely probe the spin texture of both the ground- and excited-states. Using SRT, we for the first time demonstrate the complete phase diagrams of the ground-state spin polarization as a function of magnetic fields and filling factors *ν*. Our phase diagrams reveal unusual composite-fermion (CF) phases both in the $N = 0$ and $N = 1$ Landau levels (LLs). In particular, the fully-polarized $\nu = 5/2$ and 8/3 states at a vanishingly small magnetic field indicate the unexpectedly large CF effective-mass which gives rise to the completely different correlated ground-states in the $N = 1$ LL. In order to elucidate the nature of the exotic correlations, we directly measure the Haldane's pseudopotentials from the spin-dependent excited states. We observe significant softening of the short-distance pseudopotential that provides evidence for the instability of the conventional CF phases in the $N = 1$ LL. These results establish SRT as a unique technique for investigating a rich variety of correlated electron phenomena in the QH regime.

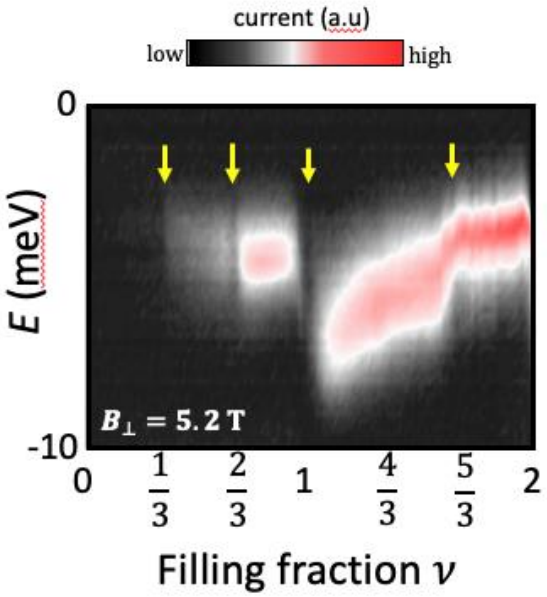

Figure 2 - Tunneling current from tunneling from the probed well into the $\nu = 1$ target well, as a function of filling factor and pulsed voltage (E). Notice the dark bands that appear at certain filling factors of the probed well (particularly at filling factors 1, 1/3, and 2/3). These dark bands indicate strong spin polarization at these filling factors.

We previously created a double-well structure that we created for studying momentum resolved tunneling and unusual quantum Hall states (e.g. even-denominator Fractional Quantum Hall states) in the 2DES. This structure is shown in figure 1. We have used this same structure for performing spin resolved tunneling. To perform spin resolved tunneling, we utilize an unusual capability of our pulsed tunneling measurements: we can measure tunneling into and out of electrical insulators. In the double-well system shown in Fig. 1, we tune the electron density of one of the wells (call it the QHF – "quantum Hall ferromagnet" well) to be at filling factor $\nu = 1$. It acts as a perfect ferromagnet(*1*) in which we can consider all electronic states of one spin (call it "spin-up") are occupied while there is no occupancy of spin-down states. So, charges tunneling from the other well (call it the "probed well") can only tunnel into the N=1 Landau level if they have spin down. We determined that there exists a sum rule – the integral of the tunneling current as a function of pulse voltage over a Landau level is proportional to the number of spin-down electrons in the probed well. Using as a normalization tunneling into an empty well (rather than a $\nu = 1$ well), we can determine the spin polarization within the probed 2D system.

Figure 2 shows the tunneling current from tunneling from the probed well into the $\nu = 1$ target well, as a function of filling factor and pulsed voltage (E). Notice the dark bands that appear at certain filling factors of the probed well (particularly at filling factors 1, 1/3, and 2/3). These dark bands indicate strong spin-polarization at these filling factors. Figure 3 shows the extracted spin polarization. Notice the peak in the spin polarization at filling factor 1. This arises from skyrmion formation.

Remarkably, we can measure polarization spectra so rapidly (much more rapidly and for more filling factors than prior methods(*2*, *3*)) that we obtain sufficient data to plot them as a function of both magnetic field strength and electron density (see Figure 4). The spin polarization in the lowest Landau level (the N=0 Landau level: filling factors between zero and two) generally agrees well with composite fermion theory. However, there are some important differences (e.g. we appear to be seeing skyrmions at filling factor 1/3). The bigger differences happen in the N=1, Landau level. In those cases, we unexpected behavior at several filling factors. Filling factor 5/2, of great interest for potential topological computing applications(*4*), remains spin polarized down to very low magnetic fields (~1.5 Tesla) and 8/3 is unexpectedly(*5*) spin polarized.

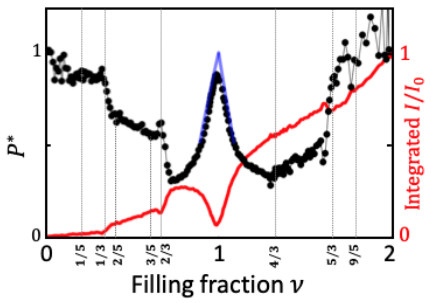

Figure 3. Integrated current from data such as that shown in Figure 2 (red) and extracted spin polarization of the probed well (black).

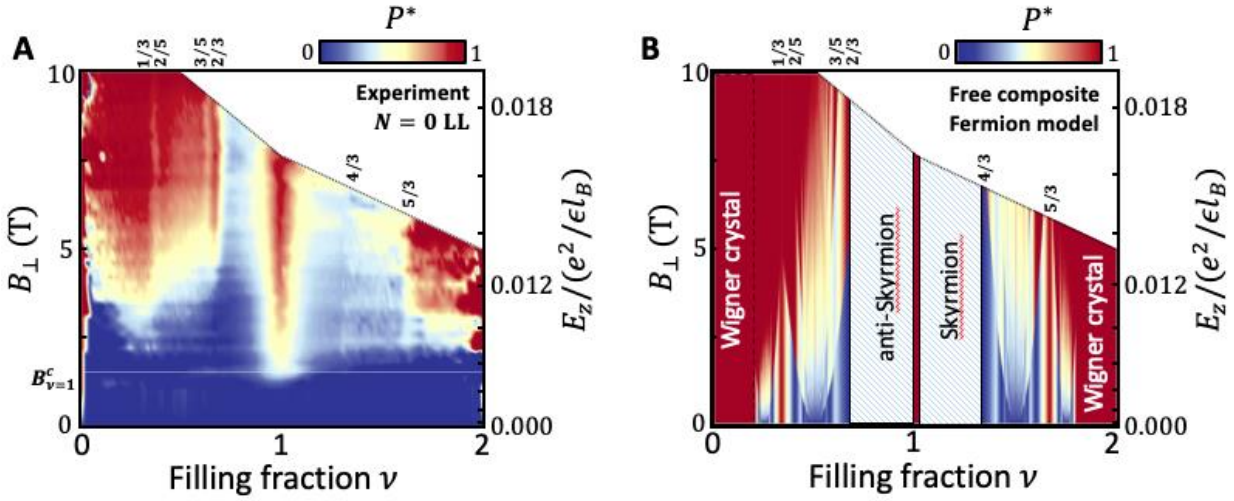

Figure 4. (A) Experimentally determined spin polarization of the lowest Landau level for a range of magnetic fields. (B) Theoretical prediction of the spin-polarization based on composite fermion theory.

Paired States at the Edges of a Mini-2D Electron System

We have worked to press our tunneling measurements to the single electron regime. We have created laterally large and low disorder quantum well based quantum dots to study single electron additions to two-dimensional electron gas systems. Electrons tunnel into these dots across an AlGaAs tunnel barrier from a single n+ electrode. Using single-electron capacitance spectroscopy (SECS) in a dilution refrigerator, we identify capacitance peaks for the addition of the first electron to a dot and record subsequent peaks in the addition spectrum up to occupancies of thousands of electrons. We have observed a remarkable phenomenon in these dots. (1) Coulomb blockade peaks arise from entrance of two electrons into quantum dots rather than one; (2) at and near filling factor 5/2 and at fixed gate voltage, these twice-height peaks appear uniformly with a periodicity of h/2e. At other filling factors in the range $2 < \nu < 5$, the mean periodicity for the twice-height electron peaks remains h/2e, but the twice-height peaks are instead further bunched into pairs, with pairs

spaced h/e apart. The unusual 2-electron Coulomb blockade peaks suggest a novel pair tunneling effect that involves electron correlations that arise in the quantum dot.

Future Plans

We will continue measurements of spin-polarization in higher Landau levels to detect signatures of charge stripe and bubble phases, along with our pulsed tunneling spectroscopy and momentum resolved tunneling spectroscopy (MERTS). We will continue or focus on fractional quantum Hall states interesting for topological quantum computing such as the 5/2 state. We have learned how to make measurements the Haldane pseudopotentials underlying such states by identifying the spin-polarization of higher-energy features that we observe in the tunneling spectrum. Such data will help us understand the basic conditions for creating the 5/2 state and also charged stripe and bubble phases in higher Landau levels. Finally, we have been working on a new method (involving creation of a tunnel-diode-like structure) for making low resistance contacts to electrodes in 2D holes samples built on top of an n+ substrate, and success with such contacts will facilitate performing MERTS measurements on Wigner Crystal samples.

References

1. Z. F. Ezawa, G. Tsitsishvili, Quantum Hall ferromagnets. *Rep. Prog. Phys.* **72**, 086502 (2009).

2. S. E. Barrett, G. Dabbagh, L. N. Pfeiffer, K. W. West, R. Tycko, Optically Pumped NMR Evidence for Finite-Size skyrmions in GaAs Quantum Wells near Landau Level Filling $\nu=1$. *Phys Rev Lett*. **74**, 5112–5115 (1995).

3. L. Tiemann, G. Gamez, N. Kumada, K. Muraki, Unraveling the Spin Polarization of the N = 5/2 Fractional Quantum Hall State. *Science*. **335**, 828–831 (2012).

4. C. Nayak, S. H. Simon, A. Stern, M. Freedman, S. Das Sarma, Non-Abelian anyons and topological quantum computation. *Rev. Mod. Phys.* **80**, 1083 (2008).

5. T. D. Rhone, J. Yan, Y. Gallais, A. Pinczuk, L. Pfeiffer, K. West, Rapid Collapse of Spin Waves in Nonuniform Phases of the Second Landau Level. *Phys. Rev. Lett.* **106**, 196805 (2011).

Publications in the last 2 years

1. J. Jang, H. M. Yoo, L. N. Pfeiffer, K. W. West, K. W. Baldwin, R. C. Ashoori, Full momentum- and energy-resolved spectral function of a 2D electronic system. *Science*. **358**, 901–906 (November 15, 2017).

2. H. M. Yoo, L. N. Pfeiffer, K. W. West, K. W. Baldwin, R. C. Ashoori, Complete spin phase diagram of the fractional quantum Hall liquid, (in preparation - putting final touches on paper and will submit shortly for publication).

Exposing the electronic properties of topologically non-trivial and correlated compounds: a quest for topological superconductivity.

Luis Balicas, National High Magnetic Field Lab and Florida State University

Program Scope

There are a number of proposals for realizing a superconducting (SC) state characterized by, for example, a $p + ip$ pairing symmetry whose vortex core is predicted to possess a localized quasiparticle at zero energy which is mathematically described by a Majorana operator. Some of the proposals for quantum computation rely on the existence of massless Dirac quasiparticles, e.g. in the surface of topological insulators, to be condensed into a SC state via the proximity effect. Here, we propose to identify good candidates for a superconducting pairing symmetry containing a triplet component. We also propose to unveil the existence of bulk topological electronic states in conducting systems in order to harvest their quasiparticles for bulk superconductivity. There are a number of compounds predicted to display topologically non-trivial electronic structures, e.g. T_d-$MoTe_2$, that are claimed to possess Weyl (type II)-like electronic dispersion(s) close to the Fermi level. We propose to clarify if its lack of inversion symmetry, combined with a possible topological electronic structure, leads to topological SC. There are a number of other bulk compounds claimed to display Dirac, Dirac type-II, Weyl, Weyl type-II, Dirac nodal line and multifold fermions. We will evaluate their properties and Fermi surfaces in order to correlate these with calculations and to expose their topological character. Subsequently, we will attempt to induce topological superconductivity via intercalation and/or chemical substitution**.**

Recent Progress

We synthesized and studied [1] the Fermi surface of WP_2 which was originally predicted [2] to display a type-II Weyl semimetallic state. WP_2 exhibits a very low residual resistivity which leads perhaps to the largest nonsaturating magnetoresistivity $\rho(H)$ ever reported for any compound. The angular dependence of the SdH frequencies is found to be in excellent agreement with first-principles calculations when the electron and hole bands are shifted with respect to the Fermi level. This small discrepancy could have implications for the predicted topological character of this compound, since it would eliminate the band crossings that led to the original type-II Weyl prediction if one assumed a rigid band shift.

We have also grown very high quality single-crystals of the type-II Weyl semimetallic candidate T_d-$MoTe_2$ finding that its superconducting transition temperature correlates with the inverse of its residual resistivity, or that the higher ρ_0 the smaller the T_c suggesting unconventional superconductivity [3]. Measurements of the de Haas van Alphen effect reveals a Fermi surface in marked contrast with both density functional theory calculations and angle resolved photoemission experiments. We attribute these discrepancies to the role of electronic correlations [4] (not included in the DFT calculations) and to the inability by DFT to correctly

capture the electronic coupling between conducting planes in layered materials which increases their effective dimensionality affecting the geometry of their Fermi surface.

Measured the bulk Fermi surfaces of the MAl_3 (where M = V, Nb, Ta) compounds [5] which are found to display an excellent agreement with DFT thus indicating that these compounds indeed are Dirac type-II semimetals [6]. Equally, we determined with great level of detail the Fermi surface of both $PdTe_2$ and $PtTe_2$ finding that the first compound displays an excellent agreement with DFT which is not the case for the second one. Overall, our results support the notion that these compounds also are Type-II Dirac systems [7]. The same can be said about $NiTe_2$ which display nearly linear magnetoresistivity [8]. We characterized in great detail the electronic structure of $NbIrTe_4$ finding that this is possibly the best candidate for a type-II Weyl state from the perspective of quantum oscillatory phenomena [9].

Future Plans

Recently, we synthesized high quality single-crystals of orthorhombic α-RhSi which has the same stoichiometry as the non-symmorphic and cubic β-RhSi, a compound that was recently claimed to display a number of band degeneracies at high symmetry points in the Brillouin zone leading to Weyl Fermions displaying higher pseudospins and very long Fermi arcs on the surface [10]. It turns out that α-RhSi preserves roto-inversion symmetry, and as consequence display a number of Dirac nodes with non-trivial pseudospins. In the short term we will be focused on the full characterization of this compound.

References

[1] R. Schönemann *et al*., Phys. Rev. B **96**, 121108(R) (2017).

[2] G. Autès et al., Phys. Rev. Lett. **117**, 066402 (2016).

[3] D. Rhodes *et al*., Phys. Rev. B **96**, 165134 (2017).

[4] N. Xu *et al*., Phys. Rev. Lett. **121**, 136401 (2018).

[5] K.-W. Chen *et al*., Phys. Rev. Lett. **120**, 206401 (2018).

[6] T. R. Chang *et al*., Phys. Rev. Lett. **119**, 026404 (2017).

[7] W. Zheng *et al*., Phys. Rev. B **97**, 235154 (2018).

[8] W. Zheng *et al*. (in preparation).

[9] R. Schönemann *et al*., Phys. Rev. B **99**, 195128 (2019).

[10] G. Chang *et al*., Phys. Rev. Lett. **119**, 206401 (2017); P. Tang *et al*., ibid **119**, 206402 (2017).

Publications (from 08/2017 to 08/2019)

1. *Giant Anisotropic Magnetoresistance due to Purely Orbital Rearrangement in the Quadrupolar Heavy Fermion Superconductor PrV_2Al_{20},* Y. Shimura, Q. Zhang, B. Zeng, D. Rhodes, R. Schönemann, M. Tsujimoto, Y. Matsumoto, A. Sakai, T. Sakakibara, K. Araki, W. Zheng, Q. Zhou, L. Balicas, and S. Nakatsuji, Phys. Rev. Lett. **122**, 256601 (2019).

2. *Bulk Fermi surface of the Weyl type-II semimetallic candidate $NbIrTe_4$,* R. Schönemann, Y.-C. Chiu, W. Zheng, V. L. Quito, S. Sur, G. T. McCandless, J. Y. Chan, and L. Balicas, Phys. Rev. B **99**, 195128 (2019).

3. *Superconducting phase diagram of H_3S under high magnetic fields*, S. Mozaffari, D. Sun, V. S. Minkov, A. P. Drozdov, D. Knyazev, J. B. Betts, M. Einaga, K. Shimizu, M. I. Eremets, L. Balicas and F. F. Balakirev, Nat. Commun. **10**, 2522 (2019).

4. *Superconductivity at 250 K in lanthanum hydride under high pressures*, A. P. Drozdov, P. P. Kong, V. S. Minkov, S. P. Besedin, M. A. Kuzovnikov, S. Mozaffari, L. Balicas, F. F. Balakirev, D. E. Graf, V. B. Prakapenka, E. Greenberg, D. A. Knyazev, M. Tkacz, and M. I. Eremets, Nature **569**, 528 (2019).

5. *Fermi surface of the flat-band intermetallics $APd_3(A=Pb,Sn)$,* K. Wei, K.-W. Chen, J. N. Neu, Y. Lai, G. L. Chappell, G. S. Nolas, D. E. Graf, Y. Xin, L. Balicas, R. E. Baumbach, and T. Siegrist, Phys. Rev. Materials **3**, 041201(R) (2019).

6. *Magnetic anisotropy of the alkali iridate Na_2IrO_3 at high magnetic fields: Evidence for strong ferromagnetic Kitaev correlations*, S. D. Das, S. Kundu, Z. Zhu, E. Mun, R. D. McDonald, G. Li, L. Balicas, A. McCollam, G. Cao, J. G. Rau, H.-Y. Kee, V. Tripathi, and S. E. Sebastian, Phys. Rev. B **99**, 081101(R) (2019).

7. *One-dimensional tellurium chains: Crystal structure and thermodynamic properties of $PrCu_xTe_2$ ($x \sim 0.45$)*, R. Baumbach, L. Balicas, G. T. McCandless, P. Sotelod, Q. R. Zhang, J. Evans, D. Camdzic, T. J. Martin, J. Y.Chan, R. T.Macaluso, J. Solid State Chem. **269**, 553 (2019).

8. An*omalous Metamagnetism in the Low Carrier Density Kondo Lattice $YbRh_3Si_7$,* B. K. Rai, S. Chikara, X. Ding, I. W. H. Oswald, R. Schönemann, V. Loganathan, A. M. Hallas, H. B. Cao, M. Stavinoha, T. Chen, H. Man, S. Carr, J. Singleton, V. Zapf, K. A. Benavides, J. Y. Chan, Q. R. Zhang, D. Rhodes, Y. C. Chiu, L. Balicas, A. A. Aczel, Q. Huang, J. W. Lynn, J. Gaudet, D. A. Sokolov, H. C. Walker, D. T. Adroja, P. Dai, A. H. Nevidomskyy, C.-L. Huang, and E. Morosan, Phys. Rev. X **8**, 041047 (2018).

9. *Detailed study of the Fermi surfaces of the type-II Dirac semimetallic candidates XTe_2 (X=Pd, Pt)*, W. Zheng, R. Schönemann, N. Aryal, Q. Zhou, D. Rhodes, Y.-C. Chiu, K.-W. Chen, E. Kampert, T. Förster, T. J. Martin, G. T. McCandless, J. Y. Chan, E. Manousakis, and L. Balicas, Phys. Rev. B **97**, 235154 (2018).

10. *Bulk Fermi Surfaces of the Dirac Type-II Semimetallic Candidates MAl_3 (Where M = V, Nb, and Ta)*, K.-W. Chen, X. Lian, Y. Lai, N. Aryal, Y.-C. Chiu, W. Lan, D. Graf, E. Manousakis, R. E. Baumbach, and L. Balicas, Phys. Rev. Lett. **120**, 206401 (2018).

11. *Spectroscopic evidence for two-gap superconductivity in the quasi-1D chalcogenide $Nb_2Pd_{0.81}S_5$*, E. Park, S. Lee, F. Ronning, J. D Thompson, Q. Zhang, L. Balicas, X. Lu, and T. Park, J. Phys. Condens. Matter **30**, 165401 (2018).

12. *Converting topological insulators into topological metals within the tetradymite family*, K.-W. Chen, N. Aryal, J. Dai, D. Graf, S. Zhang, S. Das, P. Le Fèvre, F. Bertran, R. Yukawa, K. Horiba, H. Kumigashira, E. Frantzeskakis, F. Fortuna, L. Balicas, A. F. Santander-Syro, E. Manousakis, and R. E. Baumbach, Phys. Rev. B **97**, 165112 (2018).

13. *Evidence for negative thermal expansion in the superconducting precursor phase SmFeAsO*, H. D. Zhou, P. M. Sarte, B. S. Conner, L. Balicas, C. R. Wiebe, X. H. Chen, T. Wu, G Wu, R. H. Liu, H. Chen and D. F. Fang, J. Phys.: Condens. Matter **30**, 095601 (2018).

14. *Fermi surface in the absence of a Fermi liquid in the Kondo insulator SmB_6*, M. Hartstein, W. H. Toews, Y.-T. Hsu, B. Zeng, X. Chen, M. Ciomaga Hatnean, Q. R. Zhang, S. Nakamura, A. S. Padgett, G. Rodway-Gant, J. Berk, M. K. Kingston, G. H. Zhang, M. K. Chan, S. Yamashita, T. Sakakibara, Y. Takano, J.-H. Park, L. Balicas, N. Harrison, N. Shitsevalova, G. Balakrishnan, G. G. Lonzarich, R. W. Hill, M. Sutherland, S. E. Sebastian, Nat. Phys. **14**, 166 (2018).

15. *Fermi surface in the absence of a Fermi liquid in the Kondo insulator SmB_6*, M. Hartstein, W. H. Toews, Y.-T. Hsu, B. Zeng, X. Chen, M. Ciomaga Hatnean, Q. R. Zhang, S. Nakamura, A. S. Padgett, G. Rodway-Gant, J. Berk, M. K. Kingston, G. H. Zhang, M. K. Chan, S. Yamashita, T. Sakakibara, Y. Takano, J.-H. Park, L. Balicas, N. Harrison, N. Shitsevalova, G. Balakrishnan, G. G. Lonzarich, R. W. Hill, M. Sutherland, S. E. Sebastian, Nat. Phys. **14**, s166 (2018).

16. *Bulk Fermi surface of the Weyl type-II semimetallic candidate γ−$MoTe_2$*, D. Rhodes, R. Schönemann, N. Aryal, Q. Zhou, Q. R. Zhang, E. Kampert, Y.-C. Chiu, Y. Lai, Y. Shimura, G. T. McCandless, J. Y. Chan, D. W. Paley, J. Lee, A. D. Finke, J. P. C. Ruff, S. Das, E. Manousakis, and L. Balicas, Phys. Rev. B **96**, 165134 (2017).

17. *Fermi surface of the Weyl type-II metallic candidate WP_2*, R. Schönemann, N. Aryal, Q. Zhou, Y.-C. Chiu, K.-W. Chen, T. J. Martin, G. T. McCandless, J. Y. Chan, E. Manousakis, and L. Balicas, Phys. Rev. B **96**, 121108(R) (2017).

18. *Electronic in-plane symmetry breaking at field-tuned quantum criticality in $CeRhIn_5$*, F. Ronning, T. Helm, K. R. Shirer, M. D. Bachmann, L. Balicas, M. K. Chan, B. J. Ramshaw, R. D. McDonald, F. F. Balakirev, M. Jaime, E. D. Bauer, and P. J. W. Moll, Nature **548**, 313 (2017).

Probing Excitons in Confined Environments with Photon-Resolved Methods

Moungi Bawendi, Massachusetts Institute of Technology - Department of Chemistry, 77 Massachusetts Avenue, 02139 Cambridge, MA.

Program Scope

Our research focuses on the fundamental science and applications of colloidal quantum dots (QDs) with size-tunable quantum confined electronic structure. We take a cross-disciplinary approach; developing novel synthetic methods, new characterization strategies and applications of QDs. Partially as a result of our work, semiconducting QDs have made commercial inroads as display technologies and fluorescent biological markers. [1,2] This program focuses on our spectroscopy research, which is focused on extracting a fundamental understanding of the optical properties of QDs through the development of novel spectroscopic methods, emphasizing understanding how synthetic and environmental heterogeneities influence QD properties. One recent advance in our research has been the development of novel photon resolved correlation spectroscopies that allow us to extract the physics of photo-excited QDs with unprecedented time and spectral resolution from the photon stream of individual QDs.

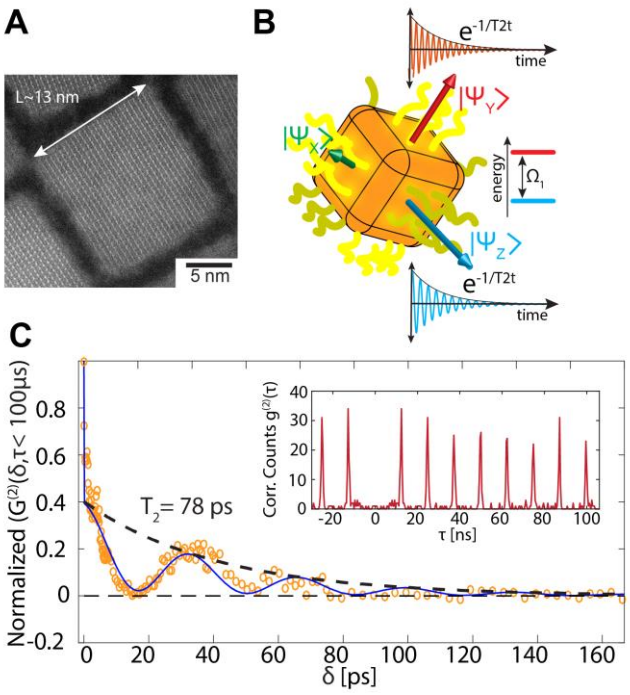

In recent years, the advent of quantum information science (QIS) has motivated our work even further, since control and minimization of dephasing mechanisms is crucial for producing quantum emitters (QEs) that are capable of generating indistinguishable photons - building blocks of modern quantum information schemes. [3]

Recent Progress

The development of practical optical quantum technologies requires the reproducible and scalable production of single quantum emitters with long optical coherence times that can be readily integrated with devices[3]. We recently demonstrated the superior optical properties of chemically-made, colloidal lead halide perovskite (CsPbX3, X=Cl, Br, I) quantum dots (PQDs) (above figure, A) as single emitters. [4] Using photon-correlation Fourier spectroscopy (PCFS) at low temperatures, we found that PQDs exhibit long optical coherence times and small exciton fine-structure splittings (B, C) [5]. The long coherence and short radiative emission lifetimes (210 ps) render the PQD emission linewidth near the Fourier transform limit. Moreover, we show that spectral diffusion is drastically reduced

compared to other colloidal quantum dots and that the majority (50-80%) of photons is emitted coherently. This fraction of coherent photons is already comparable to silicon vacancy centers in diamond, which are common emitters in quantum photonics. Broadly, our results suggest that, while all other colloidal quantum dot materials suffer from prohibitively incoherent emission, PQDs can be explored as sources of indistinguishable single photons that can be processed from solution onto virtually any substrate and easily coupled with hybrid nano-photonic components like waveguides or plasmonic gap cavities.

Future Plans

Our previous work on PQDs opens up a research program aimed at improving and using PQDs as quantum emitters. For our immediate next steps, we follow a two-pronged approach of i) investigating the pure-dephasing process of single PQDs to rationally optimize the intrinsic photon coherence of PQDs and ii) demonstrating two-photon interference and polarization-entangled photon pairs generated with PQDs.

i) Understanding the origins of pure dephasing in PQDs likely holds the key to reaching transform-limited emission. In general, two dephasing mechanisms have been proposed to play an important role depending on the exact material architecture for colloidal QDs. Some have argued that strong spin-orbit coupling and spin-noise can mediate a fast spin-flip between excitonic fine-structure states resulting in a loss of coherence. [6] Borri et al. [7] reported that low frequency acoustic phonon-mediated exchange between fine-structure states is the main mechanism of dephasing using photon-echo spectroscopy. We propose measuring the optical dephasing time T2 as a function of temperature for PQDs with various fine-structure splittings of the ground-state emissive triplet with PCFS. This will allow us to unambiguously establish the correlation between these two parameters to discern between the spin-noise and phonon-mediated exciton dephasing mechanism. Moreover, we will explore the synthetic control over the fine-structure splitting.

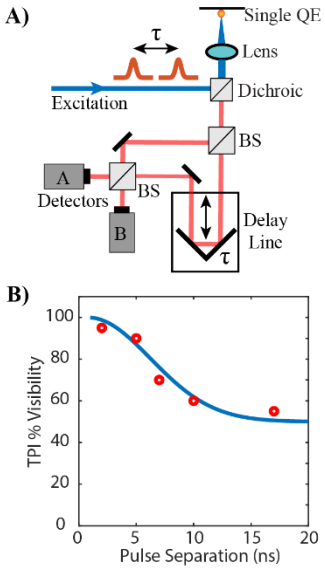

ii) One of the most important metrics of quantum emitters for QIS applications is their ability to produce indistinguishable photon pairs. Traditionally, the hallmark experiment to determine photon-indistinguishability is the Hong-Ou-Mandel (HOM) effect, [8] which measures a fourth-order correlation function of the emitted photon stream to produce a characteristic dip feature (HOM dip) at short inter-photon delays, informing on the ultimate degree of photon indistinguishability. Although a powerful characterization tool, the HOM experiment does not elucidate how the indistinguishability fluctuates in time due to processes such as fast spectral diffusion. Moreover, such characterization has never been demonstrated on colloidal quantum dots acting as QEs. Accessing information on the

dynamics of the HOM dip can provide direct evidence as to how mechanisms like spectral diffusion or exciton dephasing influence the ability of PQD QEs to produce indistinguishable photons. The above figure (A) depicts our experimental approach for interfering two-photons from the same PQDs with varying temporal distance τ. (B) shows the hypothetical two-photon interference visibility for different τ informing on botht he maximum photon-indistinguishability and spectral diffusion on timescales faster than accessible in our previous PCFS experiments. The long coherence time of PQDs also suggests the possibility of polarization entangled photon-pairs via the biexciton cascade (figure to the right). We will gauge how PQDs can be harnessed as entangled photon sources by measuring the entanglement finesse of PQDs while tuning the fine-structure splitting of the PQD with electric and magentic fields.

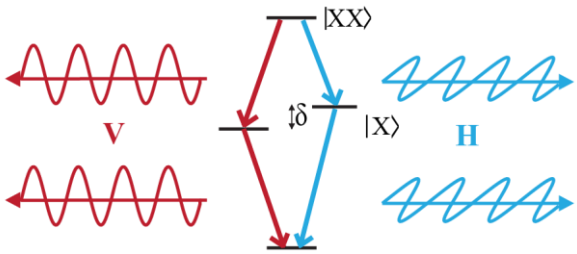

Our work will establish PQDs as color-tunable quantum-light sources and pave the way for their reliable production and integration with nano-photonic platforms.

References

[1] Coe-Sullivan, S.; Liu, W.; Allen, P.; Steckel, J. S. ECS J. Solid State Sci. Technol. 2012, 2 (2), R3026– R3030.

[2] Alivisatos, A. P.; Gu, W.; Larabell, C. Annu. Rev. Biomed. Eng. 2005, 7 (1), 55–76.

[3] Aharonovich I.; Englund D.; Toth M.; Nature Photonics 2016, (10), 631-641.

[4] Utzat, H.; Shulenberger, K; Achorn, O.; Nasilowski, M.; Sinclair, T.; Bawendi, M.; Nano Letters 2017, 17, 11, 6838-6846.

[5] . Utzat, H.; Sun, W; Kaplan, A.E.K.; Krieg, F; Ginterseder, M.;Klein, N.D.; Shulenberger, K.E.; Perkinson C.F.; Kovalenko, M.V.; Bawendi, M.G.; Science 2019, 363, 6431, 1068-1072.

[6] Accanto, N.; Maisa, F. Moreels, I.; Hens, Z. Langbein, W.; Borri, P.; ACS Nano 2012, 6 (6), 5227-5233.

[7] Borri, P.; Langbein, W.; Muljarov, E.A.; Zimmermann, R.; Physica Status Solidi b 2006, 243 (15), 3890-3894.

[8] Hong, C.; Ou Z. Y.; Mandel L.; Physical Review Letters 1987, 59, 2044.

Publications

1. Chen, Y.; Montana, D. M.; Wei, H.; Cordero, J. M.; Schneider, M.; Le Guével, X.; Chen, O.; Bruns, O. T.; Bawendi, M. G. Shortwave Infrared in Vivo Imaging with Gold Nanoclusters. Nano Lett. 2017, 17 (10), 6330–6334. doi:10.1021/acs.nanolett.7b03070 6.

2. Utzat, H.; Shulenberger, K. E.; Achorn, O. B.; Nasilowski, M.; Sinclair, T. S.; Bawendi, M. G. Probing Linewidths and Biexciton Quantum Yields of Single Cesium Lead Halide Nanocrystals in Solution. Nano Lett. 2017, 17 (11), 6838–6846. doi:10.1021/acs.nanolett.7b03120

3. Freyria, F. S.; Cordero, J. M.; Caram, J. R.; Doria, S.; Dodin, A.; Chen, Y.; Willard, A. P.; Bawendi, M. G. Near-Infrared Quantum Dot Emission Enhanced by Stabilized Self-Assembled J-Aggregate Antennas. Nano Lett. 2017, 17 (12), 7665–7674. doi:10.1021/acs.nanolett.7b03735

4. Chen, Y.; Cordero, J. M.; Wang, H.; Franke, D.; Achorn, O. B.; Freyria, F. S.; Coropceanu, I.; Wei, H.; Chen, O.; Mooney, D. J.; et al. A Ligand System for the Flexible Functionalization of Quantum Dots via Click Chemistry. Angew. Chem. Int. Ed Engl. 2018, 57 (17), 4652–4656. doi:10.1002/anie.201801113

5. Carr, J. A.; Franke, D.; Caram, J. R.; Perkinson, C. F.; Saif, M.; Askoxylakis, V.; Datta, M.; Fukumura, D.; Jain, R. K.; Bawendi, M. G.; et al. Shortwave Infrared Fluorescence Imaging with the Clinically Approved near-Infrared Dye Indocyanine Green. Proc. Natl. Acad. Sci. U. S. A. 2018, 115 (17), 4465–4470. doi:10.1073/pnas.1718917115

6. Doria, S.; Sinclair, T. S.; Klein, N. D.; Bennett, D. I. G.; Chuang, C.; Freyria, F. S.; Steiner, C. P.; Foggi, P.; Nelson, K. A.; Cao, J.; et al. Photochemical Control of Exciton Superradiance in LightHarvesting Nanotubes. ACS Nano 2018, 12 (5), 4556–4564. doi:10.1021/acsnano.8b00911

7. Shulenberger, K. E.; Bischof, T. S.; Caram, J. R.; Utzat, H.; Coropceanu, I.; Nienhaus, L.; Bawendi, M. G. Multiexciton Lifetimes Reveal Triexciton Emission Pathway in CdSe Nanocrystals. Nano Lett. 2018, 18 (8), 5153–5158. doi:10.1021/acs.nanolett.8b02080

8. Bertram, S.N.; Spokoyny, B.; Franke, D.; Caram, J.R.; Yoo, J.J.; Murphy R.P.; Grein, M.E.; and Bawendi, M.G. Single Nanocrystal Spectroscopy of Shortwave Infrared Emitters, ACSNano 2018 ASAP. doi: 10.1021/acsnano.8b07578

9. Utzat, H.; Sun, W; Kaplan, A.E.K.; Krieg, F; Ginterseder, M.;Klein, N.D.; Shulenberger, K.E.; Perkinson C.F.; Kovalenko, M.V.; Bawendi, M.G.; Coherent Single Photon Emission from Colloidal Lead Halide Perovskite Quantum Dots, Science 2019, 363, 6431, 1068-1072. DOI: 10.1126/science.aau7392.

Transient Studies of Nonequilibrium Transport in Two-Dimensional Semiconductors

Jonathan P. Bird, University at Buffalo

Program Scope

The overarching objective of this research is to investigate emergent carrier phenomena in different two-dimensional (2D) systems, under conditions where they are driven far from equilibrium. The description of nonequilibrium transport has long represented one of the most enduring challenges in condensed-matter physics, in large part due to the need to invoke the role of complex many-body phenomena (electron-phonon and electron-electron coupling) in this regime. In this project, we have explored aspects of this problem in a variety of different two-dimensional systems. These include the modulation-doped two-dimensional electrons gas, or 2DEG, in GaAs/AlGaAs heterostructures; the electron and hole systems in graphene and its related heterostructures, and; the strongly-confined electron layers in transition-metal dichalcogenide (MoS_2 and WS_2) and trichalcogenide (TiS_3) materials. Significant understanding has been achieved in a number of different areas, as we elaborate upon in the next section. A defining feature of much of this research has been an approach to problem solving in which novel experimental techniques (such as transient electrical pulsing and scanning-probe microscopy) are combined with the development (in collaboration with colleagues from condensed-matter theory) of sophisticated models.

Recent Progress

<u>Negative differential conductance due to inter-valley scattering in WS_2 under high fields</u>

Negative differential conductance (NDC) is one of the most prominent nonequilibrium phenomena exhibited by semiconductors, and arises from the scattering of hot carriers between different valleys of the conduction band. In our work published in Ref. 1, we pointed out that monolayer transition-metal dichalcogenides (TMDs) have conduction-band structures that should favor NDC, before going on to demonstrate this effect in monolayer WS_2. After processing these materials to allow electrical measurement, their current-voltage characteristics were studied and were found to exhibit NDC at room temperature. For a quantitative understanding of this behavior, we performed ensemble Monte-Carlo simulations of the high-field transport, showing how the NDC could be correlated to the increasing transfer of hot carriers to a satellite valley under high electric fields. An intriguing aspect of our experiments was found to be a dependence of the NDC on thermal annealing, with the negative conductance being most prominent for unannealed crystals. This was analyzed in terms of the influence of strain on the hot-carrier transport, specifically by considering how internal strain affects the equilibrium (K) and satellite (T) valleys. Our main finding was that the appearance of NDC can be dependent upon the energy separation of these valleys, since this determines the initial population of the satellite (T) valley at thermal equilibrium [1]. As such, our work therefore provides another nice example of how control of strain in 2D materials may be used to effectively modulate their physical properties.

Incipient localization due to scattering from frozen-phonon disorder in quantum point contacts

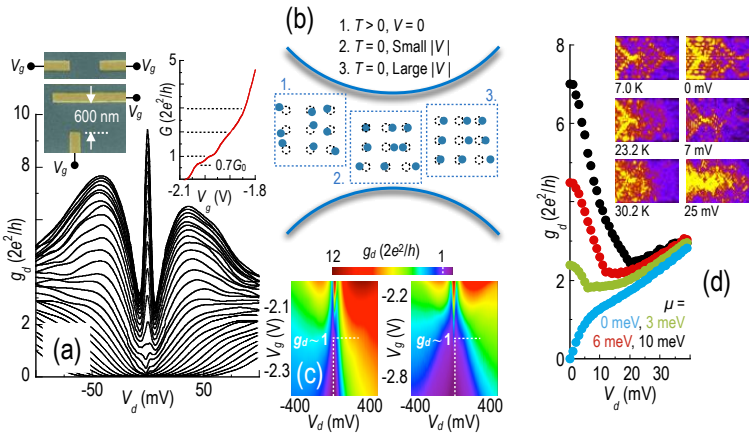

Fig. 1. (a) Differential conductance of a QPC at 4.2 K. Insets are electron micrographs of different QPC geometries. (b) Distinct disorder realizations, corresponding to different regimes of temperature and biasing. These "snapshots" denote the instantaneous displacement of atoms from equilibrium. (c) Contour plots showing differential conductance for the two QPC geometries of Fig. 1(a). (d) Calculated differential conductance as a function of source-drain bias and for different chemical potentials in the QPC. Insets show probability density in the QPC for various T (left column) and V_d (right column) [2].

An interesting discovery made in studies of nonequilibrium of transport in GaAs 2DEGs has involved our demonstration of a giant zero-bias anomaly (ZBA) in quantum point contacts (QPCs) [2]. An example of this behavior is shown in Fig. 1(a), where we plot (at 4.2 K) the differential conductance of a typical QPC at multiple gate voltages. This voltage "squeezes" the narrow conducting channel formed by the QPC gates, reducing the number of one-dimensional sub-bands involved in conduction, and leading to a systematic reduction in conductance. The most dramatic aspect of this data is a large ZBA, which causes the conductance to drop precipitously when the drain bias is raised from zero to just a few mV (for either polarity). We have described this effect in terms of an incipient localization phenomenon, which arises from the capacity of phononic disorder to function as a source of coherent scattering in the QPC channel. Central to this picture is the fact that, at the low temperatures of interest here, ballistic electrons injected into the QPC transit through it on time scales faster than the characteristic period of atomic vibration, allowing this latter motion to be thought of as a "frozen", instantaneous, form of disorder (see Fig. 1(b)). The strength of this disorder increases with increasing temperature, and can moreover be manipulated *in situ* by application of the drain voltage, which steadily imparts momentum from drifting electrons to the phonon system. Building on these considerations, we formulated [2] a model of nonequilibrium transport through a two-dimensional nanoconstriction, with a random potential controlled by temperature and bias. The differential conductance associated with this bias-dependent disorder was calculated using nonequilibrium Green functions, as illustrated in Fig. 1(d). In spite of the microscopic simplicity of our model the calculations clearly capture the essential features of our experiments, most notably the giant ZBA. Although not shown here, a crucial conclusion of our analysis [2] is that this anomaly arises from a bias-driven crossover to incipiently localized transport. Since the slow phonon disorder that lies at the heart of this phenomenon should be present in other nanoscale systems, such as molecular conductors, metallic nanojunctions, and nanotubes, the concepts developed here should find broad application to such systems.

Transient hot carrier transport in the Moire bands of graphene/h-BN heterostructures

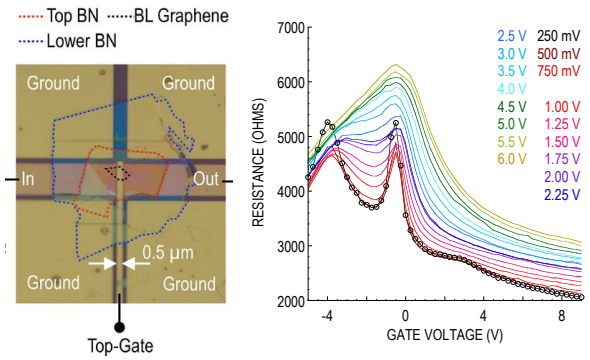

Fig. 2. Shown left is an encapsulated graphene/h-BN device with its various layers indicated by dotted lines of different color. Figure reproduced from [3]. Shown right are Dirac curves measured by transient pulsing at 77 K in graphene with complete h-BN encapsulation and edge contacts. Measurements were obtained using single-shot pulses (4-ns duration), with the amplitudes indicated by the different colors in the plot. The line with symbols indicates the density of data points involved in the measurement. Channel length and width are 1- and 4-µm, respectively. Unpublished data from the Bird group.

One of the primary objectives of research in this latest performance period has been to investigate the details of hot-carrier transport in graphene encapsulated in hexagonal boron nitride (h-BN). In our work published in Ref. 3, we used an approach of transient electrical pulsing to study the dynamics of hot carriers on time scales down to the nanosecond range. Our work revealed a significantly enhanced immunity in these devices, to current degradation due to hot-carrier effects, establishing the superiority of h-BN as a supporting dielectric for graphene [3]. As an illustration of the behavior exhibited in these experiments, in Fig. 2 we show the results of pulsed measurements of an edge-contacted graphene/h-BN device. This figure represents the results of measurements of the Dirac curve of one such device at 77 K, where the optical phonons of graphene are strongly damped. Data were obtained by the application of short (4-ns), single-shot, pulses to the device, at the various pulse amplitudes indicated in the inset. For the smallest pulse amplitude (250 mV, black line with open symbols), where this excitation should be minimal, the Dirac curve exhibits multiple peaks, features that we do not observe for graphene devices fabricated on SiO_2. As the amplitude of the applied pulse is increased, this structure in the Dirac curve is steadily suppressed, until one ultimately recovers (for pulses in excess of ~4 V) a single peak that is located close to zero gate voltage (consistent with minimal chemical doping in this sample). Our working hypothesis is that the multiple structure seen in the Dirac curve near equilibrium conditions (i.e. at small pulse amplitudes in Fig. 2) is a signature of quantum interference of carriers in the presence of Moiré bands, arising from the incommensurability of the graphene and h-BN crystal structures. To study this problem, we are currently extending our measurements to lower temperatures (as low as 3 K) than that shown in Fig. 2; although not shown here, the multi-peak structure apparent in Fig. 5 is less prominent at room temperature, suggesting that cooling to 3 K should, conversely, enhance its features even more strongly than at 77 K. Under such conditions, the possibility should exist to use our approach of transient pulsing to explore the dynamics of hot carriers in the Moiré bands. Such “bias spectroscopy” should provide a means to probe the miniband structure of the resulting superlattice and we are currently pursuing measurements of this problem.

Future Plans

Our plan for the coming period of DOE support is motivated by our most recent work [4], in which we have explored various aspects of (nonequilibrium) carrier transport in nanostructured samples of titanium trisulfide (TiS_3). A layered transition-metal trichalcogenide, this material exhibits a quasi-1D character, in which the Ti atoms in the three-dimensional (3D) crystal may be viewed as being oriented in isolated 1D chains. The chains are bound together in 2D sheets that are coupled by weak van-der-Waals-like bonding into a 3D crystal [4]. This one-dimensional nature endows the crystal with interesting collective transport properties, including evidence of a metal-insulator transition and charge-density wave (CDW) formation [4]. An advantageous feature of these materials is their capacity to be isolated in nanostructured form, allowing the physics of CDW formation to be strongly manipulated, by electrical gating and by structural control. It is this capability that motivates our studies, which address the novel behavior that emerges in CDW systems as we approach the idealized 1D limit originally envisaged by Peierls.

Publications (Two-Year List)

1. G. He, J. Nathawat, C.-P. Kwan, H. Ramamoorthy, R. Somphonsane, M. Zhao, K. Ghosh, U. Singisetti, N. Perea-López, C. Zhou, A. L. Elías, M. Terrones, Y. Gong, X. Zhang, R. Vajtai, P. M. Ajayan, D. K. Ferry, and J. P. Bird, "*Negative differential conductance & hot-carrier avalanching in monolayer WS_2 FETs*", Scientific Reports **7**, 11256 (2017).
2. Y.-H. Lee, S. Xiao, K. W. Kim, J. L. Reno, J. P. Bird, and J. E. Han, "*Giant zero bias anomaly due to coherent scattering from frozen phonon disorder in quantum point contacts*", Physical Review Letters **123**, 056802 (2019).
3. J. Nathawat, M. Zhao, C.-P. Kwan, S. Yin, N. Arabchigavkani, M. Randle, H. Ramamoorthy, G. He, R. Somphonsane, N. Matsumoto, K. Sakanashi, M. Kida, N. Aoki, Z. Jin, Y. Kim, G.-H. Kim, K. Watanabe, T. Taniguchi, and J. P. Bird, "*Transient response of h-BN-encapsulated graphene transistors: signatures of self-heating and hot-carrier trapping*", ACS Omega **4**, 4082 – 4090 (2019).
4. M. Randle, A. Lipatov, A. Kumar, C.-P. Kwan, J. Nathawat, B. Barut, S. Yin, K. He, N. Arab-chigavkani, R. Dixit, T. Komesu, J. Avila, M. C. Asensio, P. A. Dowben, A. Sinitskii, U. Singisetti, and J. P. Bird, "*Gate-controlled metal-insulator transition in TiS_3 nanowire field-effect transistors*", ACS Nano **13**, 803 – 811 (2019).
5. R. Somphonsane, H. Ramamoorthy, G. He, J. Nathawat, C.-P. Kwan, N. Arabchigavkani, Y.-H. Lee, J. Fransson, and J. P. Bird, "*Evaluating the sources of graphene's resistivity using differential conductance*", Scientific Reports **7**, 10317 (2017).
6. R. Somphonsane, H. Ramamoorthy, G. He, J. Nathawat, S. Yin, J. P. Bird, C.-P. Kwan, N. Arab-chigavkani, B. Barut, M. Zhao, Z. Jin, and J. Fransson, "*Universal voltage scaling due to self-averaging of the quantum corrections in graphene*", Scientific Reports, revision requested, under preparation; arXiv:1802.09922.

One-dimensional topological nanomaterials and superconductivity

Judy J. Cha; Department of Mechanical Engineering & Materials Science, Yale University

Program Scope

The overall scope of the project is to realize nanowires of topological materials, such as topological crystalline insulator SnTe [1], Weyl semimetals WTe_2 and $MoTe_2$ [2], and topological superconductors and to probe the nature of their topological surface states and superconducting state, exploiting the one-dimensional nature of the nanowires. To this end, efforts have been dedicated to improve the synthesis and doping of topological nanowires with control over the morphology and carrier density, followed by characterizations of basic transport properties of the synthesized topological nanowires. Proximity-induced superconductivity of the synthesized SnTe nanowires was studied in Josephson junction devices in collaborations with James R. Williams at the University of Maryland, College Park and Liang Fu at MIT.

Recent Progress

Research progress over the last year includes synthesis of narrow SnTe nanowires, which were critical for observing novel superconductivity in SnTe; synthesis of Weyl semimetal WTe_2 and $MoTe_2$ nanowires and characterizations of their transport properties; and the observation of novel $s \pm is'$ superconductivity in SnTe nanowires (in collaboration with James Williams and Liang Fu). Another notable achievement over the last year is a review on topological nanomaterials, published in Nature Reviews Materials this year. In this review, we critically examined the challenges that must be overcome for topological nanostructures for device applications and compared the benefits and disadvantages of using spin-orbit coupled semiconducting nanowires versus topological insulator nanowires for controlling Majorana bound states.

Synthesis of narrow SnTe nanowires. We have been making SnTe nanowires over the last several years via chemical vapor deposition (CVD) growth using gold nanoparticles as nucleation catalysts [3-5]. However, we lacked good control over the dimension and morphology of the nanowires during growth. Typically, the width of the nanowires ranged between 100 nm to 400 nm and these nanowires were synthesized along with SnTe micro-crystals and nanoplates, which we are not interested in. To study the surface states in detail, making narrow and long SnTe nanowires with high yield is important, which would enable a clear observation of the Aharanov-Bohm oscillations expected from the surface states. Thus, we explored ways to improve our synthesis to make high yield of narrow SnTe nanowires whose widths would be smaller than ~ 100 nm. This was achieved by introducing a second annealing

step during growth. We first grew SnTe microcrystals and large nanowires using 20 nm gold nanoparticles using the standard CVD growth recipe we developed. Then, we annealed the growth substrates, which contain the SnTe microcrystals, second time in the presence of SnTe and InTe source powders. After second annealing, the SnTe microcrystals disappeared and the growth substrate was densely covered with narrow SnTe or In-doped SnTe nanowires whose widths were much smaller than before, ranging between ~ 60 nm to ~ 200 nm (Figure 1). We attribute this to the formation of Au-Sn-Te nanoparticles during the first annealing step, which then act as efficient nucleation centers for the narrow SnTe nanowires during the second annealing step. These nanowires were essential for observing the *s* ± *is'* superconductivity, which will be discussed later. A manuscript is in preparation (#1 under Publications).

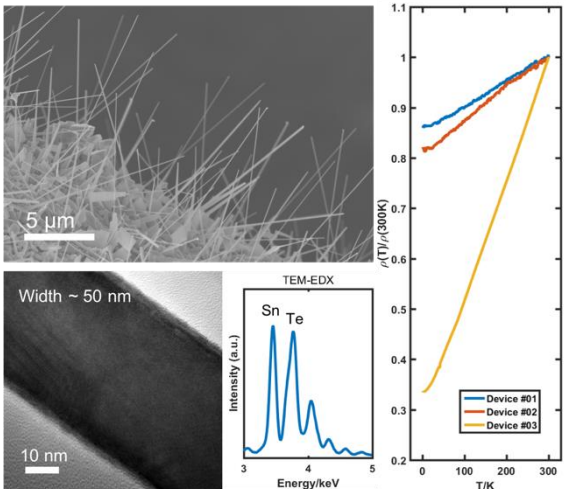

Figure 1. High yield of narrow SnTe nanowires with widths below ~ 100 nm. The residual resistance ratio is higher for narrow nanowires, suggesting less contribution from the bulk carriers.

Synthesis of WTe_2 and $MoTe_2$ nanowires. WTe_2 and $MoTe_2$ in the 1T' phase are Weyl semimetals, which possess topologically protected surface Fermi arcs [2]. We aimed to increase the contribution of the topological surface states to the transport signal by making nanowires of WTe_2 and $MoTe_2$. The eventual goal is to induce superconductivity in the nanowires by Te-vacancy doping or cation intercalation. A conventional CVD approach of co-evaporation of metal oxides (WO_3 or MoO_3 powders) and Te powder turned out to be challenging due to the low reactivity of tellurium-based transition metal dichalcogenides. Thus, we developed a conversion reaction to synthesize the nanowires. First, WO_3 and MoO_3 nanowires were synthesized by CVD. Then, the metal oxide nanowires were tellurized by annealing them in the presence of Te vapor with H_2 carrier gas (Figure 2). Formation of reactive HTe_2 helps to strip the oxygen from the metal oxide nanowires, converting WO_3 and MoO_3 to WTe_2 and $MoTe_2$ nanowires. Transport properties of the synthesized WTe_2 and $MoTe_2$ were characterized using a pseudo 4-terminal device to show that the intrinsic conductivity of the nanowires is actually lower than those of flakes exfoliated from bulk crystals. This suggests reduced electron mobility of the nanowires due to surface oxidation. Currently, *in situ* tellurium coating is being explored to alleviate the degradation induced by surface oxidation. We published the results in ACS Nano this year (#2 under Publications).

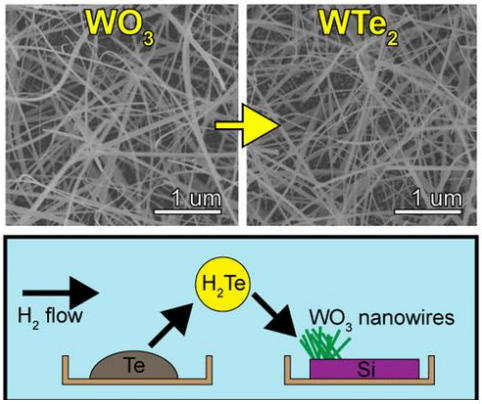

Figure 2. Conversion of WO_3 nanowires to WTe_2 nanowires by tellurization.

Novel superconductivity in SnTe nanowires. The proposed project seeks to study the nature of the superconductivity induced in SnTe nanowires and verify the predicted topological superconductivity. We provided our narrow SnTe nanowires and superconducting In-doped SnTe nanowires to James R. Williams at the University of Maryland, College Park for Josephson junction studies. The Josephson behaviors using SnTe nanowires as weak links were distinct from conventional behaviors. First, the DC Josephson effect showed that the positive and negative values of the critical current, I_{DC}, were different, which is not expected in conventional overdamped junctions (Figure 3A). Second, the magnetic diffraction pattern showed a local minimum of I_{DC} at a zero magnetic field and a maximum I_{DC} at a finite magnetic field of 16 mT, in contrast to the conventional Fraunhofer-like patterns (Figure 3B). Lastly, the AC Josephson effect shows Shapiro steps at the half values of the quantum flux.

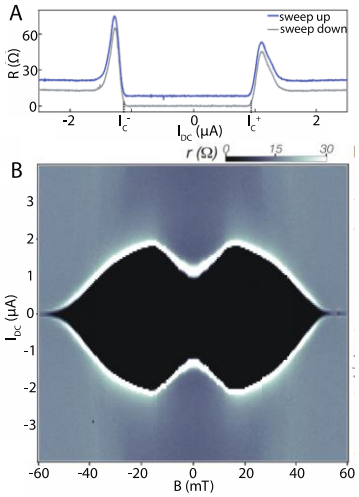

Figure 3. Josephson effects of SnTe nanowires suggest novel superconductivity.

The systematic breakdown of the three Josephson effects points to the presence of novel *s* $\pm$ *is'* superconductivity, which can arise in SnTe that possess even numbers of Dirac surface states. Momentum-preserving, Umklapp scattering between two Dirac surface states can explain our observations. We also confirmed that Majorana bound states are realized, evident in the disappearance of the first Shapiro step at a finite magnetic field. Liang Fu at MIT developed the theory to explain the data, obtained in James Williams' group. Our findings are uploaded in arXiv, and a revised version of the arXiv manuscript is submitted for peer-review (#3 under Publications).

Future Plans

We will continue our collaborations with James Williams and Liang Fu to study the novel superconductivity observed in SnTe nanowires. We noticed that the novel Josephson effects were pronounced in narrow nanowires, while the effects were small or not observed in wider nanowires. Thus, we hypothesize that the contribution of the surface states is critical for our observations. We will work together to study the detailed nature of this finding. The next step would be to braid Majorana bound states in these nanowires as the Josephson junction studies confirmed the presence of Majorana bound states. Schemes to braid the Majorana bound states and detect the braiding will be devised, and appropriate SnTe nanowires (whether branched or long wires with local magnetic fields) will be synthesized for the experiments.

We will continue to improve transport properties of synthesized WTe_2 and $MoTe_2$ nanowires by *in situ* Te coating. Transport characterizations, such as the analysis of the residual resistance ratio and the strength of the magnetoresistance, will be carried out to gauge the crystal quality and the degree of surface oxidation on these nanowires. At the same time, Li^+ intercalation into

WTe_2 and $MoTe_2$ flakes will be carried out to determine if superconductivity will be induced at the right concentration of Li ions. The induced superconductivity may be topological in nature. Flakes are easier to start with, compared to nanowires, so they serve as good test samples.

Recently, we synthesized triple-point topological metal, MoP [6], in nanostructures. While single-crystalline, the synthesized nanostructures are porous, which we think is due to the synthesis route we have developed. We will optimize the synthesis to improve the crystalline quality of MoP nanowires and nanoplates, and measure their transport properties.

References

[1] Phys. Rev. Let.. 106, 106802 (2011).
[2] Phys. Rev. B 92, 161107(R) (2015).
[3] Nano Lett. 14, p.4183-4188 (2014).
[4] Nano Lett. 15, p.3827-3832 (2015).
[5] APL Materials 5, 076110 (2017).
[6] Nature Commun. 10:2475 (2019).

Publications

1. P. Liu, D. Hynek, J. M. Woods, L. Wang, J. J. Cha, "Synthesis of narrow SnTe nanowires with high yield by secondary annealing," in preparation (2019).
2. J. M. Woods, D. Hynek, P. Liu, J. J. Cha, "Synthesis of WTe_2 nanowires with increased electron scattering," ACS Nano 13, p.6455-6460 (2019).
3. C. J. Trimble, M. T. Wei, N. F. Q. Yuan, S. S. Kalantre, P. Liu, J. J. Cha, L. Fu, J. R. Williams, "Josephson detection of $s \pm is'$ superconductivity in SnTe nanowires," arXiv:1907.04199 (2019), submitted to Science.
4. P. Liu, J. R. Williams, J. J. Cha, "Topological nanomaterials," Nature Reviews Materials 4, p.479-496 (2019).
5. Y. Zhou, J. V. Pondick, J. Lius Silva, J. M. Woods, D. J. Hynek, G. Matthews, X. Shen, Q. Feng, W. Liu, Z. Lu, Z. Liang, B. Brena, Z. Cai, M. Wu, L. Jiao, S. Hu, H. Wang, C. Moyses Araujo, J. J. Cha, "Unveiling the interfacial effects for enhanced hydrogen evolution reaction on the MoS_2/WTe_2 hybrid structures," Small 15, 1900078 (2019).
6. S. Yazdani, M. Yarali, J. J. Cha, "Recent progress on in situ characterizations of electrochemically intercalated transition metal dichalcogenides," Nano Research doi:10.1007/s12274-019-2408-6 (2019).
7. P. Liu, Y. Xie, E. Miller, Y. Ebine, P. Kumaravadivel, S. Sohn, J. J. Cha, "Dislocation-driven SnTe surface defects during chemical vapor deposition growth," Journal of Physics and Chemistry of Solids 128, p.351-359 (2019).
8. Y. Zhou, J. Lius Silva, J. M. Woods, J. V. Pondick, Q. Feng, Z. Liang, W. Liu, L. Lin, B. Deng, B. Brena, F. Xia, H. Peng, Z. Liu, H. Wang, C. Moyses Araujo, J. J. Cha, "Revealing the contribution of individual factors to hydrogen evolution reaction catalytic activity," Advanced Materials 30, 1706076 (2018).

Investigation of topologically trivial and non-trivial spin textures and their relationships with the topological Hall effect

TeYu Chien, Yuri Dahnovsky, William Rice, Jinke Tang, and Jifa Tian

Department of Physics & Astronomy, University of Wyoming, Laramie WY 82071

Program Scope

This proposal has two main goals: (1) to investigate methods to create a variety of spin textures, both topologically trivial and non-trivial, and (2) to establish the relationships between the created spin textures and the ***topological Hall effect*** (**THE**) signals. These goals will be achieved by utilizing the ***van der Waals*** (**vdW**) ***two-dimensional*** (**2D**) magnetic materials, such as CrX_3 (X=I, Br, and Cl) and Fe_3GeTe_2, transferred onto various substrates with different interactions to create a wide range of spin textures. The created spin textures will be characterized by ***spin-polarized scanning tunneling microscopy*** (**SPSTM**) as well as by signs of magneto-Raman measurements and the Hall resistivity measurements will be conducted through Hall bar devices. The relationship between the THE signal and the created spin textures will be established.

Magnetic skyrmions are topologically non-trivial spin textures with potential application for high-density memory [1–4] and logic elements for computing [5–7]. The magnetic skyrmion is protected by its topology, meaning it is very difficult to be destroyed [8]. Furthermore, magnetic skyrmions can be manipulated by a spin-polarized current [9] and require several orders of magnitude smaller current than that of the magnetic domain walls [3,10], which significantly reduces energy dissipation. All these properties are making magnetic skyrmion a strong candidate that could revolutionize the computing and memory/storage technologies. To achieve that, two important fundamental questions need to be answered: (1) What kind of ingredients are needed to create magnetic skyrmion? and (2) Knowing the ingredients, or essential parameters required for skyrmion creation, how can one design a material or a material system which will show magnetic skyrmions? Answering these fundamental questions are keys to the successful applications of magnetic skyrmion and is one of the two main focuses of this proposal.

So far, the detection of the magnetic skyrmions is not trivial, typically done with expensive and time consuming techniques. Understanding and establishing an electrical way to detect skyrmions is essential to the device applications. In contrast to the normal Hall effect, which is created by the Lorentz force, and the anomalous Hall effect, which is influenced by magnetization, the THE was first observed in the presence of non-collinear spin texture. The scalar spin chirality in the non-collinear spin texture can induce a non-trivial Berry phase and an associated virtual magnetic flux, which gives rise to the THE [11].

In literature, THE has been discussed in various magnetic systems, including magnetic skyrmions [12,13], ferromagnetic/paramagnetic bilayers [14], ***topological insulator*** (**TI**) heterostructures [15], and non-coplanar antiferromagnets [16]. While the THE is attributed to

certain spin textures, the relationships between the topologically non-trivial spin textures to the measured THE signals have not been established and understood [17]. In short, *the ability of creating desired spin textures* as well as *the ability to identify topologically non-trivial spin textures from Hall measurements* are desirable in the scientific community and for device applications, which are the two central goals of this project.

In order to achieve the two central goals, we have the following major objectives:
(1) Achieve desired spin textures in a 2D magnetic material based heterostructures consisting of the atomic-thin 2D magnetic materials and other 2D/3D functional materials;
(2) Gain understanding, delineate the confusion, and seek answers to critical questions regarding the origin of the THE signals; and
(3) Determine the characteristic features of THE that can be used for electronic detection of magnetic skyrmions.

Recent Progress

Atomic resolution STM and multi-peak features revealed in the d*I*/d*V* spectrum measured on $CrBr_3$ flakes*:*

Before performing SPSTM measurements for each material system, it is important to carry out atomic or nm resolution STM measurements to gain a baseline comparison and initial understanding of the materials systems, both topographically and electronically (d*I*/d*V* spectrum and mapping). Also, the SPSTM signal is very subtle, a high quality atomic resolution STM images can prove the feasibility of the subsequence SPSTM measurements. Recently, we have started to study $CrBr_3$ flakes prepared by mechanical exfoliation method and revealed atomic resolution images as well as high quality d*I*/d*V* spectrum. Figure 1(a) shows the crystal structure of $CrBr_3$; while Fig. 1(b) shows the large scale topography STM images. The step heights are measured to be ~0.59 nm, which is consistent with the height of the $CrBr_3$ monolayer.

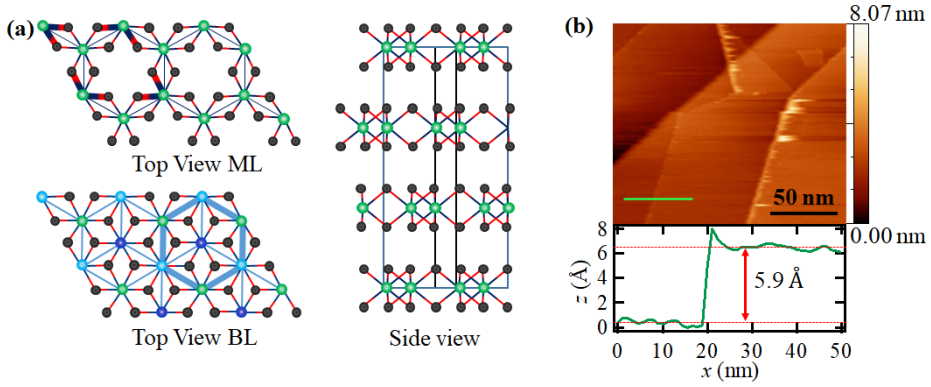

Figure 1. (a) Crystal structure of $CrBr_3$. (b) Large scale topography showing step height of ~0.59 nm.

The atomic resolution images are shown in Fig. 2(a). It is noted that though the image quality is not noise-free, the atomic features are visible and agree with the crystal structure, as shown in the zoom-in topography overlaid with the crystal structure (right panel of Fig. 2(a)). The overlaid crystal structure is a bilayer $CrBr_3$ model, indicating that the STM measurements are

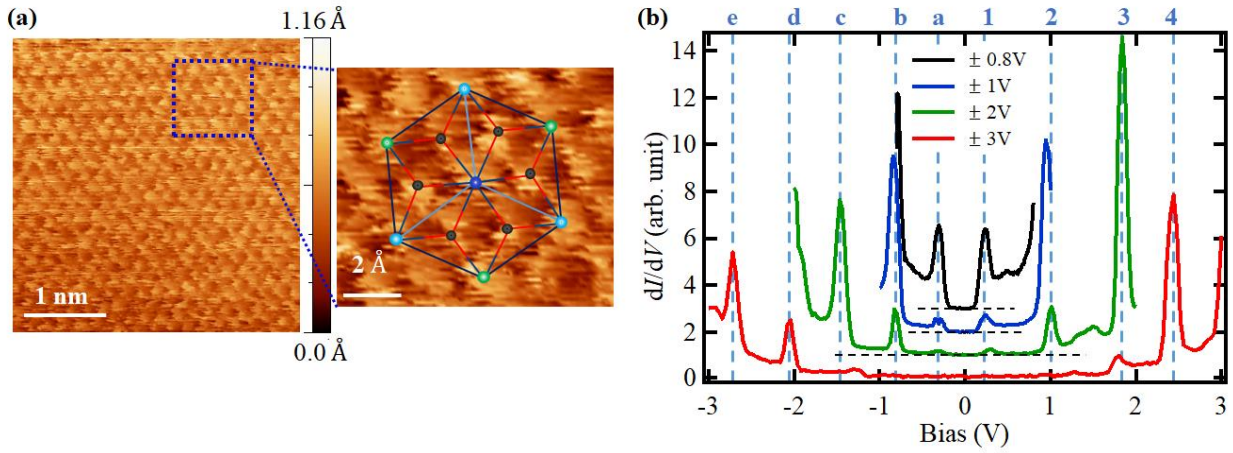

Figure 2. (a) Atomic resolution topography of $CrBr_3$ with the crystal structure overlaid in the zoom-in image (right panel). (b) dI/dV spectra measured at 77 K with various bias range in order to visualize all peaks within ±3 V range.

sensitive to the second layer $CrBr_3$. The low quality atomic resolution topography is a result of the combination of poor conductive $CrBr_3$ and lack of degassing preparation prior to STM measurements (to prevent from the heat damage in ultra-high vacuum environment). Figure 2(b) shows the d*I*/d*V* spectra measured at 77 K with various bias range. In order to clearly observe all the features within the bias range of ±3 V, the various range bias measurements are needed. At this temperature, the crystal structure is rhombohedral (space group $R\bar{3}$) and in the paramagnetic phase (the magnetic transition temperature was reported to be ~32 K). Further analysis of the peak positions revealed that all the reported optical transition energies can be matched to a certain pair of conduction-valence band peak pairs in Fig. 2(b). Note that this multi-peak DOS is very unusual and cannot be reproduced with DFT calculation (not shown here). In particular, the peaks "*1*" and "*a*" are missing in all reported DFT calculated DOS. The origin of these two peaks and the multi-peak DOS in $CrBr_3$ requires further study.

Figure 3 (a) and (b) show the topography and d*I*/d*V* mapping of a monolayer $CrBr_3$ measured at 77 K. The clear d*I*/d*V* contrast (Fig. 3(b)) unambiguously distinguishes the monolayer $CrBr_3$ flake from the substrate HOPG. The d*I*/d*V* spectrum (Fig. 3(c)) measured on the monolayer $CrBr_3$ exhibits a similar shape as the HOPG d*I*/d*V* spectrum with humps in positive bias side

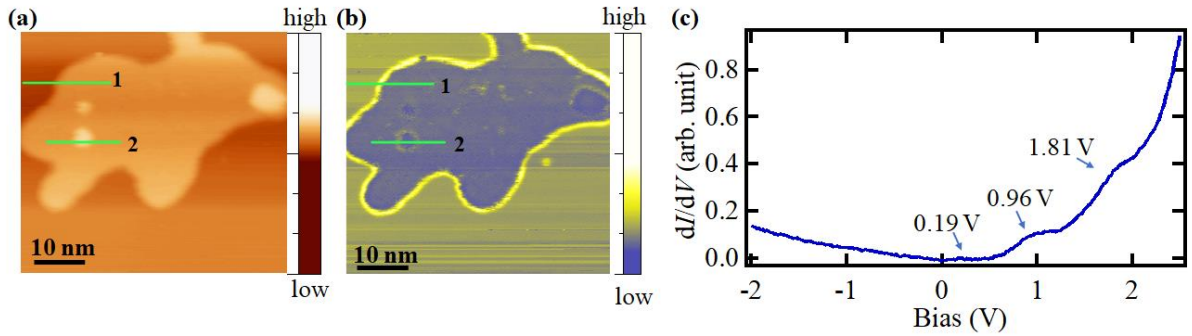

Figure 3. Monolayer and bilayer $CrBr_3$ (a) topography and (b) d*I*/d*V* mappings measured at 77 K. (c) d*I*/d*V* point spectrum of monolayer $CrBr_3$ on HOPG with bias ranging from -2 V to 2.5 V.

matching the measured peaks on bulk d*I*/d*V* spectrum (Fig. 2(b)). We believe that the combined spectral features are due to the interactions between the monolayer $CrBr_3$ and the underneath HOPG layer. This observation further confirms the importance of the second layer materials on the electronic properties. The detail analysis in the line profiles in topography and dI/dV mappings confirmed that the smaller apparent height of the monolayer $CrBr_3$ compare with that in the bulk is due to the electronic artifact. Also, edge degradations are clearly observed in the monolayer and bilayer $CrBr_3$ measurements, as shown in Fig. 3. In particular, the edges are shown to be curved and higher d*I*/d*V* contrast in Fig. 3(b).

Future Plans

SPSTM has been successfully demonstrated in Chien's lab using Cr/W tip. The next step in this project is to utilize the SPSTM to visualize the spin textures formed in the 2D magnetic materials in contacting with various substrates. We will mainly use the Cr/W tip prepared by intentionally crashing the clean W tip into Cr(100) single crystal. The Cr(100) single crystal will also be used to confirm that we have successfully prepared spin-polarized STM tip before measuring the targeting samples. A clean W for ordinary STM measurements will also be used for double checking the observed spin textures. The low-temperature STM (LTSTM) system in Chien's lab is capable of measuring at 4 K. An upgrade of this system to capable of applying 0.15-0.4 T magnetic field is expected to be finished in Fall 2019. With this capability, magnetic skyrmion may be induced in some system with moderate magnetic field application, if not found as the ground state. For systems require a higher magnetic field, Chien is a regular user in the Center for Nanoscale Materials at Argonne National Laboratory where a high magnetic field (6 T) and low temperature (4 K) system is available. Chien is a currently active user of this particular instrument.

References

[1] F.Ma, Y.Zhou, H. B.Braun, andW. S.Lew, Nano Lett. **15**, 4029 (2015).
[2] H. B.Braun, Adv. Phys. **61**, 1 (2012).
[3] T.Schulz, R.Ritz, A.Bauer, M.Halder, M.Wagner, C.Franz, C.Pfleiderer, K.Everschor, M.Garst, andA.Rosch, Nat. Phys. **8**, 301 (2012).
[4] A.Fert, N.Reyren, andV.Cros, Nat. Rev. Mater. **2**, 17031 (2017).
[5] N.Nagaosa andY.Tokura, Nat. Nanotechnol. **8**, 899 (2013).
[6] A.Fert, V.Cros, andJ.Sampaio, Nat. Nanotechnol. **8**, 152 (2013).
[7] W.Jiang, G.Chen, K.Liu, J.Zang, G. E.Suzanne, andA.Hoffmann, Phys. Rep. **704**, 1 (2017).
[8] K.VonBergmann, A.Kubetzka, O.Pietzsch, andR.Wiesendanger, J. Phys. Condens. Matter **26**, 394002 (2014).
[9] J.Iwasaki, M.Mochizuki, andN.Nagaosa, Nat. Commun. **4**, 1463 (2013).
[10] F.Jonietz, S.Mühlbauer, C.Pfleiderer, A.Neubauer, W.Münzer, A.Bauer, T.Adams, R.Georgii, P.Böni, R. A.Duine, K.Evershor, M.Garst, andA.Rosch, Science (80-.). **330**, 1648 (2010).
[11] P.Bruno, V. K.Dugaev, andM.Taillefumier, Phys. Rev. Lett. **93**, 096806 (2004).
[12] S.Mühlbauer, B.Binz, F.Jonietz, C.Pfleiderer, A.Rosch, A.Neubauer, R.Georgii, andP.Böni, Science (80-.). **323**, 915 (2009).

[13] D.Liang, J. P.Degrave, M. J.Stolt, Y.Tokura, andS.Jin, Nat. Commun. **6**, 8217 (2015).
[14] J.Matsuno, N.Ogawa, K.Yasuda, F.Kagawa, W.Koshibae, N.Nagaosa, Y.Tokura, andM.Kawasaki, Sci. Adv. **2**, e1600304 (2016).
[15] K.Yasuda, R.Wakatsuki, T.Morimoto, R.Yoshimi, A.Tsukazaki, K. S.Takahashi, M.Ezawa, M.Kawasaki, N.Nagaosa, andY.Tokura, Nat. Phys. **12**, 555 (2016).
[16] C.Sürgers, G.Fischer, P.Winkel, andH.V.Löhneysen, Nat. Commun. **5**, 3400 (2014).
[17] Y.Yun, Y.Ma, T.Su, W.Xing, Y.Chen, Y.Yao, R.Cai, W.Yuan, andW.Han, Phys. Rev. Mater. **2**, 034201 (2018).

Publications

None, new project.

Towards a Universal Description of Vortex Matter in Superconductors

PI Leonardo Civale, Co-PI Boris Maiorov
MPA Division, Condensed Matter and Magnet Science,
Los Alamos National Laboratory, Los Alamos, NM 87545
e-mail: lcivale@lanl.gov

Program Scope

The goal of our project is to obtain a universal description of superconducting vortex matter in the presence of potential pinning wells produced by material inhomogeneities. Our strategy is to compare and contrast systems with vastly different properties under a broad spectrum of conditions, with the purpose of establishing a general picture that could not be achieved through studying individual systems. Our approach is basic-science oriented and has strong technological impact. The relevance of this study goes beyond understanding existing materials, as any yet-to-be-discovered superconductor will share most of the vortex physics.

Superconducting vortices are one of the clearest manifestations of quantum mechanics in condensed matter, and an archetypical model system where the 'particle' density and interactions can be readily tuned by changing H and T. Although their existence was already well established in the 1960s, the study of vortex matter only became a large research field after the discovery of the oxide high temperature superconductors (HTS), motivated by the fascinating vortex physics that emerges from the large influence of thermal fluctuations, orders of magnitude larger than in conventional superconductors. Fluctuations have two main effects: they make vortices vibrate around their equilibrium positions in the lattice, eventually melting it into a vortex liquid at the phase transition line $H_m(T)$, and they produce a rich and fast nonequilibrium dynamics in the vortex solid phases.

Building upon our previous progress, we are now ready to make bold steps towards understanding the role of fluctuations on vortex physics at extreme conditions, drastically enhancing our capability for predicting, controlling and designing the behavior of vortex matter.

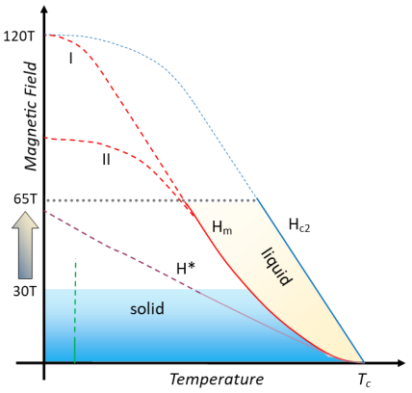

Fig. 1: Phase diagram of an HTS. Solid lines: Known boundaries. Dotted lines: possible extrapolations. Vertical green line: possible thermal-quantum dynamics crossover. Blue shade: region where most of the vortex pinning studies have been performed. Yellow shade: currently explored region of the vortex liquid.

Recent Progress

The superconducting phase extends up to the upper critical field $H_{c2}(T)$, which in HTS is very large, exceeding 100T at low T (Fig. 1), and vortex matter exists over most of it. However, experimental studies of vortex pinning and critical current density (J_c), using DC magnets, have been limited to ~ 30T. Pulsed-field magnets have allowed *linear electrical transport* studies up to much higher fields[1], but those measurements only provide information about $H_m(T)$, $H_{c2}(T)$ and the liquid

phase limited by them; they tell us nothing about the solid phase below $H_m(T)$, where vortices are pinned ($J_c > 0$) and thus the linear resistivity is zero. So, the shocking conclusion is that, after 33 years, ***we only know about 1/3 of the HTS phase diagram***. A similar statement can be made for Fe-based HTS[2], and even more so for the recently discovered almost-room-temperature hydrogen-based superconductors[3,4,5].

We have recently developed the first capability in the world to measure *nonlinear* electrical transport (current-voltage, *I-V* curves) in pulsed fields[16]. This suddenly doubles the accessible portion of the phase diagram, opening up the opportunity to explore vortex pinning, the nature and dimensionality of the vortex solid phases, and the critical phenomena associated with vortex solid-liquid phase transition[6,7], potentially up to 100T. Performing these studies in coated conductors (CCs) is also key for developing high-field DC superconducting magnets[8].

The big technical challenge posed by these studies had precluded until now; all previous measurements of vortex matter in pulsed fields had been limited to the linear response. We developed a technique for sub-microsecond smart *I-V* measurements that enables the determination of J_c in pulsed fields[16]. At the core of this success is a low-noise field programmable gate array (FPGA) that enables taking multiple *I -V* curves in one field pulse (~ 50 ms) while ensuring the voltage never exceeds a predetermined maximum value to preclude sample damage (Fig. 2a).

We performed studies on $YBa_2Cu_3O_7$ films with $BaZrO_3$ nanorods grown by pulsed laser deposition (PLD) [Fig. 2b] and $Y_{0.77}Gd_{0.23}Ba_2Cu_3O_7$ CCs with 3% $BaHfO_3$ nanoparticles, grown by metal organic deposition (MOD) [Fig. 2c]. To validate our method, we collected pulsed-field *I-V* curves at fields that can be accessed in DC magnets (Fig. 2b). The agreement between both sets of curves is very good. We were able to obtain *I -V* curves and J_c up to 65 T, the highest field at which a J_c had ever been measured. Our results show that fluctuations dominate the response not only in the liquid, but also *over most of the solid phases* [above $H^*(T)$ in Fig. 1]. Moreover,

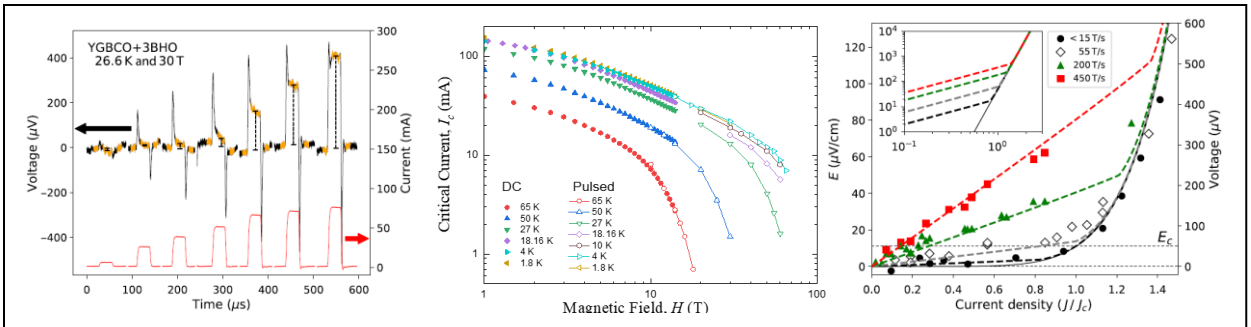

Fig. 2 (a) FPGA-based, fast *I -V* curves measurements. Source current pulses (~ 25 μs long, red lines) and corresponding raw-voltage pulses (black lines), taken at the peak field of 30 T pulses. The voltage is averaged, and the background is subtracted over the regions highlighted in orange. The dashed black lines represent the resulting average voltage amplitude. **(b)** Critical current vs. field for a PLD $YBa_2Cu_3O_7$ film with $BaZrO_3$ nanorods, using a 11 μV/cm criterion. Full symbols: DC field. Open symbols: pulsed field. **(c)** Dependence of the *I -V* curves for a MOD $Y_{0.77}Gd_{0.23}Ba_2Cu_3O_7$ CC with 3% $BaHfO_3$ nanoparticles on the magnetic field change rate $\dot{H} \equiv dH/dt$. Symbols: experimental points at 26.6 K and 30 T peak field. For large $\dot{H}$ values the *I -V* curve is initially ohmic, whereas data at $\dot{H} \leq 15$ T/s (closest to peak field) show the expected power-law. Dashed lines: model (no free parameters). Solid black line: theoretical curve for $\dot{H} = 0$.

the persistence of these fluctuations to low T (~1.8K) casts doubts on the accepted knowledge of their thermal origin, and points to the relevance of magnetic-field induced fluctuations.

Determining J_c from an *I-V* curve assumes that vortices are pinned and then moved by the force produced by the applied DC current, i.e., that over the timescale of a current pulse vortex motion is caused predominantly by the applied current and not by the fast-changing field. The effect of a large $\dot{H} \equiv dH/dt$ on the *I -V* curves is seen in Fig. 2c. At low $\dot{H}$ the *I -V* curves shape is the expected power law $V \propto I^n$ [$\Rightarrow E = E_c(J/J_c)^n$] with a well-defined J_c, whereas at higher $\dot{H}$ the initial part of the *I -V* curve becomes ohmic (linear in *J*). The power-law is recovered at high *J*. We developed a theoretical model that completely captures the changes with $\dot{H}$. Using the J_c and *n*-value obtained at low $\dot{H}$ and the sample geometry, we obtained the dashed lines in Fig. 2c *with no free parameters*. The dependence of the *I -V* shape with $\dot{H}$ impacts the ability to determine $J_c(H)$ using the entire field pulse. The maximum $\dot{H}$ at which the *I -V* curves exhibit the power-law and thus can be used in determining J_c (at a given E_c) is inversely proportional to the strip width.

Future Plans

The new hot topic in superconductivity are the hydrogen-based compounds, with T_cs as high as ~ 260 K[3,4,5]. This is essentially room temperature, the holy grail of superconducting materials discovery. We will apply our knowledge of vortex pinning and dynamics to these materials. We already have the samples at LANL (T_c ~ 220K), from M. Eremets' group (Germany)[5]. Of course, the crystalline quality of these early samples is low, and the initial results will have to be revised as they improve over time. But the superconductivity research community have successfully navigated through similar situations after the discovery of the oxide HTS, MgB_2, and the Fe-based HTS. Building upon what we learned in those previous cases, we will apply a combination of non-linear transport and magnetization to obtain some basic but very important information about vortex matter at almost room temperature, including grain connectivity, in-field J_c and flux creep rates. These compounds become superconducting only at very high pressures; the available samples are already inside pressure cells appropriate for transport studies.

References

1. M. Miura *et al*., "Vortex liquid-glass transition up to 60 T in nano-engineered coated conductors grown by metal organic deposition", *Appl. Phys. Lett*. **96**, 072506 (2010).
2. S.A. Baily *et al*., "Psuedoisotropic upper critical field in cobalt-doped SrFe2As2 epitaxial films", *Phys. Rev. Lett*. **102**, 117004 (2009).
3. M. Somayazulu *et al*., "Evidence for Superconductivity above 260 K in Lanthanum Superhydride at Megabar Pressures", *Phys. Rev. Lett*. **122**, 027001 (2019).
4. A. P. Drozdov *et al*., "Superconductivity at 250 K in lanthanum hydride under high pressures", *Nature* **569**, 528 (2019).
5. S. Mozaffari *et al*., "Superconducting Phase-Diagram of H3S under High Magnetic Fields", *Nature Commun*. **10**, 2522 (2019).
6. See G. Blatter, M.V. Feigel'man, V.B. Geshkenbein, A.I. Larkin and V.M. Vinokur, "Vortices in high-temperature superconductors", *Rev. Mod. Phys*. **66**, 1125 (1994) and references therein.

7. D.R. Nelson and V.M. Vinokur, “Boson localization and correlated pinning of superconducting vortex arrays”, *Phys. Rev. B* **48**, 13060 (1993).
8. S. Hahn *et al*., “45.5-tesla direct-current magnetic field generated with a high temperature superconducting magnet”, *Nature* **570**, 496 (2019).

Publications

9. “Tuning nanoparticle size in perovskite thin films for efficient energy applications”, M. Miura, B. Maiorov, M. Sato, M. Kanai, T. Kato, T. Kato, T. Izumi, S. Awaji, P. Mele, M. Kiuchi and T. Matsushita, *NPG Asia Materials* **9**, e447 (2017).
10. “Nuclear magnetic resonance investigation of the novel heavy fermion system Ce2CoAl7Ge4”, A.P. Dioguardi, P. Guzman, P.F.S. Rosa, N.J. Ghimire, S. Eley, S.E. Brown, J.D. Thompson, E.D. Bauer, and F. Ronning, *Phys. Rev. B* **96**, 245132 (2017).
11. “Accelerated vortex dynamics across the magnetic 3D-to-2D crossover in disordered superconductors”, S. Eley, R. Willa, M. Miura, M. Sato, M. Leroux, M.D. Henry and L. Civale, *npj Quantum Materials* (2018) 3:37; doi:10.1038/s41535-018-0108-1.
12. “In-depth study of the H - T phase diagram of Sr4Ru3O10 by magnetization experiments”, F. Weickert, L. Civale, B. Maiorov, M. Jaime, M.B. Salamon, E. Carleschi, A.M. Strydom, R. Fittipaldi, V. Granata and A. Vecchione, *Physica B - Condensed Matter* **536**, 634 (2018).
13. “Glassy Dynamics in a heavy ion irradiated $NbSe_2$ crystal”, S. Eley, K. Khilstrom, R. Fotovat, Z.L. Xiao, A. Chen, D. Chen, M. Leroux, U. Welp, W-K. Kwok and L. Civale, *Scientific Reports* **8**, 13162 (2018).
14. “Designing Nanomagnet Arrays for Topological Nanowires in Silicon”, L.N. Maurer, J.K. Gamble, L. Tracy, S. Eley and T.M. Lu, *Phys Rev. Appl*. **10**, 054071 (2018).
15. “Localized magnetic moments in metallic SrB_6 single crystals”, J. Stankiewicz, P. Schlottmann, A. Arauzo, M. J. Martinez Perez, P.F.S. Rosa, L. Civale and Z. Fisk, *J. Phys.: Condens. Matter* **31**, 065602 (2019).
16. “Dynamics and Critical Currents in Fast Superconducting Vortices at High pulsed Magnetic Fields”, M. Leroux, F.F. Balakirev, M. Miura, K. Agatsuma, L. Civale and B. Maiorov, *Phys. Rev. Applied* **11**, 054005 (2019).
17. “Pushing the limits for the highest critical currents in superconductors”, L. Civale, *PNAS* **116**, 10201 (2019) - (commentary).
18. “Competing Interface and Bulk Effects Driven Magnetoelectric Coupling in Vertically Aligned Nanocomposites”, A. Chen, Y. Dai, A. Eshghinejad, Z. Liu, Z. Wang, J. Bowlan,1 E. Knall, L. Civale, J.L. MacManus-Driscoll, A.J. Taylor, R.P. Prasankumar, T. Lookman, J. Li, D. Yarotski and Q.X. Jia, *Advanced Science,* 1901000, DOI: 10.1002/advs.201901000 (2019).
19. “Intrinsic anisotropy versus effective pinning anisotropy in $YBa_2Cu_3O_7$ thin-films and nanocomposites”, E. Bartolomé, F. Vallés A. Palau, V. Rouco, N. Pompeo, F.F. Balakirev, B. Maiorov, L. Civale, T. Puig, X. Obradors and E. Silva, *Phys. Rev. B* **100**, 054502 (2019).
20. “Strong magnetoelastic effect in $CeCo_{1-x}Fe_xSi$ as Néel order is suppressed”, V.F. Correa, A.G. Villagrán Asiares, D. Betancourth, S. Encina, P. Pedrazzini, P.S. Cornaglia, D.J. García, J.G. Sereni, B. Maiorov, N. Caroca Canales and C. Geibel, submitted to *Phys. Rev. B* (2019); https://arxiv.org/abs/1903.01383.

Electronic interactions and pairing in superconductors.

Dan Dessau, University of Colorado, Boulder

Program Scope

The goal of this project is to perform experimental studies of the electronic interactions and pairing in high temperature superconductors, topological superconductors, and materials close to a superconducting instability. We primarily utilize high-resolution angle-resolved photoemission (ARPES), both at synchrotron radiation sources around the world as well as utilizing our unique laser-ARPES facility at the University of Colorado. The developments of this technique that we have pioneered will enable this new round of studies.

The origin of the superconducting pairing in cuprate superconductors remains unknown after 30 years. It is hypothesized that this pairing ultimately arises from the strong electronic correlations, and that this pairing can best or only be understood by a detailed experimental study of these correlations and all possible signatures of the pairs. In the last DOE grant cycle we developed ARPES into a true electron "self-energy spectroscopy" – for the first time bringing access to the full energy-dependent and momentum-dependent fully-causal electron self-energies. With our new technology, we thus have the clearest window yet into the electronic correlations or interactions of an electronic material, with our previous results showing a strong positive feedback effect on the pairing from the correlations, strengthening a conventional pairing mechanism or potentially allowing a fully electronic pairing mechanism. This work also has enabled us to make the first simultaneous extraction of the size, shape, and density of the pairs.

With the unique superconductivity in the strongly correlated cuprates, the question arises whether other materials with a similar electronic structure and similar correlations may also superconduct – a quest that may not only find a new superconductor but which could shed great light on the origin of correlated high temperature superconductors. Our preliminary work as well as that of others indicates that layered nickelates are especially promising, so this is another area of emphasis for us.

An especially important type of superconductivity is topological superconductivity, as these can potentially support Majoranas that would be highly useful for quantum computation. Our program also thus includes the study of topology, topological surface states, etc. We presented the first experimental evidence for a new type of topological surface state on the edge of the T_c=39K superconductor MgB_2, making it potentially the highest temperature topological superconductor.

Recent Progress

We developed and applied a new two-dimensional (EDC and MDC combined) ARPES fitting technology, utilizing it to extract gaps, bare-band dispersion, and the fully-causal complex self-energies $\Sigma'(\omega)$ and $\Sigma''(\omega)$ in a lightly underdoped T_c=85K BSCCO cuprate superconductor [1]. These self energies are obtained with full and inherent Kramers-Kronig self-consistency

(i.e. causality), with an ~ 2 orders of magnitude reduction in free fitting parameters compared to traditional EDC & MDC fitting methods. In this way, we have turned ARPES into a true "self energy spectroscopy", i.e. a tool to access the electronic correlations and interactions.

Fig 2 shows the temperature dependence of pairing gaps and self-energies of the data of **Fig 1**. Panel A shows that upon cooling from high temperature and the onset of pairing gaps (yellow), there is a conversion of the incoherent diffusive Σ" (red) to the coherent band renormalization and kinks of Σ' (blue) – this conversion is a new effect that we detailed here. The data also suggests a

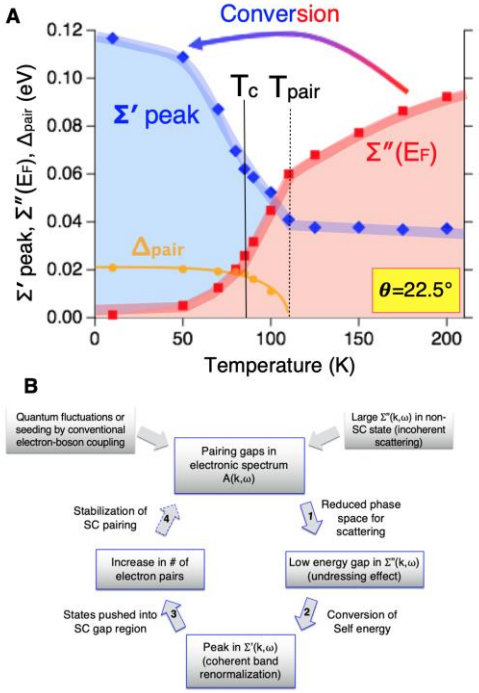

Fig 2. (**A**) Upon cooling from high temperature and the onset of pairing gaps (yellow), there is a conversion of the incoherent diffusive Σ" (red) to the coherent band renormalization and kinks of Σ' (blue). **(B)** Proposed positive feedback effect between the spectra A(k,ω) and self-energies Σ(k,ω), enhancing and stabilizing the SC pairing.

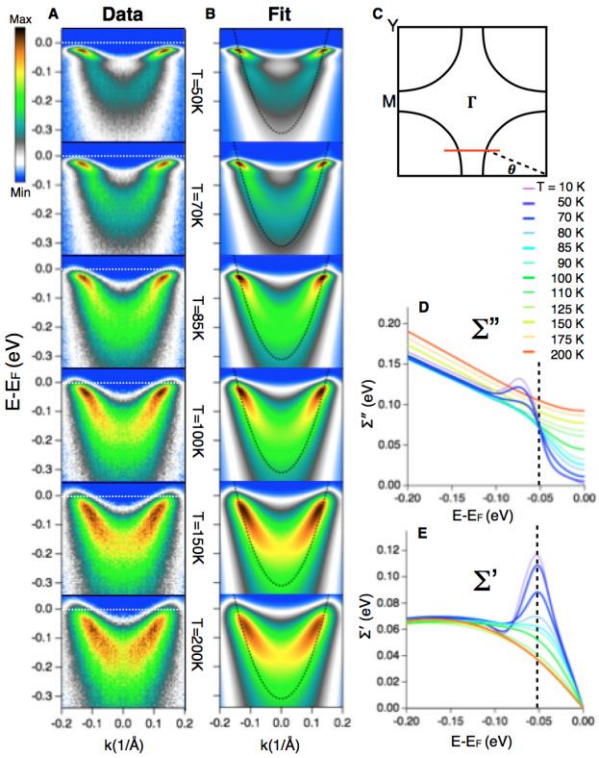

Fig 1. Development and application of ARPES into a "self energy spectroscopy" allowing us to access the full self-energies Σ" (panel D) and Σ' (panel E) vs. frequency and temperature from raw ARPES data (panel A). Sample was a Tc=85K Pb-BSCCO cuprate superconductor [1].

positive feedback effect (panel B) between the spectra A(k,ω) and self-energies Σ(k,ω) that should enhance and stabilize the SC pairing. This mechanism is possible because of, or enhanced by, the huge incoherent scattering rate Σ"(k,ω) present in the strange metal incoherent normal state.

The new technology described in **Figs 1** and **2** allowed us to obtain many new parameters of the superconducting pairs. **Fig 3** shows the shape and size of the Cooper pairs in a cuprate superconductor as extracted from our ARPES data [2]. The pairs extend quite far near the nodal direction, with drastically decreasing size when moving towards

scale of 4.5Å is seen for the antinodal pairs – a length on the order of the lattice parameter. The ultrashort antinodal length scale is maintained for all doping levels studied indicating this is likely a universal property of the Cooper pairs (panel c).

In addition to the cuprates, we have been studying the layered nickelates [3]. **Fig 4a1** shows the experimental Fermi surface (schematic in **4a2**) of the trilayer nickelate $La_4Ni_3O_{10}$, compared to the Fermi surface of the cuprate superconductor $Bi_2Sr_2CaCu_2O_8$ (panel **b1, b2**). While many aspects of the Fermi surface are similar, the nickelate has some extra pieces of Fermi surface that we argue may poison any possible superconductivity in these compounds.

Fig 5 shows our ARPES results from the T_c=39K superconductor MgB_2, obtained via edge-on cleaves. In this work we discovered a novel "waterslide" Dirac nodal-line topological surface state in MgB_2 (schematic in panel a),

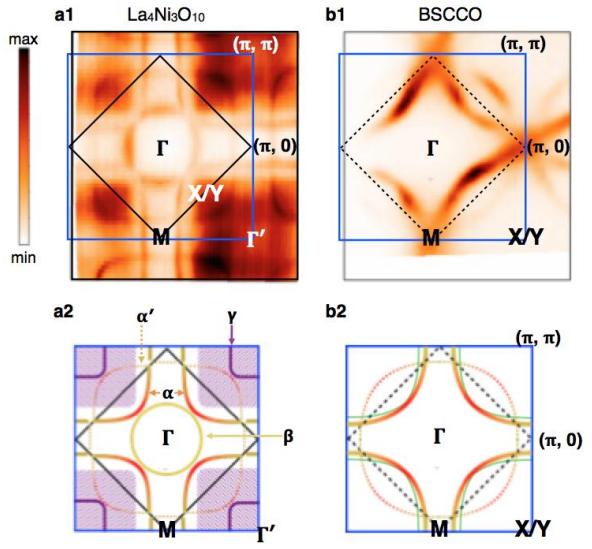

Fig 4. Fermi surface map of $La_4Ni_3O_{10}$. Compared to that of the optimally doped cuprate $(Bi,Pb)_2Sr_2CaCu_2O_8$ (BSCCO). The β and γ bands in $La_4Ni_3O_{10}$ are not observed in the cuprates and may poison any possible superconductivity in $La_4Ni_3O_{10}$. From [3].

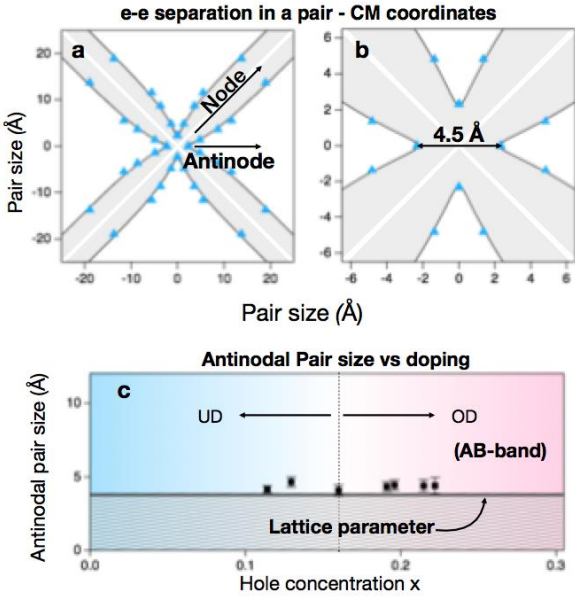

Fig 3. Shape and size of Cooper pairs of a cuprate superconductor, as extracted from ARPES [2]. An ultrashort length scale of 4.5Å is seen for the antinodal pairs – a length on the order of the lattice parameter. The ultrashort antinodal length scale is maintained for all doping levels studied indicating this is likely a universal property of the Cooper pairs.

with the theory and raw data shown in panels (b-d) and (e-g) respectively [4]. We argue that because of its intimate contact to the bulk superconducting state, this topological surface state is likely to go superconducting via the proximity effect – if confirmed this would be a novel type of topological superconducting state with by far the highest Tc so far known. Other work not discussed here was done as well [5-7].

Future Plans

We will keep advancing the state-of-the art of experiment, analysis, and understanding of a range of superconducting and topological materials. In the cuprates we have developed another new analysis method that is allowing us to access many more parameters of the Cooper pairs. For

the nickelates we are making very good progress studying a related layered nickelate $La_4Ni_3O_8$ that does not have the extra "bad" bands of $La_4Ni_3O_{10}$. Further studies of the topological edge states of MgB_2 have the potential to confirm this as a high temperature topological superconductor.

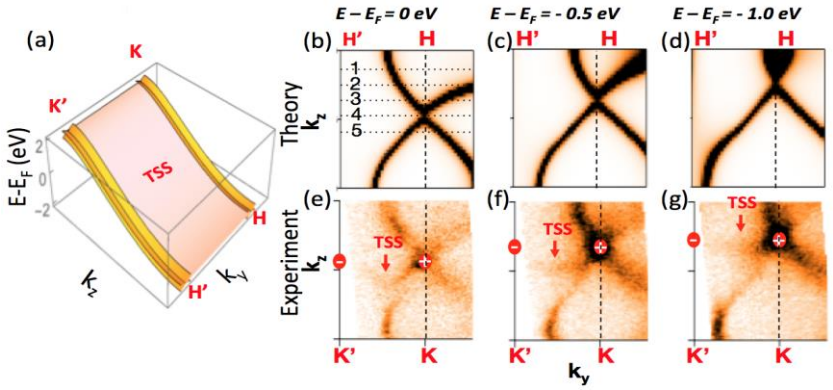

Fig 5. Edge-on ARPES discovers a novel "waterslide" Dirac nodal-line topological surface state in MgB_2. a) A schematic of the waterslide surface state. (b-d) Theoretical prediction of the bulk bands for three different binding energies. (e-g) Experimental observation of the bulk bands as well as an additional topological surface state (TSS) that connects two nodal lines (points in these planes). [4]

Publications/References

1. Haoxiang Li, X Zhou, Stephen Parham, T. J. Reber, Helmuth Berger, Gerald Arnold, Daniel S. Dessau, "Coherent organization of electronic correlations as a mechanism to enhance and stabilize high temperature cuprate superconductivity" (Nature Communications **9**, 26 (2018)
2. Haoxiang Li, X. Zhou, S. Parham, K. N. Gordon, R. D. Zhong, J. Schneeloch, G. D. Gu, Y. Huang, H. Berger, G. B. Arnold, D. S. Dessau "Starfish-shaped Cooper pairs with ultrashort antinodal length scales in cuprate superconductors" arXiv:1809.02194 (Under review)
3. Haoxiang Li, Xiaoqing Zhou, Thomas Nummy, Junjie Zhang, Victor Pardo, Warren E. Pickett, J. F. Mitchell, D. S. Desssau[SEP]"Fermiology and Electron Dynamics of Trilayer Nickelate ($La_4Ni_3O_{10}$)" Nature Comm 8, 704 (2017) Doi:10.1038/s41467-017-00777-0
4. X. Zhou, K. Gordon, K-K Jin, Ha. Li, D. Narayan, H. Zhao, H. Zheng, H. Huang, G. Cao, N. D. Zhigadlo, F. Liu, and D. S. Dessau, "Observation of Topological Surface State in High Temperature Superconductor MgB_2" http://arxiv.org/abs/1805.09240 (under review)
5. Haoxiang Li, Xiaoqing Zhou, Stephen Parham, Thomas Nummy, Justin Griffith, Kyle Gordon, Eric L. Chronister, Daniel. S. Dessau. "Spectroscopic Evidence of Pairing Gaps to 60 Kelvin or Above in Surface-Doped p-Terphenyl Crystals" Phys Rev B (to appear)
6. C. Hu, X.Zhou, P. Liu, J. Liu, P. Hao, E. Emmanouilidou, H. Sun, Y. Liu, H. Brawer, A. P. Ramirez, H. Cao, Q. Liu, D.S. Dessau, Ni Ni "A van der Waals antiferromagnetic topological insulator with weak interlayer magnetic coupling" arXiv:1905.02154 (under review)
7. X. Zhou, Q. Liu, Q.S. Wu, T. Nummy, H. Li, J. Griffith, S. Parham, J. Waugh, E. Emmanouilidou, B. Shen, O. V. Yazyev, N. Ni, D.S. Dessau "Coexistence of Tunable Weyl Points and Topological Nodal Lines in Ternary Transition-Metal Telluride TaIrTe4" Phys. Rev. B 97, 241102(R) (2018).

Patent Application:

1. J. Waugh, D. S. Dessau, S. P. Parham, T. Nummy, J. Griffith, X. Zhou, H. Li. "High Speed Two-Dimensional Event Detection and Imaging with an Analog Interface" International Patent application number PCT/US18/23146 Filed Mar 19, (2018).

THz Plasmonics and Topological Optics of Weyl Semimetals

H. D. Drew, CNAM University of Maryland, College Park, MD

Program Scope

THz magneto-optical properties of 3D topological Weyl semimetals are under investigation. Both FTIR spectroscopy and THz pump-probe measurements are being used. The electronic band structure is characterized spectroscopically through FTIR zero-field reflectance and/or cyclotron resonance measurements. The studies include the dynamic chiral pumping and the study of the predicted novel magneto-electric effects arising from the underlying Berry curvature and magneto plasmonic effects in the absence of an applied magnetic field. Chiral pumping in the extreme quantum limit is being studied on Weyl semimetals to directly probe the chiral N=0 Landau level. Non-linear pump-probe measurements are used to measure the chiral pumping lifetime. The unique THz effects predicted in these materials may have important applications in THz technology.

Recent Progress

Solids with topologically robust electronic states exhibit unusual electronic and optical transport properties that do not exist in other materials. A particularly interesting example is chiral charge pumping, the so-called chiral anomaly, in recently discovered topological Weyl and Dirac semimetals, where simultaneous application of parallel DC electric and magnetic fields creates an imbalance in the number of carriers of opposite topological charge (chirality). Using THz optical spectroscopy and time resolved measurements on the Weyl semimetal TaAs in a

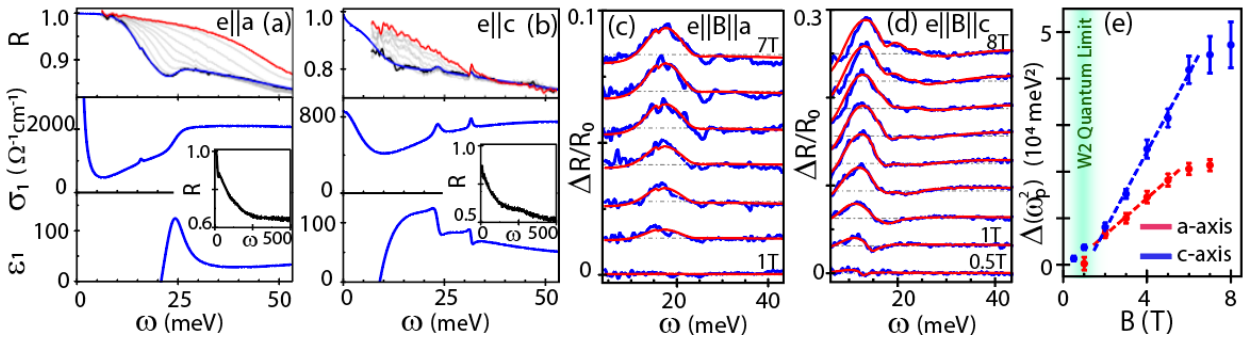

Panels a. and b. show the reflectance and optical conductivity and real part of the dielectric function of TaAs vs. magnetic field in the Faraday geometry for e||a and e||c. Panels c. and d. shows the differential reflectance as a function of magnetic field. Panel e. gives the change in Drude weight with B field for the two orientations of e||B.

magnetic field, we optically interrogate the chiral anomaly. Blue-shifts of the screened plasma frequency are observed. The blue shifts originate from an enhancement of the free carrier Drude weight, which is spectrally resolved from the scattering rate. The Drude weight enhancements agree with the theoretical predictions of chiral pumping[2]. Also, the Drude weight enhancement is accompanied by a reduction of the interband spectral weight in accordance with the f-sum rule, providing further confirmation of Drude enhancement. A departure from linear field-dependence of the Drude weight is observed at the highest fields in the quantum limit, providing direct evidence of field-dependent Fermi velocity of the chiral Landau level. Using time-resolved terahertz measurements on the Weyl semimetal TaAs in a magnetic field, we optically interrogate the chiral anomaly by dynamically pumping the chiral charges and monitoring their subsequent relaxation. Theory based on Boltzmann transport shows that the observed effects originate from an optical nonlinearity in the chiral charge pumping process. Our measurements reveal that the chiral population relaxation time is much greater than 1 ns. The observation of terahertz-controlled chiral carriers with long coherence times and topological protection suggests the application of Weyl semimetals for quantum optoelectronic technology.

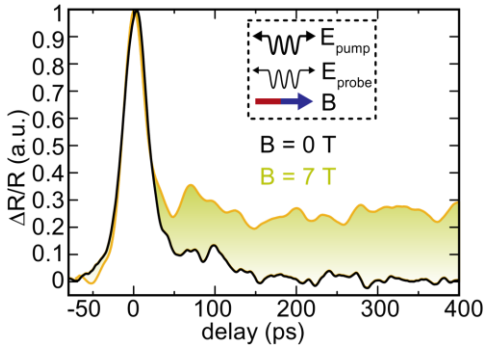

Chiral anomaly geometry. Epump || Eprobe || B (varying B). Pump-induced increase in probe reflection for B=0 T (black) and B=7 T (yellow) in arbitrary units as a function of pump-probe time delay. The pump-probe trace at B= 7 T exhibits a very slow response (>>1 ns).

Future Plans

We plan to characterize other new Weyl and Dirac systems that are coming on line. The community is looking for the "hydrogen atom" of the Weyl semimetal. CoSi is one promising new system which features Weyl node spacing comparable to the Brillouin zone size. This system may be suitable for study of the predicted chiral plasmons that arise from the Berry curvature in Weyl materials[1]. In another experiment gates will be applied to the samples in order to study the Fermi arc surface states by modulation reflectance spectroscopy at THz frequencies.

References

1. "Chiral anomaly and classical negative magnetoresistance of Weyl metals"
D. T. Son and B. Z. Spivak, PHYSICAL REVIEW B 88, 104412 (2013).

2. "*Helicons in Weyl semimetals"*, F. M. D. Pellegrino, M. Katsnelson, and M. Polini, PHYSICAL REVIEW B 92, 201407(R) (2015).

Publications

"Three-dimensional Dirac cone carrier dynamics in Na_3Bi and Cd_3As_2" G. S. Jenkins, C. Lane, B. Barbiellini, A. B. Sushkov, R. L. Carey, Fengguang Liu, J. W. Krizan, S. K. Kushwaha, Q. Gibson, Tay-Rong Chang, Horng-Tay Jeng, Hsin Lin, R. J. Cava, A. Bansil, and H. D. Drew, Phys. Rev. B 94, 085121 (2016).

"*Optical evidence of the chiral magnetic anomaly in Weyl semimetal TaAs*", A. L. Levy, A. B. Sushkov, Fengguang Liu, Bing Shen, Ni Ni, H. D. Drew, and G. S. Jenkins, arXiv preprint arXiv:1810.05660 (2018), and PRB in print.

"*Nonlinear Optical Control of Chiral Charge Pumping in a Topological Weyl Semimetal*", M. Mehdi Jadidi, Mehdi Kargarian, Martin Mittendorf Yigit Aytac, Bing Shen, Jacob C. Kronig-Otto, Stephan Winnerl, Ni Ni, Alexander L. Gaeta, Thomas E. Murphy, and H. Dennis Drew, arXiv:1905.02236 and Nature Comm. In print.

Microwave spectroscopy of correlated 2D electron systems in semiconductors and graphene

L.W. Engel, NHMFL/FSU and Cory Dean, Columbia University

Program Scope

Two-dimensional electrons can form a wide variety of correlated states, particularly in systems for which the disorder can be kept extremely small. These systems include semiconductor heterostructures and more recently graphene, in particular when it is encapsulated in clean BN. This project is aimed at studying electron solids and other correlated states by means of broadband microwave spectroscopy. The main method of performing this spectroscopy utilizes transmission lines like that pictured in Figure 1. The archetypical state which displays striking features in its microwave spectrum is the Wigner solid (WS) [1-7] that occurs at the high magnetic field (B), low filling factor (ν) termination of the series of fractional quantum Hall effect states in GaAs. We will refer to the low ν terminating state of a fractional quantum Hall effect (FQHE) series as the "low ν insulator". The insulating property of an electron solid is due to pinning by disorder, and the microwave features of WS are due to pinning modes [5-9], which are small oscillations of the solid within the potential that pins it.

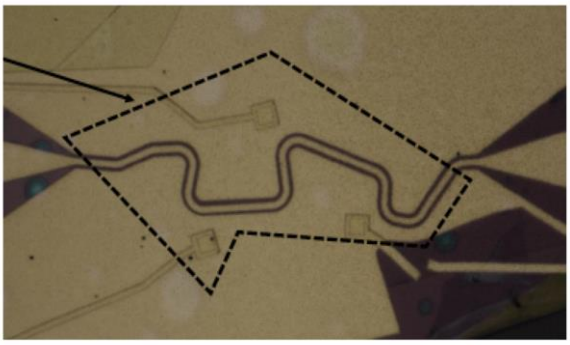

Figure 1 Photomicrograph of a coplanar waveguide transmission line on top of a BN graphene stack. The transmission line has driven center conductor and grounded side planes, and couples capacitively to the 2D electron system beneath it. Light areas are metal. The dotted line is the outline of the graphene flake.

Many other states of two-dimensional electron systems (2DES) in GaAs are electron solids and display pinning mode resonances. In GaAs pinning modes have been seen for "bubble" phases [8], with two carriers per lattice site, and for WS [9-12] within the integer quantum Hall effect, which exists in the presence of one or more filled Landau levels, and which can be composed of skyrmions [12]. There is recent evidence in graphene of IQHE WS including skyrmions [13] and bubble phases [14] from dc transport in graphene. Microwave study of such phases in graphene, including searching for pinning modes, is a major goal of this project.

Electron solids are not the sole object of our proposed microwave spectroscopic study of graphene. For bilayer graphene in its nominally eightfold degenerate lowest LL in high B, intra LL cyclotron modes have been predicted [15]. In such modes orbital quantum numbers couple to

microwave frequency radiation even at high B. This cyclotron resonance frequency is predicted to be controllable by gates, hence it is voltage controlled. Furthermore, for twisted bilayer graphene (TBLG) [16,17] superconducting states may be studied with microwaves, potentially to obtain superconducting fluid densities, or to look at the temperature dependence in conductivity, which may exhibit a peak [18] giving information on the type of superconductivity.

The project also includes continuation of microwave study of WS in semiconductor quantum wells (QWs), as a collaboration between Engel and M. Shayegan of Princeton University. This work focuses on the system of AlAs [19], which has ellipsoidal valleys oriented at right angles to each other, in-plane. This produces an anisotropic band mass with axes that can be changed *in situ* with strain, depending on which valley is populated. AlAs s offers a variety of apparent solid phases, including a low ν insulator, and also a likely bubble phase in the first Landau level [20]. Observation of pinning modes pinning modes in these phases would verify they are electron solids, and considerably narrow down the possibilities that have been advanced to explain them. Further, the *in situ* strain can be used to access the Ising type quantum Hall ferromagnetism near the zero-strain point, at which population is balanced between the valleys, and to study the effect of the ferromagnetism on electron solids, especially near ν=1 and at low ν.

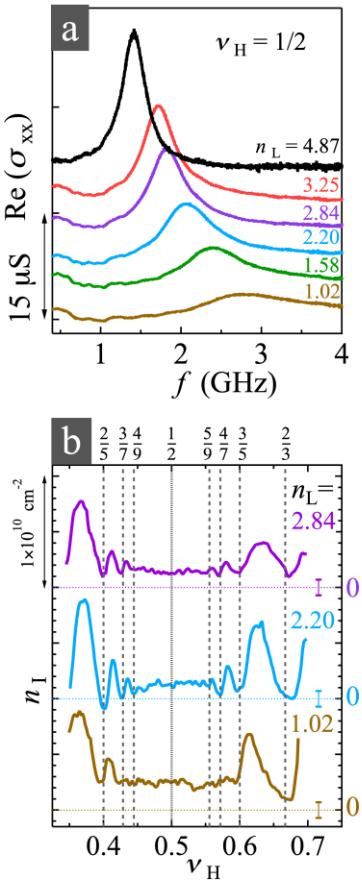

Figure 2 a) Spectra, Re(σ_{xx}) vs frequency, f, spectra for majority-layer filling ν_H=1/2 for several minority-layer densities, n_L, shown in units of 10^{10} cm^{-2}. Traces are vertically offset for clarity. b) Charge density of images in majority layer vs majority-layer filling factor, n_H, for several n_L. n_I=n_L-n_{dyn}, where n_{dyn} is calculated from the resonance integrated intensity.

Recent Progress

a) GaAs double QW with asymmetrically populated layers

Our recent paper [21] showed that in double quantum well samples whose carrier density is much larger in one layer than it is in the other, it is possible to have a composite fermion (CF) metal with filling ν =1/2 in the majority layer, but a WS state in the minority layer. We have studied the pinning resonance of the minority layer in detail for double wells set up in this way. The minority-layer pinning mode frequency, f_{pk}, dips when there are fractional quantum Hall states (FQHS) in the majority layer. We analyze the resonance to calculate the charge density, that produces the pinning mode in two ways, one (called n_{stat}) from f_{pk} alone , and one (called n_{dyn}) from the integrated absorption of the

resonance line. With n_L the minority layer density, the interpretation is that at each lattice site there is some positive local charge density superposed on the majority layer, forming essentially an image lattice, whose measured charge density, n_I, is shown in Figure 2b.

We find pinning modes signifying the presence of a WS both when the majority layer is a CF metal and when it is in a gapped FQHS. The difference between the pinning modes in the presence of these majority-layer states is remarkably slight. Even for a majority-layer CF metal, screening is closest to that expected from a dielectric substrate rather than that of a nearby metal gate, and we show such screening can be modeled by image charges of only around 10% of a WS site charge, as can be seen from Figure 2b. This result is unexpected because the CF metal and solid are so close together, only about one lattice constant of the solid away. If a normal metal were at that distance, the WS would be drastically different than one that is in the presence of a nearly inert, gapped FQHS at low temperature; instead we find the 2/3 FQHS and the CF metal have pinning mode frequencies different by at most ~10%. Our work [21] has been published in *Science Advances*.

b) Measurements of graphene

In collaboration with Scott Dietrich, now at Villanova, we have measured a number of graphene BN stacks using coplanar waveguide transmission lines like the one shown in Figure 1. While there have been issues with the smallness of the microwave signal variations and with resonances in the graphene mounting setup, we have found it is possible to resolve many FQHS [22] even at microwave frequency, as shown in Figure 3 for monolayer graphene.

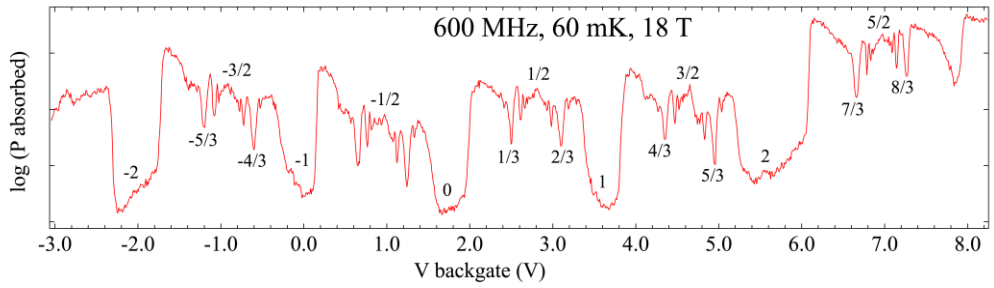

Figure 3. Preliminary data on monolayer graphene in BN: Absorbed power vs backgate voltage through a CPW containing single layer graphene, at 18 T, bath temperature approximately 50 mK. A graphite layer was used in the CPW to isolate metal from the BN on top of the graphene, reducing the level of disorder in the device. A graphite backgate was also used.

Future Plans

Future plans call for a postdoc, mutually supervised by Engel and Dean, to work in graphene, engaging in a search for pinning or propagating phonon modes in electron solid phases in high magnetic field, and also in the studies of the newly-discovered superconducting and insulating phases of TBLG. This postdoc will address the technical problems of broadband measurements in graphene including in high magnetic field. These measurements are much

more challenging than they are in GaAs owing to the small size of high quality graphene samples.

References

1. Y. E. Lozovik and V. I. Yudson, JETP Letters 22, 11 (1975).
2. P. K. Lam and S. M. Girvin. Phys. Rev. B **30** 473 (1984).
3. D. Levesque, J. J. Weis, and A. H. MacDonald, Phys. Rev. B **30,**1056 (1984).
4. H. Fukuyama and P. A. Lee, Phys. Rev. B, **18** 6245 (1978).
5. E. Y. Andrei et al., Phys. Rev. Lett. **60**, 2765 (1988).
6. F. I. B. Williams et al., Phys. Rev. Lett. **66,** 3285 (1991).
7. P. D. Ye et al., Phys. Rev. Lett. **89**, 176802 (2002).
8. R. M. Lewis et al., Phys. Rev. Lett. **89**, 136804 ((2002).
9. Yong Chen et al., Phys. Rev. Lett. **91**, 016801 (2003).
10. J. Jang, et al. Nature Physics **13**, 3470 (2016).
11. L. Tiemann, T. D. Rhone, N. Shibata, and K. Muraki, Nature Physics **10**, 648 (2014).
12. Han Zhu et al., Phys. Rev. Lett. **104**, 226801 (2010).
13. Haoxin Zhou et al. ArXiv: 1904.11485 (2019).
14. Shaowen Chen et al., Phys. Rev. Lett. **122**, 026802 (2019)
15. Y. Barlas et al., Phys. Rev. Lett. **101** 097601 (2008).
16. Y. Cao, et al., Nature **556**, 43 (2018).
17. M. Yankowitz et al., Science **363** 1059 (2019).
18. P. J. Hirschfeld, W. O. Putikka, and D. J. Scalapino, Phys. Rev. Lett., **71** 3705 (1993).
19. M. Shayegan et al., Physica Status Solidi (b) **243** 3629 (2006). [
20. Md. Shafayat Hossain et al.. Phys. Rev. Lett. **121**, 256601 (2018).
21. A. T. Hatke et al., Science Advances **5**, 2848 (2019).
22. X. Du et al., Nature **462**, 192 (2009).

Publications

- A. T. Hatke, Yang Liu, L. W. Engel, L. N. Pfeiffer, K. W. West, K.W. Baldwin, and M. Shayegan, "Microwave spectroscopic observation of a Wigner solid within the $\nu=1/2$ fractional quantum Hall effect", Phys. Rev. B **95**, 045417 (2017).
- H. Deng, L. W. Engel, L. N. Pfeiffer, K. W. West, K. W. Baldwin,and M. Shayegan, "Critical filling factor for the formation of a quantum Wigner crystal screened by a nearby layer", Phys. Rev. B **98**, 081111(R) (2018).
- A. T. Hatke, Y. Liu, L. W. Engel, L. N. Pfeiffer, K. W. West, K. W.Baldwin and M. Shayegan, "Wigner solids of wide quantum wells near Landau filling $\nu = 1$", Phys. Rev. B **98**, 195309 (2018).
- A. T. Hatke, H. Deng, Yang Liu, L. W. Engel, L. N. Pfeiffer, K. W.West, K. W. Baldwin and M. Shayegan, "Wigner solid pinning modes tuned by fractional quantum Hall states of a nearby layer", Science Advances **5**, 2848 (2019).
- H. Deng, L. N. Pfeiffer, K. W. West, K. W. Baldwin, L. W. Engel and M. Shayegan, "Probing the melting of a two-dimensional quantum Wigner crystal via its screening efficiency", Phys. Rev. Lett. **122**, 116601 (2019).

Program Title: Novel Synthesis of Quantum Epitaxial Heterostructures by Design

Principle Investigator: Chang-Beom Eom
Mailing Address: Room 2166 ECB, 1550 Engineering Drive, University of Wisconsin-Madison, Madison, WI 53706
E-mail: eom@engr.wisc.edu

Program Scope

Quantum materials such as unconventional superconductors, interfacial 2D electron gases (2DEGs), and multiferroics have been fertile ground for new discoveries. Our overarching goal is to develop novel synthesis routes that will create a new generation of epitaxial quantum thin film heterostructures for study of fundamental science and for development of new applications. These films can be of comparable or higher quality than available bulk single crystals, but more importantly film deposition conditions can be maintained far from equilibrium, so that metastable phases (nonexistent in nature) can be obtained by epitaxial stabilization of thin films. But these novel systems are usually sensitive to thin film heterostructure constraints, including interaction with the substrate, the difficulty in controlling point defects, and the challenge of forming atomically perfect interfaces.

Our hypothesis is that designing substrate interactions, controlling and identifying point defects, and working toward atomically perfect interfaces will reveal new phenomena and fundamental intrinsic properties of quantum materials arising from dimensionality, anisotropy, and electronic correlations. We have begun to implement some of these approaches, and have already demonstrated strain engineering of the Fe-based superconductor $BaFe_2As_2$, and made the first direct observation of the two-dimensional hole gas (2DHG) at an oxide interface. As a next step, we have developed a unique free-standing oxide stacked membrane fabrication technique to apply large dynamic strain, implemented a chemical pulsed laser deposition (CPLD), and begun to understand a route to new discoveries through control of highly perfect and defect free films and heterostructures. The **thrusts** of our proposed new work develop these advances, and expand into new materials systems:
(1) Novel CPLD Synthesis Route for oxide interface strain control, and oxide hole doping.
(2) Interface- and Strain engineered Fe-based superconductors

Recent Progress

Point Defect Control of Oxide-based Quantum Heterostructures

Point defects have played a major role in tuning the properties of materials over the last few decades. In quantum heterostructures based on complex oxides, however, the ability to control individual point defects continues to be challenging, due partially to non-stoichiometry issues in oxides. Here, we demonstrate the ability to tune point defects in oxide-based quantum heterostructure $LaAlO_3/SrTiO_3$ (LAO/STO), using a newly-developed chemical pulsed laser deposition (CPLD) growth technique. X-ray diffraction and Raman spectroscopy show that there is a wide process window of controlling the stoichiometry of STO without its structural change. Depth-resolved cathodoluminescence spectroscopy reveals that STO films grown at higher Titanium tetraisopropoxide (TTIP) flux has a higher ratio of antisite Ti/Sr vacancy with lower concentration of oxygen vacancies, which leads to higher electron mobility of two-dimensional electron gas at the interface of LAO/STO at low temperature, resulting in clear Shubnikov–de Haas oscillations. This result provides an essential part of the development of the next-generation complex oxide thin films and their heterostructures to investigate novel quantum phenomena.

We choose a LAO/STO heterostructure as a model system to demonstrate a point defect control of STO layer with a newly-developed chemical pulsed laser deposition (CPLD) growth technique. CPLD uses TTIP as a Ti source during laser ablation of a SrO target. The mechanism of CPLD growth for STO is related to that of hybrid MBE, where TTIP can only be adsorbed and

decomposed to form STO on SrO-terminated surface, whereas it would be desorbed on TiO_2-termiated one. Using this technique, we were able to precisely tune point defects in STO.

We have grown homoepitaxial 25 u.c. $SrTiO_3$ thin films on (001) $SrTiO_3$ single crystal substrates. Figure 1a shows out-of-plane θ-2θ XRD patterns of $SrTiO_3$ films vs. TTIP inlet pressure. Peaks other than those from the single crystal substrate likely arise from cation off-stoichiometry, as the $SrTiO_3$ lattice parameter is highly sensitive to stoichiometry. The results indicate a stoichiometric $SrTiO_3$ growth window over a wide range of TTIP gas inlet pressure where $SrTiO_3$ film peaks overlap those of the $SrTiO_3$ substrate.

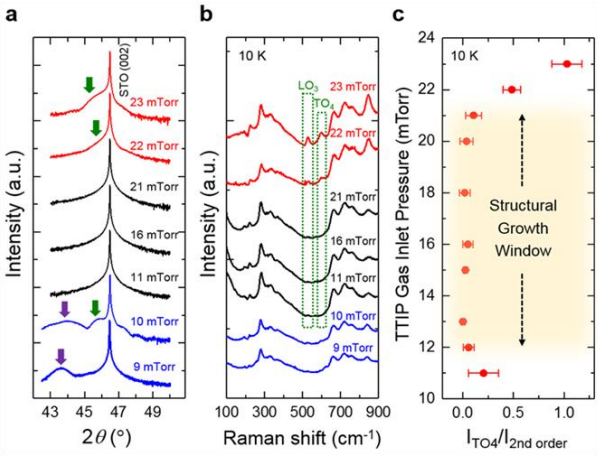

Figure 1. a, XRD patterns of $SrTiO_3$ films near (002) reflection. **b**, Raman spectra at 10 K. Data from Sr-rich, stoichiometric, Ti-rich $SrTiO_3$ (determined by XRD) films are represented in blue, black, red, respectively. **c**, Normalized TO_4 intensity in Raman spectra (**b**) as a function of TTIP inlet pressure. Yellow area is a stoichiometric growth window determined by Raman spectra at 10 K.

Variable-temperature Raman spectroscopy was performed to investigate signatures of inversion symmetry breaking due to point defects. $SrTiO_3$ is a cubic perovskite (space group Pm-3m) with 12 optical phonon modes. Because of odd modal symmetry with respect to the inversion center, 1st order Raman peaks are not present in the ideal $SrTiO_3$ structure. Point defects which break the inversion symmetry of $SrTiO_3$ can thus be detected by 1st order peaks in Raman spectra, *e.g.* the LO_3 or TO_4 modes. Raman spectrae of $SrTiO_3$ films measured at 10 K are shown in Fig. 2b. The intensity of the LO_3 and TO_4 peaks in Ti-rich $SrTiO_3$ films is higher outside the flux growth region of 11 to 21 mTorr, in agreement with the XRD stoichiometric growth process window.

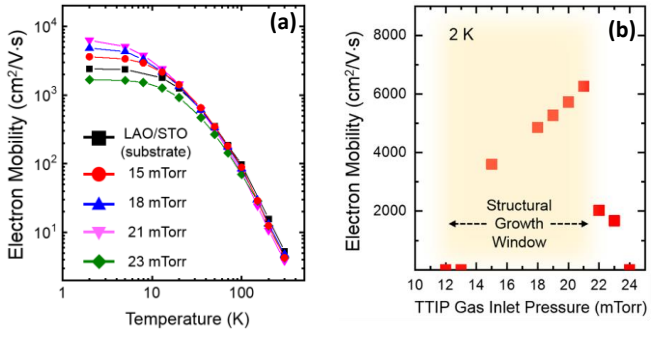

Fig. 2. (a) Electron mobility at the interface of $LaAlO_3/SrTiO_3$ substrate and $LaAlO_3$/MOPLD-grown $SrTiO_3/SrTiO_3$ substrate. TTIP gas inlet pressures of 15-23 mTorr were employed for growing $SrTiO_3$ films (b) $LaAlO_3$/ $SrTiO_3$ mobility at 2 K for various TTIP pressures.

Using the $SrTiO_3$ films as templates, epitaxial $LaAlO_3$ layers were grown on $SrTiO_3$ by conventional PLD to investigate the effect of point defects on 2DEG properties . The highest electron mobility of ~6,200 $cm^2/V{\cdot}s$ at 2 K (21 mTorr TTIP gas inlet pressure) (Fig. 2a) is substantially higher than the typical 2,400 $cm^2/V{\cdot}s$ without the TTIP process. The defect concentration inferred from the electron mobility monotonically decreases with increasing TTIP pressure within the structural growth window, as shown in Fig. 2b. We believe that point defect concentration varies within the structural growth window, resulting in the dramatic mobility enhancement.

We performed depth-resolved cathodoluminescence (DRCLS) to directly measure the point defects and their spatial distribution in STO films. Figure 3a shows DRCLS spectra of the LAO/STO samples with STO grown at 15 and 21 mTorr TTIP inlet pressure of. There is a clear difference in intensities between the 15 and 21 mTorr samples within the energy range from ~1.5

to ~3.4 eV when the spectra were normalized by the band gap (3.6 eV) energy. In Fig. 3b, relative point defect densities of Ti_{Sr}^{2+}, V_O^{2+} are plotted as a function of TTIP inlet pressures for the growth of STO films. As the TTIP inlet pressure is increased, the amount of Ti_{Sr}^{2+} is increased whereas the amount of V_O^{2+} is decreased. The electron mobility value measured at 2 K is again plotted in Fig. 3c for comparison. It is clear that lower concentration of V_O in STO is responsible for higher electron mobility at the interface of LAO/STO.

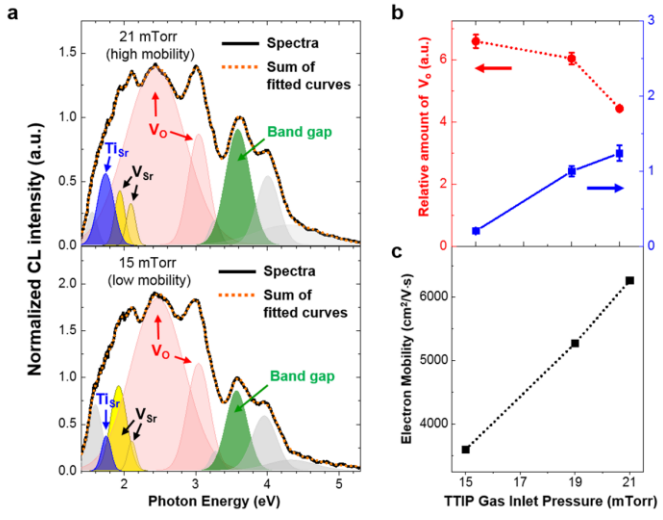

Fig. 3. (a) DRCLS Spectra of LAO 5 u.c./MOPLD-grown STO/ (001) STO substrate at 15, 21 mTorr TTIP gas inlet pressure. (b) Relative defect concentration of STO films as a function of TTIP gas inlet pressure during the growth, evaluated by summation of V_O^{2+} and V_O-R peak areas normalized with respect to the bandgap area near 3.6 eV. The relative ratio of Ti_{Sr}/V_{Sr} was evaluated by calculating the area of $Ti_{Sr}^{2+}/(V_{Sr}^{-}+V_{Sr}^{2-})$ (c) Electron mobility at 2 K in LAO/STO as a function of TTIP gas inlet pressure.

Since STO is one of the most widely used single crystals for growth of oxides, the point defect control by CPLD provides a way of making high quality STO for: (1) producing a template of STO on any substrate to integrate oxide in electronic (2) in principle because the quality of STO is superior that single crystals one can avoid buying expensive single crystals of STO, but rather producing them with CPLD.

Future Plans

(1) Novel CPLD Synthesis Route for advances in oxide films and heterostructures

We are continuing to develop a chemical pulsed laser deposition (CPLD) growth process that is showing dramatically lower concentration of point defects in complex oxide thin films. The higher quality epitaxial films and heterostructures described here remove several roadblocks that have limited the development of new science using quantum materials.

(2) Strain control of the $LaAlO_3/SrTiO_3$ interfacial two-dimensional electron gas

We will use our CPLD synthesis technique to understand the relation between point defect and electron gas properties, and to synthesize high-mobility electron gases to explore the effect of strain on fundamental aspects.

(3) Strain and Interface Engineered Unconventional Superconducting Quantum Heterostructures

Our new synthesis routes now allow exploration of strain- and electric-field dependent superconducting properties; such as (1) Giant strain control and investigation of the superconducting mechanism by lattice distortion and symmetry constraints in strain-engineered pnictides (2) the interaction of monolayer FeSe with strain- and interface engineered SrTiO3 films.

Publications (which acknowledge DOE support)

1. X. Yang, C. Vaswani, C. Sundahl, M. Mootz, L. Luo, J. H. Kang, I. E. Perakis, C. B. Eom & J. Wang, "Lightwave-driven gapless superconductivity and forbidden quantum beats by terahertz symmetry breaking" *Nature Photonics*, published on July 1, (2019)
2. X. Yang, X. Zhao, C. Vaswani, C. Sundahl, B. Song, Y. Yao, D. Cheng, Z. Liu, P. P. Orth, M. Mootz, J. H. Kang, I. E. Perakis, C.-Z. Wang, K.-M. Ho, C. B. Eom, and J. Wang,

"Ultrafast nonthermal terahertz electrodynamics and possible quantum energy transfer in the Nb_3Sn superconductor, *Phys. Rev. B* **99**, 094504 (2019)
3. Jiaxin Zhu, Jung-Woo Lee, Hyungwoo Lee, Lin Xie, Xiaoqing Pan, Roger A. De Souza, Chang-Beom Eom and Stephen S. Nonnenmann, "Probing vacancy behavior across complex oxide heterointerfaces" *Science Advances*, **5**, eaau8467 (2019)
4. D. Lee, B. Chung, Y. Shi, G. Y. Kim, N. Campbell, F. Xue, K. Song, S. Y. Choi, J. P. Podkaminer, T. H. Kim, P. J. Ryan, J. W. Kim, T. R. Paudel, J. H. Kang, D. A. Tenne, E. Y. Tsymbal, M. S. Rzchowski, L. Q. Chen, J. Lee, and C. B. Eom, "Isostructural metal-insulator transition" *Science* **362**, 1037 (2018).
5. J. H. Kang, L. Xie, Y. Wang, H. Lee, N. Campbell, J. Jiang, P. J. Ryan, D. J. Keavney, J. W. Lee, T. H. Kim, X. Pan, E. E. Hellstrom, D. C. Larbalestier, M. S. Rzchowski, Z. K. Liu, and C. B. Eom, "Control of Epitaxial $BaFe_2As_2$ Atomic Configurations with Substrate Surface Terminations" *Nano Letters* **18**, 6347 (2018).
6. T. Asaba, Z. Xiang, T.H. Kim, M. S. Rzchowski, C. B. Eom, and L. Li, "Unconventional Ferromagnetism in epitaxial (111) $LaNiO_3$" *Physical Review B* **98**, 121105 (2018).
7. T. Li, A. Lipatov, H. Lu, H. Lee, J. W. Lee, E. Torun, L. Wirtz, C. B. Eom, J. Íñiguez, A. Sinitskii, and A. Gruverman, "Optical Control of Polarization in Ferroelectric Heterostructures" *Nature Communications* **9**, 3344 (2018).
8. X. Yang, C. Vaswani, C. Sundahl, M. Mootz, P. Gagel, L. Luo, J. H. Kang, P. P. Orth, I. E. Perakis, C. B. Eom, and J. Wang, "Terahertz-light quantum tuning of a metastable emergent phase hidden by superconductivity" *Nature Materials* **17**, 586 (2018).
9. D. Lee, H. Wang, B. A. Noesges, T. J. Asel, J. Pan, J. W. Lee, Q. Yan, L. J. Brillson, X. Wu, and C. B. Eom, "Identification of a functional point defect in $SrTiO_3$" *Physical Review Materials* **2**, 060403(R) (2018).
10. D. T. Harris, N. Campbell, R. Uecker, M. Brützam, D. G. Schlom, A. Levchenko, M. S. Rzchowski, and C. B. Eom, "Superconductivity-localization interplay and fluctuation magnetoresistance in epitaxial $BaPb_{1-x}Bi_xO_3$ thin films" *Physical Review Materials* **2**, 041801(R) (2018).
11. Y. Y. Pai, H. Lee, J. W. Lee, A. Annadi, G. Cheng, S. Lu, M. Tomczyk, M. Huang, C. B. Eom, P. Irvin, and J. Levy, "One-Dimensional Nature of Superconductivity at the $LaAlO_3/SrTiO_3$ Interface" *Physical Review Letters* **120**, 147001 (2018).
12. H. Lee, N. Campbell, J. Lee, T. J. Asel, T. R. Paudel, H. Zhou, J. W. Lee, B. Noesges, J. Seo, B. Park, L. J. Brillson, S. H. Oh, E. Y. Tsymbal, M. S. Rzchowski, and C. B. Eom, "Direct observation of a two-dimensional hole gas at oxide interfaces" *Nature Materials* **17**, 231 (2018).
13. G. Cheng, A. Annadi, S. Lu, H. Lee, J. W. Lee, M. Huang, C. B. Eom, P. Irvin, and J. Levy, "Shubnikov–de Haas–like Quantum Oscillations in Artificial One-Dimensional $LaAlO_3/SrTiO_3$ Electron Channels" *Physical Review Letters* **120**, 076801 (2018).
14. H. Lu, D. Lee, K. Klyukin , L. Tao, B. Wang, H. Lee, J. Lee, T. R. Paudel, L. Q. Chen, E. Y. Tsymbal, V. Alexandrov, C. B. Eom, and A. Gruverman, "Tunneling Hot Spots in Ferroelectric $SrTiO_3$" *Nano Letters* **18**, 491 (2018).
15. S. Ryu, H. Zhou, T. R. Paudel, J. Irwin, J. P. Podkaminer, C. W. Bark, D. Lee, T. H. Kim, D. D. Fong, M. S. Rzchowski, E. Y. Tsymbal, and C. B. Eom, "In-situ probing of coupled atomic restructuring and metallicity of oxide heterointerfaces induced by polar adsorbates" *Applied Physics Letters* **111**, 141604 (2017).
16. M. Tomczyk, R. Zhou, H. Lee, J. W. Lee, G. Cheng, M. Huang, P. Irvin, C. B. Eom, and J. Levy, "Electrostatically tuned dimensional crossover in $LaAlO_3/SrTiO_3$ heterostructures" *APL Materials* **5**, 106107 (2017).

Program Title: Correlated Materials - Synthesis and Physical Properties

Principle Investigators: I. R. Fisher, T. H. Geballe, S. A. Hartnoll, A. Kapitulnik, S. A. Kivelson, and K. A. Moler
Institution: Geballe Laboratory for Advanced Materials, and Departments of Applied Physics and Physics, Stanford University, and the Stanford Institute for Materials & Energy Science, SLAC National Accelerator Laboratory.
Emails: irfisher@stanford.edu, geballe@stanford.edu, hartnoll@stanford.edu, aharonk@stanford.edu, kivelson@stanford.edu, kmoler@stanford.edu

Program Scope

An enduring aim of our FWP has been to discover and understand the nature, causes and consequences of emergent behavior in strongly correlated quantum materials, especially in relation to the occurrence of superconductivity. We do this by incorporating synthesis, measurement and theory to coherently address 'big' questions at the heart of these issues. We use cutting edge, often unique, experimental probes to uncover novel forms of electronic order in a variety of complex materials. Our theoretical work provides a framework to understand the rich variety of possible ordered states, and guides our ongoing measurements and synthesis efforts. Broad areas of interest during the last few years have included quantum phase transitions; electronic nematic order in strongly correlated materials; the inter-relation of charge order, quenched disorder, and superconductivity; and anomalous transport properties in strongly correlated materials.

Recent Progress

1. Electronic nematicity

During FY19, building on our pioneering work (both theoretical and experimental) using antisymmetric strain as a longitudinal field for nematic order [2], we went on to demonstrate that *orthogonal* antisymmetric strain (i.e. B_{1g} symmetry, relative to the B_{2g} symmetry nematic order in the Fe-pnictides) is an effective tuning parameter for electronic nematic order [18]. It rapidly suppresses the critical temperature of the nematic phase transition in Fe-based superconductors, providing a completely new means to access any associated quantum phase transition. These combined and collaborative theoretical [3] and experimental [18] insights open a wide new vista for exciting experiments probing the effects of nematic fluctuations proximate to a nematic quantum critical point.

During FY19 we also published three papers describing completely new experimental approaches to the measurement of relevant physical properties for electronic nematic systems. Each one of these new techniques actually has a much wider range of applicability, which we are already beginning to build upon in our ongoing studies of other quantum materials. The first provides access to a completely new physical property, the *dynamic* nematic susceptibility via AC elastoresistivity measurements [14]. The second, describes an extension to the Fisher-Langer relation by considering strain-derivatives of the internal energy [20]. These ideas were then

extended in a third publication focusing specifically on the AC elastocaloric effect [23], opening another wide new vista for exploring phase transitions (and QPTs) in quantum materials.

In addition to the above, we also explored vortex pinning as a window on in-plane anisotropy. Strong vortex pinning in Fe-based materials like FeSe could be useful for technological applications and could provide clues about the coexistence of superconductivity and nematicity. To characterize the pinning of individual, isolated vortices, we simultaneously applied a local magnetic field and imaged the vortex motion with scanning SQUID susceptibility. We found that the pinning is highly anisotropic: the vortices move easily along directions that are parallel to the orientations of twin domain walls and pin strongly in a perpendicular direction [22].

2. Inter-relation of charge order, quenched disorder, and superconductivity

We established a phase diagram for a model system exhibiting unidirectional incommensurate CDW order on a nominally tetragonal lattice, for which disorder can be introduced via intercalation. STM measurements on a spectrum of crystals revealed the progressive proliferation of topological defects in the CDW state induced by this intercalation, and evidence for a nematic Bragg glass phase [24]. This work potentially connects to theoretical notions of fragile superconductivity for systems with competing incommensurate density wave order [21].

Related theoretical work addressed a generalization of Anderson's theorem for disordered superconductors [15], and bounds on the critical temperature for e-ph mediated systems [4,16].

3. Imaging emergent spatially modulated textures

A major component of our research involves application of cutting edge tools to map spatial variation of relevant physical properties. For $LaAlO_3/SrTiO_3$ we showed that the transition temperature of the superconductivity at those interfaces is modulated by the $SrTiO_3$ structure domains [8]. We also found that both thin films and bulk single crystals of $La_{2-x}Ba_xCuO_4$ have micron-scale stripes of spatially modified superfluid density [9]. Finally, we mapped the superfluid density and its dependence on strain and temperature in Sr_2RuO_4 [12], finding that the cusp that would be expected for a multi-component order parameter is absent.

In a separate study, using a home-built mini-MBE system that is integrated with our STM, we deposited single layer bismuth on $NbSe_2$ [5]. The Bi layer grew conforming to the underlying substrate's lattice, thus was subjected to strain, which resulted in a rippled structure.

4. New insight into the Superconductor-Insulator Transition

Hall effect studies in thin superconducting films revealed new insight into the superconductor to insulator quantum phase transition (SIQPT), and into the anomalous metallic phase for weaker disordered films. For strong disorder we find a true SIQPT exhibiting self-duality at the transition and a Hall-charge-insulator/Hall-vortex-insulator phases on the two sides of the transition. For weak disorder, an anomalous metallic phase with (almost precise) particle-hole symmetry is revealed above the true superconducting phase [1]. More generally, we summarized the state of the field and our perspectives in a Colloquium article [19].

Future Plans

During FY20 we will continue and expand our collaborative investigations of…

- electronic nematicity, in particular with relation to nematic quantum phase transitions in Fe-based superconductors and other related materials;
- the inter-relation of charge order, quenched disorder, and superconductivity, in particular in the context of cuprate HTSCs and disordered 'model' CDW systems;
- anomalous charge transport and thermal transport in strongly correlated materials, in particular in the presence of highly anharmonic phonons and short range CDW correlations.

Publications

We list below a selection of publications resulting from DOE sponsored research from the last two years (FY18 and FY19)

1) *Superconductor to weak-insulator transitions in disordered Tantalum Nitride films*, Nicholas P. Breznay, Mihir Tendulkar, Li Zhang, Sang-Chul Lee, Aharon Kapitulnik, Phys. Rev. B **96**, 134522 (2017).
2) *Critical divergence of the symmetric (A_{1g}) nonlinear elastoresistance near the nematic transition in an iron-based superconductor*, J. C. Palmstrom, A. T. Hristov, S. A. Kivelson, J.-H. Chu, and I. R. Fisher, Phys. Rev. B **96**, 205133 (2017).
3) *Transverse fields to tune an Ising-nematic quantum phase transition*, Akash V. Maharaj, Elliott W. Rosenberg, Alexander T. Hristov, Erez Berg, Rafael M. Fernandes, Ian R. Fisher, and Steven A. Kivelson, PNAS vol. **114** no. 51, 13430–13434 (2017).
4) *Breakdown of Migdal-Eliashberg theory; a determinant quantum Monte Carlo study*, I. Esterlis, B. Nosarzewski, E. W. Huang, B. Moritz, T. P. Devereaux, D. J. Scalapino, and S. A. Kivelson, Phys. Rev. B **97**, 140501 (2018).
5) *Bursting at the seams: Rippled monolayer bismuth on $NbSe_2$*, Alan Fang, Carolina Adamo, Shuang Jia, Robert J. Cava, Shu-Chun Wu, Claudia Felser, and Aharon Kapitulnik, Science Advances **4**, eaaq0330 (2018).
6) *Polar Kerr effect from Time-Reversal Summetry Breaking of the Heavy Fermion Superconductor $PrOs_4Sb_{12}$* E. M. Levenson-Falk, E. R. Schemm, Y. Aoki, M. B. Maple, and A. Kapitulnik, Phys. Rev. Lett. **120**, 187004 (2018).
7) *Pair density waves in superconducting vortex halos*, Y. Wang, S. D. Edkins, M. H. Hamidian, J. C. S. Davis, E. Fradkin, and S. A. Kivelson, Phys. Rev. B **97**, 174510 (2018).
8) *Modulation of superconducting transition temperature in $LaAlO_3/SrTiO_3$ by $SrTiO_3$ structural domains*, H. Noad, P. Wittlich, J. Mannhart, K.A. Moler, Journal of Superconductivity and Novel Magnetism, https://doi.org/10.1007/s10948-018-4730-8 – Published online 19 June 2018
9) *Spatially modulated susceptibility in thin film $La_{2-x}Ba_xCuO_4$*, Samantha I. Davis, Rahim R. Ullah, Carolina Adamo, Christopher A. Watson, John R. Kirtley, Malcolm R. Beasley, Steven A. Kivelson, and Kathryn A. Moler, Phys. Rev. B **98**, 014506 (2018).

10) *Temperature-induced inversion of the spin-photogalvanic effect in WTe_2 and $MoTe_2$,* Sejoon Lim, Catherine R. Rajamathi, Vicky Süß, Claudia Felser, Aharon Kapitulnik, Phys. Rev. B **98**, 121301(R) (2018).

11) *Two-stage proximity induced gap-opening in topological insulator - insulating ferromagnet $(Bi_xSb_{1-x})_2Te_3$ - EuS bilayers*, Qi I. Yang and Aharon Kapitulnik, Phys. Rev. B **98**, 081403 (R) (2018).

12) *Micron-scale measurements of low anisotropic strain response of local T_c in Sr_2RuO_4,* Christopher A. Watson, Alexandra S. Gibbs, Andrew P. Mackenzie, Clifford W. Hicks, and Kathryn A. Moler, Phys. Rev. B **98**, 094521 (2018).

13) *Phases of a phenomenological model of twisted bilayere graphene*, J.F. Dodaro, S. A. Kivelson, Y. Schattner, X-Q Sun, and C. Wang, Phys. Rev. B **98**, 75154 (2018).

14) *Measurement of elastoresistivity at finite frequency by amplitude demodulation*, Alexander T. Hristov, Johanna C. Palmstrom, Joshua A. W. Straquadine, Tyler A. Merz, Harold Y. Hwang, and Ian R. Fisher, Review of Scientific Instruments **89**, 103901 (2018).

15) *Superconductivity in the doped t-J model: Results for four-leg cylinders*, H-C. Jiang, Z-Y. Weng, and S. A. Kivelson, Phys. Rev. B 98, 140505 (2018).

16) *Generalization of Anderson's theorem for disordered superconductors*, J. F. Dodaro and S. A. Kivelson, Phys. Rev. B **98**, 174503 (2018).

17) *A bound on the superconducting trqansition temperature*, I. Esterlis, S. A. Kivelson, and D. J. Scalapino, NPJ Quantum Materials 3, 59 (2018).

18) *Symmetric and antisymmetric strain as continuous tuning parameters for electronic nematic order*, M. S. Ikeda, T. Worasaran, J. C. Palmstrom, J. A. W. Straquadine, P. Walmsley, and I. R. Fisher, Phys. Rev. B **98**, 245133 (2018).

19) *Colloquium: Anomalous metals: Failed Superconductors,* A. Kapitulnik, S. A. Kivelson, and B. Spivak, Rev. Mod. Phys. **91**, 11002 (2019).

20) *Elastoresistive and elastocaloric anomalies at magnetic and electronic-nematic critical points*, Alexander T. Hristov, Matthias S. Ikeda, Johanna C. Palmstrom, Philip Walmsley, and Ian R. Fisher, Phys. Rev. B **99**, 100101(R) (2019). (Editors' Suggestion)

21) *Fragile superconductivity in the presence of weakly disordered charge density waves*, Y. Yue and S. A. Kivelson, Phys. Rev. B 99, 144513 (2019).

22) *Imaging anisotropic vortex dynamics in FeSe*, Irene P. Zhang, Johanna C. Palmstrom, Hilary Noad, Logan Bishop-Van Horn, Yusuke Iguchi, Zheng Cui, Eli Mueller, John R. Kirtley, Ian R. Fisher, and Kathryn A. Moler, Phys. Rev. B **100**, 024514 (2019).

23) *AC Elastocaloric effect as a probe for thermodynamic signatures of continuous phase transitions*, Matthias S. Ikeda, Joshua A.W. Straquadine, Alexander T. Hristov, Thanapat Worasaran, Johanna C. Palmstrom, Matthew Sorensen, Philip Walmsley, Ian R. Fisher, Accepted for publication in Rev. Sci. Instrum., arXiv:1903.00791

24) *Disorder Induced Suppression of CDW Long Range Order: STM Study of Pd-intercalated $ErTe_3$,* Alan Fang, Joshua A. W. Straquadine, Ian R. Fisher, Steven A. Kivelson, and Aharon Kapitulnik, arXiv:1901.03471

Digital Synthesis: A Pathway to Create and Control Novel States of Condensed Matter

Anand Bhattacharya, Dillon D. Fong
Materials Science Division, Argonne National Laboratory

Program Scope: Digital Synthesis is a strategy to create materials in an atomic layer-by-layer fashion to tailor new properties. Using this approach, we can control local dipole electrostatic fields *within* a unit cell, create cation-ordered analogs of known materials, and control charge transfer and band lineup in heterostructures between different materials. In short, our program seeks to create new materials out of known ingredients to yield novel properties and to manipulate these properties with external fields and currents.

Recent Progress: Our program has advanced fundamental understanding in the areas of oxide thin film synthesis and defect interactions at surfaces and heterointerfaces. We describe highlights in these areas.

In situ synchrotron X-ray studies of growth: Molecular beam epitaxy (MBE) is a synthesis technique that permits the control of materials growth one atomic plane at a time [1]. Achieving this level of precision requires an *in situ* means of monitoring the growth process, which is normally accomplished with reflection high energy electron diffraction. A more powerful means of monitoring synthesis is with the use of synchrotron X-rays, which not only allows monitoring of the growth mode, but also provides atomic-scale snapshots of the processes taking place during deposition. In Ref. [2], we describe the heteroepitaxial growth on $LaTiO_3$ on $SrTiO_3$ (001), starting with either a LaO or TiO_2 monolayer (**Figure 1**). We find that the behavior cannot be described by the layer-by-layer growth mode but a more complex mechanism due to the TiO_2 double layer at the surface of $SrTiO_3$ (001).

Defect control in heterostructures: Defects in complex oxides can strongly impact behavior, and improved control over them can be a powerful means of tailoring properties. We discovered that one can carefully manipulate oxygen vacancies with an electric field to form or break electrical pathways within an oxide, thereby providing a powerful means of achieving memristive functionality [3]. We also have written reviews on this topic in Refs. [4-6].

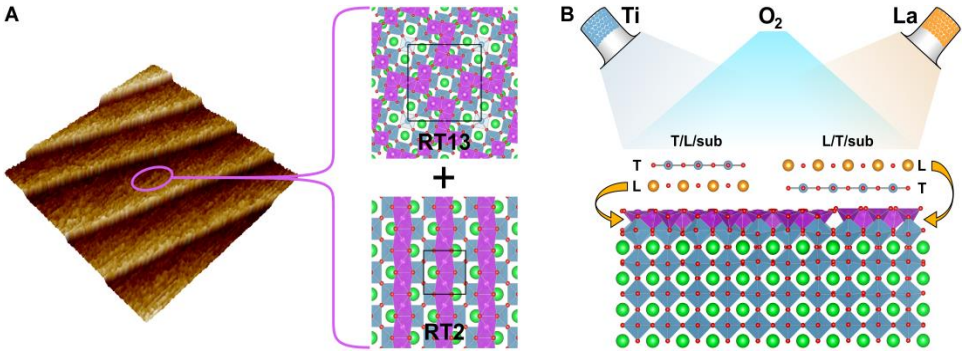

Figure 1 (A) Bare $SrTiO_3$ (001) surface after following the standard etch-and-anneal procedure showing 0.4 nm steps. (B) Schematic of $LaTiO_3$ growth by oxide MBE following either the TiO_2/LaO (T/L) or LaO/TiO_2 (L/T) growth sequence at 700°C in a background of 1×10^{-7} torr O_2 [2].

Future Plans

The goal of future work is to determine how to effectively control both the atomic and electronic structure of materials *during*

synthesis as well as to understand defect dynamics in these systems. Below, we describe two areas of interest.

In situ atomic and electronic structure: Much of our prior *in situ* results are based on surface X-ray diffraction (SXRD) and are structural in nature: the equipment necessary for X-ray scattering differs greatly from that required for electronic structure measurements such as angle-resolved photoemission spectroscopy (ARPES). If one wishes to correlate atomic structure with electronic structure, the samples are often exposed to air, leading to adsorbed contaminants and altered structural and electronic depth profiles. Exploiting both a new vacuum transfer system for the MBE chamber and a new hard X-ray photoelectron spectroscopy system (HAXPES) mounted directly on a pulsed laser deposition (PLD) system, we are uniquely positioned to make significant headway in the field of *in situ* synthesis studies.

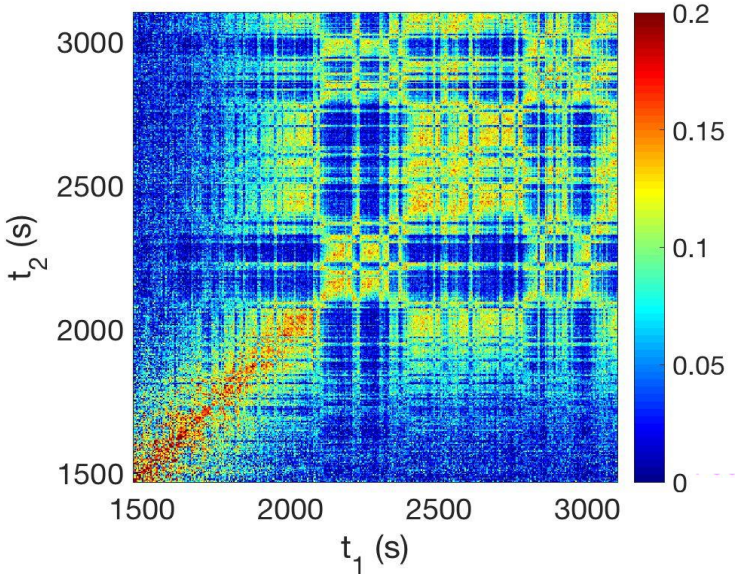

Figure 2 Two-time correlation map measured at the $SrCoO_x$ 00½ reflection at 360°C. The gas environment was switched from oxygen to nitrogen at 1600 s.

Defect dynamics: After the APS upgrade, the X-rays will be more coherent in nature – i.e., the incoming X-rays will be more like plane waves, such that the phase can be recovered after the scattering process. This will allow a wealth of remarkable possibilities for science, including improved coherent diffraction imaging (CDI) and greatly improved X-ray photon correlation spectroscopy (XPCS). XPCS is particularly conducive to *in situ* studies, as it permits the investigation of dynamics during the growth process: that is, one will be able to measure the *time fluctuations* of species as they deposit, migrate, and incorporate into the material. We recently conducted XPCS measurements of oxygen vacancy dynamics in the $SrCoO_x$ system, grown on $(LaAlO_3)_{0.3}(Sr_2AlTaO_6)_{0.7}$ (001) (**Figure 2**). This unique measurement shows how defects (and consequently the SrCoOx phase) fluctuate in controlled temperature and chemical environments. After the upgrade, we will be able to conduct such studies *during* synthesis, providing a one-of-a-kind probe for understanding how atoms incorporate into the surface.

References

1. D. G. Schlom, *APL Materials* **3,** 062403 (2015).
2. S. Cook et al., *Sci. Adv.* **5,** eaav0764 (2019).
3. H. Liu et al., *ACS Nano* **12,** 4938 (2018).
4. S. V. Kalinin et al., *Rep. Prog. Phys.* **81,** 036502 (2018).
5. T. K. Andersen et al., *Surf. Sci. Rep*. **73,** 213 (2018).

6. H.-T. Zhang et al., *Adv. Phys. X* **4,** 1523686 (2018).

FWP 58920 Publications (Since 03/2017)

1. I. C. Tung, G. Luo, J. H. Lee, S. H. Chang, J. Moyer, H. Hong, M. J. Bedzyk, H. Zhou, D. Morgan, D. D. Fong, and J. W. Freeland, *Phys. Rev. Mater*. **1,** 053404 (2017).
2. J. Kim, B. Hou, C. Park, C. B. Bahn, J. Hoffman, J. Black, A. Bhattacharya, N. Balke, H. Hong, J. H. Kim, and S. Hong, *Scientific Reports 7*, 44805 (2017).
3. D. Hong , C. Liu , J. E. Pearson , and A. Bhattacharya, *App. Phys. Lett.* **111**, 232408 (2017). (Featured Article)
4. S. M. Wu, A. Luican-Mayer, and A. Bhattacharya, *App. Phys. Lett.* **111**, 23109 (2017).
5. S. V. Kalinin, Y. Kim, D. D. Fong, and A. Morozovska, *Rep. Prog. Phys*. **81,** 036502 (2018).
6. T. K. Andersen, S. Y. Cook, E. Benda, H. Hong, L. D. Marks, and D. D. Fong, *Rev. Sci. Instrum.* **89,** 033905 (2018).
7. T. K. Andersen, D. D. Fong, and L. D. Marks, *Surf. Sci. Rep.* **73,** 213 (2018).
8. H. Liu, Y. Dong, M. J. Cherukara, K. Sasikumar, B. Narayanan, Z. Cai, B. Lai, L. Stan, S. Hong, M. K. Y. Chan, S. K. R. S. Sankaranarayanan, H. Zhou, and D. D. Fong, *ACS Nano* **12,** 4938 (2018).
9. T. K. Andersen, S. Wang, M. R. Castell, D. D. Fong, and L. D. Marks, *Surf. Sci.* **675,** 36 (2018).
10. C. Liu, S. M. Wu, J. E. Pearson, J.S. Jiang, N. d'Ambrumenil, and A. Bhattacharya, *Phys. Rev.* B (R) **98**, 060415 (2018). (Editor's Suggestion)
11. Y. Zhu, J. D. Hoffman, C. E. Rowland, H. Park, D. A. Walko, J. W. Freeland, P. J. Ryan, R. D. Schaller, A. Bhattacharya, and H. Wen. *Nature Communications* **9**, 1799 (2018).
12. J. D. Hoffman, S. M. Wu, B. J. Kirby, and A. Bhattacharya, *Phys. Rev. Applied* **9**, 044041 (2018).
13. B.H Savitzky, I. El Baggari, C. B Clement, E. Waite, B. H. Goodge, D. J. Baek, J. P. Sheckelton, C. Pasco, H. Nair, N. J. Schreiber, J. D. Hoffman, A. S. Admasu, J. Kim, S.-W. Cheong, A. Bhattacharya, D. G. Schlom, T. M. McQueen, R. Hovden, and L. F. Kourkoutis, *Ultramicroscopy* **191**, 56 (2018).
14. H. Chang, N. Shirato, Y. Zhang, J. Hoffman, D. Rosenmann, J. W. Freeland, A. Bhattacharya, V. Rose, and S.-W. Hla, *Appl. Phys. Lett.* **113**, 061602 (2018).
15. G. Fabbris, N. Jaouen, D. Meyers, J. Feng, J. D. Hoffman, R. Sutarto, S. G. Chiuzbăian, A. Bhattacharya, and M. P. M. Dean, *Phys. Rev.* B **98**, 180401(R) (2018). (Editors' Suggestion)
16. H. Liu, Y. Dong, D. Xu, E. A. Karapetrova, S. Lee, L. Stan, P. Zapol, H. Zhou, and D. D. Fong, *Adv. Mater.* **30,** 1804775 (2018).
17. H.-T. Zhang, Z. Zhang, H. Zhou, H. Tanaka, D. D. Fong, and S. Ramanathan, *Adv. Phys. X* **4,** 1523686 (2018).

18. T. Wang, A. Prakash, Y. Dong, T. Truttmann, A. Bucsek, R. James, D. D. Fong, J.-W. Kim, P. J. Ryan, H. Zhou, T. Birol, and B. Jalan, *ACS Appl. Mater. Inter.* **10,** 43802 (2018).

19. S. Y. Cook, M. T. Dylla, R. A. Rosenberg, Z. R. Mansley, G. Jeffrey Snyder, L. D. Marks, and D. D. Fong, *Adv. Elect. Mater.* **5,** 1800460 (2019).

20. C. Liu, F. Wrobel, J. D. Hoffman, D. Hong, J. E. Pearson, E. Benckiser, and A. Bhattacharya, *Phys. Rev.* B (R) **99**, 041114 (2019).

21. A. Lopez-Bezanilla, L. F. Arsenault, A. Bhattacharya, P. B. Littlewood, and A. J. Millis, *Phys. Rev.* B **99**, 035133 (2019).

22. S. Y. Cook, K. Letchworth-Weaver, I.-C. Tung, T. K. Andersen, H. Hong, L. D. Marks, and D. D. Fong, *Science Advances* **5,** eaav0764 (2019).

23. Y. Zhu, J. G. Connell, S. Tapavcevic, P. Zapol, A. Sharafi, N. Taylor, J. Sakamoto, L. A. Curtiss, D. D. Fong, J. W Freeland, and N. M. Markovic, *Adv. Energy Mater.* **9,** 1803440 (2019).

24. Y. Chen, J. A. Tilka, Y. Ahn, J. Park, A. Pateras, T. Zhou, D. E. Savage, I. McNulty, M. V. Holt, D. M. Paskiewicz, D. D. Fong, T. F. Kuech, and P. G. Evans, *J. Phys. Chem. C* **123,** 7447 (2019).

25. H. Xu, Z. Zhang, Y. Dong, C. Zeng, D. D. Fong, and Z. Luo, *Appl. Phys. Lett.* **114,** 242901 (2019).

26. D. Hong, C. Liu, J. E. Pearson, A. Hoffmann, D. D. Fong, and A. Bhattacharya, *Appl. Phys. Lett.* **114,** 242403 (2019).

27. Y. Dong, Z. Ma, Z. Luo, H. Zhou, D. D. Fong, W. Wu, and C. Gao, *Adv Mater Interfaces* 1900644 (2019).

28. S. H. Chang, S. K. Kim, Y.-M. Kim, Y. Dong, C. M. Folkman, D. W. Jeong, W. S. Choi, A. Y. Borisevich, J. A. Eastman, A. Bhattacharya, and D. D. Fong: *APL Mater.* **7,** 071117 (2019).

29. Y. Hu, G. Zhong, Y.-S. Guan, J. N. Armstrong, C. Li, C. Liu, A. N'Diaye, A. Bhattacharya, and S. Ren, *Small* **15**, 1900299 (2019).

30. *"In operando studies of CO oxidation on epitaxial $SrCoO_{2.5+\delta}$ thin films"*, C. M. Folkman, S. H. Chang, H. Jeen, E. Perret, P. M. Baldo, Carol Thompson, J. A. Eastman, H. N. Lee, and D. D. Fong (to appear in *APL Materials*)

31. *"Experimental setup combining in situ hard X-ray photoelectron spectroscopy and real-time surface X-ray diffraction for characterizing atomic and electronic structure evolution during complex oxide heterostructure growth"*, G. Eres, C. M. Rouleau, Q. Lu, Z. Zhang, E. Benda, H. N. Lee, J. Z. Tischler, and D. D. Fong (to appear in *Review of Scientific Instruments*)

Creating and Interfacing Designer Chemical Qubits

Sponsoring Institution: Northwestern University
Principal Investigator: Danna Freedman | Northwestern University
Co-Investigators: William Dichtel | Northwestern University; Mark Hersam, | Northwestern University; Jeffrey Long | University of California, Berkeley; James Rondinelli | Northwestern University; Michael Wasielewski | Northwestern University

i) Program Scope

A. Summary of Approach. Creating and understanding new materials is essential for the realization of quantum information science (QIS). Central to this goal, is creating qubits with designer attributes, building upon the previous successes within this field by bringing spatial control to qubit design. To that end, the goal of this project is the chemical synthesis of atomically-precise arrays of qubits integrated with a 2D substrate primed for system integration. Our approach is centered on imbuing qubits with spatial precision by designing bottom-up arrays of qubits using an interdisciplinary materials theory and synthetic chemistry approach within an iterative paradigm based on active exchange of data and materials among team members with synthesis, computation, and qubit characterization. Specifically, we use chemical synthesis to create metal-organic (**Freedman, Long**) and organic radical-based (**Dichtel, Wasielewski**) arrays of qubits that are interfaced with surfaces of functional 2D materials (**Hersam**) with compositions, geometries, dimensionalities by electron-structure theory (**Rondinelli**).

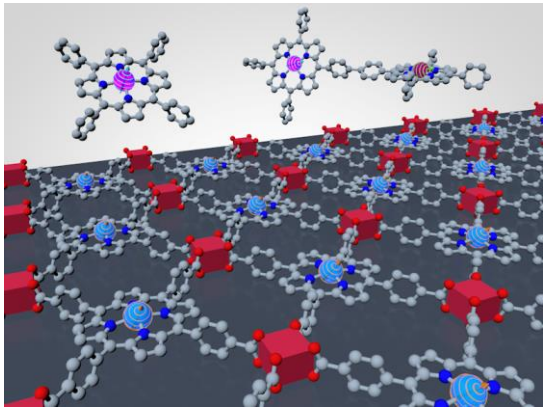

Figure 1.Graphical depiction of the central goals of the project.

B. Enumeration of Scientific Objectives. The transformative ability of chemistry to impact quantum information science lies within the intertwined combination of atomic scale control and the ability to produce arrays of thousands of qubits from a single synthetic process (**Figure 1**). Advances in synthetic chemistry and control over molecular-based materials will be harnessed to establish new framework-based qubit platforms. Our team combines expertise in synthesis, measurement, and theory to create a rapid measurement feedback cycle for evaluation of materials for quantum information science. Specifically, we are actively pursuing the following objectives:

Objective 1: Create a network of qubits using COF and MOF approaches

Objective 2: Generate fundamental insight into quantum properties of networks through molecular model studies

Objective 3: Interface qubits with surfaces

C. Methods. Toward achieving our ambitious goal, we are actively addressing numerous fundamental questions, each relying on the intersection of synthesis and measurement. Specifically, we rationally design qubit monomers and arrays, both to understand the relationship between single qubits and arrays of qubits and to understand surface–qubit interactions. The team is comprised of experts in synthetic chemistry, materials physics, magnetism and optical spectroscopy, and we leverage and unite prior advances in the development and deployment of novel spin and electronic systems to the qubit design challenge. PI **Freedman** is a synthetic

inorganic chemist, who pursues the synthesis and design of new coordination compounds, with a focus on model species; **Long** is a framework chemist with expertise in 2D arrays, who develops metal–organic frameworks (MOFs); **Dichtel** is a polymer materials chemist with expertise in 2D arrays, who develops covalent–organic frameworks (COFs); **Wasielewski** is a physical chemist, who provides spectroscopic expertise and qubit assessment; **Hersam** is a materials scientist, who interfaces the molecules and materials with substrate surfaces; and **Rondinelli** is a materials physicist, who examines the electronic structure and spin textures of the qubit design parameters.

ii) Recent Progress

Objective 1: Create a defect-free array of qubits

To create an array of qubits we are harnessing organic and coordination chemical synthesis in complementary directions, using metal-organic framework based systems and with organic radicals. Within the metal-organic frameworks, the **Harris** group discovered the first 2D zirconium-based metal-organic framework with a hexagonal lattice topology. This terphenyl dicarboxylate-based linker has two methoxy groups on the central phenyl ring, which can be potentially demethylated to form hydroquinone. These candidate radicals are spatially arranged in a kagomé topology, with a distance of 2.0 nm between the nearest neighbors. The 2D nature of this array makes it easier to interface this compound with a surface. Additional studies will focus on the impact of dimensionality on coherence.

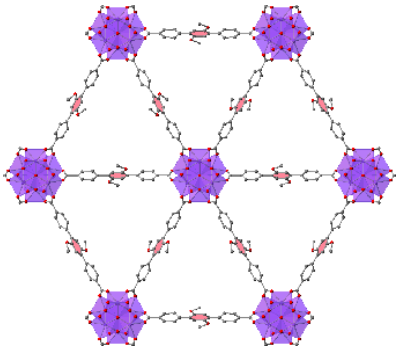

Figure 2. Structure of the 2D kagome metal organic framework with potential radicals every 2 nm

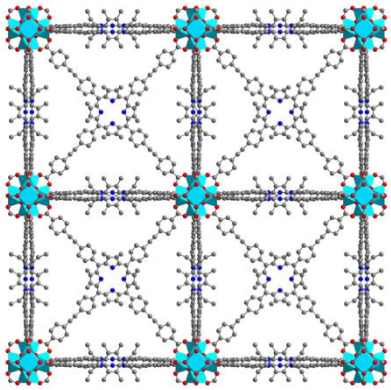

Figure 3. Framework featuring candidate qubits every 19.56 Å

Using a metal based approach, **Freedman** developed a framework housing metal based qubits every 19.56 Å (Figure 2). This system builds on our previous results demonstrating the impact of spin-spin interactions in a MOF with qubits every 13.5 Å. This is a fantastic new platform to probe the impact of coupling of the metal based orbital to the framework and spin-spin interactions. Within the covalent framework direction, we designed a more reactive pyridine-containing amine-based node, which **Dichtel** already used to make a dozen new macrocycles. We are now working on preparing an aldehyde-based dihydrophenazine linker, which we will next condense with the new node to make radical-containing macrocycle structures.

Objective 2: Molecular model studies

One key advantage of molecular chemistry is the ability to both create arrays of qubits and understand fundamental interactions through the creation of model complexes. The facile synthetic control offered by synthetic chemistry allows us to perform fundamental investigations. Here, we sought to create molecular model complexes to understand the interaction of qubits. This work is highly collaborative with **Freedman**, **Harris**, **Long**, and **Dichtel** synthesizing model systems, **Freedman** and **Wasielewski** measuring these compounds and **Rondinelli** providing theoretical support throughout. Freedman synthesized three molecules featuring two spectrally distinct qubit

candidates, shown in Figure 4. These molecules will enable us to quantify the impact of spin-spin interactions in a two qubit system. Preliminary data demonstrate the ability to manipulate both qubit candidates within each molecule, with coherence extending to high temperature. Our molecules also feature two important design parameters, they are soluble in CS_2, thereby offering a nuclear spin free environment for fundamental studies, and support gate operations that can be

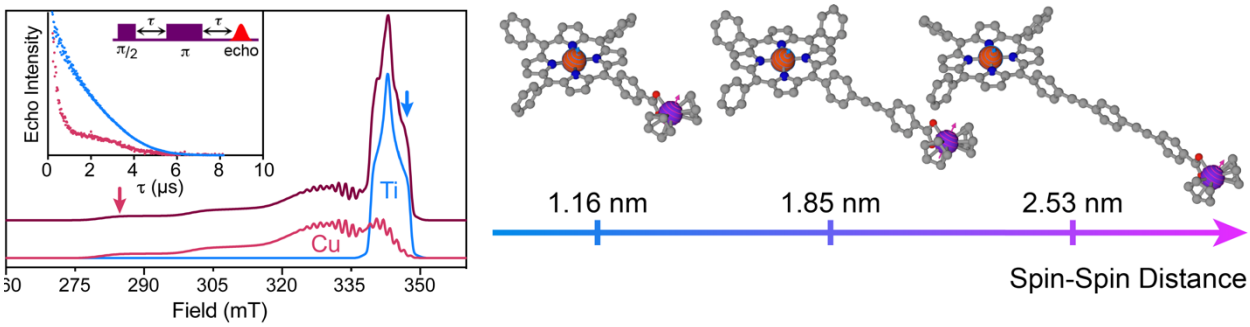

Figure 4. Series of molecules featuring two spectrally addressable separate candidate qubits with increasing distances between the metal notes. Collaborative work, Freedman, Wasielewski, Rondinelli

executed on commercial spectrometers.

Organic chemistry approaches enable us to create small molecular networks of qubits, for example six member rings where we can probe the interaction of small numbers of qubits with each other. Towards that end, **Dichtel** designed a more reactive pyridine-containing amine-based node, which **Dichtel** already used to make a dozen new macrocycles. Preliminary continuous wave experiments demonstrate the formation of radicals and enable quantization of the number of radicals in these rings (Figure 5).

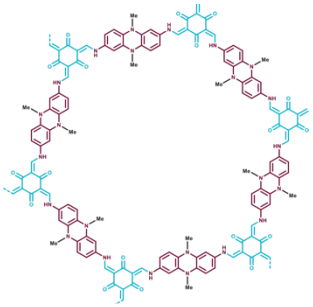

Figure 5. Macrocycle with a ring of six candidate qubits that are well spaced

Wasielewski is pursuing a parallel path to molecules designed to execute gate operations. For example, We have developed a photogenerated electron(triplet)-nuclear qubit pair, naphthalene-diketophosphepin (NDP), in order to implement the two qubit CNOT quantum gate. The molecule, NDP, rapidly intersystem crosses to form a triplet state following photo-excitation, this can provide an initially well-defined starting state thereby avoiding the need to prepare pseudo-pure states2 in order to perform the gate operations. In addition, NDP contains a single phosphorous nucleus which is well separated from other nuclear spin and is easily addressable.

Objective 3: Interface qubits with surfaces

We are interfacing qubits with surfaces in two complementary directions, interfacing molecules with surfaces and understanding the impact of surface electronics on the coherence properties of molecules and interfacing arrays with surfaces. In the first approach **Freedman** and **Rondinelli** are studying a series of planar molecules to understand the impact of surfaces on coherence properties. **Hersam** is subliming those molecules onto surfaces for further study (Figure 6). In the second approach, interfacing arrays with surfaces,

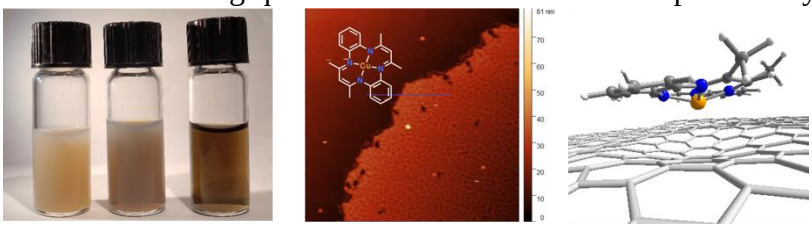

Figure 6. Suspensions of 2D materials, planar molecule on a surface and calculations of planar molecules on surfaces

Hersam and **Dichtel** are exploring the in solvo synthesis of a range of COFs in 2D material dispersions. COFs have been synthesized in colloidal suspensions of hexagonal boron nitride (hBN), while trisaminophenylamine-phenyldialdehyde (TAPA-PDA) COFs, trisaminophenylbenzene-phenyldialdehyde (TAPB-PDA) COFs, and thienoisoindigopyrene (TIIP) COFs have been synthesized in colloidal suspensions of the 2D transition metal dichalcogenides MoS_2 and WS_2 . The crystallinity of the resulting COFs has been verified with synchrotron X-ray scattering at the Advanced Photon Source. **Hersam** has also successfully exfoliated MOFs synthesized by **Harris** down to the few-layer level. Therefore, ongoing work is attempting to exfoliate few-layer MOFs in an inert atmosphere, after which they will be encapsulated with hBN to enable ambient characterization with methods such as magneto-optical Kerr effect (MOKE) measurements.

iii) Future Plans

Key immediate goals and questions

Objective 1: Create a network of qubits using COF and MOF approaches

(1) Execute measurements and calculations on arrays of MOF and COF qubits we synthesized.
(2) What is the impact of 2D vs 3D networks on coherence?
(3) What is the impact of spin-spin distance in networks of qubits?
(4) How does do lanthanides vs. transition metals impact these dynamics

Objective 2: Generate fundamental insight into quantum properties of networks through molecular model studies

(1) Complete two qubit study, execute gate operations
(2) Complete study of planar radical molecules
(3) Execute complex gate operations on organic species

Objective 3: Interface qubits with surfaces

(1) Complete study of series of molecular qubits on surfaces
(2) Understand impact of substrate on molecular coherence properties
(3) Probe MOFs and COFs on surfaces

(iv) References

NA

(V) Publications

(1) Spin-Selective Photoinduced Electron Transfer in Organic Diradicals, N. T. La Porte, J. A. Christensen, M. D. Krzyaniak, B. K. Rugg, and M. R. Wasielewski, *submitted J. Phys. Chem. B.*
(2) Stabilizing Naphthalenediimide Radical within a Tetracationic Cyclophane, T. Jiao, K. Cai, J. N. Nelson, Y. Jiao, Y. Qiu, G. Wu, C. Cheng, D. Shen, Y. Feng, Z. Liu, M. R. Wasielewski, J. F. Stoddart, and H. Li, *submitted J. Am. Chem. Soc.*
(3) Strong π-Backbonding Enables Record Magnetic Exchange Coupling Through Cyanide Valdez-Moreira, J. A.; Thorarinsdottir, A. E.; DeGayner, J. A. Lutz, S. A.; Chen, C.-H.; Losovyj, Y. Pink, M.; Harris, T. D.; Smith, J. M. *submitted J. Am. Chem. Soc*

Program Title: Electronic Structure and Spin Correlations in Novel Magnetic Structures

Principal Investigators: David J. Sellmyer (University of Nebraska) in collaboration with PI George Hadjipanayis (University of Delaware); Co-PI: Ralph Skomski (University of Nebraska); Address: Nebraska Center for Materials and Nanoscience, University of Nebraska, Lincoln, NE 68588-0298; E-mail: dsellmyer@unl.edu

Program Scope

This project is focused on advancing through fundamental research the discovery and understanding of new materials important in magnetism and nanoscience. The specific focus is on nanometer-length-scale and real structure control of new or metastable structures as a means of creating materials with high magnetization, high spin polarization, large magnetocrystalline anisotropy and high ordering temperatures. Innovative aspects of the research include synthesis of new magnetic nanostructures with special non-equilibrium fabrication techniques. The proposed research consists of two main parts. The first is aimed at preparation and properties of complex or metastable transition-metal compounds where anisotropic crystal structures and nanostructuring are expected to lead to novel magnetic properties. Several types of systems are being explored including new magnetic phases based on CoSn and CoSi that exhibit Griffiths-phase paramagnetism, quantum-phase transitions, and high-temperature ferromagnetism. The second part is focused on exploring new nanostructured magnets where confinement effects and novel structures lead to new magnetic phases with potential applications in permanent magnetism or catalysis. Our research is based on a continuing collaboration in experimental and theoretical work between groups at the Universities of Nebraska and Delaware. A broad set of experiments is performed over a wide temperature range. These include structural characterization by x-ray diffraction, analytical and high-resolution electron microscopy, Lorentz microscopy and transport measurements. Magnetic measurements include dc magnetization to fields of 7 T between 4.2 and 1000 K with SQUID and PPMS magnetometry. The results are correlated with theoretical work using first-principle density-functional theory (DFT) and analytical simulations to study spin polarization, magnetic nanostructures, anisotropies, magnetic interactions, and magnetization reversal mechanisms

Recent Progress

Background: Our recent work has focused on the synthesis and properties of nanostructures of magnetic compounds having new or metastable crystal structures as well as on bulk magnetic compounds. We have used a variety of growth routes including non-equilibrium processes such as cluster deposition, sputtering and rapid quenching from the melt. A few examples of our recent research are discussed below to highlight the important physics and technological aspects of these new phases and nanostructured magnetic materials.

1. New Quantum-Phase-Transition Systems and High-Temperature Skyrmions

Discussion: We have investigated non-collinear and spiral magnetism in several systems including MnSi [1], $Co_{1+x}Sn$ [12], $Co_{1+x}Si_{1-x}$ [23] and $Fe_{3+x}Co_{3-x}Ti_2$ (x = 0,2,3) [9]. In Co-Sn, the onset of ferromagnetism in cobalt-tin alloys has been studied experimentally and theoretically. The $Co_{1+x}Sn$ alloys were prepared by rapid quenching from the melt and form a modified hexagonal NiAs-type crystal structure for $0.45 \leq x \leq 1$. [Fig. 1a] The magnetic behavior is described analytically and by DFT using supercells and the coherent-potential approximation. The excess of Co concentration x, which enters the interstitial 2d sites in the hypothetical NiAs-ordered parent alloy CoSn, yields a Griffiths-like phase and, above a quantum critical point ($x_c \approx 0.65$), a quantum phase transition to ferromagnetic order. [Fig. 1b] Quantum critical exponents are determined on the paramagnetic and ferromagnetic sides of the transition and related to the nature of the magnetism in itinerant systems with different types of chemical disorder. The work on Co-Si has been motivated by the

fact that magnets with chiral crystal structures and helical spin structures have much potential as spin-electronics materials, but their relatively low magnetic-ordering temperatures are a disadvantage. While cobalt has long been recognized as an element that promotes high-temperature magnetic ordering, most Co-rich alloys are achiral and exhibit collinear rather than helimagnetic order. Crystallographically, the B20-ordered compound CoSi is an exception due to its chiral structure, but it does not exhibit any kind of magnetic order. Here we use non-equilibrium processing to produce B20-ordered $Co_{1+x}Si_{1-x}$ with a maximum Co solubility of $x = 0.043$. Above a critical excess Co content ($x_c = 0.028$), the alloys are magnetically ordered, and for $x = 0.043$, a critical temperature $T_c = 328$ K is obtained, the highest among all B20-type magnets. The crystal structure of the alloy supports spin spirals caused by Dzyaloshinski–Moriya interactions, and from magnetic measurements we estimate that the spirals have a periodicity of about 17 nm. Our DFT calculations explain the combination of high magnetic-ordering temperature and short periodicity in terms of a quantum phase transition in which there is weakened exchange between the spin-polarized excess-cobalt spins through the host matrix. Fig. 1c and d shows the evidence for skyrmions and resulting phase diagram.

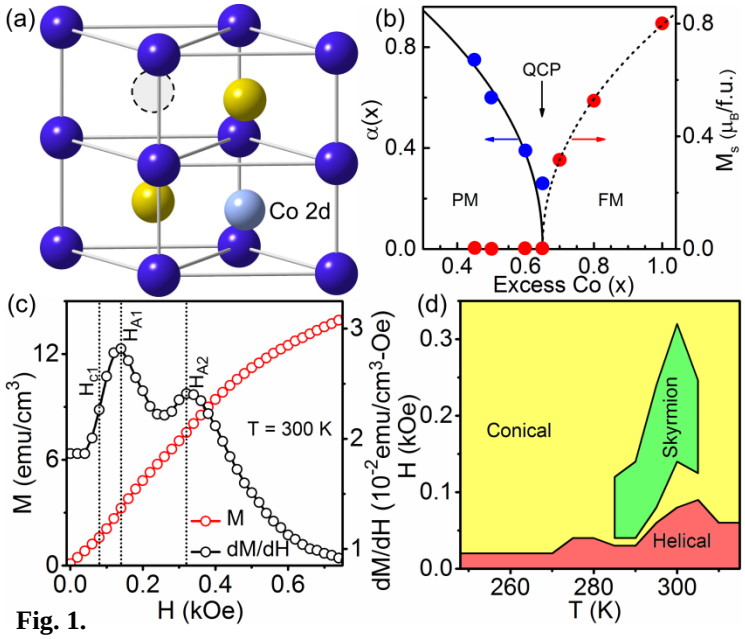

Fig. 1.
Co-Sn: (a) Structure: blue (Co), yellow (Sn), light blue (excess Co); (b) Quantum phase transition: $M \sim H^{\alpha}$, $\propto \sim (x_c\text{-}x)^{0.47}$ (para), $M_S \sim (x\text{-}x_c)^{0.47}$ (ferro)
Co-Si: (c) *M(H)* and d*M*/d*H* for x = 0.043. Skyrmions exist between H_{A1} and H_{A2}; (d) Phase diagram for skyrmions (green)

Significance: These systems represent a new class of materials with controllable magnetic transitions and in Co-Si chiral magnetism with room-temperature skyrmions, which may have spintronics or quantum-information applications.

2. Magnetism in Novel Nanostructures

Discussion: The ability to use non-equilibrium synthetic and controlled thermal processes has led to new magnetic nanostructured magnetic materials with intriguing properties. We report here recent results on Mn_5Ge_3 [3] and Co_2Ge [25] compounds. We have prepared isolated Mn_5Ge_3nanostructures with sizes in the range of 7.2 nm to 12.6 nm. The saturation magnetization and magnetocrystalline anisotropy increase significantly with particle size, from $M_s = 31$ kA/m to 172 kA/m and from $K = 0.4 \times 10^5$ J/m^3 to 2.9×10^5 J/m^3 as the particle size increases. In contrast, the Curie temperature does not vary much with size. [Fig. 2] Because of their relatively high anisotropy, all of the particles exhibit low-temperature coercivities varying from 0.04 T in the smallest particles to 0.13 T in the largest particles, compared to the nearly zero coercivity of the bulk sample. A tentative explanation of the observed magnetization increase with size is provided by a simple core-shell model with a 2.8-nm shell having zero magnetization.

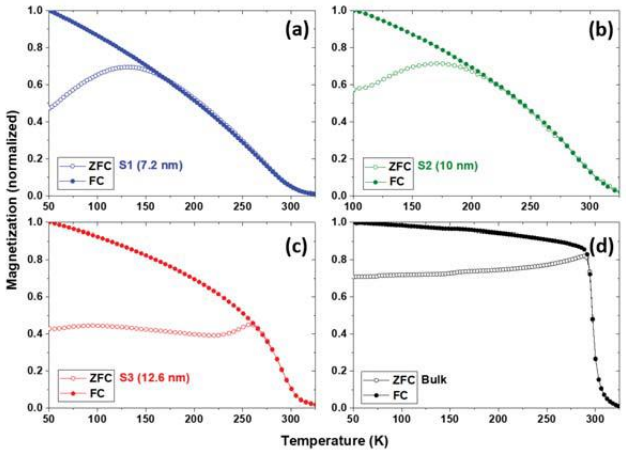

Fig 2. Temperature-dependent magnetization curves of the particles (**a**) 7.2 nm; (**b**) 10 nm; (**c**) 12.6 nm; and (**d**) powdered bulk measured at 0.05 T.

In the case of Co_2Ge, as-made particles with an average size of 5.5 nm exhibit a mixture of hexagonal and orthorhombic crystal structures. Thermomagnetic measurements showed that the as-made particles are superparamagnetic at room temperature with a blocking temperature of around 30 K. When the particles are annealed at 823 K for 12 h, their size is increased to 13 nm and they develop a new orthorhombic crystal structure, with a Curie temperature of 815 K. This is drastically different from bulk Co-Ge compounds which are ferromagnetic only at cryogenic temperatures. XRD and elemental mapping measurements suggest the formation of a new Co-rich orthorhombic phase with increased *c/a* ratio in the annealed particles and this is believed to be the reason for the drastic change in their magnetic properties.

Significance: Size effects and new crystal structures of the type studied here have significant potential as new materials for spin-electronics and rare-earth free permanent-magnet materials.

Future Plans

We will continue to produce new nanostructured Mn-X, Co-X, and Co(Fe) -based magnetic compounds of fundamental and technological importance. A further investigation will be carried out to understand the effects of size confinement on the ground-state electronic structure and associated spin correlations in nanoclusters and nanostructured materials in which complex interactions including Dzyaloshinski-Moriya effects may exist. We will also continue our studies on new sustainable magnetic materials from earth-abundant elements.

Selected References Acknowledging DOE Support (25 of 32 publications in 2018-19)

1. B. Das, B. Balasubramanian, R. Skomski, P. Mukherjee, S. Valloppilly, G. Hadjipanayis, and D. Sellmyer, "Effect of Size Confinement on Skyrmionic Properties of MnSi Nanomagnets," Nanoscale **10**, 9504-9508 (2018).
2. R. Skomski, P. Kumar, B. Balamurugan, B. Das, P. Manchanda, P. Raghani, A. Kashyap, and D. J. Sellmyer, "Exchange and Magnetic Order in Bulk and Nanostructured Fe_5Si_3," J. Magn. Magn. Mater. **460**, 438-447 (2018).
3. O. Tosun, M.S. Fashami, B. Balamurugan, R. Skomski, D.J. Sellmyer, G.C. Hadjipanayis, "Structure and Magnetism of Mn_5Ge_3 Nanoparticles," Nanomaterials **8**, 241 (10 pgs.) (2018).
4. J. Cui, M. Kramer, L. Zhou, F. Liu, A. Gabay, G. Hadjipanayis, B. Balasubramanian, D. Sellmyer, "Current Progress and Future Challenges in Rare-Earth-Free Permanent Magnets," Acta Materialia **158**, 118-137 (2018).
5. Y. Jin, Y. Yang, S. Valloppilly, S-H. Liou, D. Sellmyer, "Room-Temperature Magnetic Heusler Compound $Fe_2Ti_{0.5}Co_{0.5}Si$ with Semiconducting Behavior," J. Magn. Magn. Mater. **474**, 343-346 (2019).
6. A. Kashyap, R. Pathak, D. Sellmyer, and R. Skomski, "Theory of Mn-Based High-Magnetization Alloys," IEEE Trans. Magn. **54**, 2102106 (2018) (Intermag Invited Talk).
7. Y. Jin, R. Pathak, S. Valloppilly, P. Kharel, A. Kashyap, R. Skomski, and D. Sellmyer, "Unusual Perpendicular Anisotropy in the Heusler Compound Co_2TiSi," J. Phys. D: Appl. Phys. **52**, 035001 (8 pp.) (2019).
8. F.M. Abel, V. Tzitzios, E. Devlin, S. Alhassan, D.J. Sellmyer, G.C. Hadjipanayis, "Enhancing

the Ordering and Coercivity of $L1_0$ FePt Nanostructures with Bismuth Additives for Applications Ranging from Permanent Magnets to Catalysts," ACS Appl. Nano Mater. **2**, 3146−3153 (2019).

9. H. Wang, B. Balasubramanian, R. Pahari, R. Skomski, Y. Liu, A. Huq, D. Sellmyer and X. Xu, "Noncollinear Spin Structure in $Fe_{3+x}Co_{3-x}Ti_2$ (x = 0, 2, 3) from Neutron Diffraction," Phys. Rev. Mater. **3**, 064403 (2019).
10. A. Ullah, B. Balamurugan, W. Zhang, S.S. Valloppilly, X.-Z. Li, R. Pahari, L.-P. Yue, A. Sokolov, D.J. Sellmyer, and R. Skomski, "Crystal Structure and Dzyaloshinski-Moriya Micromagnetics," IEEE Trans. Magn. **55**, 7100305 (5 pp.) (2019).
11. R. Skomski, B. Balamurugan, D. Sellmyer, "Physics of Nanomagnets," in *21st Century Nanoscience – A Handbook: Nanophysics Sourcebook* (Volume 1), K. Sattler, Ed., CRC Press (2019).
12. R. Pahari, B. Balasubramanian, R. Pathak, M.C. Nguyen, S. Valloppilly, R. Skomski, A. Kashyap, C-Z. Wang, K-M. Ho, G. Hadjipanayis, and D. Sellmyer, "Quantum Phase Transition and Ferromagnetism in $Co_{1+x}Sn$," Phys. Rev. B **99**, 184438 (10 pp.) (2019).
13. B. Das, R. Choudhary, R. Skomski, B. Balasubramanian, A. Pathak, D. Paudyal, and D. Sellmyer, "Anisotropy and Orbital Moment in Sm-Co Permanent Magnets," Phys. Rev. B **100**, 024419 (8 pp.) (2019).
14. D. Salazar, A. Martín-Cid, J.S. Garitaonandia, T.C. Hansen, J.M. Barandiaran, G.C. Hadjipanayis, "Role of Ce Substitution in the Magneto-Crystalline Anisotropy of Tetragonal $ZrFe_{10}Si_2$," J. Alloys and Compounds **766**, 291–296 (2018).
15. C. Wang, H. Zheng, H. Ding, X. Hu, G.C. Hadjipanayis, B. Wang, J. Chen, X. Cui, "Effects of B Addition on the Microstructure and Magnetic Properties of Fe-Co-Mo Alloys," J. Alloys and Compounds **766**, 649–655 (2018).
16. D. Salazar, A. Martín-Cid, R. Madugundo, J. M. Barandiaran, G. C. Hadjipanayis, "Coercivity Enhancement in Heavy Rare Earth-Free NdFeB Magnets by Grain Boundary Diffusion Process," Appl. Phys. Lett. **113**, 152402 (2018).
17. A.M. Gabay, G.C. Hadjipanayis, "Recent Developments in RFe_{12}-Type Compounds for Permanent Magnets," Scripta Materialia **154**, 284–288 (2018).
18. A. M. Gabay, G. C. Hadjipanayis, "Assessment of Off-Stoichiometric $Zr_{33-x}Fe_{52+x}Si_{15}$ C_{14} Laves Phase Compounds as Permanent Magnet Materials," AIP Advances **8**, 056204 (2018).
19. B.T. Lejeune, R. Barua, I.J. McDonald, A.M. Gabay, L.H. Lewis, G.C. Hadjipanayis, "Synthesis and Processing Effects on Magnetic Properties in the Fe_5SiB_2 System," J. Alloys and Compounds **731**, 995–1000 (2018).
20. A.M. Schönhöbel, R. Madugundo, O.Yu. Vekilova, O. Eriksson, H.C. Herper, J.M. Barandiaran, G.C. Hadjipanayis, "Intrinsic Magnetic Properties of $SmFe_{12-x}V_x$ Alloys with Reduced V Concentration," J. Alloys and Compounds **786**, 969–974 (2019).
21. A.M. Gabay, G.C. Hadjipanayis, "Semi-Hard Magnetic Nanocomposites Based on Out-of-Equilibrium $Fe_{2+\delta}Nb$ and $Fe_{2+\delta}Ta$ Laves Phases," AIP Advances **9**, 035143 (2019).
22. A.M. Schönhöbel, R. Madugundo, A.M. Gabay, J.M. Barandiarán, G.C. Hadjipanayis, "The Sm-Fe-V Based 1:12 Bulk Magnets," J. Alloys and Compounds **791**, 1122–1127 (2019).
23. B. Balasubramanian, R. Skomski, G. Hadjipanayis, D. Sellmyer *et al.*, "Chiral Magnetism and High-Temperature Skyrmions in B20-Ordered Co-Si" (submitted).
24. A.M. Gabay, G.C. Hadjipanayis, J. Cui, "New Anisotropic MnBi Permanent Magnets by Field-Annealing of Compacted Melt-Spun Alloys Modified with Mg and Sb" (submitted).
25. O. Tosun, B. Balasubramanian, R. Skomski, D.J. Sellmyer, G.C. Hadjipanayis, "Magnetic and Structural Properties of Melt-Spun Co-Ge Alloys" (submitted).

Stripe Antiferromagnetism and Disorder in the Mott Insulator $NaFe_{1-x}Cu_xAs$ (x < 0.5)

Yizhou Xin, Ingrid Stolt, Yu Song, Pengcheng Dai, W. P. Halperin
Depart. of Physics and Astronomy, Northwestern University, Evanston IL 60208, USA}
Depart. of Physics and Astronomy and Rice Center for Quantum Materials, Rice University, Houston TX 77005, USA

Program Scope

This program at Northwestern University is focused on correlated electron physics and materials physics with emphasis on the interplay between magnetism and superconductivity. Our experimental tools include nuclear magnetic resonance (NMR), especially at very high magnetic field, and crystal growth and characterization, complemented by neutron scattering. The systems we study in the current program are a mercury based high temperature superconductor, $HgBa_2CuO_{4+x}$, and pnictide superconductors in the Na111 family, $NaFe_{1-x}Cu_xAs$; both of which have superconducting states that evolve from antiferromagnetic correlations. The Hg-cuprate has a special place as a truly high temperature superconductor ($T_{c,opt}$ = 93 K) and simultaneously a tetragonal crystal structure. In collaboration with colleagues at Los Alamos we have very high quality single crystals which we process at Northwestern for doping control and oxygen isotope exchange including NMR with ^{17}O, ^{63}Cu, and ^{199}Hg. Measurements are performed up to 14 T magnetic field at Northwestern and these are extended to above 30 T at the National High Magnetic Field Laboratory (NHMFL) in Tallahassee, Florida. We have been interested in charge and spin order and vortex structure in our recent work supported by this grant. Currently, we explore the magnetic character of the bound states in the vortex core, a challenging experimental and theoretical problem. Our approach is to improve our resolution by expanding the number of probe nuclei that sample the vortex core by increasing the density of vortices at ultra-high magnetic field.

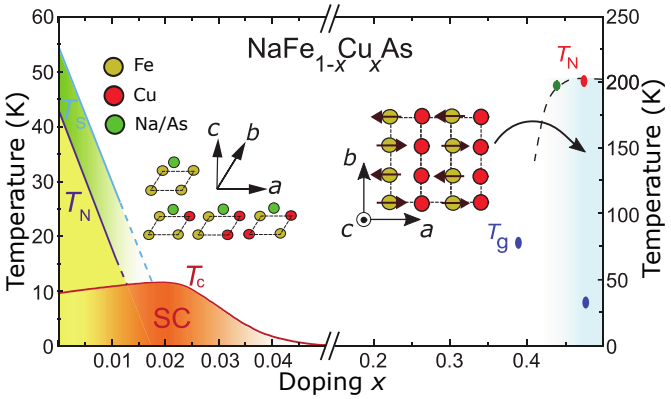

Figure 1. Phase diagram shows superconducting regions and magnetic ordering at high doping. T_N and T_g are AFM and spin-glass transitions from NMR.

The second current project is to investigate the nature of magnetic order resulting from Mott-like physics recently reported in highly Cu doped $NaFe_{1-x}Cu_xAs$ with x ~ 0.5. This unique compound provides an smooth evolution from superconductivity to localized spin-dominated electronic excitations with increased doping an unusual behavior among pnictides. We show that magnetic clusters associated with copper concentration drive a number of magnetic transitions. We confirm the report from neutron scattering of antiferromagnetic long range order at T_N = 200 K for x = 0.48 and we have discovered cluster spin-glass behavior for x ~ 0.39 at T_g = 80 K. Interestingly, we discovered that for slight differences for x less than 0.5, *i.e.* x = 0.48, there are correspondingly defects which also form a spin-glass at T_g = 30 K but these are manifest in the strongly one-dimensional antiferromagnetic background; a rather unique phenomenon. More importantly, with the aid of numerical simulations, we show that copper end-chain effects, defects

from the incomplete formation of copper chains, are responsible for the spin-glass disorder expressed within the antiferromagnetic crystal. These results are the focus of this extended abstract.

Recent Progress

An important step in understanding the physics of iron-based superconductors is to investigate the connection between superconductivity and magnetism. The heavily Cu-doped pnictide, $NaFe_{1-x}Cu_xAs$ (phase diagram displayed in Fig. 1) becomes a Mott insulator that exhibits both real space Fe-Cu stripe ordering and long-range antiferromagnetism (AFM) below $T_N \approx 200$ K for x close to 0.5 [1–3]. Later work shows the importance of the interplay of electronic correlations and spin-exchange coupling [4, 5]. This is the only known Fe-based material for which superconductivity can be smoothly connected to a Mott-insulating state with increasing dopant. Our recent investigation [6] has shown a systematic development of AFM Fe-Cu clusters with increasing Cu dopant at low copper concentrations. Here we report nuclear magnetic resonance (NMR) and magnetization measurements for $x \geq 0.39$ that identify antiferromagnetic and spin-glass transitions complemented by numerical simulation. They reveal stripe antiferromagnetism and structural evolution, as well as the link between them, consistent with neutron scattering. With NMR we can characterize spin dynamics from spin-lattice and spin-spin relaxation and have discovered spin-glass behavior associated with small deviations from stoichiometry, x ~ 0.5, that correspond to end-chain defects.

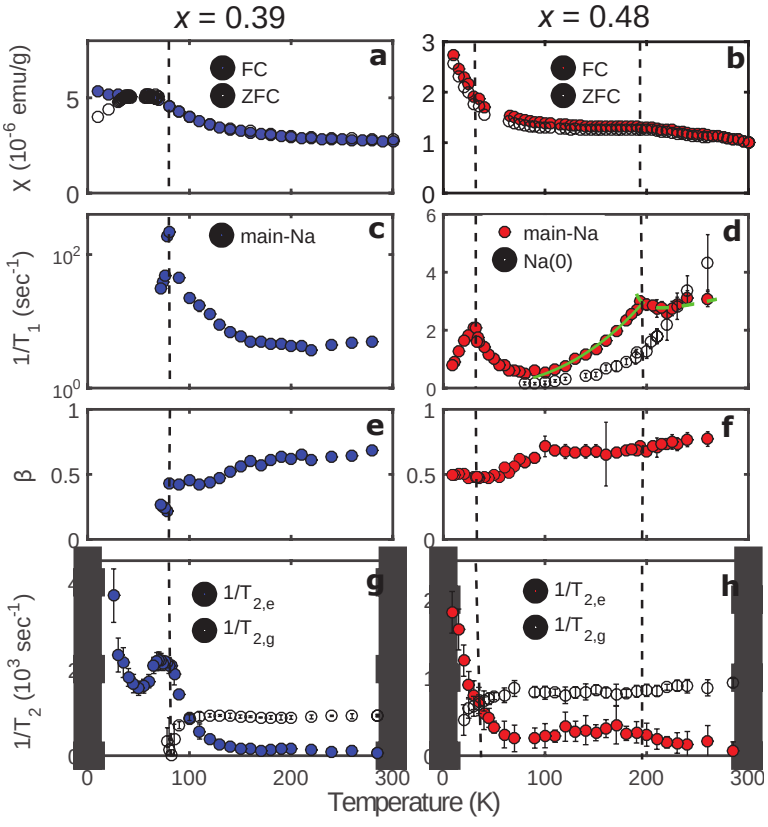

Figure 2. NMR ^{23}Na relaxation and magnetic susceptibility, showing evidences of magnetic transitions (dashed lines).

As indicated in Fig. 1, the ^{75}As and ^{23}Na nuclei are located on opposite sides of the Fe layer and are both coupled to the electronic spins at four nearest-neighbor sites in the Fe-Cu plane via transferred hyperfine interaction. Our ^{23}Na NMR spectra, nuclear spin-lattice ($1/^{23}T_1$), and spin-spin ($1/^{23}T_2$)) relaxation rates, figure 2, show evidence in the x = 0.48 compound for a stripe-ordered Mott insulator that has a Néel transition temperature at 200 K, first identified by neutron scattering [1–3] for x = 0.44 and demonstrated at x = 0.48 from our NMR measurements. We find that the long-range three-dimensional AFM order for x = 0.48 coexists with a spin-glass phase at lower temperatures than its spin-glass transition T_g = 30 K, due to

magnetic frustration in the Fe-Cu plane. In contrast the compound, x = 0.39, forms a cluster spin-glass with a much higher transition temperature, T_g = 80 K. Aided by numerical simulation, our analysis of the ^{75}As NMR spectra shows a clear splitting of the distribution of hyperfine fields, for x = 0.48, Fig. 3a, that indicates existence of staggered magnetization induced by imperfect stripes of non-magnetic Cu dopants, similar to that in cuprates [7–10].

Measurements of magnetic susceptibility Fig. 2a for x = 0.39 are a classic indication of a spin-glass. These are matched with NMR measurements of spin dynamics coupled to ^{23}Na via a relatively weak hyperfine field, through $^{23}T_1$ and $^{23}T_2$ relaxation, Fig.2c,e,g. These results provide a robust identification of this transition as a cluster spin-glass arising from the magnetic clusters that we had previously identified in our NMR report with lower Cu doping (x= 0.13, 0.18, and 0.24) [6].

Identification of stripe magnetic order follows from the measurement of a hyperfine field splitting of the ^{75}As NMR spectra shown in Fig. 3a along with numerical simulations for end-chain defects in Cu chains, Fig. 3b. This work is posted on the arXiv and submitted to Phys. Rev. Lett.

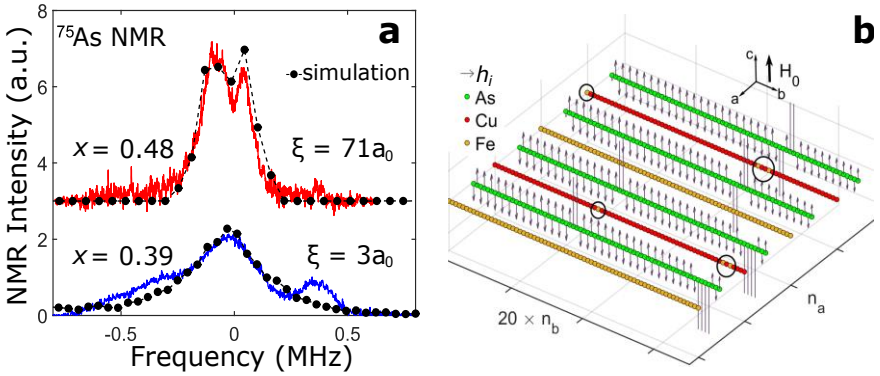

Figure 3. Hyperfine field splitting at the As site (a) and its spatial distribution from numerical simulation (b). For x substantially less than 0.5 magnetism in this compound is highly disordered in contrast to x = 0.48 where a narrower but split doublet appears in ^{75}As NMR. The correlation length ξ from the simulation is shown in units of the lattice constant.

Future Plans

Our interpretation of the NMR spectra, aided by numerical simulation, must be improved in two important ways. The staggered susceptibility model in contrast to local magnetic order can be differentiated by their dependence on the external magnetic field. We plan to extend this work to 30 T at the NHMFL where we have in the past been a regular user. This field study changes the Larmor frequency by a factor of two. The spin dynamics of a classic spin-glass is manifest in a frequency dependence of the spin-glass transition temperature. We will measure the dependence of the $1/^{23}T_1$, Na spin-lattice relaxation rate on frequency of both x = 0.48 and 0.39 crystals. Additionally we will investigate the vortex core of $HgBa_2CuO_{4+x}$ with spatially resolved oxygen NMR, $1/^{17}T_1$ [11].

References

[1] Y. Song, Z. Yamani, C. Cao, Y. Li, C. Zhang, J. S. Chen, Q. Huang, H. Wu, J. Tao, Y. Zhu, *et al.*, *Nature Communications* **7**, 13879 (2016).

[2] C. E. Matt, N. Xu, B. Lv, J. Ma, F. Bisti, J. Park, T. Shang, C. Cao, Y. Song, A. H. Nevidomskyy, P. Dai, L. Patthey, N. C. Plumb, M. Radovic, J. Mesot, and M. Shi, *Phys. Rev. Lett.* **117**, 097001 (2016).

[3] R. Yu, J.-X. Zhu, Q. Si, *Current Opinion Solid State and Materials Science* **17**, 65 (2013).

[4] S. Zhang, Y. He, J.-W. Mei, F. Liu, and Z. Liu, *Phys. Rev. B* **96**, 245128 (2017).

[5] A. Charnukha, Z. P. Yin, Y. Song, C. D. Cao, P. Dai, K. Haule, G. Kotliar, and D. N. Basov, *Phys. Rev. B* **96**, 195121 (2017).

[6] Y. Xin, I. Stolt, J.A. Lee, Y. Song, P. Dai, W.P. Halperin, *Phys. Rev. B* **99**, 155114 (2019).

[7] M.-H. Julien, T. Feher, M. Horvati c, C. Berthier, O. N. Bakharev, P. S egransan, G. Collin, and J.-F. Marucco, *Phys. Rev. Lett.* **84**, 3422 (2000).

[8] J. Bobroff, H. Alloul, Y. Yoshinari, A. Keren, P. Mendels, N. Blanchard, G. Collin, and J.-F. Marucco, *Phys. Rev. Lett.* **79**, 2117 (1997).

[9] R. E. Walstedt, R. F. Bell, L. F. Schneemeyer, J. V. Waszczak, W. W. Warren, R. Dupree, and A. Gencten, *Phys. Rev. B* **48**, 10646 (1993).

[10] D. K. Morr, J. Schmalian, R. Stern, C.P. Slichter, *Phys. Rev. B* **58**, 11193 (1998).

[11] V.F. Mitrovic, E.E. Sigmund, M. Eschrig, H.N. Bachman, W.P. Halperin, A.P. Reyes, P. Kuhns, and W.G. Moulton, *Nature* **413**, 501 (2001).

Publications

1. Stripe Antiferromagnetism and Disorder in the Mott Insulator $NaFe_{1-x}Cu_xAs$ ($x \sim 0.5$), Yizhou Xin, Ingrid Stolt, Yu Song, Pengcheng Dai, and W.P. Halperin, submitted to *Phys. Rev. Lett.* arXiv:1908.07035v1
2. Vortex Lattices and Broken Time-Reversal Symmetry in a Topological Superconductor, K. E. Avers, W. J. Gannon, S.J. Kuhn, W.P. Halperin, J.A. Sauls, C.D. Dewhurst, J. Gailano, G. Nagy, U. Gasser, and M.R. Eskildsen, *Nature Physics*, submitted (2019), arXiv: 1812.05690.
3. Toward the Mott State with Magnetic Cluster Formation in Heavily Cu-doped $NaFe_{1-x}Cu_xAs$, Yizhou Xin, Ingrid Stolt, Jeongseop A. Lee, Yu Song, Pengcheng Dai, and W.P. Halperin, *Phys. Rev. B* **99**, 155114 (2019).
4. Location of the Oxygen dopant in high temperature superconductor $HgBa_2CuO_{4+x}$ from ^{199}Hg NMR, Ingrid Stolt, Jeongseop A. Lee, A.M. Mounce, Yizhou Xin, and W. P. Halperin, *Physica C: Superconductivity and its Applications* **555**, 24-27 (2018).
(after January 1, 2017 and before August 20, 2019, as stated in each case)
5. Spin Susceptibility of the Topological Superconductor UPt_3 from Polarized Neutron Diffraction, W. J. Gannon, W.P. Halperin, M.R. Eskildsen, Pengcheng Dai, U.B. Hansen, K. Lefmann, and A. Stunault, *Phys. Rev. B* **96**, 041111(R) (2017). published July 10, 2017
6. Coherent Charge and Spin Density Waves in Underdoped $HgBa_2CuO_{4+x}$ J. A. Lee,Y. Xin, I. Stolt, W.P. Halperin, A. P. Reyes, P. L. Kuhns, and M. K. Chan, *New Journal of Physics*, **19**, 033024 (2017). published March 16, 2017
7. Magnetic Field Induced Vortex Lattice Transition in $HgBa_2CuO_{4+x}$ J. A. Lee, Y. Xin, I. Stolt, W.P. Halperin, A. P. Reyes, P. L. Kuhns, and M. K. Chan, *Phys. Rev. B*, **95**, 024512 (2017). published January 23, 2017.

Science of 100 Tesla

Neil Harrison, Los Alamos National Laboratory

Program Scope

Here we are concerned with classes of layered materials in which significant scientific progress requires access to magnetic fields of order 100 T. These include (i) layered superconductors such as the cuprates [1] and iron-based superconductors [2], in which unconventional pairing predominantly takes place within isolated layers, (ii) materials in which the bonding between layers is of the van der Waals type such as graphite or (iii) systems in which the physical properties change dramatically upon exfoliation [3-5]. In the layered unconventional superconductors, strong pairing and short coherence lengths lead to very high superconducting upper critical fields that necessitate magnetic fields of order 100 T to access the physics of the normal state [1]. There is mounting evidence that superconductivity nucleates around a singular point, referred to as a quantum critical point [6-8]. One of our goals is to identify the order parameter or the change in symmetry responsible for quantum criticality in the cuprates, which remains a major milestone in quantum matter [1], and is likely to be accomplished only by the application of a very strong magnetic field. In graphite, the weak interlayer tunneling accompanying the van der Waals bonding of multiple layers produces a semimetallic state exhibiting tiny sections of Fermi surface [9] from what would otherwise be a Dirac dispersion in a monolayer [3]. The inverse cyclotron length greatly exceeds the sizes of the compensated Fermi surface sections at 100 T, which drives this system deep into the quantum limit — producing numerous phase transitions and the possible realization of an excitonic insulator [10-12]. Our goal here is to identify the nature of the relationship between the order parameter and the Landau-quantized orbital degrees-of-freedom. In the transition metal dichalcogenides, exfoliation produces single monolayers that are transformed into a direct-gap semiconductor, with additional valley degrees of freedom resulting from the lattice symmetry [10]. Optical spectroscopy provides a means to probe fundamental properties of these monolayers, such as the effective masses or dielectric strength, through the formation of optically excited excitons. However, owing to the effective masses and electron-hole binding energies being substantially larger than, for example, GaAs or GaN [13], magnetic fields of order 100 T are required to induce a substantial diamagnetic shift [14].

Recent Progress

Graphite — a quasi-two-dimensional material in which individual layers of graphene are weakly connected by van der Waals interactions — is another area in which we have recently made significant progress. Weak van der Waals interactions transform the Dirac dispersion of neutral graphene into a compensated semimetal (see Fig. 4) whose small Fermi surface pockets are sufficiently small to reach the quantum limit at $B \approx 7$ T [15]. Hence, a magnetic field of order 100 T drives this material much deeper into the ultraquantum limit than what can be achieved in most other semimetals. At $B > 7$ T, the electronic structure is reduced to the lowest electron and hole Landau levels, with a significant Zeeman splitting between minority-spin and majority-spin carriers. It had previously been discovered [15] that a magnetic field of around ~ 25 T (applied along the crystalline *c*-axis) causes graphite to undergo a phase transition into an insulating phase. In the most recent high magnetic field studies, graphite has been found to undergo a cascade of phase transitions between various different phases [10], labeled A, B and C in Fig. 4. Each of these appears to have a different physical origin and to have different electrical transport properties. We recently utilized the different angular responses of the spin and orbital degrees-of-freedom to the orientation of the magnetic field to show that phase A in Fig. 4 forms

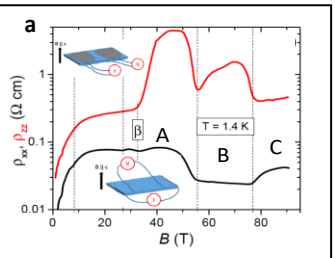

Figure 1. Electrical transport of graphite.

in the vicinity of the depopulation of the minority-spin electron and hole Landau levels at $B_o = 46$ T [11]. At $B > B_o$, quasiparticles pair across a gap in the minority-spin electronic density-of-states, causing the system to behave like an excitonic insulator crossing over from the weak to the strong coupling regimes. At magnetic fields above ~ 54 T, phase B has the unusual property of exhibiting insulating behavior only along the crystalline *c*-axis direction (orthogonal to the layers). Finally, at magnetic fields above ~ 75 T, phase C appears always to remain metallic. Despite the extreme Zeeman splitting of the spin-polarized Landau level states at $B > B_o$, the transition between B and C depends only on the coupling of the magnetic field to the orbital degrees of freedom, pointing to a strongly coupled spin-singlet excitonic insulator state.

Future Plans

In graphite, while numerous phases have been discovered at high magnetic fields [10], the natures of the various order parameters remain unknown. One of the phases, labeled B in Fig. 4, has a near-constant conductivity per layer that is quantitatively similar to that expected for the quantized conductance e^2/h, thereby warranting studies on samples with more precisely controlled current and voltage contacts. Focused ion beam (FIB) lithography, as successfully applied to TaAs, provides one viable means for carrying this out.

References

[1] B. Keimer, S. A. Kivelson, M. R. Norman, S. Uchida & J. Zaanen, From quantum matter to high-temperature superconductivity in copper oxides. *Nature* **518**, 179 (2015).

[2] D. C. Johnston, The puzzle of high temperature superconductivity in layered iron pnictides and chalcogenides. *Adv. Phys*. **59**, 803 (2010).

[3] K.S. Novoselov *et al*., Two-dimensional gas of massless Dirac fermions in graphene. *Nature* **438**, 197 (2005).

[4] A. Splendiani *et al*., Emerging Photoluminescence in monolayer MoS_2. *Nano. Lett*. **10**, 1271 (2010).

[5] K. F. Mak, C. Lee, J. Hone, J. Shan, & T. F. Heinz, Atomically thin MoS_2: A new direct gap semiconductor. *Phys. Rev. Lett*. **105**, 136805 (2010).

[6] B.J. Ramshaw *et al*., Quasiparticle mass enhancement approaching optimal doping in a high-T_c superconductor. *Science* **348**, 317 (2015).

[7] B. Michon *et al*., Thermodynamic signatures of quantum criticality in cuprate superconductors. *Nature* **567**, 218 (2019).

[8] S. Licciardello *et al*., Electrical resistivity across a nematic quantum critical point. *Nature* **567**, 213 (2019).

[9] S. Uji, J.S. Brooks, Y. Iye, Field-induced phase transition in Kish graphite. *Physica B* **246-247**, 299 (1998).

[10] Z. Zhu *et al*., Graphite in 90 T: Evidence for Strong-Coupling Excitonic Pairing. *Phys. Rev. X* **9**, 011058 (2019).

[11] Z. Zhu *et al*., Magnetic field tuning of an excitonic insulator between the weak and strong coupling regimes in quantum limit graphite. *Scientific Reports* **7**, 1733 (2017).

[12] Z. Pan, X.-T. Zhang, R. Shindou, Theory of metal-insulator transitions in graphite under high magnetic field. *Phys. Rev. B* **98**, 205121 (2018).

[13] A. D. Yoffe, Low-dimensional systems: quantum size effects and electronic properties of semiconductor microcrystallites (zero-dimensional systems) and some quasi-two-dimensional systems. *Adv. Phys*. **42**, 173 (1993).

[14] M. Goryca *et al*., Revealing exciton masses and dielectric properties of monolayer semiconductors with high magnetic fields. *Preprint*: arXiv:1904.03238.

[15] H. Yaguchi & J. Singleton, A high-magnetic-field- induced density-wave state in graphite. *J. Phys. Condens. Matter* **21**, 344207 (2009).

Publications

1) Reply to "Comment on 'Magnetotransport signatures of a single nodal electron pocket constructed from Fermi arcs';" N. Harrison & S. E. Sebastian, *Physical Review B* **96**, 146502 (OCT 2017).

2) Quantum limit transport and destruction of the Weyl nodes in TaAs; B. J. Ramshaw *et al.*, *Nature Communications* **9**, 2217 (JUN 2018).

3) Robustness of the biaxial charge density wave reconstructed electron pocket against short-range spatial antiferromagnetic fluctuations; N. Harrison, *Physical Review B* **97**, 245150 (JUN 29 2018).

4) Highly Asymmetric Nodal Semimetal in Bulk SmB_6; N. Harrison, *Physical Review Letters* **121**, 026602 (JUL 9 2018).

5) Structure-property relations in multiferroic $[(CH_3)_2NH_2]M(HCOO)_3$ (*M* = Mn, Co, Ni); K. D. Hughley *et al*., *Inorganic Chemistry* **57**, 11569 (SEP 2018).

6) Graphite in 90 T: Evidence for Strong-Coupling Excitonic Pairing; Z. Zhu *et al*., *Physical Review X* **9**, 011058 (MAR 2019).

7) Magnetoelastic coupling in URu_2Si_2: Probing multipolar correlations in the hidden order state. M. Wartenbe *et al. Physical Review B* **99**, 235101 (JUN 2019).

8) Field Angle tuned Metamagnetism and Lifschitz transitions in UPt_3. B. S. shivaram1, L. Holleis, V. W. Ulrich, J. Singleton, M. Jaime, *Scientific Reports* **9**, 8162 (JUN 2019).

9) Phonon mode links ferroicities in multiferroic $[(CH_3)_2NH_2]Mn(HCOO)_3$; K. D. Hughey *et al*., *Physical Review B* **96**, 180305 (NOV 2017).

10) Fermi surface in the absence of a Fermi liquid in the Kondo insulator SmB_6; M. Hartstein *et al*., *Nature Physics* **14**, 166 (FEB 2018).

11) Quantum oscillations from the reconstructed Fermi surface in electron-doped cuprate superconductors; J. S. Higgins *et al*., *New Journal of Physics* **20**, 043019 (APR 2018).

12) Scaling law for excitons in 2D perovskite quantum wells; J. C. Blancon *et al*., *Nature Communications* **9**, 2254 (JUN 2018).

13) Metastable states in the frustrated triangular compounds $Ca_3Co_{2-x}Mn_xO_6$ and $Ca_3Co_2O_6$; :J. W. Kim *et al*., *Physical Review B* **98**, 024407 (JUL 2018).

14) Field-induced canting of magnetic moments in $GdCo_5$ at finite temperature: first-principles calculations and high-field measurements; C. E. Patrick *et al*., *Journal of Physics-Condensed Matter* **30**, 32LT01 DOI:10.1088/1361-648X/aad029 (AUG 2018).

15) Electronic phase separation and magnetic-field-induced phenomena in molecular multiferroic $(ND_4)_2FeCl_5{\cdot}D_2O$; W. Tian *et al.*, *Physical Review B* **98**, 054407 (AUG 2018).

16) Scale-invariant magnetoresistance in a cuprate superconductor; P. Giraldo-Gallo *et al*., *Science* **361**, 479 (AUG 2018).

17) Magnetic field-induced ferroelectricity in $S = 1/2$ kagome staircase compound $PbCu_3TeO_7$; K. Yoo *et al*., *npg Qauntum Materials* **3**, 45 (SEP 2018).

18) Quantum oscillations of electrical resistivity in an insulator; Z. Xiang *et al*., *Science* **362**, 65

(SEP 2018).
19) Frustration and Glasslike Character in $R\mathrm{In}_{1-x}\mathrm{Mn}_x\mathrm{O}_3$ (R = Tb, Dy, Gd); P. Chen *et al*., *Inorganic Chemistry* **57**, 12501 (OCT 2018).
20) Magnetoresistance Scaling Reveals Symmetries of the Strongly Correlated Dynamics in $\mathrm{BaFe}_2(\mathrm{As}_{1-x}\mathrm{P}_x)_2$; I. M. Hayes *et al*., *Phyical Review Letters* **121**, 197002 (NOV 2018).
21) High magnetic fields for fundamental physics; R. Battestia *et al*., *Physics Reports* **765–766**, 1 (NOV 2018).
22) Evidence of incoherent carriers associated with resonant impurity levels and their influence on superconductivity in the anomalous superconductor $\mathrm{Pb}_{1-x}\mathrm{Tl}_x\mathrm{Te}$; P. Giraldo-Gallo *et al*., *Physical Review Letters* **121**, 207001 (NOV 2018).
23) Anomalous Metamagnetism in the Low Carrier Density Kondo Lattice $\mathrm{YbRh}_3\mathrm{Si}_7$; B. K. Rai *et al*., *Physical Review X* **8**, 041047 (DEC 2018)
24) Enhancement of the effective mass at high magnetic fields in CeRhIn_5; L. Jiao *et al*., *Physical Review B* **99**, 045127 (JAN 2019).
25) Magnetic order and enhanced exchange in the quasi-one-dimensional molecule-based antiferromagnet $\mathrm{Cu(NO_3)_2(pyz)_3}$; B. M. Huddart *et al*., *Physical Chemistry Chemical Physics* **21**, 1014 (JAN 2019).
26) Physical properties of $\mathrm{Sm}_x\mathrm{B}_6$ single crystals; J. Stankiewicz, M. Evangelisti, P. F. S. Rosa, P. Schlottmann & Z. Fisk, *Physical Review B* **99**, 045138 (JAN 2019).
27) Unconventional Field-Induced Spin Gap in an S = 1/2 Chiral Staggered Chain; J. Liu *et al*., *Physical Review Letters* **122**, 057207 (FEB 2019).
28) Spin dynamics and field-induced magnetic phase transition in the honeycomb Kitaev magnet α-$\mathrm{Li}_2\mathrm{IrO}_3$; S. Choi *et al*., *Physical Review B* **99**, 054426 (FEB 2019).
29) Non-saturating quantum magnetization in Weyl semimetal TaAs; C.-L. Zhang *et al*., *Nature Communications* **10**, 1028 (MAR 2019).
30) Fermi surface, possible unconventional fermions, and unusually robust resistive critical fields in the chiral-structured superconductor AuBe; D. J. Rebar *et al*., *Physical Review B* **99**, 094517 (MAR 2019).
31) Three-dimensional character of the Fermi surface in ultrathin $\mathrm{LaTiO_3/SrTiO_3}$ heterostructures; M. J. Veit, M. K. Chan, B. J. Ramshaw, R. Arras, R. Pentcheva & Y. Suzuki, *Physical Review B* **99**, 115126 (MAR 2019).
32) Quantum oscillations in flux-grown SmB_6 with embedded aluminum; S. M. Thomas *et al*., *Physical Review Letters* **122**, 166401 (APR 2019)
33) Correlation between scale-invariant normal-state resistivity and superconductivity in an electron-doped cuprate; T. Sarkar, P. R. Mandal, N. R. Poniatowski, M. K. Chan, R. L. Greene, *Science Advances* **5**, eaav6753 (MAY 2019).
34) Emergent bound states and impurity pairs in chemically doped Shastry-Sutherland system; Z. Shi *et al*., *Nature Commun*. 9, 2439 (JUN 2019).
35) Comprehensive magnetic phase diagrams of the polar metal $\mathrm{Ca_3(Ru_{0.95}Fe_{0.05})_2O_7}$; S. Lei *et al*. *Physical Review B* **99**, 224411 (JUN 2019).

Program Title: Non-Equilibrium Magnetism: Materials and Phenomena

PI: Frances Hellman; Co-PIs Jeff Bokor, Peter Fischer, Steve Kevan, Sujoy Roy (added 2019), Sayeef Salahuddin, Lin-Wang Wang; Materials Sciences Division, LBNL

Program Scope: This program focuses on the fundamental science of non-equilibrium magnetic materials and phenomena in films with strong spin-orbit interactions in the presence of interfacially-induced inversion symmetry breaking. It encompasses design, fabrication, measurement, and modeling of static and dynamic magnetic properties of these systems (Fig. 1). We focus on thermodynamic and dynamic control of magnetization, spin accumulation, and topological spin textures, addressing three interrelated thrusts: i) understanding and controlling the free energy landscape of chiral spin textures; ii) designing ferromagnet/non-magnet heterostructures with strong spin-orbit coupling that exhibit strong spin accumulation; iii) producing highly non-equilibrium magnetic phases in these structures by fsec external excitation. Optical, electron, and x-ray techniques provide nanoscale resolution and msec-fsec time scales.

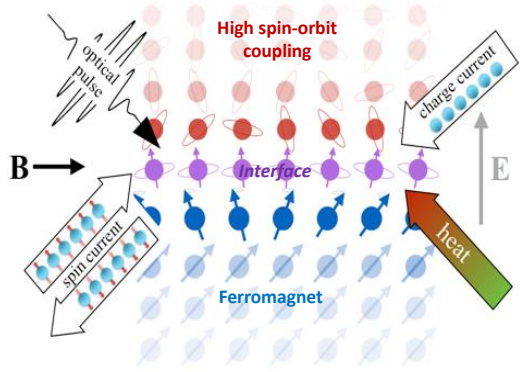

Fig. 1 Interface between ferromagnet (or other magnet) and high spin orbit coupling material, subject to optical, electrical, or heat pulses, and E or B fields.[Hellman *et al.* RMP, 2019]

Recent Progress (select results)

1. Experiments and *ab initio* theory were used to study the atomic, electronic, and magnetic structure of amorphous Fe-Ge and Fe-Si (40-75 at.% Fe). These show enhanced magnetism, spin polarization, and anomalous Hall effect (AHE, Fig. 2), compared to crystalline counterparts, as well as non-collinear spin structure. These results highlight the unappreciated importance of spin-orbit coupling and resultant DMI in non-crystalline materials. Theory suggests that there is an intrinsic AHE, typically represented by Berry phase curvature in momentum space but more universally expressed as a spin-orbital correlation function, captured theoretically as a density of curvature, and is not only present but prominent in these non-crystalline materials.

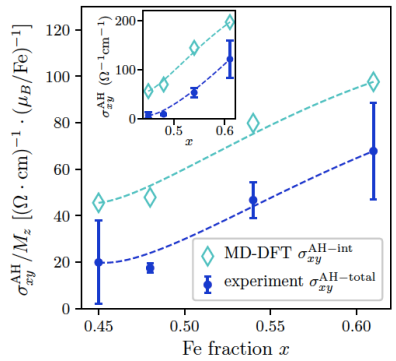

Fig. 2 Theoretical and experimental anomalous Hall effect in amorphous Fe-Ge. [Bouma, subm PRB]

2. Generalizing interfacial DMI effects to complex multicomponent systems we demonstrated chiral ferrimagnetism in Ir(Pt)/*a*-Gd-Co/Pt films. Symmetric (Pt/*a*-Gd-Co/Pt) and asymmetric (Ir/*a*-GdCo/Pt) multilayers were characterized by X-ray magnetic circular dichroism (XMCD) spectroscopy at the ALS and Lorentz transmission electron microscopy (L-TEM) at the Molecular Foundry/NCEM. We developed and applied an analysis based on exit wave reconstruction that is superior in terms of spatial and contrast resolution to the commonly used transport-of-intensity equation. We showed that thin (2nm) *a*-Gd-Co films preserve ferrimagnetism while stabilizing chiral domain walls through a significant interfacial DMI. Depending on rare-earth composition, chiral Néel or chiral hybrid Bloch-Néel walls were found in asymmetric stacks.

3. We showed spin-orbit torque (SOT) switching of ferrimagnetic *a*-$Gd_x(Fe_{90}Co_{10})_{100-x}$ films for both TM-rich and RE-rich samples. Results indicated, surprisingly, that the sign of the SOT

switching follows the total magnetization, although transport-based techniques such as anomalous Hall effect are only sensitive to the transition metal (TM) magnetization.

4. We showed that for helicity-independent all-optical switching (HI-AOS) of *a*-Gd-Fe-Co films, the incident laser pulse duration can be as long as 15 psec, much longer than in previous work. We also showed switching can be triggered by diffusion of electronic heat currents from adjacent laser-heated layers, and that psec demagnetization of Co/Pt ferromagnetic thin films and switching of *a*-Gd-Fe-Co films is induced by psec pulses of pure electric current, unambiguously confirming the process as purely thermal.

5. We discovered new ferrimagnetic alloys that exhibit HI-AOS: *a*-Gd_xCo_{1-x} and *a*-$(Gd_{1-x}Tb_x)_{22}Co_{78}$. We observed a dramatic increase in the speed of switching of *a*-Gd-Co patterned into nanodots with dimensions down to 200 nm. In *a*-$(Gd_{1-x}Tb_x)_{22}Co_{78}$, the high Gilbert damping for Tb was expected to suppress switching, but instead we observed reliable switching for Tb concentrations as high as 18%, with a critical fluence that increased with *x* (Fig. 3), results reproduced by theory. Initial experiments using fsec XMCD for *a*-$(Gd_{1-x}Tb_x)_{22}Co_{78}$ were performed at the BESSY II slicing X-ray beamline; individual switching dynamics for Gd, Tb, and Co were measured, analysis underway. These results provide insight into the not-well understood fundamental mechanism for HI-AOS.

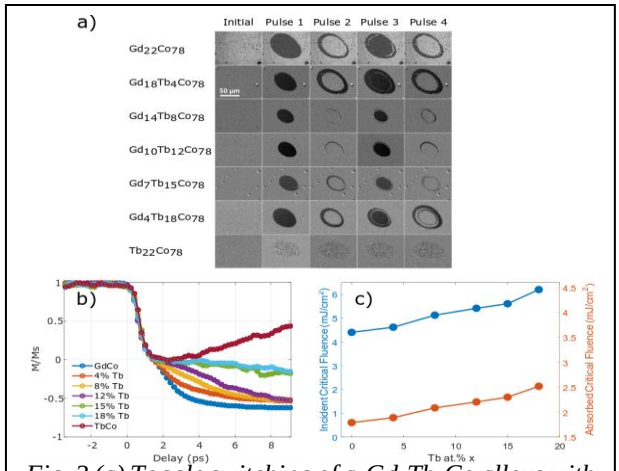

Fig. 3 (a) Toggle switching of a-Gd-Tb-Co alloys with increasing Tb at.% showing HI-AOS up to 18 at.%Tb, above which the critical fluence (c) exceeds the threshold for film damage. b) shows increasingly slow re-magnetization with increasing Tb at.%.

6. We carried out real-time time dependent density functional theory (rt-TDDFT) simulation for laser induced demagnetization of Ni. Previous rt-TDDFT simulations failed to reproduce the experimentally observed large (~45%) demagnetization using the experimental laser fluence, a long-standing problem in this field. Our simulation, with an improved algorithm which allows larger systems, reveals that initial disorder tilting of the spin plays a critical and unappreciated role, and that electron-electron interactions are extremely important in demagnetization.

Future (select) Plans

1. ***Intrinsic anomalous Hall effect, Spin Hall effect and SOT in amorphous TM-Si, Ge:*** The high anomalous Hall effect associated with density of curvature suggests a large intrinsic spin Hall effect and SOT in related alloys. We will measure *spin Hall effect* in and *spin-orbit torque* by *a*-Fe-Ge and *a*-Fe-Si through second harmonic measurements. We have also found *a*-Co-Ge to be non-magnetic up to 63 at.% Co, similar to its crystalline counterparts; we will look for the theoretically-predicted *orbital* Hall effect; recent theory indicates a combination of MOKE and XMCD would effectively detect a orbital Hall signal. New theoretical methods will also be investigated to calculate the AHE in such amorphous systems.

2. ***Spin textures in amorphous TM-Si, Ge alloys:*** We will explore the role of spin-orbit coupling in the evolution of helical and topological phases in *a*-TM-Ge, Si alloys as a function of magnetic field and temperature. Preliminary Lorentz TEM and x-ray scattering of *a*-Fe_xGe_{1-x} show stripes, skyrmions and chiral behavior, analogous to what is seen in B20 phase FeGe crystals. All magnetic interactions in these amorphous counterparts can be tuned over a wide range by varying composition; we are specifically interested in phases where exchange, dipole, anisotropy, and

thermal energies compete. Entropy stored in the resulting thermal fluctuations can stabilize new phases and textures. Resonantly tuned coherent soft X-ray scattering, LTEM, and PEEM are powerful tools to probe static textures and their spontaneous fluctuations.

3. ***Three dimensional (3D) magnetic structures:*** There is strong evidence that for a deep understanding of even traditional skyrmions, the full three-dimensional configuration has to be taken into account e.g. chiral bobbers, skyrmion tubes, hybrid Bloch/Néel domain wall, Bloch points and lines. We will continue to develop and utilize advanced X-ray spectromicroscopy techniques, as well as state-of-the-art Lorentz TEM at the MF/NCEM to obtain all 3 spatial components of spin, with nanoscale spatial resolution.

4. ***Target skyrmions (TSks) as precursor to hopfions***: We used structural imprinting (the coupling of a structurally confined magnetic structure, e.g. a nanodisk, to a magnetic thin film system via interlayer exchange coupling or stray field interaction) to modify and control local spin textures, and observed TSks with magnetization rotation up to 4π, higher order than common skyrmion textures. TSks are possible candidates for hopfions, which are complex topologically protected magnetic structures with a spin frustration that involves all three dimensions; appropriately designed heterostructures should enable these.

5. ***Manipulation of SOT by symmetry breaking:*** Spin currents and torques depend on both the crystal space group of the high spin-orbit material as well as the atomic point group *local* to heavy atoms (high SOC) within the unit cell. For epitaxial heavy metal/FM systems, the spin-torques on the FM depends not only on anti-damping torques created by spin-current generated via the spin Hall effect but also from inverse spin galvanic effects (ISGE) sensitive to changes in the crystal space group and local point group symmetries. Examples where symmetry-breaking may lead to unconventional torques is metallic pyrochlore iridates $Bi_2Ir_2O_6O'$ and $Pb_2Ir_2O_6O'$.

6. ***Ultrafast Optical Switching:*** We previously demonstrated ultrafast optical switching of Co/Pt multilayer ferromagnets by exchange coupling to an *a*-Gd-Fe-Co ferrimagnet layer. Other groups reported similar results that were attributed to spin current emitted from the *a*-Gd-Fe-Co layer into the ferromagnet layer (ultrafast spin-Seebeck effect) causing that layer to switch. We will fabricate multilayer magnetic heterostructures using a variety of exchange coupling and spin-transport layers to test this model. The BESSY-II x-ray femtoslicing beamline will allow us to measure dynamics in the different layers of such a heterostructure.

7. ***Ultrafast Dynamics of antiferromagnets:*** We will use novel fsec laser pump-probe methods to characterize ultrafast dynamics of antiferromagnets in response to ultrafast laser and electrical excitation. To pump the AFM-heterostructures with THz electrical fields and currents, we will embed AF heterostructures into coplanar waveguide structures with integrated ultrafast photoconductive switches. We will study the ultrafast dynamics of AF heterostructures with heavy metals. By passing THz electrical currents through a heterostructure that contains a strong SOC metal, we can generate THz spin-currents and SOTs, while transiently "softening" the AF order via ultrafast non-equilibrium excitation.

8. ***Theoretical studies of femtosecond demagnetization and switching:*** We will continue *real-time time-dependent density functional theory (*rt-TDDFT) to study spin dynamics as it avoids the pitfall of analytical and perturbation theories which often ignore electron-electron interactions. Our goals are to connect spin dynamics with electronic structure dynamics, and to bridge *ab initio* with phenomenological spin dynamics described by LLG. We will use rt-TDDFT to study angular momentum transfer between spin, orbit, and lattice; as well as between different elements and materials. These rt-TDDFT simulations will answer fundamental questions related to the validity of the three-temperature model, and distinguish spin temperature from electronic temperature.

Publications since last ECMP (Oct 2017-Sept 2019): (PI, co-PI's shown in bold)

A) Publications primarily supported and intellectually driven by this FWP

1. R.B.Wilson, J. Gorchon, Y. Yang, Ch.-H. Lambert, **S. Salahuddin, J. Bokor**, *Ultrafast Magnetic Switching of GdFeCo with Electronic Heat Currents*, Phys Rev B 95, 180409(R) (2017)
2. Z. Chen, W. Jia, and **L.-W. Wang**, *SGO: An ultrafast engine for atomic structure global optimization by differential evolution*, Computer Physics Communications 219 35 (2017)
3. **F. Hellman**, A. Hoffmann, Y. Tserkovnyak, G. S. D. Beach, E. E. Fullerton, C. Leighton, A. H. MacDonald, D. C. Ralph, D. A. Arena, H. A. Durr, **P. Fischer**, J. Grollier, J. P. Heremans, T. Jungwirth, A. V. Kimel, B. Koopmans, I. N. Krivorotov, S. J. May, A. K. Petford-Long, J. M. Rondinelli, N. Samarth, I. K. Schuller, A. N. Slavin, M.D. Stiles, O.Tchernyshyov, A. Thiaville, B.L.Zink, *Interface-Induced Phenomena in Magnetism*, Rev Mod Phys 89, 025006 (2017)
4. R. B. Wilson, Y. Yang, J. Gorchon, C.-H. Lambert, **S. Salahuddin**, and **J. Bokor**, *Electric Current Induced Ultrafast Demagnetization*, Phys Rev B 96, 045105 (2017)
5. **P. Fischer**, *Magnetic imaging with polarized soft x-rays*, J Phys D **50** 313002 (2017)
6. Z. Chen, J. Li, S.-S. Li, and **L.-W. Wang**. *Curve line search for atomic structure relaxation*, Phys. Rev. B 96, 115141 (2017)
7. J. Gorchon, C.-H. Lambert, Y. Yang, A. Pattabi, R. B. Wilson, **S. Salahuddin**, and **J. Bokor**, *Single shot ultrafast all optical magnetization switching of ferromagnetic Co/Pt multilayers*, Appl. Phys. Lett. **111**, 02401(2017)
8. N. Roschewsky, C.-H. Lambert and **S. Salahuddin**, *Spin-orbit torque switching of ultra large-thickness ferrimagnetic GdFeCo*, Phys. Rev. B **96**, 064406, 2017.
9. A. Ceballos, Z. Chen, O. Schneider, C. Bordel, **L.-W. Wang, F. Hellman**. *Effect of Strain and Thickness on the Transition Temperature of Epitaxial FeRh Thin-Film*, Appl. Phys. Lett. 111, 172401 (2017)
10. J. Karel, D. S. Bouma, J. Martinez, Y. N. Zhang, J. A. Gifford, J. Zhang, G. J. Zhao, D. R. Kim, B. C. Li, Z. Y. Huang, R. Q. Wu, T. Y. Chen, and **F. Hellman**. *Enhanced Spin Polarization of Amorphous Fe_xSi_{1-x} Thin Films Revealed by Andreev Reflection Spectroscopy*, Phys. Rev. Mat. 2, 064411 (2018)
11. R. Streubel, C.-H. Lambert, N. Kent, P. Ercius, A. T. N'Diaye, C. Ophus, **S. Salahuddin** and **P. Fischer**. *Experimental Evidence of Chiral Ferrimagnetism in Amorphous GdCo Films*, Adv. Mat. 30, 1800199 (2018). Frontispiece https://doi.org/10.1002/adma.201870200
12. Z. Chen and **L.-W. Wang**. *Material genome explorations and new phases of two-dimensional MoS_2, WS_2 and ReS_2 monolayers*, Chem. Mat. 30, 18, 6242 (2018)
13. R. Streubel, N. Kent, S. Dhuey, A. Scholl, **S. Kevan** and **P. Fischer**. *Spatial and Temporal Correlations of XY Macro Spins*, Nano Letters 18, 12, 7428 (2018). Cover artwork.
14. J.C.T Lee, S.K. Mishra, V.S. Bhat, R. Streubel, B. Farmer, X. Shi, L.E. De Long, I. McNulty, **P. Fischer**, **S.D. Kevan, S. Roy**, *Textured heterogeneity in squared artificial spin ice*, Phys Rev B 99, 024406 (2018)
15. Noah Kent, Robert Streubel, Charles-Henri Lambert, Alejandro Ceballos, Soong-Gun Je, Scott Dhuey, Mi-Young Im, Felix Büttner, **Frances Hellman, Sayeef Salahuddin, Peter Fischer**, *Generation and stability of structurally imprinted target skyrmions in magnetic multilayers*, APL 115, 112404 (2019).
16. D. S. Bouma, Z. Chen, B. Zhang, F. Bruni, M. E. Flatte, R. Streubel, **L.-W. Wang**, R. Q. Wu, and **F. Hellman**, *Itinerant ferromagnetism and intrinsic anomalous Hall effect in amorphous iron-germanium*, submitted Phys. Rev. B 2019.
17. Z. Chen, J.W. Luo, **L.-W. Wang**, *The role of magnetic disorder in ultrafast demagnetization*, accepted Sci. Adv. 5, eaau8000 (2019).
18. Z. Chen, **L.-W. Wang**, *Revealing angular momentum transfer channels and timescales in the ultrafast demagnetization process of ferromagnetic semiconductors*, PNAS 2019.

B) Select Collaborative Publications (15 total)

1. A. Fernández-Pacheco, R. Streubel, O. Fruchart, R. Hertel, **P. Fischer**, and R. P. Cowburn, *Three-dimensional nanomagnetism*, Nature Comm 8:15756 (2017)
2. Y. Yang, R. B. Wilson, J. Gorchon, C.-H. Lambert, **S. Salahuddin**, and **J. Bokor**. *Ultrafast Magnetization Reversal by Picosecond Electrical Pulses*, Sci. Adv. 3, e1603117 (2017).
3. J. C. T Lee, S. J. Alexander, **S. D. Kevan, S. Roy**, B. J. McMorran, *Laguerre–Gauss and Hermite–Gauss soft X-ray states generated using diffractive optics*, Nature Photonics (2018).
4. M.-Y. Im, H.-S. Han, M.-S. Jung, Y.-S. Yu, S. Lee, S.Yoon, W. Chao, **P. Fischer**, J.-I Hong, K.-S. Lee, *Dynamics of the Bloch point in an asymmetric permalloy disk*, Nat. Comm. 10, 593 (2019).

5. X. Liu, N. Kent, A. Ceballos, R. Streubel, Y. Jiang, Y. Chai, J. Forth, **F. Hellman**, S. Shi, D. Wang, B.A. Helms, P.D. Ashby, **P. Fischer**, T.P. Russell, *Reconfigurable Ferromagnetic Liquid Droplets*, Science 365, 264 (2019).

Ultrafast Spectroscopy of Pnictides in High Magnetic Field: Strongly Nonequilibrium Physics in the 25 Tesla Split Florida-Helix Magnet

David J. Hilton[1,2] and Ilias E. Perakis[1] [1]Department of Physics, The University of Alabama at Birmingham, Birmingham AL 35294, USA and [2]Department of Physics, Baylor University, Waco, TX 76798, USA

Program Scope

Topology-protected surface transport of ultimate thinness in three-dimensional topological insulators (TIs) is breaking new ground in quantum science and technology. Yet a challenge remains on how to disentangle and selectively control surface helical spin transport from the bulk contribution. Here, we demonstrated ultrafast THz manipulation of coherent transport in topologically protected surface states. In particular, mid-infrared and terahertz (THz) photoexcitation of intraband transitions was used to enable ultrafast manipulation of surface THz conductivity in Bi_2Se_3. The unique, transient electronic state is characterized by frequency-dependent carrier relaxations that directly distinguishes the faster than the bulk surface channel. We analyzed the theoretical aspects in order to guide the experiment and understand the significance of the experimental results, so that ultra-broadband, wavelength-selective pumping can be applied to emerging topological systems for separation and control of the protected transport. This work is described in detail in Luo, L., Yang, X., Liu, X., Liu, Z., Vaswani, C., Cheng, D., Mootz, M., Zhao, X., Yao, Y., Wang, C.-Z., Ho, K.M., Perakis, I.E., Dobrowolska, M., Furdyna, J.K., Wang, J., "*Ultrafast manipulation of topologically enhanced surface transport driven by mid-infrared and terahertz pulses in Bi_2Se_3,* " Nature Communications **10**, 607 (2019).

In the next application of our modeling code, we analyzed the terahertz (THz) electrodynamics of a moderately clean A15 superconductor (SC) following ultrafast excitation to manipulate quasiparticle (QP) transport. In the lattice-distorted martensitic normal state, below the critical temperature for transition from a cubic lattice metallic phase, a photo enhancement of the THz conductivity occurs for optical pump pulses. However, the opposite is observed for THz pumping. This experimental result, analyzed theoretically here, demonstrates a wavelength-selective nonthermal control of conductivity that is distinct from sample heating. The photo enhancement persists up to an additional critical temperature, above the SC one, from a competing electronic order. In the SC state, the fluence dependence of pair-breaking kinetics together with an analytic model provides an implication for a "one photon to one Cooper pair" non-resonant energy transfer during the 35-fs laser pulse. We attributed this to strong electron-phonon coupling and influence of phonon condensation.This work is described in Yang, X., Zhao, X., Vaswani, C., Sundahl, C., Song, B., Yao, Y., Cheng, D., Liu, Z., Orth, P.P., Mootz, M., Kang, J.H, Perakis, I.E, Wang, C.-Z, Ho, K.-M, Eom, C.B, Wang, J, "*Ultrafast nonthermal*

terahertz electrodynamics and possible quantum energy transfer in the Nb_3Sn superconductor, " Physical Review B **99**, 094504 (2019)

Ultrafast terahertz (THz) pump-probe spectroscopy reveals an unusual out-of-equilibrium Cooper pair nonlinear dynamics and a nonequilibrium state driven by femtosecond (fs) photoexcitation of superconductivity (SC) in iron pnictides. Following fast SC quench via hot-phonon scattering, a second, abnormally slow (many hundreds of picoseconds), SC quench regime is observed prior to any recovery. Importantly, a nonlinear pump fluence dependence is identified for this remarkably long pre-bottleneck dynamics that is sensitive to both doping and temperature. Using quantum kinetic modeling we showed that the buildup of excitonic inter-pocket correlation between electron-hole (e-h) quasiparticles (QP) quenches SC after fs photoexcitation, which leads to a controllable long-lived, many-QP excitonic state. This was publised in Yang, X., Luo, L., Mootz, M., Patz, A., Bud'Ko, S.L., Canfield, P.C., Perakis, I.E., Wang, J. "*Nonequilibrium Pair Breaking in Ba $(Fe_{1-x}Co_x)_2As_2$ Superconductors: Evidence for Formation of a Photoinduced Excitonic State*,," Physical Review Letters 121, 267001 (2018)

Here we showed theoretically and confirmed experimentally how light-induced supercurrents can chart a path forward for electromagnetic design of emergent phases and collective modes required for quantum engineering applications. The necessary spatial-temporal modulation of the order parameter phase and amplitude remained elusive so far, but here we showed that it manifests itself via high harmonic (HH) modes beyond equilibrium symmetry. In particular, we drive moving condensate macroscopic states via light–induced sub-cycle dynamical symmetry breaking and oscillating nonlinear photocurrents. Particularly, these quantum states with broken inversion symmetry are controlled via Cooper pair acceleration by asymmetric in pulse temporal profile and multi-cycle terahertz (THz) excitations. The supercurrentcarrying states which evolve during a lightwave cycle exhibit three distinguishing features: Anderson pseudo-spin precessions forbidden by equilibrium symmetry, strong HH coherent oscillations assisted bythe pairing interaction, and long-lived gapless superfluidity with minimal condensate quench. This work indicates that lightwave acceleration and tuning of persistent photocurrents can be extended for quantum control of high-T_c cuprate and iron-based superconductors and topological matter. This work has been recently published in X. Yang, C. Vaswani, C. Sundahl, M. Mootz, L. Luo, J. H. Kang, I. E. Perakis, C. B. Eom and J. Wang, "*Lightwave-Driven Gapless Superconductivity and Forbidden Quantum Beats by Terahertz Symmetry Breaking*,," Nature Photonics **86**, 1 (2019).

References

1. X. Yang, X. Zhao, C. Vaswani, C. Sundahl, B. Song, Y. Yao, D. Cheng, Z. Liu, P. P. Orth, M. Mootz, J. H. Kang, I. E. Perakis, C. Z. Wang, K. M. Ho, C. B. Eom, and J. Wang, "*Ultrafast nonthermal terahertz electrodynamics and possible quantum energy transfer in the Nb_3Sn superconductor*," Phys. Rev. B **99**, 094504 (2019).
2.

Publications

1. Yang, X., Luo, L., Mootz, M., Patz, A., Bud'Ko, S.L., Canfield, P.C., Perakis, I.E., Wang, J. "*Nonequilibrium Pair Breaking in Ba $(Fe_{1-x}Co_x)_2As_2$ Superconductors: Evidence for Formation of a Photoinduced Excitonic State*,," Physical Review Letters 121, 267001 (2018).
2. X. Yang, C. Vaswani, C. Sundahl, M. Mootz, L. Luo, J. H. Kang, I. E. Perakis, C. B. Eom and J. Wang, "*Lightwave-Driven Gapless Superconductivity and Forbidden Quantum Beats by Terahertz Symmetry Breaking*,," Nature Photonics **86**, 1 (2019).
3. Yang, X., Zhao, X., Vaswani, C., Sundahl, C., Song, B., Yao, Y., Cheng, D., Liu, Z., Orth, P.P., Mootz, M., Kang, J.H, Perakis, I.E, Wang, C.-Z, Ho, K.-M, Eom, C.B, Wang, J, "*Ultrafast nonthermal terahertz electrodynamics and possible quantum energy transfer in the Nb_3Sn superconductor*, " Physical Review B **99**, 094504 (2019).
4. Luo, L., Yang, X., Liu, X., Liu, Z., Vaswani, C., Cheng, D., Mootz, M., Zhao, X., Yao, Y., Wang, C.-Z., Ho, K.M., Perakis, I.E., Dobrowolska, M., Furdyna, J.K., Wang, J., "*Ultrafast manipulation of topologically enhanced surface transport driven by mid-infrared and terahertz pulses in Bi_2Se_3*, " Nature Communications **10**, 607 (2019).

Project Title: Single Molecule Investigations and Manipulation of Magnetic and Superconducting Molecular Systems on Surfaces

Principal Investigator: Saw Wai Hla
Mailing Address: 251B Clippinger Lab, Physics & Astronomy Department, Ohio University, Athens, OH 45701.
Email: hla@ohio.edu

i) Program Scope

This proposal seeks to advance our understanding and control over charge and energy transfer processes as well as spintronic behaviors of exotic molecular materials including individual molecular machines and molecular superconductors on materials surfaces. For the molecular machine research, we investigate individual molecular motors, and molecular transport devices operating at the quantum regime on surfaces using advanced scanning probe techniques at low temperature in ultrahigh environment. For molecular superconductivity research, we study atomic level interactions between the molecular superconducting clusters and two dimensional electron gas as well as manipulation of molecular charge density waves. As a part of the project, we also develop novel instrumentation techniques such as synchrotron X-ray tunneling microscopy and spectroscopy to advance our fundamental understanding of materials properties in quantum regimes. Our project includes both conventional and innovative components, and the achievements of these projects will impact on fundamental understanding of charge and energy transfer processes in exotic molecular materials for potential applications in energy sciences.

ii) Recent Progress

Synthetic molecular machines are fascinating and have a great promise to revolutionize scientific and technological fields. The molecular machines designed to operate on materials surfaces can convert energy into motion and they may be useful to incorporate into solid state devices. The immense interest on this research area is evident by the 2016 Nobel Prize in Chemistry awarded for the "design and synthesis of molecular machines". We have contributed a number of important results in this area supported by the previous DOE funded projects [1,2]. Here, we develop a multi-component molecular propeller that enables unidirectional rotation suitable to operate on a material surface when energized. Our molecular propeller is composed of three components. A ratchet shape molecular gear as a base, a tri-blade propeller, and a ruthenium atom acting as an atomic ball bearing. The rotor blades of the propeller are composed of three indazole groups that are arranged in a chelating tripodal manner and bind to a ruthenium (Ru) atom in a facial mode while retaining thioester (SEt) groups at the opposite ends (Fig. 1a and 1b). The stator is composed of a cyclopentadienyl center (Cp) with five *p*-bromophenylene ($Cp(PhBr)_5$) units covalently attached to it. The Ru atom is coordinated to both the stator and to the three propeller blades (Fig. 1).

An important aspect of molecular machine development is to test the mechanical properties and operations of individual molecular machines. In particular, fundamental understandings on how charge and energy transfer are taken place and how the transferred energy is utilized for mechanical motion at the single machine level are critically important for the progress of this research field. We use three scanning tunneling microscope (STM) tip manipulation schemes;

electric field induced rotation, inelastic electron tunneling induced rotation, and rotation by mechanical force to investigate unidirectional rotation of the molecular propeller one-at-a-time basis. In the electric field induced rotations, the propeller rotates by using the electrical energy supplied from the STM tip. Here, the propeller can be rotated by the tip scanning with a high voltage above ±1V during acquisition of images, as well as by positioning the tip statically above or beside the molecule. The threshold electric field of 0.25 V/Å required for the rotation is determined from the slope of the linear relationship between the negative threshold voltage and the tip height. Using this value, the electrical energy stored in the molecular propeller is calculated as -0.66 eV.

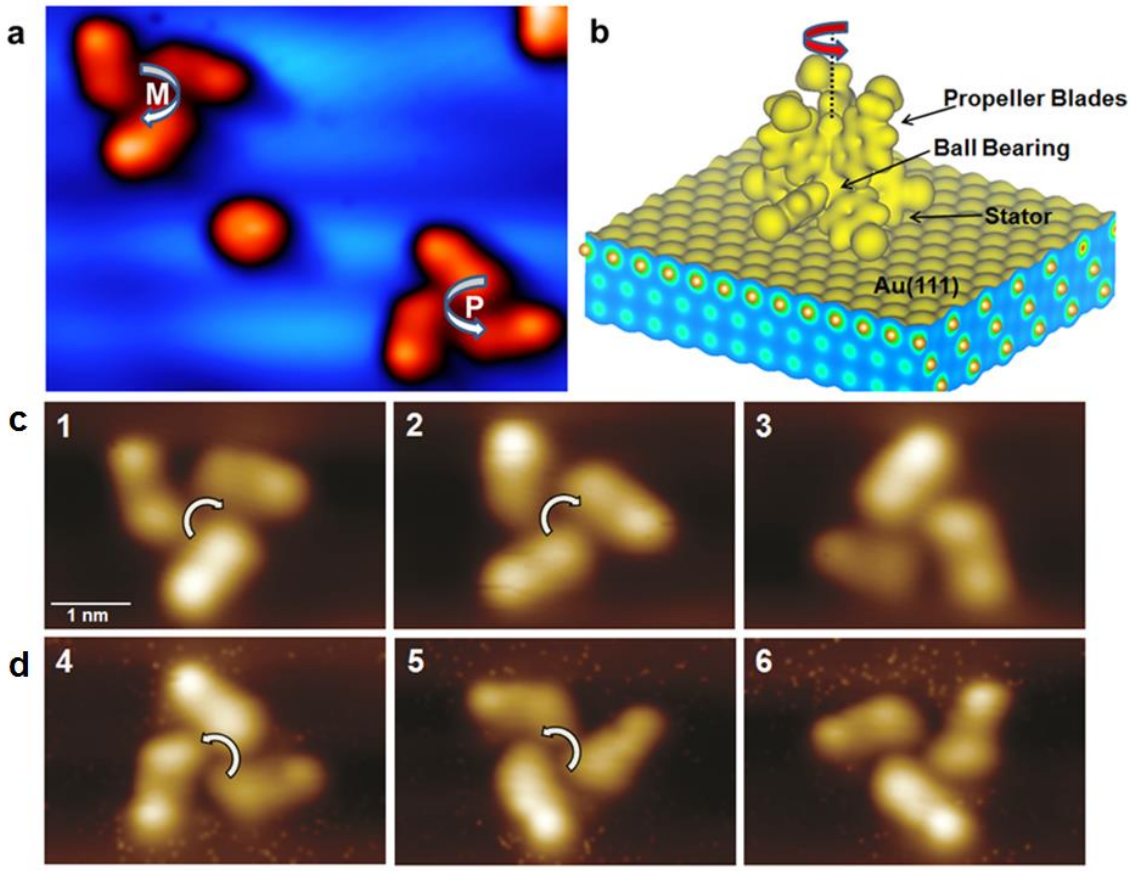

FIG. 1. **a**, *STM image of two molecular propellers on Au(111) showing left (M) and right (P) handed chirality. b, A calculated 3D charge density of propeller. c, and d: Clockwise and counterclockwise rotations.*

While a low current is used for the electric field induced rotation, inelastic tunneling electron induced rotation are performed with a high current above 2nA at positive biases. The IET induced rotation is initiated by the transfer of electron energy from inelastic tunneling electrons via temporary electron attachment to the lowest unoccupied molecular orbital (LUMO) of the molecular propeller. For the force induced rotations, a mechanical energy supplied from the STM tip via a tip-molecule contact triggers the rotation events. The step-wise mechanical rotation of the molecular propeller further provides information on the detailed rotation mechanism, which reveals that swinging of the propeller blades occur before proceeding to a full rotation (Fig. 2). Moreover, we are able to directly visualize the rotation steps of the individual propellers for both left and right handed geometries (Fig. 1c and 1d). The experimental results are corroborated by density functional theory calculations of the molecular propeller structure on the surface, which

reveals tilting of the stator phenyl rings resulted in forming a ratchet shape gear (Fig. 1b). The rotational direction of the molecular propeller is then dictated by this ratchet shape gear leading to clockwise or counterclockwise rotations of the propeller blades when it is energized. Moreover, by means of scanning tunneling microscope manipulation, the rotation steps of individual molecular propellers are directly visualized, which confirms the unidirectional rotations of both left and right handed molecular propellers into clockwise and anticlockwise directions respectively.

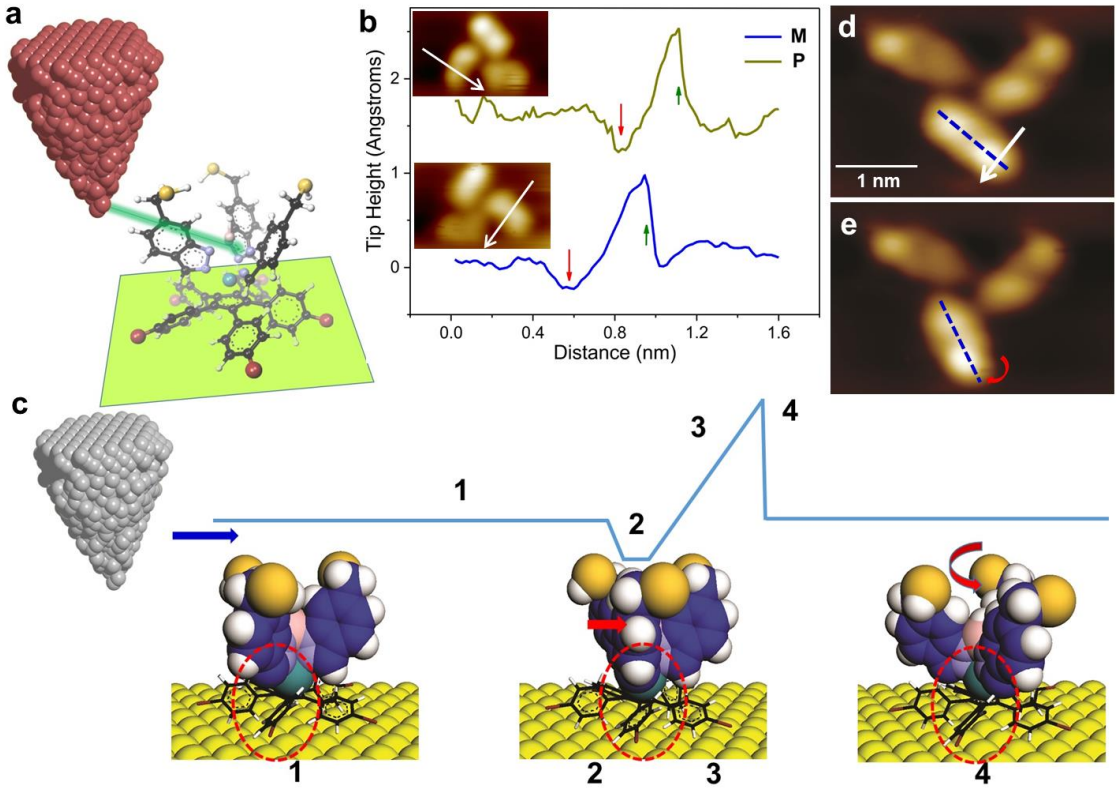

FIG. 2. ***a***, A drawing depicting the mechanical rotation. **b,** Mechanical manipulation signals during a single step rotation of M and P propellers. Inset: The arrows indicate the path and direction of manipulations. **c**, The mechanical rotation process. The dashed circles indicate the propeller bottom and the position of a phenyl ring underneath. **d,** STM image before and '**e**' after a single propeller blade rotation. White arrow in '**d**' indicates the manipulation direction.

iii) Future Plans

We are completing a number of research works under this project. For spintronic behavior of molecular motors, we have completed the DFT theory investigations of transient Kondo effect (experiments have previously been completed). We have also completed the electronic structural investigations of molecular charge density waves and molecular superconductivity related phenomena in a new charge transfer organic salt system on Ag(111) surface using low temperature tunneling microscopy and tunneling spectroscopy. For the molecular magnetism, we have measured spintronic behavior of Co-porphyrin (TBrPP-Co) molecules adsorbed on Fe film grown on Au(111) substrate by using the nascent synchrotron X-ray scanning tunneling microscopy (SX-STM) method at the world first user dedicated XTIP beamline in Advanced Photon Source, where the PI is responsible for part of the design and construction of this beamline. We have recently secured a beamtime allocation in Fall 2019 to simultaneously image magnetic, elemental,

structural, and chemical contrast of individual magnetic molecules and molecular motors using SX-STM technique. Results from these experiments are expected to make significant impact on our understanding of charge and energy transfer processes occurring in quantum regimes as well as control over these process to design novel materials and systems.

iv) References

[1] Y. Zhang, H. Kersell, R. Stefak, J. Echeverria, V. Iancu, U.G.E. Perera. Y. Li, A. Deshpande, K.-F. Braun, G. Rapenne, C. Joachim, & S.-W. Hla. ***Nature Nanotechnology*** **11**, 706-711 (2016).

[2] U.G.E. Perera. F. Ample, H. Kersell, Y. Zhang, G. Vives, J. Echeverria, M. Grisolia, G. Rapenne, C. Joachim, & S.-W. Hla. ***Nature Nanotechnology*** **8**, 46-51 (2013).

v) List of Publications Acknowledging Current DOE Grant (from 09/2017 to date)

1. Y. Zhang, J. P. Calupitan, T. Rojas, R. Tumbleson, G. Erbland, C. Kammerer, T. M. Ajayi, S. Wang, L. A. Curtiss, A. T. Ngo, S. E. Ulloa, G. Rapenne, & S.- W. Hla. A chiral molecular propeller designed for unidirectional rotations on a surface. ***Nature Communications*** **10**, 3742 (2019).

2. Y. Zhang, S. Wang, K.-F. Braun, and S.-W. Hla. Molecular flexure and atom trapping with sexiphenyl molecules by scanning tunneling microscope manipulation. ***Surf. Sci.*** **678**, 215-221 (2018).

3. J. Niederhausen, Y. Zhang, F.C. Kabeer, Y. Garmshausen, B.M. Schmidt, Y. Li, K.-F. Braun, S. Hecht, A. Tkatchenko, N. Koch, and S.-W. Hla. Subtle fluorination of conjugated molecules enables stable nanoscale assemblies on metal surfaces. ***J. Phys. Chem. C*** **122**, 19902-18911 (2018).

4. A.T. Ngo, T. Skeini, V. Iancu, P.C. Redfern, L.C. Curtiss, and S.-W. Hla. Manipulation of origin of life molecules: Recognizing single molecule conformations in β-carotene and clhorophyll-a/β-carotene clusters. ***ACS Nano*** **12**, 217-225 (2018).

5. H. Chang, N. Shirato, Y. Zhang, J. Hoffman, D. Rosenmann, J.W. Freeland, A. Bhattacharya, V. Rose, and S.-W. Hla. X-ray magnetic circular dichroism and near-edge X-ray absorption fine structure of buried interfacial magnetism measured by using a scanning tunneling microscope tip. ***Appl. Phys. Lett.*** **113**, 061602 (2018).

6. Y. Li, A. Ngo, A. DiLullo, K.Z. Latt, H. Kersell, B. Fisher, P. Zapol, S.E. Ulloa, and S.-W. Hla. Anomalous Kondo resonance mediated by semiconducting graphene nanoribbons in a molecular heterostructure. ***Nature Communications*** **8**, 946 (2017).

7. H. Kersell, N. Shirato, M. Cummings, H. Chang, D. Miller, D. Rosenmann, S.-W. Hla, and V. Rose. Detecting element specific electrons from a single cobalt nanocluster with synchrotron X-ray scanning tunneling microscopy. ***Appl. Phys. Lett.*** **111**, 103102 (2017).

Strong Negative Magnetization in Magnetic Heterostructures

Mikel Holcomb, Department of Physics & Astronomy, West Virginia University
Co-PI: Aldo Romero, Department of Physics & Astronomy, West Virginia University

Program Scope

Oxygen vacancies play a significant, yet not always well understood, role in many complex oxide systems.[1,2] The research goal of this work is to understand how oxygen vacancies affect magnetization and magnetoelectric coupling in $La_xSr_{1-x}MnO_3$ (LSMO) and LSMO/$BaTiO_3$ model heterostructures with a collaborative experimental and theoretical approach. Electrical control of this magnetic material is actually not surprising if we also observe that pure $SrMnO_3$ was theoretically predicted,[3] and later experimentally corroborated,[4] to be, by itself, one of the few single-phase multiferroic materials when a small strain is applied. Similar systems, including those Holcomb has studied, are well known to produce magnetoelectric coupling.[5,6] Even though, experimentally, it has been found that oxygen content can have a significant effect on LSMO properties,[7,8] there is not a great deal of experimental comparison between the theoretically obtained electronic properties of LSMO and the oxygen concentration. During this study, we discovered a giant negative magnetization that is persistent throughout many films. While this negative magnetization was previously attributed to coupling with the ferroelectric material, we have also observed it in LSMO films on several substrates, and is likely not unique to LSMO. This negative magnetization only occurs for small applied magnetic fields, as would be encountered for typical device applications. This change in sign can also double the efficiency of any device sensitive to the change in magnetization, since the change in magnetization is doubled due to having access to both directions.

Recent Progress

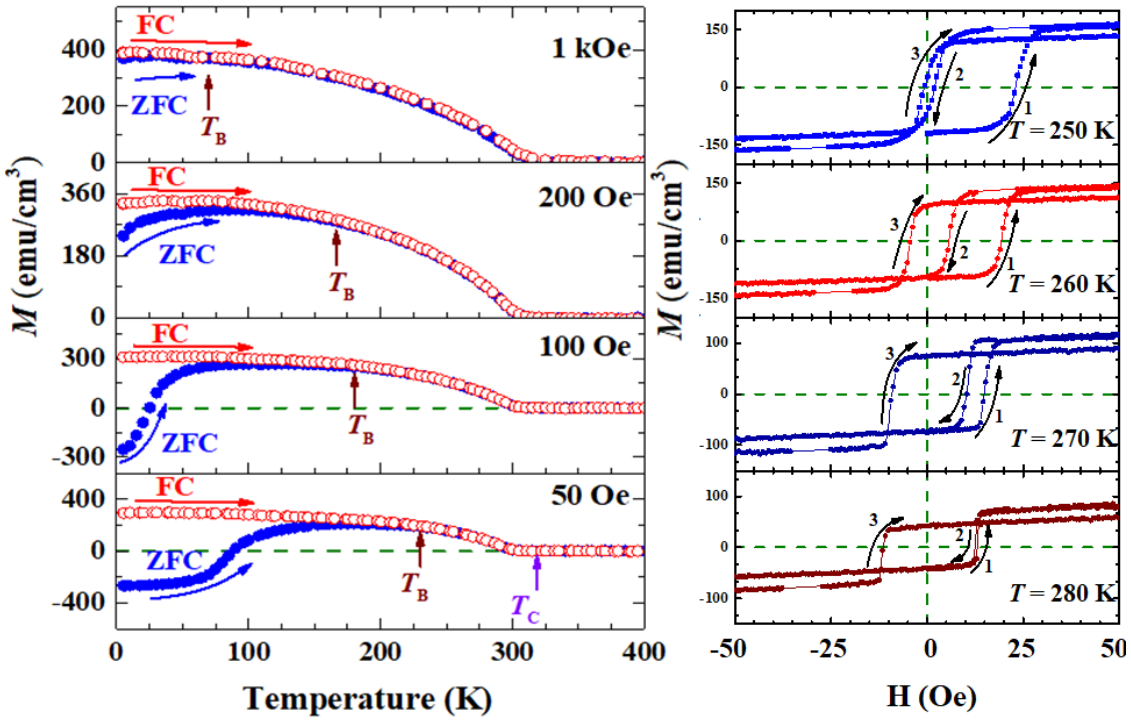

Figure 1: Magnetization with temperature and applied magnetic field for a 7.6 nm film of LSMO on $SrTiO_3$. With this treatment, negative magnetization is observed at low fields.

Depending on the sample thickness and when small external fields are applied, strong negative magnetization can be observed at low or high temperatures, including room temperature. This negative magnetization in both temperature regimes can be observed in Figure 1. Low temperature negative magnetization is observed in magnetization versus temperature curves, which are measured in a small field. However, if that field is slowly turned on as in hysteresis measurements, the negative magnetization stays through the whole temperature range. We have also confirmed this negative magnetization with both synchrotron radiation and neutron scattering measurements. An important point is that our observed negative magnetization is not removed by field cycling, which means it must be considered for technological applications. Considering that many current and future magnetic applications require small magnetic fields, it is critical to understand how the low field dynamics affect magnetization. Oxygen content affects both the saturation and negative magnetizations.

In addition to the sensitivity to oxygen content, the $La_{1-x}Sr_xMnO_3$ material family possesses a rich phase diagram that is sensitive to the Sr doping concentration. The combination of the study of oxygen and Sr content may help separate the roles of several mechanisms. The substitution of Sr^{2+} into $La^{3+}Mn^{3+}O_3^{2-}$ alters the chemical environment to include Mn^{4+}. The re-balance of charge creates a hole-doped, multivalent system. In the case of $La_{0.7}Sr_{0.3}MnO_3$ (LSMO) the balance between the Mn^{3+} and Mn^{4+} states leads to a dominant double-exchange magnetic interaction. Likewise, the excess in hole states encourages their mobility as charge carriers. These factors lead the system to take on a strongly ferromagnetic half-metal phase, having potential in spintronics. In our work we have focused on studying the role of oxygen vacancies in the magnetic structure of LSMO. In order to isolate the effects of the vacancies, the virtual crystal approximation was used to model the La/Sr atoms as it is implemented in VASP. We have studied oxygen vacancies in bulk LSMO for concentrations of 4%, 8% and 16% and under the presence of epitaxial strain between -5% and 5%. In each case, the vacancies were created using a symmetry based approach to consider only the configurations that are symmetrically inequivalent. We have calculated the changes in magnetic moment, orbital projected electronic structure, and electrical conductivity for the lowest energy configurations in each of the cases. From these calculations it was found that the presence of vacancies tends to increase the magnetic moment, to decrease the electrical conductivity, and to transition towards short range or long range antiferromagnetic order with increasing vacancy concentration. Additionally, the system tends towards orbital ordering in the presence of a vacancy as demonstrated in Figure 2.

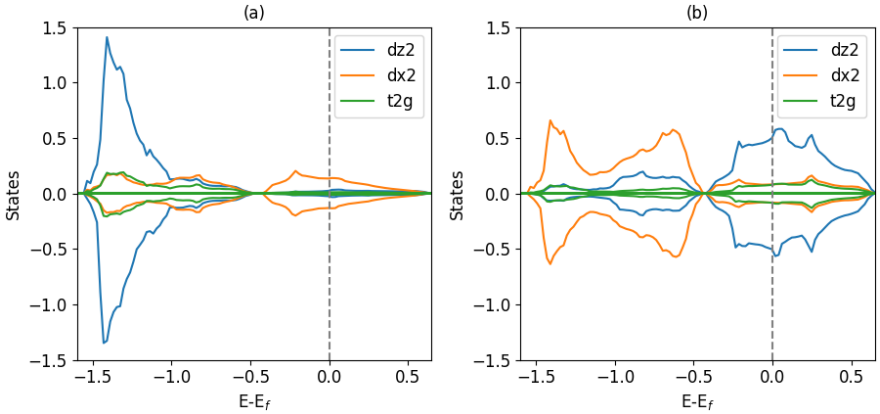

Figure 2: Orbital projected DOS for one vacancy per unit cell for Mn (a) neighboring the vacancy and (b) away from the vacancy.

Future Plans

The primary goal of our no cost extension period is to finish up a few experiments and calculations that will allow us to wrap up several papers on understanding these oxygen vacancy effects. Ongoing, we

are calculating the magnetic exchange coupling parameters in an effort to clarify the correlations between the vacancies, magnetic order, and orbital occupation, using a Green's function approach in a Wannier function basis is used as implemented in the TB2J code. Using the results found in the bulk material, We are interested in the impact of oxygen vacancy defects on the ferroelectric and magnetic structure and the magnetoelectric coupling in heterostructures of LSMO with polar materials. By first considering the effects of the vacancies in the bulk material, observations in the LSMO heterostructures can be distinguished and attributed among the presence of vacancies, epitaxial strain, interface effects, and substrate polarization. We have created heterostructures between ferromagnetic LSMO and ferroelectric $BaTiO_3$ (BTO). The structures were built from 5 unit cells of Ba-O terminated BTO. Structural optimizations are ongoing for 9 variations of pristine LSMO/BTO. The structure combinations are comprised of 3 different thicknesses of LSMO and 3 variations of the polarization. By considering LSMO layers of 4, 6 and 8 unit cells, the effects of film thickness can also be investigated. Likewise, the two polarization directions of BTO as well as the paraelectric phase are considered in order to learn the effect of the polarization and switching on the vacancies. After the ground-states for the pristine structures are obtained, we will introduce vacancies according to the minimum energy trends found in the bulk study. Calculations from each of the structure combinations will be correlated to draw conclusions on the control over vacancy migration, ferroic structures, and conductivity for the polar interface. Similarly, we are now also calculating the vibrational properties of the alloy. For that, we are using several methods to check which one is able to describe the thermal properties correctly. We are using the frozen core method as implement in PHONOPY, where the forces are obtained from VASP. We are also using density functional perturbation theory as implemented in VASP. Last resource is to use a renormalize value of the interatomic force constants of the alloy based on the dynamical matrices of the pristine materials.

References

1. Pacchioni G, "Oxygen Vacancy: The Invisible Agent on Oxide Surfaces," *Chem Phys Chem* **4**, 1041 (2003).
2. Jeen H, Choi WS, Biegalski MD, Folkman CM, Tung IC, Fong DD, Freeland JW, Shin D, Ohta H, Chisholm MF, and Lee HN, "Reversible Redox Reactions in an Epitaxially Stabilized $SrCoO_x$ Oxygen Sponge," *Nature Materials* **12**, 1057 (2013).
3. Lee JH and Rabe KM, "Epitaxial-Strain-Induced Multiferroicity in $SrMnO_3$ from First Principles," *Phys. Rev. Lett.* **104**, 207204 (2010).
4. Becher C, Maurel L, Aschauer U, Lilienblum M, Magén C, Meier D, Langenberg E, Trassin M, Blasco J, Krug IP, Algarabel PA, Spaldin NA, Pardo JA and Fiebig M, "Strain-induced Coupling of Electrical Polarization and Structural Defects in $SrMnO_3$ Films," *Nature Nanotechnology* **10**, 661–665 (2015).
5. Zhou J, Tra VT, Dong S, Trappen R, Marcus MA, Jenkins CA, Wolfe E, Frye C, Polisetty S, Lin J-L, Chu Y-H and Holcomb MB, "Thickness Dependence of $La_{0.7}Sr_{0.3}MnO_3/PbZr_{0.2}Ti_{0.8}O_3$ Magnetoelectric Interfaces," *Applied Physics Letters* **107**, 141603 (2015).
6. Huang C-Y, Zhou J, Tra VT, White R, Trappen R, N'Diaye AT, Spencer M, Frye C, Cabrera GB, Nguyen V, LeBeau JM, Chu Y-H, Holcomb MB, "Imaging Magnetic and Ferroelectric Domains and Interfacial Spin in Magnetoelectric $La_{0.7}Sr_{0.3}MnO_3/PbZr_{0.2}Ti_{0.8}O_3$ Heterostructures," *J. Phys.: Conden. Matt.* **27**, 504003 (2015).
7. De Léon-Guevara AM, Berthet P, Berthon J, Millot F, Revcolevschi A, Anane A, Dupas C, Le Dang K, Renard JP and Veillet P, "Influence of Controlled Oxygen Vacancies on the Magnetotransport and Magnetostructural Phenomena in La0.85Sr0.15MnO3−δ Single Crystals," *Phys. Rev. B* **56**, 6031 (1997).
8. Wilson ML, Byers JM, Dorsey PC, Horwitz JS, Chrisey DB and Osofsky MS, "Effects of Defects on Magnetoresistivity in La0.7Sr0.3MnO3," *J. Appl. Phys.* **81**, 4971 (1997).

Publications

1. Yousefi S, Singh S, Garcia-Castro AC, Trappen R, Mottaghi N, Cabrera G, Huang C-Y, Kumari S, Bhandari G, Bristow A, Romero A, Holcomb MB, "Surface recombination in ultra-fast carrier dynamics of perovskite oxide $La_{0.7}Sr_{0.3}MnO_3$ thin films," *ACS Nano* **13** (3), 3457 (2019). https://pubs.acs.org/doi/10.1021/acsnano.8b09595

2. Sarraf SY, Trappen R, Kumari S, Bhandari G, Mottaghi N, Huang CY, Cabrera GB, Bristow AD, Holcomb MB, "Application of wavelet analysis on transient reflectivity in ultra-thin films," *Optics Express* **27**, 14684 (2019). https://doi.org/10.1364/OE.27.014684
3. Pradhan DK, Mishra AK, Kumari S, Basu A, Somayazula M, Gradauskaite E, Smith RM, Gardner J, Turner PW, N'Diaye AT, Holcomb MB, Katiyar RS, Zhou P, Srinivasan G, Gregg JM, Scott JF, "Studies of Multiferroic Palladium Perovskites," *Scientific Reports* **9**, 1685 (2019). https://doi.org/10.1038/s41598-018-38411-8
4. Trappen R, Garcia-Castro AC, Tra V, Huang C-Y, Ibarra-Hernandez W, Penn A, Singh S, Zhou J, Cabrera G, Chu Y-H, LeBeau J, Dong S, Romero A, Holcomb MB, "Electrostatic potential and valence modulation in $La_{0.7}Sr_{0.3}MnO_3$ thin films," *Scientific Reports* **8**, 14313 (2018). https://rdcu.be/7HKI
5. Mottaghi N, Trappen R, Kumari S, Huang C-Y, Yousefi S, Cabrera G, Azizha M, Haertter A, Johnson M, Seehra MS, Holcomb MB, "Observation and interpretation of negative remanant magnetization and inverted hysteresis loops in a thin film of $La_{0.7}Sr_{0.3}MnO_3$," *J. of Phys. Cond. Matt.*, **30,** 405804 (2018). http://iopscience.iop.org/article/10.1088/1361-648X/aade14
6. Mottaghi N, Seehra MS, Trappen R, Kumari S, Huang C-Y, Yousefi S, Cabrera G, Romero AH, Holcomb MB, Insights into the magnetic dead layer in $La_{0.7}Sr_{0.3}MnO_3$ thin films from temperature, magnetic field and thickness dependence of their magnetization," *AIP Advances* **8**, 056319 (2018). https://doi.org/10.1063/1.5005913
7. Ibarra-Hernandez W, Hajinazar S, Avendano-Franco G, Bautista-Hernandez A, Kolmogorov AN, Romero AH, "Structural search for stable Mg-Ca alloys accelerated with a neural network interatomic model," *Physical Chemistry Chemical Physics* **20**, 27545 (2018) https://doi.org/10.1039/c8cp05314f
8. Singh S, Wu QS, Yue CM Romero AH, Soluyanov AA, "Topological phonons and thermoelectricity in triple-point metals," *Physical Review Materials* **2**, 114204 (2018). https://doi.org/10.1103/PhysRevMaterials.2.114204
9. Trappen R, Zhou J, Tra VT, Huang C-Y*, Marcus M, Chu Y-H, Dong S, and Holcomb MB, "Nondestructive depth-dependent atomic valence determination by synchrotron techniques," *Journal of Synchrotron Radiation* **25** (2018). https://onlinelibrary.wiley.com/doi/abs/10.1107/S1600577518011724
10. Reparaz JS, da Silva KP, Romero AH, Serrano J, Wagner MR, Callsen G, Choi SJ, Speck JS, Goni AR, "Comparative study of the pressure dependence of optical-phonon transverse-effective charges and linewidths in wurtzite InN," *Physical Review B* **98**, 165204 (2018). https://doi.org/10.1103/PhysRevB.98.165204
11. Singh S, Espejo C, Romero AH, "Structural, electronic, vibrational, and elastic properties of graphene/MoS2 bilayer heterostructures," *Physical Review B* **98**, 155309 (2018). https://doi.org/10.1103/PhysRevB.98.155309
12. Garcia-Castro AC, Ibarra-Hernandez W, Bousquet E, Romero AH, "Direct Magnetization-Polarization Coupling in $BaCuF_4$," *Physical Review Letters* **121**, 117601 (2018). https://doi.org/10.1103/PhysRevLett.121.117601
13. Romero AH and Verstraete MJ, "From one to three, exploring the rungs of Jacob's ladder in magnetic alloys," *European Physical Journal B* **91**, 193 (2018). https://doi.org/10.1140/epjb/e2018-90275-5
14. Rodriguez-Fernandez C, Almokhtar M, Ibarra-Hernandez W, de Lima MM, Romero AH, Asahi H, Cantarero A, "Isotopic Heft on the B-1/ Silent Mode in Ultra-Narrow Gallium Nitride Nanowires," *Nano Letters* **18**, 5091 (2018). https://doi.org/10.1021/acs.nanolett.8b01955
15. Payne A, Avendano-Franco G, Bousquet E, Romero AH, "Firefly Algorithm Applied to Noncollinear Magnetic Phase Materials Prediction," *Journal of Chemical Theory and Computation* **14**, 4455 (2018). https://doi.org/10.1021/acs.jctc.8b00404
16. Trevino P, Garcia-Castro AC, Lopez-Moreno S, Bautista-Hernandez A, Bobocioiu E, Reynard B, Caracas R, Romero AH, "Anharmonic contribution to the stabilization of Mg(OH)(2) from first principles," *Physical Chemistry Chemical Physics* **20**, 17799 (2018). https://doi.org/10.1039/c8cp02490a
17. Di Gennaro M, Miranda AL, Ostler TA, Romero AH, Verstraete, "Competition of lattice and spin excitations in the temperature dependence of spin-wave properties," *Physical Review B* **97**, 214417 (2018). https://doi.org/10.1103/PhysRevB.97.214417
18. Pramanik P, Singh S, Joshi DC, Mallick A, Pisane K, Romero AH, Thota S, Seehra MS, "Cubic phase stability, optical and magnetic properties of Cu-stabilized zirconia nanocrystals," *Journal of Physics D Applied Physics* **51**, 225304 (2018). https://doi.org/10.1088/1361-6463/aac004
19. Singh S, Valencia-Jaime I, Pavlic O, Romero AH, "Elastic, mechanical, and thermodynamic properties of Bi-Sb binaries: Effect of spin-orbit coupling," *Physical Review B* **97**, 054108 (2018). https://doi.org/10.1103/PhysRevB.97.054108
20. Ouma CNM, Singh S, Obodo KO, Amolo GO, Romero AH, "Controlling the magnetic and optical responses of a MoS2 monolayer by lanthanide substitutional doping: a first-principles study," *Physical Chemistry Chemical Physics* **19**, 25555 (2017). https://doi.org/10.1039/c7cp03160b

Search for 3D Topological Superconductors using Laser-Based Spectroscopy

Principal Investigator: David Hsieh
Mailing Address: 1200 E. California Blvd., MC 149-33, California Institute of Technology, Pasadena, CA 91125
E-mail: dhsieh@caltech.edu

(i) Program Scope

The goal of this program is to experimentally identify novel parity-breaking electronic liquid crystalline (PB-ELC) phases of matter in strongly spin-orbit coupled correlated electron systems, which have been predicted to be precursors to the elusive three-dimensional topological superconducting state[1,2]. In 2015, it was theoretically proposed that several different classes of PB-ELCs could exist and might be realized in certain 5*d* transition metal oxide compounds[3]. In 2017, we uncovered the first evidence of a PB-ELC belonging to the "multipolar nematic" class in $Cd_2Re_2O_7$[4]. Over the past two years, we have focused on searching for additional families of PB-ELCs and devising methods to tune them towards a 3D topological superconducting state.

(ii) Recent Progress

Evidence of the decoupled electron mechanism in the polar metal $LiOsO_3$

A PB-ELC with a vector order parameter belongs to the "ferroelectric" class[3]. However metals that spontaneously develop a polar axis are exceedingly rare because any charge polarization will typically be screened by free carriers. In 2013, the first example of a material that undergoes a spontaneous non-polar to polar metal transition was reported in $LiOsO_3$ across a critical temperature T_c = 140 K[5]. Owing to the presence of strong spin-orbit coupling and correlations in $LiOsO_3$, it was suggested that its low temperature phase may be a ferroelectric PB-ELC[3]. To better understand the low temperature phase, we first addressed the question of how a polar axis can coexist with metallicity. Previous theoretical works have suggested that such non-polar to polar metal transitions can occur if the free carriers are decoupled from the soft transverse optical phonons responsible for polar order[6,7]. However, this so-called decoupled electron mechanism (DEM) has yet to be experimentally observed. To test the DEM picture in $LiOsO_3$, we performed ultrafast optical pump-probe experiments on a single crystal, which are capable of ascertaining how efficiently photo-generated carriers relax via various phonon decay channels and are therefore well-suited to study how the electron phonon coupling strength varies across different phonon modes in $LiOsO_3$. By analyzing the reflectivity transients using a three-temperature model, we found that intra-band photo-carriers in $LiOsO_3$ relax by selectively coupling to only a subset of its phonon spectrum, leaving as much as 60 % of the lattice heat capacity decoupled. This decoupled heat capacity is shown to be consistent with a previously undetected and partially displacive transverse optical polar mode, indicating the DEM in $LiOsO_3$. These results could aid in the identification and design of larger families of ferroelectric type PB-ELC candidates.

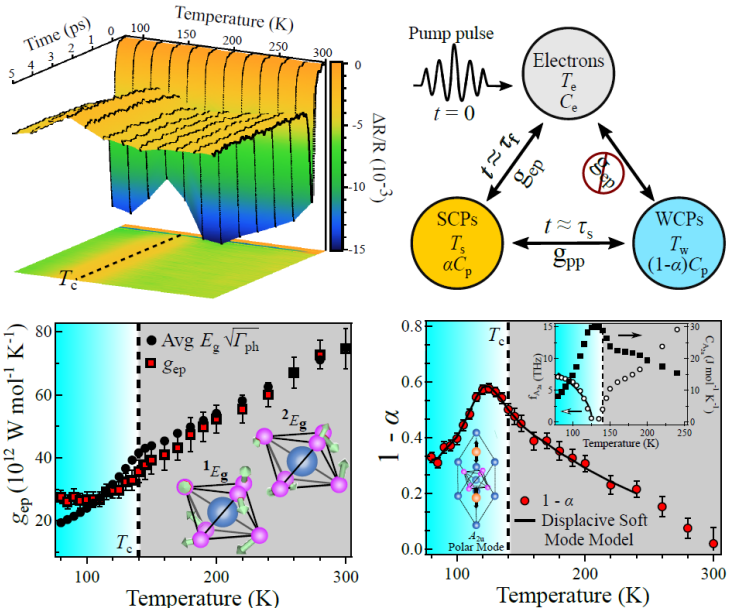

Top: Time-resolved reflectivity data of $LiOsO_3$ (left) and a three-temperature model of the relaxation dynamics (right) in which the photo-carriers selectively couple to a subset of strongly coupled phonons (SCPs) through electron-phonon coupling, whereas the remaining weakly coupled phonons (WCPs) only thermalize via coupling with the SCPs.

Bottom: Electron-phonon coupling (left) and uncoupled heat capacity (right) extracted through the application of the three-temperature model. This analysis revealed that excited electrons only couple to Os and O phonon modes and not to the Li soft mode responsible for polar order.

Detecting polar fluctuations in the para-electric phase of $LiOsO_3$

Although our time-resolved optical reflectivity studies indicate the presence of a displacive transverse optical polar mode associated with Li ion displacements in $LiOsO_3$, this mode was not detected by previous Raman spectroscopy experiments[8]. This suggests an order-disorder character to the transition at T_c, where local electric dipole moments are already formed far above T_c and long-range polar order is established at T_c through short-range dipolar interactions. To experimentally test this scenario, we sought to detect the presence of short-range dipole-dipole correlations above T_c in the para-electric phase. Although a direct detection of polar fluctuations is challenging, its presence can be inferred through changes in the lattice structure owing to electrostriction. Rotational anisotropy second harmonic generation (RA-SHG) is a technique that is particularly adept at resolving small changes in lattice structure with mode specificity[9]. By performing detailed angle-of-incidence dependent RA-SHG measurements on a $LiOsO_3$ single crystal, we found that electrostriction onsets near 220 K, indicating that local electric dipole moments are formed well above T_c. Moreover we found that the drastic changes in the RA patterns that are observed in this interval arise from anisotropic changes in the Os-O and Li-O bond polarizabilities upon cooling, possibly due to spatially anisotropic dipole-dipole correlations. These results confirm a significant order-disorder character of the polar transition and, more generally, showcase a novel approach to measuring polar fluctuations.

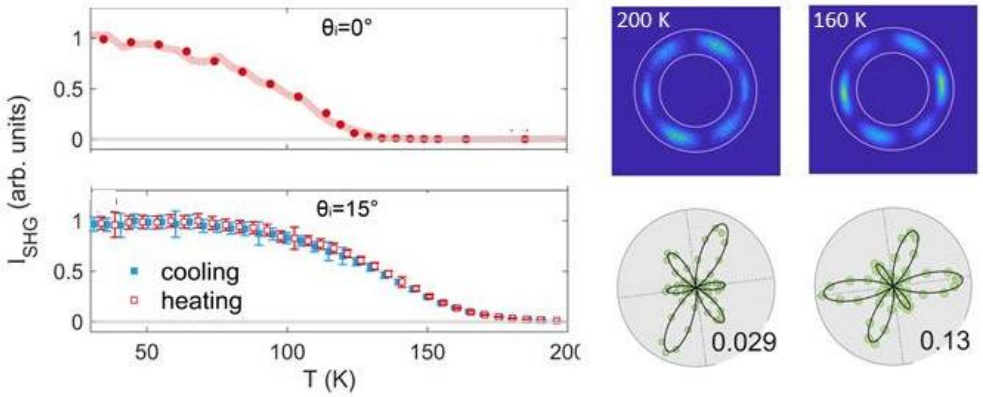

Left: Temperature dependence of SHG intensity from $LiOsO_3$ for normal (top) and oblique (bottom) angle-of-incidence geometry. The oblique geometry is sensitive to the electric quadrupole SHG contribution, which encodes the electrostriction above T_c.
Right: Raw (top) and radially integrated (bottom) RA-SHG data at 200 K and 160 K, showing a drastic change in shape takes place inside the fluctuation window.

(iii) Future Plans

To study the role correlations play in driving the polar transition of $LiOsO_3$, which is important for assessing the possibility of it hosting a ferroelectric PB-ELC phase, we will tune the electronic bandwidth using pressure and track characteristics of the transition using the optical spectroscopy methods described above. We are also interested in performing RA-SHG measurements on $Cd_2Re_2O_7$ under pressure to study if and how the multipolar nematic phase boundary intersects the superconducting dome that is known to exist in the temperature versus pressure phase diagram[10]. This will provide insight into whether a 3D topological superconducting state is stabilized. Over the past year, we optimized and tested a home-built diamond anvil cell based high pressure optical cryostat that can reach a pressure of at least 17 GPa and can be tuned *in situ*. A laser-based ruby fluorescence system has also been built and electronically controlled optics are set up to allow periodic sampling of the cell pressure during measurement without changing cryostat alignment. We are currently characterizing the system performance using a test sample and will be moving on to study $LiOsO_3$ and $Cd_2Re_2O_7$ next.

(iv) References

1. Kozii, V. & Fu, L. Odd-Parity Superconductivity in the Vicinity of Inversion Symmetry Breaking in Spin-Orbit-Coupled Systems. *Phys. Rev. Lett.* **115**, 207002 (2015).
2. Wang, Y., Cho, G. Y., Hughes, T. L. & Fradkin, E. Topological superconducting phases from inversion symmetry breaking order in spin-orbit-coupled systems. *Phys. Rev. B* **93**, 134512 (2016).
3. Fu, L. Parity-Breaking Phases of Spin-Orbit-Coupled Metals with Gyrotropic, Ferroelectric, and Multipolar Orders. *Phys. Rev. Lett.* **115**, 026401 (2015).

4. Harter, J. W., Zhao, Z. Y., Yan, J.-Q., Mandrus, D. G. & Hsieh, D. A parity-breaking electronic nematic phase transition in the spin-orbit coupled metal $Cd_2Re_2O_7$. *Science* **356**, 295–299 (2017).
5. Shi, Y. *et al.* A ferroelectric-like structural transition in a metal. *Nat. Mater.* **12**, 1024–1027 (2013).
6. Anderson, P. W. & Blount, E. I. Symmetry Considerations on Martensitic Transformations: 'Ferroelectric' Metals? *Phys. Rev. Lett.* **14**, 217–219 (1965).
7. Puggioni, D. & Rondinelli, J. M. Designing a robustly metallic noncenstrosymmetric ruthenate oxide with large thermopower anisotropy. *Nat. Commun* **5**, (2014).
8. Jin, F. *et al.* Raman phonons in the ferroelectric-like metal $LiOsO_3$. *Phys Rev B* **93**, 064303 (2016).
9. Harter, J. W., Niu, L., Woss, A. J. & Hsieh, D. High-speed measurement of rotational anisotropy nonlinear optical harmonic generation using position-sensitive detection. *Opt. Lett.* **40**, 4671 (2015).
10. Malavi, P. S., Karmakar, S. & Sharma, S. M. $Cd_2Re_2O_7$ under high pressure: Pyrochlore lattice distortion-driven metal-to-nonmetal transition. *Phys. Rev. B* **93**, 035139 (2016).

(v) Publications supported by BES

1. N. J. Laurita, A. Ron, J. Shan, D. Puggioni, N. Z. Koocher, K. Yamaura, Y. Shi, J. M. Rondinelli & D. Hsieh. Evidence for the weakly coupled electron mechanism in an Anderson-Blount polar metal. *Nature Comm.* **10**, 3217 (2019).
2. K. Frohna, T. Deshpande, J. W. Harter, W. Peng, B. Barker, J. Neaton, S. Louie, O. Bakr, D. Hsieh & M. Bernardi. Inversion symmetry and bulk Rashba effect in methylammonium lead iodide perovskite single crystals. *Nature Comm.* **9**, 1829 (2018).
3. J. W. Harter, D. M. Kennes, H. Chu, A. de la Torre, Z. Y. Zhao, J.-Q. Yan, D. G. Mandrus, A. J. Millis & D. Hsieh. Evidence of an improper displacive phase transition in $Cd_2Re_2O_7$ via time-resolved coherent phonon spectroscopy. *Phys. Rev. Lett.* **120**, 047601 (2018).

Symmetry Engineering of Topological Quantum States

Jin Hu, University Arkansas

Program Scope

Topological band theory has bridged condensed matter and high energy physics. Dirac, Weyl, and Majorana fermions have found their counterparts in Dirac semimetals, Weyl semimetals, and topological superconductors. The topological character of the bands creates symmetry-protected band crossings with linearly dispersing electronic states, giving rise to exotic phenomena including chiral anomaly and surface Fermi arcs, as well as technologically useful properties such as high mobility and large linear magnetoresistance.

The protected band crossings in topological semimetals, i.e., the Dirac or Weyl points, are guaranteed by specific crystal symmetries and/or time-reversal symmetry (TRS). Symmetry breaking is expected to create, split, and annihilate Dirac/Weyl points in topological semimetals, but experimental studies have been hindered because of the difficulties to induce symmetry-breaking perturbations, particularly for crystal symmetry, in a controllable manner in most topological semimetals. In this project, the PIs propose to probe the intimate connection between symmetry and topological electronic states in topological semimetals. We propose to pursue crystal symmetry-breaking and TRS-breaking with synergistic experimental and theoretical efforts. For crystal symmetry-breaking, we will induce crystal symmetry-breaking strain in both bulk and 2D samples by using a strain apparatus and flexible substrates, respectively. For TRS-breaking, we use magnetic substitution and magnetic proximity effect in heterostructures for bulk and 2D samples respectively. We expect the realization of various new topological quantum states such as weak topological insulator, two-dimensional topological insulator (i.e., quantum spin Hall insulator), TRS-breaking Weyl state, and quantum anomalous Hall insulator via symmetry engineering.

Recent Progress

We studied how topological phase is coupled with symmetry in ZrSiS. In this work, we performed combined high-pressure magneto-transport measurements, Raman spectroscopy, x-ray diffraction, and first-principles calculations to reveal the connection between topological states and crystalline symmetry.

As shown in Fig. 1, using daphne 7373 as pressure medium for hydrostatic pressure application, our high-pressure magneto-transport and quantum oscillation experiments reveal transition-like, sharp changes in multiple quantities near a critical pressure of 7 GPa, including magnetoresistance, residual resistivity, Berry phase, effective mass, and quantum mobility. All

these observations point out to a transition from non-trivial topological state to trivial phase under pressure. To reveal the driven force of such transition, we have performed structure analysis by high pressure synchrotron x-ray diffraction on powder samples obtained from grounding single crystals. Although a structure transition has not been observed up to 40 GPa, we found an anomaly near 7 GPa in lattice constant ratio c/a obtained from the x-ray spectra refinement (Figs. 2a-b). Surprisingly, such anomaly is gone when switching to neon gas as pressure medium. Similar trend has also been observed in Raman spectrum. As shown in Figs. 2c-d, a linear dependence of Raman peak shift with pressure has been probed when using neon gas, while anomalies occur for the case of daphne, again around 7 GPa.

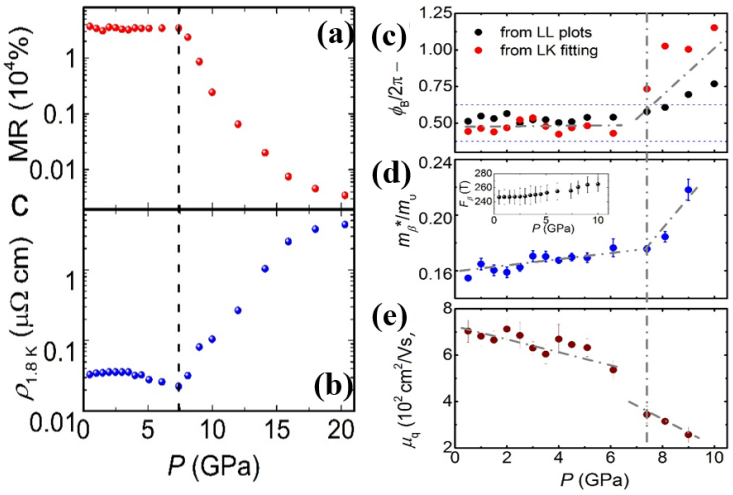

Fig. 1 Pressure dependence of (a) Normalized magnetoresistance, (b) residual resistivity at T = 1.8K, (c) Berry phase, (d) effective mass, and (c) quantum mobility. All show transition-like behavior near 7 GPa.

Given XRD and Raman spectra probe the crystal lattice, the coincidence of the anomalies near the same critical pressure in structure characterization (Fig. 2) and electronic properties (Fig. 1) implies an intimate connection between lattice and electronic state. Particularly, the sharp transition in electronic properties without drastically modification of lattice strongly implies a symmetry-breaking driven topological phase transition. Considering that neon gas is known to provide much better hydrostatic pressure over a wider range than daphne 7373, we conclude that it is the pressure gradient produced by daphne that create symmetry-breaking strain in ZrSiS, which consequently lead to a topological phase transition. This is further reinforced by our

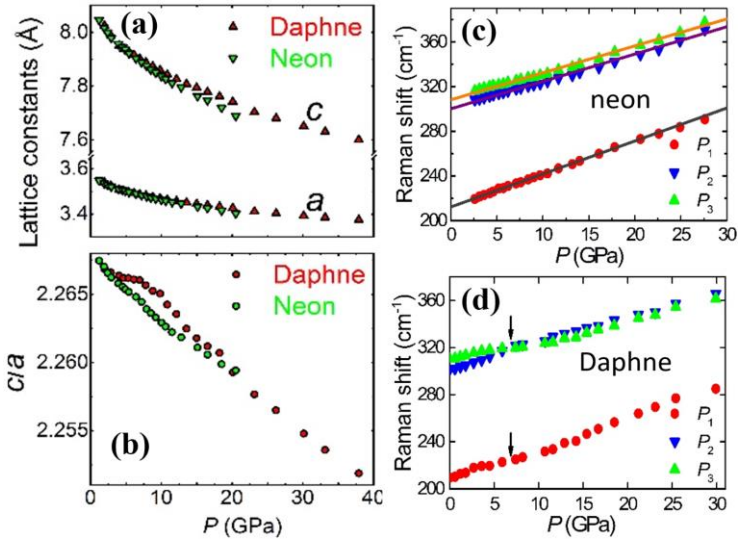

Fig. 2 (a-b) Pressure dependence of lattice constants and c/a ratio under pressure mediums of daphne liquid and neon gas. An anomaly near 7 GPa in c/a appears when using daphne. (c-d) Pressure dependence of the Raman peaks under daphne and neon. Anomalies near 7 GPa appear for daphne.

first principles calculations, which found the shear strain due to non-prefect hydrostatic compression would lead to both the mirror- and inversion-symmetry breaking. This finding provides the first direct experimental evidence for crystal symmetry protection for the topological semimetal state, which is at the heart of topological relativistic fermion physics.

Future Plans

We will extend the symmetry-breaking study by using the controllable uniaxial strain. Unlike (quasi)hydrostatic pressure, applying uniaxial strain could selectively break particular symmetry(ies) that closely related to the topological electronic state. The magnitude of strain could be read out by a capacitance stain meter, while the lattice deformation and corresponding symmetry breaking could be revealed by high precision synchrotron x-ray diffraction. Transport experiments, including quantum oscillation, chiral anomaly, and planar Hall effect will be performed to examine the evolution of the topological states.

In addition to the study on bulk single crystals, we will also use flexible substrate to apply uniaxial strain in nano-flakes. We will exfoliate thin flake of the ZrSiS-topological nodal-line family materials on flexible substrate such as Kapton, and apply *in situ* strain by using a nano positioner inside a cryostat, which enables the simultaneous strain application and low temperature magneto-transport measurement. Similar to bulk samples, the strain engineering of the topological states will be revealed by quantum oscillation, chiral anomaly, and planar Hall effect measurements.

References

C. C. Gu, J. Hu, X. L. Chen, Z. P. Guo, Y. H. Zhou, C. An, Y. Zhou, R. R. Zhang, C. Y. Xi, Q. Y. Gu, C. Park, H. Y. Shu, W. G. Yang, L. Pi, Y. H. Zhang, Z. R. Yang, J. Sun, Z. Q. Mao, and M. L. Tian, Exp*erimental evidence of crystal symmetry protection for the topological nodal line semimetal state in ZrSiS*, Phys. Rev. Lett. submitted

Publications

*The project DE-SC0019467 was started in Oct, 2018. The following lists publications over the past 11 months:

- S. H. Lee, Y. Zhu, Y. Wang, L. Miao, H. Yi, T. Pillsbury, S. Kempinger, J. Hu, C.A. Heikes, P.A. Quarterman, W. Ratcliff, J.A. Borchers, H. Zhang, X. Ke, D. Graf, N. Alem, C-Z Chang, N. Samarth and Z. Mao, *Spin scattering and noncollinear spin structure-induced intrinsic anomalous Hall effect in antiferromagnetic topological insulator* $MnBi_2Te_4$, Physical Review Research **1**, 012011(R) (2019)

- J. Hu, S.-Y. Xu, N. Ni, and Z. Mao, *Transport of Topological Semimetals*, Annual Review of Materials Research, **49**, 207-252 (2019)
- C. C. Gu, J. Hu, X. L. Chen, Z. P. Guo, Y. H. Zhou, C. An, Y. Zhou, R. R. Zhang, C. Y. Xi, Q. Y. Gu, C. Park, H. Y. Shu, W. G. Yang, L. Pi, Y. H. Zhang, Z. R. Yang, J. Sun, Z. Q. Mao, and M. L. Tian, Exp*erimental evidence of crystal symmetry protection for the topological nodal line semimetal state in ZrSiS*, Physical Review Letters, in revision

The Short-Wavelength Magnon Spectrum in YIG

J. B. Ketterson
Northwestern University

Extended Abstract

Program Scope

The major goal of this project is to verify, and follow up on, reports by the groups of B. Hillebrands and S. O. Demokritov in Germany that a dynamic Bose- Einstein Condensate (BEC) of magnons forms in yttrium iron garnet (YIG), a ferrimagnetic material known for its unusually narrow resonance linewidths. In the reported experiments a parametric microwave excitation process was used to generate an initial magnon distribution, the time evolution of which was probed by Brillouin light scattering. The primary observation was a resolution- limited buildup of spectral density at the minimum in the backward volume magnon dispersion relation. This minimum occurs due to the combined effects of the negative linear dispersion associated with this magnetostatic volume mode at longer wavelengths giving way to the positive quadratic dispersion associated with the exchange interaction at shorter wavelengths; these two behaviors result in a minimum in the dispersion relation at some finite wavevector, thereby fulfilling this requirement for BEC.

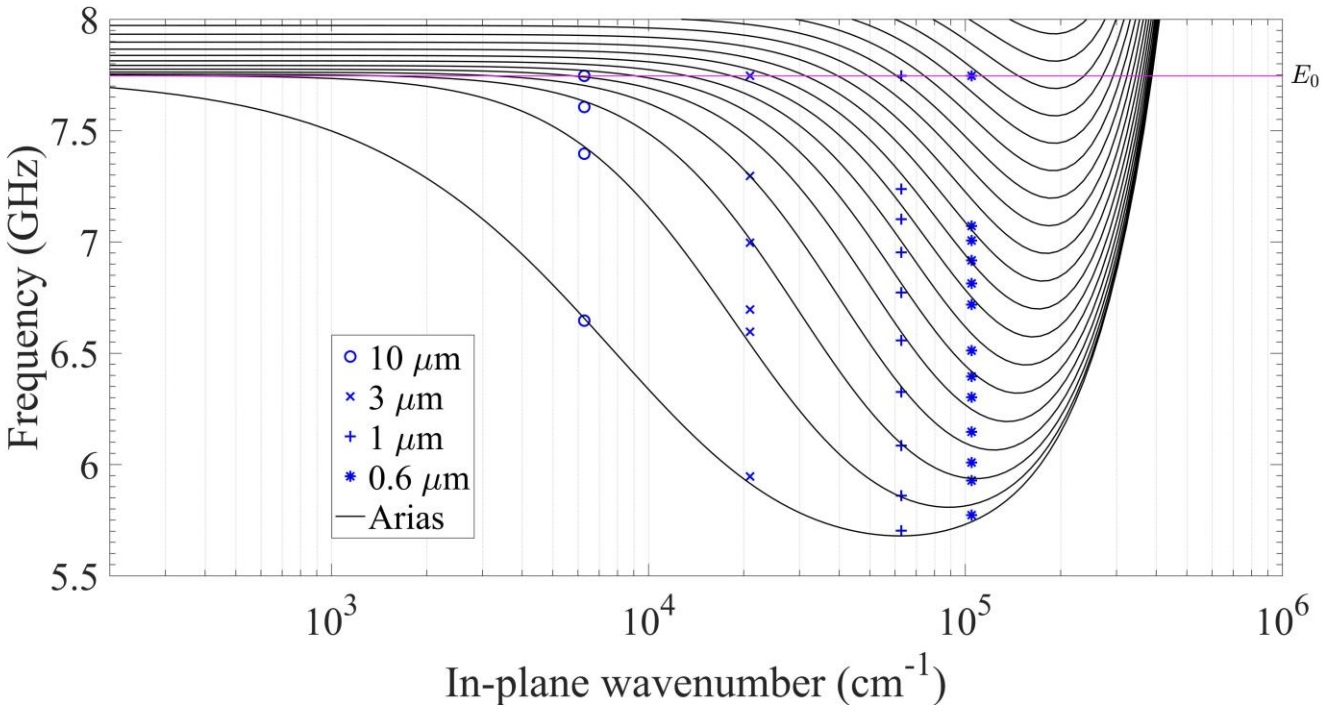

Recent Progress

The initial focus of our efforts to observe magnon BEC with purely microwave techniques is to i) better under the dispersion in the region where the condensation occurs and ii) gain a better understanding of the parametric pumping process. In connection with the first of these goals we prepared a set of wave-vector-specific multi-element antennas and characterized

the dispersion of spin waves in an yttrium iron garnet film at submicron lengths and resolved the dispersion relations of multiple backward volume modes, particularly in the region of their minima. The techniques developed now facilitate the characterization of spin waves at length scales limited only by available lithography and at a spectral resolution that greatly exceeds that of Brillouin scattering. The data obtained are in excellent agreement with theoretical predictions based on a model Hamiltonian as well as those obtained by an algebraic solution the dipole/exchange boundary value problem by Aries as shown in the figure.

In connection with the second goal, we have studied the minimum frequency associated with the backward volume (BV) spin wave branch for the magnetic field lying in plane and parallel to the wave vector (the so called backward volume geometry) as well as for out-of-plane field angles. We find that there is a drastic change in the efficiency of parametric excitation between two different pumping frequency regimes in which the uniform precession frequency lies either higher than or lower than the uniform FMR frequency.

As a part of a third effort we used a 50 micron multi-element antenna, to measure the *angular dependence* of propagating magnetostatic spin waves, both in-plane and out-of-plane and compared the measurements with existing theoretical models. For most magnetic field directions theory and experiment agree reasonably well. However, there is a range of magnetic field directions where differences between theory and experiment becomes large.

Future Plans

We will attempt to detect coherent magnons at the minimum in the dispersion curve in the coming year. We have already begun to pattern new antennas that are better matched to the position of the minimum. Attempts with the current antenna, which is mismatched by several percent were not successful. In addition we think it may be possible to detect BEC with novel edge detection technique and samples with polished edges to facilitate this approach are being prepared.

References

Publications

Tracking the Suhl instability versus angle and frequency for the backward volume mode in an yttrium iron garnet film
Jinho Lim, Wonbae Bang, Jonathan Trossman, C. C. Tsai, and John B. Ketterson
Submitted to Journal of Applied Physics.

Magnetostatic spin-waves in an yttrium iron garnet thin film: Comparison between theory and experiment for arbitrary field directions
Jinho Lim, Wonbae Bang, Jonathan Trossman, Dovran Amanov, C. C. Tsai, Matthias B. Jungfleisch, Axel Hoffmann, and John B. Ketterson
Submitted to Journal of Applied Physics

Phase detection of spin waves in yttrium iron garnet and metal induced nonreciprocity

Jonathan Trossman, Jinho Lim, Wonbae Bang, John B. Ketterson, and C. C. Tsai
Journal of Applied Physics 125, 053905 (2019)
https://doi-org.turing.library.northwestern.edu/10.1063/1.5080449

Study of Surface Character of Micrometer-Scale Dipole-Exchange Spin Waves in an Yttrium Iron Garnet Film
Jinho Lim, Wonbae Bang, Jonathan Trossman, Andreas Kreise, Matthias Benjamin Jungfleisch, Axel Hoffmann, C. C. Tsai, and John B. Ketterson
IEEE Transactions on Magnetics, VOL. 55, NO. 2, FEBRUARY 2019 6100504

Direct detection of multiple backward volume modes in yttrium iron garnet at micron scale wavelengths
Jinho Lim, Wonbae Bang, Jonathan Trossman, Andreas Kreisel, Matthias Benjamin Jungfleisch, Axel Hoffmann, C. C. Tsai, and John B. Ketterson
Phys. Rev. B 99, 014435 – Published 28 January 2019

Propagation of magnetostatic spin waves in an yttrium iron garnet film for out of-plane magnetic fields
Wonbae Bang, Jinho Lim, Jonathan Trossman, C.C. Tsai, John B. Ketterson
Journal of Magnetism and Magnetic Materials **456** 241–250 (2018).

Excitation of the three principal spin waves in yttrium iron garnet using a wavelength specific multi-element antenna
Wonbae Bang, Matthias B. Jungfleisch, Jinho Lim , Jonathan Trossman, C. C. Tsai, Axel Hoffmann, and John B. Ketterson
AIP Advances 8, 056015 (2018); https://doi.org/10.1063/1.5007101

Forward volume and surface magnetostatic modes in an yttrium iron garnet film for out-of-plane magnetic fields: Theory and experiment
Jinho Lim, Wonbae Bang, Jonathan Trossman, Dovran Amanov, and John B. Ketterson
AIP Advances 8, 056018 (2018); https://doi.org/10.1063/1.5007263

Effects of an adjacent metal surface on spin wave propagation
Jonathan Trossman, Jinho Lim, Wonbae Bang, J. B. Ketterson, C. C. Tsai, and S. J. Lee
Advances 8, 056024 (2018); https://doi.org/10.1063/1.5007253

Measurements of long-wavelength spin waves for the magnetic field in the Damon-Eshbach, backward-volume and forward-volume geometries of an yttrium iron garnet film
Wonbae Bang, Jinho Lim, Jonathan Trossman, Dovran Amanov, Matthias B. Jungfleisch, Axel Hoffmann, and John B. Ketterson,
Journal of Applied Physics 123, 123902 (2018);
https://doiorg.turing.library.northwestern.edu/10.1063/1.5019752

Superconductivity & Magnetism

W. –K. Kwok; Co-PIs: U. Welp, A. E. Koshelev, V. Vlasko-Vlasov, Z. -L. Xiao
Materials Science Division, Argonne National Laboratory, 9700 S. Cass Ave., Argonne IL 60439

Program Scope

This program explores novel physical phenomena associated with superconductivity and its interplay with magnetism, determines the origins of these phenomena and explores innovative applications for superconductivity. It combines synergies among synthesis, characterization, theory and simulation to produce fast-track results on frontier research topics. Our current goal is to discover and control novel physical phenomena in unconventional superconductors and vortex matter. We use controlled *heterogeneity* such as disorder induced by particle irradiation and magnetic texturing via patterned nano-magnets to probe competing order and intertwined phases in high-temperature superconductors, topological materials and vortex matter without affecting the underlying crystal-lattice constants. We are currently focused on investigating the competition of charge density waves and superconductivity in 1/8 doped LBCO, the phase diagram of the novel magnetic superconductor $RbEuFe_4As_2$ and the gap structure of emergent superconductivity in doped topological insulators. Furthermore, in vortex matter, we are exploring various magnetic textures derived from artificial spin-ice structures to probe new vortex functionality out of hybrid ferromagnetic/superconducting structures. We maintain leading programs in experiment and theory, with each deriving strong benefit from close mutual cooperation.

Recent Progress

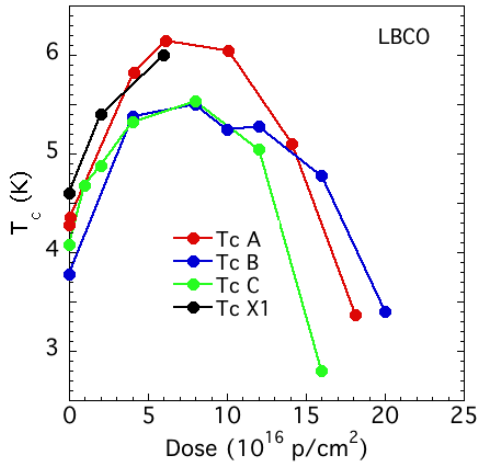

Fig. 1: Dependence of T_c of four crystals (A, B, C, X1) of $La_{1.875}Ba_{0.125}CuO_4$ (LBCO) on the dose of irradiation with 5-MeV protons.

A hallmark of highly correlated electron system is that their properties result from the interplay of various degrees of freedom including electronic, orbital, lattice, and/or spin. As relevant energy scales are frequently comparable, different types of order may be present simultaneously. A well-known example is the emergence of charge-density wave (CDW) and spin-density wave (SDW) correlations in cuprate superconductors. Following the initial observation of stripe charge and spin order in the $La_{2-x}Sr_xCuO_4$ family [1], modulated charge distributions have been discovered in virtually all families of cuprate superconductors [2,3] and are found to be expressed strongest near 1/8 doping. It has been proposed that near 1/8-doping, an intertwined pair-density wave state arises in which the spatial charge modulation is inherently coupled to a spatial modulation of the superconducting order parameter, yielding a pair density wave (PDW) state [4,5]. This intertwined state is expected to have vanishing Meissner effect and to be highly sensitive to disorder [5]. In effect, the observed T_c and Meissner effect are believed to be caused by residual disorder in the sample. While the commonly observed magnetic field and doping dependence suggest that charge order and a uniform superconducting state

compete, no studies have yet found that T_c actually increases when the CDW/PDW is suppressed and the intertwining is broken.

Here, we use electron scattering due to defects created by particle irradiation to tune the balance between charge correlations and superconducting pairing. As shown in Fig. 1, the irradiation with MeV-protons causes an *increase* of T_c of 1/8-doped $La_{2-x}Ba_xCuO_4$ by almost 50 % [3]. This behavior is in sharp contrast with the behavior expected of a d-wave superconductor, for which scattering by both magnetic and nonmagnetic defects suppresses T_c. At the same time, our XRD studies on pristine and irradiated crystals reveal the strong suppression of the charge density wave. Our results thus make an unambiguous case for the strong detrimental effect of the CDW on bulk superconductivity in $La_{1.875}Ba_{0.125}CuO_4$. Furthermore, using high-frequency susceptibility measurements, we find enhanced 3-D coupling induced by irradiation, consistent with the notion that the CDW is part of a PDW state, see Fig. 2.

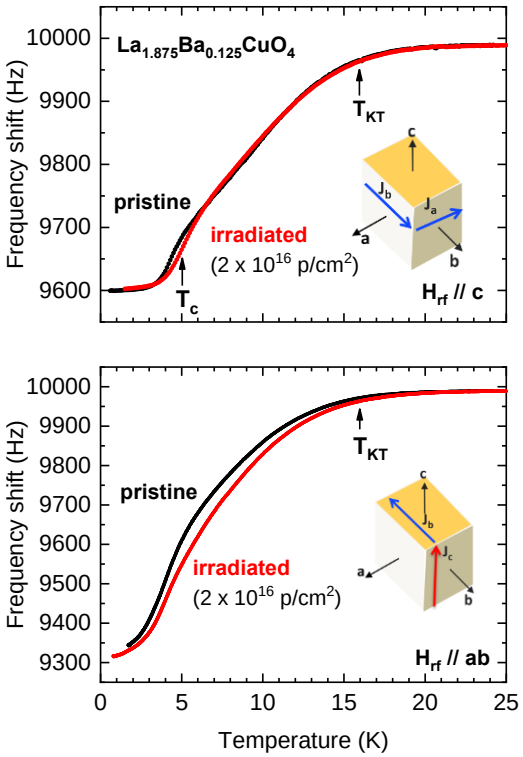

Fig. 2: Superconducting screening as measured with high-frequency susceptibility. The comparison of data taken with the rf-field applied parallel and perpendicular to the CuO_2-planes reveals enhanced three-dimensional coupling in the irradiated sample, suggestive of the suppression of a PDW state.

Future Plans

In future work, we will extend these studies to other cuprates that have demonstrated charge order. These studies will give information on what kind of T_c-enhancement can be achieved due to the suppression of CDW and probe if T_c can approach the pseudo-gap temperature, at least in some parts of the phase diagram. By modifying the type of irradiation and thermal annealing of the samples, we will minimize the detrimental effect of pair-breaking scattering, especially due to point defects. We will also investigate iron-based superconductors, in particular 122-type materials, which are characterized by an extended range of microscopic coexistence of SDW order and superconductivity in the underdoped part of the doping phase diagram. Theoretical work [6] has suggested that in the underdoped regime where superconductivity emerges from a pre-existing SDW, both orders compete. For certain ranges of the order parameter anisotropy and intra- and inter-band scattering rates, disorder is expected to suppress the SDW and enhance T_c.

References

[1] J. M. Tranquada, et al., *Evidence for stripe correlations of spins and holes in copper-oxide superconductors*, Nature **375**, 561 (1995).

[2] recent review: C. Proust, L. Taillefer, *Ground states of cuprate superconductors*, Annu. Rev. Condens. Matter Phys. **10**, 409 (2019).

[3] M. Leroux, et al., *Disorder raises the critical temperature of a cuprate superconductor*, PNAS **116**, 10691 (2019) and references therein.

[4] E. Fradkin, et al., *Colloquium: Theory of intertwined order in high temperature superconductors*, Rev. Mod. Physics **87**, 457 (2015).
[5] E. Berg, et al., *Striped superconductors: how spin, charge and superconducting orders intertwine in the cuprates*, New J. Phys. **11**, 115004 (2009).
[6] V. Mishra, *Effect of disorder on superconductivity in the presence of spin-density wave order*, Phys. Rev. **B 91**, 104501 (2015); R. M. Fernandes, et al., *Enhancement of T_c by disorder in underdoped iron pnictide superconductors*, Phys. Rev. **B 85**, 140512(R) (2012); M. Hoyer, et al., *Effect of weak disorder on the phase competition in iron pnictides*, Phys. Rev. **B 89**, 214504 (2014).

Publications

1. *Separation of Electron and Hole Dynamics in the Semimetal LaSb*, F. Han, J. Xu, A. S. Botana, Z. L. Xiao, Y. L. Wang, W. G. Yang, D. Y. Chung, M. G. Kanatzidis, M. R. Norman, G. W. Crabtree, and W. K. Kwok, Phys. Rev. **B 96**, 125112 (2017).
2. *Robust nodal superconductivity in the doped topological insulator $Nb_xBi_2Se_3$*, M. P. Smylie, K. Willa, H. Claus, A. Snezhko, I. Martin, W.-K. Kwok, Y. Qiu, Y. S. Hor, E. Bokari, P. Niraula, A. Kayani, and U. Welp, Phys. Rev. **B 96**, 115145 (2017).
3. *Reentrant metallic behavior in the Weyl semimetal NbP*, J. Xu, D. E. Bugaris, Z. L. Xiao, Y. L. Wang, D. Y. Chung, M. G. Kanatzidis and W. K. Kwok, Phys. Rev. **B 96**, 115152 (2017).
4. *Parallel magnetic field suppresses dissipation in superconducting nanostrips*, Y. L. Wang, A. Glatz, G. J. Kimmel, I. S. Aranson, L. R. Thoutam, Z. -L. Xiao, G. R. Berdiyorov, F. M. Peeters, G.W. Crabtree, and W. -K. Kwok, PNAS **114**, E10274 (2017).
5. *An increase in T_c under hydrostatic pressure in superconducting doped topological insulator $Nb_{0.25}Bi_2Se_3$*, M. P. Smylie, K. Willa, K. Ryan, H. Claus, W.-K. Kwok, Y. Qiu, Y. S. Hor, and U. Welp, Physica C-Superconductivity and its Applications Vol **543**, 58. (2017).
6. *Nanocalorimeter platform for in-situ specific heat measurements and x-ray diffraction at low temperature*, *K. Willa*, Z. Diao, *D. Campanini*, U. Welp, R. Divan, M. Hudl, Z. Islam, W.-K. Kwok, A. Rydh, Reviews of Scientific Instruments **88**(12), 125108 (2017).
7. *Guiding thermo-magnetic avalanches with soft magnetic stripes*, V. K. Vlasko-Vlasov, F. Colauto, T. Benseman, D. Rosenmann, W.-K. Kwok, Phys. Rev **B 96**, 214510 (2017).
8. *Thick $Bi_2Sr_2CaCu_2O_{8+\delta}$ films grown by liquid-phase epitaxy for Josephson THz applications*, Y. Simsek, V. Vlasko-Vlasov, A. E. Koshelev, T. Benseman, Y Hao, I. Kesgin, H. Claus, J Pearson, W-K Kwok and U Welp, Supercond. Sci. & Technol. **31**(1), 015009 (2018).
9. *Strong-pinning regimes by spherical inclusions in anisotropic type-II superconductors* R. Willa, A. E. Koshelev, I. A. Sadovskyy, A. Glatz, Superconductor Science & Technology **31**(1), 014001. (2018).
10. *Superconductivity, pairing symmetry, and disorder in the doped topological insulator $Sn_{1-x}In_xTe$ for $x\geq 0.10$*, M.P. Smylie, H. Claus, W. -K. Kwok, E. R. Louden, M. R. Eskildsen, A. S. Sefat, R. D. Zhong, J. Schneeloch, G. D. Gu, E. Bokari, P. M. Niraula, A. Kayani, C. D. Dewhurst, A. Snezhko and U. Welp, Phys. Rev **B 97**, 024511 (2018).
11. *Superconducting and normal-state anisotropy of the doped topological insulator $Sr_{0.1}Bi_2Se_3$* M. P. Smylie, K. Willa, H. Claus, A. E. Koshelev, et al., Scientific Reports **8**, 7666 (2018).
12. *Single Crystal Growth and Study of the Ferromagnetic Superconductor $RbEuFe_4As_4$*, J.-K. Bao, K. Willa, M. P. Smylie, H. Chen et al., Crystal Growth and Design **18**(6), 3517 (2018).
13. *Switchable geometric frustration in an artificial-spin-ice/superconductor hetero-system*, Y. – L. Wang, X. Ma, J. Xu, Z. -L. Xiao, et al., Nature Nanotechnology **13**, 560-565 (2018).

14. *Pressure-induced isostructural phase transition and charge transfer in superconducting FeSe*, Z. Yu, M. Xu, Z. Yan, H. Yan, et al., Journal of Alloys and Compounds **767**, 811-819 (2018).
15. *Superconductivity and Structural Conversion with Na and K Doping of the Narrow-Gap Semiconductor $CsBi_4Te_6$*, H. Chen, et al., Chemistry of Materials **30**(15), 5293 (2018).
16. *Electronic and structural response to pressure in the hyperkagome-lattice*, F. Sun, H. Zheng, Y. Liu, E. D. Sandoval, C. Xu, J. Xu**,** C. Q. Jin, C., et al., Phys. Rev. **B 98**, 085131(2018).
17. *Anisotropic superconductivity and magnetism in single-crystal $RbEuFe_4As_4$*, M. P. Smylie, J. -K. Bao, K. Ryan, Z. Islam, H. Claus, Y. Simsek, et al., Phys. Rev. **B 98**, 104503 (2018).
18. *Peak effect due to competing vortex ground states in superconductors with large inclusions*, R. Willa, A. E. Koshelev, I. A. Sadovskyy, A. Glatz, Phys. Rev. **B 98**, 054517 (2018).
19. *Nanocalorimetric Evidence for Nematic Superconductivity in the Doped Topological Insulator $Sr_{0.1}Bi_2Se_3$*, K. Willa, R. Willa, K. W. Song, G. D. Gu, et al., Phys. Rev. **B 98**, 184509 (2018).
20. *Extreme asymmetry of Neel domain walls in multilayered films of diluted magnetic semi-conductor (Ga, Mn)(As, P)*, V. Vlasko-Vlasov, et al., Phys. Rev. **B 98**, 180411 (2018).
21. *Chemical stability and superconductivity in Ag-sheathed $CaKFe_4As_4$ superconducting tapes*, Z. Cheng, C. Dong, et al., Superconductor Science and Technology **32**, 015008 (2018).
22. *Negative Longitudinal Magnetoresistance in GaAs Quantum Wells*, J. Xu, M. Ma, M. Sukonov, Z. -L. Xiao, Y. -L. Wang, D. Jin, W. Zhang, et al., Nature Communications **10**, 287 (2019).
23. *High Hole Mobility and Nonsaturating Giant Magnetoresistance in the New 2D Metal $NaCu_4Se_4$ Synthesized by a Unique Pathway*, H. Chen, J. Rodrigues, A. Rettie, T. -B. Song, D. Chica, X. Su, et al., Journal of the American Chemical Society, **141** (1), 635 (2019).
24. *Competition between orthorhombic and re-entrant tetragonal phases in underdoped $Ba_{1-x}K_xFe_2As_2$ probed by the response to controlled disorder*, E. I. Timmons, M. A. Tanatar, K. Willa, S. Teknowijoyo, Kyuil Cho, et al., Phys. Rev. **B 99** (5), 054518 (2019).
25. *Particle Irradiation Induced Defects in High Temperature Superconductors*, P. M. Niraula, E. Bokari, S. Iqbal, L. Paulius, et al., MRS Advances DOI: 10.1557/adv.2019.143 (2019).
26. *Disorder Raises the Critical Temperature of a Cuprate Superconductor*, M. Leroux, V. Mishra, J. P.C. Ruff, H. Claus, M. P. Smylie, C. Opagiste, P. Rodiere, et al., PNAS **116**, 10691 (2019).
27. *Self-induced Magnetic Flux Structure in the Magnetic Superconductor $RbEuFe_4As_4$*, V. K. Vlasko-Vlasov, A. E. Koshelev, M. Smylie, et al., Phys. Rev. **B 99**, 134503 (2019).
28. *A Natural 2D Heterostructure $[Pb_{3.1}Sb_{0.9}S_4][AuxTe_{2-x}]$ with Large Transverse Non-saturating Negative Magnetoresistance and High Electron Mobility*, H. Chen, J. He, C. D. Malliakas, C. C. Stoumpos, et al., Journal of the American Chemical Society **141** (18), 17544-7553 (2019).
29. *Strongly fluctuating moments in the high-temperature magnetic superconductor $RbEuFe_4As_4$* K. Willa, R. Willa, J.-K. Bao, A. E. Koshelev, et al., Phys. Rev. **B 99**, 180502R (2019).
30. *Orbital Flop in Rare Earth Monopnictide CeSb*, J. Xu, F. Wu, J. -K. Bao, F. Han, Z. -L. Xiao, I. Martin, Y. -Y. Lyu, Y. -L. Wang, D. Y. Chung, et al., Nat. Comm. **10**, 2875 (2019).
31. *Programmable bias field induced by symmetry breaking in ferromagnetic semiconductor films*, S. Dong, Y. Wang, S.-K. Bac, et al., Physical Review Materials **3**, 074407 (2019).
32. *Strong magnon-photon coupling in ferromagnet-superconducting resonator thin-film devices*, Y. Li, T. Polakovic, Y. -L. Wang, J. Xu, et al., Physical Review Letters (in-press 2019).
33. *Phase transition preceding magnetic long-range order in the double perovskite Ba_2NaOsO_6* K. Willa, R. Willa, I. R. Fisher, et al., Physical Review B-Rapid Commun. (in press 2019).
34. *Anisotropic upper critical field of pristine and proton-irradiated single crystals of the magnetically ordered superconductor $RbEuFe_4As_4$*, M. P. Smylie, A. E. Koshelev, K. Willa, W.-K. Kwok, J.-K. Bao, D. Y. Chung, et al., Physical Review B (in-press, 2019).

Magnetometry Studies of Quantum Correlated Topological Materials in Intense Magnetic Fields

Lu Li
University of Michigan

Program Scope

This project investigates the fundamental nature of quantum correlated topological materials by torque magnetometry in intense magnetic fields. The project aims to answer this question: does strong electronic interaction lead to novel topological quantum states? In particular, our project will address the following three questions:

1. Does strong electronic correlation help make a topological material?
2. Do topological insulators stay insulating or become semimetals under magnetic fields?
3. Does a strong electronic correlation lead to new electronic and magnetic states?

These questions test the *hypothesis* that, in quantum material, strong electronic interaction creates unique topological quantum states.

This project aims to use advanced experimental torque magnetometry techniques to give conclusive evidence in the novel electronic and magnetic states in quantum correlated topological materials. Our research starts with magnetic torque and resistance measurements in intense magnetic fields to explore the magnetic response of quantum correlated topological material. With these efforts, we hope to carry out these following tasks:

1: Detecting quantum oscillations of the bulk and the surface states in quantum correlated topological materials;

2: Revealing the origin of quantum oscillations in quantum correlated topological materials;

3: Searching for novel electronic and magnetic ground states in quantum correlated topological materials.

Answering all the three key questions, the research lays the foundation for the understanding of the novel electronic state in the correlated topological quantum materials. Topological materials host peculiar physical properties that particularly suited for future low-dissipation electronics [1, 2]. The highly conductive surface states are topologically protected against impurity scattering. As a result, electronic devices based on topological phases have the potential to exceed the performance of conventional silicon-based field-effect transistors, with faster operation speed, lower power consumption, and higher integration density. Furthermore, in the rare earth compounds and transition metal oxides, the enhanced electronic interaction may lead to novel phases of matter and new multi-functionalities. The interaction-driven topological phases combine the beauty of symmetry protected topological states with potentially strong electronic correlation. Many new topological phases are predicted in correlated systems, such as Weyl-Kondo semimetal, quantum anomalous Hall system, topological Mott insulator, and topological superconductor. Uncovering these effects will lead to a significant advance in fundamental research of correlated quantum materials and lay the material foundation for quantum information science.

Recent Progress

(1). Discovery of Quantum Oscillations in Both Magnetization And Resistivity in Strongly Correlated Insulator Ytterbium Dodecaboride YbB_{12}.

Electrons in solid materials obey the Fermi-Dirac statistics. At zero temperature, the Fermi energy marks the position of the highest occupied energy level. These conduction electrons, acting as the charge carriers in metals, can be further driven into cyclotron motion under magnetic field and consequently experience an energy quantization called Landau quantization. By contrast, the Fermi energy in an insulator resides in the band gap in which no electronic states exist. As a result, the population of conduction electrons decays exponentially with the thermal activation weakened

upon cooling down, and Landau quantization is not expected at low temperature as all the carriers depleted. Our manuscript [1] reports a rare exception of this textbook scenario. By applying intense magnetic fields on mixed valent Kondo insulator ytterbium dodecaboride YbB_{12}, we discovered Landau quantization in both magnetization and electrical resistivity, as shown in Fig. 1. Our result reveals a mysterious dual nature of the ground state in YbB_{12}: it is both a charge insulator and a strongly correlated metal.

Furthermore, we studied the low-temperature thermal transport property of this material to reveal the unconventional nature of the ground state. Our study [2] applied low-temperature heat-transport measurements to discover gapless, itinerant, charge-neutral excitations in the ground state of YbB_{12}. At zero field, sizeable linear temperature-dependent terms in the heat capacity and

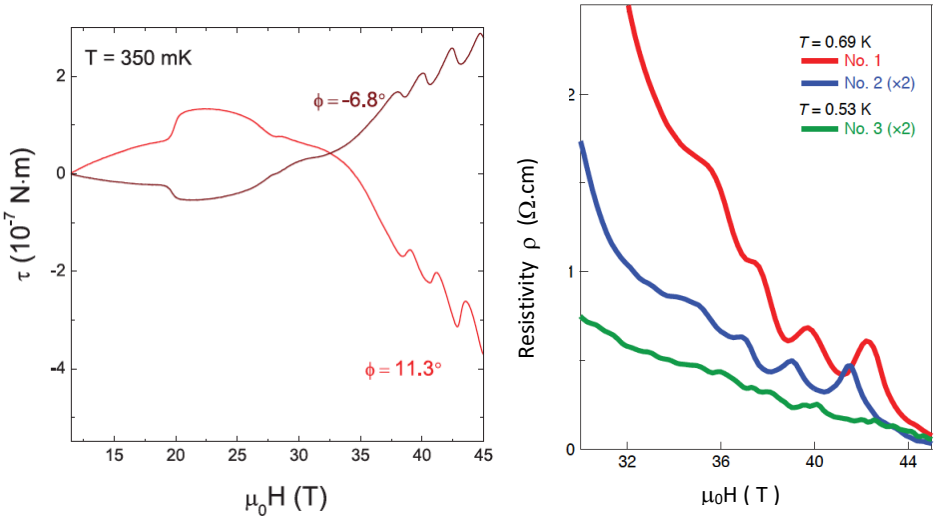

Figure 1.

(Left): Quantum Oscillations in Magnetic Torque τ of YbB_{12}

(Right): Quantum Oscillations in Electrical Resistivity ρ of YbB_{12}

thermal conductivity are resolved in the zero-temperature limit, indicating the presence of gapless fermionic excitations with an itinerant character. Remarkably, linear temperature-dependent thermal conductivity leads to a spectacular violation of the Wiedemann–Franz law: the Lorenz ratio is 104–105 times larger than that expected in conventional metals, indicating that YbB_{12} is a charge insulator and a thermal metal. Moreover, we find that these fermions couple to magnetic fields, despite their charge neutrality. Our findings expose novel quasiparticles in this unconventional quantum state.

(2). Development of torque differential magnetometry with quartz tuning forks.

We advanced our high field magnetometry technique with our recent invention of **torque differential magnetometry** [3]. The biggest challenge for the capacitive torque magnetometry measurement is vibration noise. The soft cantilevers generally resonant around 1 Hz, making them easily coupled to the mechanical noises. We solved the problem by using a highly resonant cantilever to detect the magnetic force. The approach has a significant advantage. The high-*Q* resonance eventually decouples the cantilever response from the noisy electrical and mechanical environment. Quartz tuning forks are the high-*Q* resonator in commercial quartz watches. As shown in Fig. 2a, we break the quartz tuning fork packages to get the forks and then glue them permanently to heavy substrates. With the sample glued to the fork tip that is excited by a radio-frequency AC voltage, a sharp resonance is observed in both the current amplitude and the phase (Fig. 2b). Under magnetic fields, the magnetic torque from the sample brings additional damping on the resonant fork, leading to a shift in the resonant frequency and subsequently changes in the phase of the current. As a result, the phase shift measures directly $d\tau/d\theta$, the differential of the

magnetic torque τ with respect to the magnetic field title angle θ. Fig. 3c shows an example of the current phase from a tuning fork with a piece of single crystal bismuth mounted. This result reveals a quantum oscillation pattern due to the Landau quantization of the carriers in bismuth. (3) Discovery of rotational symmetry breaking of magnetization oscillation amplitude in strongly correlated insulator samarium hexaboride SmB_6

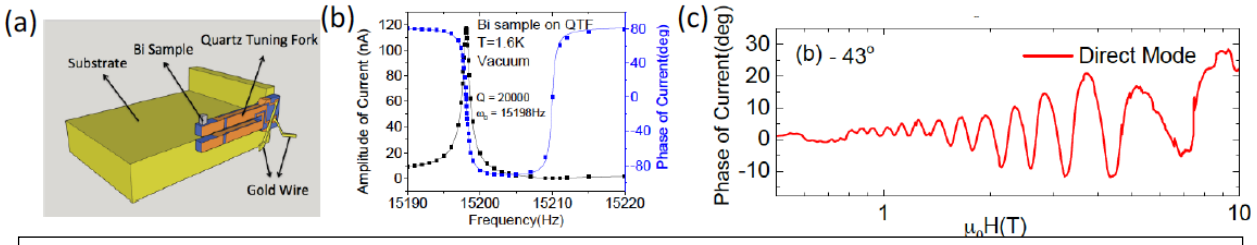

Figure 2. Preliminary results of quartz tuning fork (QTF) torque differential magnetometry. (a) Setup sketch of a QTF mounted with a bismuth (Bi) crystal. One prong of the QTF is firmly glued on an L-shape substrate. The Bi sample is attached on top of the free moving prong. (b) Resonance curve of QFT with Bi crystal attached. *Q*-factor is found to be about 20000. (c) Driven by an AC voltage at the resonant frequency, the QTF generates a current. The current phase is plotted against the magnetic field *H*, showing an oscillatory pattern coming from the Landau level quantization of single crystal bismuth. Taken from Ref. [4]

The Kondo insulator samarium hexaboride (SmB_6) has been intensely studied in recent years as a potential candidate of a strongly correlated topological insulator. One of the most exciting phenomena observed in SmB_6 is the clear quantum oscillations appearing in magnetic torque at a low temperature despite the insulating behavior in resistance. These quantum oscillations show multiple frequencies and different effective masses. The origin of quantum oscillation is, however, still under debate with evidence of both two-dimensional Fermi surfaces and three-dimensional Fermi surfaces. In our manuscript [4], we carry out angle-resolved torque magnetometry measurements in a magnetic field up to 45 T and a temperature range down to 40 mK. With the magnetic field rotated in the (010) plane, the quantum oscillation frequency of the strongest oscillation branch shows a fourfold rotational symmetry. However, in the angular dependence of the amplitude of the same branch, this fourfold symmetry is broken and, instead, a twofold symmetry shows up, which is consistent with the prediction of a two-dimensional Lifshitz- Kosevich model. No deviation of Lifshitz-Kosevich behavior is observed down to 40 mK. Our results suggest the existence of multiple light-mass surface states in SmB_6, with their mobility significantly depending on the surface disorder level.

Future Plans

[1] Revealing the origin of quantum oscillations in these strongly correlated insulators

One particular question we would like to address is the origin of the quantum oscillations in Kondo insulator YbB_{12}. We will carry out *in situ* resistivity measurement to understand the underlying novel physics. The preliminary data shows the *T*-dependence of the electrical resistivity of YbB_{12} in high magnetic fields where quantum oscillations appear. The ρ-T curves still follow the semiconducting trend, i.e., ρ increases by three orders of magnitude with T decreasing from 12 K to 0.5 K. However, the resistive upturn is closer to a power-law dependence, as expected by the theory of the disorder-driven semimetal phase in the narrow gap insulator. We will track this dependence at various magnetic field directions for YbB_{12} and other quantum correlated topological materials. Furthermore, the theory of disorder-driven semimetal phase in Kondo insulator has a direct prediction on the effective mass. As discussed above, the samples with higher disorder level would have a higher effective mass. This prediction can be tested. We will determine the effective masses in both magnetization oscillation and resistivity oscillations for samples with different disorder levels. That would give a direct verification of the theories.

[2] Determining how the correlated insulating ground state change under intense magnetic fields

Most of the quantum correlated topological materials are mixed valence Kondo insulators. Intense magnetic fields increase the Zeeman energy, and if the *g*-factor is large enough, the Zeeman energy can match the insulating gap in an experimentally accessible field. As a result, the insulator turns into a simple metal. The preliminary data shows magnetic field driven transition observed in both resistivity and magnetic torque of YbB_{12} in intense magnetic fields. The surprising feature is that the transition field changes with magnetic field orientation. The YbB_{12} crystals have a cubic structure. If the magnetic response is linear, this simple crystal structure should not lead to anisotropy. As a result, the *g*-factor is expected to stay the same for different magnetic field orientations. This puzzle called for a detailed angular mapping of the transition fields, which would help reveal the origin of quantum oscillations in Kondo insulators, and other quantum correlated topological materials.

References

[1] Z. Xiang, *et al.* "Quantum Oscillations of Electrical Resistivity in an Insulator", Science, 362, 65 (2018)

[2] Y. Sato, *et al.* "Unconventional thermal metallic state of charge-neutral fermions in an insulator", Nature Physics, DOI:10.1038/s41567- 019-0552-2 (2019)

[3] L. Chen, *et al.* "Torque Differential Magnetometry Using the qPlus Mode of a Quartz Tuning Fork", Physical Review Applied, 9, 024005 (2018)

[4] Z. Xiang, *et al.* "Bulk Rotational Symmetry Breaking in Kondo Insulator SmB6", Physical Review X, 7, 031054 (2017)

Publications

1. Tomoya Asaba, BJ Lawson, Colin Tinsman, Lu Chen, Paul Corbae, Gang Li, Y Qiu, YS Hor, Liang Fu, Lu Li. "Rotational Symmetry Breaking in a Trigonal superconductor Nb-doped Bi_2Se_3", Physical Review X, 7, 011009 (2017)

2. Z. Xiang, B. J. Lawson, T. Asaba, Lu Chen, C. Shang, X. H. Chen, Lu Li. "Bulk Rotational Symmetry Breaking in Kondo Insulator SmB_6", Physical Review X, 7, 031054 (2017)

3. Lu Chen, F. Yu, Z. Xiang, Tomoya Asaba, Colin Tinsman, B. J. Lawson, Paul M. Sass, Weida Wu, B. L. Kang, Xianhui Chen, Lu Li. "Torque Differential Magnetometry Using the qPlus Mode of a Quartz Tuning Fork", Physical Review Applied, 9, 024005 (2018)

4. Tomoya Asaba, Yongjie Wang, G. Li, Z. Xiang, Colin Tinsman, Lu Chen, S. Zhou, S. Zhao, D. Laleyan, Yi Li, Zetian Mi, Lu Li. "Magnetic Field Enhanced Superconductivity in Epitaxial Thin Film WTe_2", Scientific Reports, 8, 6520 (2018)

5. Z. Xiang, Y. Kasahara, Tomoya Asaba, B. J. Lawson, Colin Tinsman, Lu Chen, G. Li, S. Yao, Y. L. Chen, F. Iga, John Singleton, Y. Matsuda, Lu Li. "Quantum Oscillations of Electrical Resistivity in an Insulator", Science, 362, 65 (2018)

6. H. Boschker, T Harada, T Asaba, R Ashoori, AV Boris, H Hilgenkamp, ME Holtz, CR Hughes, Lu Li, DA Muller, H. Nair, P. Peith, X Renshaw Wang, DG Schlom, A Soukiassian, J Mannhart, Ferromagnetism and conductivity in atomically thin $SrRuO_3$, Physical Review X, 9, 011027 (2019)

7. Y. Sato, Z. Xiang, Y. Kasahara, T. Tanigguchi, S. Kasahara, Lu Chen, Tomoya Asaba, Colin Tinsman, O. Tanaka, Y. Mizukami, T. Shibauchi, F. Iga, J. Singleton, Lu Li, Y. Matsuda. "Unconventional thermal metallic state of charge-neutral fermions in an insulator", Nature Physics, DOI:10.1038/s41567- 019-0552-2 (2019)

Study of topological and unconventional superconductors in nanoscale

Qi Li

Department of Physics, Pennsylvania State University, University Park, PA 16802

Project scope

The goal of the program is to study proximity-induced or intrinsic topological superconductivity and other unconventional superconductors in nanoscale systems. The systems explored are known topological insulators, strong spin-orbit coupling (SOC) systems or large Rashba effect, and thin films with enhanced T_c from their bulk value in nanoscales. Three families of systems studied are inducing topological superconductivity in Bi_2Te_3 nanotubes, two-dimensional electron gases (2DEGs) at transition metal oxide interfaces with (111) orientation with large SOC or Rashba effect, and superconductivity in very thin TiOx and monolayer FeSe, both of which have higher T_c in thin films than corresponding bulks. All three families of materials have been predicted and some demonstrated to have topological orders.

Bi_2Te_3 is a topological insulator as demonstrated by Angle Resolved Photoemission Spectroscopy. However, transport signature of the topological surface states is often hindered by the bulk conduction. Our previous studies[1] have shown that in nanotube geometry, the bulk conduction can be suppressed by disorder and large surface to volume ratio, and the surface states can dominate the transport at low temperatures. For this grant period, we have studied inducing superconductivity in Bi_2Te_3 nanotubes and other topological phase samples with Nb contacts to seek the signature of Majorana fermions. Transition metal oxide with (111) orientation has hexagonal structure, similar to topological insulator Bi_2Se_3 and graphene, which has been predicted to display exotic phases and properties.[2] We have fabricated $SrTiO_3$ (111) interface 2DEGs with high mobility and studied quantum transport at high magnetic fields to explore those intriguing properties as well as superconductivity in the system. TiO (111) films have been shown to display much higher T_c (7.4K) than that of the bulk, highlighting the role interfaces and boundaries can play in enhancing T_c in thin films. We have studied how oxygen content and the thickness affect the superconducting transition in $TiO_{1+\delta}$ thin films. In particular, the samples display semiconducting behavior before the superconducting transition, which is different from the metallic systems. Detailed studies on the scaling behavior of the superconductor-to-insulator transition have been conducted to reveal the nature of the quantum phase transitions.

Recent Progress

Shubnikov-de Hass oscillations in 2D electron gases at $SrTiO_3$ (111) interface. We have created high mobility two-dimensional electron gases with mobility up to 18000 $cm^2V^{-1}s^{-1}$ at (111)-oriented $SrTiO_3$ interface. $SrTiO_3$ is a band insulator, but conducting electron gas can be formed at the interfaces with a variety of other insulators. We have studied the Shubnikov-de Hass

(SdH) oscillations at National High Magnetic Field Lab up to 60 T (pulse field). Due to the high mobility of the system, pronounced SdH oscillations can be observed from a relatively low magnetic field of ~ 2 T at low temperature. Distinct from the multiple frequency oscillations at $SrTiO_3$ (001) interface, longitudinal resistance (R_{xx}) versus $1/B$ of $SrTiO_3$ (111) electron gas has a single oscillation frequency as revealed by fast Fourier transformation (FFT) of the SdH oscillations. The FFT spectrum exhibits a single peak at around 26 T, which corresponds to a low quantum carrier density of ~ 1.3×10^{12} cm^{-2} via the Onsager relation. The single frequency feature is further demonstrated by plotting the relationship between the position of resistance peak/dip ($1/B_p$) and the filling factor (n). Notably, the lowest Landau level is achieved at high magnetic field above ~ 27 T in the samples. When the magnetic field is above the lowest filling level, the magnetoresistance changes to a different state at higher fields.

Quantum oscillations were also measured in a dilution refrigerator system till 18 T. Plateau-like structures appear in Hall resistance and are accompanied by dips in longitudinal resistance, which is a signature of quantum Hall effect.

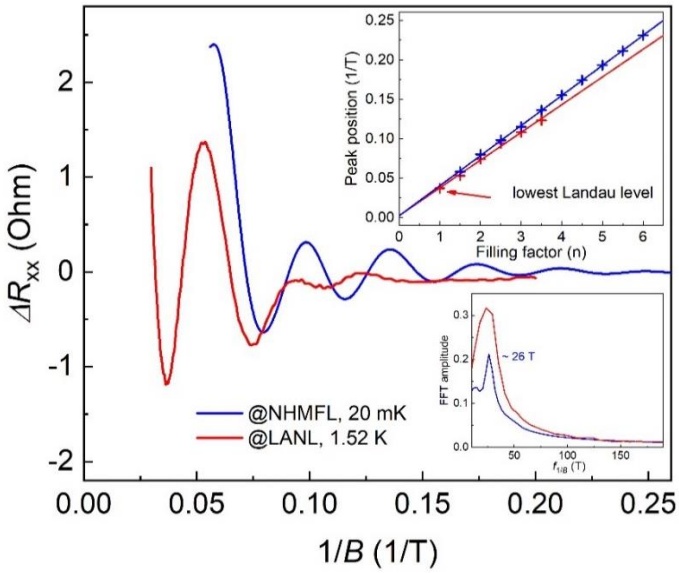

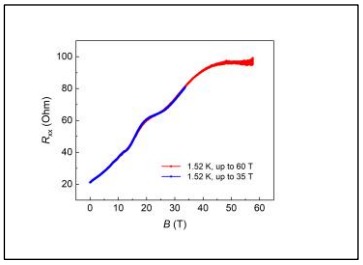

Fig. 2. Resistance as a function of magnetic field up to 60 T (pulse field). A clear change of Rxx v.s. B behavior is seen at ~40 T where the lowest Landau level has been filled.

Fig. 1. Background subtracted R_{xx} v.s. $1/B$, exhibiting clear periodicity SdH oscillations in $SrTiO_3$ (111) electron gas. The red curve is measured up to 60 T (pulse field) but only plotted till 35 T where no more oscillation exists at higher field. The blue curve is measured up to 18 T (DC field, 20 mK) with much lower noise than the pulse field data. Upper inset: the position of resistance peak/dip ($1/B_p$) v.s. the filling factor (n). The lowest Landau level is achieved in this system above ~ 27 T. Lower inset: the FFT spectrum of SdH oscillation, showing a peak at ~ 26 T.

<u>Superconductor-insulator transition and Quantum Griffiths singularity in epitaxial TiO thin films with different oxygen content and thicknesses</u>

Superconductor-insulator transition (SIT) is closely related to the competition between superconductivity and carrier localization in intrinsically disordered thin films. Superconducting epitaxial $TiO_{1+\delta}$ thin films were fabricated by a pulsed-laser deposition and the effect of oxygen and thickness on the superconducting transition has been studied. Increasing oxygen content leads

to an increase of disorder, a reduction of carrier density, and therefore a decrease of superconducting transition temperature. SIT emerges in $TiO_{1+\delta}$ films with increasing oxygen content and its critical resistance is close to the quantum resistance $h/(2e)^2$ ~6.45 kΩ/□. The scaling analyses of magnetic field-tuned SIT exhibit the increase of critical exponent products zv with increasing disorder. On the other hand, superconductor-metal transition with an unconventional diverging dynamical critical exponent was recently discovered and interpreted as the signature of quantum Griffiths singularity (QGS). QGS has been so far observed in limited materials with metallic normal states. In TiO thin films, the normal state before the superconducting transition is insulating as the resistance increase with decreasing temperature. In this system, we have also observed that the magnetic field tuned SIT has a diverging dynamical critical exponent, an evidence of QGS, although the critical magnetic field H_c tends to saturate as the temperature approaching 0 K, which is different from the upturn trend of H_c observed in SMT systems. This may be due to the weaker Josephson coupling of the ordered superconducting islands (rare regions) in an insulating normal state background. The results extend the QGS scenario from only SMT systems to SIT systems, and provide evidences to conclude that the QGS might be commonly observed in disordered superconducting thin films.

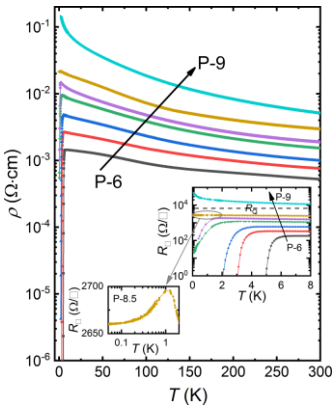

Fig. 3. Temperature dependent resistivities of $TiO_{1+\delta}$ films with different oxygen content. Right inset: The enlarged view of sheet resistances for TiO films at low temperatures, and the critical quantum resistance. Left inset: Enlarged sheet resistance below 2 K for the circled region.

<u>Proximity inducing superconductivity in Bi_2Te_3 nanotube and topological materials with Nb</u>

We have explored to induce superconductivity into Bi_2Te_3 nanotubes with Nb contacts and combination of Nb and Au contacts by using e-beam lithography. Previously, we have observed induced topological superconductivity in bi-layer $NbSe_2/Bi_2Se_3$ thin films. However, to our biggest surprise, we observed a sudden increase of the nanotube resistance when the Nb became superconducting. The anomalous resistance increase disappears when the temperature is above the superconducting transition or the applied magnetic field is larger than the Hc_2 of Nb, indicating that the effect is solely related to the interaction of topological surface states with the superconducting state of Nb. The origin of the effect is subject to further studies. Separately, quantum anomalous Hall insulator in contact with Nb has also been studied. The observed half-quantized conductance has been discussed in regard to the possible interpretation for non-Majorana Fermions verses Majorana Fermions.

Future Plans

We plan to study the gating effect on the SdH oscillations, Quantum Hall effect, and superconductivity in $SrTiO_3$ (111) 2D electron gases. We also plan to fabricate and study 2D electron gases based on 5*d* electron metal oxide systems which have much stronger spin-orbit coupling than that of $SrTiO_3$. Superconductivity of the two systems will be studied with gate tuning of the carrier concentration. We plan to complete the study of induced superconductivity and the

anomalous effect observed in Bi_2Te_3 nanotubes for different nanotube diameter size using Nb and other superconducting contact leads.

Reference

1. Renzhong Du, Hsiu-Chuan Hsu, Ajit C. Balram, Yuewei Yin, Sining Dong, Wenqing Dai, Weiwei Zhao, DukSoo Kim, Shih-Ying Yu, Jian Wang, Xiaoguang Li, Suzanne E. Mohney, Srinivas Tadigadapa, Nitin Samarth, Moses H.W. Chan, Jainendra. K. Jain, Chao-Xing Liu, and Qi Li "Robustness of Topological Surface States Against Strong Disorder Observed in Bi_2Te_3 Nanotubes, *Phys. Rev. B* 93, 195402 (2016).
2. D. Doennig, W.E. Pickett, and R. Pentcheva, "Massive symmetry breaking in LaAlO3/SrTiO3(111) quantum wells: a three-orbital strongly correlated generalization of graphene" Phys. Rev. Lett. 111, 126804 (2013).

Publications (acknowledge DOE support)

1. Yuewei Yin and Qi Li, "A Review on All-perovskite Multiferroic Tunnel Junctions", Materiomics 3, 245-254 (2017).
2. Weichuan Huang, Yue-Wen Fang, Yuewei Yin, Bobo Tian, Wenbo Zhao, Chuangming Hou, Chao Ma, Qi Li, Evgeny Y. Tsymbal, Chun-Gang Duan, Xiaoguang, "Synapse Based on Magnetoelectrically Coupling Memristor", *ACS Appl. Mater. Interfaces* 10, 5649-5656 (2018)**.**
3. Y. J. Fan, C. Ma, T. Y. Wang, C. Zhang, Q. L. Chen, X. Liu, Z. Q. Wang, Q. Li, Y. W. Yin, and X. G. Li "Quantum superconductor-insulator transition in titanium monoxide thin films with a wide range of oxygen contents,", *Phys. Rev. B* **98**, 064501 (2018).
4. Chao Zhang, Yunjie Fan, Tianyi Wang, Xiang Liu, Qi Li, Yuewei Yin1, Xiaoguang Li, "Distinct superconductor-insulator transition with quantum Griffiths singularity in TiO epitaxial thin films with insulating normal states", NPG Asia Materials, accepted (2019)
5. M. Kayyalha, D. Xiao, R. X. Zhang, J. Shin, J. Jiang, F. Wang, Y.-F. Zhao, L. Zhang, K. M. Fijalkowski, P. Mandal, M. Winnerlein, C. Gould, Q. Li, L. W. Molenkamp, M. H. W. Chan, N. Samarth, C.- Z. Chang, "Absence of Evidence for Chiral Majorana Fermion in Quantum Anomalous Hall Insulator and Superconductor Hybrid Structures," Science, accepted (2019).

Manuscript submitted (selected)

1. S. Kumari, D. K. Pradhan, S. Liu, M. M. Rahaman, P. Zhou, D. K. Pradhan, A. Kumar, G. Srinivasan, Qi Li, R. S. Katiyar, and J. F. Scott **"**Room Temperature Magnetoelectricity in Transition Metal Doped Ferroelectrics" submitted to Nat. Commun. (2019).
2. L. Miao, J. Wang, R. Du, Y. Yin, W. Zhao, M.H. Chan, and Qi Li "Band filling and electric field effects on anisotropic magnetoresistance of two-dimensional electron gases at SrTiO3 (111)-, (110)-, and (001)-oriented surfaces" submitted to *npj Quantum Materials* (2018).
3. Renzhong Du, Ludi Miao, Yuewei Yin, and Qi Li "Anomalous Resistance Increase on Bi2Te3 Nanotubes under the Proximity to Superconductors" Nano Lett. unpublished.

Chiral Materials and Unconventional Superconductivity

Lead PI: Qiang Li
Co-PIs: Genda Gu and Tonica Valla
Condensed Matter Physics & Materials Science Division, Brookhaven National Laboratory
e-mail: qiangli@bnl.gov

i) Program Scope

This program studies electronic transport properties of chiral materials and unconventional superconductors. A unique feature of chiral materials is that their low-energy quasi-particles possess an additional quantum number that goes by the name of handedness or chirality – a definitive projection of spin on momentum direction. The powerful notion of chirality underpins a wide palette of new and useful phenomena, among which is non-dissipative charge transport, enabled by the newly discovered chiral magnetic effect (CME).[1,2] Recently, we proposed that the chirality may be utilized to construct a new type of qubit – the chiral qubit – potentially capable of operating at THz frequency and at room temperature.[3] To this end, the program aims at providing the basic understanding of chiral fermions transport process under various stimulus, including chemical potentials, thermal gradient, magnetic field, strain, and optical means. Unconventional superconductivity arises in superconductors having, for example, order parameter with a non-zero angular momentum. To this end, the focus of the program is to look for the exotic states of matter in order to exploit their true potential. Our approach has been developed through synthesizing chiral materials and unconventional superconductors in both single crystals and thin film forms, and subsequently characterizing them using a range of techniques including transport, electron and optical spectroscopy. Experimental activities are strongly coupled with a collaborative effort on theory and computation, providing new strategies for designing robust electronic materials capable of transporting nearly non-dissipative electrical current more efficiently for energy applications and quantum computing.

ii) Recent Progress

Topological phase transition and long coherence time in $ZrTe_5$ – Since the discovery of chiral magnetic effect (CME) in condensed matters by our group in 2014,[1] $ZrTe_5$ has become a rich platform for investigating transport properties of chiral fermions and topological phase transition. Recent first-principles calculations have shown that the small gap between the conduction and valence band at the Γ point in $ZrTe_5$ can be made to close or open by a small change in crystal lattice constant and symmetry, leading to phase transitions from strong topological insulators (TI) to Dirac semimetal, then to weak TI.[4] We have been exploring methods of inducing topological phase transition in $ZrTe_5$, and enhancing chiral particles' coherence time (chirality flipping time) - a key parameter for the chiral qubit. We successfully realize the field driven Weyl states by using ultra-fast electromagnetic (EM) radiation that allows us to measure the chirality flipping time directly in Dirac semimetals. Enhanced coherence time of chiral charges and polarization dependent photocurrent are observed in $ZrTe_5$. The experimental results appear to be consistent with the results from the first principle calculations.

3D quantum Hall effect (QHE) in $ZrTe_5$ at the extreme quantum limit – The discovery of the QHE in 2D electronic systems[5] has given topology a central role in modern condensed matter physics. Although the possibility of generalizing the QHE to 3D electronic systems[6] was proposed decades ago, it has not been demonstrated experimentally until its realization in our

$ZrTe_5$ bulk crystal. This discovery is a part of our effort in searching for exotic states at the extreme quantum limit, where only the lowest Landau level is occupied. By fine tuning chemical potential, we are able to make the Femi surface sufficient small in bulk $ZrTe_5$ single crystals to reach the quantum limit under a few tenth of Tesla magnetic field, that allows us to perform low-temperature electric-transport measurements at the extreme quantum limit in moderate field. In this regime, shown in Fig. 1, a nearly dissipationless longitudinal resistivity (red), is accompanied by a well-developed Hall resistivity (blue) plateau proportional to half of the Fermi wavelength along the field direction. This response is the signature of the 3D QHE and strongly suggests a Fermi surface instability driven by enhanced interaction in the extreme quantum limit.[7] A key question follows: Does QHE exist in 2D $ZrTe_5$?

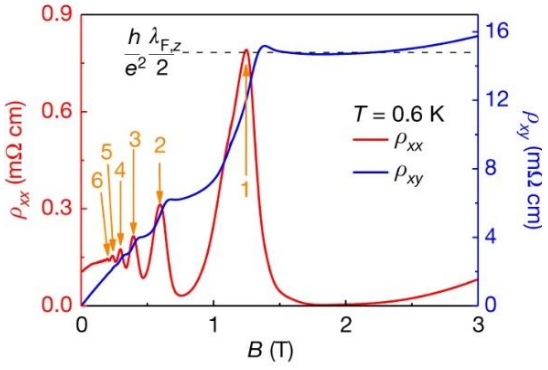

Fig. 1 3D quantum Hall effect in bulk $ZrTe_5$: Longitudinal resistivity, $\rho_{xx}(B)$ (red, left axis) and Hall resistivity $\rho_{xy}(B)$ (blue, right axis) as a function of magnetic field at temperature 0.6 K.[7]

Role of dimensionality in the transport coefficients of chiral materials – The CME requires chiral fermions that exist in 3D, but not 2D materials. How do CME and QHE evolve with a change in dimensionality? To answer these questions, we are investigating the thickness dependence of longitudinal magneto-resistivity and Hall coefficients. Works on monolayer and a few layers of chiral and superconducting materials are in progress.

Thermopower and thermal Hall effect in $ZrTe_5$ – Recent theories predicted that Weyl semimetals in the extreme quantum limit can lead to a giant, non-saturating longitudinal thermopower.[8] We have been investigating the thermal transport properties in $ZrTe_5$ since the discovery of CME. We observed no-saturating and large thermopower S in $ZrTe_5$ in magnetic field, shown in Fig. 2. Normalized $S(B)/S(B = 0)$ exhibits an oscillatory feature consistent with the Shubnikov-de Haas (SdH) oscillation evident at around 2 T in magnetic field dependence of resistivity ρ_{xx}. In progress are measurements of the Nernst coefficients, and thermal Hall effect – an orthogonal temperature gradient produced by an applied thermal gradient across a solid under a magnetic field – in $ZrTe_5$.

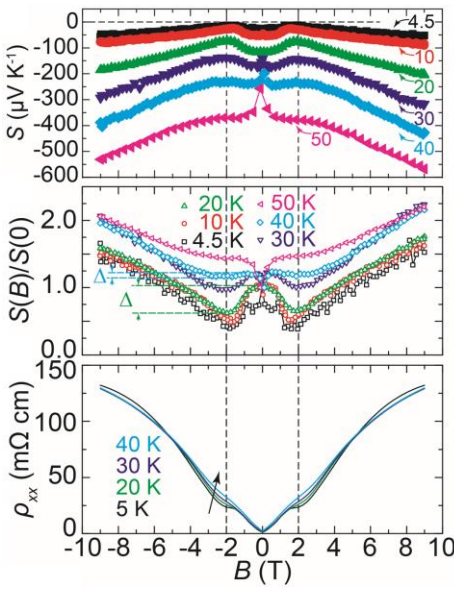

Fig. 2 Thermopower S (top and middle) and resistivity ρ_{xx} (bottom) as a function of magnetic field B in $ZrTe_5$,

The chiral qubit: quantum computing with chiral anomaly – The quantum chiral anomaly enables a nearly non-dissipative current in the presence of chirality imbalance. Recently, we proposed to utilize the chiral anomaly for the designs of qubits potentially capable of operating at THz frequency and at room temperature with a coherence time to gate time ratio of about 10^4.

The proposed "Chiral Qubit" is a micron-scale ring made of a Weyl or Dirac semimetal, with the $|0\rangle$ and $|1\rangle$ quantum states corresponding to the symmetric and antisymmetric superpositions of quantum states describing chiral fermions circulating along the ring clockwise and counter-clockwise (Fig. 3). A fractional magnetic flux through the ring induces a quantum superposition of the $|0\rangle$ and $|1\rangle$ quantum states. The entanglement of qubits can be implemented through the near-field THz frequency electromagnetic fields (EMF). We show that the Hamiltonian of the chiral qubit is similar to that of the superconducting qubit. This means that quantum gates can be implemented in a traditional way, and the algorithms developed for superconducting quantum processors will apply. The main challenge in implementing the chiral qubit is a relatively short coherence time of chiral states, which is determined by the chirality flipping time. Currently, we are investigating the mechanisms of chirality flipping, while developing both theoretical and experimental methods to enhance the coherence time in various chiral materials.

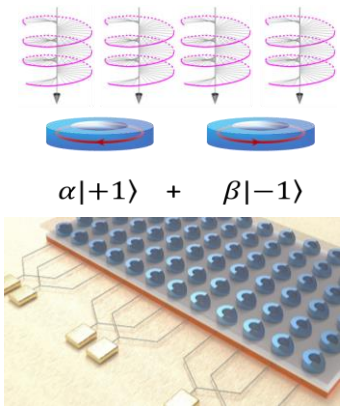

Fig. 3 A conceptual diagram of the chiral qubit and its arrays: The clockwise and counter-clockwise currents in a ring form the base states controlled by circular polarized EMF coupled to THz resonators (not shown)[3]

Ultra-quantum-metal phase in stripe ordered superconductors – Do charge modulations compete with electron pairing in unconventional high-temperature superconductors? We investigated this question by suppressing superconductivity (SC) in a stripe-ordered $La_{1.875}Ba_{0.125}CuO_4$ at low temperature with high magnetic fields. We found that, with increasing field, loss of 3D SC order is followed by reentrant 2D SC and then an ultra-quantum-metal (UQM) phase.[9] Circumstantial evidence suggests that the latter state is bosonic and associated with the charge stripes. Metallic conduction with zero Hall response is due to the incoherent hopping of electron pairs. An alternative model for the UQM is that the application of a sufficient strong magnetic field to the odd-frequency-paired pair-density wave state leads to formation of a low-temperature metallic state, in which the metallic conduction is the result of quasi-particles.[10] Since the pairs do not carry entropy, while quasi-particles do, measurement of the thermal Hall effect may be able to separate these two models apart. We are in the process of building thermal Hall instrument that can operate in very high field for investigating entropy transfer in unconventional superconductors and chiral materials, such as $ZrTe_5$. This powerful entropy probe can also be used to explore magnetic texture and topological excitation, such as spin chirality or fractionalized (topological) excitations, in a spin liquid.

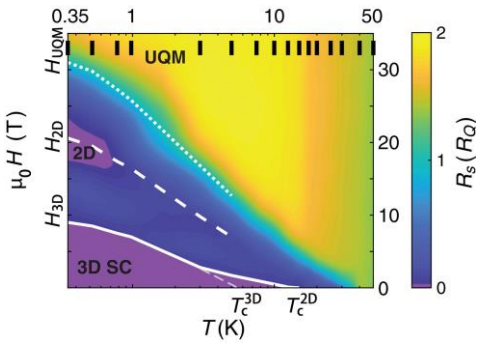

Fig. 4 Phase diagram of $La_{1.875}Ba_{0.125}CuO_4$ in contour plot of the sheet resistance R_s as a function of temperature and magnetic field. The regimes of 3D and 2D superconductivity (SC) with zero resistance are labeled; the UQM (defined in the text) phase occurs at fields above the dotted line.[9]

iii) Future Plans

Topology, strain, and transport properties of chiral materials is a key research direction of this program that will continue in order to understand the chiral flipping mechanism. This study will

lead to the methods of increasing the coherence and dephasing time of the proposed chiral qubits to a level that makes them competitive to superconducting qubits, while operating at much higher temperature.

THz and IR spectroscopy of chiral materials is an area that will see increased effort through collaborations. The emphasis is on experimental investigation of dynamics of chiral fermions, their interactions with phonons and photons. We aim at providing the basic understanding of chiral fermions in transient states, with the possibility of demonstrating Rabi oscillation in two level chiral states for the first time.

Exotic states in chiral material and unconventional superconductor junctions will be investigated to determine the order parameter symmetry in a number of unconventional superconductors, as well as to realize colossal proximity effect in chiral materials/superconductor junctions.

Ultra-quantum (bosonic) metals, spin chirality and Majorana zero modes in unconventional superconductors and their parent compounds will be investigated. This study may lead to the discovery of novel quantum states that can be utilized for the next generation of quantum computing.

iv) References

1. Q. Li et al. "Chiral magnetic effect in $ZrTe_5$" *Nature Physics* **12** 550 (2016)
2. Q. Li and D. Kharzeev, *Nuclear Physics* A **956** 107 111110 (2016)
3. Kharzeev & Li "The Chiral Qubit: quantum computing with chiral anomaly" arXiv:1903.07133
4. H. Weng, et al. Phys. Rev. X **4**, 011002 (2014); Z. Fan, et al. Sci. Rep. **7**, 45667 (2017)
5. K. Klitzing et al. Phys. Rev. Lett. **45**, 494 (1980); D. C. Tsui et al. *ibid*. **48**, 1559 (1982)
6. Halperin, Jpn. J. Appl. Phys. 26, 1913 (1987); Kohmoto et al. Phys. Rev. B **45**, 13488 (1992)
7. F. Tang, et al. Nature **569**, 537 (2019)
8. B. Skinner et al. Sci. Adv. 4, eaat2621, (2018); Kozii et al. Phys. Rev. B **99**, 155123 (2019)
9. Y. Li, et al. Advances, **5**, 6, eaav7686, DOI: 10.1126/sciadv.aav7686 (2019)
10. A. M. Tsvelik, PNAS **25**, 116 (26) 12729 (2019)

v) Publications (Aug. 2018 – July 2019, One Year)

1) D. Kharzeev and Q. Li "The Chiral Qubit: quantum computing with chiral anomaly" arXiv:1903.07133.
2) F. Tang, et al. "Three-dimensional quantum Hall effect and metal–insulator transition in $ZrTe_5$" *Nature* **569**, 537 (2019)
3) Y. Li, et al. "Tuning from failed superconductor to failed insulator with magnetic field" *Sciences Advances*, **5**, 6, eaav7686 (2019)
4) C. Zhang, et al. "Low-temperature charging dynamics of the ionic liquid and its gating effect on $FeSe_{0.5}Te_{0.5}$ superconducting films" *ACS Appl. Mater. Inter*. **11**, 19, 17979 (2019)
5) T Ozaki, et al. "Two-fold reduction of J_c anisotropy in $FeSe_{0.5}Te_{0.5}$ films using low-energy proton irradiation" *IEEE Trans. on Appl. Supercon*. **29** 5, 7300403 (2019)
6) C. Zhang, et al. "Electron and hole contributions to normal-state transport in the superconducting system $Sn_{1-x}In_xTe$" *Phys. Rev*. B **98**, 054503 (2018)

Current-Driven Interface Magneto-Electric Effect in Complex Oxide Heterostructure

F. Fang[1], Y. W. Yin[2], Qi Li[2] & G. Lüpke[1]

[1]Department of Applied Science, College of William & Mary, Williamsburg, Virginia 23187, USA.

[2]Department of Physics, Pennsylvania State University, University Park, Pennsylvania 16802, USA.

Program Scope

Engineered thin-film heterostructures designed for the electric control of magnetic properties, the so-called *magneto-electric (ME) interfaces*, present a unique route towards using the spin degree of freedom in electronic devices. This research program focuses on the study of a variety of ME coupling effects and coherent spin dynamics in a broad range of complex multiferroic oxide heterostructures using interface-specific and time-resolved nonlinear-optical techniques. Our program concentrates on two major themes: (i) to determine the interfacial ME coupling mechanism and its correlation with charge transfer, orbital states and strain states induced by the substrate or film thickness using the interface-specific magnetization-induced second-harmonic generation (MSHG) technique, and (ii) to investigate its effect on the coherent spin precession in these strongly correlated systems as a new path for fast magnetic switching utilizing the time-resolved magneto-optical Kerr effect (MOKE) technique. The coupling of the ferromagnetic (FM) conducting oxides across a polar oxide layer is interesting, because electric-field modulation of the interlayer exchange coupling introduces new functionalities. The goal of these studies is to elucidate the static and dynamic magnetic interactions and their correlations with the electronic structure and strain states at the valence and lattice mismatched interfaces, which can be artificially engineered. The science addresses issues of energy dissipation and the coupling between electronic and magnetic order in these advanced multi-functional quantum materials, of fundamental importance to our understanding of solid-state properties and has numerous applications.

Recent Progress

Here, we use MSHG technique to selectively probe the interface magnetization of n-type $BaTiO_3/La_{0.7}Sr_{0.3}MnO_3$ (BTO/LSMO) heterojunction as a function of gate voltage U_g (Fig. 1(a)). We fabricated indium-tin-oxide (ITO)(50 nm)/BTO(200 nm)/LSMO(50 nm) heterostructures epitaxially grown on $SrTiO_3$ (STO) (100) substrates by pulsed laser deposition. The ITO and

LSMO layer serve as top and bottom electrodes, respectively. Since the samples are cooled down to room temperature in a reduced oxygen atmosphere, the sufficient native oxygen vacancies in BTO are double shallow donors and will make it n-type (~10^{18}/cm^3). The MSHG technique is well suited for probing the interfacial magnetic state where both space-inversion and time-reversal symmetries are broken. For comparison, MOKE measurements are employed to detect the bulk magnetization. All measurements are performed at 80 K. Figure 1(a) displays the magnetic contrast *A* obtained from the MSHG hysteresis loops as a function of U_g. For $U_g < U_c$ (+6 V), the interfacial LSMO is in the FM state since the magnetic contrast is obvious. Above U_c the magnetic contrast *A* suddenly vanishes, indicating a magnetic transition to anti-ferromagnetic (AFM) phase since a paramagnetic phase is unlikely to occur in LSMO at 80 K due to the strong superexchange interaction of t_{2g} electrons of neighboring Mn ions. We attribute this sudden, reversible FM-to-AFM phase transition to an interface ME effect.

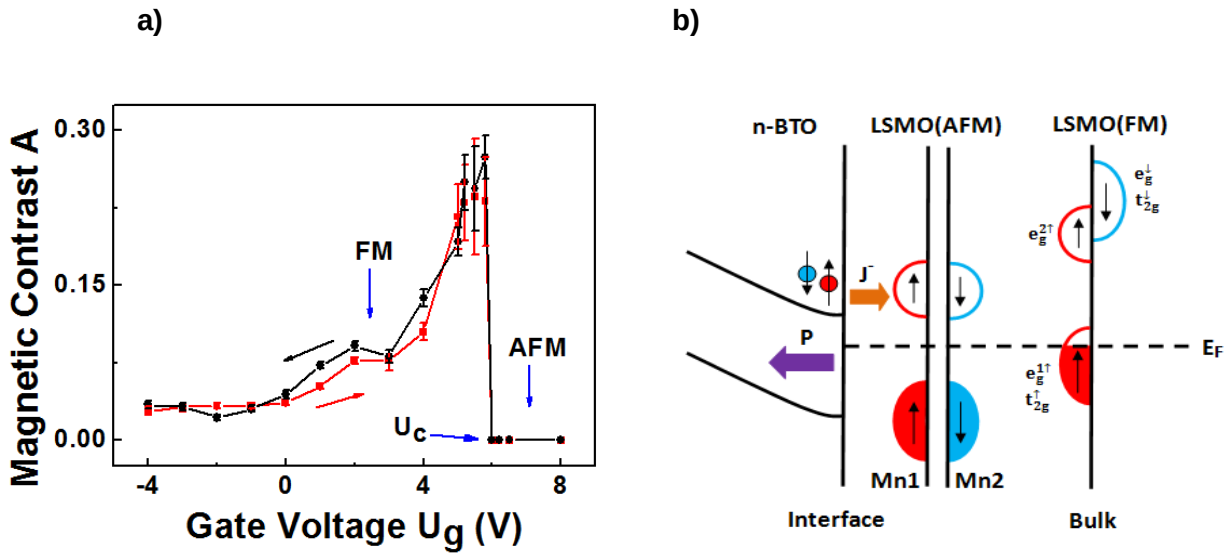

Figure 1: (a) Magnetic contrast *A* determined from MSHG hysteresis loops as a function of gate voltage U_g. The oxygen-rich BTO/LSMO heterojunction exhibits an interface magnetic transition at U_c = +6 V All of the experiments are performed at 78 K. (b) Schematic band diagram of the n-type BTO/LSMO Schottky junction for $U_g > U_c$, depicting the electron current J^-, ferroelectric polarization P, and considering an AFM-ordered LSMO interface layer and a half-metallic LSMO electrode with only spin-up states at the Fermi level E_F.

Figure 1(b) shows a schematic of the proposed band alignment at the n-type BTO/LSMO Schottky junction with positive gate voltage. The band alignment of BTO/LSMO is based on the electron affinity of BTO (3.9 eV) and metal work function of LSMO (4.8 eV), which makes the bands bend up at the interface. For ferroelectric polarization (P) pointing away from the LSMO layer, the hole accumulation biases the interfacial LSMO layer towards the AFM insulating

phase. The $La_{0.7}Sr_{0.3}MnO_3$, however, has stoichiometry that is far enough from the phase boundary and a change in magnetic order is not expected owing solely to a build-up of screening charge. At the reverse gate voltage U_g, no spin injection current occurs at the n-type BTO/LSMO interface. The nearby majority spins of Mn^{3+} and Mn^{4+} ions are double-exchange coupled, leading to a FM state.

On the other hand, for a positive gate voltage applied to the LSMO layer, an electron current (J^-) begins to flow across the BTO/LSMO heterojunction. Both, spin-up and spin-down electrons will be injected from the conduction band of BTO into the interfacial LSMO layer, since the spin polarization of LSMO surfaces extracted from transport measurements usually yield less than 95%. The majority spin-up electrons will quickly relax to the Fermi level and conduct through the LSMO layer. In contrast, the minority spin-down electrons will accumulate at the interface, since the spin-hopping process t is blocked by the strong interaction with the local spins due to the large Hund's rule coupling J_H. This will weaken the double-exchange mechanism and hence reduce the ferromagnetic coupling between Mn ions at the LSMO interface. At a critical gate voltage U_c (+6V), the injected minority spin-down electrons will reduce the double-exchange mechanism such that the AFM super-exchange interaction will dominate, and the interfacial LSMO layer will undergo a FM-to-AFM phase transition. This magnetic reconstruction will occur in the first Mn layer at the interface, since the minority spin-down electrons will strongly scatter with electrons, phonons and magnons, resulting in fast spin-flip processes. The primary one is the Elliott-Yafet-type of spin-flip scattering, which usually takes place on a time scale of a few hundred femtoseconds. For comparison, the characteristic timescales of double- and super-exchange coupling, J≈ -10 K and 7 K, can be estimated via Heisenberg relation $\tau = h/|J| \approx 4$ ps. Hence, the magnetic reconstruction will occur predominantly at the interface. This will also lead to spin frustration, with the competition between AFM coupling at the interface and FM ground state of bulk LSMO. To achieve a more energetically favorable state, the spins in the interfacial layer will cant along the spin direction of the bulk LSMO.

Future Plans

Within the current award work, we have demonstrated the excitation of coherent magnetization precession by photon-induced modulation of FM and AFM phases in LCMO thin film grown on NGO substrate at different temperatures [1]. The dynamic evolution of the bulk magnetization is well monitored in the time domain by the transient MOKE signal. From this study, we know that a transient magnetic field can be generated by photon-induced electronic excitation, which helps generate coherent spin waves in the manganite material. Based on this result, we will apply a static biasing E field on the multiferroic heterostructure to transfer charges onto or away from the interface, which might lead to an electronic orbital occupancy reconstruction, and further modulate the AFM and FM phases of the manganite layer. This will

affect the excitation behavior of spin waves by the above-mentioned photon-induced mechanism. Moreover, we will also investigate the spin precession variance caused by different boundary conditions with the appearance of interfacial ME coupling. The pinning state and alignment of interfacial spins, which can be modulated by the charge state or external E field, play an important role in determining FM spin precession eigenfrequency and damping rate. These aspects can be directly related to the switching speed and stability relevant for magnetic storage performance.

References

1. H. B. Zhao, D. Talbayev, X. Ma, Y. H. Ren, A. Venimadhav, Qi Li, and G. Lüpke, Coherent Spin Precession via Photoinduced Antiferromagnetic Interactions in $La_{0.67}Ca_{0.33}MnO_3$, Phys. Rev. Lett. 107, 207205 (2011).

Publications

1. F. Fang, Y. W. Yin, Qi Li, and G. Lüpke, Current-driven interface magneto-electric effect in complex oxide heterostructure, to be submitted.

2. F. Fang, Y. W. Yin, Qi Li, and G. Lüpke, Spin-polarized current injection induced magnetic reconstruction at oxide interface, Scientific Reports 6:40048, DOI: 10.1038/srep40048 (2017).

3. F. Fang, H. Zhai, X. Ma, Y. W. Yin, Qi Li, and G. Lüpke, Current-driven interface magnetic transition in complex oxide heterostructure, J. Vac. Sci. Technol. B 35, 04F101 (2017); doi: 10.1116/1.4976587.

Program Title: Understanding topological pseudospin transport in van der Waals' materials

Principle Investigator: Kin Fai Mak

Mailing Address: Department of Physics, Cornell University, Ithaca, NY 14853

E-mail: km627@cornell.edu

Program Scope

The goals of the program are to develop a fundamental understanding of the mechanisms of the valley pseudospin transport and to identify regimes for quantized valley Hall conductivity and pure valley pseudospin currents. Successful implementation of the program will help develop techniques to control pseudospin transport and design new pseudospin-based device concepts that may have an impact on the next-generation information technology. Two-dimensional (2D) van der Waals' materials of hexagonal structure including group-VI transition metal dichalcogenides, bilayer graphene, and graphene on hexagonal boron nitride (hBN) are the major materials of interest.

The main strategy that we use to achieve our goals consists of direct measurements of the pseudospin currents or valley Hall conductivity that is required to access the contribution to the valley Hall effect (VHE) from all the filled electronic states and the direction of the pseudospin current flow. The approach can overcome the deficiencies of the initial experiments on the VHE in monolayer molybdenum disulfide (MoS_2) [1], graphene on hBN [2] and bilayer graphene [3, 4] that measure either the change in the valley Hall conductivity induced by photoexcited carriers of given pseudospin state or the nonlocal voltage arisen from the combined VHE and inverse VHE. The direct measurement of the valley conductivity relies on the simultaneous determination of both the pseudospin polarization accumulated on the channel edges of the transistors driven by the VHE and the electron intervalley scattering time. The former can be probed by the Kerr rotation microscopy and the latter by the femtosecond two-pulse correlation of the anomalous Hall voltage generated by circularly polarized laser pulses.

The projects also involve fabrication of 2D vdW materials and their heterostructures by micromechanical exfoliation and transfer, and nanofabrication of electronic and optoelectronic devices based on these materials and structures.

Recent Progress

<u>Nonlinear anomalous Hall effect in few-layer WTe_2</u>

It is well known that the Hall effect occurs only in systems with broken time-reversal symmetry, such as materials under an external magnetic field in the ordinary Hall effect or magnetic materials in the anomalous Hall effect. Unlike the linear Hall effect that has to vanish to satisfy

the Onsager's reciprocity relation in a time-reversal invariant system, the nonlinear Hall effect (NHE), in principle, does not have to vanish. However, it requires a planar metal with a polar axis, which carries local electric polarization. Few-layer T_d-WTe_2, a 2D semimetal with broken inversion symmetry and only one mirror line in the crystal plane (Fig. 1a), satisfies this requirement. We have performed transport studies on these materials, and observed a Hall response under zero magnetic field that scales quadratically with the bias voltage (Fig. 1b). Angle-resolved measurements reveal that the Hall voltage maximizes (vanishes) when the bias current is perpendicular (parallel) to the polar axis (Fig. 1c and 1d). The observed effect can be understood as an anomalous Hall effect induced by a current induced out-of-plane magnetization so that a quadratic Hall voltage is produced. The temperature dependence of the Hall conductivity suggests that both intrinsic Berry curvature dipole, a topological quantity of Bloch bands, and extrinsic spin-dependent scatterings contribute to the observed NHE. Our results open the door for exploring topological effects in solids by nonlinear electrical transport and applications in spin-charge conversion. The result has been published in Nature Materials [5].

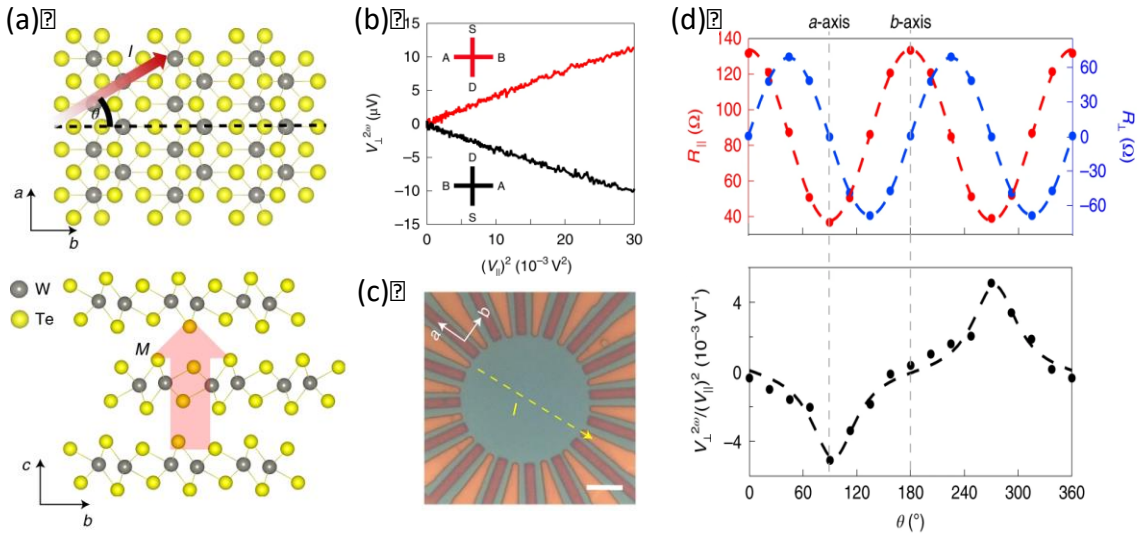

Fig. 1 (a) The polar crystal structure of few-layer T_d-WTe_2. An electrical bias perpendicular to the polar axis (black dashed line) produces an out-of-plane magnetization. (b) Quadratic dependence of the second harmonic nonlinear Hall voltage on the bias voltage. (c) Electrical device for angle-resolved transport measurements. The crystal a and b axes are shown. Scale bar corresponds to 5 microns. (d) Angle-dependent linear transport coefficients (top) and nonlinear Hall susceptibility (bottom).

Future Plans

Exciton condensation at high temperatures

Excitons in 2D transition metal dichalcogenide semiconductors are tightly bound because of the significantly reduced dielectric screening. The large exciton binding opens the door for realizing exciton condensation at temperatures much higher than other excitonic systems. We plan to carry out a series of complementary experiments to explore the properties of exciton condensates in

transition metal dichalcogenide double layers. We will also demonstrate exciton superfluidity and superconductivity, as well as to find ways to enhance the condensation temperature. Particular plans include: 1) measurement of the spatial coherence length and the condensation energy gap; 2) tuning of the interlayer exciton binding energy and the transition temperature; 3) demonstration of exciton superfluidity and high-temperature superconductivity; and 4) demonstration of the BEC to BCS crossover.

References

1. Mak, K. F., McGill, K. L., Park, J. & McEuen, P. L. The valley Hall effect in MoS_2 transistors. *Science* **344,** 1489–1492 (2014).
2. Gorbachev, R. V. *et al.* Detecting topological currents in graphene superlattices. *Science* **346,** 448–451 (2014).
3. Sui, M. *et al.* Gate-tunable topological valley transport in bilayer graphene. *arXiv*:1501.04685 (2015).
4. Shimazaki, Y. *et al.* Generation and detection of pure valley current by electrically induced Berry curvature in bilayer graphene. *arXiv:*1501.04776 (2015).
5. Kang, K., Li, T., Sohn, E., Shan, J., & Mak, K. F., "Nonlinear anomalous Hall effect in few-layer WTe_2," *Nature Mater.* **18,** 324-328 (2019)

Publications

1. G. M. Stiehl, R. Li, V. Gupta, I. El Baggari, S. Jiang, H. Xie, L. F. Kourkoutis, K. F. Mak, J. Shan, R. A. Buhrman, & D. C. Ralph, "Layer-dependent spin-orbit torques generated by the centrosymmetric transition metal dichalcogenide β-$MoTe_2$," arXiv:1906.01068 (2019).
2. T. Li, S. Jiang, N. Sivadas, Z. Wang, Y. Xu, D. Weber, J. E. Goldberger, K. Watanabe, T. Taniguchi, C. J. Fennie, K. F. Mak, & J. Shan, "Pressure-controlled interlayer magnetism in atomically thin CrI_3," *Nature Mater.* In press (2019).
3. Z. Wang, D. A. Rhodes, K. Watanabe, T. Taniguchi, J. C. Hone, J. Shan, & K. F. Mak, "Evidence of high-temperature exciton condensation in 2D atomic double layers," *Nature* In press (2019).
4. K. F. Mak, J. Shan, & D. C. Ralph, "Two-dimensional layered magnetic materials: Probing and controlling their magnetic states," *Nature Rev. Phys.* In press (2019).
5. Y. Tang, K. F. Mak, & J. Shan, "Long valley lifetime of dark excitons in single-layer WSe_2," *Nature Commun.* **10,** 4047 (2019).
6. H. H. Kim, B. Yang, S. Li, S. Jiang, C. Jin, Z. Tao, G. Nichols, F. Sfigakis, S. Zhong, C. Li, S. Tian, D. G. Cory, G.-X. Miao, J. Shan, K. F. Mak, H. Lei, K. Sun, L. Zhao, & A.

W. Tsen, “Evolution of interlayer and intralayer magnetism in three atomically thin chromium trihalides,” *Proc. Nat. Acad. Sci.* **116,** 11131-11136 (2019).

7. S. Jiang, L. Li, Z. Wang, J. Shan, & K. F. Mak, “Spin transistor built on 2D van der Waals heterostructures,” *Nature Electron.* **2,** 159-163 (2019).
8. K. Kang, T. Li, E. Sohn, J. Shan, & K. F. Mak, “Nonlinear anomalous Hall effect in few-layer WTe_2,” *Nature Mater.* **18,** 324-328 (2019).
9. D. V. Tuan, B. Scharf, Z. Wang, J. Shan, K. F. Mak, I. Zutic, & H. Dery, “Probing many-body interactions in monolayer transition-metal dichalcogenides,” *Phys. Rev. B* **99,** 085301 (2019).
10. K. F. Mak, & J. Shan, “Opportunities and challenges of interlayer exciton control and manipulation,” *Nature Nanotech.* **13,** 974-976 (2018).
11. K. F. Mak, D. Xiao, & J. Shan, “Light-valley interactions in 2D semiconductors,” *Nature Photon.* **12,** 451-460 (2018).
12. S. Jiang, L. Li, Z. Wang, K. F. Mak, & J. Shan, “Controlling magnetism in 2D CrI_3 by electrostatic doping,” *Nature Nanotech.* **13,** 549-553 (2018).
13. H. Xie, S. Jiang, J. Shan, & K. F. Mak, “Valley-selective exciton bistability in a suspended monolayer semiconductor,” *Nano Lett.* **18,** 3213-3220 (2018).
14. E. Sohn, X. Xi, W. He, S. Jiang, Z. Wang, K. Kang, J.-H. Park, H. Berger, L. Forró, K. T. Law, J. Shan, & K. F. Mak, “An unusual continuous paramagnetic-limited superconducting phase transition in 2D $NbSe_2$,” *Nature Mater.* **17,** 504-508 (2018).
15. K. F. Mak & J. Shan, “Mirrors made of a single atomic layer,” *Nature* **556,** 177-178 (2018).
16. S. Jiang, J. Shan, & K. F. Mak, “Electric-field switching of two-dimensional van der Waals magnets,” *Nature Mater.* **17,** 406-410 (2018).
17. Z. Wang, K. F. Mak, & J. Shan, “Strongly interaction-enhanced valley magnetic response in monolayer WSe_2,” *Phys. Rev. Lett.* **120,** 066402 (2018).
18. Z. Wang, Y.-H. Chiu, K. Honz, K. F. Mak, & J. Shan, “Electrical tuning of interlayer exciton gases in WSe_2 bilayers,” *Nano Lett.* **18,** 137-143 (2018).

Direct Observation of Fractional Quantum Hall Quasiparticle Braiding Statistics via Interferometry

Michael Manfra
Department of Physics and Astronomy
Schools of Electrical and Computer Engineering and Materials Engineering
Purdue University
telephone: 765-494-3016
email: mmanfra@purdue.edu

Program Scope

Utilizing a recent breakthrough in AlGaAs/GaAs heterostructure design that allows for operation of electronic Fabry-Perot interferometers with reduction of quantum dot-like charging effects while simultaneously generating sharper edge potential profiles, we have recently demonstrated Aharonov-Bohm (AB) interference of fractional quantum Hall effect edge modes. Clear demonstration of AB interference of fractional edge modes is a vital step towards demonstration Abelian and non-Abelian braiding statistics. We propose a series of interferometry experiments aimed at answering the most important questions surrounding quantum coherence and braiding statistics in quantum Hall systems. Fine control of device parameters in this new system facilitates systematic investigation of quantum coherence, edge state reconstruction, and braiding statistics. The objectives of this project are:

- Measurement of Abelian phase for the fractional quantum Hall state at $\nu=1/3$
- Exploration of the limit of interferometer size reduction while maintaining operation in Aharonov-Bohm regime
- Quantification of quantum coherency of fractional edge modes via measurement of the temperature dependence of AB oscillation amplitude and dependence on interferometer size
- Design of heterostructures and measurement of interferometers to probe non-Abelian braiding statistics at $\nu=5/2$
- Measurement of interferometers in which the edge potential prolife is systematically modified through variation of screening well-quantum well separation to study impact on edge mode reconstruction

Using a combination of heterostructure growth, mesoscopic device fabrication, and low temperature electronic transport measurements, this project aims to provide the first direct measurement of Abelian and non-Abelian braiding statistics. Information learned during this work will be crucial to determination if quantum Hall systems are capable of hosting topological qubits. Our work will also inform investigations of other topological material systems where

systematic control of epitaxial growth, device fabrication and operation are currently in more nascent stages. We hope our work may serve as a blueprint for interrogation of other topological phases needed to support next generation quantum systems.

Recent Progress

Our first generation of devices and the results obtained are shown in the figure below. The

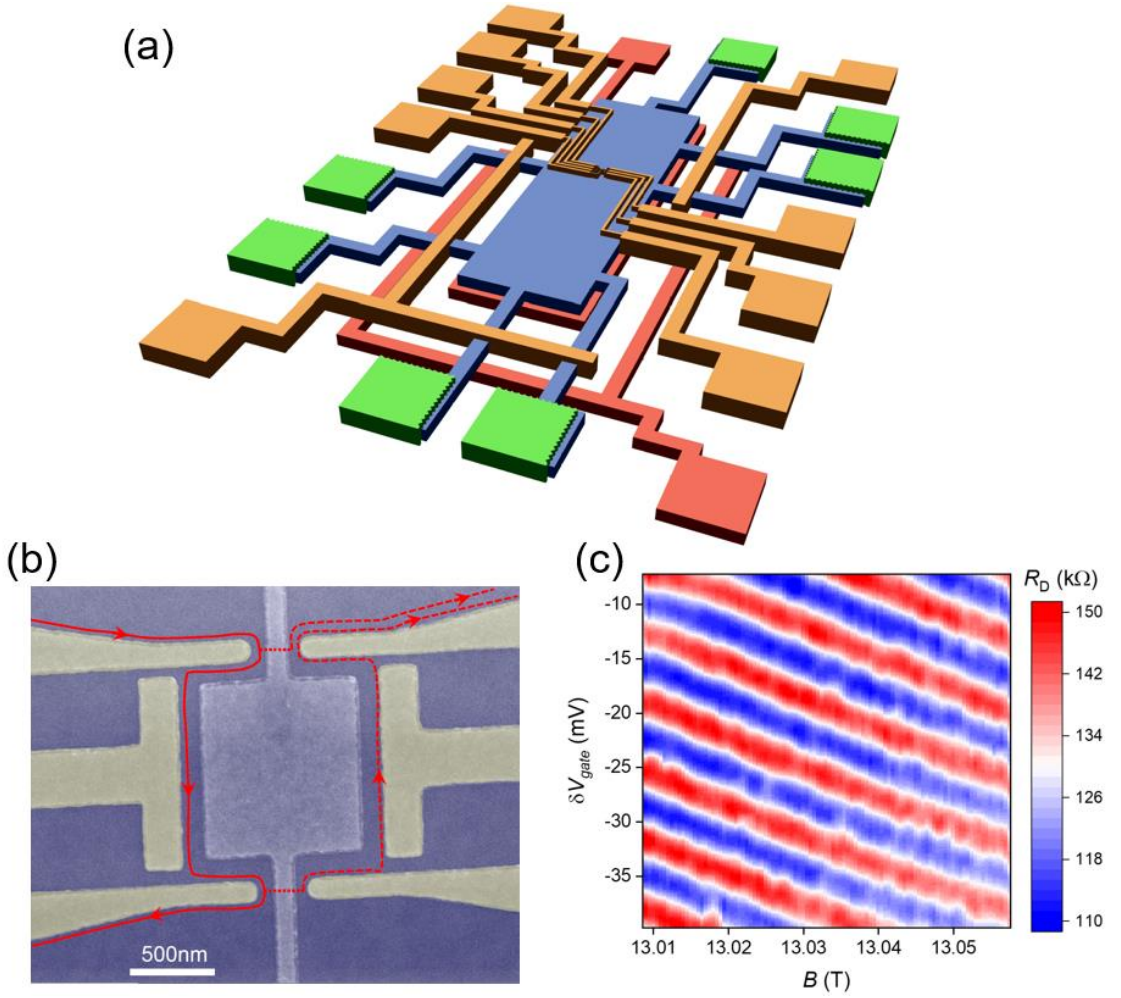

(a) Schematic of the interferometer device. The GaAs mesa is shown in blue, Ohmic contacts are shown in green, metal surface gates are shown in orange, and metal backgates are shown in red. The metal gates which extend onto the middle of the mesa are used to define the interference path, while the metal surface and backgates which extend across the arms of the Ohmic contacts are negatively biased to disconnect the contacts from the screening wells so that only the primary quantum well is probed in measurements. (b) SEM image of the interferometer, located in the middle of the mesa. The gates highlighted in yellow are negatively biased to define the interference path; red lines indicate the edge state, with the backscattered paths shown in dashed lines. (c) Resistance oscillations measured across the device as a function of magnetic field and side gate voltage at the $\nu = 1/3$ quantum Hall state.

addition of screening wells in proximity to the primary quantum well allow the interferometer to operate in Aharonov-Bohm regime. This device architecture allows experiments to be conducted in the fractional quantum Hall regime.

Future Plans

- Measurement of Abelian phase for the fractional quantum Hall state at $\nu=1/3$
- Exploration of the limit of interferometer size reduction while maintaining operation in Aharonov-Bohm regime
- Quantification of quantum coherency of fractional edge modes via measurement of the temperature dependence of AB oscillation amplitude and dependence on interferometer size
- Design of heterostructures and measurement of interferometers to probe non-Abelian braiding statistics at $\nu=5/2$
- Measurement of interferometers in which the edge potential prolife is systematically modified through variation of screening well-quantum well separation to study impact on edge mode reconstruction

Publications

J. Nakamura et al. Nature Physics **15** 563-569 (2019)

Project Title: Superconductivity and magnetism in *d*- and *f*-electron materials

Principal Investigator: M. Brian Maple
Mailing address: Department of Physics, University of California, San Diego, La Jolla, California 92093
Email: mbmaple@ucsd.edu

Program Scope

The objectives of this research program are the experimental investigation and development of a fundamental understanding of emergent phases and phenomena that are produced by competing interactions in strongly correlated electron quantum materials. The underlying physics on which these emergent phases and phenomena are based constitutes one of the most important and challenging problems in condensed matter physics. The application of pressure, temperature, atomic substitution, and magnetic fields are used to "tune" the competing interactions and emergent phenomena. A combination of materials synthesis and physical properties measurements are employed to characterize these phenomena, map out the complex phase diagrams in which they reside, determine how different phases are related to one another, probe the underlying physics, and, when possible, test relevant theoretical models.

Experimental investigations of the physics of several classes of correlated electron materials have been conducted in this research program, including: (1) Superconductivity (SC) in layered electron-doped $LnO_{0.5}F_{0.5}BiS_2$ (*Ln* = lanthanide) compounds, unconventional multiband SC with gap nodes and broken time reversal symmetry in the filled skutterudite systems $Pr_{1-x}Ln_xPt_4Ge_{12}$ (*Ln* = Ce, Eu), and unconventional SC and quantum criticality in $Ce_{1-x}Ln_xCoIn_5$ (*Ln* = Yb, Sm) systems; (2) correlated electron phenomena in filled skutterudite $LnOs_4Sb_{12}$ and "1-2-20" LnT_2Cd_{20} (*T* = Ni, Pd) "cage" compounds; (3) electronic phases that emerge from "tuning" competing interactions in the "hidden order" compound URu_2Si_2 via substitution of *T* ions for Ru (particularly, *T* = Fe, Os, Re) and application of high pressure and high magnetic fields; (4) investigation of the properties of transition metal monosilicides, particularly, the correlated electron small gap semiconductor FeSi, which appears to have a conducting surface state below 19 K; (5) ac magnetic susceptibility and specific heat measurements to low temperatures on single crystals of the quantum spin liquid pyrochlore candidate $Ce_2Zr_2O_7$ in collaboration with Prof. Pengcheng Dai of Rice University and his group.

Recent Progress

Recent progress on three projects in which emergent phenomena and phases have been observed in quantum materials is described in the following:

Conducting surface state in FeSi

The transition metal monosilicide FeSi is considered to be a strongly correlated electron semiconductor with a small energy gap of about 0.05 eV at low temperatures. One of the most intriguing physical properties of FeSi is its magnetic susceptibility, which increases with temperature above 100 K, passes through a broad maximum at ~500 K, and then exhibits Curie-Weiss behavior at higher temperatures. The electrical conductivity of FeSi also rises steeply in the same temperature interval as the magnetic susceptibility. Neutron diffraction measurements have not revealed any evidence of magnetic order in FeSi. During the past year, we have been investigating the physical properties of high quality FeSi single crystals prepared in our lab by growth in a molten Sn flux. This work yielded the discovery of a semiconducting to metallic crossover with decreasing temperature at ~19 K, which is not accompanied by any features in bulk properties [J6]. These experiments provide evidence for a conducting surface state in FeSi, reminiscent of the conducting surface state of a topological insulator.

Unconventional superconductivity of $PrPt_4Ge_{12}$

The filled skutterudite compound $PrPt_4Ge_{12}$ is a SCor with a relatively high T_c of 8 K with properties similar to those of the extraordinary correlated *f*-electron SCor $PrOs_4Sb_{12}$ (T_c = 1.86 K), discovered in our lab in 2002. Both compounds exhibit unconventional SC, characterized by time reversal symmetry breaking (TRSB), gap nodes, and multiband SC, and are considered to be leading candidates for hosting 3-D Majorana fermions. The unconventional SC of $PrPt_4Ge_{12}$ was probed by measuring the SCing- and normal-state properties of the substitutional systems $Pr_{1-x}Ln_xPt_4Ge_{12}$ for the substituents *Ln* = Ce and Eu, both of which suppress T_c with *x* towards 0 K at $x \approx 0.6$. The SC of the $Pr_{1-x}Ce_xPt_4Ge_{12}$ ($0 \leq x \leq 0.2$) system was investigated further by means of specific heat $C(T)$ measurements [R1]. Analysis of the $C(T)$ data for $x \leq 0.07$ revealed that SC develops in at least two bands; the SCing order parameter has nodes on one Fermi surface pocket and remains fully gapped on the other. Both the nodal and nodeless gaps decrease, with the nodal gap being suppressed more strongly, upon Ce substitution. The higher Ce concentration samples ($x > 0.07$) display only a nodeless gap. In the $Pr_{1-x}Eu_xPt_4Ge_{12}$ system, $C(T)$ measurements revealed that SC and short-range antiferromagnetic order coexist in the range $x \leq 0.6$ [J9].

Emergent phases generated by tuning competing interactions in URu_2Si_2

We have been involved in an investigation of the novel electronic states (excluding SC) that emerge upon tuning competing interactions in the "hidden order" (HO) *f*-electron compound URu_2Si_2 via the variation of substituent composition *x*, pressure *P* and magnetic field *H*. This produces complex temperature *T* vs. *x*, *P*, and *H* phase diagrams that contain a multitude of correlated electron phases and phenomena. For example, we discovered that substitution of isoelectronic Fe for Ru in URu_2Si_2 produces a transition from the HO to the AFM phase at $x_c \approx 0.15$ [R2], similar to that which occurs under pressure in URu_2Si_2 at $P_c \approx 1.5$ GPa. We proposed that single crystals of $URu_{2-x}Fe_xSi_2$ could provide an opportunity to study the transition from the HO to the AFM phase at ambient pressure with techniques that cannot be readily performed on URu_2Si_2 under pressure (e.g., ARPES, STM, neutron scattering, measurements in high magnetic fields, etc.), providing new information about the HO phase, whose identity has remained a mystery for over 3 decades. During the past several years, we have synthesized a series of $URu_{2-x}Fe_xSi_2$ single crystals by means of the Czochralski method in a tetra-arc furnace for investigations underway in our lab, the labs of our collaborators, and national laboratory facilities.

In one of the most intriguing experiments, the HO and AFM phases of $URu_{2-x}Fe_xSi_2$ were investigated in collaboration with Girsh Blumberg and Sean Kung at Rutgers University [R3] by means of polarization resolved Raman spectroscopy. In a previous study using this technique, the Prof. Blumberg's group obtained evidence that the HO phase in URu_2Si_2 is a "chirality density wave" [R4]. In the experiments on $URu_{2-x}Fe_xSi_2$, a collective mode of pseudovector-like A_{2g} symmetry was observed. With increasing *x*, the mode energy decreases monotonically in the HO phase, vanishes at the x_c where the HO-AFM transition occurs, and then reappears with increasing energy in the AFM phase. The mode's evolution provides evidence for a unified order parameter for both HO and AFM phases arising from the orbital degrees-of-freedom of the U 5*f* electrons.

In another important experiment that we carried out at the NHMFL facilities at FSU, Tallahassee, and LANL, the 3-D *T*-*H*-*x* phase diagram for $URu_{2-x}Fe_xSi_2$ in magnetic fields *H* up to 45 T was constructed from magnetoresistance data as a function of *T*, *H* and *x* [J3]. This work was featured in a recent NHMFL Highlight [R5].

Future Plans

Research projects planned for the future include the following:

- Preparation and investigation of the electronic and magnetic properties of transition metal monosilicides, particularly, the correlated electron narrow gap semiconductor FeSi, which has a conducting surface state recently discovered in our laboratory. Experiments will be performed in an effort to determine if the surface state of FeSi is topologically protected.
- High pressure studies of unconventional SC that emerges from magnetically ordered, charge ordered, and insulating phases in layered Fe-pnictide/chalcogenide and Bi-sulfide compounds. Some of the measurements will extend into the megabar range with diamond anvil cells. One class of experiments under consideration will focus on the effect on $T_c(P)$ of site selective doping of Fe-based SCors with electrons or holes, inspired by dramatic differences in the behavior of $T_c(P)$ observed in our site-selective doping experiments on BiS_2-based SCors. Exploratory high-pressure experiments will be carried out on selected quantum materials such as layered Fe-based compounds, transition metal oxides, and topological insulators with the goal of raising the T_c of known SCing materials or inducing SC in non-SCing materials.
- Investigation of quantum spin liquid (QSL) behavior and other emergent phenomena in geometrically frustrated compounds such as $Ln_2T_2O_7$ pyrochlores.
- Continuation of ongoing experiments on emergent phases that arise from the tuning of competing interactions in $URu_{2-x}M_xSi_2$ (M = Fe, Os, Re) single crystals and exploratory experiments on $URu_{2-x}M'_xSi_2$ (M' = Co, Ir) polycrystals.
- Synthesis of LnT_2X_{20} (Ln = Ce, Pr; T = Ti, V, Ni, Pd, Pt; X = Al, Zn, Cd) single crystals and investigation of correlated electron phenomena in these materials.
- Synthesis and study of unconventional superconductivity and correlated electron phenomena in $PrPt_4Ge_{12}$-based filled skutterudite pseudoternary compounds.

References

R1. Y. P. Singh, R. B. Adhikari, S. Zhang, K. Huang, D. Yazici, I. Jeon, M. B. Maple, M. Dzero, and C. C. Almasan, "Multiband superconductivity in the correlated electron filled skutterudite system $Pr_{1-x}Ce_xPt_4Ge_{12}$," *Phys. Rev. B* **94**, 144502 (2016).

R2. S. Ran, C. T. Wolowiec, I. Jeon, N. Pouse, N. Kanchanavatee, B. D. White, K. Huang, D. Martien, T. DaPron, D. Snow, M. Williamsen, S. Spagna, P. S. Riseborough, and M. B. Maple, "Phase diagram and thermal expansion measurements on the system $URu_{2-x}Fe_xSi_2$," *Proc. Nat. Acad. Sci.* **113**, 13348 (2016).

R3. H.-H. Kung, S. Ran, N. Kanchanavatee, V. Krapivin, A. Lee, J. A. Mydosh, K. Haule, M. B. Maple, and G. Blumberg, "Analogy Between the "Hidden Order" and the Orbital Antiferromagnetism in $URu_{2-x}Fe_xSi_2$," *Phys. Rev. Lett.* **117**, 227601 (2016).

R4. H.-H. Kung, R. E. Baumbach, E. D. Bauer, V. K. Thorsmølle, W. L. Zhang, K. Haule, J. A. Mydosh, and G. Blumberg, "Chirality density wave of the "hidden order" phase in URu_2Si_2," *Science* **347**, 1339 (2015).

R5. National High Magnetic Field Laboratory Highlight: (https://nationalmaglab.org/user-facilities/pulsed-field-facility/publications-pulsed-field/highlights-pulsed-field/hidden-order-phase

Publications (supported by BES)

Ph.D. Theses:

Four Ph.D. Theses based on BES supported research were completed during this grant period: Inho Jeon, Christian Todd Wolowiec (2017); Yuankan Fang, Naveen Pouse (2018).

Journal Articles (selected):

J1. I. Jeon, S. Ran, A. J. Breindel, P.-C. Ho, R. B. Adhikari, C. C. Almasan, B. Luong, and M. B. Maple, "Crossover and coexistence of superconductivity and antiferromagnetism in the filled-skutterudite system $Pr_{1-x}Eu_xPt_4Ge_{12}$," *Phys. Rev. B* **95**, 134517 (2017).

J2. Y. Fang, D. Yazici, I. Jeon, and M. B. Maple, "High-pressure effects on nonfluorinated BiS_2-based superconductors $La_{1-x}M_xOBiS_2$ (M = Ti and Th)," *Phys. Rev. B* **96**, 214505 (2017).

J3. Sheng Ran, Inho Jeon, Naveen Pouse, Alexander J. Breindel, Noravee Kanchanavatee, Kevin Huang, Andrew Gallagher, Kuan-Wen Chen, David Graf, Ryan E. Baumbach, John Singleton, and M. Brian Maple, "Phase diagram of $URu_{2-x}Fe_xSi_2$ in high magnetic fields," *Proc. Nat. Acad. Sci.* **114**, 9826 (2017).

J4. T. Yanagisawa, S. Mombetsu, H. Hidaka, H. Amitsuka, P. T. Cong, S. Yasin, S. Zherlitsyn, J. Wosnitza, K. Huang, N. Kanchanavatee, M. Janoschek, M. B. Maple, and D. Aoki, "Search for multipolar instability in URu_2Si_2 studied by ultrasonic measurements under pulsed magnetic field," *Phys. Rev. B* **97**, 155137 (2018).

J5. E. M. Levenson-Falk, E. R. Schemm, Y. Aoki, M. B. Maple, and A. Kapitulnik, "Polar Kerr Effect from Time Reversal Symmetry Breaking in the Heavy Fermion Superconductor $PrOs_4Sb_{12}$," *Phys. Rev. Lett.* **120**, 187004 (2018).

J6. Yuankan Fang, Sheng Ran, Weiwei Xie, Shen Wang, Ying Shirley Meng, and M. Brian Maple, "Evidence for a conducting surface ground state in high-quality single crystalline FeSi," *Proc. Nat. Acad. Sci.* **115**, 8558 (2018).

J7. Y. P. Singh, R. B. Adhikari, D. J. Haney, B. D. White, M. B. Maple, M. Dzero, and C. C. Almasan, "Zero-field quantum critical point in $Ce_{0.91}Yb_{0.09}CoIn_5$," *Phys. Rev. B* **97**, 184514 (2018).

J8. Yinming Shao, Zhiyuan Sun, Ying Wang, Chenchao Xu, Raman Sankar, Alexander J. Breindel, Chao Cao, Michael M. Fogler, Andrew J. Millis, Fangcheng Chou, Zhiqiang Li, Thomas Timusk, M. Brian Maple, and Dmitri N. Basov, "Optical signatures of Dirac nodal lines in $NbAs_2$," *Proc. Nat. Acad. Sci.* **116**, 1168 (2019).

J9. R. B. Adhikari, D. L. Kunwar, I. Jeon, M. B. Maple, M. Dzero, and C. C. Almasan, "Short-range antiferromagnetic correlations in the superconducting state of filled skutterudite alloys $Pr_{1-x}Eu_xPt_4Ge_{12}$," *Phys. Rev. B* **98**, 064506 (2018).

J10. S. Ran, G. M. Schmiedeshoff, N. Pouse, I. Jeon, N. P. Butch, R. B. Adhikari, C. C. Almasan, and M. B. Maple, "Rapid suppression of the energy gap and the possibility of a gapless hidden order state in $URu_{2-x}Re_xSi_2$," *Phil. Mag.* **99**, 1751 (2019).

J11. Z. F. Ding, J. Zhang, C. Tan, K. Huang, Q. Y. Chen, I. Lum, O. O. Bernal, P.-C. Ho, D. E. MacLaughlin, M. B. Maple, and L. Shu, "Renormalizations in unconventional superconducting states of $Ce_{1-x}Yb_xCoIn_5$," *Phys. Rev. B* **99**, 035136 (2019).

J12. Peter Kissin, Sheng Ran, Dylan Lovinger, Verner K. Thorsmølle, Noravee Kanchanavatee, Kevin Huang, M. Brian Maple, and Richard D. Averitt, "Quasiparticle relaxation dynamics in $URu_{2-x}Fe_xSi_2$ single crystals," *Phys. Rev. B* **99**, 165144 (2019).

J13. Bin Gao, Tong Chen, David W. Tam, Chien-Lung Huang, Kalyan Sasmal, Devashibhai T. Adroja, Feng Ye, Huibo Cao, Gabriele Sala, Matthew B. Stone, Christopher Baines, Joel A. T. Verezhak, Haoyu Hu, Jae-Ho Chung, Xianghan Xu, Sang-Wook Cheong, Manivannan Nallaiyan, Stefano Spagna, M. Brian Maple, Andriy H. Nevidomskyy, Emilia Morosan, Gang Chen and Pengcheng Dai, "Experimental signatures of a three-dimensional quantum spin liquid in effective spin-1/2 $Ce_2Zr_2O_7$ pyrochlore," *Nature Physics* (2019) https://doi.org/10.1038/s41567-019-0577-6

Magnetic interactions and excitations in quantum materials

Robert McQueeney, Peter P. Orth, David C. Johnston, David Vaknin, Liqin Ke, Ben Ueland, Deborah Schlagel
Ames Laboratory, Ames, IA 50011

Program Scope

A generational challenge in condensed matter physics is to reveal the interrelationship between spin and charge that plays a central role in the emergence of quantum phenomena. Overcoming this challenge requires the development of extensive insight into the microscopic origins of magnetism, including the roles of covalency and itinerancy, spin-orbit coupling, competing magnetic states and frustration, symmetry breaking, and electronic band topology. Our research program combines the synthesis and discovery of novel magnetic materials, the experimental characterization of their quantum phenomena, the determination of magnetic correlations and corresponding excitations using neutron scattering techniques, and theoretical calculations that employ first-principles electronic band structure and analytical and numerical methods. The current program scope is focused on two research thrusts; (1) Kinetic frustration and flat bands in itinerant magnets and (2) Interplay of magnetism, itinerancy and topology in magnetic materials.

Recent Progress

Thrust 1: Kinetic frustration and flat bands in itinerant magnets. Magnetic frustration in local-moment systems has gained considerable interest due to the possibility of generating quantum spin liquids, spin ices, and other unique quantum states. In *itinerant* magnetic frustration (or *kinetic frustration*), flat bands and frustration occur from destructive interference of different hopping paths of the conduction electrons, leading to the localization of electronic states [1]. The large *electronic* flat band degeneracy is lifted by electronic correlations or other interactions, making these materials susceptible to a variety of instabilities, including ferromagnetism (FM), superconductivity, charge ordering, and other entangled quantum magnetic ground states. Kinetic frustration shares certain criteria with local moment frustration, e.g., such systems are predicted to occur on geometrically frustrated lattices for antiferromagnetic (AF) ordering, with the essential difference being that kinetically frustrated magnets are metallic. As described below, the metallic nature allows for sensitive tuning of the different possible ground states via chemical substitutions.

We have discovered a class of itinerant magnets based on square-lattice cobalt pnictide metals which harbor signatures of weakly itinerant FM [2], unusual spin fluctuations [3], and magnetic frustration between FM and stripe-type AF states [P1], which are suggested to arise from flat-band driven Stoner instabilities [4]. Our recent work provides evidence for extreme magnetic frustration in $CaCo_2As_2$ [P1] and temperature driven magnetic phase competition in $SrCo_2As_2$ [P2].

We also study chemically-substituted compositions, such as $(Ca,Sr)Co_2As_2$ [P3,P4] and $Sr(Co,Ni)_2As_2$ [P5], to examine the tunable intralayer ferromagnetism driven by the proximity of flat electronic bands to the Fermi energy. Surprisingly, we find the details of the AF stacking of the FM-aligned layers involve subtle interlayer magnetic interactions which are highly sensitive to doping. In the Ni-doped case, we find a helical stacking of Co-moments [P5-P7]. We extended these studies to $EuCo_2As_2$ [P8] and $EuNi_2As_2$ [P9] where the Eu^{+2} ions carry a large spin 7/2. In the former compound we discovered that the Eu moments are significantly enhanced by ferromagnetic interactions with the Co 3*d* electrons, and in the latter we inferred that the Eu spins undergo AF order into a *c*-axis helix structure below a temperature T_N = 15 K.

Thrust 2 – Interplay of magnetism, itinerancy and topology in magnetic materials. In AF semiconductors and magnetic topological semimetals (TSMs), the coupling of localized magnetic moments to charge carriers is a primary factor controlling their transport properties. A fundamental understanding of this coupling, including the microscopic nature of the magnetic interactions and details of the spin Hamiltonian (anisotropy, energy scale of exchange interactions, hierarchy of couplings, symmetry) is critical for exploiting their functionality. For example, in magnetic topological materials, quantum magnetotransport phenomena (such as chiral anomalies) arise directly from the coupling of magnetism to topological fermions.

Our work on carrier-doped $BaMn_2As_2$-based AF semiconductors has revealed the coexistence of both local-moment AF and itinerant FM [5-8]. We have shown that the observed half-metallic FM is associated with itinerant As 4*p* electronic bands. These discoveries led to recent investigations of the magnetic TSM candidate $SrMnSb_2$ [P10] where the development of FM out of strong AF correlations, possibly enabled by hole-doping (as was found in $BaMn_2As_2$), may enable topologically protected chiral electron transport. We have found these materials to have interesting magnetic and transport properties, but they are resistant to carrier doping [P11].

Our study of magnetic topological insulators (TI) obtained the remarkable result that collective magnetic excitations can be observed by neutron scattering from the dilute magnetic TI $(Bi_{0.95}Mn_{0.05})_2Te_3$ [P12]. The discovery of stoichiometric and periodic AF-TI compounds, such as $MnBi_2Te_4$ and $MnBi_{2-x}Sb_xTe_4$, [P13-15] provide new opportunities to study the fundamental nature of magnetism in TIs from the dilute to the fully occupied limit. It is an open question as to whether the coupling between magnetism and topological fermions, or even the topological nature of Dirac or Weyl fermions themselves, can be determined through an investigation of magnetic excitations. $MnBi_2Te_4$ and $SrMnSb_2$ appear to be ideal systems to address this question.

Future Plans

Thrust 1: Our main hypothesis in Thrust 1 is that it is possible to "tune" itinerant magnetic frustration and obtain electronic states that can be potentially exploited in spintronics, quantum computing, and various other quantum-based technologies. Our future work aims at synthesizing hole- and electron-doped compositions of ACo_2As_2 compounds, such as $Sr(Co_{1-x}Ni_x)_2As_2$, to determine their magnetic and electronic ground states and the degree of frustration by magnetization, heat capacity, electronic transport, neutron diffraction, and inelastic neutron scattering (INS) measurements.

Establishing that the principles of kinetic frustration are operative in the development of different magnetic and electronic ground states in the cobalt arsenides would constitute a new paradigm in the field of frustrated magnetism. Dynamical spin susceptibilities will be calculated using first-principles methods [9] to directly compare with INS measurements and unravel the nature of spin excitations. Based on *ab initio* band structures, multi-band Hubbard-Hund models can also be constructed and investigated by analytical approaches such as the random-phase approximation or renormalization group theory. This will correlate the magnetic interactions with details of the band structure and identify the origins of observed electronic instabilities and magnetic phases.

Finally, kinetically frustrated materials are susceptible to forming a variety of sought-after quantum states, such as those with chiral or incommensurate magnetic order or even *p*-wave superconductivity. Our current work on kinetically frustrated cobalt arsenides puts us in an ideal position to expand into studies of other potential flat-band systems, such as YCo_2.

Thrust 2: We will pursue targeted experimental studies on single crystals of carrier-doped square-lattice and corrugated honeycomb lattice AF semiconductors, such as $BaMn_2As_2$ and $SrMn_2P_2$, respectively. Characterization of the magnetism and INS studies of the magnetic excitations will be performed to identify signatures of itinerant FM and its coupling to the AF spin fluctuations.

Additionally, open questions surrounding the detailed nature of the magnetic coupling in magnetic TIs and its effect on band topology and transport properties motivate our study of dilute and stoichiometric magnetic TI compounds. Our INS measurements of the magnetic excitations will be compared with *ab initio* and local-moment model calculations, beginning with the AF-TI compound $MnBi_2Te_4$ and the trivial AF semiconductor $MnSb_2Te_4$. This provides a vantage point to study dilute magnetic TIs, such as $(Bi_{1-x}Mn_x)_2Te_3$.

A demonstration that key signatures of the chiral anomaly in Weyl semimetals are observable using INS would be a highly impactful result and provide a new experimental spectroscopic method to access the chiral nature of charge carriers in topological materials. Addressing the coupling of magnetic fluctuations to topological fermions requires close coordination between INS measurements and theoretical modeling. For example, it is predicted that spin fluctuations can mix with plasmon-like, chiral charge fluctuations. We can test this prediction by measuring the dynamical spin susceptibility of a magnetic TSM in an applied magnetic field using INS.

References

[1]. Z. P. Yin, K. Haule, and G. Kotliar, Kinetic frustration and the nature of the magnetic and paramagnetic states in iron pnictides and iron chalcogenides, Nat. Mater. **10**, 932 (2011).

[2]. A. Pandey, *et al.*, Crystallographic, electronic, thermal, and magnetic properties of single-crystal $SrCo_2As_2$, Phys. Rev. B **88**, 014526 (2013).

[3]. W. Jayasekara, *et al.*, Stripe antiferromagnetic spin fluctuations in $SrCo_2As_2$, Phys. Rev. Lett. **111**, 157001 (2013).

[4]. H. Mao and Z. Yin, Electronic structure and spin dynamics of ACo_2As_2 (A = Ba, Sr, Ca), Phys. Rev. B **98**, 115128 (2018).

[5]. A. Pandey, *et al.*, $Ba_{1-x}K_xMn_2As_2$: An antiferromagnetic local-moment metal, Phys. Rev. Lett. 108 (2012).

[6]. A. Pandey, *et al.*, Coexistence of Half-Metallic Itinerant Ferromagnetism with Local-Moment Antiferromagnetism in $Ba_{0.60}K_{0.40}Mn_2As_2$, Phys. Rev. Lett. **111**, 047001 (2013).

[7]. B. G. Ueland, *et al.*, Itinerant Ferromagnetism in the As 4p Conduction Band of $Ba_{0.6}K_{0.4}Mn_2As_2$ Identified by X-Ray Magnetic Circular Dichroism, Phys. Rev. Lett. **114**, 217001 (2015).

[8]. M. Ramazanoglu, *et al.*, Robust antiferromagnetic spin waves across the metal-insulator transition in hole-doped $BaMn_2As_2$, Phys. Rev. B **95**, 224401 (2017).

[9]. L. Ke, *et al.*, Low-energy coherent Stoner-like excitations in $CaFe_2As_2$ Phys. Rev. B **83**, 060404 (R) (2011).

[10]. C.-X. Liu, P. Ye, and X.-L. Qi, Chiral gauge field and axial anomaly in a Weyl semimetal, Phys. Rev. B **87**, 235306 (2013).

Select Publications (28 total publications in the past two years)

[P1]. A. Sapkota, B. G. Ueland, V. K. Anand, N. S. Sangeetha, J. Lamsal, D. L. Abernathy, M. B. Stone, J. L. Niedziela, D. C. Johnston, A. Kreyssig, A. I. Goldman, Effective one-dimensional coupling in the highly-frustrated square-lattice itinerant magnet $CaCo_{2-y}As_2$, R. J. McQueeney, Phys. Rev. Lett. **119**, 147201 (2017) [Editors' Suggestion].

[P2]. Bing Li, B. G. Ueland, W. T. Jayasekara, D. L. Abernathy, N. S. Sangeetha, D. C. Johnston, Q.-P. Ding, Y. Furukawa, P. P. Orth, A. Kreyssig, A. I. Goldman, R. J. McQueeney, Competing paramagnetic phases and frustration the itinerant magnet $SrCo_2As_2$, Phys. Rev. B **100**, 054411 (2019).

[P3]. N. S. Sangeetha, V. Smetana, A. V. Mudring, D. C. Johnston, Anomalous Composition-Induced Crossover in the Magnetic Properties of the Itinerant-Electron Antiferromagnet $Ca_{1-x}Sr_xCo_{2-y}As_2$, Phys. Rev. Lett. **119**, 257203 (2017).

[P4]. B. Li, Y. Sizyuk, N. S. Sangeetha, J. M. Wilde, P. Das, W. Tian, D. C. Johnston, A. I. Goldman, A. Kreyssig, P. P. Orth, R. J. McQueeney, B. G. Ueland, Antiferromagnetic stacking of ferromagnetic layers and doping controlled phase competition in $(Ca,Sr)Co_2As_2$, Phys. Rev. B **100**, 024415 (2019).

[P5]. N. S. Sangeetha, L.-L. Wang, A. V. Smirnov, V. Smetana, A.-V. Mudring, D. D. Johnson, M. A. Tanatar, R. Prozorov, D. C. Johnston, Non-Fermi-liquid behaviors associated with a magnetic quantum-critical point in $Sr(Co_{1-x}Ni_x)_2As_2$ single crystals, arXiv:1907.08238.

[P6]. J. M. Wilde, A. Kreyssig, D. Vaknin, N. S. Sangeetha, B. Li, W. Tian, P. P. Orth, A. I. Goldman, D. C. Johnston, B. G. Ueland, R. J. McQueeney, Helical magnetic ordering in $Sr(Co_{1-x}Ni_x)_2As_2$, arXiv:1907.11676.

[P7]. D. C. Johnston, Magnetic Structure and Magnetization of z-Axis Helical Heisenberg Antiferromagnets with XY Anisotropy in High Magnetic Fields Transverse to the Helix Axis at Zero Temperature, Phys. Rev. B **99**, 214438 (2019).

[P8]. N. S. Sangeetha, V. Smetana, A.-V. Mudring, D. C. Johnston, Helical Antiferromagnetic Ordering in $EuNi_{1.95}As_2$ Single Crystals, arXiv:1907.04813.

[P9]. N. S. Sangeetha, V. K. Anand, E. Cuervo-Reyes, V. Smetana, A.-V. Mudring, D. C. Johnston, Enhanced moments of Eu in single crystals of the metallic helical antiferromagnet $EuCo_{2-y}As_2$, Phys. Rev. B 97, 144403 (2018) [Editors' Suggestion].

[P10]. Y. Liu, L. Zhou, T. Ma, W. E. Straszheim, D. Vaknin, R. J. McQueeney, Crystal growth, microstructure and physical properties of $SrMnSb_2$, Phys. Rev. B **99**, 065535 (2019).

[P11]. Y. Liu, F. Islam, K. W. Dennis, W. Tian, B. G. Ueland, R. J. McQueeney, D. Vaknin, Hole doping and antiferromagnetic correlations above the Neel temperature of the topological semimetal $(Sr_{1-x}K_x)MnSb_2$, Phys. Rev. B **100**, 014437 (2019).

[P12]. D. Vaknin, D. M. Pajerowski, D. L. Schlagel, K. W. Dennis, R. J. McQueeney, Two-dimensional ordering and collective magnon excitations in the dilute ferromagnetic topological insulator $(Bi_{0.95}Mn_{0.05})_2Te_3$, Phys. Rev. B **99**, 220404(R) (2019).

[P13]. J.-Q. Yan, Q. Zhang, T. Heitmann, Z. L. Huang, D. Wu, D. Vaknin, B. C. Sales, R. J. McQueeney, Crystal growth and magnetic structure of $MnBi_2Te_4$, Phys. Rev. Mater. **3**, 064202 (2019).

[P14]. J.-Q. Yan, S. Okamoto, M. A. McGuire, A. F. May, R. J. McQueeney, B. C. Sales, Evolution of structural, magnetic and transport properties in $MnBi_{2-x}Sb_xTe_4$, *Phys. Rev. B* (in press). arXiv:1905.00400.

[P15]. J.-Q. Yan, D. Pajerowski, Liqin Ke, A. M. Nedić, Y. Sizyuk, E. E. Gordon, P. P. Orth, D. Vaknin, R. J. McQueeney, Competing magnetic interactions in the antiferromagnetic topological insulator $MnBi_2Te_4$, arXiv:1908.02332.

Emerging Materials

John F. Mitchell, Daniel Phelan (Argonne National Laboratory); Nirmal Ghimire (George Mason University)

Program Scope

Emerging Materials pursues materials synthesis and single crystal growth as a driver for foundational research on newly discovered quantum materials, with an emphasis on transition metal oxides. We leverage unique tools, such as high-pressure floating zone crystal growth, to create these systems not accessible in other ways. In addition to oxides, we pursue materials-driven opportunities to address fundamental physics of topological matter found in semiconducting and semimetallic chalcogen- and pnictogen-containing systems. We concentrate along four primary research foci: (i) understanding short-range charge and magnetic states in transition metal compounds, (ii) exploring topological quantum matter, (iii) scrutinizing existing models that are used to explain 5d systems such as iridates, and (iv) expanding today's framework of disorder and random fields, to more deeply understand the impact of heterogeneity and disorder on the short-range structure of matter. To enable much of this foundational science, we continue to emphasize the need to expand the boundaries of crystal synthesis and to exploit a broad range of x-ray and neutron scattering tools to understand structural and magnetic phenomena in quantum matter.

Recent Progress

Topological Matter: The ordinary Hall effect in a conductor arises due to the Lorentz force acting on the charge carriers. In ferromagnets, an additional contribution to the Hall effect, the so-called anomalous Hall effect (AHE), appears with a size proportional to the magnetization. While the AHE is not seen in a collinear antiferromagnet, with zero net magnetization, recently it has been shown that an intrinsic AHE can be non-zero in non-collinear antiferromagnets as well as in topological materials hosting Weyl nodes.[1] The key finding of this work is a large *c*-axis anomalous Hall effect in antiferromagnetic, noncentrosymmetric $CoNb_3S_6$ (Fig. 1a) for which band structure calculations reveal the presence of Weyl nodes proximate to the fermi level (Fig 1c). Based on its chiral crystal structure and the calculated band structure, we attribute the AHE in $CoNb_3S_6$ (Fig. 1b) either to the formation of a complex magnetic texture or to the influence of the small intrinsic ferromagnetic moment on the underlying electronic band structure. $CoNb_3S_6$ is a member of a large class of intercalated transition metal dichalcogenides, where a 3*d*-transition metal sandwiches between layers of a 5d-transition metal dichalcogenide, offering a flexible new platform for building topological electronic states. We also synthesized crystals of the rare earth honeycomb magnet $Tb_3Ir_2Ga_9$. The crystal field at the non-Kramer's Tb^{3+} site generates a quasi-doublet as the ground state, j=1/2, which was confirmed by heat capacity. Interest in such j=1/2 honeycomb systems derives from their potential as Kitaev spin liquids.[2] In this case, $Tb_3Ir_2Ga_9$ behaves as an Ising magnet with M directed along the a-axis as determined by neutron diffraction below its Neél temperature, 11 K. In the ordered phase, metamagnetic steps to $M_s/2$ and M_s at H= 2.5 and 7.5 T, respectively, were found when H || a. A phenomenological spin Hamiltonian was developed to explain M(H) along

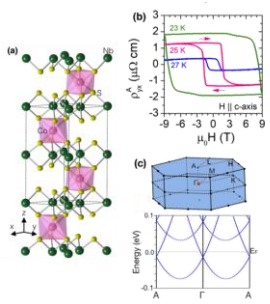

Fig. 1 (a) Crystal structure of $CoNb_3S_6$ (b) Anomalous Hall effect and its magnetic field behavior (c) DFT with spin-orbit coupling band structure showing a Weyl node highlighted near E_f at Γ.

all three principal axes. A key element of this model is the small orthorhombic distortion away from true trigonal symmetry. It is possible that spin liquid behavior could be realized were this distortion removed.

Correlated Electron Systems: We have reported the first single crystal growth of the archetype perovskite nickelate, $LaNiO_3$. We find structural, magnetic, and electronic properties similar to those reported for powders synthesized at high pressure[3] and for epitaxial thin films.[4]The magnetic susceptibility exhibits a previously unobserved broad maximum near 200 K, which may reflect some short range order of the 'breathing mode' distortion that is found as a condensed, long-range phase in the $RNiO_3$ with smaller rare earth ions. LNO crystals were also reported by the MPI-Dresden group as having an antiferromagnetic metallic ground state.[5] If true, this would be an exceptionally important result and would 'rewrite' the established physics of $LaNiO_3$; our crystals showed no sign of this signal. Subsequent studies at Argonne suggest that the antiferromagnetic behavior arises from a small concentration of second phases, such as $LaNiO_{2.5}$. Our conclusion of an extrinsic origin for the reported antiferromagnetic order has been corroborated recently by the Heidelberg group.[6] We have also extended our study of the trilayer nickel system, $La_4Ni_3O_{10}$, which we previously demonstrated has a metal-insulator transition at 105 K driven by charge stripe formation. Using single crystal polarized neutron diffraction, we now have shown that the expected spin stripes with $2q_{spin} = q_{charge}$ form concomitantly with the charge-ordered state. This contrasts with other stripe phase nickelates, where the charge orders at a temperature well above that of the spins. Collaborating with D. Haskel at the Advanced Photon Source, we measured the effect of pressure on magnetic and electronic properties of the hyperkagome iridate $Na_3Ir_3O_8$ using single crystals we prepared by vapor transport. We found a structural phase transition at ~10 GPa that results in the apparent formation of Ir-Ir pairs, a feature more often found in 4*d* oxides. Concomitantly, the expectation value of $L \bullet S$, measured through the Ir L_3/L_2 branching ratio, drops dramatically, but is still finite even at 50 GPa. This branching ratio scales with the size of the bandgap with pressure. These findings indicate that spin-orbit coupling is playing a role in dictating the electronic ground state, even at extreme pressures. Finally, we used our high-pressure zone furnace to grow crystals of $(Pr_{0.85}Y_{0.15})_{0.7}Ca_{0.3}CoO_{3-\delta}$ (PYCCO) with a metal-insulator transition that involves charge transfer between Co and Pr ions. Using inelastic neutron scattering, we measured the phonon spectrum of PYCCO and found evidence for precursor lattice distortions above the MIT that may arise from precursory changes in the Pr oxidation state, consistent with XAS measurements.[7]

Local ordering in relaxor ferroelectrics Collaborating with the MSD Neutron and X-ray Scattering FWP, we comprehensively studied the evolution of the local order that occurs in the prototypical relaxor ferroelectric system, $(1-x)PbMg_{1/3}Nb_{2/3}O_3$-$xPbTiO_3$ (PMN-*x*PT). Our goal was to understand the microscopic origins of its anomalous dielectric properties and exceptional electromechanical properties. We chose this system because its dielectric and electromechanical behaviors are strongly composition-dependent, which allowed us to correlate the local ordering with the behavior through systematic compositional studies. Crucial to this effort, large volumes of diffuse X-ray and neutron scattering were collected and analyzed for a wide span of compositions. Several important observations that are expected to have a significant impact upon the field came out of these studies. First, we observed that the 'butterfly' scattering, which has long been attributed to polar nanoregions (nanoscopic polar domains) in relaxors, does not evolve with composition in the same way as the relaxational dielectric behavior. Specifically, the butterfly scattering is maximal where the relaxational properties are minimal; therefore, the butterfly scattering is not a unique characteristic of relaxors. Second, we observed that local

antiferroelectric correlations, likely seeded by chemical ordering, strongly correlated with the relaxational dielectric properties, thereby suggesting that phase competition between antiferroelectric and ferroelectric correlations is the impetus of relaxor behavior. Third, we found that the 'butterfly' scattering was correlated with the electromechanical properties, suggesting that local ferroic order is important for ultrahigh piezoelectricity, which has implications upon the design of the next generation of piezoelectrics. Finally, we observed differences between X-ray and neutron scattering patterns that originated from contributions of oxygen ions, evidencing that they contribute to the atomic displacements present in regions of local order. We have now performed the same types of diffuse neutron and X-ray scattering measurements under applied electric fields, observing how the different components are affected by this external perturbation. Such data provide direct insight into the microscopic structural changes as the origin of electromechanical (piezoelectric) effects.

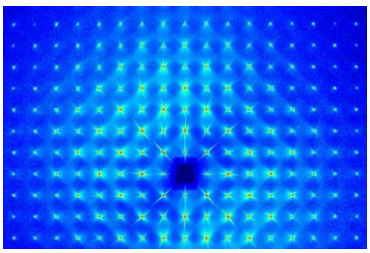

Fig 2. X-ray diffuse scattering of PMN-PT forms butterfly-like patterns indicative of correlated atomic disorder.

Other research outcomes included: achieved first crystal growth of quantum spin liquid candidate $Na_4Ir_3O_8$ showing previously overlooked evidence for Na-ion ordering; grew the first reported crystals of magnetic rare-earth doped $BaSnO_3$; Synthesized and measured structural and magnetic behavior of kagomé lattice averievite and Zn-doped analogs and found spin liquid behavior in agreement with theoretical predictions of M. Norman; discovered the first reported low-spin tetrahedron in a 5*d* transition metal oxide; grew first floating-zone crystals of $PrNiO_3$.

Future Plans

"Molecules in Solids" - orbital degeneracy lifting: We will explore the static and dynamical properties of molecular fragments contained in solids, focusing on how frustrated orbital states emerge from degenerate cluster orbital manifolds and how this frustration is lifted locally within the cluster and then coherently across the lattice.

The quest for nickelate superconductivity: We will explore highly reduced, 2-D nickelates, such as doped $RNiO_2$ (R=rare earth) in single crystal form grown from perovskites at high pressure. While superconductivity remains the goal, interrogating these and other layered systems, for example, to understand transitions between static and dynamic charge- and spin-stripes (Fig. 3).

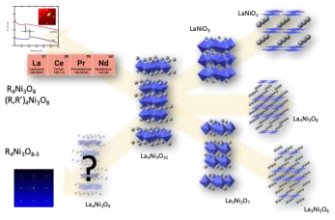

Fig. 3 Exploring layered nickelates via dimensionality, oxygen sublattice, and doping.

Topological Quantum Matter: We will pursue two research directions: (1) inspired by the behavior discovered in $CoNb_3S_6$, we explore other stuffed layered dichalcogenides and magnetic Weyl semimetals (2) we will test the potential for quantum spin liquid behavior in j=1/2 rare-earth based magnets with honeycomb lattices.

Relaxors: We will probe the microscopics of disparate classes of relaxor ferroelectric materials. We will study systems that fall into the three-dimensional Ising universality class as opposed to the more Heisenberg-like Pb-based relaxor ferroelectrics. We will also test the universality of our findings in chemically-distinct classes of compounds, particularly the Pb-free relaxor ferroelectrics compounds which are emerging as new electromechanical materials.

References: 1. K-Y Yang et al. *Phys. Rev. B* **2011**, 84, 075129; 2. S-H Jang et al. *Phys. Rev. B* **2019**, 99, 241106; 3. J-S Zhou et al. *Phys. Rev. B* **2014**, 89, 245138; 4. R. Scherwitzl et al. *Phys. Rev. Lett.* **2011**, 106, 246403; 5. H. Guo et al. *Nat. Comm.* **2018**, 9:43, 1; 6. K. Dey et al. *J. Cryst. Growth.* **2019**, 524, 125127; 7. H. Fujishiro et al. *J. Phys. Soc. Jpn.* **2012**, 81, 064709.

Publications

27 publications were supported by this FWP in the two years since the last ECMP PI meeting. Select publications most closely related to the abstract text are listed below.

1. Li, H.; Zhou, X.; Nummy, T. Zhang, J.; Pardo, V.; Pickett, W.E.; Mitchell, J.F.; Dessau, D.S. "Fermiology and Electron Dynamics of Trilayer Nickelate $La_4Ni_3O_{10}$" *Nature Communications* **2017**, 8, 704.
2. Ghimire, N. J.; Botana, A. S.; Jiang, J. S.; Zhang, J.; Chen, Y. S.; Mitchell, J. F. "Large Anomalous Hall Effect in the Chiral-Lattice Antiferromagnet $CoNb_3S_6$," *Nature Communications* **2018**, *9*, 3280.
3. Zheng, H.; Zhang, J.; Stoumpos, C. C.; Ren, Y.; Chen, Y.-S.; Dally, R.; Wilson, S. D.; Islam, Z.; Mitchell, J. F. "Controlled Vapor Crystal Growth of $Na_4Ir_3O_8$: A Three-Dimensional Quantum Spin Liquid Candidate," *Phys. Rev. Materials* **2018**, *2*, 043403.
4. Wang, Bi-Xia; Rosenkranz, S.; Rui, X.; Zhang, J.; Ye, F.; Zheng, H.; Klie, R. F.; Mitchell, J. F.; Phelan, D. "Antiferromagnetic defect structure in $LaNiO_{3-\delta}$ single crystals," *Phys. Rev. Materials* **2018**, *2*, 064404.
5. McCalla, E.; Phelan, D.; Krogstad, M. J.; Dabrowski, B.; and Leighton, C. "Electrical transport, magnetic, and thermal properties of La-, Nd-, and Pr-doped $BaSnO_{3-\delta}$ single crystals," *Phys. Rev. Materials* **2018**, *2*, 086401.
6. Sun, F.; Zheng, H.; Liu, Y.; Sandoval, E. D.; Xu, C.; Xu, J.; Jin, C. Q.; Sun, C. J.; Yang, W. G.; Mao, H. K.; Mitchell, J.F.; Kolmogorov, A.N.; Haskel, D. "Electronic and Structural Response to Pressure in the Hyperkagome-Lattice $Na_3Ir_3O_8$," *Phys. Rev. B* **2018**, *98*, 085131.
7. Botana, A. S.; Zheng, H.; Lapidus, S. H.; Mitchell, J. F.; Norman, M. R. "Averievite: A Copper Oxide Kagomé Antiferromagnet," *Phys. Rev. B* **2018**, 98, 054421.
8. Krogstad, M.; Gehring, P.; Rosenkranz, S.; Osborn, R., Ye; F., Liu, Y.; Ruff, J.; Chen, W.; Wozniak, J.; Luo, H.; Chmaissem; O., Ye; Z.; Phelan, D. "The relation of local order to material properties in relaxor ferroelectrics" *Nature Materials* **2018**, 17(8), 718-724.
9. Zheng, H., Zhang, J., Wang, B., Phelan, D., Krogstad, M., Ren, Y., Phelan, W., Chmaissem, O., Poudel, B., Mitchell, J. F. "High pO_2 Floating Zone Crystal Growth of the Perovskite Nickelate $PrNiO_3$" *Crystals* **2019**, 9(7), 324.
10. Bozin, E., Yin, W., Koch, R., Abeykoon, M., Hor, Y., Zheng, H., Lei, H., Petrovic, C., Mitchell, J.F., Billinge, S. "Local orbital degeneracy lifting as a precursor to an orbital-selective Peierls Transition" *Nature Communications* **2019**, 10(1), 1-7.
11. Phelan, D.; Krogstad, M.; Schreiber, N.; Osborn, R.; Said, A.; Zheng, H.; Rosenkranz, S. "Acoustic phonon dispersion and diffuse scattering across the valence transition of $(Pr_{0.85}Y_{0.15})_{0.7}Ca_{0.3}CoO_{3-\delta}$" *Phys. Rev. B* **2019**, 100(5), 054101.
12. Zhang, J., Pajerowski, D., Botana, A., Zheng, H., Harriger, L., Rodriguez-Rivera, J., Ruff, J., Schreiber, N., Wang, B., Chen, Y., Chen, W., Norman, M., Rosenkranz, S., Mitchell, J.F., Phelan, D. "Spin Stripe Order in a Square Planar Trilayer Nickelate" *Phys. Rev. Lett.* **2019**, 122(24), 247201.

Frustration as tuning parameter for quantum criticality

Emilia Morosan, Rice University

Program Scope

The project is focused on using magnetic frustration as a new tuning parameter for quantum criticality, with three main objectives: (1) understanding the effects of frustration and disorder on the quantum critical behavior of magnetic systems; (2) search for spin liquid states in strongly correlated systems; and (3) discover topological magnetic systems.

Recent Progress

The ordered pyrochlore lattice $Ce_2Zr_2O_7$ has been shown to embody the first experimental realization of a 3D spin liquid with minimum or no magnetic/non-magnetic chemical disorder.

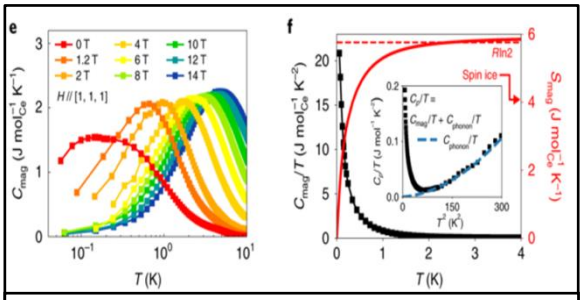

Quantum Spin Liquid $Ce_2Zr_2O_7$ magnetic specific heat C_{mag} (left) and magnetic entropy S_{mag} (red, right) indicate (1) no long range order down to 60 mK; (2) onset of coherent quantum fluctuations and (3) no spin ice behavior.

Future Plans

We will tune the frustration in this and other systems using uniaxial pressure. The rhombohedral ErRh3Si7 system we recently discovered does not order magnetically down to ~1 K, providing an alternative crystal structure to the pyrochlores, for observing the effects of frustration and possibly looking for a new spin liquid system.

References

Publications

- Bin Gao, Tong Chen, David W. Tam, Chien-Lung Huang, Kalyan Sasmal, Devashibhai T. Adroja, Feng Ye, Huibo Cao, Gabriele Sala, Matthew B. Stone, Christopher Baines, Joel A. T. Verezhak, Haoyu Hu, Jae-Ho Chung, Xianghan Xu, Sang-Wook Cheong, Manivannan Nallaiyan, Stefano Spagna, M. Brian Maple, Andriy H. Nevidomskyy, Emilia Morosan, Gang Chen and Pengcheng Dai, "Experimental signatures of a three-dimensional quantum spin liquid in effective spin-1/2 $Ce_2Zr_2O_7$ pyrochlore" Nature Physics **10**, 1038 (2019)

Program title: Spectroscopic investigations of novel electronic and magnetic materials

Principle Investigator: Janice L. Musfeldt
Affiliation: Departments of Chemistry and Physics, University of Tennessee, Knoxville TN 37996
Contact: (865) 974-3392 or musfeldt@utk.edu

Program scope

The goal of our program is to develop a fundamental understanding of the interplay between charge, structure, and magnetism in quantum materials – especially oxides and chalcogenides – in order to facilitate the development of tunable materials of scientific and technological importance. We employ a variety of spectroscopic methods to reveal properties and use external stimuli such as magnetic field, pressure, and size to tune the response. Current research directions include (i) understanding coupling processes, interface properties, and phase diagrams of multiferroic oxides, (ii) uncovering enhanced functionality from spin-orbit coupling in 4- and 5*d*-containing materials, and (iii) unveiling the response of nanoscale materials, few- and single sheet systems, and domain walls. Using these platforms, we can learn about the relationships between different ordered and emergent states, explore the dynamical aspects of coupling, and gain insight into the generality of these phenomena and their underlying mechanisms. In addition to broadening the understanding of novel solids under extreme conditions, multifunctional materials and their assemblies are of interest for a number of energy-relevant technologies.

Recent progress

Infrared nano-spectroscopy of ferroelastic domain walls in hybrid improper ferroelectric $Ca_3Ti_2O_7$: Many unique properties in functional materials arise from spatially heterogeneous electronic and magnetic states. The domains and domain walls in ferroics are but one example. This is especially true for $Ca_3Ti_2O_7$, a hybrid improper ferroelectric where the polarization arises from a trilinear coupling mechanism and abundant charged domain walls have been observed. Atomic- and piezo-force imaging reveal the different orientations of directional order parameters

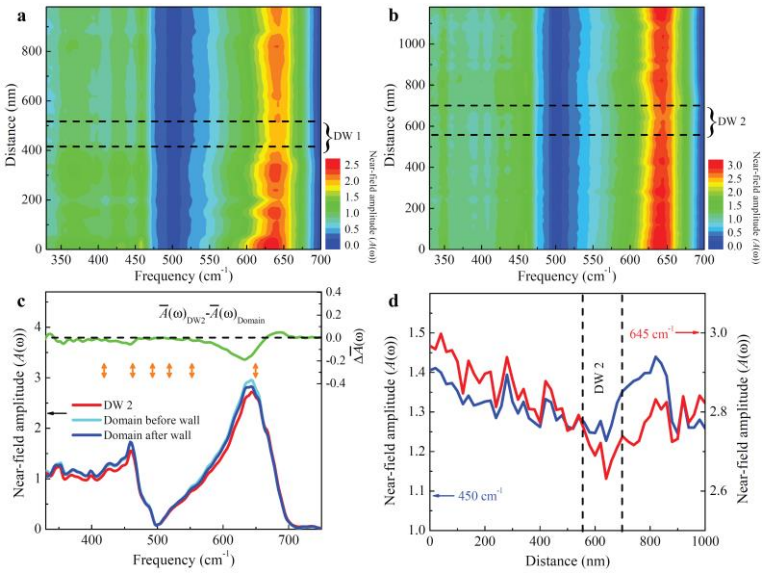

Fig. 1: Near-field infrared spectroscopy of $Ca_3Ti_2O_7$. (a,b) Contour plot of the nearfield amplitude normalized to a gold reference across two different domain walls. (c) Fixed distance cuts of the contour spectra in panel (b) showing A(ω) at the ferroelastic domain wall compared with two different point scans away from the wall. Arrows denote the calculated position of the totally symmetry modes. (d) Fixed frequency cut of the contour data in panel (b) showing how intensity at 450 and 645 cm^{-1} varies across domain wall 2.

and domain wall character, the latter of which provides a physical playground for graph theory. In order to uncover the behavior of fundamental excitations like phonons at domain walls and to explore the structural distortions that they represent, we performed synchrotron-based near-field nano-spectroscopy of the local phonon response at domain boundaries in $Ca_3Ti_2O_7$ and compared our findings with theoretical models of how the order parameter develops across the wall [Fig. 1]. Analysis of the Ti-O stretching and bending modes across the twin boundary reveals rich changes in the matrix element that we relate to the underlying modulation of the crystal structure and to the rotation of the structural order parameters. We find significant width to the residual structural distortion across the walls as well as semiconducting character. This research opens the door to broadband imaging of heterogeneity in ferroics and represents a first step to revealing the rich dynamics of domain walls in these systems. At the same time, it provides crucial information on loss mechanisms involving phonons for the development of ultra low-power devices, switches, polarizers, and computing architectures based upon domain walls.

Near-field infrared spectroscopy of single layer $MnPS_3$: The layered structures of many chalcogenides allow for exfoliation, providing a unique platform for combining the complexity of bulk materials with the tunability of few- and single-layer systems. Raman scattering is widely employed to assure sample quality, probe even-symmetry vibrational modes, and reveal confinement effects in the single layer. The odd-symmetry modes are, however, highly unexplored. In order to reveal the properties of a complex van der Waals material, we measured the near-field infrared response of MnPS3 in bulk, few-, and single-layer form and compared the results with traditional far field infrared and Raman spectroscopy and complementary lattice dynamics calculations [Fig. 2]. Trends in the activated B_u mode near 450 cm^{-1} are particularly striking, with the disappearance of this structure in the thinnest sheets. Combined with the amplified response of the A_g mode and analysis of the $A_u + B_u$ features, we find that symmetry is unexpectedly increased in single-sheet $MnPS_3$ due to the restoration of the three-fold axes of rotation. The monoclinicity of this system is thus a consequence of the long-range stacking pattern and temperature effects rather than local structure. Near-field infrared spectroscopy clearly has the potential to unlock a much wider field of investigation into the properties of atomically-thin materials.

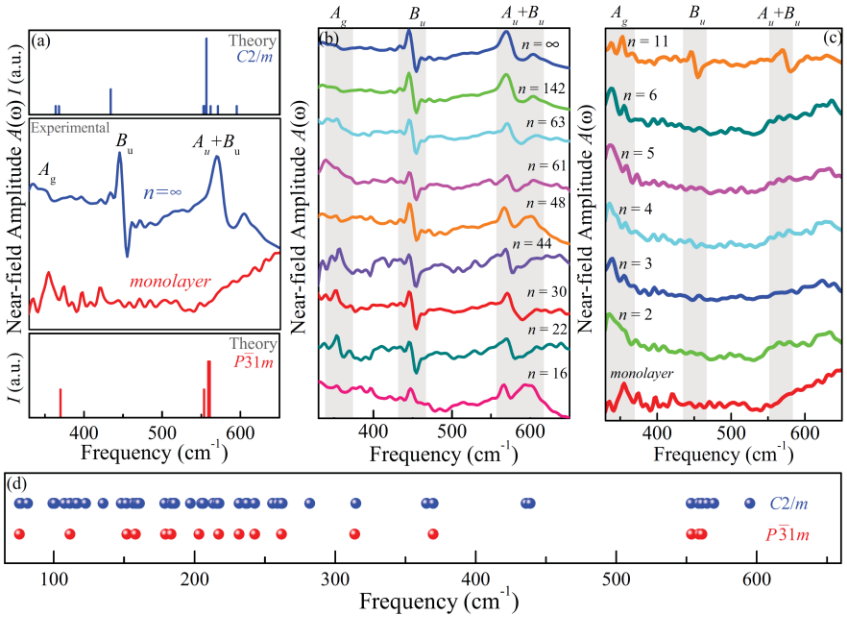

Fig. 2: (a) Near-field infrared response of bulk $MnPS_3$ compared with the monolayer. Lattice dynamics calculations highlight symmetry modifications. (b,c) Evolution of the near-field infrared spectra from bulk $MnPS_3$ ($n=\infty$) to the monolayer. Spectra are shifted for clarity. (d) Direct comparison of the predicted vibrational modes over the entire frequency range for a single sheet of $MnPS_3$ - depending on the symmetry imposed during the calculation.

Spin-lattice and electron-phonon coupling in 3*d*/5*d* **hybrid Sr_3NiIrO_6**: While 3*d* transition metal oxides are renowned for strong electron correlations, narrow band widths, and robust magnetism, 5*d*-containing oxides are recognized for strong spin-orbit coupling, increased hybridization, and larger more diffuse orbitals. When the two sets of properties are brought together in a single material, novel behavior can emerge. The 3*d*/5*d* hybrid Sr_3NiIrO_6 is a prominent example with complex magnetism and ultra-high coercive fields - up to an incredible 55 T. In this work, we bring together high field magnetization, infrared and optical spectroscopies, and first principles calculations to explore the fundamental excitations of the lattice and related coupling processes. Magneto-infrared spectroscopy reveals three phonons that display strong spin-lattice interactions. Analysis of the displacement patterns shows that they modulate the environment around the Ir centers and by so doing, reduce the energy required to modify the spin arrangement. While displacements of these modes primarily affect exchange within the chains, inspection uncovers important inter-chain motion as well. This supports the role of inter-chain interactions in the developing model for ultra-high coercivity and provides a mechanism by which it can occur. At the same time, analysis of the on-site Ir^{4+} excitations reveals vibronic coupling and extremely large crystal field parameters [Fig. 3, Table 1]. Thediffuse character of the 5*d* orbitals determines the spin structure by driving Sr_3NiIrO_6 into a low-spin state that emanates from t_{2g}-derived levels. These findings highlight the interplay between charge, structure, and magnetism in this 3*d*/5*d* hybrid and suggest that similar interactions may take place in other materials of this family.

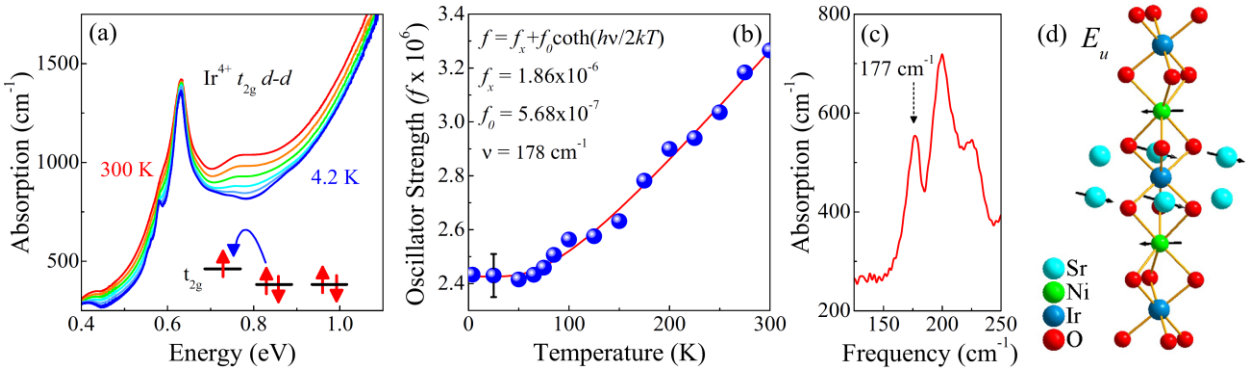

Fig. 3: (a) Optical absorption of Sr_3NiIrO_6 in the vicinity of the Ir_{4+} on-site excitations at select temperatures. (b) Oscillator strength analysis using the indicated vibronic coupling model, where ν is the coupled phonon frequency. (c) The infrared spectrum shows phonons near the extracted ν value. (d) Calculated displacement pattern for the vibronically-coupled phonon. Data in panel (a) was used to calculate the crystal field parameters in Table I.

Table 1: Summary of $10Dq$ and Racah parameters for the $3d/5d$ materials in this study compared to the crystal field parameters of other Ir-containing compounds along with information about the vibronically coupled phonons. No vibronic coupling analysis has been reported for Sr_2IrO_4 or Li_2IrO_3, and the Ni^{2+} excitations in Ni_3TeO_6 are not vibronically activated, so no phonons are implicated.

Material	Element	Electronic state	$10Dq$ (eV)	B (eV)	Coupled phonon frequency (cm^{-1})	Displacement
Sr_3NiIrO_6	Ir	$5d^5$	3.24	1.18	177	Ni in-plane motion
Sr_3CuIrO_6	Ir	$5d^5$	2.33	0.86	273	O-Ir-O bend
Sr_2IrO_4	Ir	$5d^5$	3.8	0.93	-	-
Li_2IrO_3	Ir	$5d^5$	2.7	0.95	-	-
Ni_3TeO_6	Ni	$3d^8$	1.10	0.11	-	-
α-Fe_2O_3	Fe	$3d^5$	1.59	0.09	525	In-plane, in-phase Fe-O stretch

Future plans

Several exciting efforts are planned for the coming year. They include:

- unveiling the origin of high temperature magnetism, the charge ordering pattern, and the dynamic magnetoelectric coupling constant in $(LuFeO_3)_m(LuFe_2O_4)_n$ superlattices,
- revealing the competition between metallicity, disorder, and ferroelectricity in Nb-substituted $EuTiO_3$
- imaging domain walls in ferroics like $(Lu,Sc)FeO_3$ using near field infrared techniques,
- uncovering the dynamics of the intercolant in noncentrosymmtric chiral chalcogenides like $Fe_{1/3}TaS_2$, $Cr_{1/3}NbS_2$, and $RbFe(SO_4)_2$,
- evaluating structure-property relations in atomically-thin $MnPS_3$, $MnPSe_3$, $NiPS_3$, $FePS_3$, and $CrPS_4$, and
- exploring piezochromic effects in $MnPS_3$ and related materials.

We anticipate travel to national laboratories in support of these activities including the National High Magnetic Field Laboratory (TLH + LANL), Lawrence Berkeley National Laboratory, and Brookhaven National Laboratory. Plans are also underway for meeting and workshop attendance (APS, ACS, GRC). Outreach includes service to the several different national laboratories as well as organization of the 2020 Telluride workshop on spin-orbit coupling.

Publications emanating from this grant (2018 – 2019)

1. *Charge and bonding in $CuGeO_3$ nanorods*, K. R. O'Neal, A. al-Wahish, Z. Li, G. Dhalenne, A. Revcolevschi, X. -T. Chen, and J. L. Musfeldt, Nano Lett. **18**, 3428 (2018).

2. *Magnetic field control of charge excitations in $CoFe_2O_4$* , B. S. Holinsworth, N. C. Harms, S. Fan, D. Mazumdar, A. Gupta, S. A. McGill, and J. L. Musfeldt, APL Materials **6**, 066110 (2018).

3. *Frustration and glassy character in multiferroic $RIn_{1-x}Mn_xO_3$ (R = Tb, Dy, Gd)*, P. Chen, B. S. Holinsworth, K. R. O'Neal, X. Luo, C. V. Topping, S. -W. Cheong, J. Singleton, E. S. Choi, and J. L. Musfeldt, Inorg. Chem. **57**, 12501 (2018).

4. *Large positive zero field splitting in the cluster magnet $Ba_3CeRu_2O_9$*, Q. Chen, S. Fan, J. M. Taddei, M. B. Stone, A. I. Kolesnikov, J. G. Cheng, J. L. Musfeldt, H. D. Zhou, and A. A. Aczel, J. Am. Chem. Soc. **141**, 9928 (2019).

5. *Spin-lattice and electron-phonon coupling in a 3d/5d hybrid Sr_3NiIrO_6*, K. R. O'Neal, A. Paul, A. al-Wahish, K. D. Hughey, A. L. Blockman, X. Luo, S. -W. Cheong, V. Zapf, C. V. Topping, J. Singleton, M. Ozerov, T. Birol, and J. L. Musfeldt, accepted, npj Quant. Mater.

6. *Near-field infrared spectroscopy of single layer $MnPS_3$*, S. N. Neal, H. -S. Kim, K. A. Smith, A. V. Haglund, D. G. Mandrus, H. A. Bechtel, G. L. Carr, K. Haule, D. H. Vanderbilt, and J. L. Musfeldt, accepted, Phys. Rev. B.

7. *Infrared nano-spectroscopy of ferroelastic domain walls in hybrid improper ferroelectric $Ca_3Ti_2O_7$*, K. A. Smith, E. A. Nowadnick, S. Fan, O. Khatib, S. L. Lim, N. C. Harms, S. Neal, J. K. Kirkland, M. C. Martin, C. J. Won, M. B. Raschke, S. -W. Cheong, C. J. Fennie, G. L. Carr, H. A. Bechtel, and J. L. Musfeldt, under review, Nature Comm.

Exploring superconductivity at the edge of magnetic or structural instabilities

Ni Ni

University of California, Los Angeles, Los Angeles, CA

Program Scope

Modern research of condensed matters devotes in understanding how properties of complex solids are determined by their structural and electronic degrees of freedom. Recently, since the discovery of protected surface state in bulk materials, band topology has emerged as a new organizing principle of states of matter. The entanglement of band topology and the spin, charge, orbital and lattice (SCOL) degrees of freedom have led to emergent phenomena, such as quantized anomalous Hall effect, colossal photovoltaic effect, etc. However, due to the lack of "ideal" topological materials where only minimum non-trivial nodal feature exists at the Fermi level, there are significant materials challenges facing the in-depth understanding of collective phenomena and excitations of topological materials, thus hindering the material discovery with favorable functionality arising from the non-trivial topology. The objective of this research is to design topological materials that lie at the edge of structural/magnetic instabilities, aiming at the discovery of "ideal" magnetic/superconducting topological materials and the in-depth understanding of the entanglement of band topology and SCOL degrees of freedoms through thermodynamic, transport, X-ray, and neutron measurements.

Recent Progress

1. <u>Discovery of novel antiferromagnetic topological insulator with weal saturation field.</u> Magnetic topological insulators (MTI), including Chern insulators with a Z-invariant and antiferromagnetic (AFM) topological insulators (TIs) with a Z_2-invariant, provide fertile ground for the exploration of emergent quantum phenomena such as the quantum anomalous Hall (QAH) effect, Majorana modes, the topological magnetoelectric effect, and the proximity

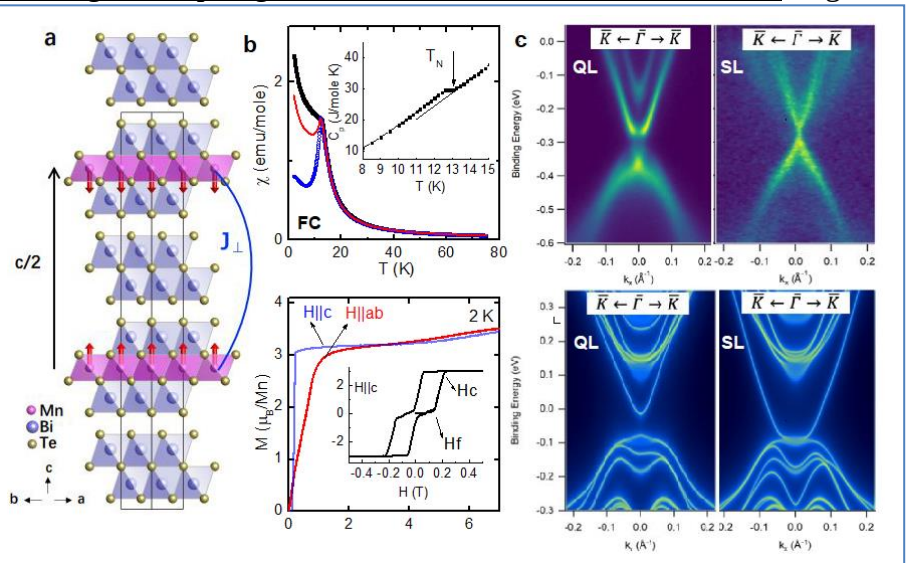

Figure 1: $MnBi_4Te_7$: (a) Crystal structure, (b) magnetic properties, (c) angular-resolved photoemission spectroscopy and DFT calculation on the QL and SL terminations, respectively.

effect. Although the QAH effect has been experimentally realized in magnetically doped topological insulator $Cr_{0.15}(Bi_{0.1}Sb_{0.9})_{1.85}Te_3$ thin films [1], it remains a challenge to realize the QAH effect at high temperatures. Recently $MnBi_2Te_4$ was discovered to be an intrinsic AFM TI [2]. In its two-dimensional (2D) limit, quantized Hall conductance originating from the topological protected dissipationless chiral edge states was realized in odd number of slab, a magnetic field of 12 T at 4.5 K or 6 T at 1.5 K, above which the AFM spins enter the forced ferromagnetic (FM) state [3].

How can we achieve the QAH effect at much lower magnetic fields in AFM TIs so that the associated emergent phenomena could be studied at more accessible conditions and the quantized Landau levels would not contaminate the QAH effect? Our recent work realized a bulk vdW material with a superlattice of alternating one [$MnBi_2Te_4$] and one [Bi_2Te_3] layers, as shown in Figure 1. This have paved a new avenue to achieve the QAH effect at low or even zero magnetic fields. We showed that $MnBi_4Te_7$ is a Z_2 antiferromagnetic topological insulator with two distinct (001) surface states from the QL [Bi_2Te_3] and SL [$MnBi_2Te_4$] termination, respectively. Strong FM fluctuations were observed above T_N (12 K). Due to its superlattice nature, in the two-dimensional limit, it serves as natural heterostructures. The extremely low out-of-plane saturation field $\approx$ 0.22 T makes it an ideal system to study the quantized anomalous Hall effect, quantum spin Hall effect and associated emergent phenomena.

2. Discovery of an ideal topological nodal line semimetal. Recently, the relativistic fermions hosted by square-net lattices of main group elements were found to have rich interplay with the magnetism in antiferromagnetic (AFM) material family of $AMnX_2$ (A=alkaline earth or rare earth elements, and X=Sb/Bi). $SrZnSb_2$ can be viewed as a nonmagnetic version of the $AMnX_2$. To examine the effect of magnetism on the existence of Dirac fermions in this group of mateirals, we have investigated quantum transport properties up to 35T for $SrZnSb_2$. Our analysis on the observed quantum oscillation reveals the nontrivial Berry phase accumulation and light effective masses of the quasiparticles in this system. The angular dependence of the de Haas van Alphen oscillations further reveals that the Fermi surfaces are quasi 2D-like, similar to those in the $AMnX_2$ materials. Interestingly, our DFT calculation suggests this compound may serve as an ideal topological nodal line semimetal since the DFT band structure shows that we can tune the Fermi level so that only the nodal line feature exist at the G point in the reciprocal space. In collaboration with Dan Dessau's group on $SrZnSb_2$, ARPES measurement has been performed. The good agreement between ARPES experiment and DFT calculation indeed suggests the non-trivial topology and nodal line feature in $SrZnSb_2$.

3. The investigation of quasi-two-dimensional materials with structural/magnetic instability. Layered pnictide materials have provided a fruitful platform to study various emergent phenomena, including superconductivity, magnetism, charge density waves, etc. We performed transport, magnetic, single crystal X-ray and neutron diffraction measurements on AAg_4As_2 (A=Sr, Eu). We have revealed the Fermi surface topology and the strong coupling of magnetism and charge carriers. Both $SrAg_4As_2$ and $EuAg_4As_2$, show a nonmagnetic phase transitions emerge

at around 110 K, likely associated with structural distortions. In $SrAg_4As_2$, quantum oscillations reveal small Fermi pockets with light effective masses. In $EuAg_4As_2$, noncollinear magnetism was revealed, where two sets of superlattice peaks. The magnetic structure below 9 K is helical along the c axis and cycloidal along the b axis with a moment of 6.4 μ_B/Eu^{2+}.

4. Collaborations with various groups in this period. Our collaboration with Burch's group (Boston College) published on Nat. Mater. has demonstrated a colossal mid-infrared bulk photovoltaic effect in microscopic devices of TaAs which produces large photocurrent. Our collaboration with Prasankumar's group (LANL) published on PRL has elucidated the relationship between the crystalline symmetry and the direction of the photocurrent.

Future Plans

We will continue our exploration and investigation on topological materials with structural/magnetic instabilities.

1. The existence of natural heterostructure $MnBi_{2n}Te_{3n+1}$ (n=1 to 4) family of alternating n[Bi_2Te_3] and [$MnBi_2Te_4$] makes this system great to investigate the effect of dimensionality and interlayer magnetic coupling on the band topology and magnetism. We will continue our investigation on the members with higher *n* numbers, aiming at discovering a FM natural heterostructure topological material.
2. By doping, intercalating and designing of new materials with the $MnBi_2Te_4$ building blocks, we will aim at the discovery of MTI with higher transition temperatures and natural heterostructure materials with alternating superconducting and topological magnetic layers.
3. In collaboration with Dan Dessau's group on $SrZnSb_2$, ARPES measurement will be performed on the $(Sr_{1-x}La_x)ZnSb_2$ (x=0.1, 0.2, 0.25) single crystals.
4. The TI material data base suggests that the sister compound of $SrAg_4As_2$, $SrAg_4Sb_2$ has nontrivial topology without structural distortion. As a comparison study, we will investigate $SrAg_4Sb_2$ and $EuAg_4Sb_2$ to reveal the role of topology and structural distortion in the transport properties.
5. We will explore chiral topological materials to investigate the effect of the chirality in the band topology.

References

[1] Chang, C.-Z. et al., Science 340, 167 (2013)

[2]Mikhail M. Otrokov, et al., arxiv: 1809.07389 (2019)

[3] Yujun Deng, et al., ArXiv:1904. 11468 (2019)

Publications

1. Eve Emmanouilidou, et. al, Phys. Rev. B 96, 224405 (2017) Activity supported by this award: bulk sample growth, structure determination, bulk transport, thermodynamic and neutron measurements as well as data analysis.
2. Bing Shen, et. al, Phys. Rev. B 98, 235130 (2018) Activity supported by this award: bulk single crystal growth, structure determination, bulk transport, thermodynamic measurements and data analysis.
3. Eve Emmanouilidou, et. al, J. Magn. Magn. Mater. **469**, 570 (2019) Activity supported by this award: bulk single crystal growth, bulk transport, thermodynamic measurements and data analysis.
4. Jinyu Liu, et. al, arXiv:1807.0254, under review, Phys. Rev. B, (2018) Activity supported by this award: bulk single crystal growth, bulk transport, thermodynamic measurements and data analysis.
5. Bing Shen, et. al, arXiv:1809.07317, Phys. Rev. Mater., under review, (2018) Activity supported by this award: bulk single crystal growth, bulk transport, thermodynamic measurements and data analysis.
6. Chaowei Hu, et. al, arXiv:1905.02154, Nature Communication, Under review, (2019) Activity supported by this award: bulk single crystal growth, bulk transport, thermodynamic measurements and data analysis.
7. Gavin B. Osterhoudt, et. al, Colossal mid-infrared bulk photovoltaic effect in a type-I Weyl semimetal, Nature Materials 18, 471 (2019) Activity supported by this award: bulk single crystal growth, bulk transport measurements and data analysis.
8. N. Sirica, et. al, Tracking ultrafast photocurrents in the Weyl semimetal TaAs using THz emission spectroscopy, Phys. Rev. Lett., 122, 197401 (2019) Activity supported by this award: bulk single crystal growth, bulk transport measurements and data analysis.
9. Sihang Liang, et. al, Phys. Rev. X **8**, 031002 (2018) Activity supported by this award: bulk single crystal growth, bulk transport measurements and data analysis.
10. Xiao-Bo Wang, et. al, Phys. Rev. B 96, 161112(R) (2017) Activity supported by this award: idea and bulk single crystal growth.
11. Xiaoqing Zhou, et. al, Phys. Rev. B 97, 241102(R) (2018) Activity supported by this award: bulk sample growth, bulk transport measurements and data analysis.
12. Shu Cai, et. al, Phys. Rev. B 99, 020503(R) (2019) Activity supported by this award: bulk single crystal growth, bulk transport measurements and data analysis.
13. Jin Hu, et. al, Annual Review of Materials Research, 49, 207 (2019) Activity supported by this award: literature research and manuscript writing.
14. Antonio L. Levy, et. al, arXiv: 1810.05660 (2018) Activity supported by this award: bulk sample growth, bulk transport measurements and data analysis.
15. Jennifer Coulter et. al, arXiv:1903.07550 (2019) Activity supported by this award: bulk single crystal growth, bulk transport measurements and data analysis.
16. M. Mehdi Jadidi, et. al, arXiv:1905.02236 (2019) Activity supported by this award: bulk single crystal growth, bulk transport measurements and data analysis.
17. Yu-Jie Hao, et. al, arXiv:1907.03722 (2019), Accepted by PRX. Activity supported by this award: bulk single crystal growth and characterization.

Project Title: Quantum Materials
Principal Investigators: James Analytis, Robert Birgeneau, Edith Bourret-Courchesne, Alessandra Lanzara, Dunghai Lee, Joel Moore, Joseph Orenstein, and R. Ramesh
Affiliations: Lawrence Berkeley National Lab and University of California, Berkeley

Program Scope
Technological advances in energy, transportation, medical and information technologies build on the foundation of materials properties. Breakthroughs in materials physics can transform these fields, as new opportunities for invention emerge from the discovery of materials that exhibit new phases and phenomena. Partially reflecting this progress, the term "quantum materials," was coined to denote *materials whose collective phases and physical properties defy a classical description.* The Quantum Materials FWP at LBNL is a leader in this dynamic field.

We have identified two broad themes as foci for our collaborative research:

Theme I: How does topology provide pathways to control transport, magnetic, and optical properties?
Our research in this area focuses on three classes of material systems: (1) chiral Weyl semimetals in which all mirror symmetries are broken, (2) time-reversal breaking systems in which frustration leads to exotic forms of non-collinear order or topological textures, and (3) superlattices of ferroelectric oxides that exhibit real space topological structures and emergent chirality with close analogy to those found in magnetic systems.

Theme II: How do interactions among the structural, charge, orbital, and magnetic degrees of freedom generate high-T_c superconductivity? How do defects, impurities, and other forms inhomogeneity affect these interactions?
The ultimate goal of our research in this area is to utilize our unique combination of synthesis, scattering, spectroscopic, and theoretical tools to disentangle the roles played by magnetic, orbital, and nematic fluctuations in generating Cooper pairing in Fe- and Cu-based superconductors.

Progress report
Nonlinear electrodynamics in Weyl semimetals
Weyl semimetals (WSMs) are currently a focus of intense research into the topological properties of crystalline solids. In these materials, breaking of either inversion or time-reversal symmetry generates three-dimensional massless chiral fermions and disconnected Fermi arcs at interfaces. While the demonstration by ARPES that WSMs and Fermi arcs exist represent major advances (Hasan *et al.*, 2017), a central question remains: do Weyl semimetals possess novel physical properties that derive from their unique topology? Our research has made significant progress towards answering this question.

Discovery of giant SHG: In our initial experiments, we studied second harmonic generation (SHG) in the semimetal TaAs. As TaAs is a non-centrosymmetric crystal with a unique polar axis, the existence of SHG is not by itself surprising. However, we found that its second-order optical conductivity, $\sigma^{(2)}$, measured with excitation photon energy $\hbar\omega = 1.5$ eV is larger by an order of magnitude than GaAs, and indeed larger than that of any crystal reported in the literature (Wu *et al.*, 2017).

SHG spectrum and nonlinear response sum rule: We performed the first nonlinear spectroscopic measurements on a Weyl semimetal, studying the dependence of $\sigma^{(2)}$ on $\hbar\omega$ in the range from

0.55-1.8 eV. We discovered that $\boldsymbol{\sigma^{(2)}(\omega)}$ **increases rapidly as the photon energy decreases, reaching a maximum at 0.7 eV that is a factor of ≈ 10 larger than we reported previously at 1.5 eV.** In analyzing these results, we discovered a new link between the spectral weight of the nonlinear conductivity and the "skew" of the polarization distribution function, a quantity closely related to the Berry curvature. These experimental and theoretical discoveries provide a new strategy for computational searches for nonlinear materials with optimal response functions (Patankar *et al.*, 2018b).

Observation of the quantized circular photogalvanic effect (QCPGE): The most direct signature of Weyl semimetal topology is the QCPGE, predicted by the Moore group. Photogalvanism refers to light-induced current driven by intrinsic asymmetry of the crystal structure. In the CPGE the current direction flips with reversal of the photon helicity. Moore and collaborators predicted that the generation rate of CPGE current from photoexcitation of an isolated Weyl node is quantized in units of e^3/h^2, independent of material parameters and photon energy. Our team, which includes groups from UC Berkeley, Temple University, and MPI Dresden, has discovered the QCPGE in the chiral Weyl material, RhSi. Our measurements of photocurrent as a function of photon energy reveal a response at low photon energy that cuts off above 0.66 eV. The shape of the CPGE spectrum and magnitude of the current are in striking agreement with theory.

Future Plans

Berry curvature, symmetry, and Weyl semimetals

Weyl semimetals (WSMs) and related topological states are a focus of our proposed research because they are systems in which the effects of Berry curvature on transport and optical properties are expected to be most pronounced. I-breaking in WSMs introduces a class of response functions that are forbidden in systems that possess a center of symmetry. We will investigate an important example of such responses: the second-order nonlinear conductivity, defined by $J^{(2)} = \sigma^{(2)}EE$, in which an inversion odd quantity (current) is related to an even one (electric field squared).

Quantized photogalvanic effects and spin dynamics in chiral topological semimetals

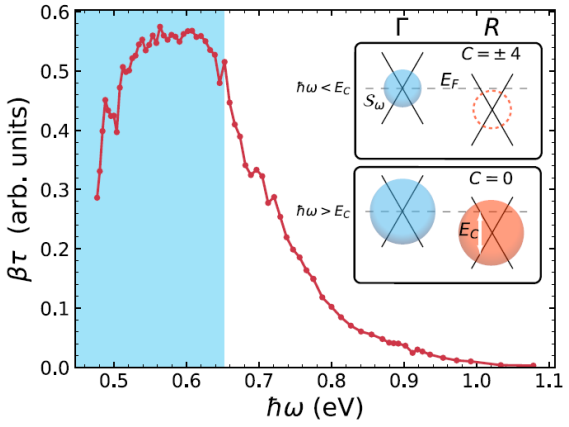

CPGE spectrum. CPGE amplitude as a function photon energy, showing abrupt quenching above 0.65 eV. The inset contains a schematic showing the surface, S in k-space defined by the available optical transitions at photon energy $\hbar\omega$. For $\hbar\omega > E_C$, S encloses two nodes of opposite chirality and has zero integrated Berry flux. Below E_C it encloses a single node and has Chern number 4. The blue shaded region in the main plot indicates the region where S! encloses only a single node.

One of the most important of the $\sigma^{(2)}$-derived effects is the CPGE. Since its initial observation (Asnin *et al.*, 1979), the CPGE has attracted attention as a means of detecting symmetry breaking as well as controlling photocurrent via light polarization. The discovery of topological invariants and Berry phases in bandstructure has led to a greatly heightened pace of research in phenomena related to the CPGE.

Recently Moore and collaborators predicted that the CPGE in chiral WSMs is directly proportional to topological charge and is quantized in units of the fundamental constants e and $\hbar$ (de Juan *et al.*, 2017). This quantization is hidden in WSMs that preserve mirror symmetry but emerges in

chiral WSMs because in such lower symmetry structures Weyl nodes with opposite topological charge need not be degenerate in energy.

(1) Verification of universality of the spectrum/new materials: It is important to test the theoretical prediction of universality of the quantized CPGE (de Juan *et al.*, 2017, Flicker *et al.*, 2018) by extending the measurements to other materials. We will begin with candidate materials within the same $P2_13$ (#198) as RhSi; these include CoSi, CoGe, and RhGe. Preliminary work indicates that these materials can be synthesized in both left and right enantiomorphs, allowing a direct test of the proportionality to chiral charge (C). In addition, we will attempt thin film synthesis of representative compounds (motivation for thin films is described below).

(2) Spin momentum locking/hydrodynamics: Chiral Weyl semimetals are new systems for controlling spin polarization and spin current with light. As emphasized above, circularly polarized light generates a charge current either parallel or antiparallel to the wavevector of the excitation light, depending on the photon helicity. Given the perfect spin-momentum locking at the Weyl cone, the photoexcited state carries a photon helicity-dependent spin current as well. This creates the possibility of measuring spin lifetimes and diffusion coefficients using time-resolved MOKE and spin transient grating measurements developed by our group. We note that particle-hole asymmetry in chiral Weyl systems creates the possibility to observe spin lifetimes far in excess of the momentum relaxation times.

Second harmonic generation in chiral topological semimetals

In the previous review period, we reported the discovery of giant SHG in the polar Weyl semimetal TaAs (Wu *et al.*, 2017). The giant response in TaAs peaks at 700 meV, above the energy where the Weyl dispersion applies (Patankar *et al.*, 2018a). In chiral semimetals the energy range of nearly perfect Weyl dispersion is much larger, providing the opportunity to probe the intrinsic SHG response of chiral Weyl fermions. As an example, the bandstructure of RhSi features a nearly perfect Weyl dispersion for energies below approximately 700 meV (Chang *et al.*, 2017). Using our recently acquired OPA/DFG laser system, we will probe the SHG response to energies low as 100 meV, allowing us to map out the spectral response of a single chiral Berry monopole.

Response of Fermi arc states: Fermi arcs that extend across the entire Brillouin zone in intricate patterns have been observed in chiral Weyl semimetals (Sanchez *et al.*, 2018). As yet there are no observations of electromagnetic or transport responses associated with these states. SHG measurements, by virtue of their sensitivity to surface symmetry, have the potential to observe such effects. We will perform experiments as a function of angle of incidence on different surface orientations to look for departures from expectations based on the symmetry of the bulk. These departures should be particularly clear in the cubic chiral Weyl materials where the bulk response is characterized by a nonlinear response tensor with a single non-vanishing component.

Literature Cited

Asnin, V. M., Bakun, A. A., Danishevskii, A. M., Ivchenko, E. L., Pikus, G. E. & Rogachev, A. A. (1979) '"Circular" photogalvanic effect in optically active crystals', *Solid State Communications,* 30, 565-70.

Chang, G., Xu, S.-Y., Wieder, B. J., Sanchez, D. S., Huang, S.-M., Belopolski, I., Chang, T.-R., Zhang, S., Bansil, A., Lin, H. & Hasan, M. Z. (2017) 'Unconventional Chiral Fermions and Large Topological Fermi Arcs in RhSi', *Physical Review Letters,* 119, 206401.

De Juan, F., Grushin, A. G., Morimoto, T. & Moore, J. E. (2017) 'Quantized circular photogalvanic effect in Weyl semimetals', *Nature Communications,* 8.

Flicker, F., De Juan, F., Bradlyn, B., Morimoto, T., Vergniory, M. G. & Grushin, A. G. (2018) 'Chiral optical response of multifold fermions', *Physical Review B,* 98, 155145.

Hasan, M. Z., Xu, S.-Y., Belopolski, I. & Huang, S.-M. (2017) 'Discovery of Weyl Fermion Semimetals and Topological Fermi Arc States', *Annual Review of Condensed Matter Physics,* 8, 289-309.

Patankar, S., Wu, L., Lu, B., Rai, M., Tran, J. D., Morimoto, T., Parker, D. E., Grushin, A. G., Nair, N. L., Analytis, J. G., Moore, J. E., Orenstein, J. & Torchinsky, D. H. (2018a) 'Resonance-enhanced optical nonlinearity in the Weyl semimetal TaAs', *Physical Review B,* 98, 165113.

Patankar, S., Wu, L., Lu, B. Z., Rai, M., Tran, J. D., Morimoto, T., Parker, D. E., Grushin, A. G., Nair, N. L., Analytis, J. G., Moore, J. E., Orenstein, J. & Torchinsky, D. H. (2018b) 'Resonance-enhanced optical nonlinearity in the Weyl semimetal TaAs', *Physical Review B,* 98.

Sanchez, D. S., Belopolski, I., Cochran, T. A., Xu, X., Yin, J.-X., Chang, G., Xie, W., Manna, K., Süß, V., Huang, C.-Y., Alidoust, N., Multer, D., Zhang, S. S., Shumiya, N., Wang, X., Wang, G.-Q., Chang, T.-R., Felser, C., Xu, S.-Y., Jia, S., Lin, H. & Zahid Hasan, M. (2018) 'Discovery of topological chiral crystals with helicoid arc states', *arXiv e-prints*. https://ui.adsabs.harvard.edu/\#abs/2018arXiv181204466S.

Wu, L., Patankar, S., Morimoto, T., Nair, N. L., Thewalt, E., Little, A., Analytis, J. G., Moore, J. E. & Orenstein, J. (2017) 'Giant anisotropic nonlinear optical response in transition metal monopnictideWeyl semimetals', *Nature Physics,* 13, 350-55.

Publications

1. K. Gotlieb, Z. L. Li, C. Y. Lin, C. Jozwiak, J. H. Ryoo, C. H. Park, Z. Hussain, S. G. Louie, A. Lanzara. "Symmetry rules shaping spin-orbital textures in surface states," *Phys. Rev. B* 95, 245142 (2017)

2. G. Affeldt, T. Hogan, C. L. Smallwood, T. Das, D. Denlinger, S. D. Wilson, A. Vishwanath, A. Lanzara. "Spectral weight suppression near a metal-insulator transition in a double layer electrondoped iridate," *Phys. Rev. B* 95, 235151 (2017)

3. D. Varjas, A. G. Grushin, R. Ilan, and J. E. Moore, "Dynamical piezoelectric and magnetopiezoelectric effects in polar metals from Berry phases and orbital moments," *Phys. Rev.Lett.* **117**, 257601 (2016)

4. T**.** Helm, P.N. Valdivia, E. Bourret-Courchesne, J.G. Analytis, R.J. Birgeneau. "The influence of magnetic order on the magnetoresistance anisotropy of Fe1+delta-xCuxTe," *Journal of physics: Condensed Matter*: 29(28): 285801 (2017).

5. M. Wang, S.J. Jin, M. Yi, Y. Song, H.C. Jiang, W.L. Zhang, H.L. Sun, H.Q. Luo, A.D. Christianson, E. Bourret-Courchesne, D.H. Lee, D.X. Yao, R.J. Birgeneau. "Strong

ferromagnetic exchange interaction under ambient pressure in BaFe2S3," *Phys Rev B* 96, 6, 060502 (2017).

6. Jonathan Cookmeyer, Joel E. Moore. "Spin Wave Analysis of Low-Temperature Thermal Hall Effect in the Candidate Kitaev Spin Liquid α-RuCl3," *Phys Rev B* 98 060412 (R) (2018).

7. B.A. Frandsen, K.M. Taddei, M. Yi, A. Frano, Z. Guguchia, Y. Rong, Q. Si, D.E. Bugaris, R. Stadel, R. Osborn, S. Rosenkranz, O. Chmaissem, and R.J. Birgeneau. "Local orthorhombicity in the magnetic *C*4 phase of the hole-doped iron-arsenide superconductor Sr1-*x*Na*x*Fe2As2," *Physical Review Letters* 119, 187001 (2017).

8. Eric Thewalt, Ian M. Hayes, James P. Hinton, Arielle Little, Shreyas Patankar, Liang Wu, Toni Helm, Camelia V. Stan, Nobumichi Tamura, James G. Analytis, and Joseph Orenstein. "Imaging anomalous nematic order and strain in optimally doped BaFe2(As, P)2," *Phys. Rev. Lett.* 121, 027001 (2018).

9. G. Affeldt, T. Hogan, J. D. Denlinger, A. Vishwanath, S. D. Wilson, A. Lanzara. "Doping dependent correlation effects in (Sr1-*x*La*x*)3Ir2O7," *Physical Review B* 97, 125111 (2018).

10. L. Moreschini, I. Lo Vecchio, N. P. Breznay, S. Moser, S. Ulstrup, R. Koch, J. Wirjo, C. Jozwiak, K. S. Kim, E. Rotenberg, A. Bostwick, J. Analytis, A. Lanzara. "Quasiparticles and charge transfer at the two surfaces of the honeycomb iridate Na2IrO3," *Physical Review B* 96, 199902 (2017).

11. M. Yi, A. Frano, D.H. Lu, Y. He, M. Wang, B.A. Frandsen, A.F. Kemper, R. Yu, Q. Si, L. Wang, M. He, F. Hardy, P. Schweiss, P Adelmann, T. Wolf, M. Hashimoto, S.-K. Mo, Z. Hussain, M. Le Tacon, A.E. Boehmer, D.-H. Lee, Z.-X. Shen, C. Meingast, and R.J. Birgeneau. "Spectral Evidence for Emergent Order in Ba1-*x*Na*x*Fe2As2," *Phys. Rev. Lett.* 121, 127001 (2018).

12. Shreyas Patankar, Liang Wu, Baozhu Lu, Manita Rai, Jason D. Tran, T. Morimoto, D. Parker, Adolfo Grushin, N. L. Nair, J. G. Analytis, J. E. Moore, J. Orenstein, Darius H. Torchinsky. "Resonance enhanced optical nonlinearity in the Weyl semimetal TaAs," *Phys. Rev. B* 98, 165113 (2018).

13. Daniel E. Parker, Takahiro Morimoto, J. Orenstein, and J.E. Moore, "Diagrammatic approach to nonlinear response with application to Weyl semimetals," Phys. Rev. B 99, 045121 (2019).

14. Zheng, Liangliang; Frandsen, Benjamin A.; Wu, Changwei; Ming Yi, Shan Wu, Qingzhen Huang, Edith Bourret-Courchesne, G. Simutis, R. Khasanov, Dao-Xin Yao, Meng Wang, and Robert J. Birgeneau " Gradual enhancement of stripe-type antiferromagnetism in the spin-ladder material BaFe2S3 under pressure" Physical Review B 98(18) 180402 (2018).

15. B. A. Frandsen, K. M. Taddei, D. E. Bugaris, R. Stadel, M Yi, A.Acharya, R. Osborn, S. Rosenkranz, O. Chmaissem, R. J. Birgeneau, Widespread orthorhombic fluctuations in the (Sr, Na)Fe2As2 family of superconductors, Physical Review B 98 180505(R) (2018).

Synthesis and Observation of Emergent Phenomena in Heusler Compound Heterostructures

Christopher J. Palmstrøm, ***Department of Electrical and Computer Engineering, University of California-Santa Barbara, Santa Barbara CA 93106***

Anderson Janotti, ***Department of Materials Science and Engineering, University of Delaware, Newark, Delaware 19716, USA***

Program Scope:

Heusler compounds are an exciting class of ternary compounds that exhibit a wide range of electrical and magnetic properties [1] including materials that can be semiconducting [2, 3], half-metallic ferromagnets [4,5], superconductors [6-10], thermoelectrics [1] and can even host topologically non-trivial ground states including nodal-lines, Weyl semi-metallic phase and triple-point fermions [1,11-15]. In the closely related crystal structures of the rare-earth monopnictides with the rock-salt structure, predictions of topological semimetals and insulators have also been made [16, 17]. Our proposed effort addresses the prediction, synthesis and characterization of these novel materials and heterostructures with quantum properties of importance to the field of Quantum Information Science through the use of high quality epitaxial single crystal films and heterostructures grown using molecular beam epitaxy combined with state-of-the art density functional theory and *in vacuo* atomic level characterization. Our approach is compatible with advanced spectroscopic tools such as angle-resolved photoemission spectroscopy (ARPES) and scanning tunneling microscopy (STM) that allows us access to pristine sample surfaces without the requirement of cleaving along with chosen surface orientations optimum for investigations of Dirac cones, Weyl points and triple point Fermions. Furthermore, through heteroepitaxial growth on high quality lattice tuned III-V semiconductor substrates, epitaxial strain will be used to tune the bulk band structure of thin Heusler films, interfaces and heterostructures. The ability to predict and synthesize these materials in a single crystal thin film form, combining them with other materials, including other Heuslers, rare-earth monopnictides and superconductors, and controllably tune their physical properties via materials engineering promise to open up avenues for the realization of multi-functional structures and novel emergent phenomena in engineered heterostructures. We are particularly interested in investigating the formation of emergent phenomena, such as two-dimensional electron and hole gases, induced superconductivity and magnetism at epitaxial interfaces.

Recent Progress:

Co based full-Heusler compounds are one of the primary candidates that have been predicted to host magnetic Weyl points [18,19]. Due to the existence of mirror symmetries (M_x, M_y, M_z, M_{xy}, M_{yz}, M_{xz}) a nodal line is expected to form if one ignores spin-orbit coupling. Addition of spin-orbit coupling generally opens up a gap in the band structure in this magnetic

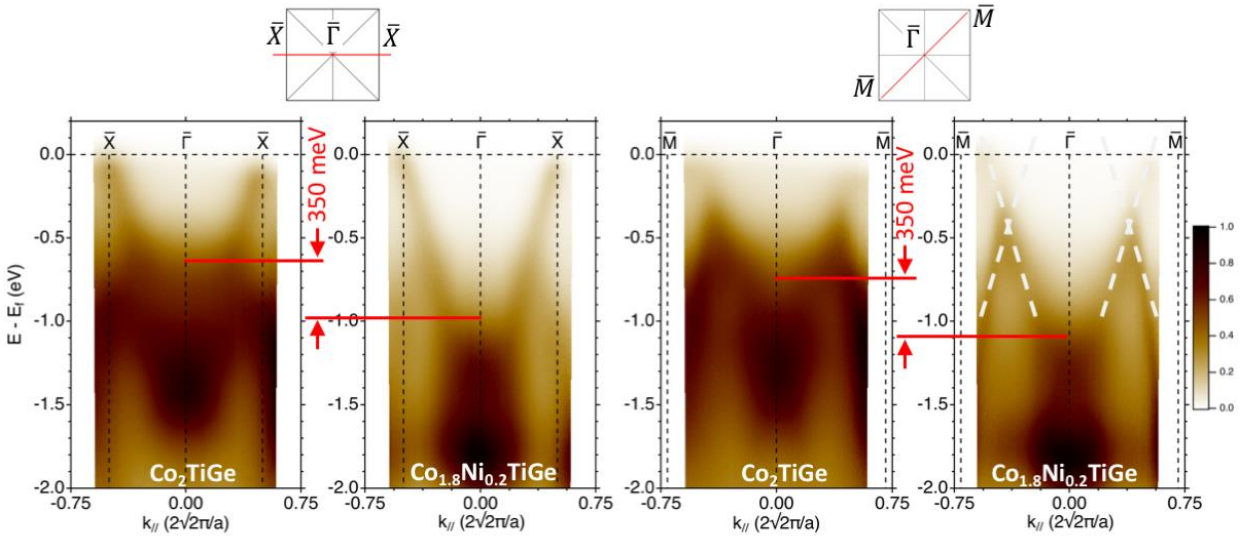

Fig. 1: ARPES energy dispersion slices collected at hv = 60 eV for for Co_2TiGe and $Co_{1.8}Ni_{0.2}TiGe$ along the (left pair) $\overline{X} - \overline{\Gamma} - \overline{X}$ and (right pair) $\overline{M} - \overline{\Gamma} - \overline{M}$ directions. Dashed white lines have been added as a guide to the eye on the far-right image.

material everywhere apart from along the direction of magnetization if it is along one of the mirror symmetry directions. It is along this direction that the band crossing is still protected, and Weyl nodes are expected to appear. Explicit calculations for one such candidate compound, Co_2TiGe, reveal three possible Weyl points for [001] magnetization direction, which are about 200-300 meV away from the Fermi level [18]. Our own DFT calculations indicate the possibility of stabilizing magnetic Weyl points in other full Heusler compounds such as Co_2MnSi and Co_2MnAl.

We have demonstrated successful synthesis of a number of such candidate compounds including Co_2TiGe [20], Co_2MnAl [21], Co_2MnSi [22,23,24,25]. Furthermore, we have also demonstrated our ability to maintain pristine sample surfaces compatible with spectroscopy tools allowing us to perform the first, to the best of our knowledge, ARPES measurements on Co_2TiGe. Our measurements suggest that the Weyl nodes are further away from the Fermi level that also explains lack of signature of the presence of Weyl points in our transport measurements of Co_2TiGe. To address this problem, we have synthesized substitutionally alloyed thin films of $Co_{2-x}Ni_xTiGe$ and utilizing ARPES measurements have shown our ability to shift the chemical potential by as much as 350 meV (Fig. 1). Further spectroscopic investigation and transport measurements of these substitutionally alloyed compounds are currently underway.

In addition, using a similar approach we have been able to shift the chemical potential in substitutionally alloyed half-Heusler topological semi-metal $Pt_{1-x}Au_xLuSb$, where we have been able to observe signatures of quantum hall effect from the topological surface states in transport measurements. We have also established our ability to control electron-hole compensation and thereby its magnetoresistance properties in ultra-thin films of LuSb, which is a topologically trivial

electron-hole compensated semimetal in the bulk [26]. Furthermore, we have been able to elucidate the modification of electronic structure by ARPES measurements in $Co_2MnSi_{1-x}Al_x$ thin films.

Future Plans:

We plan to undertake extensive transport and photoemission measurements on suitably substitutionally alloyed $Co_{2-x}Ni_xTiGe$ and $Co_2MnSi_{1-x}Al_x$ thin films to look for the presence of Weyl nodes. In addition, we are also planning to perform spin-resolved ARPES measurements and fabricate lateral spin-valve devices to probe the degree of spin polarization at the Fermi level both via spectroscopic and electrical measurements.

We are synthesizing strained PtLuSb thin films to bring about the predicted topological to trivial phase transition in bi-axial strained thin films. We plan to synthesize thin films of PtLuBi, where enhanced spin-orbit coupling will allow us to increase the inverted band gap in these compounds.

In addition, we are beginning to work on GdSb and GdBi thin films. We are interested in understanding the modification of its magnetic structure under dimensional confinement. We are also interested in investigating the feasibility of a predicted Chern insulating phase in ultra-thin films of Gd monopnictides [27].

References:

1 T. Graf, C. Felser, and S. S. P. Parkin, *Simple rules for the understanding of Heusler Compounds,* Progress in Solid State Chemistry **39,** 1 (2011).

2 H. C. Kandpal, C. Felser, and R. Seshadri, *Covalent bonding and the nature of band gaps in some half-Heusler compounds,* J. Phys. D-Appl. Phys. **39,** 776 (2006).

3 L. Offernes, P. Ravindran, and A. Kjekshus, *Electronic structure and chemical bonding in half-Heusler phases,* Journal of Alloys and Compounds **439,** 37 (2007).

4 R. A. de Groot, F. M. Mueller, P. G. van Engen, and K. H. J. Buschow, *New class of materials: half-metallic ferromagnets,* Phys. Rev. Letts. **50,** 2024 (1983).

5 I. Galanakis, P. H. Dederichs, and N. Papanikolaou, *Slater-Pauling behavior and origin of the half-metallicity of the full-Heusler alloys,* Phys. Rev. B **66,** 174429 (2002).

6 J. Winterlik, G. H. Fecher, and C. Felser, *Electronic and structural properties of palladium-based Heusler superconductors,* Solid State Communications **145,** 475 (2008).

7 T. Klimczuk, C. H. Wang, K. Gofryk, F. Ronning, J. Winterlik, G. H. Fecher, J. C. Griveau, E. Colineau, C. Felser, J. D. Thompson, D. J. Safarik, and R. J. Cava, *Superconductivity in the Heusler family of intermetallics,* Physical Review B **85,** 174505 (2012).

8 Y. Pan, A. M. Nikitin, T. V. Bay, Y. K. Huang, C. Paulsen, B. H. Yan, and A. de Visser, *Superconductivity and magnetic order in the noncentrosymmetric half-Heusler compound ErPdBi,* Epl **104,** 27001 (2013).

9 G. Xu, W. Wang, X. Zhang, Y. Du, E. Liu, S. Wang, G. Wu, Z. Liu, and X. X. Zhang, *Weak Antilocalization Effect and Noncentrosymmetric Superconductivity in a Topologically Nontrivial Semimetal LuPdBi,* Scientific Reports **4,** 5709 (2014).

10 F. F. Tafti, T. Fujii, A. Juneau-Fecteau, S. R. de Cotret, N. Doiron-Leyraud, A. Asamitsu, and L. Taillefer, *Superconductivity in the noncentrosymmetric half-Heusler compound LuPtBi: A candidate for topological superconductivity,* Physical Review B **87,** 184504 (2013).

11 H. Lin, L. A. Wray, Y. Q. Xia, S. Y. Xu, S. A. Jia, R. J. Cava, A. Bansil, and M. Z. Hasan, *Half-Heusler ternary compounds as new multifunctional experimental platforms for topological quantum phenomena*, Nature Materials **9,** 546 (2010).

12 S. Chadov, X. Qi, J. Kuebler, G. H. Fecher, C. Felser, and S. C. Zhang, *Tunable multifunctional topological insulators in ternary Heusler compounds*, Nature Materials **9,** 541 (2010).

13 W. Al-Sawai, H. Lin, R. S. Markiewicz, L. A. Wray, Y. Xia, S. Y. Xu, M. Z. Hasan, and A. Bansil, *Topological electronic structure in half-Heusler topological insulators*, Physical Review B **82,** 125208 (2010).

14 G. Q. Chang, S. Y. Xu, X. T. Zhou, S. M. Huang, B. Singh, B. K. Wang, I. Belopolski, J. X. Yin, S. T. Zhang, A. Bansil, H. Lin, and M. Z. Hasan, *Topological Hopf and Chain Link Semimetal States and Their Application to Co2MnGa*, Physical Review Letters **119,** 156401 (2017).

15 H. Yang, J. B. Yu, S. S. P. Parkin, C. Felser, C. X. Liu, and B. H. Yan, *Prediction of Triple Point Fermions in Simple Half-Heusler Topological Insulators*, Physical Review Letters **119,** 136401 (2017).

16 M. Zeng, C. Fang, G. Chang, Y.-A. Chen, T. Hsieh, A. Bansil, H. Lin, and L. Fu, *Topological semimetals and topological insulators in rare earth monopnictides*, arXiv:1504.03492**,** (2015).

17 J. Nayak, S. C. Wu, N. Kumar, C. Shekhar, S. Singh, J. Fink, E. E. D. Rienks, G. H. Fecher, S. S. P. Parkin, B. H. Yan, and C. Felser, *Multiple Dirac cones at the surface of the topological metal LaBi*, Nature Communications **8,** 139421 (2017).

18 G. Q. Chang, S. Y. Xu, H. Zheng, B. Singh, C. H. Hsu, G. Bian, N. Alidoust, I. Belopolski, D. S. Sanchez, S. T. Zhang, H. Lin, and M. Z. Hasan, *Room-temperature magnetic topological Weyl fermion and nodal line semimetal states in half-metallic Heusler Co_2TiX (X=Si, Ge, or Sn)*, Scientific Reports **6,** 38839 (2016).

19 Z. J. Wang, M. G. Vergniory, S. Kushwaha, M. Hirschberger, E. V. Chulkov, A. Ernst, N. P. Ong, R. J. Cava, and B. A. Bernevig, *Time-Reversal-Breaking Weyl Fermions in Magnetic Heusler Alloys*, Physical Review Letters **117,** 236401 (2016).

20 J. A. Logan, T. L. Brown-Heft, S. D. Harrington, N. S. Wilson, A. P. McFadden, A. D. Rice, M. Pendharkar, and C. J. Palmstrøm, *Growth, structural, and magnetic properties of single-crystal full-Heusler Co_2TiGe thin films*, J. Appl. Phys. **121,** 213903 (2017).

21 T. L. Brown-Heft, J. A. Logan, A. P. McFadden, C. Guillemard, P. Le Fèvre, F. Betran, S. Andrieu, and C. J. Palmstrøm, *Epitaxial Heusler superlattice Co_2MnAl/Fe_2MnAl with perpendicular magnetic anisotropy and termination-dependent half-metallicity*, Physical Review Materials **2,** 034402 (2018).

22 M. Oogane, A. P. McFadden, Y. Kota, T. L. Brown-Heft, M. Tsunoda, Y. Ando, and C. J. Palmstrøm, *Fourfold symmetric anisotropic magnetoresistance in half-metallic Co_2MnSi Heusler alloy thin films*, Japanese Journal of Applied Physics **57,** 063001 (2018).

23 A. Rath, C. Sivakumar, C. Sun, S. J. Patel, J. S. Jeong, J. Feng, G. Stecklein, P. A. Crowell, C. J. Palmstrøm, W. H. Butler, and P. M. Voyles, *Reduced interface spin polarization by antiferromagnetically coupled Mn segregated to the $Co_2MnSi/GaAs$ (001) interface*, Physical Review B **97,** 045304 (2018).

24 A. P. McFadden, T. Brown-Heft, D. Pennachio, N. S. Wilson, J. A. Logan, and C. J. Palmstrøm, *Oxygen migration in epitaxial CoFe/MgO/Co_2MnSi magnetic tunnel junctions*, J. Appl. Phys. **122,** 113902 (2017).

25 A. McFadden, N. Wilson, T. Brown-Heft, D. Pennachio, M. Pendharkar, J. A. Logan, and C. J. Palmstrøm, *Interface formation of epitaxial MgO/Co_2MnSi(001) structures: Elemental segregation and oxygen migration*, Journal of Magnetism and Magnetic Materials **444,** 383 (2017).

26 Shouvik Chatterjee, Shoaib Khalid, Hadass S. Inbar, Aranya Goswami, Felipe Crasto de Lima, Abhishek Sharan, Fernando P. Sabino, Tobias L. Brown-Heft, Yu-Hao Chang, Alexei V. Fedorov, Dan Read, Anderson Janotti, and Christopher J. Palmstrøm, *Weak antilocalization in quasi-two-dimensional electronic states of epitaxial LuSb thin films*, Physical Review B **99,** 125134 (2019)

27 Zhi Li, Jinwoong Kim, Nicholas Kioussis, Shu-Yu Ning, Haibin Su, Toshiaki Iitaka, Takami Tohyama, Xinyu Yang, and Jiu-Xing Zhang, *GdN thin film: Chern insulating state on square lattice*, Physical Review B **92,** 201303(R) (2015)

Publications:

1. S. Chatterjee, S. Khalid, H. S. Inbar, A. Goswami, F. C. de Lima, A. Sharan, F. P. Sabino, T. L. Brown-Heft, Y.-H. Chang, A. V. Fedorov, D. Read, A. Janotti, and C. J. Palmstrøm, *Weak antilocalization in quasi-two-dimensional electronic states of epitaxial LuSb thin films*, Physical Review B **99,** 125134 (2019)
2. B. Bonef, S. D. Harrington, D. J. Pennachio, J. S. Speck, and C. J. Palmstrom, *Nanometer scale structural and compositional inhomogeneities of half-Heusler $CoTi_{1-x}Fe_xSb$ thin films*, Journal of Applied Physics **125,** 205301 (2019).
3. Sharan, Z. G. Gui, and A. Janotti, *Formation of two-dimensional electron and hole gases at the interface of half-Heusler semiconductors*, Phys. Rev. Mater. **3,** 061602 (2019)
4. S. Khalid, F. P. Sabino, and A. Janotti, *Topological phase transition in LaAs under pressure*, Phys. Rev. B **98,** 220102 (2018).
5. M. Oogane, A. P. McFadden, Y. Kota, T. L. Brown-Heft, M. Tsunoda, Y. Ando, and C. J. Palmstrøm, *Fourfold symmetric anisotropic magnetoresistance in half-metallic Co_2MnSi Heusler alloy thin films*, Jpn. J. Appl. Phys. **57,** 063001 (2018)
6. M. Oogane, A. P. McFadden, K. Fukuda, M. Tsunoda, Y. Ando, and C. J. Palmstrøm, *Low magnetic damping and large negative anisotropic magnetoresistance in halfmetallic $Co_{2-x}Mn_{1+x}Si$ Heusler alloy films grown by molecular beam epitaxy*, Appl. Phys. Lett. **112,** 262407 (2018)
7. . K. Kawasaki, A. Sharan, L. I. M. Johansson, M. Hjort, R. Timm, B. Thiagarajan, B. D. Schultz, A. Mikkelsen, A. Janotti, and C. J. Palmstrøm, *A simple electron counting model for half-Heusler surfaces*, Science Advances **4,** eaar5832 (2018)
8. S. D. Harrington, A. D. Rice, T. L. Brown-Heft, B. Bonef, A. Sharan, A. P. McFadden, J. A. Logan, M. Pendharkar, M. M. Feldman, O. Mercan, A. G. Petukhov, A. Janotti, L. C. Arslan, and C. J. Palmstrøm, *Growth, electrical, structural, and magnetic properties of half-Heusler $CoTi_{1-x}Fe_xSb$*, Physical Review Materials **2,** 014406 (2018)
9. S. D. Harrington, J. A. Logan, S. Chatterjee, S. J. Patel, A. D. Rice, M. M. Feldman, C. M. Polley, T. Balasubramanian, A. Mikkelsen, and C. J. Palmstrom, *Electronic structure of epitaxial half-Heusler $Co_{1-x}Ni_xTiSb$ across the semiconductor to metal transition*, Applied Physics Letters **113,** 092103 (2018)
10. T. L. Brown-Heft, J. A. Logan, A. P. McFadden, C. Guillemard, P. Le Fèvre, F. Betran, S. Andrieu, and C. J. Palmstrøm, *Epitaxial Heusler superlattice Co_2MnAl/Fe_2MnAl with perpendicular magnetic anisotropy and termination-dependent half-metallicity*, Physical Review Materials **2,** 034402 (2018)

Degeneracy of the 1/8 Plateau and Antiferromagnetic Phases in the Shastry-Sutherland Magnet TmB_4

Principal Investigator: Arthur P. Ramirez, University of California Santa Cruz

Program Scope: The present work was performed as a sub-topic under the project "Tuning Quantum Fluctuations in Low-Dimensional and Geometrically Frustrated Magnets". The goal of this project is to develop methods to enhance the production of quantum fluctuations in magnetic materials at low temperatures. The proposed work includes both the study of novel geometrically frustrated magnetic systems as well as known, non-frustrated and low-dimensional systems that can be tuned, primarily by magnetic field, from a state of classical long range order into a non-ordered quantum fluctuating state.

Recent Progress: The work to date has included a number of sub-topics. First among these is the study of the Shastry-Sutherland (SS) lattice magnet TmB_4, in collaboration with P. Canfield at Ames Lab [1]. This system exhibits a phase diagram in field (H) and temperature (T) as shown in Fig. 1, where the antiferromagnetic (AF) mixed phase (MP) and ferromagnetic (FI) phases are indicated. The FI phase has a magnetization plateau with $M = M_s/2$, where M_s is the saturation moment, and the shaded region is a phase with $M = M_s/8$. Whereas many materials possess magnetization plateaus, TmB_4 has gained much attention due to this so-called 1/8 fractional plateau phase (1/8-FPP) [2, 3]. This phase has been compared to a similar phase in another SS magnet $SrCu_2(BO_3)_2$ [4-6], which in turn has been described by a number of models [7, 8] including a topological Chern-Simons theory of triplon crystallization [9]. We are studying TmB_4 because it allows us to draw analogies to $SrCu_2(BO_3)_2$ while also working at a smaller H field than where this system's 1/8-FPP is found, 25T, thus enabling a larger range of high precision measurements.

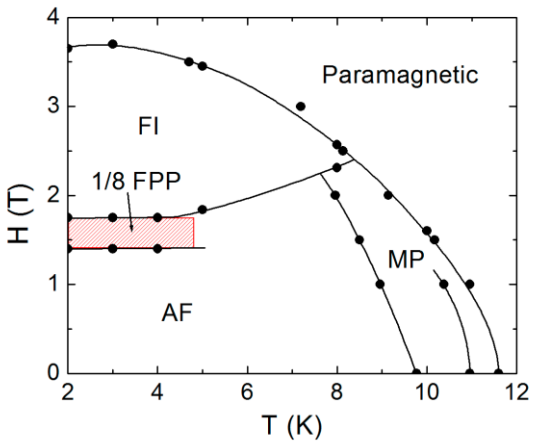

Fig. 1 Phase diagram of TmB_4 in the H-T plane. In the red-shaded region, the magnetization is 1/8 of the saturation value.

In addition to the 1/8-FPP, TmB_4 has also exhibited plateaus at fractions such as 1/9 and 1/11, as well as hysteresis between data taken on sweeping H up and down [2]. Realizing that magnetization measurements are susceptible to domain effects and other signals not representative of the majority spins, we sought to understand the nature of the 1/8-FPP from a thermodynamic standpoint. In Fig. 2 we show both magnetization and specific heat (C) data in the H and T range encompassed by the 1/8-FPP, as a function of H. We see that, at the lowest T studied, 2K, M assumes the value $1/8M_s$ with little hysteresis. The behavior of $C(H)$ is also reflective of a static phase in this region with a thermodynamically large number of spins being affected at the upper and lower phase boundaries. As T increases, however, hysteresis becomes, paradoxically, more pronounced and, on H up-sweeps, a seemingly continuous range of M-plateau values is observed. At the same time, $C(H)$ starts to behave differently and, most surprisingly, its signature at the lower boundary vanishes at 3K. This behavior is summarized in the phase diagram of the 1/8-FPP shown in Fig. 3 which shows well defined thermodynamic phase boundaries on H down-sweeps, but an ill-formed lower phase

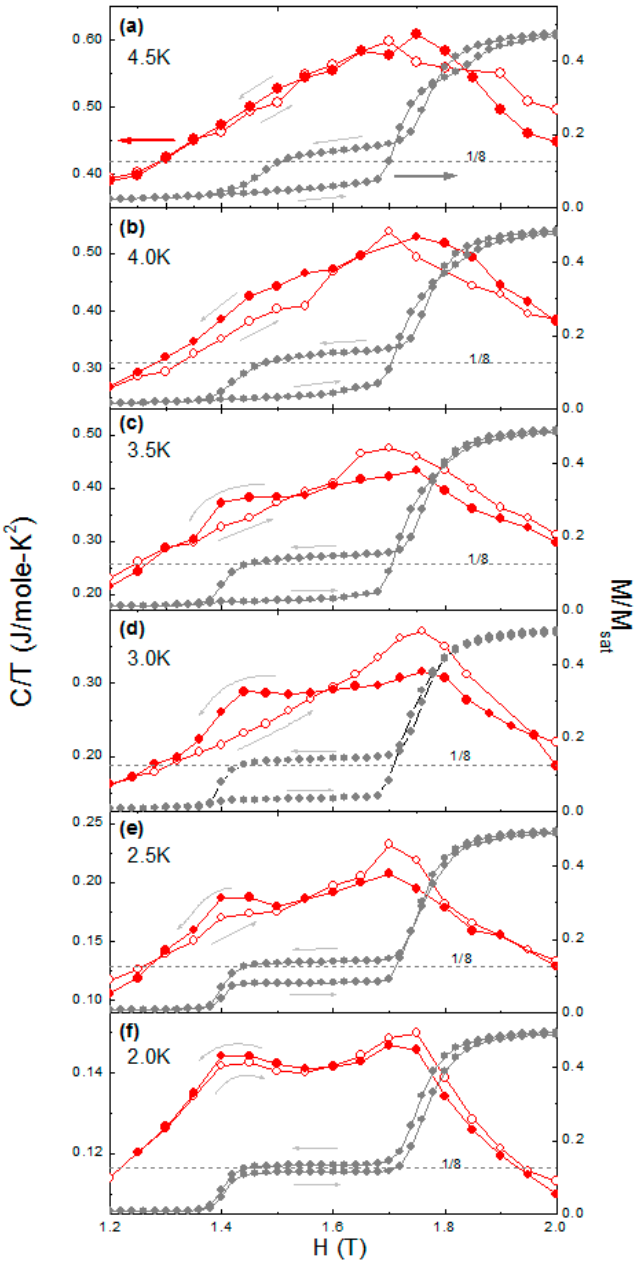

Fig. 2 - Specific heat of TmB_4, divided by temperature, C/T, and magnetization, M, as a function of magnetic field H, for various temperatures encompassing the FPP.

boundary on up sweeps. The conclusion of this work is that the 1/8-FPP is a meta-stable phase. In our paper, we show that the total spin energy of the 1/8-FPP differs from that of the AF phase by less than the thermal energy in this region, which supports the notion of a meta-stable 1/8-FPP. The existence of arbitrary size fractions, accessible via history-dependent field processing, places strong constraints on possible theories for explaining such plateaus, as well as for future experimental study of related systems.

Recent Progress – Based on the TmB_4 work, we are presently investigating the 1/3-FPP in CeSb [10], also in collaboration with P. Canfield at Ames Lab. This phase is associated with an extremely flat *M*-plateau, which we are studying using both thermodynamic and transport probes. In particular, we have developed the capability to explore this and other materials using non-local conductivity measurement techniques, targeted towards the discovery and elucidation of topological phases of matter. In this work, we have found evidence for a collective modification of the spin texture in the middle of the FPP. This collective effect is characterized by step in *M* that, while involving only one percent of the spins, is extremely sharp as a function of *H*, which allows for its identification. We have validated this effect also using Hall resistance measurements, which strongly suggest a topological origin. Further work on this system will invoke non-local probes to explore the interplay of topological order and thermodynamic order.

Other progress has been made in low-dimensional magnets. We recently observed at the *H*-induced quantum critical point (QCP) in the quasi-1D system copper elpasolite ($K_2PbCu(NO_2)_6$),

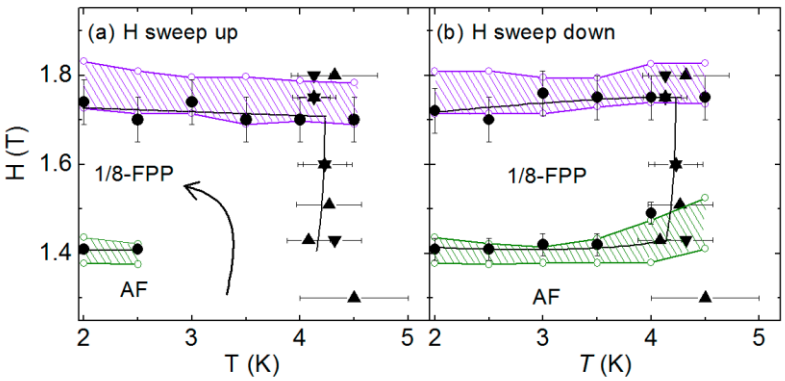

Fig. 3. The phase diagram around the 1/8 FPP as determined by specific heat measurements, denoted by solid black symbols. The circles are obtained from $C(H)$ in Fig. 2 and the up (down) triangles denote the peaks in $C(T)$. Other symbols are derived from $M(H)$.

an anomalously large entropy anomaly [11]. We also identified the "double-peak" phenomenon in $C(H)$ at the QCP, and showed its relationship to the Tonks gas of free fermions in 1D. We showed how this entropy anomaly is a by-product of the H-induced shift of short-range-order development to lower T. In subsequent work on pyridine-N complex compounds containing Cu s = 1/2 spins, we show how this shift occurs not only in quasi-1D magnets, but also in quasi-2D magnets. One conclusion of this work is that, by using H as a tuning parameter, it is possible to explore much larger classes of magnets than those with extreme low-D character since the QCP suppresses the classical 3D order, revealing quantum low-D behavior. This work has been done in collaboration with T. Siegrist (FSU), Joel Miller (Univ Utah) and A. Sandvik (Boston Univ).

Other work under this project is the search for quantum spin and topological behavior in intermediate-valence systems. For SmB_6, touted as possessing a neutral Fermi surface [12], we have made substantial progress in performing difficult specific heat measurements in high fields. These measurements of the density of states will either reveal the behavior of exotic itinerant excitations or serve to constrain future theories. This work is being done in collaboration with N. Fortune (Smith College), Z. Fisk (UC Irvine) and P. Rosa (LANL). Another intermediate valence material, SmS [13], has been discussed as a platform for possible topological Kondo insulator states [14, 15]. We have explored the series of compounds $Sm_{1-x}Eu_xS$ which span from non-magnetic SmS to ferromagnetic EuS. We find that, while M and resistivity (ρ) obey Vegard's law behavior, the lattice constant displays an anomalous minimum not centered at x = 0.5, but at 0.25. This implies a magnetic interaction among Eu ions and the excited state of Sm, a possible 3-body magnetic polaron. This work has been done in collaboration with T. Siegrist (FSU).

Another area of investigation is the origin of spin anisotropy in collective systems, and in particular the pseudobrookite phase Fe_2TiO_5. This system exhibits purely Ising-like spin glass (SG) freezing despite its Fe^{3+} spins being Heisenberg-like [16]. Using neutron scattering, we found that, above the SG transition, the spins exhibit a short-range magnetic Bragg peak, the inferred correlation length of which is largest in the direction transverse to SG freezing, creating surfboard-shaped nano-sized ordered regions (Fig. 4). The only reasonable interpretation of these data is that the transverse spin response of the surfboard region is the degree of freedom that freezes, a picture that represents a dramatic departure from mean field SG theories which assume the atomic spin as freezing. This result has broad implications for how SG states are described, especially in systems with strong geometrical frustration. In addition, it demonstrates a new route for creating spin anisotropy, an important ingredient for large-energy-product permanent magnets. Specifically, it shows how anisotropy can arise in an emergent degree of freedom formed by spatial correlations.

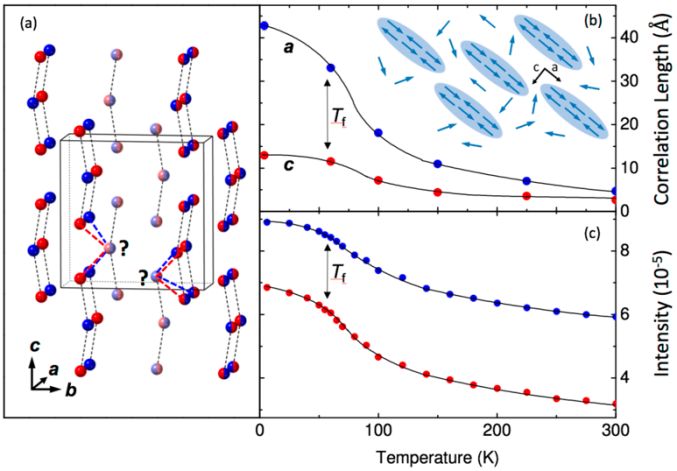

Fig. 4 Left: Proposed Fe^{3+} spin arrangement in Fe_2TiO_5, assuming ordered Fe site occupancy. Upper Right: Correlation length in the a and c directions (SG order occurs only in the c-direction). Inset: Proposed two-spin model, where short range order occurs in surfboard-shaped regions and the remaining spins are paramagnetic down to low temperatures. Lower Right: The scattering intensity in the a and c directions.

Future Work In future work we will continue to explore ways to induce quantum fluctuations using *H* fields as a tuning parameter. In particular, we will use *H* to tune in quantum behavior in transverse field Ising model systems. Here we will study TmB_4 with higher quality samples than are presently available by working with synthesis collaborators. Another planned experiment involves applying a transverse *H* field to the Dy spins in $DyBa_2Cu_3O_7$ under the hypothesis that the superconducting Cu-O planes will enforce the transverse orientation. Samples suitable for *C*(*T*,*H*) measurements at ultra-low *T* have been made by R. Jin (LSU) and are presently being annealed for high integrity in the Cu-O planes. Other work will involve applying our newly operating non-local conductivity apparatus to search for topological states. This technique has been discussed in the literature but not widely implemented as a tool for screening materials.

References

[1] J. Trinh, et al., *Physical Review Letters* **121,**(2018).
[2] K. Siemensmeyer, et al., *Physical Review Letters* **101,**(2008).
[3] K. Wierschem, et al., *Physical Review B* **92,**(2015).
[4] H. Kageyama, et al., *Physical Review Letters* **82,** 3168 (1999).
[5] S. Miyahara, and K. Ueda, *Physical Review B* **61,** 3417 (2000).
[6] T. Momoi, and K. Totsuka, *Physical Review B* **62,** 15067 (2000).
[7] P. Corboz, and F. Mila, *Physical Review Letters* **112,**(2014).
[8] Z. T. Wang, and C. D. Batista, *Physical Review Letters* **120,**(2018).
[9] G. Misguich, T. Jolicoeur, and S. M. Girvin, *Physical Review Letters* **87,** art. no. (2001).
[10] T. A. Wiener, and P. C. Canfield, *Journal of Alloys and Compounds* **303,** 505 (2000).
[11] N. Blanc, et al. *Nature Physics* **14,** 273 (2018).
[12] M. Hartstein, et al, *Nature Physics* **14,** 166 (2018).
[13] M. B. Maple, and D. Wohlleben, *Physical Review Letters* **27,** 511 (1971).
[14] Z. Li, J. Li, P. Blaha, and N. Kioussis, *Physical Review B* **89,**(2014).
[15] C. J. Kang, H. C. Choi, K. Kim, and B. I. Min, *Physical Review Letters* **114,**(2015).
[16] U. Atzmony, et al., *Physical Review Letters* **43,** 782 (1979).

Publications

[1] J. Trinh, S. Mitra, C. Panagopoulis, T. Kong, P.C. Canfield, A.P. Ramirez, *Physical Review Letters* **121,**(2018)

Engineering topologically protected superconducting states

Leonid P. Rokhinson, Purdue University

Program Scope

An ultimate long-term objective of the proposed research is to develop qubits which are inherently protected from environmental noises. The most publicized approach is to develop qubits based on non-abelian excitations, where non-locality of Majorana or higher-order non-abelian excitations protects qubit from local sources of decoherence. While there is mounting experimental evidence that Majorana excitations can be realized in solid-state systems, non-abelian nature of excitation statistics, a key ingredient of topologically protected quantum computing, is yet to be demonstrated. *The first objective of the program is to design devices to probe statistics of what we think are Majorana excitations.* An alternative approach is to encode quantum information in a discreet number of quantum states, each consisting of a superposition of a large number of coherent states. It has been shown theoretically that operations on such qubits belong to the same class of Clifford algebra as Majorana-based qubits, and can be processed fault tolerantly. *The second objective of the program is to devise protected qubits based on abelian π-periodic superconducting elements.* While the first objective has a strong intellectual appeal to discover excitations with non-abelian statistics, the second objective provides a route to design and demonstrate a protected qubit without reliance on a yet-to-be-discovered physics.

Recent Progress

My program review presentation will be focused on our progress toward the second objective, development of a topologically protected qubits based on abelian anyons. At the heart of such qubit is a π-periodic device that can be constructed from two anharmonic Josephson junctions. We have studied JJs formed from topological insulator with Nb electrodes. First we optimized contact fabrication to achieve high transparency of TI/superconductor contacts and demonstrated multiple Andreev reflection (up to 13 peaks!) in short JJs [3]. We also discovered unexpected enhancement of critical current at low temperatures in TI nanoribbons (TINR) JJs, see Fig. 1. The enhancement is attributed to the presence of $k > 0$ modes in a long-junction regime and suppression of $k = 0$ transmission (short-junction regime) in TINRs [1].

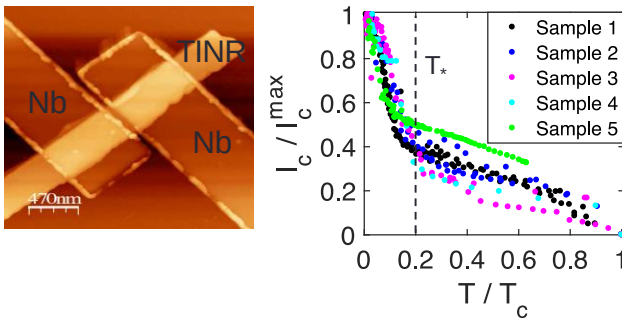

Fig.1 AFM micrograph of TI nanoribbon JJs. Scaled Ic(T) plot shows universal enhancement of critical current at low temperatures in multiple devices.

Current-phase relation (CPR) in TI-based JJs was studied using asymmetric SQUID geometry shown in Fig. 2. We found that for large TI flakes ($> 1\ \mu$m) CPR is very anharmonic, see Fig. 1, while for JJ fabricated using TI nanoribbons (100nm-wide) CPR is almost sinusoidal. To understand the difference we performed detailed modeling of both cases and found that low laying energy states (due to almost continuous energy quantization of surface states in large flakes) are responsible for the skewed CPR [4]. With this understanding of the underlying physics we can proceed with the demonstration of a π-SQUID.

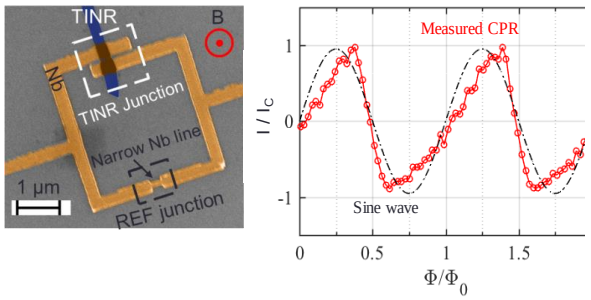

Fig. 2. SEM micrograph of an asymmetric SQUID with a TI-based JJ in one arm a Dayem bridge as a reference junction. CPR in a large TI flake junction is highly anharmonic (red dots).

Finally, we studied TINR JJs in axial magnetic field. In our earlier work we demonstrated $0-\pi$ Aharonov Bohm oscillations in TINRs which was a conformation of the existence of protected surface states. In the device shown in Fig. 3 we reproduced $0-\pi$ AB oscillations for normal contacts but we found only $0-$phase Little-Park-like oscillations for superconducting contacts. Majorana fermions are expected to be formed in the $\pi-$phase. This observation, combined with strong modulation of I_c by gate voltage, questions the attribution of the I_c modulation by electrostatic gating to the change of the number of transmitting channels in semiconductor, both in TINRs and in other nanowire JJs. This finding may be important for the interpretation of the zero bias modes observed in nanowire semiconductor/superconductor hybrids.

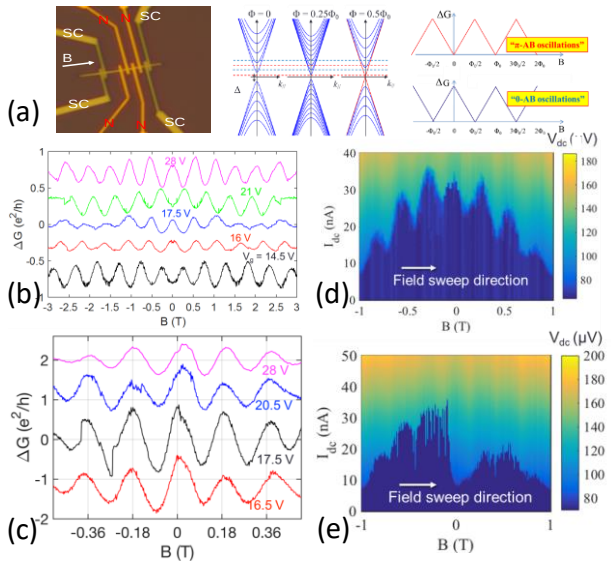

Fig. 3. (a) In TINR we expect opening and closing of the gap at zero energy as a function of gate voltage, which is seen as a $0-\pi$ swithing of AB oscillations (b). No such switching is observed for superconducting contacts (c). Little-Park oscillations are seen for slow I/V scans (>10 min/scan), suppression of Ic is observed for fast scans (e).

Finally, we observed modulation of critical current in TINRs as a function of axial magnetic field, Fig. 3d. The period of these oscillations is found to be ~2.5 of the period of AB oscillations measured on the same TINR. Moreover, when field crossed zero I_c becomes suppressed and restores to its equilibrium value exponentially slow with characteristic time scales of 10-15 minutes. These long time scales are currently not understood.

Future Plans

Recently we received high quality InAs/Al wafers from our collaborators and we are planning to devote most of the effort toward the first objective of the program, detection of the non-abelian statistics. If time permits or we encounter unforeseen problems with InAs/Al device fabrication and/or quality we will continue working on the development of π −SQUIDs and demonstration of superconducting devices with π −periodic current-phase relation.

Publications

[1] Morteza Kayyalha, Mehdi Kargarian, Aleksandr Kazakov, Ireneusz Miotkowski, Victor M. Galitski, Victor M. Yakovenko, Leonid P. Rokhinson, Yong P. Chen, "Anomalous low-temperature enhancement of supercurrent in topological-insulator nanoribbon Josephson junctions: evidence for low-energy Andreev bound states" Phys. Rev. Lett. **122**, 047003 (2019)

[2] Tailung Wu, Zhong Wan, Aleksandr Kazakov, Ying Wang, George Simion, Jingcheng Liang, Kenneth W. West, Kirk Baldwin, Loren N. Pfeiffer, Yuli Lyanda-Geller, and Leonid P. Rokhinson, "Formation of helical domain walls in the fractional quantum Hall regime as a step toward realization of high-order non-Abelian excitations" Phys. Rev. B **97**, 245304 (2018)

[3] Luis A. Jauregui, Morteza Kayyalha, Aleksander Kazakov, Ireneusz Miotkowski, Leonid P. Rokhinson, Yong P. Chen, "Gate-tunable supercurrent and multiple Andreev reflections in a superconductor-topological insulator nanoribbon-superconductor hybrid device", Appl. Phys. Lett. **112**, 093105 (2018)

[4] Morteza Kayyalha, Aleksandr Kazakov, Ireneusz Miotkowski, Sergei Khlebnikov, Leonid P. Rokhinson, Yong P. Chen, "Observation of highly skewed current-phase relation in superconductor-topological insulator-superconductor Josephson junctions" Under review in Nature Quantum Materials, arXiv:1812.00499 (2018)

[5] M. Kotiuga, Z. Zhang, J. Li, F.M.R Simoes, H. Zhou, R. Sutarto, F. He, Q. Wang, Y. Sun, Y. Wang, N.A. Aghamiri, S.B. Hancock, L.P. Rokhinson, D. Landau, Y. Abate, J.W. Freeland, R. Comin, S. Ramanathan, K.M. Rabe, *"Carrier localization in perovskite nickelates from oxygen vacancies"*, submitted to PNAS

Program Title: Quantum Order and Disorder in Magnetic Materials

Principal Investigator: Thomas F. Rosenbaum, California Institute of Technology

Program Scope

Disorder, competing interactions, and geometrical frustration on the mesoscopic scale can have profound macroscopic consequences, leading to materials with novel electronic, optical, and magnetic properties. Inhomogeneous quantum systems are particularly appealing in this context because they have a proclivity for stable self-organization on scales from nanometers to microns, and they can exhibit pronounced fluctuations away from equilibrium. With the right choice of materials, there are manifest opportunities for tailoring the macroscopic response and for garnering insights into fundamental quantum properties such as coherence and entanglement. We seek here to explore and exploit model, disordered, and frustrated magnets where magnetic domains in the concentrated limit and coherent spin clusters in the dilute limit stably detach themselves from their surroundings, leading to extreme sensitivity to finite frequency excitations and the ability to encode information. We take advantage of the ability to tune quantum tunneling with a "knob" in the laboratory, a field applied transverse to the ordering axis of magnetic dipoles. By driving the systems into the nonlinear regime, it is possible to parse tunneling pathways, decoherence from the thermodynamic spin bath, and the underlying structure of the complex free energy landscape. Moreover, by tuning the spin concentration along with the tunneling probability, it should be possible to study the competition between quantum entanglement and random field effects. A combination of ac susceptometry, dc magnetometry, Barkhausen noise measurements, and non-linear Fano experiments as functions of temperature, magnetic field, frequency, excitation amplitude, dipole concentration, and disorder should address issues of stability, overlap, coherence, and control.

Recent Progress

(A) Magnetic Domain Dynamics in an Insulating Quantum Ferromagnet. A wide range of systems, from hard magnets to soft matter, from fluids to power grids, exhibit avalanche behavior when driven out of equilibrium. The statistics and form of these avalanches can be used to reveal the nature of the underlying energy landscape and dynamics. Barkhausen noise, driven by avalanches of ferromagnetic domain motion, is perhaps the best studied realization of this general phenomenon (Fig. 1). In conventional metallic ferromagnets, drag effects arising from eddy-current back action dominate the dynamics, but realizing either a drag-free response or alternative drag mechanisms remains an important avenue for investigation. Here we measure Barkhausen noise in an insulating Ising ferromagnet, $LiHo_{0.44}Y_{0.56}F_4$. An insulator cannot support eddy currents, and, indeed, we find that the ensemble average over long-duration avalanche events just below the Curie temperature approaches a symmetric lineshape, as expected for a drag-free response (Fig. 2). This limit has not been observed in metallic ferromagnets. At lower temperatures and for short duration events, we do observe clear drag effects, which cannot arise from eddy currents. By studying the temperature dependence in different time regimes and comparing to the well-understood microscopic Hamiltonian of this model Ising magnet, we are able to propose the presence of two coexisting drag mechanisms:

one arising from quantum-fluctuation-induced domain wall broadening and the other from random-field-induced domain wall pinning. The disparate nature of the drag mechanisms discussed here can be probed in more detail by exploiting one of the key features of the Li(Ho,Y)F_4 family: the ability to tune the strength of both the quantum fluctuations and the random fields via application of an external magnetic field applied transverse to the Ising axis. The relative importance of the two effects can be controlled via the transverse field, the temperature, and the degree of yttrium substitution. Continuously tuning the drag behavior within a single system offers a valuable experimental substrate for comparing classical and quantum Barkhausen noise.

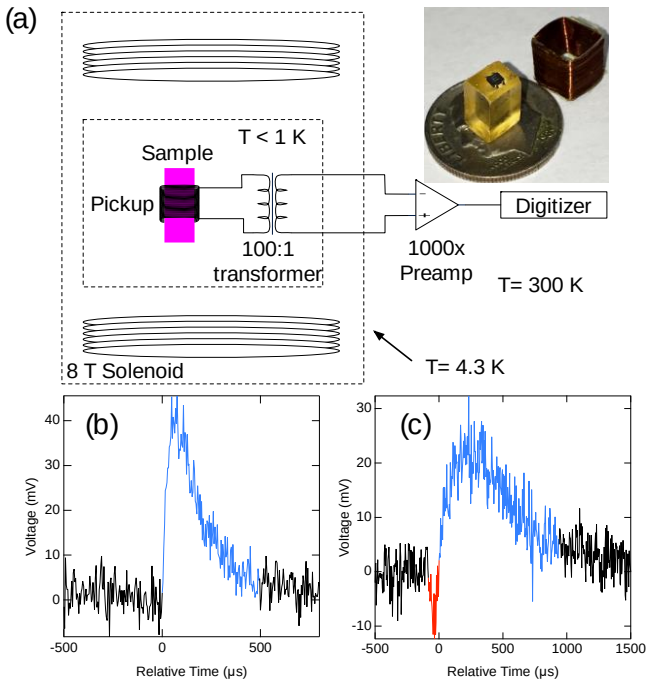

Fig. 1: Measurement of Barkhausen noise with circuitry, sample, and representative events (short and long duration).

Fig. 2: Evolution of ensemble avalanche lineshapes as a function of temperature and event duration, showing the onset of drag effects.

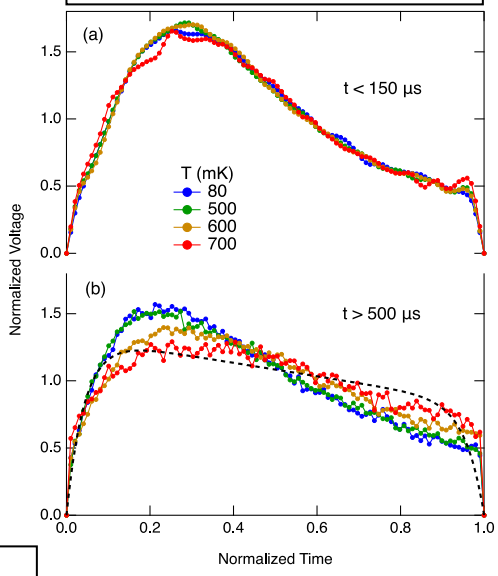

(B) Nonlinear Dynamics in a Disordered Quantum Magnet. Quantum states cohere and interfere. Quantum systems composed of many atoms arranged imperfectly rarely display these properties. Here we demonstrate an exception in a disordered quantum magnet that divides itself into nearly isolated subsystems. We probe these coherent clusters of spins by driving the system beyond its linear response regime at a single frequency and measuring the resulting "hole" in the overall linear spectral response. The Fano shape of the hole encodes the incoherent lifetime as well as coherent mixing of the localized excitations. For the disordered Ising magnet, $LiHo_{0.045}Y_{0.955}F_4$, the quality factor Q for spectral holes can be as high as 100,000. We tune the dynamics of the quantum degrees of freedom by sweeping the Fano mixing parameter q through zero via the amplitude of the ac pump as well as a static external transverse magnetic field (Fig. 3). The zero-crossing of q is associated with a dissipationless response at the drive frequency, implying that

the off-diagonal matrix element for the two-level system also undergoes a zero-crossing. The identification of localized two-level systems in a dense and disordered dipolar-coupled spin system pushes the search forward for potential qubit platforms emerging from strongly-interacting, many-body systems.

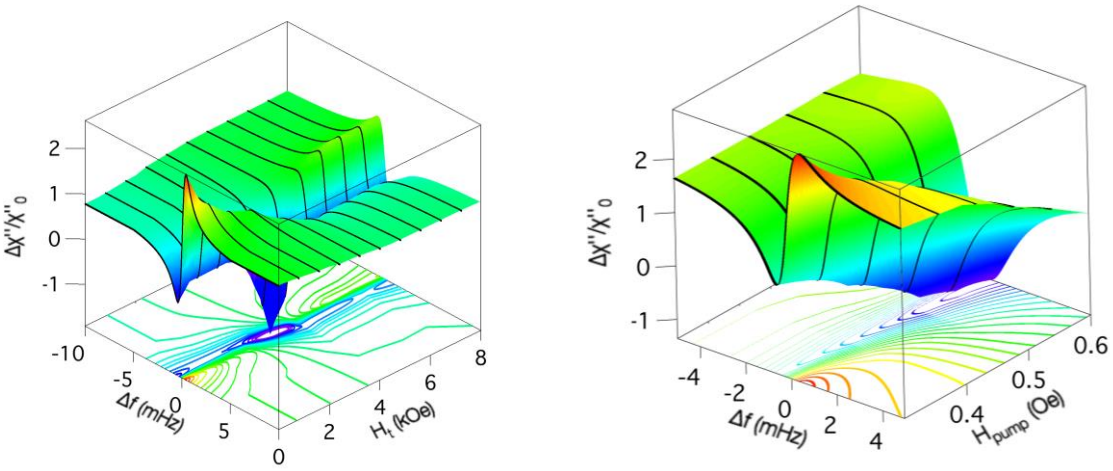

Fig. 3: Evolution of the Fano resonance, arising from quantum interference between relaxation pathways, with transverse magnetic field (left) and ac pump amplitude (right). The zero crossings represent a decoupling of coherent, strongly-localized spin clusters from their environment, with lifetimes of seconds.

Future Plans

A quantum quench is the rapid tuning of a quantum parameter, such as magnetic field, that drives a material out of equilibrium and creates excitations, e.g., quasiparticles, vortices, and magnetic domain walls. Over the past decade, intense interest has focused on how the quench rate and material parameters, such as particle interactions, determine the density and character of excitations created during the quench, and how equilibrium is eventually established. An area of particular focus and potential impact involves measuring quenches across a phase transition, which is believed to give rise to universal behavior irrespective of microscopic material details. The Kibble-Zurek effect predicts that the density of excitations created during a quench scales as a power-law that depends on the critical exponents associated with the phase transition and the dimensionality. To date, the only reported tests of the theory are for lower-dimensional, cold atom systems. We believe that we are poised to explore the non-equilibrium dynamics of quantum quenches in the bulk, three-dimensional quantum ferromagnet, $LiHoF_4$, with a statistically-significant number of spins. This system also affords the ability to introduce the effects of disorder with the partial substitution of non-magnetic yttrium for magnetic holmium.

The experiment involves a rapid quench from paramagnet to ferromagnet, where the formation of domains occurs by quantum tunneling of domain walls rather than thermal excitations. There are two major experimental problems: (1) Finding a T=0 equilibrium phase transition from paramagnet to ferromagnet. We solve this problem by driving the Curie temperature to zero in our Ising magnet with a magnetic field applied transverse to the Ising axis, which then serves as the quantum tuning parameter, and (2) Quenching sufficiently quickly (microseconds) through the quantum phase transition to be able to record the growth dynamics of the magnetic domains.

Ramping a magnetic field rapidly at the required Tesla field scales is experimentally impossible because of the inductance of superconducting magnets. Eddy current heating would also ensue, potentially driving the system out of the quantum regime.

It is the second challenge that we believe that we have surmounted. Below T = 0.4 K, the nuclear spins of the Ho atoms are slaved to the electronic spins. We apply a microwave field to the $LiHoF_4$ crystal at a frequency that inverts the population of nuclear spins (Fig. 4), thereby reducing the effective magnetic moment and, hence, the transverse field needed to drive the quantum phase transition. Now the phase boundary itself moves in the presence of a fixed transverse field. This technique only relies on tuning the microwave field in a resonant cavity, with timescales below a microsecond.

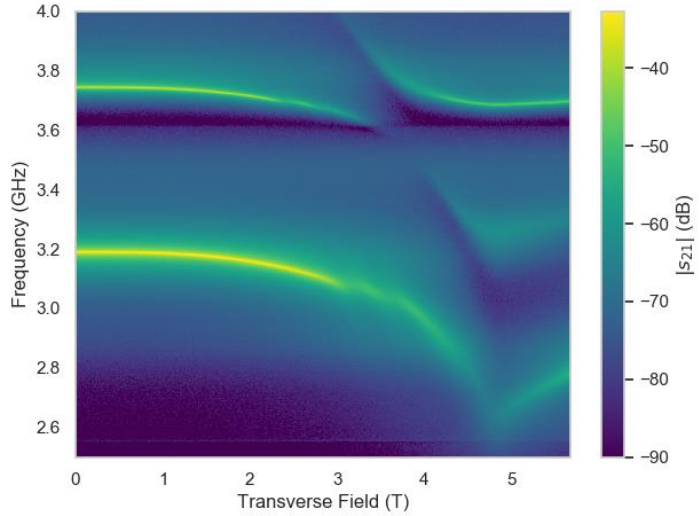

Fig. 4: Density plot of the magnitude of the transmission parameter s_{21} through a bimodal 3D lumped element resonator showing strong coupling to the electronuclear soft mode in $LiHoF_4$ at T = 0.1 K. A significant reduction in the mode transmission near a frequency of 3.5 GHz and 4 T transverse field corresponds well to the calculated soft mode energy, and a pair of less-prominent absorption peaks are visible. These peaks only appear below T = 0.25 K, suggesting that they correspond to excitations between hyperfine levels.

Publications

1. "Multiple Superconducting States Induced by Pressure in Mo_3Sb_7," Y. Feng, Y. Wang, A. Palmer, L. Li, D.M Silevitch, S. Calder, and T.F. Rosenbaum, Phys. Rev. B **95**, 125102 (2017).
2. "Nonlinear Dynamics in a Disordered Quantum Magnet," D.M. Silevitch, C. Tang, G. Aeppli, and T.F. Rosenbaum, Nature Commun., in press.
3. "Design of a Loop-Gap Resonator with Bimodal Uniform Fields Using Finite Element Analysis," M.M. Libersky, D.M. Silevitch, and A. Kouki, IEEE Trans. on Magnetics, in press.
4. "Magnetic Domain Dynamics in an Insulating Quantum Ferromagnet," D.M. Silevitch, J. Xu, C. Tang, K.A. Dahmen, and T.F. Rosenbaum, Phys. Rev. B, under review.
5. "Quantum Dynamics in Strongly-Driven Random Dipolar Magnets," M. Buchhold, C. Tang, D.M. Silevitch, T.F. Rosenbaum, and G. Refael, preprint.

Program Title: Correlated Quantum Materials

Principle Investigator: B. C. Sales; Co PIs: D. Mandrus, A. F. May, M. A. McGuire, J.-Q. Yan
Materials Science and Technology Division, Oak Ridge National Laboratory, Oak Ridge, TN 37831
Email: salesbc@ornl.gov

Program Scope

Correlated quantum materials (CQM), with collective, emergent behavior like superconductivity and magnetism, are expected to form the basis for next-generation energy and information technologies. Because strong electron-electron correlations are difficult to model theoretically, experimental studies of high-quality samples are essential for advancing our understanding of such materials. The overarching goal of our research is to attain a predictive understanding of the behavior of *key* CQM. To achieve this, we have three specific research aims: (1) study the interactions and excitations in layered and cleavable magnets (2) explore those materials that combine topology and magnetism and (3) examine exotic phenomena on honeycomb or Kagome lattices. A unifying theme among the diverse topics and materials is the role of magnetism associated with partially-filled d or 4f shells. Focus is placed on the discovery and investigation of new model materials that exhibit collective phenomena and new forms of order. Our approach combines bulk materials synthesis emphasizing single crystal growth, and compositional tuning, with studies of basic physical properties using X-ray and neutron diffraction, electron microscopy, and thermodynamic and transport measurements. A deeper understanding of the physics of the most interesting materials is pursued through collaborations involving theoretical calculations, inelastic neutron scattering, scanning tunneling microscopy and angle-resolved photoemission spectroscopy. This research directly addresses the ability to control and exploit quantum mechanical behaviors targeting novel functionality, a priority research direction identified in the BES BRN on Quantum Materials. In addition, our emphasis on synthesizing complex materials addresses the challenge of mastering the science of crystalline synthesis identified in the Synthesis Science BRN.

Recent Progress in the area of Cleavable Magnets

Cleavable van der Waals bonded magnets (Newer-past year) $Fe_{5-x}GeTe_2$, $MnBi_2Te_4$, $MnBi_{2-x}Sb_xTe_4$ $MoCl_5$, $MoCl_4$, $Os_{0.55}Cl_2$ *(Older)* CrI_3, $CrCl_3$, $CrTe_3$, $RuCl_3$, $Fe_{3-x}GeTe_2$, $Ru_{1-x}Ir_xCl_3$. Single crystals of van der Waals bonded magnets are attractive for studying magnetism in the quasi-2D limit, in very thin crystals, in monolayers, and for forming heterostructures with unique functional properties. For the past year we have focused on (1) cleavable magnets that exhibit ferromagnetism at or above room temperature ($Fe_{5-x}GeTe_2$) [1], (2) possible candidates for a quantum spin liquid ($Os_{0.55}Cl_2$, $Ru_{1-x}Ir_xCl_3$) [2,3], and (3) materials that combine magnetic and topological order in a natural heterostructure ($MnBi_2Te_4$, $MnSb_2Te_4$, $MnBi_{2-x}Sb_xTe_4$) [3,4]. These natural heterostructures show great promise for demonstrating the quantum anomalous Hall effect and may be an example of an axion insulator. Development of cleavable magnetic materials also may help enable

continued advancement in miniaturization and performance enhancement of electronic devices, either as electronically active components themselves, or through interfacing with materials like graphene.

Fe_5GeTe_2: A cleavable room temperature ferromagnet. $Fe_{5-x}GeTe_2$ (x= 0.13) has a crystal structure similar to Fe_3GeTe_2, which consists of 2D slabs of Fe and Ge between layers of Te, but with a considerably more complicated hexagonal structure. The Fe_5GeTe_2 crystals are uniaxial ferromagnets above room temperature (T_c = 310 K) while nanoflakes with thicknesses of about 10 unit cells had T_c ranging from 270 - 300 K. The magnetism for the nanoflakes is determined using the anomalous Hall effect. The low temperature saturation magnetization corresponds to about 2 μ_B per Fe. Fe_5GeTe_2 has a high temperature phase and magnetic properties depend on details of the crystal growth. Crystals are grown via iodine vapor transport at a growth temperature of 750 °C. To obtain the highest T_c quenched crystals are cooled below 100 K where there is a first order irreversible change in the local structure due to strong magnetoelastic coupling. After this initial training the properties of the crystal are stable from 2 K to at least 400 K. The crystal and magnetic structure is investigated using STEM, single crystal x-ray diffraction, magnetization measurements, powder neutron diffraction and Mossbauer spectroscopy. From STEM data the average crystal structure is rhombohedral with *a* = 4.04 (2) Å, *c* =29.19(3) Å, however the local structure is complex due to disorder and the presence of short-range order due to the partial occupation of split sites.

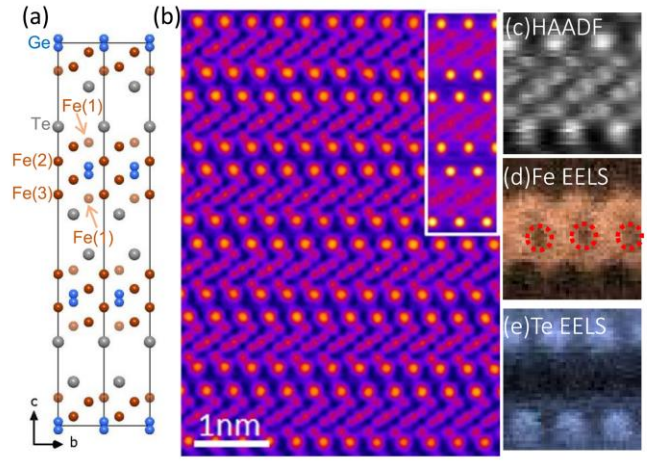

Fig. 1. STEM data used to determine local and average crystal structure of $Fe_{5-x}GeTe_2$ in conjunction with x-ray and neutron diffraction.

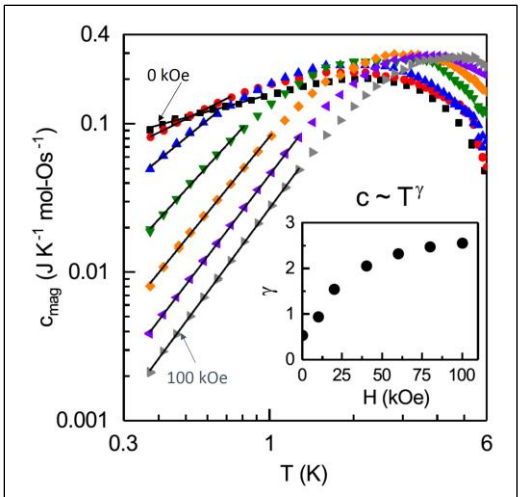

Fig. 2. C_P vs log T for 0 < H < 100 kOe. Note power-law dependence of C_p for the *insulator* $Os_{0.55}Cl_2$.

$Os_{0.55}Cl_2$: A possible quantum spin liquid analogous to $RuCl_3$ but with stronger spin-orbit coupling. In an effort to grow $OsCl_3$ as an analog to the quantum spin liquid compound α-$RuCl_3$, we grew sizable crystals that are stable in air with the composition $OsCl_{3.6}$ [2]. A detailed study of the crystallography of this phase using powder and single crystal x-ray diffraction and real-space STEM analysis indicate that the average structure is best described by the rhombohedral $CdCl_2$ structure with Os vacancies, so that the composition is best written as $Os_{0.55}Cl_2$. There is also evidence for short and long-range vacancy ordering.

Magnetization data indicate significant magnetocrystalline anisotropy due to spin-orbit coupling, antiferromagnetic correlations and no sign of magnetic order or spin freezing down to 0.4 K. Heat-capacity measurements in applied magnetic fields show only a broad field-dependent anomaly. The magnetic susceptibility and heat capacity (Fig. 2) obey power laws at low temperature and low field with exponents close to 0.5, suggesting that gapless magnetic fluctuations prevent spin freezing or ordering. Divergence of the magnetic Gruneisen parameter indicated nearness to a magnetic quantum critical point. Much of this behavior is similar to candidate spin-liquid materials such as $ZnCu_3(OH)_6Cl_2$ and $YbMgGaO_4$.

$MnBi_2Te_4$, $MnSb_2Te_4$, $MnBi_{2-x}Sb_xTe_4$: magnetic topological insulator heterostructures

There have been multiple theoretical predictions of the interesting topological behavior expected for $MnBi_2Te_4$, which combines a magnetic MnTe layer and the topological insulator Bi_2Te_3. After a careful mapping of the critical region of the Mn-Bi-Te phase diagram, we have successfully grown mm size crystals of $MnBi_2Te_4$ even though the growth window is only 10 K [4]. The properties of the crystals are investigated using magnetic, transport, scanning tunneling microscopy and spectroscopy measurements, and powder and single crystal neutron diffraction. Below T_N = 24 K, the Mn moments align ferromagnetically in the *ab* plane but antiferromagnetically along the crystallographic *c* axis with an ordered moment of 4.04 μ_B at 10 K aligned along the *c* axis in an A-type antiferromagnetic order. A spin-flop transition is observed at 35 kOe with H//c. This transition also produces a dramatic drop is both the resistivity and the Hall resistivity at 2 K. The Mn moments are completely polarized when H>78 kOe. The approximate carrier concentration of the crystals is 10^{19} electrons/cm^3, which is too large for many of the proposed applications. Using a similar growth method, however, we recently grew [5] and characterized crystals of $MnBi_{2-x}Sb_xTe_4$ for all x between 0 and 2 (Fig. 3). For $x \approx 0.63$ the carrier concentration can be tuned to low values perhaps suitable for the observation of the QAHE.

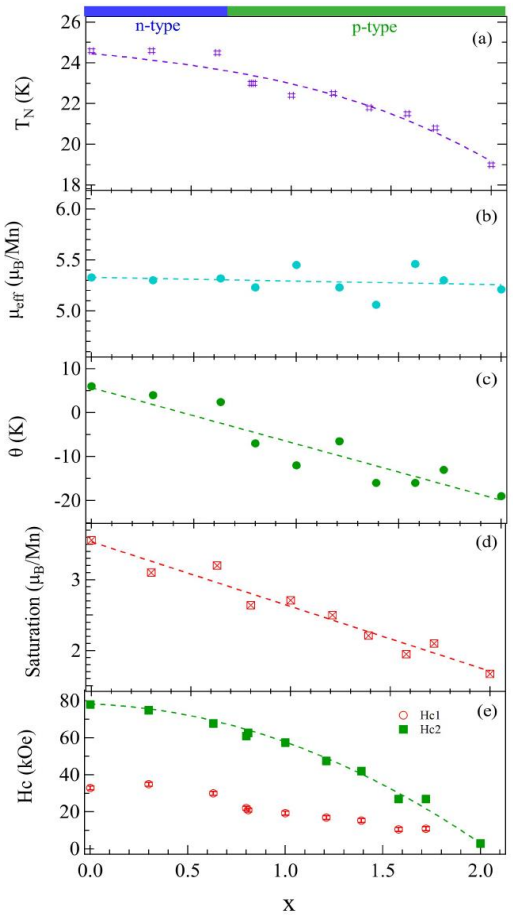

Fig. 3. Evolution of magnetic properties of $MnBi_{2-x}Sb_xTe_4$. The crossover from n-type to p-type conduction occurs near x=0.63.

Future Work

Some of our future efforts on cleavable magnets will focus of the following questions. Can the Curie temperature of Fe_5GeTe_2 be pushed even higher with suitable chemical doping

or pressure? Can the anisotropy of vdW magnets be controlled? Does the inelastic neutron signal from $Os_{0.55}Cl_2$ resemble that seen in $RuCl_3$ and $Ru_{1-x}Ir_xCl_3$? What are other experimental signatures for a QSL? Can the sample quality in $MnBi_{2-x}Sb_xTe_4$ be improved enough to observe the QAHE at He^4 temperatures?

Publications

Since July 2017, this project has fully or partially supported more than 85 refereed publications including: 3 Science, 2 Nature, 6 Nature Other (Materials, Nano, Phys., Comm.), 3 PRX, 2 PRL, 5 Nano Letts, 2 Adv. Mat., 2 ACS Nano, 1 JACS, 4 Chem. Mat., 15 PRB and 7 PRM. Publications referenced in this abstract and other selected papers with significant input from this project are listed below.

1. A.F. May, D. Ovchinnikov, Q. Zheng, R. Hermann, S. Calder, B. Huang, Z.Y. Fei, Y.H. Liu, X.D. Xu, M.A. McGuire, Ferromagnetism Near Room Temperature in the Cleavable van der Waals Crystal Fe_5GeTe_2, *ACS Nano* **13**, 4436 (2019).
2. M.A. McGuire, Q. Zheng, J.-Q. Yan, B.C. Sales, Chemical disorder and spin-liquid-like magnetism in the van der Waals layered 5d transition metal halide $Os_{0.55}Cl_2$, *Physical Review B* **99**, 214402 (2019).
3. P. Lampen-Kelley, A. Banerjee, A.A. Aczel, H.B. Cao, M.B. Stone, C.A. Bridges, J.-Q. Yan, S.E. Nagler, D. Mandrus, "Destabilization of Magnetic Order in a Dilute Kitaev Spin Liquid Candidate," *Physical Review Letters* **119**, 237203 (2017).
4. J.Q. Yan, Q. Zhang, T. Heitmann, Z.L. Huang, K.Y. Chen, J.G. Cheng, W.D. Wu, D. Vaknin, B.C. Sales, R.J. McQueeney, Crystal growth and magnetic structure of $MnBi_2Te_4$, *Physical Review Materials* **3**, 064202 (2019).
5. J. -Q. Yan, S. Okamoto, M. A. McGuire, A. F. May, R. J. McQueeney, B. C. Sales, Evolution of structural, magnetic, and transport properties in $MnBi_{2-x}Sb_xTe_4$, arXiv:1905.00400.
6. S. Mukhopadhyay, D. S. Parker, B. C. Sales, A. A. Puretzky, M. A. McGuire, L. Lindsay, "Two-channel model for ultralow thermal conductivity of crystalline Tl_3VSe_4," *Science* **360**, 1455 (2018).
7. M.E. Manley, O. Hellman, N. Shulumba, A.F. May, P.J. Stonaha, J.W. Lynn, V.O. Garlea, A. Alatas, R.P. Hermann, J.D. Budai, H. Wang, B.C. Sales, A.J. Minnich, Intrinsic anharmonic localization in thermoelectric PbSe, *Nature Communications* **10**, 1928 (2019).
8. S. Calder, A.I. Kolesnikov, A.F. May, Magnetic excitations in the quasi-two-dimensional ferromagnet $Fe_{3-x}GeTe_2$ measured with inelastic neutron scattering, *Physical Review B* **99**, 094423 (2019).
9. J.L. Niedziela, D. Bansal, A.F. May, J. Ding, T. Lanigan-Atkins, G. Ehlers, D.L. Abernathy, A. Said, O. Delaire, Selective breakdown of phonon quasiparticles across superionic transition in $CuCrSe_2$, *Nature Physics* **15**, 73 (2019).
10. T. Song, X. Cai, M. Tu, X. Zhang, B. Huang, N. Wilson, K. Seyler, L. Zhu, T. Taniguchi, K. Watanabe, M. McGuire, D. Cobden, D. Xiao, W. Yao, X. Xu, "Giant tunneling magnetoresistance in spin-filter van der Waals heterostructures," *Science* **360**, 1214 (2018).

Tuning Phase Transformations for Designed Functionality

Athena S. Sefat, Oak Ridge National Laboratory

Program Scope

Quantum materials, where quantum mechanical interactions lead to exotic properties such as magnetism and superconductivity, have demonstrated great potential for a variety of applications including magnetic sensors, permanent magnets, magnetocaloric refrigerators, and superconducting wires. Historically such functionality has been discovered serendipidously by measuring a material at very low temperatures; however, better performance and higher operating temperatures are often desirable in quantum materials. This project meets the challenge of microscopic control in quantum materials that will ultimately fulfill the promise of materials-by-design, rather than continuing along the path of serendipidous trials. This project investigates microscopic *structural parameters* (atomic-level interactions, local disorder, structural dimensionality) in order to tune advanced quantum materials. The overarching goal is to understand how chemical, electronic, and spin competitions lead to *antiferromagnetic and (unconventional) superconducting properties* in pnictide- and chalcogenide-based quantum materials. The specific aims are to (1) elucidate the role of atomic-level interactions for causing bulk antiferromagnetic or superconducting phase transitions; (2) determine the impact of local disorder and strain on materials' magnetic and superconducting temperature; and (3) investigate the effect of structural dimensionality on magnetic phase transitions. This project brings diverse expertise across ORNL in order to leverage synthesis, first-principles-based theoretical modeling, and characterization across a broad range of length scales (~cm to pm) with complementary techniques, with the vision to design advanced quantum materials. By filling the knowledge gap in fundamental details of structural parameters, the discovery of advanced quantum materials can be accelerated that is crucial to nation's economic advancement.

Recent Progress

We have discovered non-percolative local superconductivity in vanadium hole-doped $BaFe_2As_2$ (122). Although hole-doping of 122 using transition metals (such as V, Nb, Ta, Cr, and Mo) does not produce perfect conductivity, local nanometer superconducting regions cause a drop in electrical resistivity. We report scanning tunneling microscopy/ spectroscopy (STM/S) and find a coexistence of antiferromagnetic and local superconducting nanoscale regions [1]. In another study, we have discovered nanoscale chemical

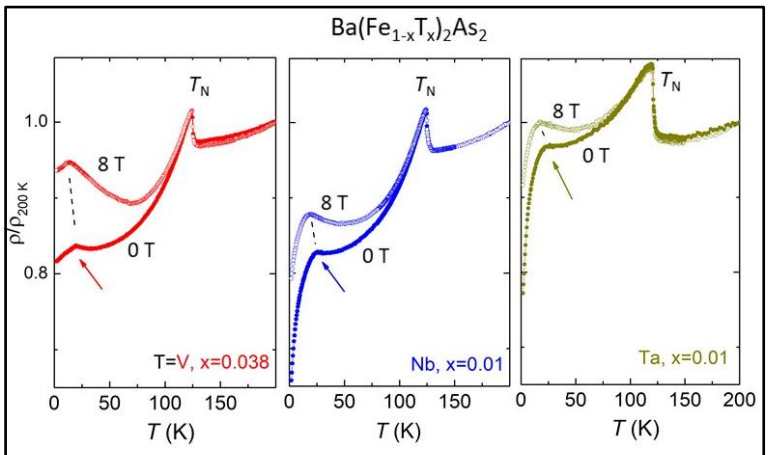

Figure 1: Temperature-dependent resistivity ρ normalized to 200 K, for $Ba(Fe_{1-x}T_x)_2As_2$ with T= V, Nb, and Ta. Data show anomalies for Néel antiferromagnetic ordering temperature (T_N), and drop feature at T^* (indicated by arrows) that does not reach zero. There is a shift of T^* with applied field of 8 Tesla.

Figure 2: Atomic-resolution STEM images showing a typical stacking fault that separates two sets of 122 crystal domains, in the *c*-direction. This defect causes an interlayer shift of 0.2*a* in the plane.

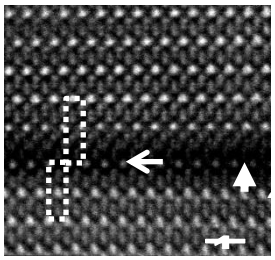

defects between FeAs-layers in 122-type crystals. These interlayer barium disorder, at nanometer regions along the *c*-crystallographic direction, are common to all 122s that should affect high-temperature superconductivity.

Future Plans

Our upcoming project goal is to understand how structural dimensionality, in rare-earth or transition-metal based materials, can lead to correlated (1) *low-D magnetism*, (2) *unconventional superconductivity*, and (3) *quantum spin liquid* behavior. Our unique approach is to synthesize novel quantum materials first, and then perform and offer the feedback mechanism through multiple length scale (cm to nm) characterization and theory. We have already submitted numerous publications under these subtopics, which are being refereed, and are referenced below [a-h].

References

[a] Sefat, A. S.; Wang, X. P.; Liu, Y.; Zou, Q.; Fu, M.; Gai, Z.; Kalaiselvan, G.; Vohra, Y.; Parker, D. S. "Lattice disorder effect on magnetic ordering of iron arsenide," [submitted]

[b] Xing, J.; Sanjeewa, L. D.; Kim, J.; Meier, W. R.; May, A. F.; Zheng, Q.; Custelcean, R.; Stewart, G. R.; Sefat, A. S. "Synthesis, magnetization and heat capacity of triangular lattice materials $NaErSe_2$ and $KErSe_2$," [submitted]

[c] Sanjeewa, L. D.; Garlea, V. O.; Fishman, R. S.; McGuire, M.; Xing, J.; Cao, H.; Kolis, J. W.; Sefat, A. S. "Observation of Large Magnetic Anisotropy and Magnetization Plateau in $SrCo(VO_4)(OH)$: A Structure with Quasi One-Dimensional Magnetic Chain," [submitted]

[d] Parker, D. S.; Sanjeewa, L. D.; Wang, X.; Cooper, V. R.; Liu, Y., Sefat, A. S. "Insulating antiferromagnetism in VTe," [submitted].

[e] Zou, Q.; Fu, M.; Wu, Z.; Li, L.; Parker, D. S.; Sefat, A. S.; Gai, Z. "Competitive and Cooperative electronic states in $Ba(Fe_{1-x}T_x)_2As_2$ with T=Co, Ni, Cr," [submitted to *Nature Communications*].

[f] Taddei, K. M.; Sanjeewa, L. D.; Lei, B.-H.; Fu, Y.; Zheng, Q.; Singh, D. J.; Sefat, A. S.; de la Cruz, C. "Superconductivity in quasi-one-dimensional KCr_3As_3 through hydrogen doping," [submitted].

[g] Pellizzeri, T. M. S.; Sanjeewa, L. D.; Pellizzeri, S.; McMillen, C. D.; Garlea, V. O.; Ye, F.; Sefat, A. S.; Kolis, J. W. "Single crystal neutron and magnetic measurements of $Rb_2Mn_3(VO_4)_2CO_3$ and $K_2Co_3(VO_4)_2CO_3$ with mixed honeycomb and triangular magnetic lattices," [submitted]

[h] Sanjeewa, L. D.; Sefat, A. S.; Smart, M.; McGuire, M. A.; McMillen, C. D.; Kolis, J. W. "Synthesis, structure and magnetic properties of $Ba_3M_2Ge_4O_{14}$ (M = Mn and Fe): Quasi-one-dimensional zigzag chain compounds," [submitted].

Publications

[1] Sefat, A. S.; Nguyen, G. D.; Parker, D. S.; Fu, M. M.; Zou, Q.; Li, A.-P.; Cao, H. B.; Sanjeewa, L. D.; Li, L.; Gai, Z. "Local superconductivity in vanadium iron arsenide," *Physical Review B* [accepted], https://journals.aps.org/prb/accepted/7607eY2aP771c772d12e7643828a77173f3f2fd7d.

[2] Zheng, Q.; Chi, M.; Ziatdinov, M.; Li, L.; Maksymovych, P.; Chisholm, M. F.; Kalinin, S. V.; Sefat, A. S. "Nanoscale interlayer defects in iron arsenides," *Journal of Solid State Chemistry* **277** (2019), 422.

[3] Li, A.; Yin, J.-X.; Wang, J.; Wu, Z.; Ma, J.; Sefat, A. S.; Sales, B. C.; Mandrus, D. G.; McGuire, M. A.; Jin, R.; Zhang, C.; Dai, P.; Lv, B.; Chu, C. -W.; Liang, X.; Hor, P. -H.; Ting, C. -S.; Pan, S. H. "Surface terminations and layer-resolved tunneling spectroscopy of the 122 iron pnictide superconductors," *Physical Review B* **99** (2019), 134520.

[4] Mirmelstein, A.; Kolesnikov, A. I.; Ehlers, G.; Abernathy, D. L.; Matvienko, V.; Sefat, A. S.; Podlesnyak, A. "Dynamic Magnetic response across the pressure-induced structural phase transition in CeNi," *Physical Review B* **99** (2019), 024401.

[5] Taddei, K. M.; Sanjeewa, L.; Kolis, J.W.; Sefat, A. S.; de la Cruz, C.; Pajerwski, D. M. "Local-Ising type magnetic order and metamagnetism in the rare-earth pyrogermanate $Er_2Ge_2O_7$," *Physical Review Materials* **3** (2019), 014405.

[6] Ijaduola, A. O.; Shipra, R.; Sefat, A. S. "Effect of pressure on the superconducting properties of $Tl_2Ba_2Ca_2Cu_3O_{9-\delta}$," *Crystals* **9** (2019), 4.

[7] Kim, J. S.; VanGennep, D.; Hamlin, J. J.; Wang, X.; Sefat, A. S.; Stewart, G. R. "Unusual effects of Be doping in the iron-based superconductor FeSe," *Journal of Physics: Condensed Matter* **30**, 445701 (2018).

[8] Nikitin, S. E.; Wu, L. S.; Sefat, A. S.; Shaykhutdinov, K. A.; Lu, Z.; Meng, S.; Pomjakushina, E. V.; Conder, K.; Ehlers, G.; Lumsden, M. D.; Kolesnikov, A. I.; Barilo, S.; Guretskii, S. A.; Inosov, D. S.; Podlesnyak, A. "Decoupled spin dynamics in rare-earth orthoferrite $YbFeO_3$: Evolution of magnetic excitations through the spin-reorientation transition," *Physical Review B* **98**, 064424 (2018).

[9] Felder, J. B.; Smith, M. D.; Sefat, A.; zur Loye, H. C. "Magnetic and thermal behavior of a family of compositionally related zero-dimensional fluorides," *Solid State Sciences* **81** (2018), 19.

[10] Taddei, K. M.; Xing, G.; Sun, J.; Fu, Y.; Li, Y.; Zheng, Q.; Sefat, A. S.; Singh, D. J.; de la Cruz, C. "Frustrated structural instability in superconducting quasi-one-dimensional $K_2Cr_3As_3$," *Physical Review Letters* **121**, 187002 (2018).

[11] Smylie, M. P.; Claus, H.; Kwok, W. -K.; Louden, E. R.; Eskilden, M. R.; Sefat, A. S.; Zhong, R. D.; Schneeloch, J.; Gu, G. D.; Bokari, E.; Niraula, P. M.; Kayani, A.; Dewhurst, C. D.; Snezhko, A.; Welp, U. "Superconductivity, pairing symmetry, and disorder in the doped topological insulator $Sn_{1x}In_xTe$ for $x \geq 0.10$," *Physical Review B* **97**, 024511 (2018).

[12] Dzubak, A. L.; Mitra, C.; Chance, M.; Kuhn, S.; Jellison, G.E.; Sefat, A.S.; Krogel, J.T.; Reboredo, F.A. "$MnNiO_3$ revisited with modern theoretical and experimental methods," *The Journal of Chemical Physics* **147**, 174703 (2017).

[13] Sundar, S.; Mosqueira, J.; Alvarenga, A. D.; Sonora, D.; Sefat, A. S.; Salem-Sugui, S. "Study of the second magnetization peak and the pinning behavior in $Ba(Fe_{0.935}Co_{0.065})_2As_2$ pnictide superconductor," *Superconductor Science & Technology* **30**, 125007 (2017).

[14] Taddei, K. M.; Zheng, Q.; Sefat, A.S.; de la Cruz, C. "Coupled structural, magnetic and superconducting order in quasi-one-dimensional $K_2Cr_3As_3$," *Physical Review B* **96**, 180506 (2017).

[15] Wu, L. S.; Nikitin, S. E.; Frontzek, M.; Kolesnikov, A. I.; Ehlers, G.; Lumsden, M. D.; Shaykhutdinov, K. A.; Guo, E.-J.; Savici, A. T.; Gai, Z.; Sefat, A. S.; Podlesnyak, A. "Magnetic ground state of the Ising-like antiferromagnet $DyScO_3$," *Physical Review B* **96**, 144407 (2017).

Magneto-optical Study of Correlated Electron Materials in High Magnetic Fields

Principal Investigator: Dmitry Smirnov; Co-PI: Zhigang Jiang

Address: National High Magnetic Field Laboratory, Tallahassee, FL 32312

Email: smirnov@magnet.fsu.edu

Program Scope

This program is focused on studying electronic structure, low-energy excitations, and many-body effects in novel electronic materials via magneto-optical spectroscopy. Our research interest span over two broad and interconnected areas, (i) properties of Dirac and Weyl fermions in topological materials, and (ii) atomically thin materials with the valley degree of freedom and strong spin-orbit coupling.

Recent Progress

Magneto-Infrared Spectroscopy of Topological Materials: Case Study of Coupled Weyl Points in Semimetal NbP

Weyl semimetals (WSMs) have attracted great attention in the search of three-dimensional zero-gap materials with nontrivial band topology. In a topological WSM, the conduction band and valence band touch in the bulk at discrete Weyl points (WPs) connected by Fermi arcs at the surface. Because the WPs always come in pairs, the coupling between the two WPs can significantly modify the band dispersion. Specifically, when the linear band from each WP overlaps, the band symmetry is reduced from the spherical symmetry of isolated WP to the axial symmetry of two coupled WPs. To demonstrate the essential role of the coupling effect between WPs, we consider the case of niobium phosphide (NbP), belonging to the archetypal WSM family of nonmagnetic transition-metal monopnictides (TX: T = Ta, Nb; X = As, P). The combination of low Fermi energy and small separation between WPs [1] makes NbP an excellent platform for a case study of coupled WPs physics. First, we studied the most experimentally accessible configuration, that is, when the magnetic field ($\boldsymbol{B}$) is applied perpendicular to the separation of all 12 WP pairs, $\boldsymbol{B} \parallel \boldsymbol{c} \perp \boldsymbol{k_W}$ **.** Our band structure analysis predicted several unique spectroscopic features originated from the coupled WPs. Experimentally, the infrared (IR) magneto-spectroscopy measurements revealed spectral features that cannot be explained within the picture of isolated WPs. These findings are consistently captured by the model of coupled WPs. Such coupling results in band hybridization, gap opening, avoided level crossing, and new selection rules for optical transitions. These results emphasize the importance of coupling between WPs for fundamental understanding of Weyl fermions in realistic condensed matter systems. Next, we extended our study to other orientations, $\boldsymbol{B} \parallel \boldsymbol{a}$ or $\boldsymbol{B} \parallel \boldsymbol{b}$. Now, the magnetic field is parallel to half of the WP pairs and perpendicular to the other half, which results in a very rich structure of inter Landau level (LL) transitions observed experimentally. Intriguingly, we observed new

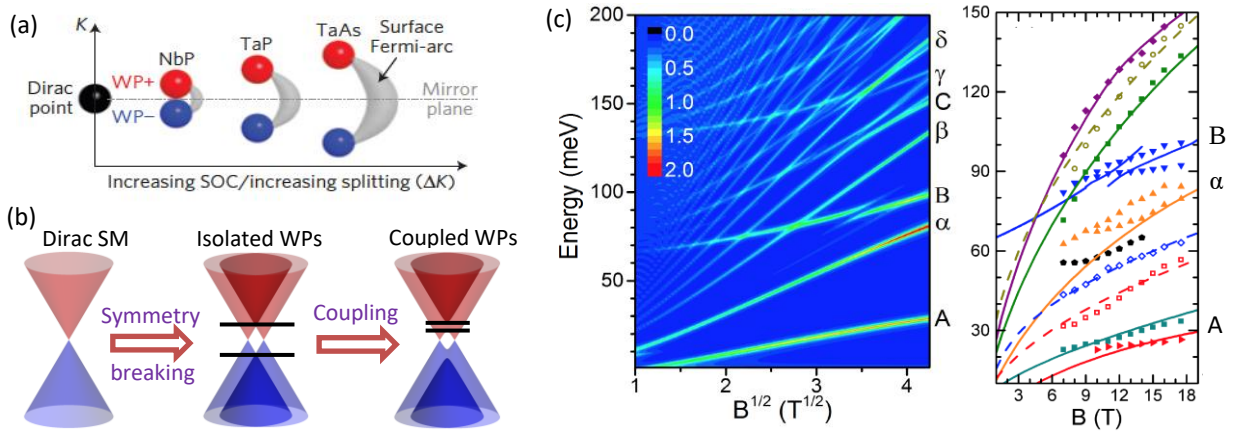

(a) Separation of Weyl points in transition-metal monopnictides. Adopted after Ref. [1]. (b) Separation of Weyl points and gap openings resulting from symmetry breaking and coupling effects. (c) Inter Landau level transitions (left – theory, right – experiment) unveiling new spectral features unique for coupled Weyl points in NbP.

transitions in the reflectance spectra measured in Voigt geometry and when the IR light is linearly polarized parallel to the magnetic field direction. These features have a distinct absorption-like Lorentzian lineshape and, thus, could be related to the topological surface states. The results are being analyzed.

Magneto-Infrared Spectroscopy of Topological Materials: Topological phase transition in $ZrTe_5$

Zirconium pentatelluride ($ZrTe_5$) has attracted substantial interest in the wave of Dirac and topological material exploration due to the theoretical prediction of a large-gap quantum spin Hall insulator phase in its monolayer form [2]. Theory also predicts that the electronic structure of bulk $ZrTe_5$ resides near the phase boundary between weak and strong topological insulators (TIs) [3]. This topological phase transition depends on the strength of the interlayer coupling, which can be continuously tuned by applying external pressure or varying the temperature. The unambiguous experimental identification of the topological phase transition in $ZrTe_5$ is still lacking. Motivated by theoretical predictions [3] and recent temperature dependent magneto-transport [4] and zero-field IR spectroscopy [5] studies, we focused our experimental development efforts on the implementation of variable temperature IR magneto-spectroscopy (limited so far to liquid helium temperatures). The far-IR setup developed in collaboration with Dr. M. Ozerov (NHMFL) became operational very recently. Our first experimental campaign was very successful. We were able to follow the evolution of inter-LL transitions in $ZrTe_5$ in a very broad temperature range and detect continuous closing and reopening of the band gap. This behavior is qualitatively consistent with the picture a temperature-driven topological phase transition from a weak to a strong topological insulating state.

Spectroscopic determination of valley and Zeman splitting in graphene

Monolayer and bilayer graphene remain among the best experimental platforms to study 2D Dirac fermions due to their high mobility and additional valley or pseudospin degrees of freedom. Broken-symmetry states realized at high magnetic fields, particularly at the charge neutrality point

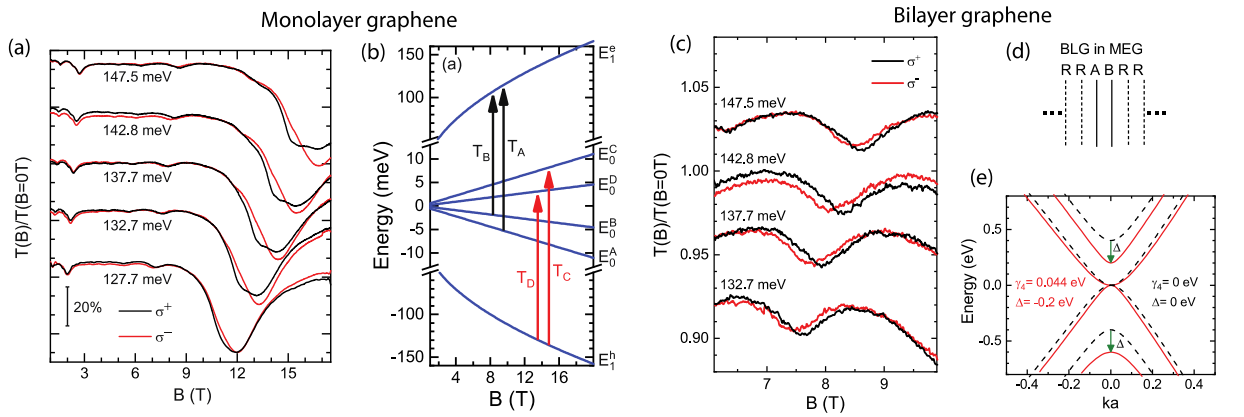

(a) CP-resolved magneto-transmission spectra measured at different incident photon energies revealing splitting of zeroth LL in MLG. (b) Landau fan diagram of MLG near charge neutrality. The four-fold splitting of the n = 0 LL results in four modes spectrally resolved in the experiment. (c) CP-resolved spectra of the m = 2 LL in BLG. (d) Schematics of the stacking order between BLG layers (AB) and rotational stacked graphene layers (R) in MEG. (e) Low-energy band structure of BLG with (red) and without (black) electron-hole asymmetry.

of graphene, have long been a focal point of research. High-field and high-resolution spectroscopies enabling direct comparison with theory are the preferred techniques to probe the nature of the broken-symmetry states in graphene.

The direct evidence to date of the four-fold splitting of the zeroth LL only comes from the electronic transport and tunneling spectroscopy measurements. Here, we use the circular-polarization (CP) resolved magneto-IR spectroscopy of quasi-neutral multilayer epitaxial graphene (MEG) to probe the valley and Zeeman splittings of graphene LLs. Moreover, CP-resolved magneto-spectroscopy yielded important information on the electron-hole asymmetry of the material's band structure due to its selective activation of the electron-like or hole-like transitions. Our experiments revealed spectroscopically a four-fold splitting of the zeroth LL transition in monolayer graphene (MLG), resulting from the lifting of the valley and spin degeneracy and the broken electron-hole symmetry. By analyzing the magnetic field dependence of the transition energies, we deduce a possible scenario that involves valley splitting at the charge neutrality and enhanced Zeeman splitting in the electron and hole sub-LLs, and extract their effective *g*-factors. The CP-resolved measurements of bilayer graphene (BLG) inclusions uncover an even larger electron-hole asymmetry, with an opposite sign to the monolayer. We show that the asymmetry could be strongly influenced by the stacking orientation of the bilayer (with respect to the neighboring layers), making it a possible design parameter for future epitaxial graphene band engineering.

Future Plans

Probing energy, symmetry and dispersion of low-lying excitations and studying topological phase transitions in novel electronic materials via magneto-optical spectroscopy is a longstanding goal of this program. In the next funding period, we plan to investigate spectroscopically topological phase transitions in a broader parameter space (magnetic field, temperature, pressure), while

continuing to explore exotic optically excited states in atomically thin materials and structures, including systems with moiré "textured" unit cells or "twist-angle" engineered bands.

References

[1] Z.K. Liu *et al.* Nature Materials **15**, 27 (2017)
[2] H. M. Weng, X. Dai, and Z. Fang, Phys. Rev. X **4**, 011002 (2014)
[3] Z. Fan, Q.-F. Liang, Y. B. Chen, S.-H. Yao, and J. Zhou, Scientific Reports **7**, 45667 (2017)
[4] N.L. Nair *et al.* Phys. Rev. B **97**, 041111(R) (2018)
[5] B. Xu *et al.* Phys. Rev. Lett. **121**, 187401 (2018)

Publications

1. "Landau Quantization in Coupled Weyl Points: A Case Study of Semimetal NbP", Y. Jiang, Z.L. Dun, S. Moon, H.D. Zhou, M. Koshino, D. Smirnov, Z. Jiang, Nano Letters **18**, 7726 (2018)
2. "Valley and Zeeman Splittings in Multilayer Epitaxial Graphene Revealed by Circular Polarization Resolved Magneto-Infrared Spectroscopy", Y. Jiang, Z. Lu, J. Gigliotti, A. Rustagi, L. Chen, C. Berger, W. de Heer, C. Stanton, D. Smirnov, Z. Jiang, submitted to Nano Letters (2019)
3. "Magnetic field mixing and splitting of bright and dark excitons in monolayer $MoSe_2$", Z. Lu, D. Rhodes, Z. Li, D.V. Tuan, Y. Jiang, J. Ludwig, Z. Jiang, Z. Lian, S.F. Shi, J. Hone, H. Dery, D. Smirnov, submitted to 2D Materials, arXiv: 1905.10439v1 (2019)
4. "Zeeman-Induced Valley-Sensitive Photocurrent in Monolayer MoS_2", X.X. Zhang *et al,* Phys. Rev. Lett. **122**, 127401 (2019)
5. "Luminescent Emission of Excited Rydberg Excitons from Monolayer WSe_2", S.Y. Chen, Z. Lu *et al*, Nano Letters **19**, 2464 (2019)
6. "Gate Tunable Dark Trions in Monolayer WSe_2", E. Liu *et al*, Phys. Rev. Lett. **123**, 027401 (2019).
7. "Engineering Dirac Materials: Metamorphic $InAs_{1-x}Sb_x/InAs_{1-y}Sb_y$ Superlattices with Ultralow Bandgap", S. Suchalkin *et al,* Nano Letters **18**, 412 (2018)
8. "Metamorphic narrow-gap InSb/InAsSb superlattices with ultra-thin layers", M. Ermolaev *et al,* Appl. Phys. Lett., **113**, 213104 (2018)
9. "Anomalously large resistance at the charge neutrality point in a zero-gap InAs/GaSb bilayer", W. Yu *et al*, New J. Phys. **20,** 053062 (2018).
10. "Revealing the biexciton and trion-exciton complexes in BN encapsulated WSe_2", Z. Li, T.Wang, Z. Lu, *et al*, Nature Communications **9**, 1271 (2018)
11. "Efficient generation of neutral and charged biexcitons in encapsulated WSe_2 monolayers. Nature Communications", Z. Ye *et al*, Nature Communications **9**, 21001 (2018)

1. Title: ER46317: "Spin-Polarized Scanning Tunneling Microscopy Studies of Magnetic, Electronic, and Spintronic Phenomena in Nitride Systems"

PI: **Arthur R. Smith**

Address: **Ohio University**
Nanoscale & Quantum Phenomena Institute
Department of Physics & Astronomy
Athens, OH 45701

E-mail: **smitha2@ohio.edu**

2. Program Scope

The scope of this project is to investigate the structural, electronic, and spin magnetic properties of nitride-related material systems, in particular magnetic nitrides, magnetic gallium nitrides, and related elemental magnetic materials. The project seeks to explore, image, and even manipulate the ferromagnetic, antiferromagnetic, and ferrimagnetic structures of these material systems. An important goal is to develop these materials as advanced spintronic systems which may have future energy-related applications. In order to probe these systems, this project makes use of scanning tunneling microscopy (STM) and especially spin-polarized STM (SP-STM). The latter is a powerful technique which can provide spin information on surfaces with atomic-scale resolution. Combining ultra-high vacuum SP-STM together with *in-situ* molecular beam epitaxial growth, diverse nitride-related material systems can be explored in a pristine state.

3. Recent Progress

- **A *Investigation of Possible Spin Kondo effect in Iron on Antiferromagnetic Chromium Nitride***

We are investigating a possible spin Kondo effect in iron deposited on CrN surfaces. First we have established the magnetic properties of CrN (001) thin films grown by MBE in our chamber, finding it to be clearly antiferromagnetic with a Néel temperature of 270 +/- 2 K which is strongly correlated with a structural transition from cubic (RT) to orthorhombic (LT) and an electronic transition from semiconducting (RT) to metallic (LT). We published a comprehensive paper on this topic in 2017 together with both experimental collaborators (NIST-Gaithersburg/ neutron scattering) and theoretical collaborators (Mexico/ first-principles) [pub #89].

Preliminary data for the possible spin Kondo effect in this system is shown in Fig. 1 where (a) & (b) show the smooth RHEED pattern and LT-STM image of the CrN(001) surface, respectively. Iron deposited on the surface leads to small islands as seen in (c) & (d). The *dI/dV* curve of the CrN substrate area between islands reveals a smooth U-shaped valley near 0 mV and a peak

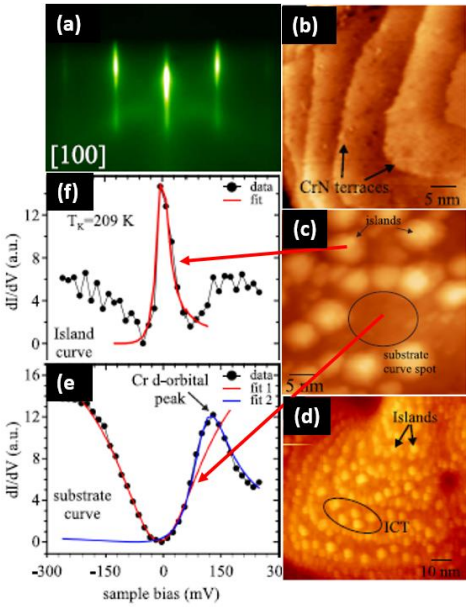

Fig. 1 (a) Streaky RHEED of CrN(001) with (b) LT-STM image; (c) & (d) show islands after depositing Fe on CrN; *dI/dV* spectroscopy on bare CrN region (e) and Fe/CrN islands (f).

near 105 mV as seen in (e). This characteristic lineshape is thought to be related to nitridated Cr *d*-orbitals and is similar to what is seen on oxygenated chromium as reported by Hanke *et al* [1].

The *dI/dV* of the island areas is shown in Fig. 1(f) where we see a sharp peak at the Fermi level. Occasionally a sharp dip (not shown) is seen rather than a sharp peak. A Fano line shape is fit to the sharp peak seen in (f), with an extracted Kondo parameter T_K of 209 K. Additional work is underway to provide more evidence for a Kondo resonance.

Kondo physics has been explored greatly with the use of scanning tunneling spectroscopy, particularly for magnetic single atoms or molecules on non-magnetic metal substrates [2,3]. But in this case, we know that CrN is antiferromagnetic at low temperatures. Theory suggests that the islands we see in Fig. 1 are in fact Cr islands with deposited Fe atoms substituting for Cr atoms. Since chromium is also antiferromagnetic, this could mean that our *dI/dV* spectroscopy results correspond to an antiferromagnetic Cr/ CrN surface with imbedded Fe impurities (just underneath the surface).

- ***Strain-controlled energy of spin-polarized DOS peak for 2D-MnGaN – a room temperature ferromagnetic monolayer***

We recently demonstrated the first-ever observation of a 2D *room-temperature-ferromagnetic monolayer* of MnGaN (2D-MnGaN). The sample was grown by MBE on GaN, and studied by SP-STM and first-principles theory. We resolved the ferromagnetic domains using SP-STM, demonstrated magnetic hysteresis using small *out-of-plane* magnetic fields, observed magnetic rim states, and measured magnetic DOS profiles using tunneling spectroscopy which are in excellent agreement with the predicted spin-polarized & spin-split DOS peaks obtained from first-principles theory. This work was published online in December 2017 in *Nano Letters* [pub #90]**.**

More recently, we have investigated the dependence of the magnetization anisotropy on *in-plane* lattice strain. First of all, we have observed from the spectroscopy measurements that the position of the spin-polarized Mn DOS peak varies from spectrum to spectrum, as seen in Fig. 2(A) where different peak energies are observed ranging from -1.69 eV up to -1.22 eV (relative to the Fermi level).

Using atomic resolution STM, we have also found that significant strain variations exists within the 2D-MnGaN. As compared to an ideally periodic hexagonal lattice, the 2D-MnGaN lattice displays spacing variations from atom to atom, as shown in the atom spacing histogram in Fig. 2(B). This spacing distribution is highly non-Gaussian and much broader than for typical surfaces.

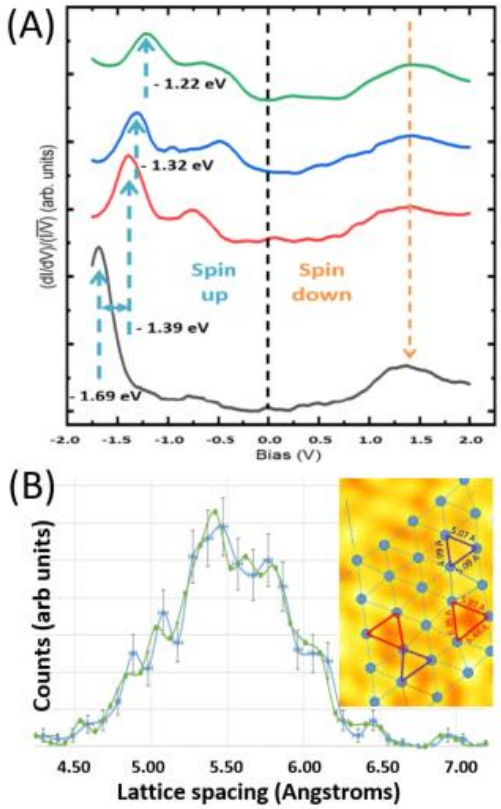

Fig. 2. (A) dI/dV spectroscopy of 2D-MnGaN showing variations of the position of the spin-polarized filled states energy peak; (B) highly non-Gaussian lattice spacing distribution directly measured on the surface using atomic resolution STM images.

Finally, via our Argentinean theory collaboration, we have found that the peak energy variations are linked directly to the lattice spacing distribution. Theoretical calculations for local lattice strains show that for *in-plane* strains, the spin-polarized density of states peak moves closer to the Fermi level. Qualitative and semi-quantitative agreement is found between the experimental and theoretical results. Furthermore, it is also

discovered that the sign of the *in-plane* strain controls the magnetic anisotropy of the Mn atoms, which can flip the Mn spins from *in-plane* to *out-of-plane*.

- ***Development of Difference-Ratio Method for Determining Crystalline Anisotropies and Antiferromagnetic Spin Alignment: Application to Topologically Antiferromagnetic Cr(001) c(2×2)***

It is often the case in spin-polarized STM measurements that the state of the tip spin will flip or change its angle during the measurements. This behavior can be put to good use in order to determine crystalline anisotropies and spin alignment of the surface spins. To that end, we have developed a method we refer to as the difference-ratio (*DR*) method.

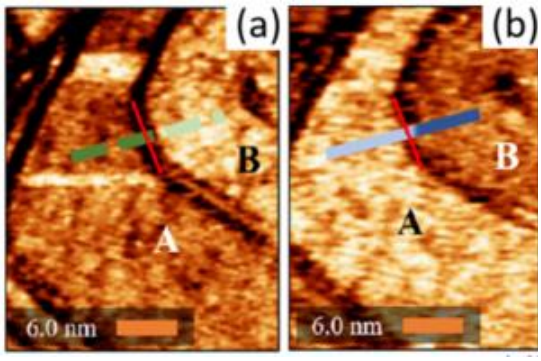

Fig. 3 *dI/dV* images of stepped terraces on Cr(001) c(2×2) surface. (a) tip state 1 where terrace A is dark and B is bright; (b) tip state 2 where terrace A is bright and B is dark.

The basis of the *DR* method is to take the difference between *dI/dV* levels for any two regions of the surface and ratio that to the difference between *dI/dV* levels for any two other regions of the surface; these can be the same two regions but don't have to be. The beauty is that taking the ratio cancels out the unknown pre-factors, especially the spin polarizations of sample (P_S) and tip (P_T). The result is fully 3-dimensional, and the resulting *DR* is a ratio of differences between cosines of angles between tip and sample vectors of the respective regions.

The general equation is the following:

$$DR = \frac{\frac{dI}{dV}_R^T - \left(\frac{dI}{dV}\right)_{R'}^{T'}}{\frac{dI}{dV}_{R''}^{T''} - \frac{dI}{dV}_{R'''}^{T'''}} = \frac{cos\theta_R^T - cos\theta_{R'}^{T'}}{cos\theta_{R''}^{T''} - cos\theta_{R'''}^{T'''}} \qquad Eq.(1)$$

In this equation, the *R*'s correspond to sample regions while the *T*'s correspond to tip states.

Shown in Fig. 3 are SP-STM *dI/dV* map images for the Cr(001) c(2x2) surface prepared in our lab and imaged at 4.2 K. We can see that the tip has changed between the 2 images. Applying the *DR* method, we first let *R* and *R'* equal region A, *R''* and *R'''* equal region B, *T* and *T''* equal tip state 1, and *T'* and *T'''* equal tip state 2. It can be shown using trigonometric identities that the RHS of *Eq.* (1) should equal -1 if region A and region B have 180° opposite spin polarization. We find experimentally that $DR = -0.94 \pm 0.3$, thus verifying the antiferromagnetism in our sample.

4. Future Plans

In general, each project in our lab should move from the initial growth study, to the structural investigation, and then on to the measurement of electronic and spin magnetic properties. Current and future efforts are therefore aimed at the use of *dI/dV* spectroscopy and *dI/dV* mapping, combined with magnetic STM tips and measurements under applied magnetic fields.

To further support a Kondo effect in Fe/CrN, we could take *dI/dV* measurements over a range of temperatures and look for peak broadening. But even such data may remain inconclusive. A second way to prove a Kondo resonance is to perform *dI/dV* measurements under large applied

magnetic fields, looking for peak splitting as the Zeeman energy exceeds the Kondo energy. We plan to try this in our LT-STM (field up to 4.5 T). Further, we plan to obtain spin-resolved information on and around the islands (spatial dependence) using magnetic STM tips, also as a function of applied magnetic fields, and including both *dI/dV* maps and atomic resolution images.

For MnGaN-2D, besides publishing our results for the strain/ peak energy/ anisotropy results, we would like to probe the local magnetic anisotropy at the atomic scale using SP-STM. Then apply *out-of-plane* magnetic fields to align the spins while performing *dI/dV* spectroscopy.

5. References

[1] T. Hänke, M. Bode, S. Krause, L. Berbil-Bautista, and R. Wiesendanger, "Temperature-dependent scanning tunneling spectroscopy of Cr(001): Orbital Kondo resonance versus surface state," Phys. Rev. B **72**, 085453 (2005).

[2] V. Madhavan, W. Chen, T. Jamneala, M. F. Crommie, N. S. Wingreen, "Tunneling into a single magnetic atom: spectroscopic evidence of the Kondo resonance," Science **280**, 567 (1998).

[3] U.G.E. Perera, H. J. Kulik, V. Iancu, L. G. G. V. Dias da Silva, S. E. Ulloa, N. Marzari, and S.-W. Hla, "Spatially Extended Kondo State in Magnetic Molecules Induced by Interfacial Charge Transfer, Phys. Rev. Lett. **105**, 106601 (2010).

6. Publications of DOE sponsored research (2017-2019)

Papers listed below are shown in reverse chronological order, with the numbering defined based on paper #1 = A.R. Smith's first paper. Full publication list can be seen at: http://www.phy.ohiou.edu/~asmith/publist.html.

94. Nitrogen-induced reconstructions on the Cr (001) surface, Emiliano Ventura-Macias*, J. Guerrero-Sánchez, Joseph P. Corbett, Arthur R. Smith, and Noboru Takeuchi, *Applied Surface Science* **484**, 578 (2019).
93. Dislocation Structures, Interfacing, and Magnetism in the $L1_0$-MnGa on eta-perp-Mn_3N_2 bilayer, J. P. Corbett, J. Guerrero-Sanchez, J. C. Gallagher, A.-O. Mandru, A. L. Richard, D. C. Ingram, F. Yang, N. Takeuchi, and A. R. Smith, *Journal of Vacuum Science & Technology A* **37**, 031102 (2019).
92. Applying a Difference Ratio Method in Spin-Polarized Scanning Tunneling Microscopy to Determine Crystalline Anisotropies and Antiferromagnetic Spin Alignment in Cr(001) c(2x2), Joseph P. Corbett and Arthur R. Smith, *Journal of Magnetism & Magnetic Materials* **465**, 626 (2018).
91. Structural, Electronic, and Magnetic Properties of the CrN(001) Surface: First-principles Studies, Rodrigo Ponce-Perez, Khan Alam, Gregorio H. Cocoletzi, Noboru Takeuchi, and Arthur R. Smith, Applied Surface Science **454**, 350 (2018).
90. A Two-Dimensional Manganese Gallium Nitride Surface Structure Showing Ferromagnetism at Room Temperature, Yingqiao Ma, Abhijit V. Chinchore, Arthur R. Smith, María Andrea Barral, and Valeria Ferrari, *Nano Letters* **18**, 158 (2018).
89. Structural and Magnetic Phase Transitions in Chromium Nitride Thin Films Grown by RF Nitrogen Plasma Molecular Beam Epitaxy, K. Alam, S. M. Disseler, W. D. Ratcliff, J. A. Borchers, R. Ponce-Perez, G. H. Cocoletzi, N. Takeuchi, A. Foley, A. Richard, D. C. Ingram, and A. R. Smith, *Phys Rev B* **96**, 104433 (2017).

Hybrid Electro- and Acousto-Dynamical Systems for Quantum Optical Networks (HEADS-QON, feasibility)

Maria Spiropulu, Shang-Yi Ch'en Professor of Physics
California Institute of Technology, 626 395 2471, smaria@caltech.edu
Caltech (M. Spiropulu, O. Painter), Harvard (M. Loncar), Berkeley (N. Yao)

ABSTRACT

We propose a research program that will study the feasibility of novel multi-layer quantum transduction and memory schemes, and explore how to utilize them to realize advanced quantum network architectures. The program aims to be a feasibility study of novel, sustained, dense, and efficient quantum information generation, storage, retrieval, relay and distribution.

A notable part of the proposal's novelty is anchored on original ideas and device conceptual designs that turn the phononic-sourced challenges into an opportunity pathfinder towards optimized transduction chains over a broad range of length and energy/temperature scales. The proposal involves theory building and conceptual design and laboratory implementation of transduction systems as well as designing a path towards integration, commissioning and benchmarking in a scalad quantum network setup.

Quantum networks, both integrated on a chip and distributed over long distances, rely on efficient storage, processing, retrieval and communication of quantum information, thus requiring long lived quantum memories, efficient and low loss quantum communication channels, and fast and fault tolerant quantum processors. Currently, these elements of the net- work are implemented using different types of qubits. Optically addressable spin qubits, including negatively charged silicon-vacancy (SiV) color center in diamond (Figure 1a), have emerged as one of the most promising quantum memory platforms, owing to their long coherence times. Recently, ultra-high quality factor (Q) mechanical resonators, have also been proposed as a memory platform (Figure 1b). Photons at telecommunication wavelength (≈ 1.55μm) remain the best information carriers for distances exceeding several meters, due to low propagation loss of optical fibers. Finally, the most powerful quantum processors are currently implemented with superconducting qubits, e.g. transmons (Figure 1d), that are interfaced via microwave photons. Therefore, quantum networks rely crucially on efficient transduction of information between different qubit platforms. Currently explored transduction schemes rely on converting quantum information to optical photons, and thus require efficient optical interfaces to spins, transmons, and microwave photons. While this approach is justified in the case of distributed quantum networks, where the quantum information needs to be carried over long distance via optical fiber, it is unclear if it is suited for realization of hybrid on-chip networks. Despite great progress that has been made in the field of integrated photonics, finite losses of on-chip optical waveguides and resonators still limit the efficacy (efficiency and fidelity) of photon mediated quantum transduction schemes.

Our vision in the HEADS-QON proposal is to study the utilization of mechanical/ acoustic modes of nanofabricated mechanical systems, to mediate interactions between qubits on the same chip. While there is a large body of work dedicated to engineering interactions of quantum system with photons inside nanofabricated devices, not much has

been done to engineer their interactions with phonons. Importantly, phonons can couple to variety of quantum systems (e.g. spin, charge, flux), and thus can be used to transfer the quantum states between them. This could enable hybrid quantum networks that capitalize on the strengths of each system. We will leverage this to develop novel hybrid architectures based upon acousto-dynamical transducers involving driven strain fields (Figure 1a), piezo- electric interactions (Figure 1e and g), and surface acoustic waves (Figure 1f), Our basic science feasibility program seeks to understand how to utilize coherent phonons as on-chip information carriers. This provides a paradigm shift in the way quantum networks are realized since interactions with phonons are typically considered detrimental to the coherence of quantum systems, and therefore are avoided. In addition, we will push the state of the art in photon mediated distributed quantum networks by exploring new types of quantum transcievers (Figure 1f) that rely on state of the art nanophotonic and electro-optic devices.

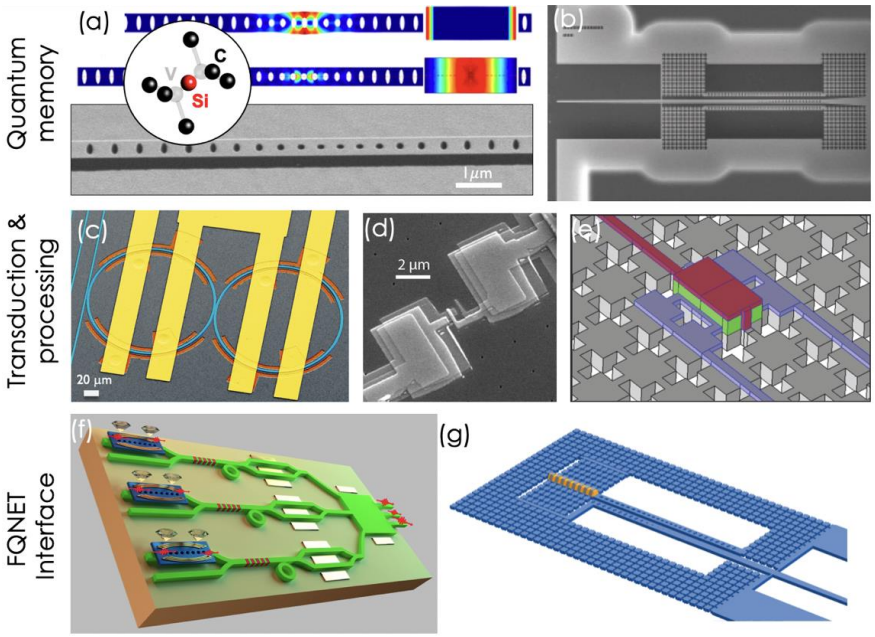

Figure 1. HEADS-QON program will study (a) silicon vacancy (SiV) color centers embedded in diamond optomechanical cavities and (b) silicon optomechanical crystals as quantum memory and (d) superconducting transmon as a quantum processor. We will study transduction between memory and processing unit mediated via (a) strain, (c) electro-optic effect, (e) piezo-electric effect. (f) Quantum optical transcievers based on hybrid diamond-lithium niobate nanophotonics platform for generation, frequency translation & shaping, temporal shaping, and routing of single photons and (g) microwave-optical quantum transducers will also be studied with an eye of possible utilization at a scaled quantum system like FQNET.

(Figure 1c). These will replace discrete optical components currently used at FQNET thus enabling orders of magnitude higher communication rates.

Selected Recent Relevant Publications of PIs

- G. S. MacCabe, H. Ren, J. Luo, J. D. Cohen, H. Zhou, A. Sipahigil, M. Mirhosseini, and O. Painter, arXiv:1901.04129 (2019).
- M. Mirhosseini, E. Kim, V. S. Ferreira, M. Kalaee, A. Sipahigil, A. J. Keller, and O. Painter, Nat. Comms. 9, 3706 (2018).
- M. J. Burek, J. D. Cohen, S. M. Meenehan, T. Ruelle, S. Meesala, J. Rochman, H. A. Atikian, M. Markham, D. J. Twitchen, M. Lukin, O. J. Painter, and M. Lonar, Optica 12, 1404 (2016).
- M. Mirhosseini, E. Kim, X. Zhang, A. Sipahigil, P. B. Dieterle, A. J. Keller, A. Asenjo-Garcia, D. E. Chang, and O. Painter, arXiv:1809.09752 (2018)
- K. Fang, J. Luo, A. Metelmann, M. H. Matheny, F. Marquardt, A. A. Clerk, and O. Painter, Nature Physics 13, 465 (2017).
- B. Machielse, S. Bogdanovic, S. Meesala, S. Gauthier, M. J. Burek, G. Joe, M. Chalupnik, Y. I. Sohn, J. Holzgrafe, R. E. Evans, C. Chia, H. Atikian, M. K. Bhaskar, D. D. Sukachev, L. Shao, S. Maity, M. D. Lukin, and M. Loncar, arXiv:1901.09103v2 (2019)
- M. A. Lemonde, S. Meesala, A. Sipahigil, M. J. A. Schuetz, M. D. Lukin, M. Loncar, and P. Rabl, Physical Review Letters 120, 213603 (2018).
- M. Zhang, C. Wang, R. Cheng, A. Shams-Ansari, and M. Loncar, Optica 4, 1536 (2017)
- B. Desiatov, A. Shams-Ansari, M. Zhang, C. Wang, and M. Loncar, Optica 6, 380 (2019)
- C. Wang, M. Zhang, X. Chen, M. Bertrand, A. Shams-Ansari, S. Chandrasekhar, P. Winzer, and M. Loncar, Nature 562, 101 (2018)
- S. Hsieh, P. Bhattacharyya, C. Zu, T. Mittiga, T. J. Smart, F. Machado, B. Kobrin, T. O. Hhn, N. Z. Rui, M. Kamrani, S. Chatterjee, S. Choi, M. Zaletel, V. V. Struzhkin, J. E. Moore, V. I. Levitas, R. Jeanloz, N. Y. Yao, arXiv:1812.08796

Nanoscale Electrical Transfer and Coherent Transport Between Atomically-Thin Materials

Douglas R. Strachan, Department of Physics and Astronomy, University of Kentucky

Program Scope

The working paradigm of the electronics field over the last 50 years has been the steady reduction in size of their components, yet as the size of electronics are reduced towards nanoscale dimensions electrical contacts are increasingly important, and their resistances are major obstacles to achieving faster and more efficient devices. It is widely expected that this steady reduction in size will soon involve the incorporation of the new class of atomically-thin materials (such as, graphene, nanotubes, and the dichalcogenides) into future electronics. At this extreme limit of miniaturization, the interfaces to electrical contacts will likely become the critical barriers to improved performances and energy efficiencies. The case in which both the device material and the contact comprise an atomically-thin material is particularly exciting, as this nanostructure has the potential to realize controlled coherent transport at the electrode-channel interface, enabling very high conductivities over extremely short length scales; in essence pushing the limit of miniaturization of the electrode thickness can in this situation be exploited as an advantage rather than being an obstacle.

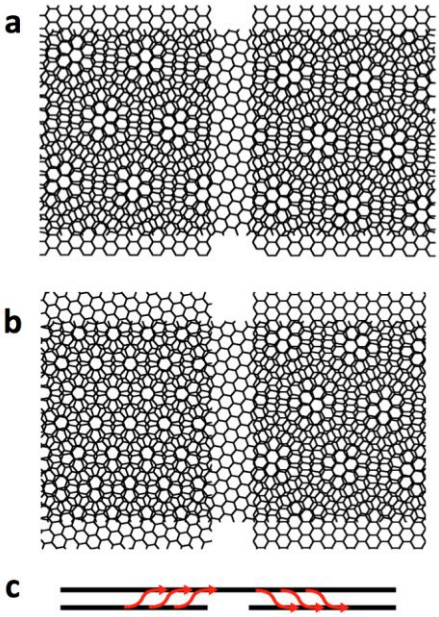

Figure 1. (a) Conceptual top-down illustration of commensurate nanogap junction electrodes. Both sides of the nanogap junction have the same Moiré lattice. (b) Conventional nanogap junctions do not have the same crystal orientation for both electrodes, and result in different crystal interfaces on either side of the junction. (c) Side view illustration of a bi-layer nanogap heterostructure where the current is shown flowing from the bi-layer region to the single-layer channel, and then returning to the bi-layer on the other side of the junction.

At these extremely small scales, the interplay between the 2D-heterostrucuture electrode and the channel has tremendous potential for probing and generating new emergent quantum phenomena. For example, these commensurate nanoscale heterostructures could be ideally suited for the development of highly-ordered Josephson junctions (JJs) made from the recently discovered magic-angle twisted bi-layer graphene.[1] While these magic-angle twisted JJs could be useful devices for quantum information applications, they also could reveal the symmetry of the underlying order parameter of this fascinating emergent quantum phenomena.

The objective of the current project is to utilize highly-ordered atomically-thin commensurate nanoscale electrodes to probe and control the coherent electron transfer to another atomically-thin material. An illustration of a commensurate electrode pair is illustrated in Fig. 1a, with the typical electrode configuration shown (for contrast) in Fig. 1b and a bi-layer side-view example in Fig. 1c. The work utilizes etched nanogaps within a pristine 2D material resulting in two commensurate regions, as in Fig 1a, on either side of a junction.[2] To fulfill the objective of this project, two aims are being pursued to determine the electron transport between commensurate electrodes through channel materials comprising two prototypical atomically-thin materials with different dimensionalities; one-dimensional nanotubes, and atomically-thin 2D materials. This two-aim research effort will provide fundamental complementary understanding of coherent transfer processes as the dimensionality of the electrical interface is varied.

Recent Progress

1D-2D commensurate nanogap heterojunctions: With the recent discovery of superconductivity and Mott insulation within magic-angle twisted bi-layer graphene, there has been tremendous interest in investigating systems near to lattice alignment between adjacent layers. To achieve commensurate nanogap junction interfaces with near lattice alignments, we are utilizing crystallographically aligned nanotubes grown across etched nanogaps within few-layer graphene films.[3] Figure 2a shows an AFM scan of one of our recent devices, with an enlarged image of the nanotube/graphene-nanogap junction in the inset. The transport across these junctions shows enhanced transconductance compared to the bare few-layer graphene electrodes (as seen in Fig. 2b). We are currently working with several similar samples to apply lateral forces to the nanotubes at the junction in order to induce a small lattice twists at at the interface and to probe such twisted nanoscale heterostructures.

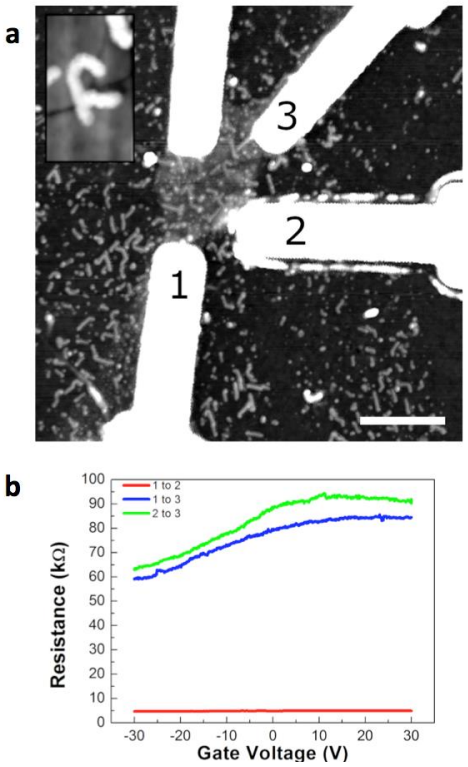

Figure 2. 1D-2D commensurate heterojunction formed with etched few-layer graphene (FLG) nanogap electrodes and crystallographically-grown nanotubes. (a) AFM image of nanotubes over etched FLG nanogaps with metallic electrodes connected to junctions (scale bar is 500 nm) and enlarged image of junction is shown in the inset. (b) Transport measurements show enhanced gate response and dissipation across nanotube heterostructure junction in comparison to measurements made on the same side of the junction.

2D commensurate nanogap heterojunctions: Towards the second aim of the project, we have recently constructed commensurate electrode junctions from crystallographically etched few-layer graphene interfaced with a bi-layer of MoS_2. The sample construction and results (which are currently being prepared for journal submission) are summarized in Fig. 3. These show that we can obtain high transconductance across the junction consistent with some of the best performing 2D semiconductor devices.[4] Similar devices utilizing graphene channels have also been constructed and are closely related to our future proposed work to develop magic-angle twisted bi-layer graphene Josephson junctions (JJs), as discussed below.

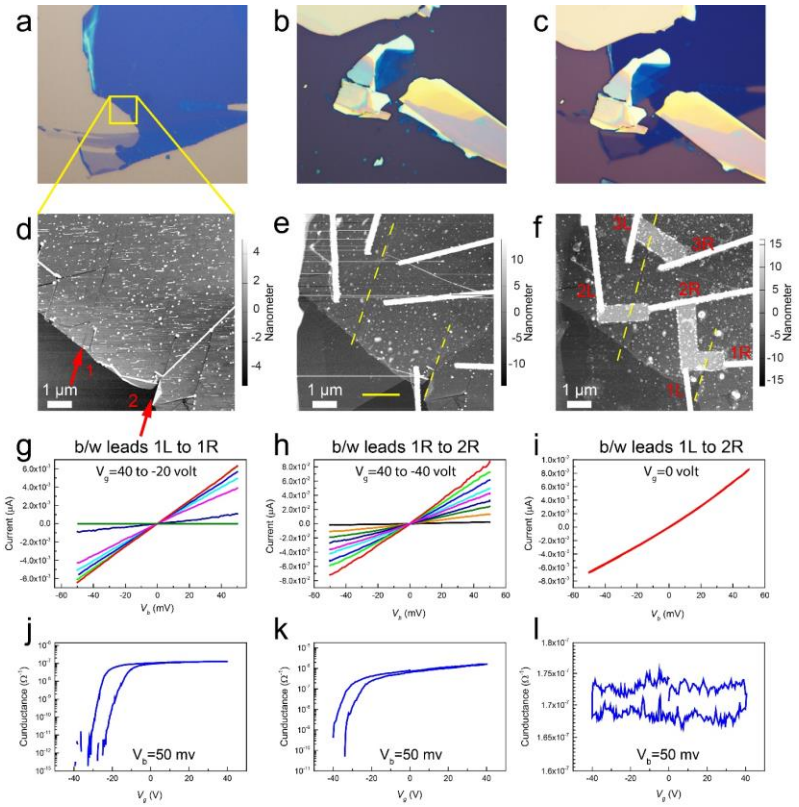

Figure 3. 2D commensurate heterojunction formed with etched few-layer graphene (FLG) nanogap electrodes and bi-layer MoS_2. (a-c) Optical images of 2D heterostructure formation with AFM image in (d) showing etched nanogaps (red arrows) in FLG. (e) Image shows MoS_2 bilayer placed over the etched nanogaps, metallic electrodes (white lines), and location of nanogaps (dashed lines). (f) Final plasma etched devices (the three light regions). (g-l) Transport measurements of lower-right device in (f) showing strong gate dependence across the junction (j-k), but no detectable gate response on the same side of the junction (l).

Etched hBN nanogaps for commensurate 2D heterojunctions beyond graphene: We have developed etched nanogaps in the 2D dielectric hBN through catalytic etching, as summarized in Fig. 4 and published.[5] Such structures can be used to apply a commensurate lattice perturbation to another 2D material on either side of the etch hBN nanogap.

Future Plans

Josephson Junctions of magic angle twisted bi-layer, order parameter symmetry determination, and emergent phenomena at commensurate junctions for quantum information sciences: The etched commensurate graphene electrodes we are developing in this project hold tremendous promise in providing fundamental insight into the superconductivity of the fascinating and recently developed magic-angle bi-layers systems. By placing a single layer with a small relative

twist angle onto an etched graphene nanogap (like shown in Figs. 1a and 1c), we should be able to construct two magic-angle superconducting regions separated by a short single-layer graphene barrier – thus resulting in a Josephson Junction. Such JJs are of fundamental importance to understanding magic-angle superconductivity, as they can provide insight into the symmetry of the order parameter,[6] which is currently a hotly debated issue within this rapidly growing field. The development of these magic-angle JJs could also lead to emergent phenomena at their interfaces along with devices relevant to quantum information sciences.

References

[1] Y. Cao, V. Fatemi, S. Fang, K. Watanabe, T. Taniguchi, E. Kaxiras, P. Jarillo-Herrero, *Unconventional superconductivity in magic-angle graphene superlattices*, Nature, 556 43-+ (2018).
[2] D.P. Hunley, A. Sundararajan, M.J. Boland, D.R. Strachan, *Electrostatic Force Microscopy and Electrical Isolation of Etched Few-Layer Graphene Nano-Domains*, Appl. Phys. Lett., 105 243109 (2014).
[3] D.P. Hunley, M.J. Boland, D.R. Strachan, *Integrated Nanotubes, Etch Tracks, and Nanoribbons in Crystallographic Alignment to a Graphene Lattice*, Adv Mater, 27 813-818 (2015).
[4] B. Stampfer, F. Zhang, Y.Y. Illarionov, T. Knobloch, P. Wu, M. Waltl, A. Grill, J. Appenzeller, T. Grasser, *Characterization of Single Defects in Ultrascaled MoS2 Field-Effect Transistors*, Acs Nano, 12 5368-5375 (2018).
[5] A. Ansary, M. Nasseri, M.J. Boland, D.R. Strachan, *Parallel boron nitride nanoribbons and etch tracks formed through catalytic etching*, Nano Research, 11 4874-4882 (2018).
[6] C.C. Tsuei, J.R. Kirtley, *Pairing symmetry in cuprate superconductors*, Reviews of Modern Physics, 72 969-1016 (2000).

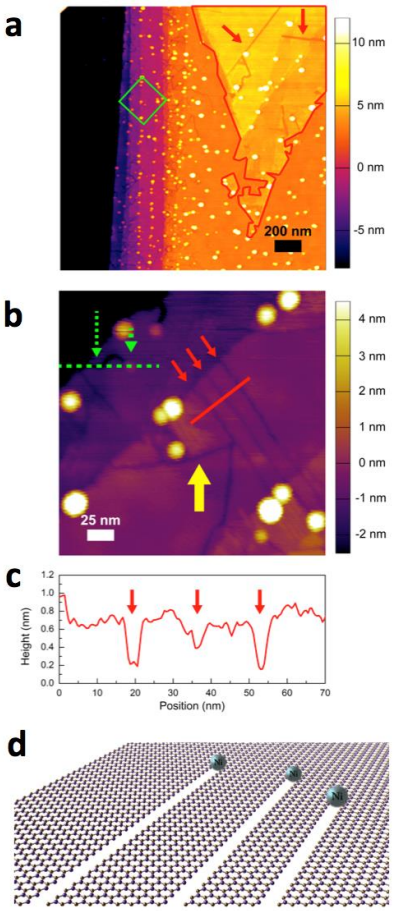

Figure 4. Etched nanogaps within hBN. (a-c) Results showing nanogaps etched into hBN layers with illustration in (d).

Publications

1 M. Nasseri, A. Ansary, M. J. Boland, and D. R. Strachan, "Aligned van der Waals Coupled Growth of Carbon Nanotubes to Hexagonal Boron Nitride", *Advanced Materials Interfaces* **5**, 1800793 (2018).

2 A. Ansary, M. Nasseri, M. J. Boland, and D. R. Strachan, "Parallel Boron Nitride Nanoribbons and Etch-Tracks Formed Through Catalytic Etching" *Nano Res.*, **11**, 4874-4882 (2018).

3 M. J. Boland, J. L Hempel, A. Ansary, M. Nasseri, and D. R. Strachan, "Graphene Used as a Lateral Force Microscopy Calibration Material in the Low-Load Non-Linear Regime", *Review of Scientific Instruments* **89**, 113902 (2018).

Quantum and non-equilibrium phenomena in nanoscale systems driven by current

Sergei Urazhdin, Emory University

Program Scope

The program aims to identify and characterize quantum and non-equilibrium phenomena in nanoscale systems that have been traditionally interpreted in terms of the classical (or semiclassical) and/or quasi-equilibrium approximations. The originally proposed research focused on the contributions of quantum magnetization fluctuations in ferromagnets to spin transfer effect – excitation of magnons (quantized magnetization fluctuations) by spin currents. The existence of such a quantum spin transfer (QST) effect was inferred from the analysis of current-dependent resistance in magnetic nanostructures at cryogenic temperatures, and shown by theoretical calculations performed by the PI and confirmed by several other groups [1-4]. Follow-up measurements showed that current-induced nonequilibrium phonons may have provided an unexpected contribution to the experimentally observed behaviors. Therefore, the scope of the project has been extended to also analyze the nonequilibrium phonon distribution generation by phonons in micro- and nano-structures.

Recent Progress

The main recent finding is the observation of a piecewise-linear dependence of resistance on current, inconsistent with Joule heating, at cryogenic temperatures in several planar and vertical nanostructures, including thin-film Pt, Au, and Permalloy wires on Si, SiO_2, and sapphire substrates [Fig.1], as well as in resistive vertical nanocontacts [Fig.2]. These measurements confirmed the general nature of the observed behaviors, which can be explained by the strongly nonequilibrium distribution of phonons generated by current. The phonons quasi-ballistically escape from the microstructures, before they can thermalize. Their population, and thus current-dependent resistance increase, is determined by the electron scattering rate, which is proportional to current.

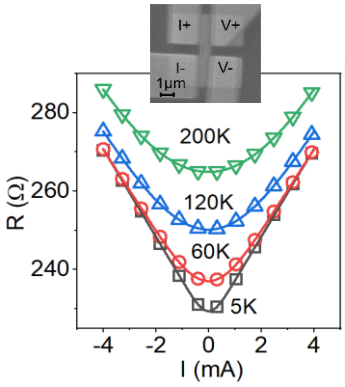

Fig.1. Resistance vs current for a 5 nm-thick Pt microwire on Si, at the labeled values of temperature. Inset: SEM micrograph of the wire.

The linear dependence becomes smeared out with increasing temperature, but remains inconsistent with Joule heating even near ambient conditions. The performed analysis has led to a semi-quantitative understanding of the observed phenomena, providing insight into electron and phonon transport, and electron-phonon scattering. For instance, the slope of the linear

dependence provides information about phonon relaxation, while the thermal smearing provides information about the characteristic energy transfer in electron-phonon scattering. The observed smearing is about 20 times smaller than expected based on the Drude-Sommerfeld approximation, raising questions about our understanding of electron transport even in simple nanostructures.

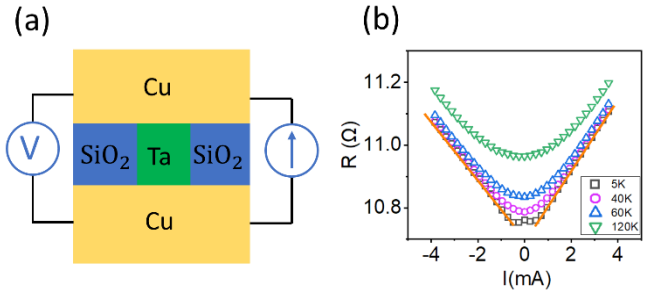

Fig.2. (a) Schematic of a nanofabricated resistive point contact. (b) Resistance vs current for a 10 nm-thick Ta nanocontact, at the labeled values of temperature.

The current-dependence of resistance in vertical nanocontacts was also found to be asymmetric with respect to the current direction [e.g. the slope in Fig.2(b) at I>0 is 10% higher than at I<0], which demonstrated the importance of linear momentum transfer in electron-phonon scattering, resulting in phonon drag.

Future Plans

The planned studies of QST will avoid indirect magnetoresistive measurements that can be misleading because of the similarity with the phonon contribution. One of the approaches will be based on the spin torque ferromagnetic resonance (ST-FMR) technique [5], in which the resonance frequency (or field) provides direct information about the current-dependent effective magnetization, directly related to the current-driven magnon population. In a qualitatively different approach, the effects of current on marginally stable nanomagnets will be investigated. In the subcritical (activated) regime, the current-induced magnetization reversal in such systems may be expected to be a quasi-equilibrium process determined by the total magnetic energy, which at cryogenic temperatures is likely dominated by QST.

In a completely different setting, QST effects may be expected to be much more significant in antiferromagnets (AF) than ferromagnets, because of the much higher characteristic dynamical frequencies. Two approaches will be taken to exploring these systems. First, the spin transport through conductive (AF) may be expected to bear signatures of QST, for example, in the dependence on the energies of the current-carrying electrons. Second, an indicator of the dynamical magnetization state such as exchange bias or magnetic viscosity [6] can be utilized as a measure of current-induced effects.

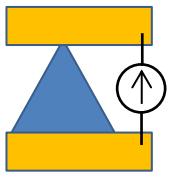

Fig.3. Structure for the analysis of phonon drag.

The plans also include further exploration of current effects on the phonon distribution in nanostructures. One significant issue is why the thermal effects are 20 times smaller than expected based on the Drude-Sommerfeld modes. This issue will be address by studying materials with simple free-electron band structure, such as Au, Ag, and/or Cu. Another potentially significant effect – the phonon drag effect associated with linear momentum

transfer in the phonon generation process – will be explored in spatially asymmetric structures, for example, in a planar "phonon diode" shown in Fig.3.

References

[1] A. Zholud, R. Freeman, R. Cao, A. Srivastava, S. Urazhdin "Spin transfer due to quantum magnetization fluctuations", Phys. Rev. Lett., **119**, 257201 (2017).

[2] A. Qaiumzadeh and A. Brataas "Quantum magnetization fluctuations via spin shot noise", Phys. Rev. B **98**, 220408(R) (2018)

[3] S.A. Bender, R.A. Duine, and Y. Tserkovnyak "Quantum-kinetic theory of spin-transfer torque and magnon-assisted transport in nanoscale magnetic junctions", Phys. Rev. B **99**, 024434 (2019)

[4] P. Mondal, U. Bajpai, M. D. Petrović, P. Plecháč, and B.K. Nikolić "Quantum spin transfer torque induced nonclassical magnetization dynamics and electron-magnetization entanglement", Phys. Rev. B **99**, 094431 (2019)

[5] J.C. Sankey, P.M. Braganca, A.G.F. Garcia, I.N. Krivorotov, R.A. Buhrman, and D.C. Ralph "Spin-transfer-driven ferromagnetic resonance of individual nanomagnets", PRL **96**, 227601 (2006).

[6] 6. S. Urazhdin, W.Li, L. Novozhilova "Magnetic freezing transition in a CoO/Permalloy bilayer revealed by transverse ac susceptibility", J. Magn. Magn. Mater. **476**, 75-85 (2019).

Publications

1. G.X. Chen, R. Freeman, A. Zholud, S. Urazhdin "Nonequilibrium phonon distribution in current-driven nanostructures", submitted (2019), arXiv:1907.00224.

Designing Metastability: Coercing Materials to Phase Boundaries

T. Zac Ward, Oak Ridge National Laboratory

Program Scope

Crystalline materials are defined by their highly ordered microscopic arrangement of atoms. Functionality is then dictated by how the constituent atoms and their spatial relationship to one another affects the electrons in the material. The often strong coupling between spin, charge, orbital, and lattice degrees of freedom in transition metal oxides (TMOs) creates a particularly high sensitivity to slight variations in the crystal composition and structure. The crystal lattice—including the coupled effects of lattice parameter, symmetry, strain state, and octahedral rotations—is thus one of the most important degrees of freedom in these materials. Effective control over lattice parameters not only facilitates the understanding of multiple interactions in strongly correlated systems, but also creates new phases and emergent behaviors: ranging from metal-insulator transitions to superconductivity to multiferroicity. Lattice engineering through epitaxy and/or chemical pressure induced by isovalent substitution are widely used methods of controlling lattice parameters in TMOs and have demonstrated great functional importance. However, these routes can be a tedious trial and error process that require multiple samples to be grown while only allowing discrete symmetry configurations dictated by available substrate and the Poisson effect. These methods also rule out the ability to continuously and/or locally control a material's structure and resulting function. In other words, we have many technologically important materials which are highly sensitive to small structural perturbations but no means of applying these structural perturbations systematically to explore and ultimately design explicit structure-driven functionalities.

This project is aimed at creating, understanding, and utilizing previously inaccessible structural distortions in strongly correlated oxides, with the goal of obtaining new and highly controllable functional properties. We examine how structural changes induce emergent metastabilities using both top-down and bottom-up approaches. The specific aims of this project are: (1) to design metastable ferroic states, (2) to understand local inhomogeneity's role in emergent functionalities, and (3) to understand the mechanisms of structural distortions under strain doping. This work will provide previously hidden insights into the structure-function relationship of correlated quantum materials while providing a means of designing coexisting local functionalities in a single crystal wafer. Together, these aims will provide significant insight into the role of strain and local disorder in determining properties of TMO systems.

Recent Progress

Our effort is motivated by the ability to exert unprecedented control over crystal symmetries related to single axis lattice expansion and octahedra rotation through strain doping; the availability of exceptional tools to analyze materials across multiple length scales; and the need for a fundamental understanding of how local structural distortions create macroscopic functionality. Selected highlights of recent progress are listed as follows:

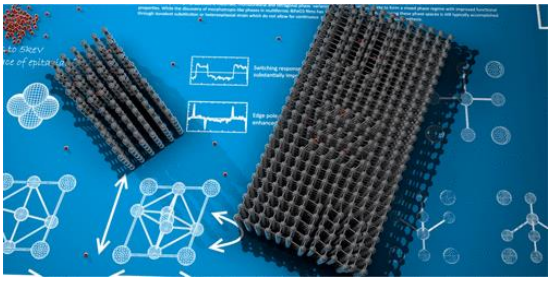

Fig. 1 Represented here, a $BiFeO_3$ lattice(grey) can be reversibly driven through a morphotropic phase boundary with single axis expansion mediated by He(red) irradiation.

On-demand design of crystal phase metastability: Post-synthesis and iterative control of lattice energy enables the design of metastable states. [1] The ability to set lattice energies in correlated systems permits new routes in the design of

magnetic, electronic, and optical properties critical to future information storage, sensing, and computing applications.

Interstitial helium is used to control the type and ratio of competing crystallographic phases in epitaxial multiferroic $BiFeO_3$ films. Slight changes to lattice energy can be continuously and iteratively manipulated post-synthesis, which permits the creation of monolithic lattices with coexisting crystal phases of nearly degenerate energy, such as those residing at a morphotropic phase boundary [Fig. 1]. These findings should be universally applicable to virtually any thin-film system where competing crystal phases are used to generate or enhance functionality. This pool of systems includes any type of ferroic material where lattice distortion affects order parameters, but may also be extended to more unconventional systems such as materials showing magnetic morphotropic phase boundaries or martensitic phase transformations.

Manipulating spin anisotropy with symmetry: The coupling between a material's lattice and its underlying spin state links structural deformation to magnetic properties; however, traditional strain engineering does not allow the continuous, post-synthesis control of lattice symmetry needed to fully utilize this fundamental coupling in device design. Uniaxial lattice expansion induced by post-synthesis low energy helium ion implantation is shown to provide a means of bypassing these limitations. [2] Magnetocrystalline energy calculations are used *a priori* to design a material's preferred magnetic spin orientation. The efficacy of this approach is experimentally confirmed in a spinel $CoFe_2O_4$ model system where the epitaxial film's magnetic easy axis is continuously manipulated between the out-of-plane (oop) and in-plane (ip) directions as lattice tetragonality moves from ip to oop with increasing strain doping [Fig. 2]. Macroscopically gradual and microscopically abrupt changes to preferential spin orientation are demonstrated by combining ion irradiation with simple beam masking and lithographic procedures. The ability to design magnetic spin orientations across multiple length scales in a single crystal wafer using only crystal symmetry considerations provides a clear path toward the rational design of spin transfer, magnetoelectric, and skyrmion-based applications where magnetocrystalline energy must be dictated across multiple length scales. We are currently exploring this concept as a means of manipulating DMI in heterostructures.

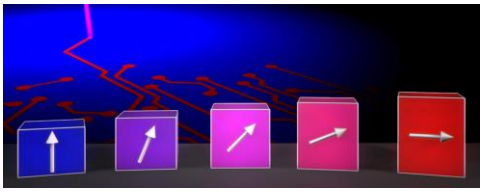

Fig. 2 Strain doping permits the design of lattice symmetries in single crystal films by giving control over magnetic anisotropy energies. Represented here are magnetic easy axis direction in $CoFe_2O_4$ as uniaxial out-of-plane strain is applied with He irradiation.

Extreme disorder in single crystal perovskites: Entropy stabilization is used to create single crystal complex oxide materials where one or more cation sublattices are populated by five or more elements. [Fig. 3] Our initial work demonstrated the first example of a single crystal perovskite oxide with an equiatomic five element B-site population. [3] Films of $Ba(Zr_{0.2}Sn_{0.2}Ti_{0.2}Hf_{0.2}Nb_{0.2})O_3$ were shown to be single phase with excellent crystallinity and atomically abrupt interfaces to the underlying substrates. Atomically resolved electron energy loss spectroscopy mapping showed uniform and random distribution of all B-site cations. This is ongoing work aimed at gaining a deeper

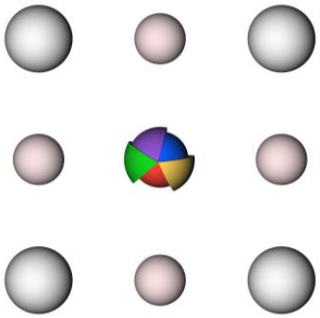

Fig. 3 Representation is of ABO_3 perovskite planes showing single element occupied A-site (grey), equiatomic quintenary B-site (rainbow), and oxygen (pink).

understanding of the role of disorder in the formation and stabilization of competing functional phases. The ability to stabilize complex crystal structures with this level of configurational disorder offers new possibilities for designing materials from a much broader combinatorial cation pallet while providing a fresh avenue for fundamental studies in strongly correlated quantum materials where local disorder can play a critical role in determining macroscopic properties.

Future Plans

The use of strain doping has become routine in our labs. Currently, we are focusing on using this technique to manipulate orbital population in correlated materials to understand functional responses to local distortions. One specific area that this is showing interesting results is when applied to the control of DMI in magnetic heterostructures.

We also plan to broaden our efforts at understanding disorder in quantum materials by stabilizing new highly disordered single crystal films using entropy stabilization synthesis approaches. We expect to have the first examples of single crystal entropy stabilized spinels, pyrochlores, and layered RP phases very soon. This ability to evenly distribute five or more cations onto a single sublattice in these complex crystal structures opens new possibilities for functional design strategies while providing access to fundamental studies seeking to understand how diverse local coupling environments can work to generate macroscopic responses, such as those driven by electron-phonon channels and complex exchange interaction pathways.

References

[1] A. Herklotz, S. F. Rus, N. Balke, C. Rouleau, E.-J. Guo, A. Huon, S. KC, R. Roth, X. Yang, C. Vaswani, J. Wang, P. P. Orth, M. S. Scheurer, and T. Z. Ward, Nano Lett. **19**, 1033 (2019).

[2] A. Herklotz, Z. Gai, Y. Sharma, A. Huon, S. F. Rus, L. Sun, J. Shen, P. D. Rack, and T. Z. Ward, Adv. Sci. **5**, 1800356 (2018).

[3] Y. Sharma, B. L. Musico, X. Gao, C. Hua, A. F. May, A. Herklotz, A. Rastogi, D. Mandrus, J. Yan, H. N. Lee, M. F. Chisholm, V. Keppens, and T. Z. Ward, Phys. Rev. Mater. **2**, 060404(R) (2018).

Publications

1. A. Herklotz, S.F. Rus, N. Balke, C. Rouleau, E.J. Guo, A. Huon, S. KC, R. Roth, X. Yang, C. Vaswani, J. Wang, P.P. Orth, M.S. Scheurer, T.Z. Ward, *Designing Morphotropic Phase Composition in $BiFeO_3$*, Nano Letters **19**, 1033 (2019).
2. A. Herklotz, Z. Gai, Y. Sharma, A. Huon, S.F. Rus, L. Sun, J. Shen, P.D. Rack, T.Z. Ward, *Designing Magnetic Anisotropy through Strain Doping*, Advanced Science **5**, 1800356 (2018).
3. Y. Sharma, A.T. Wong, A. Herklotz, D.K. Lee, A.V. Ievlev, L. Collins, H.N. Lee, S. Dai, N. Balke, P.D. Rack, T.Z. Ward, *Ionic Gating of Ultrathin and Leaky Ferroelectrics*, Advanced Materials Interfaces **6**, 1801723 (2019).
4. Y. Sharma, B.L. Musico, X. Gao, C. Hua, A.F. May, A. Herklotz, A. Rastogi, D. Mandrus, J. Yan, H.N. Lee, M.F. Chisholm, M. Keppens, T.Z. Ward, *Single-crystal high entropy perovskite oxide epitaxial films*, Physical Review Materials **2**, 060404(R) (2018).
5. C. Zhang, P. Pudasaini, A. Oyedele, A. Ievlev, L. Xu, A. Haglund, J.H. Noh, A.T. Wong, K. Xiao, T.Z. Ward, D. Mandrus, H. Xu, O. Ovchinnikova, P. Rack, *Ion Migration Studies in*

Exfoliated 2D Molybdenum Oxide via Ionic Liquid Gating for Neuromorphic Device Applications, ACS Applied Materials & Interfaces **10**, 22623 (2018).
6. E.J. Guo, M.A. Roldan, T. Charlton, Z. Liao, Q. Zheng, H. Ambaye, A. Herklotz, Z. Gai, T.Z. Ward, H.N. Lee, and M.R. Fitzsimmons, *Removal of Magnetic Dead Layer by Geometric Design*, Advanced Functional Materials 1800922 (2018).
7. A.R. Lupini, B.M. Hudak, J. Song, H. Sims, Y. Sharma, T.Z. Ward, S.T. Pantelides, P.C. Snijders, *Direct Imaging of Low-Dimensional Nanostructures*, Microscopy and Microanalysis **24**, 90 (2018).
8. J. Spiegelberg, J.C. Idrobo, A. Herklotz, T.Z. Ward, W. Zhou, J. Rusz, *Local low rank denoising for enhanced atomic resolution imaging*, Ultramicroscopy **187**, 34 (2018).
9. W. Zhao, S. Bi, N. Balke, P.D. Rack, T.Z. Ward, S.V. Kalinin, S. Dai, G. Feng, *Understanding Electric Double Layer Gating Based on Ionic Liquids: from Nanoscale to Macroscale*, ACS Applied Materials & Interfaces **10**, 43211 (2018).
10. E.J. Guo, R.D. Desautels, D. Keavney, A. Herklotz, T.Z. Ward, M.R. Fitzsimmons, H.N. Lee, *Switchable orbital polarization and magnetization in strained $LaCoO_3$ films*, Physical Review Materials **3**, 014407 (2019).
11. Z. Liao, E. Skoropata, J. Freeland, E.-J. Guo, R. Desautels, X. Gao, C. Sohn, A. Rastogi, T.Z. Ward, T. Zou, T. Charlton, M. Fitzsimmons, H.N. Lee, *Large orbital polarization in nickelate-cuprate heterostructures by dimensional control of oxygen coordination*, Nature Communications **10**, 589 (2019).
12. F. Lan, H. Chen, H. Lin, Y. Bai, Y. Yu, T. Miao, Y. Zhu, T.Z. Ward, Z. Gai, W. Wang, L. Yin, E.W. Plummer, J. Shen, *Observing a previously hidden structural phase transition onset through heteroepitaxial cap response*, Proceedings of the National Academy of Sciences **116**, 4141 (2019).
13. E.J. Guo, R. Desautels, D. Keavney, M.A. Roldan, B.J. Kirby, D. Lee, Z. Liao, T. Charlton, A. Herklotz, T.Z. Ward, M.R. Fitzsimmons, H.N. Lee, *Nanoscale ferroelastic twins formed in strained $LaCoO_3$ films*, Science Advances **5**, eaav5050 (2019).
14. W.L. Boldman, C. Zhang, T.Z. Ward, D.P. Briggs, B.R. Srijanto, P. Brisk, P.D. Rack, *Programmable Electrofluidics for Ionic Liquid based Neuromorphic Platform*, Micromachines **10**, 478 (2019).
15. Z.Q. Liu, J. Liu,i, M. Biegalski, J. Hu, S. Shang, Y. Ji, J. Wang, S. Hsu, A.T. Wong, M. Cordill, B. Gludovatz, C. Marker, H. Yan, Z. Feng, L. You, M. Lin, T.Z. Ward, Z. Liu, C. Jiang, L. Chen, R. Ritchie, H.M. Christen, R. Ramesh, *Electrically Reversible Cracks in an Intermetallic Film Controlled by an Electric Field*, Nature Communications **9**, 41 (2018).
16. E.J. Guo, R. Desautels, D. Lee, M. Roldan, Z. Liao, T. Charlton, H.A. Ambaye, J.J. Molaison, R. Boehler, D. Keavney, A. Herklotz, T.Z. Ward, H.N. Lee, M.R. Fitzsimmons, *Exploiting symmetry mismatch to control magnetism in a ferroelastic heterostructure*, Physical Review Letters **122**, 187202 (2019).
17. B. Musicó, Q. Wright, T.Z. Ward, A. Grutter, E. Arenholz, D. Gilbert, D. Mandrus, V. Keppens, *Tunable magnetic ordering through cation selection in entropic spinel*, Physical Review Materials (In Press).

Charge inhomogeneity in correlated electron systems: charge order or not

PI: Barrett O. Wells
Department of Physics and Institute of Materials Science
University of Connecticut, Storrs, CT 06269-3046
barrett.wells@uconn.edu

Program Scope

The goal of this program is to develop an understanding of how and why conduction electrons arrange themselves in correlated electron systems, with particular emphasis on superconducting and closely related materials. Our strategy is to explore materials in which dopants can be controlled in a manner that leads to interesting properties. A primary path towards this goal is to compare the properties of similar compounds doped with highly mobile oxygen defects versus static cation substitutions. While charge and spin order are common in both, doping via oxygen defects often leads to electronic phase separation. In the cases we study, oxygen can be incorporated topotactically, at lower temperatures within an already formed crystalline network.

The systems we study include unconventional superconductors and related materials, mostly transition metal oxides. We have a long running interest in the unique cuprate superconductor $La_{2-x}Sr_xCuO_{4+y}$, co-doped with both Sr on La sites and excess oxygen. Samples with adequate excess oxygen spontaneously phase separate into lower doped, stripe-like magnetic phases and non-magnetic high T_C superconducting phases. In some sense, the separated regions are notably pure examples of each phase making an interesting test-bed for new developments on the cuprates. We also investigate related compounds, looking for universal properties in doped Mott insulators and related strongly correlated metals. This has led to studies of 214 nickelates, 113-perovskite cobaltates that also can be charge doped though either cation substitution or oxygen defect formation.

Recent Progress

The study of a given type of compound with differing dopants has two distinct advantages. One is that studying samples with the same overall charge doping level achieved by using different mixtures of dopant ions we can specify effects that are purely electronic versus those that depend upon a particular substitution chemistry. Secondly, samples with mobile oxygen dopants often form large scale phase separated regions, often associated with inhomogeneities that only exist over the nanoscale in samples with cation substitutional dopants. This allows for the identification of true ground states and then a marker of features associated with the differing most-stable phases.

Separation of static versus magnetic stripe response (publication #3 below)

The importance of, and connection between, the static charge order found in most cuprate compounds doped near 0.125 holes per Cu ($n_h = 1/8$) and the dynamic magnetism broadly prevalent in the cuprates has been a long standing issue. We present detailed neutron scattering studies of the static and dynamic stripes in the high-temperature superconductor, La_2CuO_{4+y}, which is known to separate into a magnetic phase like the nh-0.125 cation doped 214 compounds and a superconducting phase like optimally doped nh = 0.16 compounds. [1] In this sample we observe that the dynamic stripes do not disperse towards the static stripes in the limit of

vanishing energy transfer. In addition, the rotation away from the Cu-O-Cu bond direction is different for the static and magnetic stripes. The basic result is shown in Fig. 1 below.

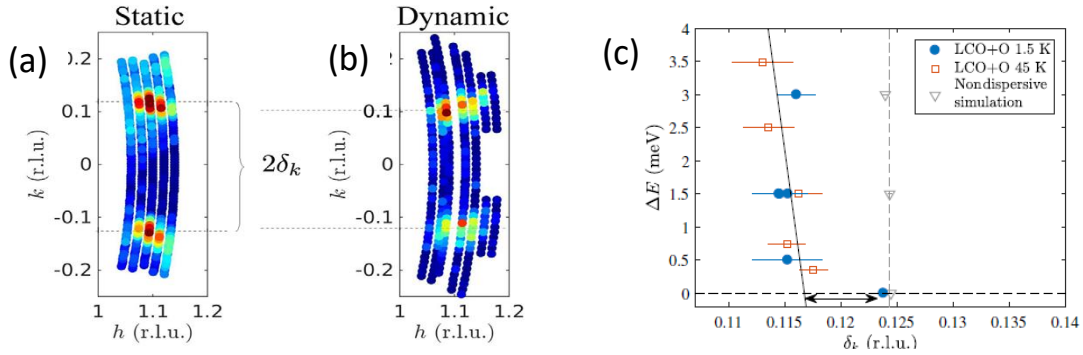

Fig 1. a) and b): Two dimensional intensity maps of the magnetic scattering in La2CuO4+y for the elastic (static) case (a) and the inelastic (dynamic) case with DE = 1.5 meV.
c. A summary of the measured magnetic dispersion at two temperatures, above and below TC. The zero energy transfer peak is only present in the low temperature data set and does not align with the inelastic dispersion.

Therefore, the dynamic stripes observed in neutron scattering experiments are not the Goldstone modes associated with the broken symmetry of the simultaneously observed static stripes. Our analysis indicates that the signals originate from different domains in the sample. These observations seem to follow from real-space electronic phase separation in the crystal, where the static stripes in one phase are pinned versions of the dynamic stripes in the other, having slightly different periods. Our results explain earlier observations of unusual dispersions in underdoped $La_{2-x}SrxCuO_4$ (x = 0.07) [2] and $La_{2-x}BaxCuO_4$ (x = 0.095). [3]

Charge order in electronically phase separated $La_{2-x}Sr_xCuO_{4+y}$ (Publication #2 below)

Over the past few years charge order (CO) has been found in most cuprate superconductors doped to have 1/8th hole per planar Cu site. [1] An important exception has been La_2CuO_{4+y}, doped with large amounts of excess oxygen. As noted above, this material spontaneously phase separates into non-superconducting regions with stripe-like magnetism and optimally doped superconducting regions. [2] The magnetic regions ought to also have well-developed charge order if the stripe picture holds, but several searches failed to find CO.

Through a careful study of freshly cleaved samples, we have been able to find charge order peaks in a sample of La_2CuO_{4+y}, whose near surface regions was doped close to an overall hole concentration near 1/8th hole per Cu. Samples whose near surface region was doped nearer to 0.16 holes per Cu showed no such charge order peak. Fig. 2 shows a basic q-scan over the peak and the temperature dependence of the intensity. The stripes in this superoxygenated sample have similar ordering temperatures as in other cuprates (both charge and spin), but exist within regions that do not have the structural LTT phase to provide pinning sites for stripe order.

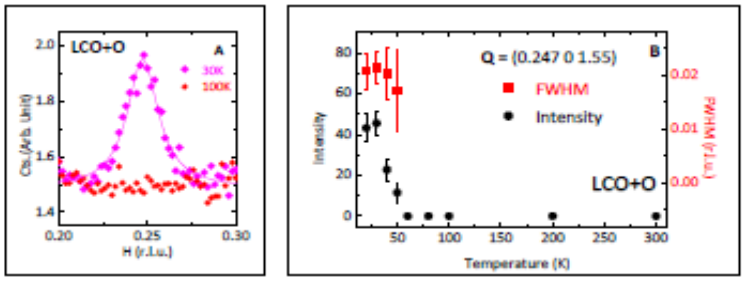

Fig. 2. Left: Q scan over the charge order peak at two temperatures.
Right: temperature dependence of the charge order peak intensity and peak width.

Field Induced Magnetism and Phase Separation in $La_{1.94}Sr_{0.06}CuO_{4+y}$ (in progress)

For some time it has been known that an applied magnetic field induces and continually increases a static magnetic state in cuprates doped near $n_h = 0.125$. [4-6] A long-standing issue has been to understand this effect, with a common explanation that the applied field increases the strength of the magnetism, the local moment, throughout the sample. We have conducted a joint neutron scattering and muon spin rotation measurement of this magnetism in a superoxygenated sample known to be prone to electronic phase separation between a magnetic and optimally doped superconducting state.

The particular sample used in this study was approximately $La_{1.94}Sr_{0.06}CuO_{4.05}$ such that the total hole doping was near the optimal $n_h = 0.16$. At zero field, the sample exhibited little to no static magnetic state by either neutron scattering or muon spin rotation, and was near fully superconducting. Under the application of an applied field, the magnetic neutron signal increased linearly up to the maximum field available of 15T. This is at roughly consistent with the increase in neutron signal seen in $La_{2-x}Sr_xCuO_4$ and related samples, though more linear in field. A piece of the same sample was used in a field-dependent muon spin rotation study. In this case, a static magnetic phase was also induced upon application of a field. The muon data indicate a constant local field and a linearly increasing fraction of the sample that becomes magnetic. Thus, our interpretation is that the increased magnetism under a field is due to an induced phase separation, with the field serving to localize doped holes effectively shifting the samples position in the temperature-doping phase diagram. Fig. 2 below gives the essential muon data and summary plot of the field-induced magnetism.

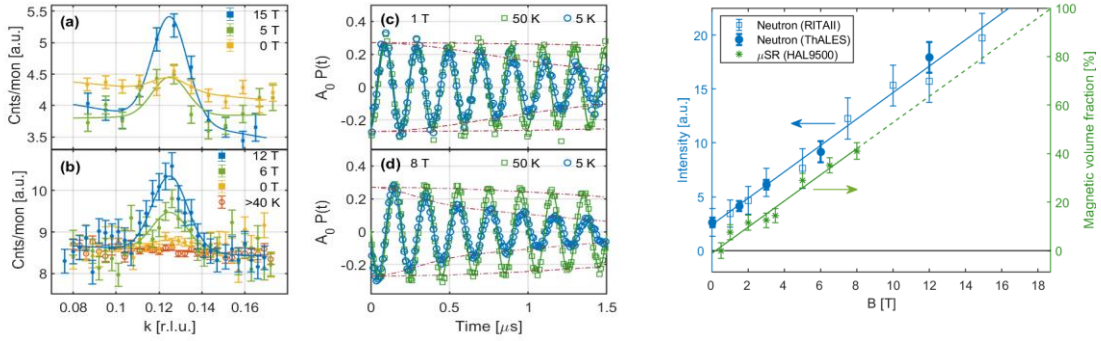

Fig. 3. (a) and (b): Elastic neutron magnetic peak at different fields showing intensity growing with field. (c) and (d): field dependent muon spin rotation profiles at B = 1T (c) and 8 T (d). (e) A summary plot of the neutron intensity versus field and the muon magnetic volume fraction versus field.

Future Plans

We are currently working to finish several manuscripts. One is the joint muon/neutron study of magnetism in the cuprates under an applied field as described above. Another is on the presence of a phonon softening in a superoxygenated cuprate indicating coupling between electrons and dynamic charge stripes. Finally was are working to bring to publication a manuscript on the relationship between charge order and phase separation in the oxygen deficient, doped Mott insulator $SrCoO_{3-y}$.

References

1. Hashini E. Mohottala, et al, *Nature Materials* **5**, 377 (2006).
2. H. Jacobsen, et al., *Phys. Rev. B* **92**, 174525 (2015).
3. Z. Xu, et al., *Phys. Rev. Lett*. **113**, 177002 (2014).
4. B. Lake et al., *Nature* **415**, 299 (2002).
5. A. T. Roemer et al., *Phys. Rev. B* **87**, 144513 (2013).
6. J. Chang, et al., *Phys. Rev. Lett*. **102**, 177006 (2009).
7. Jörg Fink et al., "Phase diagram of charge order in $La_{1.8-x}Eu_{0.2}Sr_xCuO_4$ from resonant soft x-ray diffraction" *Phys. Rev. B* **83**, 092503 (2011).
8. A. Achkar et al., "Nematicity in stripe-ordered cuprates probed via resonant x-ray scattering" *Science* **351**, 576 (2016).
9. C. He et al., "Doping fluctuation-driven magneto-electronic phase separation in $La_{1-x}Sr_xCoO_3$ single crystals" *Europhys. Lett*. **87**, 27006 (2009).
10. Jonathan M. Edge et al., "Quantum Critical Origin of the Superconducting Dome in $SrTiO_3$" *Phys. Rev. Lett.* **115**, 247002 (2015).

Publications

1. F.J. Rueckert, F. Z. He, B. Dabrowski, W. A. Hines, J. I. Budnick, and B. O. Wells "Charge order and phase separation in $SrCoO_3$" under review *Phys. Rev. B*. Web: https://arxiv.org/abs/1707.04336
2. Zhiwei Zhang, William A. Hines, Joseph I. Budnick, R. Sutarto, F. He, F. C. Chou, and B. O. Wells, "Nematicity and Charge Order in Superoxygenated $La_{2-x}Sr_xCuO_{4+y}$" *Phys. Rev. Lett*. 121, 067602 (2018). Web: https://doi.org/10.1103/PhysRevLett.121.067602
3. H. Jacobsen, S. L. Holm, M.-E. Lăcătuşu, A. T. Rømer, M. Bertelsen, M. Boehm, R. Toft-Petersen, J.-C. Grivel, S. B. Emery, L. Udby, B. O. Wells, and K. Lefmann, "Distinct Nature of Static and Dynamic Magnetic Stripes in Cuprate Superconductors" *Phys. Rev. Lett*. 120, 037003 (2018). Web: https://doi.org/10.1103/PhysRevLett.120.037003
4. P. J. Ray, N. H. Andersen, T. B. S. Jensen, H. E. Mohottala, Ch. Niedermayer, K. Lefmann, B. O. Wells, M. v. Zimmermann, F. C. Chou, and L. Udby, "Staging superstructures in high-Tc Sr/O co-doped $La_{2-x}Sr_xCuO_{4+y}$" *Phys. Rev. B* **96**, 174106 (2017). Web: https://doi.org/10.1103/PhysRevB.96.174106
5. Zhiwei Zhang, William A. Hines, Joseph I. Budnick, David M. Perry, and Barrett O. Wells, "Direct evidence for the source of reported magnetic behavior in "CoTe"" *AIP Advances* **7**, 125322 (2017). Web: https://doi.org/10.1063/1.4997161

Two works in progress as noted in the text.

Imaging Electron Motion in 2D Materials

PI: Robert M Westervelt
Co-PI: David Bell
John A Paulson School of Engineering and Applied Sciences
Harvard University, Cambridge MA 02138

Program Scope

The goal of our research program is to image the motion of electrons in 2D materials using a liquid-He cooled scanning probe microscope (SPM). Using this approach, we can track the ballistic paths of electrons (and holes) in graphene. We can also identify, locate, and characterize quantum dots formed by gates or disorder.

To image an electron trajectory, we use capacitive coupling to an AFM tip to deflect the electron path as it flows between two point-contacts, causing it to miss the second contact. An image is obtained by displaying the change in conductance *vs.* tip position. We can also locate and characterize a quantum dot that holds an integer number of electrons in the Coulomb blockade regime, by using tip motion to move electrons on or off the dot. The image dot conductance shows a bullseye pattern of Coulomb blockade conductance peaks *vs.* tip position, and their radial spacing determines the physical size of the dot.

Recent Progress

Imaging Andreev Reflection in Graphene from a Superconducting Contact

An important goal for quantum information science is to find ways to coherently transport quantum information from one place to another. Andreev scattering provides a way to coherently transmit electrons through a normal (N) metal via collisions with a superconducting (S) contact. An electron from the normal metal that arrives at the contact is reflected as a hole and also transmits a Cooper pair into the superconductor. Graphene provides an attractive alternative to conventional metals, because it is extraordinarily thin and strong, and because electrons travel ballistically over comparatively long distances.

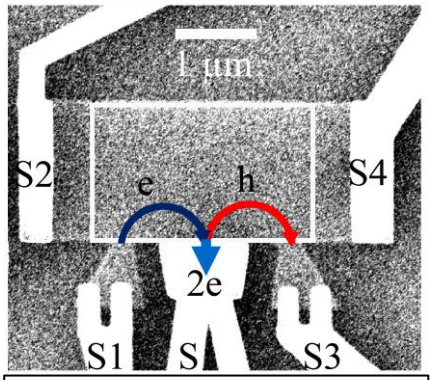

Fig. 1 SEM image of graphene sample with superconducting contacts showing Andreev scattering of an electron into a hole.

We have used our cooled scanning probe microscope to image Andreev scattering in graphene from a superconducting sample. (Bhandari et al. 2019). Figure 1 shows a graphene sample with superconducting contacts. Magnetic focusing in a perpendicular magnetic field B is used to define cyclotron orbits for electrons (and holes)

traveling between three point-contacts along the lower side. Andreev scattering of an electron into a hole in the graphene is illustrated by the blue and red trajectories.

SPM Images of Andreev scattering in graphene are shown in Fig. 2. Magnetic focusing of electrons into cyclotron orbits that travel between the two outer contacts is shown in the top panel. The tip scatters electrons to reduce their flow (red), and no Andreev scattering is observed. On the second magnetic focusing peak at twice the magnetic field, the bottom panel shows Andreev scattering from the center superconducting contact. Electrons are transformed into holes, and the tip now increases the flow of electrons (blue) by scattering holes. When superconductivity is destroyed by going above the critical temperature T_c, Andreev scattering disappears, and the tip-imaged flow of holes (blue) changes a flow of electrons (red).

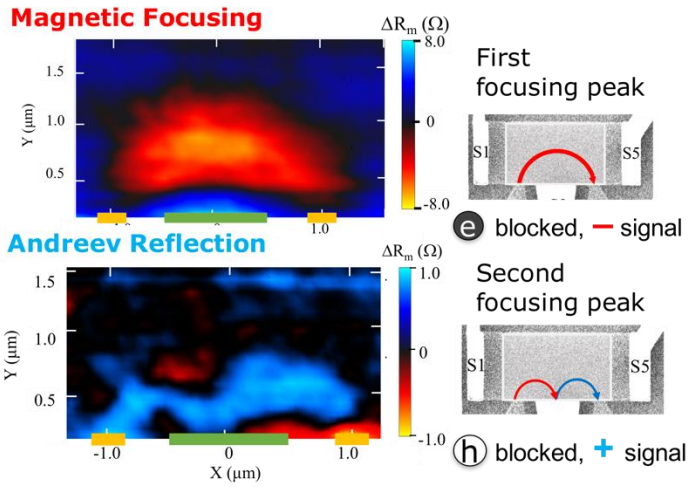

Fig. 2 (top) Cooled SPM image of electron flow on the first magnetic focusing peak that shows a cyclotron orbit connecting the two outer contacts. The tip reduces the transmission (red) by scattering electrons. (bottom) SPM image of flow between the outer contacts on the second focusing peak, where Andreev reflection has converted the electrons into holes. The tip now increases transmission of electrons (blue) by scattering holes.

Collimating Contacts in Graphene for Electrons, and for Holes

Graphene opens the way for ballistic electrons, where electrons (or holes) travel along predictable trajectories within a device. However, electrons enter graphene at all possible angles from a conventional contact. To create a beam of electrons traveling in one direction, we have developed a collimating contact, shown in Fig. 3. Of the electrons emitted into graphene at the narrow end, only those traveling straight ahead enter the device, electrons at larger angles are absorbed by the grounded zigzag-shaped contacts along the sides. Collimation can be turned off by floating the zigzag side contacts.

Images of electron flow through graphene as they travel from the top to bottom contact demonstrate how collimation occurs. Figure 4 presents an array of images vs. magnetic field *B* and electron density *n* for the collimated and uncollimated cases. Bending of the trajectories by the magnetic field provides a measure of the angular width of the electron beam emitted by the contact – when the beam misses the lower contact, the image disappears. For the uncollimated contact, the electron beam is quite wide – analysis shows that it covers an angular half width

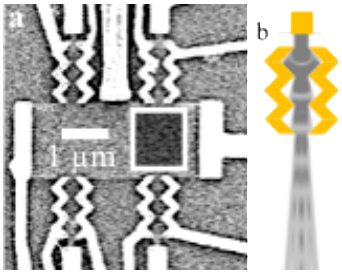

Fig. 3 (a) SEM image of hBN encased graphene device with 4 collimating contacts (b) Ray tracing simulation of a collimating contact.

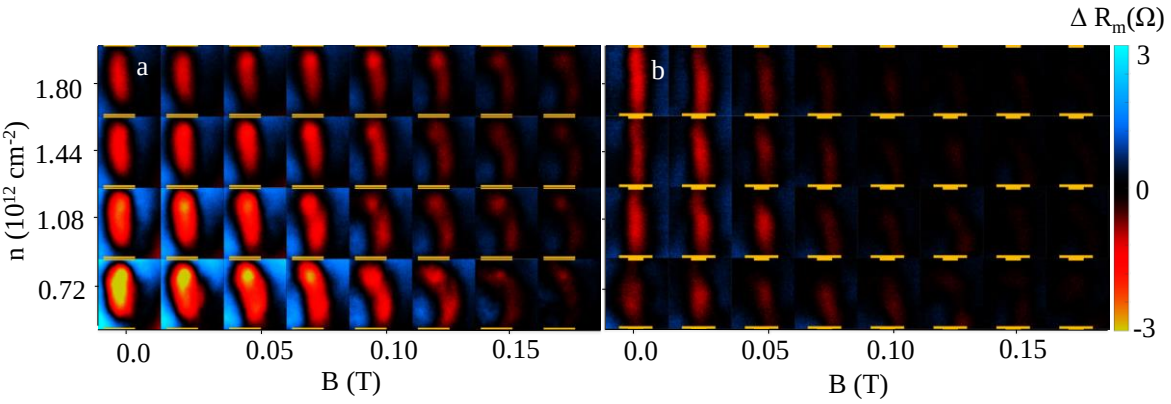

Fig. 4 (a) Cooled Scanning Probe Microscope Images of electron flow between the top and bottom contacts (white box) at 4.2K. (a) Electron flow with collimation turned off (b) Electron flow for a collimating Contact. (Bhandari et al. 2D Materials 5(2), 021003 (2018)).

54°. However, when collimation is turned on, the images disappear at much smaller *B* fields and the angular half width is reduced to 9°. The ability to image the electron flow using our cooled SPM will open the way to the design of electronic devices based on electron beams, a bit like vacuum tubes.

The collimating contact can also inject a narrow beam of holes into graphene (Bhandari *et al.* 2019). Figure 5 presents an array of images of electron flow between the top and bottom contacts vs. magnetic field *B* and density, along with a corresponding set of simulated images. The data and simulations agree quite well. The SPM tip acts to focus the flow of holes downstream. The focusing creates blue regions of high flow in the images when the tip directs holes into the receiving contact, and red images of low flow when the B field bends them away.

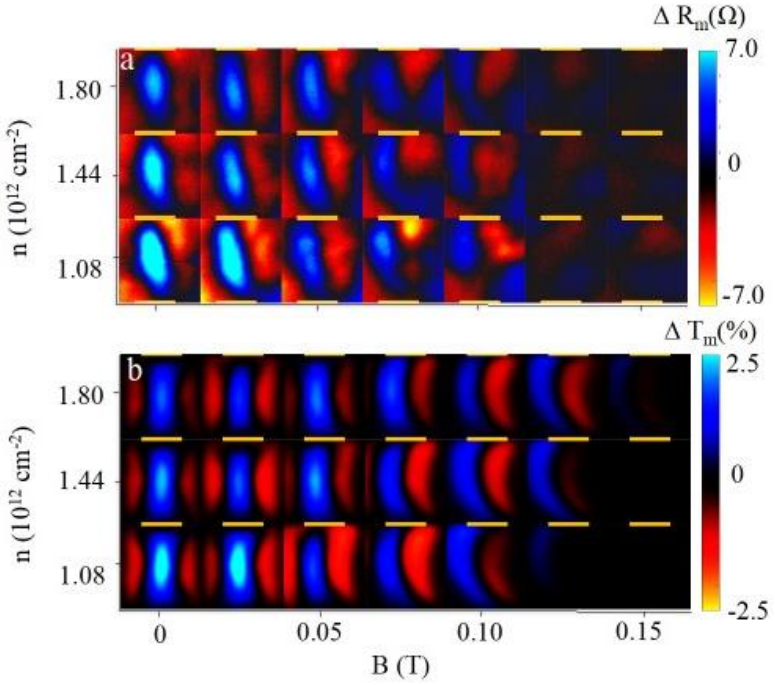

Fig. 5 (top) experimental at 4.2K and (lower) simulated images of hole flow through graphene between the top and bottom contacts. A magnetic field *B* curves hole paths away from the bottom contact.

Future Plans

We plan to direct our experiments in a new direction: imaging electron jets in graphene. Recent experiments (Ma *et al.* 2019) and theory (Lewandowski and Levitov 2018) on photoexcited graphene have shown that the relaxation of hot electrons can form jets directed in a

particular direction determined by the edge geometry. When the Fermi energy lies above the Dirac point, electron-electron scattering typically pushes electrons to the side. However, when the Fermi energy touches the Dirac point, energy relaxation can only occur along a line that maintains the original direction, producing a directed jet of electrons. Using our cooled SPM, we plan to image electron jets in graphene devices shaped to form jets in well-defined directions.

References

Sagar Bhandari, Mary Keenan Kreidel, Gil-Ho Lee, Kenji Watanabe, Takashi Taniguchi, Philip Kim, Robert M. Westervelt, "Imaging Hole Motion in Graphene," (2019).

Sagar Bhandari, Gil-Ho Lee, Kenji Watanabe, Takashi Taniguchi, Philip Kim, Robert M. Westervelt, "Imaging Andreev Reflection in Graphene", (2019).

Cyprian Lewandowski, L. S. Levitov, "Photoexcitation Cascade and Quantum-Relativistic Jets in Graphene," Phys. Rev. Lett. **120**, 076601 (2018).

Qiong Ma, Chun Hung Lui, Justin C. W. Song. Yuxuan Lin, Jian Feng Kong, Yuan Cao, Thao H. Dinh, Nityan L. Nair, Wenjing Fang, Kenji Watanabe, Takashi Taniguchi, Su- Yang Xu, Jing Kong, Tomás Palacios, Nuh Gedik, Nathaniel M. Gabor, Pablo Jarillo-Herrero, "Giant intrinsic photoresponse in pristine graphene," Nature Nanotechnology **14**, 145-150 (2019).

Publications

1. Sagar Bhandari and Robert M. Westervelt, "Imaging Electron Motion in Graphene," Special Issue *Hybrid Quantum Materials and Devices*, Semiconductor Science and Technology, Vol. 32 No. 2 (IOP Science, 2017) doi:10.1088/1361-6641/32/2/024001.

2. Sagar Bhandari, Gil-Ho Lee, Philip Kim and Robert M. Westervelt, "Analysis of Scanned Probe Images of Magnetic Focusing in Graphene," Proc. Int. Conf. Superlattices, Nanostructures and Nanodevices (ICSNN 2016), Hong Kong, Journal of Electronic Materials 46(7), 3827-3841 (2017), doi: 10.1007/s11664-017-5350-y.

3. Sagar Bhandari, Andrew Lin, Robert M. Westervelt, "Investigating the Transition Region in Scanned Probe Microscope Images of the Cyclotron Orbit in Graphene," Proc. Int. Conf. on Nanoscience and Technology (ICN+T), Busan, Korea, J. Nanoelectronics and Optoelectronics 12(9), 952-955 (2017), doi: 10.1166/jno.2017.2158.

4. Sagar Bhandari, Ke Wang, Kenji Watanabe, Takashi Taniguchi, Philip Kim and Robert M. Westervelt, "Imaging Electron Motion in a Few Layer MoS_2 Device," Proc Int. Conf. Physics of Semiconductors, Beijing, China (ICPS 2016), J. Phys.: Conf. Ser. 864(1), 012031 (2017), doi:10.1088/1742-6596/864/1/012031.

5. Sagar Bhandari, Ke Wang, Kenji Watanabe, Takashi Taniguchi, Phillip Kim, Robert M. Westervelt, "Imaging Quantum Dot Formation in MoS_2 Nanostructures", Nanotechnology 29(42), (2018); doi: 10.1088/1361-6528/aad79f

6. Sagar Bhandari, Gil-Ho Lee, Kenji Watanabe, Takashi Taniguchi, Philip Kim, Robert M. Westervelt, "Imaging Electron Flow from Collimating Contacts in Graphene," 2D Materials 5(2), 021003 (2018), doi: 10.1088/2053-1583/aab38a.

Spin Orbit Torque in Ferromagnet/Topological-Quantum-Matter Heterostructures

John Q. Xiao[1], Branislav Nikolic[1], Stephanie Law[2], and Matt Doty[2]
[1]Department of Physics and Astronomy, [2]Department of Materials Science Engineering, University of Delaware, Newark, DE 19716.

Program Scope

The major goals of the project are: (1) to develop ferromagnet and ferromagnet insulator FM(i)/topological insulator (TI) heterostructures; (2) to system investigate and understand spin orbit torque (SOT) in TI/FM with in-plane magnetization and FMi/TI with PMA; (3) Use X-ray in Advance Photon Source (APS) in Argonne National Lab (ANL) to investigate the electronic and magnetic structures in FM(i)/TI systems; (4) to use our novel time-resolved low-temperature electrical pump-optical probe instrument to investigate spin dynamics and magnetization switching behaviors; (5) to calculate SOT and spin dynamics in the TI/FM systems we explore experimentally and use the results to identify promising new structures for experimental investigation.

Recent Progress

During this research period we have worked on achieving all 5 goals listed above. We briefly summarize them below, followed by more details on results to be reported in PI meeting.

1. We have demonstrated that growing Bi_2Se_3 TI thin films on lattice-matched trivially-insulating $(Bi_{1-x}In_x)_2Se_3$ buffer layers reduces the trivial carrier density while simultaneously increasing carrier mobility. We have grown quality GaAs//Bi_2Se_3/FM (CoFeB, NiFe) films which lead to large second harmonic signals and allow us to implement bias-dependence studies.
2. There are two most important experimental findings in this research period: (a) we are close to identify the contributions to observed large second harmonic signals and (b) we have established the linear relationship between the second harmonic signal and quantum coherence length of TI.
3. We have performed X-ray synchrotronic studies using Advance Photon Source at Argonne National Lab (ANL) on TmIG/Bi_2Se_3 and TmIG/Pt bilayers. We have not observed magnetic proximity effect at the interface in TmIG/Bi_2Se_3. However, we have identified interesting interfacial phenomena in TmIG/Pt bilayers, reflecting magnetization compensation in TmIG, related spin Hall magnetoresistance, and interesting spin configurations in TmIG.
4. We have developed a theory of spin pumping in ferromagnet/topological-insulator heterostructures with precessing magnetization. This makes it possible to compute the effective spin mixing conductance that is often extracted in experiments, but it cannot be computed from standard scattering theory that is applicable only in the absence of strong spin-orbit coupling effects at the interface. We have also demonstrated first-principles quantum transport computation of spin-orbit torque in realistic ferromagnet/monolayer-spin-orbit-material, which is computationally less expensive than ferromagnet/topological-insulator system and it allows us to tune the formalism. Our screening over several bilayer combinations shows that Co/WSe_2 is the optimal combination which maximizes spin-orbit torque. We have also demonstrated how to extract the full angular dependence of spin-orbit torque beyond standard field-like and antidamping-like components.

In the following, we present more details on two important experimental findings: i.e. (a) the contributions to second harmonic Hall signal (SHH) and (b) the linear relationship between SHH and quantum coherence length of TI; and on theory development.

With quality GaAs//Bi_2Se_3/CoFeB films, we have observed large SHH at various temperatures as shown in Figure 1. These SHHs are traditionally used to extract SOTs where 1/H dependence at above 70K is due to field-like (FL) SOT (τ_{FL}) and the offset ($V_y^{2\omega}$), as indicated in Figure 1(b), is due to damping-like (DL) SOT (τ_{DL}). Based on this approach, we can conclude that τ_{FL} is observed at T > 70K and a large τ_{DL} is observed at T < 70K. The later also becomes pronounced for thin Bi_2Se_3 layer less than 8 nm and is attributed to TI surface states (TSS). Further, the extracted SOT efficiency ranges from 0.5 to 50, a huge improvement over that observed in heavy metals such as W, Pt, which have SOT efficiency of about 0.07.

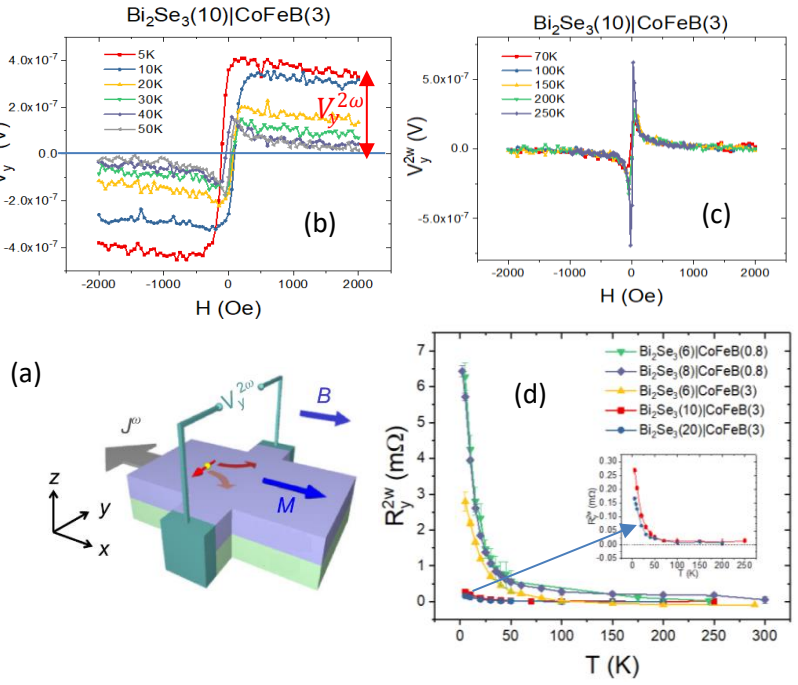

Figure 1, (a) schematics for second harmonic Hall measurements; (b) and (c) second harmonic Hall measurements of GaAs//Bi_2Se_3(10nm)/CoFeB(3nm) samples at different temperatures and (d) the temperature dependence of second harmonic resistance. The inset enlarges the results of samples with Bi_2Se_3 thickness of 10 and 20nm.

Most recently, it is argued that the large $V_y^{2\omega}$ could also arise from magnon scattering. To identify the origin, we performed detailed high field study and the results are presented in Figure 2. We do not observe 1/H dependence as predicted by SOT model. Instead, $V_y^{2\omega}$ remains to be constant up to 1T and decreases linearly with field at above 1T. These results suggest the existence of magnon scattering. However, we could not rule out the contributions from SOT. The ideal tool to confirm and separate these two contributions is MOKE based spin orbit torque magnetometer, which only measures the magnetization reorientation and is independent of magnon scattering. Such a measurement is currently underway.

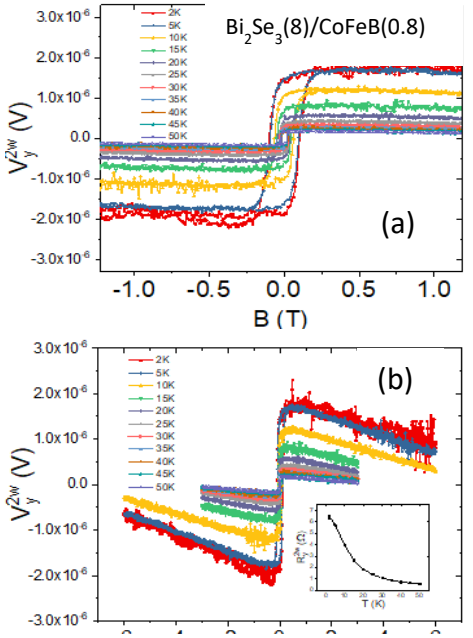

Figure 2, SHHs as function of the magnetic field up to (a) 1T and (b) 6T at various temperatures for Bi_2Se_3(8)/CoFeB(0.8) sample. The inset shows the temperature dependence of the second harmonic Hall resistance.

Regardless the contributions to $V_y^{2\omega}$, the detailed contribution from TI remains elusive. For example, if there is SOT contribution, why there is overwhelming τ_{DL} instead of τ_{FL} which is more expected from spin-momentum locking of TSS. On the other end, if there is large asymmetric magnon scattering of Dirac fermions on TSS, why SHH is so strong and persistent in TI as thin as 6nm where the bottom and top surfaces are believed to be coupled. To address these questions, we carefully look at the relationship between SHH and the coherence length of TI.

The quantum coherence length (l_ϕ) can be extracted from weak antilocalization (WAL) measurement as shown Figure 3 (a) and (b). The relationship between second harmonic Hall resistance and coherence length is shown in Figure 3 (c). It is first time that a linear relationship is observed. Several addition features can also be revealed with close examination of the results: (1) while there appears no major difference in $l_\phi(T)$ for TIs of different thickness, there seems to have two regions with very different slopes, separating thin (≤8nm) and thick (>10nm) TIs in linear dependence between $R^{2\omega}$ and l_ϕ; (2) the extracted critical $l_\phi(R^{2\omega} = 0)$is much larger than the TI thickness. Is this the criteria for coupled 2 conducting channels as we extracted from WAL measurements (not shown)? Is two conducting channels arises from two surface states or surface+bulk of TI? We are currently performing theoretical studies to gain insights of these phenomena.

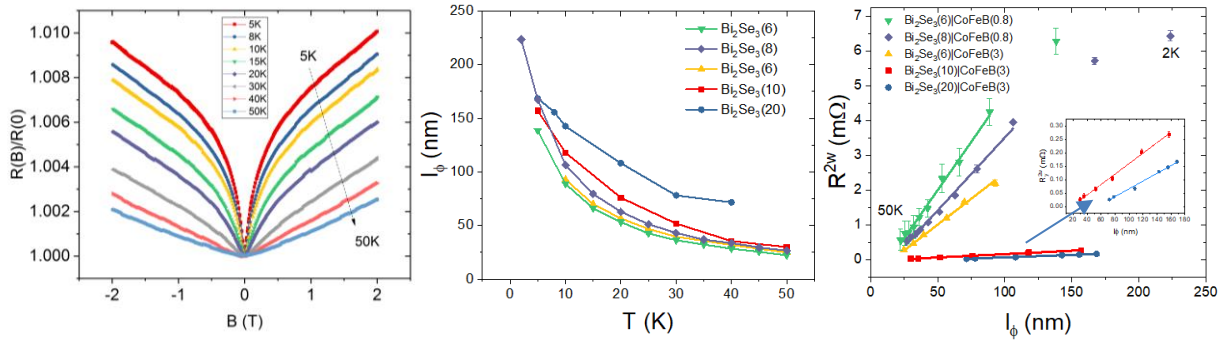

Figure 3, (a) magnetoresistance for Bi_2Se_3(10nm) showing weak antilocalization effect, (b) extracted coherence length as a function of the temperature, and (c) the linear relationship between second harmonic Hall resistance and coherence length for various TI/FM samples.

Future Plans

We will perform low temperature MOKE studies to confirm and separate the SOT contributions to second harmonic Hall signal, understand the origin of the linear relationship between the second harmonic Hall signal and coherence length of TI, and disseminate results via publications and talks. We will extend the investigation in GGG//Bi:TmIG/TI. Particularly, we will measure the coherence length of TI on Bi:TmIG via weak antilocalization measurements and SOT behavior via MOKE spin torque magnetometer. We will attempt to establish the relationship between SOT and coherence length, determine the compensation temperatures of magnetization (T_M) and angular moment (T_A) via MOKE technique and FMR measurements, and SOT behaviors across T_M and T_A.

We will continue to write beam proposal to access synchrotron X-ray beam time in APS. Collaborating with beamline scientist we will attempt to perform dynamic measurements.

We will compute angular dependence of spin-orbit torque components in ferromagnet/topological-insulator (such as Co/Bi_2Se_3) and ferromagnet/Weyl-semimetal (such as Py/WTe_2) bilayers. Motivated by the recent discovery of two-dimensional ferromagnets, such as CrI_3 or $Cr_2Ge_2Te_6$, we will also calculate spin-orbit torque on them in the presence of topological insulator, which could provide systems with minimal dissipation for spin-orbit torque operated devices.

Publications

1. Y. Wang, T.P. Ginley, C. Zhang, S. Law, "*Transport properties of $Bi_2(Se_{1-x}Te_x)_3$ thin films grown by molecular beam epitaxy*", J. Vac. Sci. Technol. B 35, 02B106, 2017.
2. K. Dolui, B.K. Nikolic, "*Spin-memory loss due to spin-orbit coupling at ferromagnet/heavy-metal interfaces: Ab initio spin-density matrix approach",* PRB**96**, 22, 220403(R), 2017.
3. J. M. Marmolejo-Tejada, K. Dolui, P. Lazic, P.-H. Chang, S. Smidstrup, D. Stradi, K. Stokbro, and B. K. Nikolic, "*Proximity band structure and spin textures on both sides of topological-insulator/ferromagnetic-metal interface and their transport probes*", Nano Lett, 17, 9, 5626, 2017.
4. Wang, Y., Ginley, T., and Law, S. "*Growth of high-quality Bi_2Se_3 topological insulators using $(Bi_{1-x}In_x)_2Se_3$ buffer layers*" J. Vac. Sci. Tech. B, 36, 02D101 (1/30/2018). *Selected as an Editor's Pick*
5. Ginley, T., Wang, Y., Wang, Z., and Law, S. "Dirac plasmons and beyond: the past, present, and future of plasmonics in 3D topological insulators" MRS Comm, 8, 782-794 (2018).
6. Wang, Y. and Law, S. "Optical properties of $(Bi_{1-x}In_x)_2Se_3$ thin films" Optical Materials Express, 8, 2570-2578 (2018). *Selected as an Editor's Pick.*
7. Branislav K. Nikolic, Kapildeb Dolui, Marko D. Petrovic, Petr Plechác, Troels Markussen, and Kurt Stokbro, "*First-Principles Quantum Transport Modeling of Spin-Transfer and Spin-Orbit Torques in Magnetic Multilayers"* Chapter in Handbook of Materials Modeling, W. Andreoni and S. Yip (Eds), Springer, Cham, 2019.
8. H. Celik, H. Kannan, T. Wang, A.R. Mellnik, X. Fan, X. Zhou, D.C. Ralph, M.F. Doty, V.O. Lorenz, and J.Q. Xiao, "*Vector-Resolved Magnetooptic Kerr Effect Measurements of Spin-Orbit Torque",* IEEE Transactions on Magnetics, 55, 1, 4100105, 2019.
9. K. Dolui, U. Bajpai and B. K. Nikolic, Spin-mixing conductance of ferromagnet/topological-insulator and ferromagnet/heavy-metal heterostructure: A first-principles Floquet-nonequilibrium Green function approach, arXiv:1905.01299 (2019).
10. Xinran Zhou, Hang Chen, Yu-Sheng Ou, Tao Wang, Rasoul Barri, Harsha Kannan, John Q. Xiao, and Matthew F. Doty, *Investigation of spin orbit torque driven dynamics in ferromagnetic heterostructures",* submitted to J. of Magn. Mat. Mat. 2019.

QPress: Quantum Press for Next-Generation Quantum Information Platforms

Amir Yacoby, Harvard University (Principal Investigator)

Philip Kim, Harvard University (Co- Investigator)

Tim Kaxiras, Harvard University (Co- Investigator)

William Wilson, Harvard University (Co- Investigator)

Joseph Checkelsky, MIT (Co- Investigator)

Pablo Jarillo-Herrero, MIT (Co- Investigator)

Alán Aspuru-Guzik, University of Toronto (Co- Investigator)

Program Scope

This program aims to develop the fundamental science of layered materials and the QPress- an approach for making new layered material structures by stacking constituent component 2D materials. As shown in Fig. 1, this involves developing DFT methods for predicting and understanding 2D materials, synthesis of high quality source materials for 2D layers, developing the science of assembling 2D stacks, characterizing 2D materials, and machine learning / AI techniques to accelerate the materials process, all of which are currently being performed.

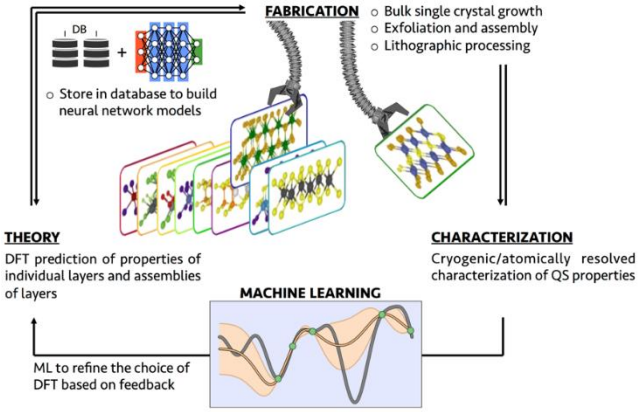

Figure 1 – Iterative process of QPress

Recent Progress

We have made progress in a number of directions in the QPress project. From the viewpoint of DFT, one achievement has been the characterization of a new type of dislocation relevant for isolated 2D sheets: a "ripplocation" (*1*). As shown in Fig. 2, the dominant defects in a typical 2D material such as MoS_2 have been studied from quantum mechanical calculations based on DFT. A surprising result is that the dominant S vacancy which can arise in terms of energetic favorability is charge neutral. This is

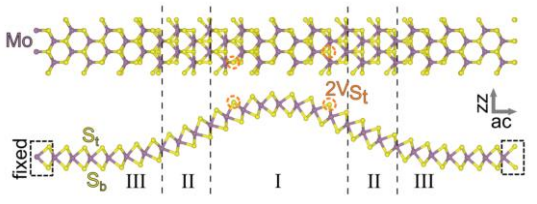

Figure 2 – Ripplocation in MoS_2

important for understanding the types of defects which may arise with the exfoliation and manipulation of 2D sheets.

From the viewpoint of accelerated characterization of 2D materials, we have also made significant advances in deep-learning based optical identification of 2D materials (*2*). As shown in Fig. 3(a), we have studied a variety of layered materials which upon mechanical exfoliation (Fig. 3(b)) we have imaged optically (Fig. 3(c)). We use information about these materials determined with other techniques in terms of layer thickness to train a neural network to analyze new images. These images are fed in to a neural network (Fig. 3(d)) which can then output the expected material and layer thickness. We found a fidelity above 90% for this process, suggesting its implementation may rapidly accelerate the identification of target layers.

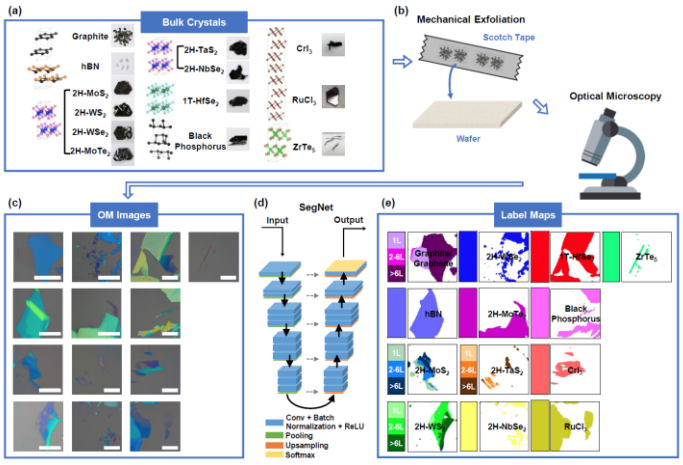

Figure 3 – Depiction of deep-learning driven optical identification of 2D materials.

In terms of improving 2D materials, we have developed a new commensurate superlattice transition metal dichalcogenide (TMD) $Ba_3Nb_5S_{13}$ (*3*), shown as viewed from cross-sectional TEM in Fig. 4. This bulk single crystal material realizes a commensurate superlattice of hexagonal NbS_2 monolayers and insulating Ba_6NbS_8 spacer layers. Unlike previously studied misfit layer compounds, there is a commensurate relationship between the two lattices, leading to a high degree of electronic quality. This material is also a superconductor, and realizes clean limit superconductivity not previously observed for the TMD class. This suggests a larger class of high quality TMDs may be possible to develop.

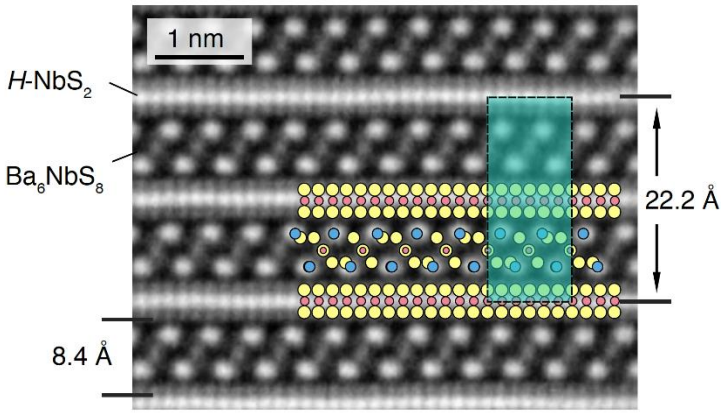

Figure 4 – Cross sectional TEM image of $Ba_3Nb_5S_{13}$.

Future Plans

Our future plans include the continued development of advanced DFT for 2D materials, with a focus on implementing machine learning methods to accelerate such calculations. We will also work on the development of advanced characterization toward the identification of methods

to probe topological superconductors. We will continue the development of high quality 2D source materials. We will also continue to collaborate with Brookhaven National Laboratory on their development of the QPress tool.

References

1. G. A. Tritsaris, M. G. Şensoy, S. N. Shirodkar, E. Kaxiras, First-principles study of coupled effect of ripplocations and S-vacancies in MoS2. *Journal of Applied Physics*. **126**, 084303 (2019).

2. B. Han, Y. Lin, Y. Yang, N. Mao, W. Li, H. Wang, V. Fatemi, L. Zhou, J. I.-J. Wang, Q. Ma, Y. Cao, D. Rodan-Legrain, Y.-Q. Bie, E. Navarro-Moratalla, D. Klein, D. MacNeill, S. Wu, W. S. Leong, H. Kitadai, X. Ling, P. Jarillo-Herrero, T. Palacios, J. Yin, J. Kong, Deep Learning Enabled Fast Optical Characterization of Two-Dimensional Materials. *arXiv:1906.11220 [cond-mat, physics:physics]* (2019) (available at http://arxiv.org/abs/1906.11220).

3. A. Devarakonda, H. Inoue, S. Fang, C. Ozsoy-Keskinbora, T. Suzuki, M. Kriener, L. Fu, E. Kaxiras, D. C. Bell, J. G. Checkelsky, Evidence for clean 2D superconductivity and field-induced finite-momentum pairing in a bulk vdW superlattice. *arXiv:1906.02065 [cond-mat]* (2019) (available at http://arxiv.org/abs/1906.02065).

Publications

1. G. A. Tritsaris, M. G. Şensoy, S. N. Shirodkar, E. Kaxiras, First-principles study of coupled effect of ripplocations and S-vacancies in MoS2. Journal of Applied Physics. 126, 084303 (2019).

2. B. Han, Y. Lin, Y. Yang, N. Mao, W. Li, H. Wang, V. Fatemi, L. Zhou, J. I.-J. Wang, Q. Ma, Y. Cao, D. Rodan-Legrain, Y.-Q. Bie, E. Navarro-Moratalla, D. Klein, D. MacNeill, S. Wu, W. S. Leong, H. Kitadai, X. Ling, P. Jarillo-Herrero, T. Palacios, J. Yin, J. Kong, Deep Learning Enabled Fast Optical Characterization of Two-Dimensional Materials. arXiv:1906.11220 [cond-mat, physics:physics] (2019) (available at http://arxiv.org/abs/1906.11220).

3. A. Devarakonda, H. Inoue, S. Fang, C. Ozsoy-Keskinbora, T. Suzuki, M. Kriener, L. Fu, E. Kaxiras, D. C. Bell, J. G. Checkelsky, Evidence for clean 2D superconductivity and field-induced finite-momentum pairing in a bulk vdW superlattice. arXiv:1906.02065 [cond-mat] (2019) (available at http://arxiv.org/abs/1906.02065).

August, 2019

Novel SP^2-bonded Materials and Related Nanostructures

PI: Alex Zettl, Lawrence Berkeley National Laboratory and UC Berkeley. Co PI's: Marvin Cohen, Lawrence Berkeley National Laboratory and UC Berkeley; Michael Crommie, Lawrence Berkeley National Laboratory and UC Berkeley; Alessandra Lanzara, Lawrence Berkeley National Laboratory and UC Berkeley; Steven Louie, Lawrence Berkeley National Laboratory and UC Berkeley

Program Scope

Experimental and theoretical investigation of nanostructures based on sp^2-bonded carbon and boron nitride, and related layered or low-D materials. Experimental approaches encompass synthesis, and characterization utilizing STM, AFM, ARPES, TEM, transport, and mechanical properties. Theory includes ab-initio approaches.

Recent Progress

We have expanded our investigation of the few-chain limit of quasi–one-dimensional transition metal trichalcogenides (TMTs). The chains are created by vapor transport growth within the hollow cores of carbon and BN nanotubes which prevent oxidation, facilitate characterization, and can serve as charge transfer media. Our initial study of NbSe3[1] found static and dynamic structural torsional waves not found in bulk $NbSe_3$ crystals. We have investigated the related TMT compound $HfTe_3$ via high resolution transmission electron microscopy and band structure calculations[2]. Interestingly, $HfTe_3$ does not display the long-wavelength torsional wave that occurs in $NbSe_3$. Unexpectedly, for $HeTe_3$ there occurs a metal-insulator transition at critical chain number n=4, i.e. the system is metallic only when 4 or more chains are present.

We have locally confined and characterized massive Dirac Fermions within bilayer graphene quantum dots defined by circular p-n junctions through the use of scanning tunneling microscopy (STM)-based methods[3]. The p-n junctions are created via a flexible technique that enables realization of exposed quantum dots in bilayer graphene/hBN heterostructures. The quantum dots exhibited sharp spectroscopic resonances that disperse in energy as a function of applied gate voltage. Spatial maps of these features showed prominent concentric rings with diameters that can be tuned by an electrostatic gate. This behavior is

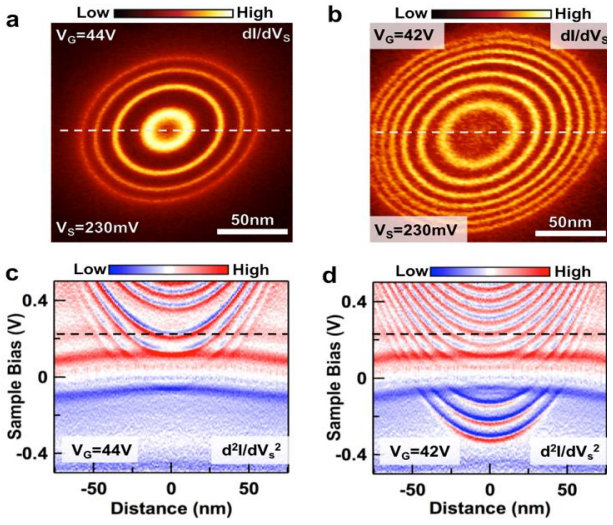

Fig. 1. dI/dV map of electronic states in bilayer graphene trapped in a p-n junction created by an STM tip. From Ref. 3.

explained by single-electron charging of localized states that arise from the quantum confinement of massive Dirac Fermions within our exposed bilayer graphene quantum dots. Using a combination of scanning tunneling spectroscopy measurements and theoretical modeling, we have also characterized how graphene's massless charge carriers screen individual charged calcium atoms[4]. A backgated graphene device allows direct visualization of how the screening length for a single charged atom on graphene is tuned by carrier density. These results provide insight into electron-impurity and electron-electron interactions in a relativistic setting and have significant consequences for other graphene-based electronic devices.

Hexagonal boron nitride (h-BN) can be successively stacked in sheets, but virtually all synthesis methods for h-BN lead to the so-called AA' stacking sequence. Of great theoretical and experimental interest are potential alternative stacking sequences for h-BN. We have theoretically examined the atomic and electronic properties of all possible distinct stacking sequences for h-BN. The cohesive energy, electronic band structure, and dielectric response tensor are investigated[5]. This complements our experimental discovery of methods to reliably grow, using CVD, large area AB-stacked h-BN[5].

Future Plans

In van der Waals heterostructure Moire superlattices, the electronic band structures can be easily varied by changing the twist angle, leading to flat bands formation, enhanced Coulomb interaction, Mott like insulating states and even superconductivity. While several theoretical predictions exist to date on the evolution of band structure and Fermi surface topology as a function of twisting angle, very little exist from an experimental point of view. We will use ARPES and nano-ARPES to measure the electronic structure of twisted superlattices and will study how it evolves by changing the twisting angle. Particular attention will be given to the evolution of the mini flat bands, van hove singularities and Fermi surface topology to understand what is driving the Mott like insulating state and eventually the superconducting ground state at the magic angle.

We propose to explore the non-equilibrium Doppler effect of Dirac electron plasmons in graphene. Strongly biased graphene can sustain a large current, which results in a highly non-equilibrium distribution of charge carriers. The electron distribution will feature a finite average velocity. This can lead to a plasmonic Doppler effect, where the frequency degeneracy of the counter-propagating plasmonic modes is lifted due to broken time-reversal symmetry. This effect should exist in all materials under bias when electrons are driven by an external electric field to form electrical current, but it is usually negligible in conventional metals because the plasmon velocity is extremely high (i.e. typically close to the speed of light) and the electron drifting velocity is rather low. Graphene offers an ideal model system to realize the plasmonic Doppler effect.

We will explore single photon emission in engineered hBN specimens. Of interest is how strain, tailored defect structure, and functionalization affect the emission spectrum. UV through visible wavelengths will be investigated. This project will also explore novel collective plasmon excitations and their non-equilibrium behavior in graphene and carbon nanotube systems. The study will involve synergistic optical spectroscopy, ab initio theory, scanning

tunneling spectroscopy, electrical and mechanical characterization, chemical functionalization, and photoemission.

Our initial studies of few chains of $NbSe_3$ and $HfTe_3$ inside nanotubes suggest that other TMTs will yield exciting results. For example, TMTs such as TaS_3 have shown transitions due to CDW formation. Some TMTs are not stable in bulk, but there is a possibility that they can be stabilized within the confines of a cylindrical nanotube. We propose a comprehensive experimental and theoretical investigation of the TMT family in the few to single chain limit. We also wish to explore experimentally and theoretically transition metal dichalcogenides (TMDs) confined within the hollow core of nanotubes.

References

[1] T. Pham, S. Oh, P. Stetz, S. Onishi, C. Kisielowski, M. L. Cohen, and A. Zettl. "Torsional instability in the single-chain limit of a transition metal trichalcogenide," Science 361, pp 263 - 266 (2018) doi: 10.1126/science.aat4749
[2] Scott Meyer, Thang Pham, Sehoon Oh, Peter Ericus, Christian Kisielowski, Marvin L Cohen, Alex Zettl. Metal-insulator transition in quasi-one-dimensional $HfTe_3$ in the few-chain limit Phys. Rev. B 100, 041403(R) (2019) doi: https://doi.org/10.1103/PhysRevB.100.041403
[3] J. Velasco, Jr., J. Lee, D. Wong, S. Kahn, H.-Z. Tsai, J. Costello, T. Umeda, T. Taniguchi, K. Watanabe, A. Zettl, F. Wang, and M. F. Crommie. "Visualization and Control of Single-Electron Charging in Bilayer Graphene Quantum Dots," Nano Letters 18 (8), pp 5104 - 5110 (2018) doi: 10.1021/acs.nanolett.8b01972
[4] 7. D. Wong, F. Corsetti, Y. Wang, V. W. Brar, H. Tsai, Q. Wu, R. K. Kawakami, A. Zettl, A. A. Mostofi, J. Lischner, and M. F. Crommie. Spatially resolving density-dependent screening around a single charged atom in graphene. Phys Review B 95, 205419 (2017)
[5] S. M. Gilbert, T. Pham, M. Dogan, S. Oh, B. Shevitski, G. Schumm, S. Liu, P. Ericus, S. Aloni, M. L. Cohen, and A. Zettl. Alternative stacking sequences in hexagonal boron nitride. 2D Materials 6, 021006 (2019) doi: https://doi.org/10.1088/2053-1583/ab0e24

Publications

1) Saly Turner, Hu Long, Brian Shevitski, Thang Pham, Maydelle Lorenzo, Ellis Kennedy, Shaul Aloni, Marcus Worsley, and Alex Zettl, "Density Tunable Graphene Aerogels Using a Sacrificial Polycyclic Aromatic Hydrocarbon" Phys. Status Solidi B 254, 11 1700203 (2017)
2) H. Ryu, J. Hwang, D. Wang, A. S. Disa, J. Denlinger, Y. Zhang, S.-K. Mo, C. Hwang, and A. Lanzara. "Temperature-Dependent Electron–Electron Interaction in Graphene on SrTiO3" Nano Lett., 17 (10) 5914–5918 (2017)
3) A. M. Yan, C. S. Ong, D. Y. Qiu, C. Ophus, J. Ciston, C. Merino, S. G. Louie, and A. Zettl. "Dynamics of Symmetry-Breaking Stacking Boundaries in Bilayer MoS2," Journal of Phys. Chem. C 121, 22559 (2017)
4) G. Dunn, K. Shen, H. Reza Barzegar, W. Shi, J.N. Belling, T. N. H. Nguyen, E. Barkovich, K. Chism, M. M. Maharbiz, M. R. DeWeese, and A. Zettl. "Selective Insulation of Carbon Nanotubes," Phys. Status Solidi B 254, 107202 (2017)

5) S.M. Gilbert, G. Dunn, A. Azizi, T. Pham, B. Shevitski, E. Dimitrov, S. Liu, S. Aloni and A. Zettl. “Fabrication of Subnanometer-Precision Nanopores in Hexagonal Boron Nitride,” Nature Scientific Reports 7, 15096 (2017)
6) S. M. Gilbert, S. Liu, G. Schumm, and A. Zettl. “Nanopatterning Hexagonal Boron Nitride with Helium Ion Milling: Towards Atomically-Thin, Nanostructured Insulators,” MRS Advances 3, pp 327 - 331 (2018)
7) T. Pham, S. Oh, P. Stetz, S. Onishi, C. Kisielowski, M. L. Cohen, and A. Zettl. “Torsional instability in the single-chain limit of a transition metal trichalcogenide,” Science 361, pp 263 - 266 (2018)
8) D. Wong, Y. Wang, W. Jin, H.-Z. Tsai, A. Bostwick, E. Rotenberg, R.K. Kawakami, A. Zettl, A. A. Mostofi, J. Lischner, and M.F. Crommie. “Microscopy of hydrogen and hydrogen-vacancy defect structures on graphene devices,” Phys. Rev. B. 98, 155436 (2018). DOI: 10.1103/PhysRevB.98.155436
9) J. Velasco, Jr., J. Lee, D. Wong, S. Kahn, H.-Z. Tsai, J. Costello, T. Umeda, T. Taniguchi, K. Watanabe, A. Zettl, F. Wang, and M. F. Crommie. “Visualization and Control of Single-Electron Charging in Bilayer Graphene Quantum Dots,” Nano Letters 18 (8), pp 5104 - 5110 (2018)
10) D.W. Latzke, C. Ojeda-Aristizabal, S. M. Griffin, J. D. Denlinger, J. B. Neaton, A. Zettl and A. Lanzara, “Observation of highly dispersive bands in pure thin film C60,” Phys. Rev. B. 99, 045425 (2019)
11) Bradford A. Barker, Aaron J. Bradley, Miguel M. Ugeda, Sinisa Coh, Alex Zettl, Michael F. Crommie, Steven G. Louie, and Marvin L. Cohen, “Geometry and electronic structure of iridium adsorbed on graphene,” Phys. Rev. B. 99, 075431 (2019)
12) S. M. Gilbert, T. Pham, M. Dogan, S. Oh, B. Shevitski, G. Schumm, S. Liu, P. Ericus, S. Aloni, M. L. Cohen, and A. Zettl, “Alternative stacking sequences in hexagonal boron nitride,” 2D Materials 6, 021006 (2019)
13) Scott Meyer, Thang Pham, Sehoon Oh, Peter Ericius, Christian Kisielowski, Marvin L Cohen, Alex Zettl, “Metal-insulator transition in quasi-one-dimensional HfTe3 in the few-chain limit” Phys. Rev. B. 100, 041403(R) (2019)

Project Title: Correlated electronic display of quantum excitations in geometrically frustrated magnets via heteroepitaxy

PI: Haidong Zhou (University of Tennessee), Co-PI: Jian Liu (University of Tennessee)

Program Scope

As the conventional semiconductor technology is approaching the end of the Moore's law, the rising of quantum computing and quantum information is believed to hold promises of solving problems of drastically increased complexities and deliver information with unhackable security. But the big question has been where the "silicon" of quantum technology is for scalable device realization. Most of the known material systems still operate in an atomic or atomic-like fashion, which is simply due to the fact that quantum states are better defined and protected in a highly confined and isolated space. In contrast, quantum objects emerging in many-body systems may survive in a much "tougher" environment that is more extended and compact since they are driven by collective states of matter.

While collective states and elementary excitations widely exist in quantum materials, entanglement is rather rare and is often associated with a high degree of incipient degeneracy that is embedded in the system in a nontrivial way. Geometrically frustrated quantum magnets (GFQMs) are one of such kinds, where the geometric frustration of the spin lattice leads to a large number of magnetic configurations that are energetically equal and force the spins to collectively choose a highly-entangled state rather than a conventional symmetry-broken ordering. For instance, the celebrated quantum spin liquid (QSL) state[1] has all the spins randomly oriented in space and time. They are free to fluctuate not individually but cooperatively through a high degree of long-range entanglement, enabling the possibility of non-abelian quasiparticle and fractional excitations known as spinons, which allows quantum mechanical encryption and transportation of information[2].

Despite extensive studies on GFQMs, they are still distance away from serious application. A main challenge is that, although more and more candidate materials are being identified, most of them are insulators and electronically inert, which is incompatible with electrical circuit that relies on moving charge carriers. The grand challenge is to find a clean method to convert the collective excitations in GFQMs into a charge signal and therefore bridges the gap from quantum magnetism to quantum device and circuit. This program is to explore a new route, combining insulating quantum magnets and correlated metals in a heterostructure, toward taming the entanglements. In such a system, the GFQM hosts exotic spin states and excitations while the correlated metals host the interacting electrons forming a liquid-like state of itinerant fermions. Due to the electronic correlation, an ensemble of itinerant quasi-electrons is often highly sensitive to spin fluctuations and on the verge of electronic instabilities. Our study will establish a new interfacial approach for metallizing quantum magnets. We will perform a systematic electronic transport study on a series of heterojunctions where spin ice and spin liquid compounds are interfaced with a correlated metal. This work will facilitate understanding of the interfacial effects that enable charge responses to exotic magnetic excitations.

Recent Progress

As a pragmatic approach, we will first focus on the heterostructures combining pyrochlore magnets and correlated metals. In pyrochlores[3], the rare earth magnetic ions form a corn-shared tetrahedral network, which is the most celebrated geometrically frustrated lattice. The first prototypical GFQM selected here is $Dy_2Ti_2O_7$ (DTO). As illustrated in Fig. 1: (i) at zero field, DTO exhibits a short-range ordered spin state for each magnetic tetrahedron with two spins pointing in and two pointing out along the <111> axis (Fig. 1(a)). This is the so called "spin ice" state since the "two-in-two-out" spin configuration is an analogy to the two short and two long H-O bonds in the ice structure[4]; (ii) with a magnetic field along the <111> axis, the spins on the triangular layers are fully polarized while the spins on the kagome layers still form the either "two-in-one-out" or "two-out-one-in" configurations on the corner-shared triangles (Fig. 1(b)). Therefore, the spin ice state now enters a "kagome spin ice" state[5]; Accordingly, the magnetization of DTO exhibits a plateau in this state at low temperatures (Fig. 1(e)); (iii) with even larger field, the system enters a polarized state with the "three-in-one-out" or "three-out-one-in" configuration on the tetrahedron (Fig. 1(c)); (iv) while a spin is flipped by local defect, thermal excitation, and/or a small magnetic field, the ice rule will be violated between the two tetrahedral, which to a good approximation can be viewed as the formation of a pair of deconfined monopoles[6] of opposite sign (Fig. 1(d)).

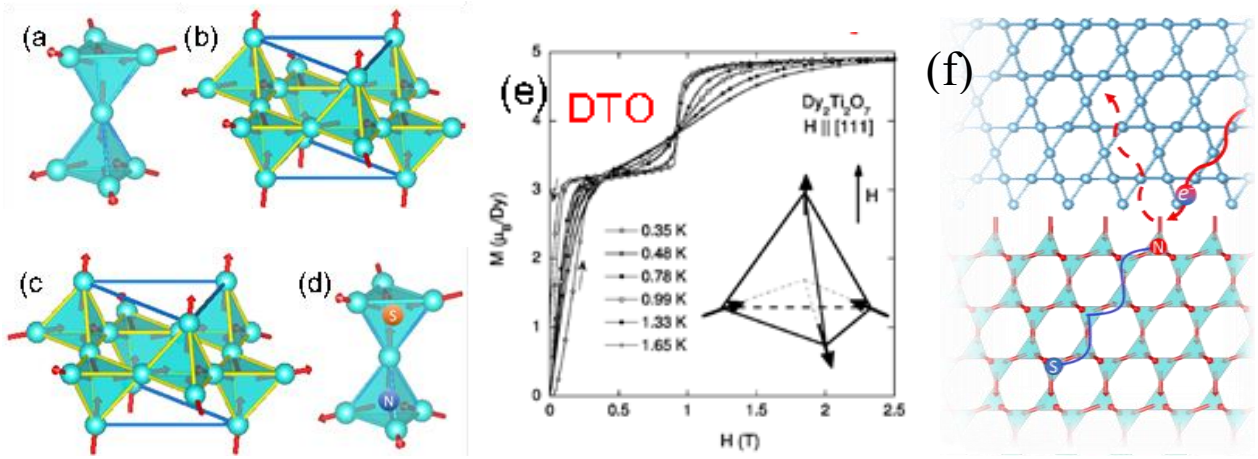

Figure 1 The spin structures for DTO as described in the main text: (a) spin ice; (b) kagome spin ice; (c) polarized state; and (d) magnetic monopole. The magnetization (e) for DTO. (f) Schematic of GFQM/correlated metal pyrochlore heterostructure, where the itinerant quasi-electron interacts with a spin ice structure through the magnetic monopole excitation.

For the correlated metal part of the heterostructure, $Bi_2Ir_2O_7$ is selected here, due to its structural compatibility with DTO as well as its strong spin-orbit coupling. Lattice mismatch is critical for heterostructure synthesis. BIO is isostructural with DTO with a lattice mismatch less than 2%, providing an ideal combination for forming heteroepitaxial interfaces (Fig.1(f)). Electronically, BIO is an exotic correlated metal[7] with a divergent magnetic susceptibility at low temperatures but no long-range order down to 50 mK. This behavior is believed to be associated with the proximity to the magnetic quantum critical point of the phase diagram of rare earth pyrochlore iridates. The transport properties of the itinerant electrons in BIO are thus expected to be highly sensitive to spin fluctuations. Indeed, the interaction between the $J_{\text{eff}} = 1/2$ electron and magnetic rare earth ion in pyrochlore iridates has been shown to cause large magnetoresistance when the

external field modulates the geometrically frustrated rare earth sublattice. While the rare earth is replaced by the nonmagnetic Bi ion in BIO, such a coupling will be present at the interface with DTO (Fig.1(f)).

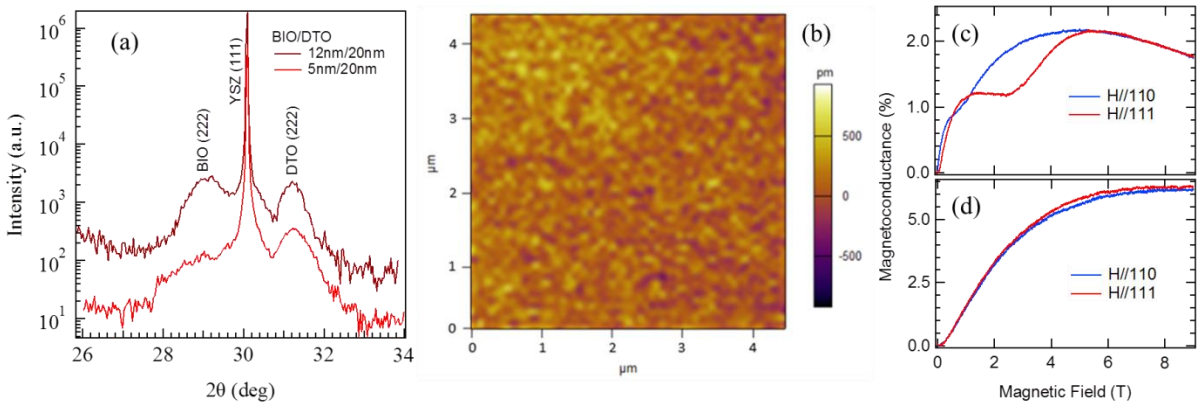

Figure 2: (a) Specular x-ray diffraction scans on BIO/DTO heterostructures grown on YZS (111) substrates. (b) A typical AFM morphology image of the surface. Magneto-conductance curves for (c) DIO 20nm/BIO 5nm and (d) YTO 20nm/BIO 5nm heterostructures with applied magnetic field along the different orientations of DTO or YTO films at 50 mK.

Recently, the PIs have tested this interfacial approach on such kind of heterostrcutures and gathered promising preliminary data. As shown by the x-ray diffraction results in Fig. 2(a), epitaxial layers of BIO and DTO have been successfully grown on YSZ substrates by pulsed laser deposition. The resulted films and heterostructures show flat surfaces (Fig. 2(b)) with a roughness less than 0.5 nm. We have tuned the thickness of the BIO layer from 12 nm to 5 nm in order to enhance the ratio of the interfacial region in the BIO layer. We were able obtained magneto-conductance measured for a 20nm/5nm DTO/BIO heterostructure at 50 mK, which clearly shows an anomalous behavior (Fig. 2(c)). Specifically, the magneto-conductance is positive for the DTO/BIO sample with significant anisotropy between 1 and 5 T. With increasing field, a step-like feature is observed with H//<111> axis from 1 to 3 T but not with H//<110>. This feature is reminiscent of the magnetization plateau of DTO (Fig.1(e)) where the Kagome spin ice state is stabilized. The magneto-conductance continues increasing upon further increasing the field and starts to saturate around 5 T, resembling the second magnetization jump to the plateau (Fig.1(e)) of the polarized state. The absence of this plateau-like conductance feature is also consistent with angular dependence of the Kagome spin ice state[8]. None of these phenomena was observed in the reference sample where the DTO layer is replaced by a nonmagnetic $Y_2Ti_2O_7$ (YTO) layer (Fig.2(d)). It is obvious that this anomalous behavior is due to the interfacial interaction between the spin state in DTO and the charge transport in BIO.

Future Plans

We will systematically investigate the magneto-transport properties of the BIO/DTO heterostructures. We will vary the BIO layer thickness from 20 to 1 nm. As the thickness decreases, the interfacial coupling will become more dominant to the electronic transport. On the other hand, such a dimensional crossover will also enhance localization effects due to the size effect. Therefore, we anticipate a metal-to-insulator crossover with an intermediate thickness where the electronic response to the spin excitations of the GFQMs will be maximized. To

determine this optimal thickness and resolve the electronic response, we will measure the temperature and field dependences of the longitudinal and transverse (Hall) resistance of the BIO films. We will monitor how the characteristic transport behavior of BIO evolves with the thickness and in the presence of the interfacial coupling. In addition, we will also vary the thicknesses of the DTO layer from 5 to 100 nm for revealing any size effect on the GFQM layer. To verify the spin state, we will perform magnetic torque and AC susceptibility measurements.

In parallel, we will use DTO single crystal as the substrate and directly deposit BIO ultrathin films on the top. This approach will fully preserve the bulk spin states of DTO such that the electronic responses of the BIO layer can be unambiguously correlated with the spin excitations in the GFQMs. The single crystal growth of pyrochlores will be conducted by using the image furnace. The crystal surface will be cut along the (111) plane for the same epitaxial interface. The same magneto-transport measurements will be performed for direct comparison. A corresponding comparison will be to replace the DTO crystal with an YTO crystal, which can be achieved through the same crystal growth and preparation process. Moreover, this will allow us to further use YTO single crystal as the substrate for depositing the DTO/BIO heterostructures, taking advantage of its almost perfect lattice match with DTO over YSZ. The comprehensive comparisons among samples with all these different designs and combinations will allow us examine the nature and robustness of the interfacial coupling. Finally, we will utilize this methodology to investigate heterostructures where the spin ice DTO is replaced by the other GFQMs, such as the QSL $Tb_2Ti_2O_7$ (TTO). Recent low temperature AC susceptibility has showed that a magnetic field along the <111> axis can induce a spin state transitions, possibly from QSL to kagome spin ice, akin to the one observed in DTO. It will be interesting to explore any possible charge responses through the interfacial coupling.

References

1. Lee, P. A. *Science* **321,** 1306–1307 (2008).
2. Kitaev, A. & Preskill, J. *Phys. Rev. Lett.* **96,** 110404 (2006).
3. Gardner, J. S., Gingras, M. J. P. & Greedan, J. E. *Rev. Mod. Phys.* **82,** 53–107 (2010).
4. Bramwell, S. T. *Science* **294,** 1495–1501 (2001).
5. Tabata, Y., Kadowaki, H., Matsuhira, K., Hiroi, Z., Aso, N., Ressouche, E. & Fåk, B. *Phys. Rev. Lett.* **97,** 257205 (2006).
6. Castelnovo, C., Moessner, R. & Sondhi, S. L. Magnetic monopoles in spin ice. *Nature* **451,** 42–45 (2008).
7. Qi, T. F., Korneta, O. B., Wan, X., DeLong, L. E., Schlottmann, P. & Cao, G. *J. Phys. Condens. Matter* **24,** 345601 (2012).
8. Fukazawa, H., Melko, R., Higashinaka, R., Maeno, Y. & Gingras, M. *Phys. Rev. B* **65,** 054410 (2002).

Publications

No publications are yet supported by the DOE as the project is newly funded.

Quantum Hall Systems In and Out of Equilibrium

Michael Zudov, University of Minnesota – Twin Cities

Program Scope

This program deals with quantum transport phenomena in semiconductor nanostructures focusing on the roles of microwave radiation, dc electric field, in-plane magnetic field, and disorder. The research expands upon the area originated by discoveries of integer and fractional quantum Hall effects [1], followed by other phenomena, such as quantum Hall stripes (QHSs) and bubbles [2], microwave-induced resistance oscillations and zero-resistance states [3], etc. The proposal is aimed to address issues of contemporary interest related to both nonequilibrium and equilibrium physics in quantum Hall systems.

Recent Progress

1. Quantum Hall stripes at high carrier densities in tilted magnetic fields [4] – While native QHSs are usually aligned along [110] crystal axis, there exist experiments [5] which have found orthogonal stripe orientation above certain carrier density (n = 3 × 10^{11} cm^{-2}). However, our recent experiments [6] in a tunable-density sample revealed that normal, [110], native stripe orientation is preserved up to the onset of the second subband population (n = 3.6 × 10^{11} cm^{-2}) and that such orientation is not affected by the in-plane magnetic field. It is thus very desirable to explore the effect of the in-plane field in the higher density regime (without populating the second subband) in which QHSs are expected to have an abnormal orientation. We have investigated several high-mobility samples with densities ranging from ~3.3 to 4.3 × 10^{11} cm^{-2}. Surprisingly, we have found that QHSs are still oriented along conventional [110] direction even at the highest density studied. We also found that the in-plane magnetic field readily reorients QHSs perpendicular to it (see Fig. 1). Upon further increase of the in-plane field, the resistance

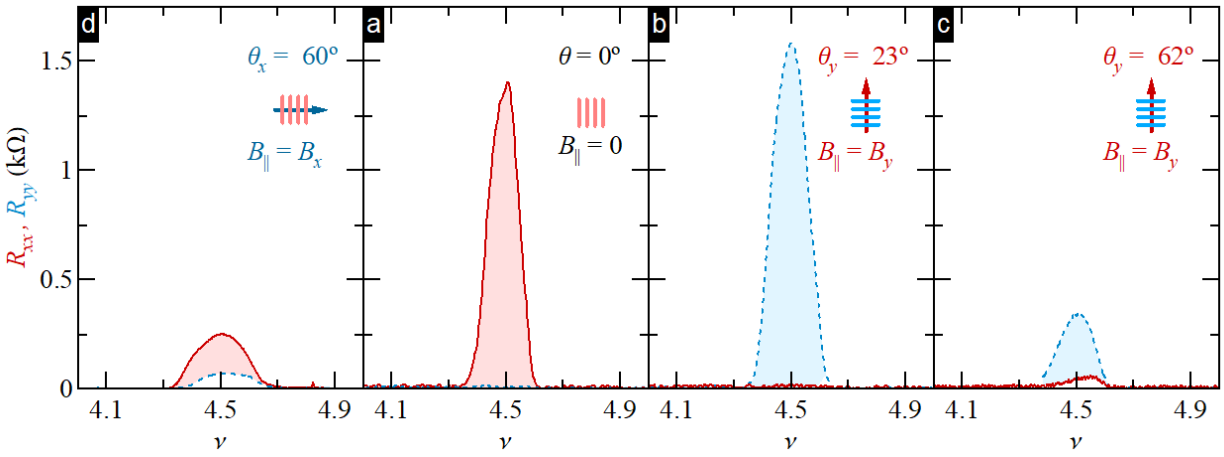

Fig. 1. R_{xx} (solid line) and R_{yy} (dotted line) vs filling factor ν at $B_{\|} = B_y$ and different tilt angles θ, as marked.

anisotropy diminished but no second reorientation was detected, in contrast to the study using a back-gated device [6]. We thus can conclude that high electron density alone is not a decisive factor for either abnormal native QHSs orientation or their alignment with respect to the in-plane field. Instead, our study suggests that quantum confinement also plays an important role [4].

2. Observation of two- and three-electron bubbles in the N = 3 Landau level [7,8] – A "bubble" phase is a generalization of a Wigner crystal containing $M \geq 2$ electrons per unit cell. While experimental evidence of such phases with $M = 2$ has emerged shortly after their prediction in 1996 [2], larger bubbles have not been identified till now. We have detected transport signatures of eight distinct bubble phases in the $N = 3$ Landau level of an $Al_xGa_{1-x}As$ quantum well with $x = 0.0015$. These phases occur near partial filling factors $\nu^\star \approx 0.2$ (0.8) and $\nu^\star \approx 0.3$ (0.7) and have $M = 2$ and $M = 3$ electrons (holes) per bubble, respectively. We speculate that a small amount of alloy disorder in our sample helps to clearly distinguish these broken symmetry states in low-temperature transport. These findings experimentally confirm a long-standing prediction of more complex bubbles and draw attention to a regime of higher Landau levels which has not yet been experimentally explored in detail.

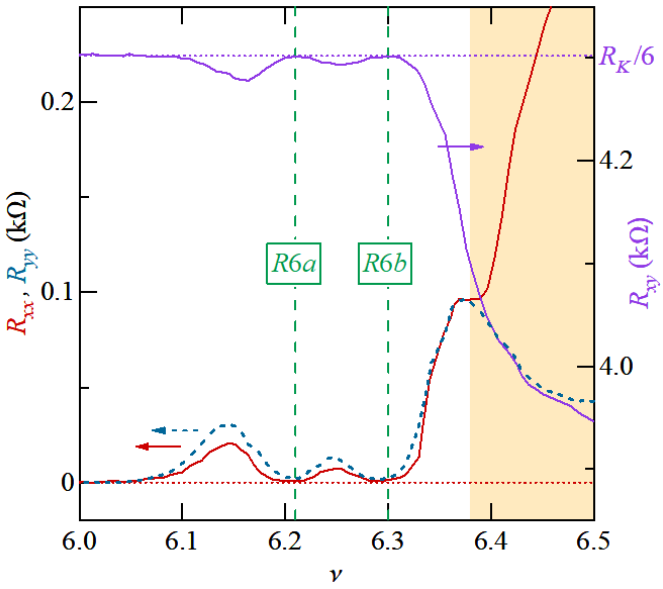

Fig. 2. R_{xx} (solid line, left axis), R_{yy} (dotted line, left axis), and Hall resistance R_{xy} (right axis) as a function of the filling factor ν at $T \approx 25$ mK. Bubble phases are marked by vertical dashed lines drawn at $\nu = 6.21$ and at $\nu = 6.30$.

3. Quantum Hall stripes with reduced transport anisotropy near filling factor $\nu = 13/2$ – QHSs form when $0.4 \leq \nu^\star \leq 0.6$ and R_{xx} (R_{yy}) usually reaches its maximum (minimum) value at $\nu^\star \approx 1/2$. However, several of our samples have consistently revealed pronounced local minimum in the R_{xx} and a maximum in R_{yy} (with $R_{xx} >> R_{yy}$) near filling factor $\nu = 13/2$ (see Fig. 3). While the anisotropy sets in at $T \geq 0.1$ K, this local extrema emerge at $T \leq 70$ mK and become stronger with decreasing temperature. Upon application of modest $B_\parallel = B_y$, R_{xx} at $\nu = 13/2$ can *increase* several times while R_{yy} becomes immeasurably small. This behavior is in vast contrast with previous studies which showed switching of the anisotropy axis under $B_\parallel = B_y$. Application of $B_\parallel = B_x$ also destroys this anomaly indicating that the orientation of $B_\parallel$ with respect to native QHSs is of secondary importance. Interestingly, these extrema usually disappear in a very similar way with increasing T; the resistance anisotropy at $\nu = 13/2$ substantially *grows* as T is raised. While the origin of these extrema remains unclear, it might be another manifestation of the recently reported nematic to smectic phase transition [9]. However, we cannot rule out other scenarios, such as competition with an anisotropic even-denominator fractional Hall state.

Future Plans

During next year we plan to conclude our studies of unusual QHSs phases with reduced transport anisotropy. In addition, we plan to investigat the role of density on QHSs reorientation under $B_{\|}$ applied perpendicular to the native QHSs. The latter should provide insight on possible coupling between $B_{\|}$-induced and native symmetry-breaking potentials. In the area of non-equilibrium transport, we plan to investigate microwave-induced resistance oscillations in a tunable-density GaAs quantum well in which the second subband can be populated.

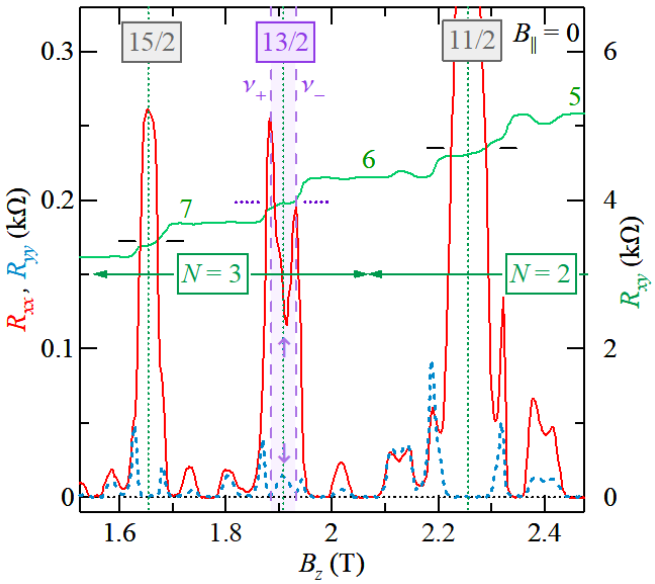

Fig. 3. R_{xx} (solid line, left axis), R_{yy} (dotted line, left axis), and R_{xy} (right axis) vs. B_z.

References

[1] K. von Klitzing, G. Dorda, and M. Pepper, Phys. Rev. Lett. **45**, 494 (1980); D.C. Tsui, H. L. Stormer, and A. C. Gossard, Phys. Rev. Lett. **48**, 1559 (1982).

[2] A. A. Koulakov, M. M. Fogler, and B. I. Shklovskii, Phys. Rev. Lett. **76**, 499 (1996); M. P. Lilly, K. B. Cooper, J. P. Eisenstein, L. N. Pfeiffer, and K. W.West, Phys. Rev. Lett. **82**, 394 (1999); R. R. Du, D. C. Tsui, H. L. Stormer, L. N. Pfeiffer, K. W. Baldwin, and K. W. West, Solid State Commun. **109**, 389 (1999).

[3] M. A. Zudov, R. R. Du, J. A. Simmons, and J. L. Reno, **64**, Phys. Rev. B 201311(R) (2001); R. G. Mani, J. H. Smet, K. von Klitzing, V. Narayanamurti, W. B. Johnson, and V. Umansky, Nature (London) **420**, 646 (2002); M. A. Zudov, R. R. Du, L. N. Pfeiffer, and K. W. West, Phys. Rev. Lett. **90**, 46807 (2003).

[4] X. Fu, Q. Shi, M. A. Zudov, Y. J. Chung, K. W. Baldwin, L. N. Pfeiffer, and K. W. West, Phys. Rev. B **98**, 205418 (2018) .

[5] J. Zhu, W. Pan, H. L. Stormer, L. N. Pfeiffer, and K. W. West, Phys. Rev. Lett. **88**, 116803 (2002).

[6] Q. Shi, M. A. Zudov, J. D. Watson, Q. Qian, and M. J. Manfra, Phys. Rev. B **95**, 161303(R) (2017).

[7] X. Fu, Q. Shi, M. A. Zudov, G. C. Gardner, J. D. Watson, and M. J. Manfra, Phys. Rev. B **99**, 151402(R) (2019).

[8] Dohyung Ro, N. Deng, J. D. Watson, M. J. Manfra, L. N. Pfeiffer, K. W. West, and G. A. Csáthy, Phys. Rev. B **99**, 201111(R) (2019).

[9] Q. Qian, J. Nakamura, S. Fallahi, G. C. Gardner, M. J. Manfra, Nat. Comm. **8**, 1536 (2017)

Publications (2017-2019)

1. X. Fu, Q. Shi, M. A. Zudov, G. C. Gardner, J. D. Watson, and M. J. Manfra, "Two- and three-electron bubbles in AlxGa1−xAs/Al0.24Ga0.76As quantum wells", Physical Review B – Rapid Communications **99**, 151402(R) (2019) [Editors' Suggestion]

2. X. Fu, Q. Shi, M. A. Zudov, Y. J. Chung, K. W. Baldwin, L. N. Pfeiffer, and K. W. West, "Quantum Hall stripes in high-density GaAs/AlGaAs quantum wells", Physical Review B **98**, 205418 (2018)

3. X. Fu, A. D. Riedl, M. D. Borisov, M. A. Zudov, J. D. Watson, G. C. Gardner, M. J. Manfra, K. W. Baldwin, L. N. Pfeiffer, and K. W. West, "Effect of low-temperature illumination on quantum lifetime in GaAs quantum wells", Physical Review B **98**, 195403 (2018)

4. X. Fu, M. D. Borisov, M. A. Zudov, J. D. Watson, and M. J. Manfra, "Effect of density on the amplitude of microwave-induced resistance oscillations", Physical Review B – Rapid Communications **98**, 121303(R) (2018)

5. M. Sammon, M. A. Zudov, and B. I. Shklovskii, "Mobility and quantum mobility of modern GaAs/AlGaAs heterostructures", Physical Review Materials **2**, 064604 (2018)

6. M. A. Zudov, Q. Shi, I. A. Dmitriev, B. Friess, V. Umansky, K. von Klitzing, and J. Smet, "Hall field-induced resistance oscillations in a tunable-density GaAs quantum well", Physical Review B – Rapid Communications **96**, 121301(R) (2017)

7. Q. Shi, M. A. Zudov, J. Falson, Y. Kozuka, A. Tsukazaki, M. Kawasaki, and J. Smet, "Nonlinear response of a MgZnO/ZnO heterostructure close to zero bias", Physical Review B **96**, 125401 (2017)

8. X. Fu, Q. A. Ebner, Q. Shi, M. A. Zudov, Q. Qian, and M. J. Manfra, "Microwave-induced resistance oscillations in a backgated GaAs quantum well", Physical Review B **95**, 235415 (2017)

9. Q. Shi, M. A. Zudov, B. Friess, J. Smet, J. D. Watson, G. C. Gardner, and M. J. Manfra "Apparent temperature-induced reorientation of quantum Hall stripes", Physical Review B – Rapid Communications **95**, 161404(R) (2017)

10. Q. Shi, M. A. Zudov, J. D. Watson, Q. Qian, and M. J. Manfra, "Effect of density on quantum Hall stripe orientation in tilted magnetic fields", Physical Review B – Rapid Communications **95**, 161303(R) (2017)

11. Q. Shi, M. A. Zudov, J. Falson, Y. Kozuka, A. Tsukazaki, M. Kawasaki, K. von Klitzing, and J. Smet, "Hall field-induced resistance oscillations in MgZnO/ZnO heterostructures", Physical Review B – Rapid Communications **95**, 041411(R) (2017)

Author Index

Participant List

Name	Organization	Email Address
Adams, Philip	Louisiana State University	pwadams9@gmail.com
Ahn, Charles	Yale University	charles.ahn@yale.edu
Analytis, James	University of California, Berkeley	analytis@berkeley.edu
Andrei, Eva	Rutgers University	eandrei@physics.rutgers.edu
Ashoori, Ray	Massachusetts Institute of Technology	ashoori@mit.edu
Balicas, Luis	National High Magnetic Field Laboratory	balicas@magnet.fsu.edu
Basov, Dmitri	Columbia University	db3056@columbia.edu
Bawendi, Moungi	Massachusetts Institute of Technology	mgb@mit.edu
Bird, Jon	University at Buffalo	jbird@buffalo.edu
Bisogni, Valentina	Brookhaven National Laboratory	bisogni@bnl.gov
Butov, Leonid	University of California, San Diego	lvbutov@physics.ucsd.edu
Canfield, Paul	AMES Laboratory	canfield@ameslab.gov
Cha, Judy	Yale University	judy.j.cha@gmail.com
Chan, Moses	Pennsylvania State University	mhc2@psu.edu
Chan, Mun	Los Alamos National Laboratory	mkchan@lanl.gov
Chien, TeYu	University of Wyoming	tchien@uwyo.edu
Civale, Leonardo	Los Alamos National Laboratory	lcivale@lanl.gov
Csathy, Gabor	Purdue University	gcsathy@purdue.edu
Dessau, Dan	University of Colorado, Boulder	dessau@colorado.edu
Dean, Cory	Columbia University	cd2478@columbia.edu
DiTusa, John	Louisiana State University	ditusa@phys.lsu.edu
Engel, Lloyd	Florida State University/National High Magnetic Field Laboratory	engel@magnet.fsu.edu
Eom, Chang-Beom	University of Wisconsin, Madison	eom@engr.wisc.edu

Finkelstein, Gleb	Duke University	gleb@phy.duke.edu
Fisher, Ian	Stanford University/SLAC National Accelerator Laboratory	irfisher@stanford.edu
Fong, Dillon	Argonne National Laboratory	fong@anl.gov
Freedman, Danna	Northwestern University	danna.freedman@northwestern.edu
Furukawa, Yuji	AMES Laboratory	furukawa@ameslab.gov
Gersten, Bonnie	US Department of Energy	bonnie.gersten@science.doe.gov
Hadjipanayis, George	University of Delaware	hadji@udel.edu
Halperin, Bill	Northwestern University	w-halperin@northwestern.edu
Harrison, Neil	Los Alamos National Laboratory	nharrison@lanl.gov
Hellman, Frances	University of California, Berkeley	fhellman@berkeley.edu
Hilton, David	University of Alabama, Birmingham	dhilton@uab.edu
Hla, Saw	Ohio University	hla@ohio.edu
Holcomb, Micky	West Virginia University	mikel.holcomb@mail.wvu.edu
Hone, Jim	Columbia University	jh2228@columbia.edu
Hsieh, David	California Institute of Technology	dhsieh@caltech.edu
Hu, Jin	University of Arkansas	jinhu@uark.edu
Hunt, Benjamin	Carnegie Mellon University	bmhunt@andrew.cmu.edu
Hwang, Harold	Stanford University/SLAC National Accelerator Laboratory	hyhwang@stanford.edu
Jarillo-Herrero, Pablo	Massachusetts Institute of Technology	pjarillo@mit.edu
Jiang, Zhigang	Georgia Institute of Technology	zhigang.jiang@physics.gatech.edu
Ketterson, John	Northwestern University	j-ketterson@northwestern.edu
Kidd, Tim	University of Northern Iowa	tim.kidd@uni.edu
Kim, Philip	Harvard University	pkim@physics.harvard.edu

Kono, Junichiro	Rice University	jth6@rice.edu
Kwok, Wai-Kwong	Argonne National Laboratory	wkwok@anl.gov
Lau, Jeanie	The Ohio State University	lau.232@osu.edu
Lee, Honyung	Oak Ridge National Laboratory	hnlee@ornl.gov
Li, Qi	Pennsylvania State University	qil1@psu.edu
Li, Qiang	Brookhaven National Laboratory	qiangli@bnl.gov
Li, Lu	University of Michigan	luli@umich.edu
Liu, Jian	University of Tennessee	jianliu@utk.edu
Lüpke, Gunter	College of William & Mary	luepke@wm.edu
Mak, Kin Fai	Cornell University	km627@cornell.edu
Manfra, Michael	Purdue University	mmanfra@purdue.edu
Maple, Brian	University of California, San Diego	mbmaple@ucsd.edu
McQueeney, Rob	AMES Laboratory	mcqueeney@ameslab.gov
Mitchell, John	Argonne National Laboratory	mitchell@anl.gov
Mitrano, Matteo	University of Illinois, Urbana-Champaign	mmitrano@illinois.edu
Morosan, Emilia	Rice University	emorosan@rice.edu
Musfeldt, Jan	University of Tennessee	musfeldt@utk.edu
Natelson, Douglas	Rice University	natelson@rice.edu
Ni, Ni	University of California, Los Angeles	nini@physics.ucla.edu
Ojeda-Aristizabal, Claudia	California State Univ., Long Beach	Claudia.Ojeda-Aristizabal@csulb.edu
Ong, Nai Phuan	Princeton University	npo@princeton.edu
Orenstein, Joe	Lawrence Berkeley National Laboratory	jworenstein@lbl.gov
Ouyang, Min	University of Maryland, College Park	mouyang@umd.edu

Paglione, Johnpierre	University of Maryland	paglione@umd.edu
Palmstrom, Chris	University of California, Santa Barbara	cpalmstrom@ece.ucsb.edu
Pechan, Michael	US Department of Energy	michael.pechan@science.doe.gov
Ralph, Dan	Cornell University	dcr14@cornell.edu
Ramirez, Art	University of California, Santa Cruz	apr@ucsc.edu
Ramshaw, Brad	Cornell University	bradramshaw@cornell.edu
Rokhinson, Leonid	Purdue University	leonid@purdue.edu
Ronning, Filip	Los Alamos National Laboratory	fronning@lanl.gov
Rosenbaum, Thomas	California Institute of Technology	tfr@caltech.edu
Sales, Brian	Oak Ridge National Laboratory	salesbc@ornl.gov
Schiffer, Peter	Yale University	peter.schiffer@yale.edu
Schuller, Ivan	University of California, San Diego	ischuller@ucsd.edu
Sefat, Athena	Oak Ridge National Laboratory	sefata@ornl.gov
Shan, Jie	Cornell University	jie.shan@cornell.edu
Shayegan, Mansour	Princeton University	shayegan@princeton.edu
Smirnov, Dmitry	National High Magnetic Field Laboratory	smirnov@magnet.fsu.edu
Smith, Arthur	Ohio University	ohiousmith@gmail.com
Spiropulu, Maria	California Institute of Technology	smaria@caltech.edu
Strachan, Doug	University of Kentucky	drst222@uky.edu
Thiyagarajan, Pappannan	US Department of Energy	p.thiyagarajan@science.doe.gov
Urazhdin, Sergei	Emory University	sergei_u@hotmail.com
Valla, Tonica	Brookhaven National Laboratory	valla@bnl.gov
Wang, Feng	Lawrence Berkeley National Laboratory	fengwang76@berkeley.edu

Ward, Zac	Oak Ridge National Laboratory	wardtz@ornl.gov
Wells, Barry	University of Connecticut	barrett.wells@uconn.edu
Welp, Ulrich	Argonne National Laboratory	welp@anl.gov
Westervelt, Bob	Harvard University	westervelt@seas.harvard.edu
Wu, Mingzhong	Colorado State University	mwu@colostate.edu
Xiao, John	University of Delaware	jqx@udel.edu
Xu, Xiaoshan	University of Nebraska, Lincoln	xiaoshan.xu@unl.edu
Yacoby, Amir	Harvard University	yacoby@g.harvard.edu
Yang, Fengyuan	The Ohio State University	yang.1006@osu.edu
Zhou, Haidong	University of Tennessee	hzhou10@utk.edu
Zudov, Michael	University of Minnesota	zudov001@umn.edu